



# **Space engineering**

---

## **Thermal design handbook - Part 5: Structural Materials: Metallic and Composite**

ECSS Secretariat  
ESA-ESTEC  
Requirements & Standards Division  
Noordwijk, The Netherlands

## Foreword

This Handbook is one document of the series of ECSS Documents intended to be used as supporting material for ECSS Standards in space projects and applications. ECSS is a cooperative effort of the European Space Agency, national space agencies and European industry associations for the purpose of developing and maintaining common standards.

The material in this Handbook is a collection of data gathered from many projects and technical journals which provides the reader with description and recommendation on subjects to be considered when performing the work of Thermal design.

The material for the subjects has been collated from research spanning many years, therefore a subject may have been revisited or updated by science and industry.

The material is provided as good background on the subjects of thermal design, the reader is recommended to research whether a subject has been updated further, since the publication of the material contained herein.

This handbook has been prepared by ESA TEC-MT/QR division, reviewed by the ECSS Executive Secretariat and approved by the ECSS Technical Authority.

## Disclaimer

ECSS does not provide any warranty whatsoever, whether expressed, implied, or statutory, including, but not limited to, any warranty of merchantability or fitness for a particular purpose or any warranty that the contents of the item are error-free. In no respect shall ECSS incur any liability for any damages, including, but not limited to, direct, indirect, special, or consequential damages arising out of, resulting from, or in any way connected to the use of this document, whether or not based upon warranty, business agreement, tort, or otherwise; whether or not injury was sustained by persons or property or otherwise; and whether or not loss was sustained from, or arose out of, the results of, the item, or any services that may be provided by ECSS.

Published by: ESA Requirements and Standards Division  
ESTEC, P.O. Box 299,  
2200 AG Noordwijk  
The Netherlands

Copyright: 2011 © by the European Space Agency for the members of ECSS

---

## Table of contents

---

<b>1 Scope</b> .....	<b>18</b>
<b>2 References</b> .....	<b>19</b>
<b>3 Terms, definitions and symbols</b> .....	<b>20</b>
3.1 Terms and definitions .....	20
3.2 Symbols.....	20
<b>4 Metallic materials</b> .....	<b>23</b>
4.1 General.....	23
4.1.1 Modifiers of thermal radiative properties .....	26
4.1.2 Cladding definitions .....	27
4.1.3 Temper designation for heat treatable aluminium alloys .....	28
4.2 Aluminium alloys .....	28
4.3 Aluminium-Copper alloys .....	85
4.4 Aluminium-Magnesium alloys.....	104
4.5 Aluminium-Zinc alloys .....	114
4.6 Magnesium-Zinc-Thorium alloys .....	131
4.7 Titanium-Aluminium-Tin alloys .....	133
4.8 Titanium-Aluminium-Tin alloys .....	144
4.9 Titanium-Aluminium-Vanadium alloys .....	151
4.10 Nickel-Chrome-Cobalt-Molybdenum alloys .....	165
4.11 Iron-Nickel alloys .....	175
<b>5 Composite materials</b> .....	<b>182</b>
5.1 List of symbols.....	182
5.2 List of matrices, prepregs and laminates quoted in this clause .....	187
5.2.1 Matrices, adhesives, potting, moulding compounds.....	188
5.2.2 Prepregs, laminates and films .....	193
5.2.3 Code list of manufacturers (or developers) .....	195
5.3 General introduction .....	197
5.3.2 Composition.....	198
5.3.3 Commercial fiber product names, descriptions and manufacturers .....	200

5.3.4	Geometry of fiber reinforcement. fabrics. abridged designation.....	205
5.4	Physical properties .....	210
5.4.1	Density.....	210
5.5	Thermal properties .....	216
5.5.1	Specific heat.....	216
5.5.2	Thermal conductivity.....	222
5.5.3	Thermal diffusivity.....	247
5.6	Thermo-elastic properties.....	256
5.6.1	Coefficient of linear thermal expansion .....	256
5.7	Thermal radiation properties of bare high strength fibers.....	319
5.7.1	Sample characterization .....	319
5.7.2	Emittance.....	319
5.7.3	Absorptance .....	321
5.8	Thermal radiation properties of bare composite materials .....	324
5.8.1	Tabulated data.....	324
5.9	Thermal radiation properties of coated composite materials.....	326
5.9.1	White painted composite materials.....	327
5.9.2	Sputtered Aluminium on graphite-epoxy composite material .....	331
5.10	Operating temperature range .....	334
5.10.1	Temperatures related to the maximum service temperature.....	335
5.11	Electrical properties .....	341
5.11.1	Electrical resistance and electrical resistivity.....	341
5.12	Prelaunch environmental effects .....	348
5.12.1	Moisture absorption and desorption .....	348
5.13	Postlaunch environmental effects .....	355
5.13.1	Ascent.....	355
5.13.2	Orbital effects .....	357
5.13.3	Re-entry effects .....	367
5.14	Thermal vacuum cycling.....	371
5.14.1	Test facilities.....	371
5.14.2	Measurement methods.....	372
5.14.3	Thermal vacuum cycling effects on the coefficient of linear thermal expansion .....	373
5.14.4	Trends in the variation of mechanical properties.....	378
5.15	Coating application.....	378
5.15.1	Pcbz conductive white paint .....	378
5.15.2	APA-2474 (TiO <sub>2</sub> white paint) .....	378
5.15.3	Wiederhold's Z-12321 .....	379

5.16 Past spatial uses .....	380
5.16.1 Intelsat v .....	380
5.16.2 Spelda (structure porteuse externe de lancement double ariane).....	381
5.16.3 CS-3A Japanese satellite .....	384
<b>Bibliography metallic materials.....</b>	<b>387</b>
<b>References composite materials.....</b>	<b>391</b>

## Figures

Figure 4-1: Specific heat, $c$ , of Aluminium as a function of temperature, $T$ .....	30
Figure 4-2: Thermal conductivity, $\kappa$ , of Aluminium as a function of temperature, $T$ .....	31
Figure 4-3: Thermal conductivity integrals of Aluminium as a function of temperature, $T$ .....	32
Figure 4-4: Thermal diffusivity, $\alpha$ , of Aluminium as a function of temperature, $T$ .....	33
Figure 4-5: Linear thermal expansion, $\Delta L / L$ , of Aluminium as a function of temperature, $T$ .....	34
Figure 4-6: Normal spectral emittance, $\varepsilon_{\lambda}'$ , of Aluminium as a function of wavelength, $\lambda$ .....	37
Figure 4-7: Normal spectral emittance, $\varepsilon_{\lambda}'$ , of Aluminium conversion coatings as a function of wavelength, $\lambda$ .....	38
Figure 4-8: Angular spectral emittance, $\varepsilon_{\lambda}'$ , of Aluminium as a function of wavelength, $\lambda$ .....	39
Figure 4-9: Normal total emittance, $\varepsilon'$ , of Aluminium as a function of temperature, $T$ .....	45
Figure 4-10: Normal total emittance, $\varepsilon'$ , of Aluminium anodized as a function of anodizing thickness, $t_c$ .....	46
Figure 4-11: Summary of data concerning the hemispherical total emittance, $\varepsilon$ , of Aluminium as a function of temperature, $T$ . From Touloukian & DeWitt (1970) [42]. .....	47
Figure 4-12: Summary of data concerning the hemispherical total emittance, $\varepsilon$ , of Aluminium conversion coatings vs. temperature, $T$ . From Touloukian, DeWitt & Hernicz (1972) [43]. .....	52
Figure 4-13: Directional spectral absorptance, $\alpha_{\lambda}'$ , of Aluminium as a function of wavelength, $\lambda$ . Data points $\nabla$ correspond to $\beta = 25^\circ$ .....	54
Figure 4-14: Absorptance to emittance ratio, $\alpha_s/\varepsilon$ , of Aluminium conversion coatings as a function of the exposure time, $t$ .....	60
Figure 4-15: Normal - normal spectral reflectance, $\rho_{\lambda}''$ , of Aluminium as a function of wavelength, $\lambda$ .....	62
Figure 4-16: Normal - normal spectral reflectance, $\rho_{\lambda}''$ , of Aluminium contact coatings as a function of wavelength, $\lambda$ .....	64
Figure 4-17: Effect of coating thickness on normal - normal spectral reflectance, $\rho_{\lambda}''$ , of Aluminium conversion coatings as a function of wavelength, $\lambda$ .....	65
Figure 4-18: Bidirectional reflectance, $\rho_{\lambda}''$ , of Aluminium contact coatings as a function of wavelength, $\lambda$ .....	66

Figure 4-19: Bidirectional spectral reflectance, $\rho_{\lambda}''$ , of Aluminium conversion coatings as a function of zenith angles, $\beta$ and $\beta'$ , of incident and reflected radiations. ....	68
Figure 4-20: Summary of data concerning normal - hemispherical spectral reflectance, $\rho_{\lambda}'$ , of Aluminium vs. wavelength, $\lambda$ . From Touloukian & DeWitt (1970) [42]. ....	69
Figure 4-21: Normal - hemispherical spectral reflectance, $\rho_{\lambda}'$ , of Aluminium conversion coatings as a function of wavelength, $\lambda$ . ....	70
Figure 4-22: Effect of UV exposure on normal - hemispherical spectral reflectance, $\rho_{\lambda}'$ , of Aluminium conversion coatings as a function of wavelength, $\lambda$ . ....	71
Figure 4-23: Effect of electron exposure on normal - hemispherical spectral reflectance of Aluminium conversion coatings as a function of wavelength, $\lambda$ . ....	72
Figure 4-24: Effect of simultaneous UV - electron exposure on normal - hemispherical spectral reflectance, $\rho_{\lambda}'$ , of Aluminium conversion coatings as a function of wavelength, $\lambda$ . ....	73
Figure 4-25: Effect of proton exposure on normal - hemispherical spectral reflectance, $\rho_{\lambda}'$ , of Aluminium conversion coatings as a function of wavelength, $\lambda$ . ....	74
Figure 4-26: Directional - hemispherical spectral reflectance, $\rho_{\lambda}'$ , of Aluminium conversion coatings as a function of wavelength, $\lambda$ . ....	75
Figure 4-27: Hemispherical - normal spectral reflectance, $\rho_{\lambda}'$ , of Aluminium contact coatings as a function of wavelength, $\lambda$ . ....	76
Figure 4-28: Bidirectional total reflectance, $\rho''$ , of Aluminium as a function of the viewing zenith angles, $\beta'$ . ....	77
Figure 4-29: Normal - normal spectral transmittance, $\tau_{\lambda}''$ , of Aluminium as a function of wavelength, $\lambda$ . ....	80
Figure 4-30: Angular spectral transmittance, $\tau_{\lambda}''$ , of Aluminium as a function of wavelength, $\lambda$ . ....	81
Figure 4-31: Electrical resistivity, $\sigma^{-1}$ , of Aluminium as a function of temperature, $T$ . ....	83
Figure 4-32: Specific heat, $c$ , of Al - 4,3 Cu - 1,5 Mg - 0,6 Mn as a function of temperature, $T$ . ....	86
Figure 4-33: Thermal conductivity, $k$ , of Al - 4,3 Cu - 1,5 Mg - 0,6 Mn as a function of temperature, $T$ . ....	87
Figure 4-34: Thermal conductivity integrals of Al - 4,3 Cu - 1,5 Mg - 0,6 Mn as a function of temperature, $T$ . ....	88
Figure 4-35: Thermal diffusivity, $\alpha$ , of Al - 4,3 Cu - 1,5 Mg - 0,6 Mn as a function of temperature, $T$ . ....	89
Figure 4-36: Linear thermal expansion, $\Delta L / L$ , of Al - 4,3 Cu - 1,5 Mg - 0,6 Mn as a function of temperature, $T$ . ....	90
Figure 4-37: Normal - spectral emittance, $\varepsilon_{\lambda}'$ , of Al - 4,3 Cu - 1,5 Mg - 0,6 Mn as a function of wavelength, $\lambda$ . ....	91
Figure 4-38: Normal total emittance, $\varepsilon'$ , of Al - 4,3 Cu - 1,5 Mg - 0,6 Mn as a function of temperature, $T$ . ....	93
Figure 4-39: Normal-normal spectral reflectance, $\rho_{\lambda}''$ , of Al-4,3 Cu-1,5 Mg-0,6 Mn, anodized, as a function of wavelength, $\lambda$ . ....	98

Figure 4-40: Normal - hemispherical spectral reflectance, $\rho_{\lambda}'$ , of Al - 4,3 Cu - 1,5 Mg - 0,6 Mn as a function of wavelength, $\lambda$ .....	99
Figure 4-41: Normal - hemispherical spectral reflectance, $\rho_{\lambda}'$ , of Al - 4,3 Cu - 1,5 Mg - 0,6 Mn, anodized, as a function of wavelength, $\lambda$ .....	100
Figure 4-42: Normal-hemispherical spectral reflectance, $\rho_{\lambda}'$ , of Al-1 Mg-0,6 Si, as received, as a function of wavelength, $\lambda$ .....	108
Figure 4-43: Normal-hemispherical spectral reflectance, $\rho_{\lambda}'$ , of Al-1 Mg-0,6 Si, grit blasted, as a function of wavelength, $\lambda$ .....	109
Figure 4-44: Normal-hemispherical spectral reflectance, $\rho_{\lambda}'$ , of Al-1 Mg-0,6 Si, chemically polished, as a function of wavelength, $\lambda$ .....	111
Figure 4-45: Normal - hemispherical spectral reflectance, $\rho_{\lambda}'$ , of Al - 1 Mg - 0,6 Si, chemically milled, as a function of wavelength, $\lambda$ .....	112
Figure 4-46: Specific heat, $c$ , of Al - 5,7 Zn - 2,5 Mg - 1,6 Cu as a function of temperature, $T$ .....	115
Figure 4-47: Thermal conductivity, $k$ , of Al - 5,7 Zn - 2,5 Mg - 1,6 Cu as a function of temperature, $T$ .....	116
Figure 4-48: Thermal conductivity integral of Al – 5,7 Zn – 2,5 Mg – 1,6 Cu as a function of temperature, $T$ .....	117
Figure 4-49: Thermal diffusivity, $\alpha$ , of Al - 5,7 Zn - 2,5 Mg - 1,6 Cu as a function of temperature, $T$ .....	118
Figure 4-50: Linear thermal expansion, $\Delta L / L$ , of Al - 5,7 Zn - 2,5 Mg - 1,6 Cu as a function of temperature, $T$ .....	119
Figure 4-51: Normal spectral emittance, $\varepsilon_{\lambda}'$ , of Al - 5,7 Zn - 2,5 Mg - 1,6 Cu as a function of wavelength, $\lambda$ .....	120
Figure 4-52: Angular spectral emittance, $\varepsilon_{\lambda}'$ , of Al - 5,7 Zn - 2,5 Mg - 1,6 Cu as a function of wavelength, $\lambda$ .....	121
Figure 4-53: Normal total emittance, $\varepsilon'$ , of Al - 5,7 Zn - 2,5 Mg - 1,6 Cu as a function of temperature, $T$ .....	122
Figure 4-54: Normal-hemispherical spectral reflectance, $\rho_{\lambda}'$ , of Al - 5,7 Zn - 2,5 Mg - 1,6 Cu conversion coatings, as a function of wavelength, $\lambda$ .....	126
Figure 4-55: Specific heat, $c$ , of Ti - 5 Al - 2,5 Sn as a function of temperature, $T$ .....	134
Figure 4-56: Thermal conductivity, $k$ , of Ti - 5 Al - 2,5 Sn as a function of temperature, $T$ .....	135
Figure 4-57: Thermal linear expansion, $\Delta L/L$ , of Ti - 5 Al - 2,5 Sn as a function of temperature, $T$ .....	136
Figure 4-58: Normal spectral emittance, $\varepsilon_{\lambda}'$ , of Ti - 5 Al - 2,5 Sn as a function of temperature, $T$ , for $\lambda = 6,65 \times 10^{-7}$ m. ....	137
Figure 4-59: Normal total emittance, $\varepsilon'$ , of Ti - 5 Al - 2,5 Sn as a function of temperature, $T$ .....	138
Figure 4-60: Normal-normal spectral reflectance, $\rho_{\lambda}''$ , of Ti - 5 Al - 2,5 Sn as a function of wavelength, $\lambda$ .....	140
Figure 4-61: Normal - hemispherical spectral reflectance, $\rho_{\lambda}'$ , of Ti - 5 Al - 2,5 Sn as a function of wavelength, $\lambda$ .....	141

Figure 4-62: Normal - hemispherical spectral reflectance, $\rho_{\lambda}'$ , of Ti - 5 Al - 2,5 Sn, anodized, as a function of wavelength, $\lambda$ .....	142
Figure 4-63: Electrical resistivity, $\sigma^{-1}$ , of Ti - 5 Al - 2,5 Sn as a function of temperature, $T$ .....	143
Figure 4-64: Specific heat, $c$ , of Ti - 6 Al - 2 Sn - 4 Zr - 2 Mo as a function of temperature, $T$ .....	145
Figure 4-65: Thermal conductivity, $k$ , of Ti - 6 Al - 2 Sn - 4 Zr - 2 Mo as a function of temperature, $T$ .....	146
Figure 4-66: Mean coefficient of linear thermal expansion, $\beta$ , of Ti - 6 Al - 2 Sn - 4 Zr - 2 Mo from room temperature to temperature $T$ .....	147
Figure 4-67: Electrical resistivity, $\sigma^{-1}$ , of Ti - 6 Al - 2 Sn - 4 Zr - 2 Mo as a function of temperature, $T$ .....	149
Figure 4-68: Specific heat, $c$ , of Ti - 6 Al - 4 V as a function of temperature, $T$ .....	152
Figure 4-69: Thermal conductivity, $k$ , of Ti - 6 Al - 4 V as a function of temperature, $T$ .....	153
Figure 4-70: Thermal conductivity integrals of Ti - 6 Al - 4 V as a function of temperature, $T$ .....	154
Figure 4-71: Thermal diffusivity, $\alpha$ , of Ti - 6 Al - 4 V as a function of temperature, $T$ .....	155
Figure 4-72: Thermal linear expansion, $\Delta L/L$ , of Ti - 6 Al - 4 V as a function of temperature, $T$ .....	156
Figure 4-73: Normal spectral emittance, $\varepsilon_{\lambda}'$ , of Ti - 6 Al - 4 V as a function of temperature, $T$ .....	157
Figure 4-74: Normal total emittance, $\varepsilon'$ , of Ti - 6 Al - 4 V as a function of temperature, $T$ ...	158
Figure 4-75: Hemispherical total emittance, $\varepsilon$ , of Ti - 6 Al - 4 V as a function of temperature, $T$ .....	160
Figure 4-76: Normal - hemispherical spectral reflectance, $\rho_{\lambda}'$ , of Ti - 6 Al - 4 V as a function of wavelength, $\lambda$ .....	162
Figure 4-77: Electrical resistivity, $\sigma^{-1}$ , of Ti - 6 Al - 4 V as a function of temperature, $T$ .....	163
Figure 4-78: Specific heat, $c$ , of Ni - 19 Cr - 11 Co - 10 Mo - 3 Ti as a function of temperature, $T$ .....	166
Figure 4-79: Thermal conductivity, $k$ , of Ni - 19 Cr - 11 Co - 10 Mo - 3 Ti as a function of temperature, $T$ .....	167
Figure 4-80: Thermal linear expansion, $\Delta L/L$ , of Ni - 19 Cr - 11 Co - 10 Mo - 3 Ti as a function of temperature, $T$ .....	168
Figure 4-81: Normal spectral emittance, $\varepsilon_{\lambda}'$ , of Ni - 19 Cr - 11 Co - 10 Mo - 3 Ti as a function of wavelength, $\lambda$ .....	169
Figure 4-82: Normal total emittance, $\varepsilon'$ , of Ni - 19 Cr - 11 Co - 10 Mo - 3 Ti as a function of temperature, $T$ .....	170
Figure 4-83: Normal-normal spectral reflectance, $\rho''_{\lambda}$ , of Ni - 19 Cr - 11 Co - 10 Mo - 3 Ti as a function of wavelength, $\lambda$ . Data points $\triangleright$ correspond to normal-hemispherical reflectance while $\blacktriangleright$ , $\blacktriangleleft$ correspond to hemispherical-normal reflectance.....	172
Figure 4-84: Specific heat, $c$ , of Fe - 36 Ni (Invar) as a function of temperature, $T$ .....	176



Figure 4-85: Linear thermal expansion, $\Delta L/L$ , of Fe - 36 Ni (Invar) as a function of temperature, $T$ .	177
Figure 4-86: Effect of the concentration of alloying elements, $c$ , on the value of the coefficient of linear expansion, $\beta$ . From MOND NICKEL Co.	178
Figure 4-87: Normal emittance, $\varepsilon_{\lambda}$ , of Fe - 36 Ni (Invar), for $\lambda = 6,7 \times 10^{-7}$ as a function of temperature, $T$ .	179
Figure 5-1: International ties between Carbon Fiber manufactures. From SENER (1984) [147].	205
Figure 5-2: Schematic of an angle plied laminate. From Chamis (1987) [67].	206
Figure 5-3: Schematic of a tri-orthogonally fiber reinforced composite. a) Straight filaments. From Domínguez (1987) [82]. b) Tapes. From Aboudi (1984) [49].	206
Figure 5-4: Main types of woven fabrics. Lengthwise (warp) yarns and crosswise (fill) yarns can be interlaced to produce woven fabrics. A fabric construction of 16 x 14 means 16 warp ends per inch and 14 fill ends per inch. a) Plain weave. Very stable. Small yarn slippage. b) Leno weave. Minimizes distortion with few yarns. c) Twill. The fabric has a broken diagonal line and, consequently, greater pliability than a plain weave. d) Crowfoot satin. Pliable and comfortable to contoured surfaces. From Domínguez (1987) [82], Weeton, Peters & Thomas (1987) [164].	207
Figure 5-5: Longitudinal (to fibers) and transverse directions for the measurement of composite properties. From Chamis (1987) [67].	209
Figure 5-6: Cryostat assemblies for measuring the thermal conductivity, $k$ . a) High- $k$ samples. b) Low- $k$ samples. From Pilling, Yates, Black & Tattersall (1979) [137]. For explanation see text.	222
Figure 5-7: Facility used to measure the thermal conductivity, $k$ , of a sample as a function of temperature in the range 90 K to 410 K. Temperature changes continuously. From Ott (1981) [132].	224
Figure 5-8: Hypodermic probe to measure the thermal conductivity of polymer melts. All the dimensions are in mm. From Lobo & Cohen (1990) [120].	225
Figure 5-9: Thermal conductivity, $k_m$ , of different matrices as a function of temperature, $T$ . Numerical values are given in Table 5-10.	236
Figure 5-10: Longitudinal thermal conductivity, $k_{f1}$ , of several advanced pitch graphite fibers vs. temperature, $T$ . The fiber designation is from Amoco Performance Products; the number stands for the fiber elasticity modulus in millions of lbs.in <sup>-2</sup> . All the data, unless otherwise stated, are from LMSC. Pitch precursor graphite fibers have a structure which approaches that of a single crystal of graphite and, thus, their thermal conductivity is very large. From McGuire & Vollerin (1990) [127].	237
Figure 5-11: Typical assembly for measuring the thermal diffusivity, $\alpha$ , of a long slender bar by use of the Angström method. From Landis (1964) [116].	247
Figure 5-12: Typical assembly for measuring the thermal diffusivity, $\alpha$ , of a disc shaped sample. From Lachi, Legrand & Degiovanni (1988) [115].	248
Figure 5-13: Thermal diffusivity, $\alpha_f$ , of different fiber cloths as a function of temperature, $T$ . Numerical values are given in Table 5-33 From Touloukian (1967) [157].	251

Figure 5-14: Experimental arrangement for the interferometric measurement of the thermal expansion. a) Specimen chamber assembly. b) Optical system. From James & Yates (1965) [108]. For explanation see text. ....	256
Figure 5-15: The ESTEC CTE 1000 facility for the measurement of the linear thermal expansion of structure up to 0,7 m long. All the dimensions are in mm. From Aalders (1989) [48]. ....	258
Figure 5-16: Linear thermal expansion, $\beta_m$ , as a function of temperature, $T$ , for four different epoxy matrices. Numerical values are given in Table 5-41. ....	269
Figure 5-17: Linear thermal expansion coefficient measured parallel to fibers, $\beta_1$ , as a function of temperature, $T$ , for some composite materials formed by the same matrix, DER 332/T403, and two different glass fiber reinforcements. Upper and lower limits of the shadowed regions are for 95% confidence. ....	278
Figure 5-18: Linear thermal expansion coefficient measured perpendicular to fibers, $\beta_2$ , as a function of temperature, $T$ , for some composite materials formed by the same matrix, DER 332/T403, and two different glass fiber reinforcements. ....	280
Figure 5-19: Linear thermal expansion coefficient measured in different directions, $\beta$ , as a function of temperature, $T$ , for similar carbon fiber reinforced composite materials. The matrix is ERLA 4617/mPDA. From Rogers, Phillips, Kingston.Lee, Yates, Overy, Sargent & McCalla (1977) [144]. ....	281
Figure 5-20: Linear thermal expansion coefficient measured parallel to fibers, $\beta_1$ , as a function of temperature, $T$ , for different fiber volume ratios, $\varphi_f$ . Fiber: Courtaulds HTS PT112/21Z; Matrix: DLS 351/BF <sub>3</sub> 400. ....	290
Figure 5-21: Linear thermal expansion coefficient measured perpendicular to fibers, $\beta_2$ , as a function of temperature, $T$ , for different fiber volume ratios, $\varphi_f$ . Fiber: Courtaulds HTS PT112/21Z; Matrix: DLS 351/BF <sub>3</sub> 400. ....	291
Figure 5-22: Linear thermal expansion coefficient measured either in plane of laminate, $\beta_1$ , or perpendicular to it, $\beta_3$ , as a function of temperature, $T$ , for similar carbon fibers reinforced composite materials. The fiber is carbon HTS PT112/21Z. From Yates, McCalla, Sargent, Rogers, Phillips & Kingston-Lee (1978)b [169]. ....	292
Figure 5-23: Linear thermal expansion coefficient, $\beta$ , of a carbon fiber reinforced unidirectional composite material, measured in plane of laminate, as a function of the direction of the measurement, $\theta$ . Matrix is Epikote 828/BF <sub>3</sub> MEA. Fibers are Torayca T300A. Temperature range is 290 K to 340 K. From Isikawa, Koyama & Kobayashi (1977, 1978) [106] & [107]. ....	299
Figure 5-24: Linear thermal expansion coefficient measured parallel to fibers, $\beta_1$ , as a function of temperature, $T$ , for two nominally identical carbon fiber reinforced composite materials produced on separate occasions and having slightly different fiber volume ratios, $\varphi_f$ . Fiber: HTSCarbon; Matrix: Fibredux 914C. ....	300
Figure 5-25: Linear thermal expansion coefficient measured perpendicular to fibers, $\beta_2$ , as a function of temperature, $T$ , for two nominally identical carbon fiber reinforced composite materials produced on separate occasions and having slightly different fiber volume ratios, $\varphi_f$ . Fiber: HTSCarbon; Matrix: Fibredux 914C. ....	301
Figure 5-26: Linear thermal expansion coefficient measured in 0° direction, $\beta_0$ , as a function of temperature, $T$ , for some carbon fiber reinforced composite	

materials with various amounts of fibers in different directions. Fiber: Courtaulds HTS, Type II; Matrix: Fibredux 914C.....	306
Figure 5-27: Linear thermal expansion coefficient, $\beta_0$ , of a two-ply ( $\pm \theta$ ) carbon fiber reinforced composite material, measured in direction $0^\circ$ of the plane of laminate, as a function of the angle ply, $\theta$ . Matrix is Hercules 3002, fibers are Hercules HT (Hercules 3002T prepreg). Temperature range is 80 K to 450 K. From Friend, Poesch & Leslie (1972) [90].....	308
Figure 5-28: Linear thermal expansion coefficient, $\beta$ , measured in several directions of the plane of laminate for an unidirectional and an angle plied carbon fiber reinforced composite material, as a function of temperature, $T$ . Matrix is Narmco 5208, fibers are Narmco T300. From Karlsson (1983) [111].....	309
Figure 5-29: Linear thermal expansion coefficient measured either parallel, $\beta_1$ , or perpendicular, $\beta_2$ , to fibers of two composites with similar epoxy matrices, but with carbon fiber or Kevlar 49 reinforcements. ....	316
Figure 5-30: Linear thermal expansion coefficient measured parallel to fibers, $\beta_1$ , as a function of temperature, $T$ , for two graphite fiber-metal and one carbon fiber-epoxy composite materials. ....	317
Figure 5-31: Linear thermal expansion coefficient measured perpendicular to fibers, $\beta_2$ , as a function of temperature, $T$ , for graphite fiber-metal and carbon fiber-epoxy composite materials. ....	318
Figure 5-32: Normal spectral absorptance, $\alpha'_{\lambda}$ , of SiO <sub>2</sub> Fabric at 310 K vs. wavelength, $\lambda$ . Sample is described in the text. From Eagles, Babjak & Weaver (1975) [85].....	320
Figure 5-33: Normal-hemispherical spectral reflectance, $\rho'_{\lambda}$ , of SiO <sub>2</sub> Fabric vs. wavelength, $\lambda$ . Sample is described in the text. From Eagles, Babjak & Weaver (1975) [85]. ....	321
Figure 5-34: Solar absorptance, $\alpha_s$ , of SiO <sub>2</sub> Fabric-Substrate composite as a function of the solar absorptance, $\alpha_{ss}$ , of the substrate. Sample: 16 Harness Satin Weave $0,38 \times 10^{-3}$ m thick, on different substrates. From Eagles, Babjak & Weaver (1975) [85]. ....	322
Figure 5-35: Absorptance/Emitatnce ratio, $\alpha_s/\varepsilon$ , solar absorptance, $\alpha_s$ , and hemispherical total emittance, $\varepsilon$ , of various mosaics of silica and carbon yarn as functions of the exposed black to total area fraction, $A_B/A$ . From Eagles, Babjak & Weaver (1975) [85].....	322
Figure 5-36: Normal spectral emittance, $\varepsilon'_{\lambda}$ , of PV 100 coating on different substrates and with different thicknesses (see Table 5-67) vs. wavelength, $\lambda$ , at 393 K. From Giommi, Marchetti, Salza & Testa (1985) [92].....	327
Figure 5-37: Normal-hemispherical spectral reflectance factor, $R'_{\lambda}$ , of PV 100 coating on different substrates and with different thicknesses vs. wavelength, $\lambda$ . From Giommi, Marchetti, Salza & Testa (1985) [92].....	329
Figure 5-38: Normal total emittance, $\varepsilon'(0)$ , of sputtered aluminium on T300/5209 graphite-epoxy composite material as a function of sputtered coating thickness, $t_c$ , and for two different textures of the supporting material. From Witte & Teichman (1989) [166]. ....	332
Figure 5-39: Normal solar absorptance, $\alpha_s$ , of sputtered aluminium on T300/5209 graphite-epoxy composite material as a function of sputtered coating	

thickness, $t_c$ , and for two different textures of the supporting material. From Witte & Teichman (1989) [166].	333
Figure 5-40: Solar absorptance to emittance ratio of sputtered aluminium on T300/5209 graphite-epoxy composite material as a function of sputtered coating thickness, $t_c$ , and for two different textures of the supporting material. From Witte & Teichman (1989) [166].	334
Figure 5-41: Tensile strength, $\sigma_t$ , vs. temperature, $T$ , of structural materials. Inert atmospheres. From DeMario (1985) [81].	335
Figure 5-42: Electrical resistivity, $\rho$ , as a function of frequency, $f$ , for a carbon-epoxy composite material. Fiber: Super A, Matrix: Fibredux 914C. Layup ( $0^\circ \pm 45^\circ$ ) 16 plies. Sample size: $\bigcirc$ :> $1,98 \times 10^{-3}$ m, $10 \times 10^{-3}$ m, $25 \times 10^{-3}$ m. $\square$ :> $1,98 \times 10^{-3}$ m, $5,5 \times 10^{-3}$ m, $25 \times 10^{-3}$ m. From Thomson (1982) [156].	345
Figure 5-43: One-dimensional and radial models of laminar diffusion through homogeneous-isotropic media.	350
Figure 5-44: Moisture content, $M$ , as a function of ambient temperature, $T$ , after 100 h of exposure to distilled water at that temperature, for several carbon fiber reinforced composites. The specimens are infinitely large rods of $6 \times 10^{-3}$ m diameter. $M_0 = 0,002$ assumed.	351
Figure 5-45: Effect of UV radiation on linear thermal expansion, $\beta$ , of Graphite/epoxy T300/SP 288 laminates. a) $\theta = 90^\circ$ , b) $\theta = (\pm 43^\circ)_s$ , c) $\theta = 0^\circ$ . Ambient pressure $10^{-4}$ Pa to $10^{-5}$ Pa. From Tennyson & Zimcik (1982) [107], Hansen & Tennyson (1983) [153].	361
Figure 5-46: Effect of UV radiation on linear thermal expansion, $\beta$ , of Kevlar/epoxy 3M SP 306 laminates. a) $\theta = 90^\circ$ , b) $\theta = (\pm 43^\circ)_s$ , c) $\theta = 0^\circ$ . Ambient pressure $10^{-4}$ Pa to $10^{-5}$ Pa. From Tennyson & Zimcik (1982) [154], Hansen & Tennyson (1983) [95].	361
Figure 5-47: Effect of electron radiation with (thick solid line) and without (thin solid line) UV exposure, on linear thermal expansion, $\beta_0$ , of graphite/epoxy and Kevlar/epoxy, $\theta = (\pm 43^\circ)_s$ . Ambient pressure $10^{-4}$ Pa to $10^{-5}$ Pa. Exposure > 1 year and 300 ESD of UV. From Hansen & Tennyson (1983) [95].	362
Figure 5-48: Linear thermal expansion, $\beta_0$ , as a function of temperature, $T$ , of T50(PAN)/F263 (0/90) <sub>2s</sub> HM graphite/epoxy laminates exposed to electron radiation. Calculated by the compiler by numerical derivation ( $\beta = d(\Delta L/L)/dT$ ) of data from Mauri & Crossman (1983) [125].	362
Figure 5-49: Graphs for estimating the depletion by atomic oxygen of a material of known Reaction Efficiency, $R_e$ . From Leger & Visentine (1986) [118].	367
Figure 5-50: Effect of the number of thermal cycles, $N$ , on the linear thermal expansion, $\beta_0$ , of $(\pm 22^\circ)_s$ T300/3M SP288 Graphite/Epoxy laminates. $300 \text{ K} \leq T \leq 370 \text{ K}$ , $p = 1,33 \times 10^{-4}$ Pa to $1,33 \times 10^{-5}$ Pa. From Tennyson & Zimcik (1982) [154], Hansen & Tennyson (1983) [95].	375
Figure 5-51: Effect of the number of thermal cycles, $N$ , on the linear thermal expansion, $\beta_0$ , of $(\pm 43^\circ)_s$ T300/3M SP288 Graphite/Epoxy laminates. $300 \text{ K} \leq T \leq 370 \text{ K}$ , $p = 1,33 \times 10^{-4}$ Pa to $1,33 \times 10^{-5}$ Pa. From Tennyson (1980) [153], Tennyson & Zimcik (1982) [154], Hansen & Tennyson (1983) [95].	375
Figure 5-52: Effect of the number of thermal vacuum cycles, $N$ , on the linear thermal expansion, $\beta_0$ , of $(\pm \theta^\circ)_s$ T300/3M SP288 Graphite/Epoxy laminates. $300 \text{ K} \leq T \leq 370 \text{ K}$ , $p = 1,33 \times 10^{-4}$ Pa to $1,33 \times 10^{-5}$ Pa. 50 cycles $\approx$ 220 days in	

vacuum. From Tennyson & Zimcik (1982) [154], Hansen & Tennyson (1983) [95].	376
Figure 5-53: Effect of the number of thermal vacuum cycles, $N$ , on the linear thermal expansion, $\beta_0$ , of $(\pm \theta)_S$ 3M SP306 Kevlar/Epoxy laminates. $300\text{ K} \leq T \leq 370\text{ K}$ , $p = 1,33 \times 10^{-4}\text{ Pa}$ to $1,33 \times 10^{-5}\text{ Pa}$ . 50 cycles $\approx$ 220 days in vacuum. From Tennyson & Zimcik (1982) [154], Hansen & Tennyson (1983) [95].	376
Figure 5-54: Comparison of predicted (-) and experimental (o) values of the linear thermal expansion, $\beta_0$ , vs. fiber angle, $\theta$ , for $(\pm \theta)_S$ 3M SP306 Kevlar/Epoxy laminates. 48 cycles $\approx$ 220 days in vacuum. $300\text{ K} \leq T \leq 370\text{ K}$ , $p = 1,33 \times 10^{-4}\text{ Pa}$ to $1,33 \times 10^{-5}\text{ Pa}$ . From Tennyson & Zimcik (1982) [171], Hansen & Tennyson (1983) [95]. Results for Graphite/Epoxy are given in Tennyson (1980) [153]. Compare also with Figure 5-27.	377
Figure 5-55: Effect of the number of thermal vacuum cycles, $N$ , on the linear thermal expansion, $\beta_0$ , of $(\pm \theta)_S$ 3M SP290 Boron/Epoxy laminates. $300\text{ K} \leq T \leq 370\text{ K}$ , $p = 1,33 \times 10^{-4}\text{ Pa}$ to $1,33 \times 10^{-5}\text{ Pa}$ . 50 cycles $\approx$ 220 days in vacuum. From Tennyson & Zimcik (1982) [154], Hansen & Tennyson (1983) [95].	377
Figure 5-56: Coefficient of the linear thermal expansion, $\beta_0$ , as a function of temperature, $T$ , for Graphite/Epoxy circular hybrid tubes, identified as Spec. No. 12 in Table 5-84 and Table 5-85, before (solid line) and after (dashed line) thermal vacuum cycling. 3000 cycles. $98\text{ K} \leq T \leq 370\text{ K}$ , $p = 1,33 \times 10^{-3}\text{ Pa}$ . From Reibaldi (1985) [141].	378
Figure 5-57: Outline of INTELSAT V communication satellite.	380
Figure 5-58: Sketch of the ARIANE 4 upper part. From Thomas & Oliver (1985) [155].	382
Figure 5-59: Exploded view of SPELDA. From Thomas & Oliver (1985) [155].	383
Figure 5-60: Sketch of the CS-3a structure. From Kawashima, Inoue & Seko (1985) [112].	384
Figure 5-61: Exploded view of CS-3a Central Thrust Tube. Prepared by the compiler after Kawashima, Inoue & Seko (1985) [112].	385

## Tables

Table 4-1: Normal Total Emittance of Aluminium	40
Table 4-2: Normal Total Emittance and Normal Solar Absorptance of Aluminium Contact Coatings	42
Table 4-3: Normal Total Emittance and Normal Solar Absorptance of Aluminium Conversion Coatings	44
Table 4-4: Hemispherical Total Emittance of Aluminium Contact Coatings	47
Table 4-5: Hemispherical total Absorptance of Aluminium	55
Table 4-6: Normal Solar Absorptance of Aluminium	57
Table 4-7: Normal Solar Absorptance of Aluminium Conversion Coatings	58
Table 4-8: Angular Solar absorptance of Aluminium	60
Table 4-9: Normal-Normal Solar Reflectance of Aluminium Conversion Coatings	78
Table 4-10: Normal-Hemispherical Solar Reflectance of Both Bulk Aluminium and Contact Coatings	79
Table 4-11: Normal Total Emittance of Al – 4,3 Cu – 1,5 Mg – 0,6 Mn, Anodized	95

Table 4-12: Hemispherical Total Emittance of Al – 4,3 Cu – 1,5 Mg – 0,6 Mn.....	95
Table 4-13: Normal Solar Absorptance of Al – 4,3 Cu – 1,5 Mg – 0,6 Mn .....	96
Table 4-14: Normal Solar Absorptance of Al – 4,3 Cu – 1,5 Mg – 0,6 Mn, Anodized .....	97
Table 4-15: Normal Hemispherical Solar Reflectance of Al – 4,3 Cu – 1,5 Mg – 0,6 Mn, Anodized.....	102
Table 4-16: Normal Total Emittance of Al – 1 Mg – 0,6 Si .....	105
Table 4-17: Hemispherical Total Emittance of Al – 1 Mg – 0,6 Si .....	106
Table 4-18: Normal Solar Absorptance of Al – 1 Mg – 0,6 Si.....	107
Table 4-19: Hemispherical Total Emittance of Al – 5,7 Zn – 2,5 Mg – 1,6 Cu Conversion Coatings. ....	124
Table 4-20: Normal Solar Absorptance and Normal-Hemispherical Solar Reflectance of Al – 5,6 Zn – 2,5 Mg 1,6 Cu.....	125
Table 4-21: Normal Solar Absorptance of Ti – 5 Al – 2,5 Sn .....	139
Table 4-22: Normal Solar Absorptance of Ti – Al – 4 V .....	161
Table 4-23: Cost of Ti – 6 Al – 4 – V compared with those of other structural metallic materials. ....	164
Table 4-24: Electrical Resistivity of Ni – 19Cr – 11Co – 10Mo – 3Ti <sup>a</sup> .....	173
Table 4-25: Linear thermal expansion coefficient of Fe – 36 Ni under different temper conditions.....	178
Table 4-26: Magnetic Properties of Fe – 36 Ni under different temper conditions. ....	180
Table 4-27: Relative Permeability of Fe – 36 Ni, measured at 400 A.m <sup>-1</sup> .....	180
Table 5-1: Abridged Designation of Single Reinforcement Laminates.....	208
Table 5-2: Density, $\rho_f$ [kg.m <sup>-3</sup> ], of High-Strength Fibers.....	210
Table 5-3: Density, $\rho_m$ [kg.m <sup>-3</sup> ], of Matrices .....	215
Table 5-4: Specific Heat, $c_f$ [J.kg <sup>-1</sup> .K <sup>-1</sup> ], of High-Strength Fibers .....	217
Table 5-5: Fused Silicia .....	218
Table 5-6: Kevlar <sup>d</sup> .....	219
Table 5-7: Specific Heat, $c_m$ [J.kg <sup>-1</sup> .K <sup>-1</sup> ], of Matrices .....	220
Table 5-8: Specific Heat, $c$ [J.kg <sup>-1</sup> .K <sup>-1</sup> ], of Composite Materials.....	221
Table 5-9: Longitudinal (1) and Transverse (2) Thermal Conductivity, of High-Strength Fibers. Tabulated Data are $k_{f1}$ [W.m <sup>-1</sup> .K <sup>-1</sup> ]/ $k_{f2}$ [W.m <sup>-1</sup> .K <sup>-1</sup> ], of Fibers .....	226
Table 5-10: Thermal Conductivity, $k_m$ [W.m <sup>-1</sup> .K <sup>-1</sup> ], of Matrices .....	228
Table 5-11: Araldite LY556.....	229
Table 5-12: DER 332/T403 (100:36) <sup>c</sup> .....	230
Table 5-13: Epitoke 210/BF <sub>3</sub> 400 <sup>b</sup> .....	230
Table 5-14: Epoxin 162 <sup>a</sup> .....	230
Table 5-15: Palatal P51 <sup>a</sup> .....	231
Table 5-16: Nylon 6 <sup>a</sup> .....	232
Table 5-17: Comco, Nylon 6/6 <sup>g,h</sup> .....	233

Table 5-18: Polypenco 101, Nylon 6/6 <sup>g,h</sup> .....	234
Table 5-19: Polypropylene <sup>a</sup> .....	235
Table 5-20: Characteristics of Composite Materials (Thermal Conductivity can be found following the links) .....	237
Table 5-21: Smoothed values of the Thermal conductivity, $k$ [W.m <sup>-1</sup> .K <sup>-1</sup> ], of the Composite Specimens Characterized in Table 5-9. ....	241
Table 5-22: Smoothed values of the Thermal conductivity, $k$ [W.m <sup>-1</sup> .K <sup>-1</sup> ], of the Composite Specimens Characterized in Table 5-9. ....	241
Table 5-23: Smoothed values of the Thermal conductivity, $k$ [W.m <sup>-1</sup> .K <sup>-1</sup> ], of the Composite Specimens Characterized in Table 5-9. ....	242
Table 5-24: Smoothed values of the Thermal conductivity, $k$ [W.m <sup>-1</sup> .K <sup>-1</sup> ], of the Composite Specimens Characterized in Table 5-9. ....	242
Table 5-25: Smoothed values of the Thermal conductivity, $k$ [W.m <sup>-1</sup> .K <sup>-1</sup> ], of the Composite Specimens Characterized in Table 5-9. ....	242
Table 5-26: Smoothed values of the Thermal conductivity, $k$ [W.m <sup>-1</sup> .K <sup>-1</sup> ], of the Composite Specimens Characterized in Table 5-9. ....	243
Table 5-27: Smoothed values of the Thermal conductivity, $k$ [W.m <sup>-1</sup> .K <sup>-1</sup> ], of the Composite Specimens Characterized in Table 5-9. ....	243
Table 5-28: Smoothed values of the Thermal conductivity, $k$ [W.m <sup>-1</sup> .K <sup>-1</sup> ], of the Composite Specimens Characterized in Table 5-9. ....	244
Table 5-29: Smoothed values of the Thermal conductivity, $k$ [W.m <sup>-1</sup> .K <sup>-1</sup> ], of the Composite Specimens Characterized in Table 5-9. ....	245
Table 5-30: Smoothed values of the Thermal conductivity, $k$ [W.m <sup>-1</sup> .K <sup>-1</sup> ], of the Composite Specimens Characterized in Table 5-9. ....	245
Table 5-31: Smoothed values of the Thermal conductivity, $k$ [W.m <sup>-1</sup> .K <sup>-1</sup> ], of the Composite Specimens Characterized in Table 5-9. ....	246
Table 5-32: Smoothed values of the Thermal conductivity, $k$ [W.m <sup>-1</sup> .K <sup>-1</sup> ], of the Composite Specimens Characterized in Table 5-9. ....	246
Table 5-33: Thermal diffusivity, $\alpha_f \times 10^6$ [m <sup>2</sup> .s <sup>-1</sup> ], of High-Strength Fibers .....	249
Table 5-34: Thermal diffusivity, $\alpha_f \times 10^6$ [m <sup>2</sup> .s <sup>-1</sup> ], of High-Strength Fibers .....	250
Table 5-35: Thermal diffusivity, $\alpha_m$ [m <sup>2</sup> .s <sup>-1</sup> ], of Matrices .....	252
Table 5-36: Thermal diffusivity, $\alpha_x \times 10^6$ [m <sup>2</sup> .s <sup>-1</sup> ], of Composite Materials.....	253
Table 5-37: Thermal diffusivity, $\alpha_x \times 10^6$ [m <sup>2</sup> .s <sup>-1</sup> ], of Composite Materials.....	254
Table 5-38: Thermal diffusivity, $\alpha \times 10^6$ [m <sup>2</sup> .s <sup>-1</sup> ], of Composite Materials .....	255
Table 5-39: Linear thermal expansion, $\beta_f$ [K <sup>-1</sup> ], and elasticity modulus, $E_f$ [Pa], of high-strength fibers .....	260
Table 5-40: Linear thermal expansion, $\beta_m$ [K <sup>-1</sup> ], elasticity modulus, $E_m$ [Pa] and Poisson's ratio, $\nu_m$ , of matrices .....	264
Table 5-41: Arrangements of the Data on Linear Thermal Expansion, $\beta$ , of Composite Materials Compiled in Table 5-42 to Table 5-60.....	270
Table 5-42: Characterization of Composite Materials (Linear Thermal Expansion is given following the links).....	271

Table 5-43: Smoothed values of the Linear Thermal Expansion Coefficient, $\beta \times 10^6$ [K <sup>-1</sup> ], of the Specimens characterized in Table 5-85. ....	274
Table 5-44: Smoothed values of the Linear Thermal Expansion Coefficient, $\beta \times 10^6$ [K <sup>-1</sup> ], of the Specimens characterized in Table 5-85. ....	274
Table 5-45: Smoothed values of the Linear Thermal Expansion Coefficient, $\beta \times 10^6$ [K <sup>-1</sup> ], of the Specimens characterized in Table 5-85. ....	275
Table 5-46: Smoothed values of the Linear Thermal Expansion Coefficient, $\beta \times 10^6$ [K <sup>-1</sup> ], of the Specimens characterized in Table 5-85. ....	275
Table 5-47: Smoothed values of the Linear Thermal Expansion Coefficient, $\beta \times 10^6$ [K <sup>-1</sup> ], of the Specimens characterized in Table 5-85. ....	276
Table 5-48: Smoothed values of the Linear Thermal Expansion Coefficient, $\beta \times 10^6$ [K <sup>-1</sup> ], of the Specimens characterized in Table 5-85. ....	277
Table 5-49: Characterization of Composite Materials (Linear Thermal Expansion is given following the links). ....	282
Table 5-50: Smoothed Values of the Linear Thermal Expansion Coefficient, $\beta \times 10^6$ [K <sup>-1</sup> ], of the Specimens Characterized in Table 5-49. ....	285
Table 5-51: Smoothed Values of the Linear Thermal Expansion Coefficient, $\beta \times 10^6$ [K <sup>-1</sup> ], of the Specimens Characterized in Table 5-49. ....	286
Table 5-52: Smoothed Values of the Linear Thermal Expansion Coefficient, $\beta \times 10^6$ [K <sup>-1</sup> ], of the Specimens Characterized in Table 5-49. ....	288
Table 5-53: Smoothed Values of the Linear Thermal Expansion Coefficient, $\beta \times 10^6$ [K <sup>-1</sup> ], of the Specimens Characterized in Table 5-49. ....	289
Table 5-54: Characterization of Composite Materials (Linear Thermal Expansion is given following the links). ....	293
Table 5-55: Smoothed Values of the Linear Thermal Expansion Coefficient, $\beta \times 10^6$ [K <sup>-1</sup> ], of the Specimens Characterized in Table 5-54. ....	295
Table 5-56: Smoothed Values of the Linear Thermal Expansion Coefficient, $\beta \times 10^6$ [K <sup>-1</sup> ], of the Specimens Characterized in Table 5-54. ....	297
Table 5-57: Characterization of Composite Materials (Linear Thermal Expansion is given following the links). ....	302
Table 5-58: Smoothed Values of the Linear Thermal Expansion Coefficient, $\beta \times 10^6$ [K <sup>-1</sup> ], of the Specimens Characterized in Table 5-57. ....	304
Table 5-59: Smoothed Values of the Linear Thermal Expansion Coefficient, $\beta \times 10^6$ [K <sup>-1</sup> ], of the Specimens Characterized in Table 5-57. ....	305
Table 5-60: Characterization of Composite Materials (Linear Thermal Expansion is given following the links). ....	310
Table 5-61: Smoothed Values of the Linear Thermal Expansion Coefficient, $\beta \times 10^6$ [K <sup>-1</sup> ], of the Specimens Characterized in Table 5-60. ....	312
Table 5-62: Smoothed Values of the Linear Thermal Expansion Coefficient, $\beta \times 10^6$ [K <sup>-1</sup> ], of the Specimens Characterized in Table 5-60. ....	313
Table 5-63: Smoothed Values of the Linear Thermal Expansion Coefficient, $\beta \times 10^6$ [K <sup>-1</sup> ], of the Specimens Characterized in Table 5-60. ....	314
Table 5-64: Smoothed Values of the Linear Thermal Expansion Coefficient, $\beta \times 10^6$ [K <sup>-1</sup> ], of the Specimens Characterized in Table 5-60. ....	315



Table 5-65: Effect of the Space Environment on Solar Absorptance, $\alpha_s$ , of Silica Fabrics .....	323
Table 5-66: Normal Total Emittance, $\varepsilon^l$ ( $\beta=0$ ), and Solar Absorptance, $\alpha_s$ , of Uncoated Plastic Materials .....	324
Table 5-67: Coated Composite Materials the Thermal Radiation Properties of Which Are Given in This Clause .....	326
Table 5-68: Normal Total Emittance, $\varepsilon^l$ ( $\beta=0$ ), of PV 100 Coating on Different Substrates and with Different Thicknesses .....	328
Table 5-69: Normal Solar Reflectance, $\rho_s$ ( $\beta=0$ ), of PV 100 Coating on Different Substrates and with Different Thicknesses .....	330
Table 5-70: Characteristic Temperatures of Neat and Reinforced Resins .....	336
Table 5-71: Electrical Resistivity, $\rho_f$ [ $\Omega.m$ ], of High-Strength Fibers .....	342
Table 5-72: Electrical Resistivity, $\rho$ [ $\Omega.m$ ], of Carbon-Epoxy Composite Materials .....	344
Table 5-73: Drill Bit Costs and Standard Drilling Hour .....	347
Table 5-74: Characterization of Composite Materials, the Maximum Moisture Content and Diffusion Constants of which are given in Table 5-75 and Table 5-76 respectively .....	352
Table 5-75: Maximum Moisture Content, $M_m$ , of the Specimens Characterized in Table 5-74 .....	353
Table 5-76: Constants $D_0$ and $C$ for the Arrhenius Expression, of the Transverse Diffusion Coefficient, $D_2$ , of the Specimens Characterized in Table 5-74 .....	353
Table 5-77: Outgassing Data for Typical Composite Materials .....	355
Table 5-78: Characterization of Materials Tested under a Vacuum Radiation Environment .....	357
Table 5-79: Summary of the Data Regarding Radiation Effects on the Coefficient of Linear Thermal Expansion for the Specimens Characterized in Table 5-78 .....	360
Table 5-80: Average Values of Linear Thermal Expansion, $\beta$ , for 75S(Pitch)/948A1(0/90) <sub>2S</sub> Graphite/Epoxy Laminates in the Temperature Range 280 K - 370 K .....	363
Table 5-81: Atomic Oxygen Reaction Efficiency Data from Reported LEO Flights and Ground Testing .....	365
Table 5-82: Weight Loss, WL (%), of Carbon Fibers After Isothermal Aging in Flowing Air .....	368
Table 5-83: Chemical Composition, Atom (%), of both T40R and Hercules AS4 Carbon Fibers, as received and oxidized, ESCA .....	370
Table 5-84: Characterization of Materials Tested under or after Thermal Vacuum Cycling .....	371
Table 5-85: Thermal Vacuum Cycling Effects on the Coefficient of Linear Thermal Expansion of the Specimens Characterized in Table 5-84 .....	373
Table 5-86: Effect of Storage on the Linear Thermal Expansion, $\beta_o$ , of the Hybrid Tubes Identified as Spec. No. 1, in Table 5-84 and Table 5-85 .....	374
Table 5-87: Effect of Thermal Cycling (either Ambient or Vacuum) on the Linear Thermal Expansion, $\beta_o$ , of the Hybrid Tubes Identified as Spec. No. 1 in Table 5-84 and Table 5-85 <sup>a</sup> .....	374

# 1

## Scope

---

In this Part 5 of the spacecraft thermal control and design data handbooks, clause 4 contains technical data on the metallic alloys used in spacecrafts is given: composition, application areas, properties and behaviour from a thermal and thermo-optics point of view, degeneration and aging. All other properties of the metallic alloys are outside the scope of this document.

Properties of composite materials combined to form heterogeneous structures are given in clause 5.

The Thermal design handbook is published in 16 Parts

ECSS-E-HB-31-01 Part 1	Thermal design handbook – Part 1: View factors
ECSS-E-HB-31-01 Part 2	Thermal design handbook – Part 2: Holes, Grooves and Cavities
ECSS-E-HB-31-01 Part 3	Thermal design handbook – Part 3: Spacecraft Surface Temperature
ECSS-E-HB-31-01 Part 4	Thermal design handbook – Part 4: Conductive Heat Transfer
ECSS-E-HB-31-01 Part 5	Thermal design handbook – Part 5: Structural Materials: Metallic and Composite
ECSS-E-HB-31-01 Part 6	Thermal design handbook – Part 6: Thermal Control Surfaces
ECSS-E-HB-31-01 Part 7	Thermal design handbook – Part 7: Insulations
ECSS-E-HB-31-01 Part 8	Thermal design handbook – Part 8: Heat Pipes
ECSS-E-HB-31-01 Part 9	Thermal design handbook – Part 9: Radiators
ECSS-E-HB-31-01 Part 10	Thermal design handbook – Part 10: Phase – Change Capacitors
ECSS-E-HB-31-01 Part 11	Thermal design handbook – Part 11: Electrical Heating
ECSS-E-HB-31-01 Part 12	Thermal design handbook – Part 12: Louvers
ECSS-E-HB-31-01 Part 13	Thermal design handbook – Part 13: Fluid Loops
ECSS-E-HB-31-01 Part 14	Thermal design handbook – Part 14: Cryogenic Cooling
ECSS-E-HB-31-01 Part 15	Thermal design handbook – Part 15: Existing Satellites
ECSS-E-HB-31-01 Part 16	Thermal design handbook – Part 16: Thermal Protection System

## 2 References

---

ECSS-S-ST-00-01	ECSS System - Glossary of terms
ECSS-E-HB-31-01 Part 4	Thermal design handbook – Part 4: <a href="#">Conductive Heat Transfer</a>
ECSS-E-HB-31-01 Part 12	Thermal design handbook – Part 12: <a href="#">Louvers</a>
ECSS-E-HB-31-01 Part 14	Thermal design handbook – Part 14: <a href="#">Cryogenic Cooling</a>

All other references made to publications in this Part are listed, alphabetically, in the **Bibliography**.

# 3

## Terms, definitions and symbols

### 3.1 Terms and definitions

For the purpose of this Standard, the terms and definitions given in ECSS-S-ST-00-01 apply.

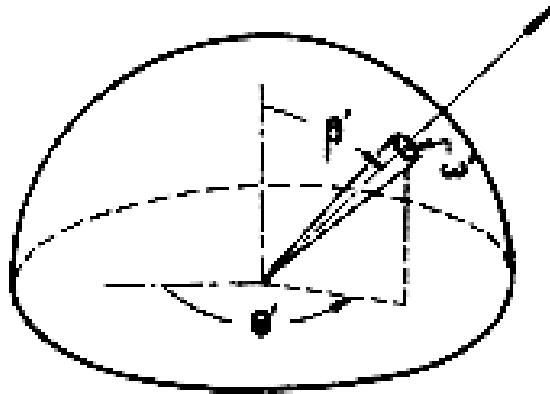
### 3.2 Symbols

$B$	magnetic induction, [T]
$E$	modulus of elasticity, [Pa]
$H$	magnetic field strength, [ $A \cdot m^{-1}$ ]
$R$	reflectance factor
$c$	specific heat, [ $J \cdot kg^{-1} \cdot K^{-1}$ ]
$k$	thermal conductivity, [ $W \cdot m^{-1} \cdot K^{-1}$ ]
$\Delta L/L$	thermal expansion
$\alpha$	thermal diffusivity, [ $m^2 \cdot s^{-1}$ ] $\alpha = k/\rho c$
$\alpha$	temperature coefficient of electrical resistivity, [ $K^{-1}$ ]
$\alpha$	hemispherical total absorptance
$\alpha'(\beta, \theta)$	directional total absorptance
$\alpha_s$	normal solar absorptance
$\alpha_\lambda(\lambda)$	hemispherical spectral absorptance
$\alpha'_\lambda(\lambda, \beta, \theta)$	directional spectral absorptance
$\beta$	mean coefficient of linear thermal expansion, [ $K^{-1}$ ]
	angle between surface normal and direction of incident flux, [angular degrees]
$\beta'$	angle between surface normal and direction of emitted, reflected or transmitted flux, [angular

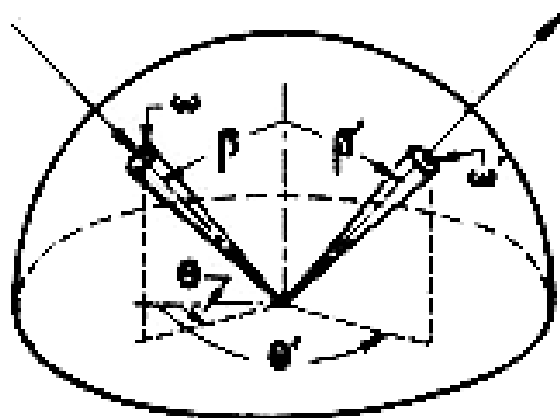
	degrees]
$\varepsilon$	hemispherical total emittance
$\varepsilon'(\beta', \theta)$	directional total emittance
$\varepsilon_\lambda(\lambda)$	hemispherical spectral emittance
$\varepsilon'_\lambda(\lambda, \beta', \theta)$	directional spectral emittance
$\theta$	azimuthal angle of incident flux, [angular degrees]
$\theta'$	azimuthal angle of emitted, reflected or transmitted flux, [angular degrees]
$\lambda$	wavelength, [m]
$\mu/\mu_0$	relative magnetic permeability
$\rho$	density, [kg.m <sup>-3</sup> ]
	hemispherical total reflectance
$\rho_\lambda(\lambda)$	hemispherical spectral reflectance
$\rho'(\beta, \theta)$	directional-hemispherical total reflectance
$\rho'(\beta', \theta)$	hemispherical-directional total reflectance
$\rho'_s$	normal-hemispherical solar reflectance
$\rho'_\lambda(\lambda, \beta, \theta)$	directional-hemispherical spectral reflectance
$\rho'_\lambda(\lambda, \beta', \theta)$	hemispherical-directional spectral reflectance
$\rho''(\beta, \theta, \beta', \theta')$	bidirectional total reflectance.
$\rho''_\lambda(\lambda, \beta, \theta, \beta', \theta')$	bidirectional spectral reflectance
$\rho''_s(\beta, \theta, \beta', \theta')$	bidirectional solar reflectance
$\sigma$	electrical conductivity, [ $\Omega^{-1}.m$ ] $\sigma^{-1}$ , electrical resistivity [ $\Omega.m$ ]
$\sigma_{ult}$	ultimate tensile strength, [Pa]
$\tau'_\lambda(\lambda, \beta, \theta, \beta', \theta')$	bidirectional spectral transmittance
$\omega$	solid angle of incident radiation beam [steradians]
$\omega'$	solid angle of emitted, reflected or transmitted radiation beam, [steradians]

The sketches below show the angles used to characterize the radiative fluxes arriving at or leaving a surface element.

Angles used to define directional emittance



Angles used to define bidirectional reflectance



# 4

## Metallic materials

---

### 4.1 General

Data for each alloy are arranged as indicated below. When no data on some property are available the heading is omitted.

#### 1. TYPICAL COMPOSITION, PERCENT

#### 2. OFFICIAL DESIGNATIONS

#### 3. PHYSICAL PROPERTIES

##### 3.1. Density

##### 3.2. Thermal properties

###### 3.2.1. Specific heat

###### 3.2.2. Thermal conductivity

###### 3.2.3. Thermal diffusivity

###### 3.2.4. Thermal expansion

###### 3.2.5. Melting range

##### 3.3. Thermal radiation properties

###### 3.3.1. Emittance

###### 3.3.1.1. Directional spectral emittance

###### 3.3.1.1.1. Normal spectral emittance

###### 3.3.1.1.2. Angular spectral emittance

###### 3.3.1.2. Directional total emittance

###### 3.3.1.2.1. Normal total emittance

###### 3.3.1.3. Hemispherical spectral emittance

###### 3.3.1.4. Hemispherical total emittance

##### 3.3.2. Absorptance

###### 3.3.2.1. Directional spectral absorptance

###### 3.3.2.1.1. Normal spectral absorptance

###### 3.3.2.2. Directional total absorptance

###### 3.3.2.2.1. Normal total absorptance

- 3.3.2.3. Hemispherical spectral absorptance
- 3.3.2.4. Hemispherical total absorptance
- 3.3.2.5. Solar absorptance
  - 3.3.2.5.1. Normal solar absorptance
  - 3.3.2.5.2. Angular solar absorptance
- 3.3.2.6. Absorptance to emittance ratio
- 3.3.3. Reflectance
  - 3.3.3.1. Bidirectional spectral reflectance
    - 3.3.3.1.1. Normal-normal spectral reflectance
    - 3.3.3.1.2. Angular (non-normal) spectral reflectance
  - 3.3.3.2. Directional-hemispherical spectral reflectance
    - 3.3.3.2.1. Normal-hemispherical spectral reflectance
    - 3.3.3.2.2. Angular-hemispherical spectral reflectance
  - 3.3.3.3. Hemispherical-directional spectral reflectance
    - 3.3.3.3.1. Hemispherical-normal spectral reflectance
  - 3.3.3.4. Hemispherical spectral reflectance
  - 3.3.3.5. Bidirectional total reflectance
    - 3.3.3.5.1. Normal-normal total reflectance
    - 3.3.3.5.2. Angular (non-normal) total reflectance
  - 3.3.3.6. Directional-hemispherical total reflectance
    - 3.3.3.6.1. Normal-hemispherical total reflectance
  - 3.3.3.7. Hemispherical-directional total reflectance
    - 3.3.3.7.1. Hemispherical-normal total reflectance
  - 3.3.3.8. Bidirectional solar reflectance
    - 3.3.3.8.1. Normal-normal solar reflectance
  - 3.3.3.9. Directional-hemispherical solar reflectance
    - 3.3.3.9.1. Normal-hemispherical solar reflectance
- 3.3.4. Transmittance
  - 3.3.4.1. Bidirectional spectral transmittance
    - 3.3.4.1.1. Normal-normal spectral transmittance
    - 3.3.4.1.2. Angular (non-normal) spectral transmittance
- 3.4. Other physical properties
  - 3.4.1. Electrical resistivity
  - 3.4.2. Magnetic properties
- 4. ENVIRONMENTAL BEHAVIOR
  - 4.1. Prelaunch



4.2. Postlaunch

5. CHEMICAL PROPERTIES

5.1. Solution potential

5.2. Corrosion resistance

6. FABRICATION

6.1. Casting

6.2. Forming

6.3. Welding

6.4. Machining

6.5. Heat treatment

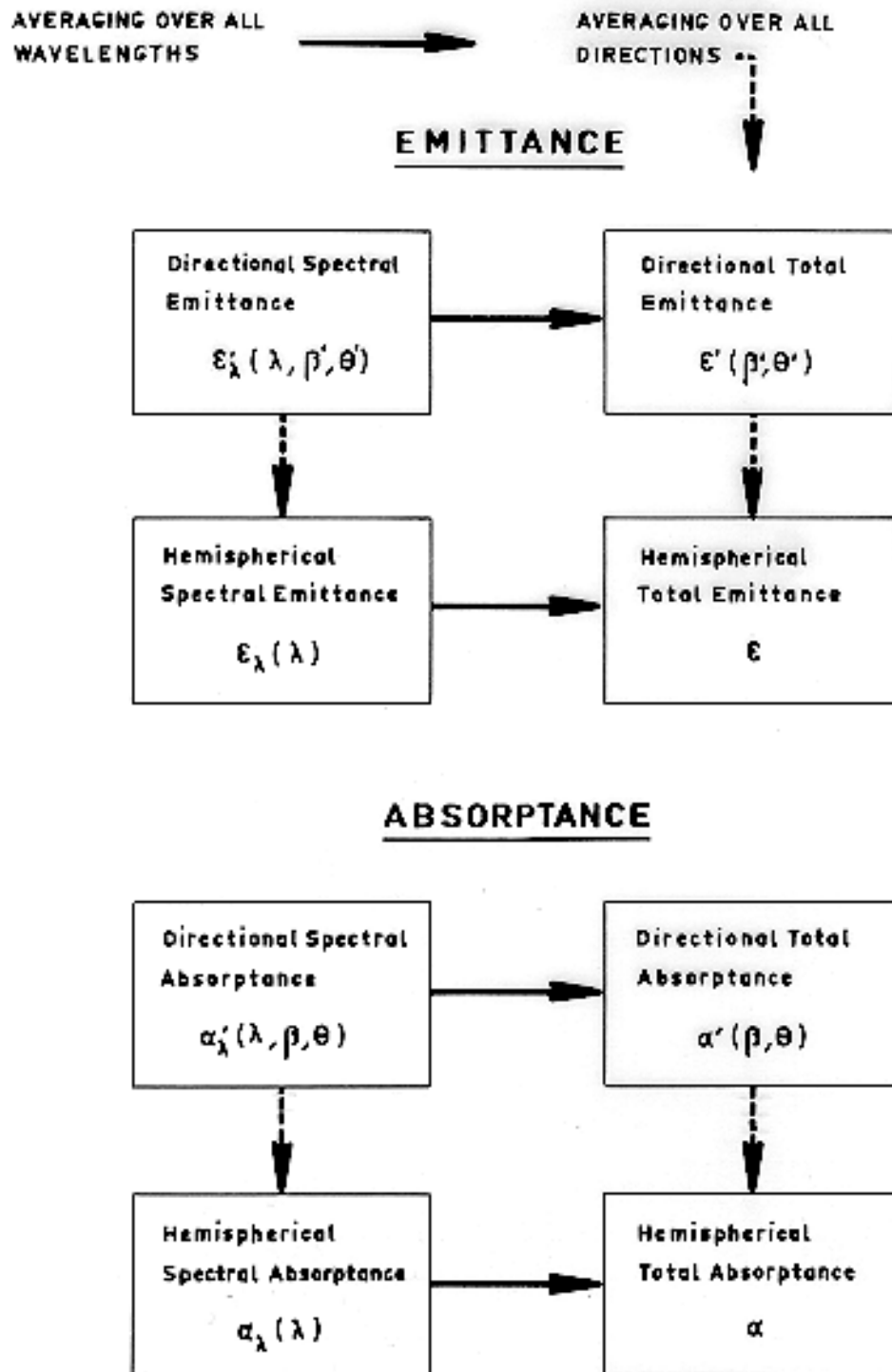
6.6. Anodizing

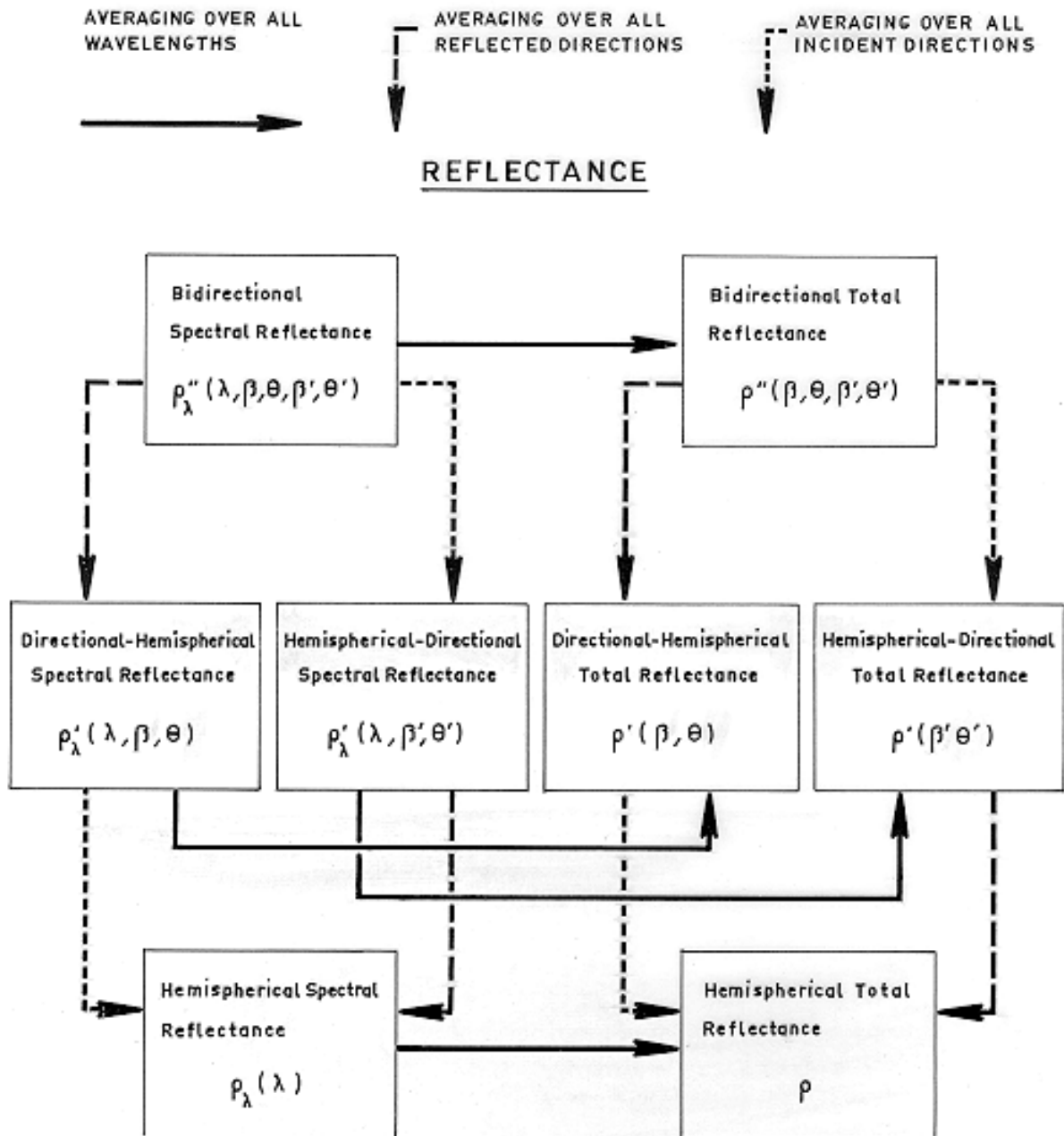
7. AVAILABLE FORMS AND CONDITIONS

8. USEFUL TEMPERATURE RANGE

9. APPLICATIONS

### 4.1.1 Modifiers of thermal radiative properties





### 4.1.2 Cladding definitions

**Clad.** A composite metallic material containing two or three layers that have been bonded together. Bonding may be achieved by co-rolling, welding, casting, heavy chemical deposition or heavy electroplating.

**Alclad.** Clad produced by bonding either a corrosion-resistant aluminium alloy or high purity aluminium to a base of a structurally stronger aluminium alloy.

**Nonclad.** Metallic material to which no other alloy has been bonded by cladding.

### 4.1.3 Temper designation for heat treatable aluminium alloys

F Condition: As fabricated.

O Condition: Annealed (wrought products only).

W Condition: Solution heat treated.

T1 Condition: Naturally aged to a stable condition.

T2 Condition: Annealed (cast products only).

T3 Condition: Solution heat treated, cold worked, and naturally aged to a substantially stable condition.

T4 Condition: Solution heat treated and naturally aged to a substantially stable condition.

T5 Condition: Artificially aged only.

T6 Condition: Solution heat treated and artificially aged.

T7 Condition: Solution heat treated and over aged.

T8 Condition: Solution heat treated, cold worked, and artificially aged. Different amounts of cold working are denoted by a second digit.

T9 Condition: Solution heat treated, artificially aged and cold worked.

T10 Condition: Artificially aged and cold worked.

## 4.2 Aluminium alloys

ALLOYS Al - 99,99. Al - 99,9. Al - 99,8. Al - 99,7. Al - 99,5. Al - 99,3. Al - 99.

This data item concerns all aluminium alloys whose aluminium content is above 99%.

1. TYPICAL COMPOSITION, PERCENT. Maximum values are given except for Aluminium.

	Al	Cu	Fe	Mn	Si	Zn	Others	
							Each	Total
Al - 99,99	>99,99	-	-	-	-	-	-	0,01
Al - 99,9	>99,9	0,02	0,07	0,01	0,07	0,03	0,01	-
Al - 99,8	>99,8	0,03	0,15	0,03	0,15	0,06	0,02	-
Al - 99,7	>99,7	0,03	0,25	0,03	0,20	0,07	0,03	-
Al - 99,5	>99,5	0,05	0,40	0,05	0,30	0,10	0,03	-
Al - 99,3	>99,3	0,10	0,60	0,05	0,30	0,10	0,05	-
Al - 99,0	>99,0	0,20	0,80	0,05	0,50	0,10	0,05	-

## 2. OFFICIAL DESIGNATIONS

	AECMA	ISO	AFNOR	AMS	BS	DIN
Al - 99,99					1	Al 99,98R S - Al 99,98R 3,0385
Al - 99,9						Al 99,9 3,0305
Al - 99,8		Al 99,8	A8		1A	Al 99,8 S - Al 99,8 3,0285
Al - 99,7		Al 99,7	A7	~4000		Al 99,7 3,0275
Al - 99,5	Al P 99,5	Al 99,5	A5	~4000	1B ~1E	Al 99,5 S - Al 99,5 3,0255 ~E - Al ~3,0257
Al - 99,3			~A45	4040 4041 4042		~S - Al 99,5Ti ~3,0805
Al - 99,0		Al 99,0 ~Al 99,0Cu	A4	~1100 4001 4003 4062 4102 4180 7220	1C	Al 99 3,0205

NOTE ~ Can be approximately included with those alloys having the indicated aluminium content.

## 3. PHYSICAL PROPERTIES

## 3.1. Density.

Al - 99,99,  $\rho = 2699 \text{ kg.m}^{-3}$ . (Pennington (1961) [29]).

Al - 99,5  $\rho = 2700 \text{ kg.m}^{-3}$ . (Kappelt (1961) [23]).

Al - 99,0  $\rho = 2710 \text{ kg.m}^{-3}$ . (Kappelt (1961) [23]).

## 3.2. Thermal properties

## 3.2.1. Specific heat

Effect of temperature on specific heat: Figure 4-1.

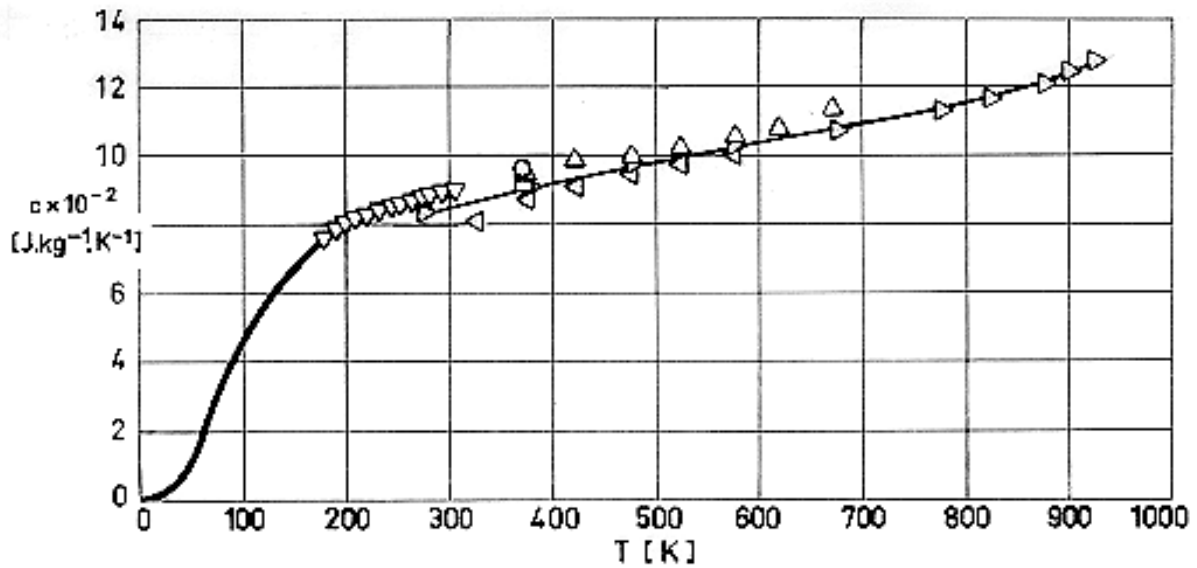


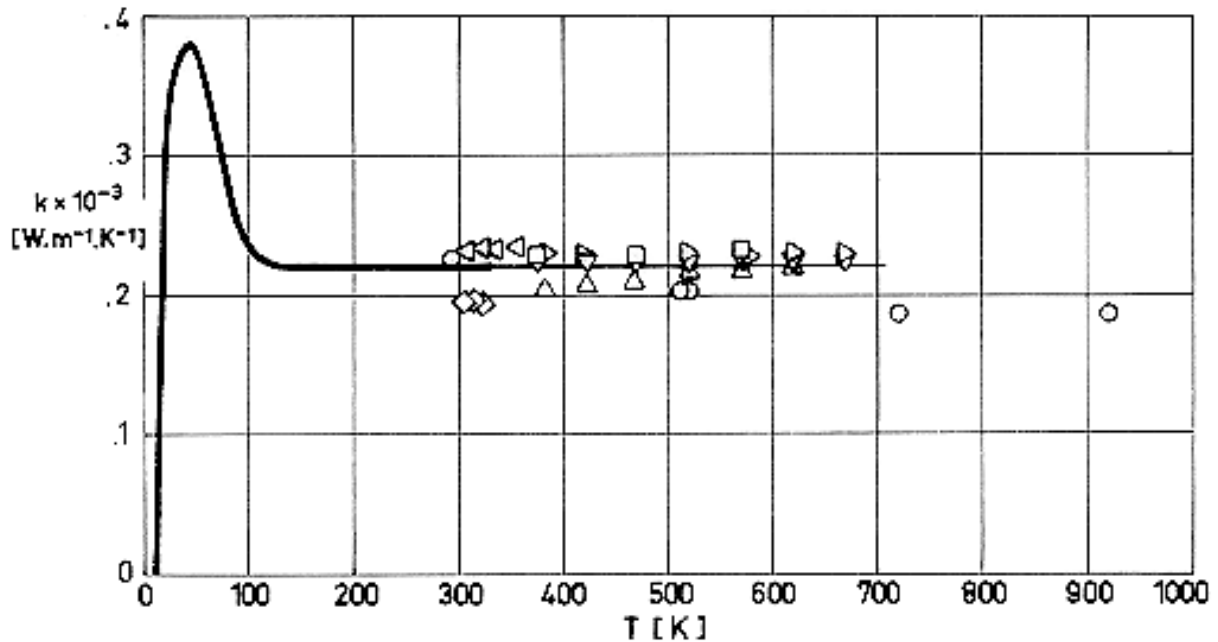
Figure 4-1: Specific heat,  $c$ , of Aluminium as a function of temperature,  $T$ .

Explanation

Key	Description	Comments	References
○	Al - 99,0		Kappelt (1961) [23].
□	Al - 99,99		Pennington (1961) [29].
△	Al - 99,99 Average of 2 samples 1) Water quenched from 873 K; annealed 100 h at 403 K. 2) Cooled from 873 K at 5 K.min <sup>-1</sup>	Reported error ≤ 1%	Touloukian (1967)a [38]
▽	Al 99,9 Single crystal. Melted and cooled 2 d in vacuum.		
▷	Al - 99,9	Reported error ± 5%	
◁		Reported error ± 5%	
—			Coston (1967) [18].

3.2.2. Thermal conductivity

Effect of temperature on thermal conductivity: Figure 4-2.



Note: non-si units are used in this figure

Figure 4-2: Thermal conductivity,  $\kappa$ , of Aluminium as a function of temperature,  $T$ .

Explanation

Key	Description	Comments	References
○	Al - 99,9	Losses evaluated by measuring unsteady state cooling of rod initially at uniform temperature.	Touloukian (1967)a [38].
□	0,04 Si - 0,03 Fe - 0,006 Cu - 0,005 Ti, and traces of Mn and Mg. Annealed 1 h at 723 K and cooled slowly.	Reported error $\pm 3\%$ .	
△	Al - 99,5 Cast at 973 K into molds at 473 K; rolled and drawn, then turn into rods.		
▽	Al - 99,9 Same treatment as above.		
▷	Al - 99,9 Same treatment as above.		
◁	Al 99,99	Reported error $\pm 1\%$ .	

Key	Description	Comments	References
◇	Commercially pure. Sample $2 \times 10^{-2}$ m in diameter and $1,8 \times 10^{-2}$ m length.	Reported error $\pm 3\%$ .	
—			Coston (1967) [18].

Thermal conductivity integrals: Figure 4-3.

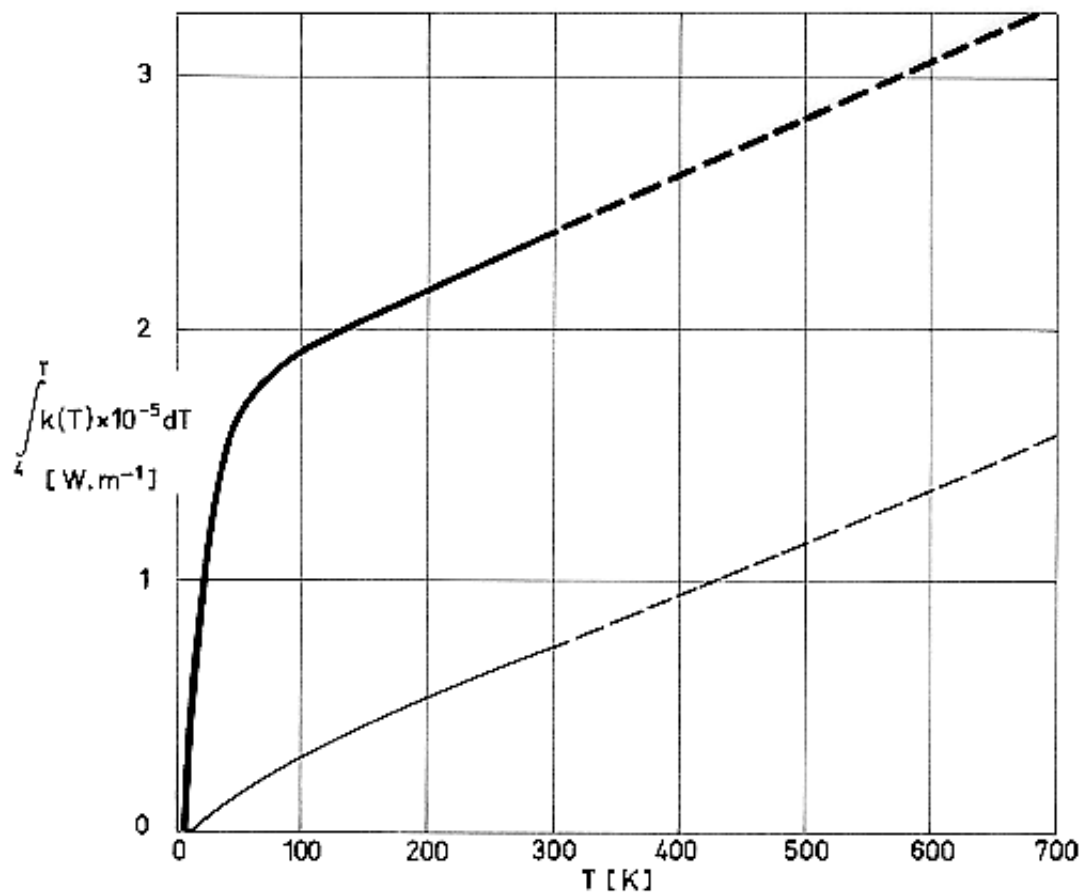


**Figure 4-3: Thermal conductivity integrals of Aluminium as a function of temperature,  $T$ .**

Explanation

—: Al - 99,99. From Coston (1967) [18].

—: Al - 99,0. From Coston (1967) [18].

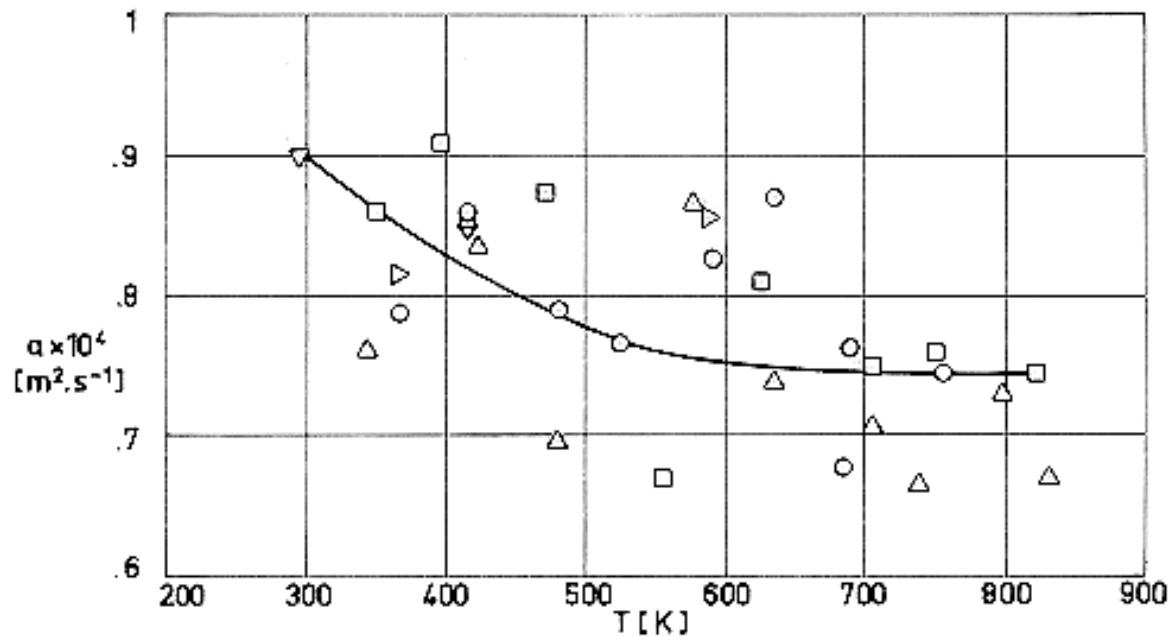
— —: Straight line whose slope has been calculated by the compiler by fitting the experimental data points ◇ and ◁ of Figure 4-2 with the least-squares method.

— —: Calculated by the compiler from data points ◇ of Figure 4-2



## 3.2.3. Thermal diffusivity.

Effect of temperature on thermal diffusivity: Figure 4-4.



Note: non-si units are used in this figure

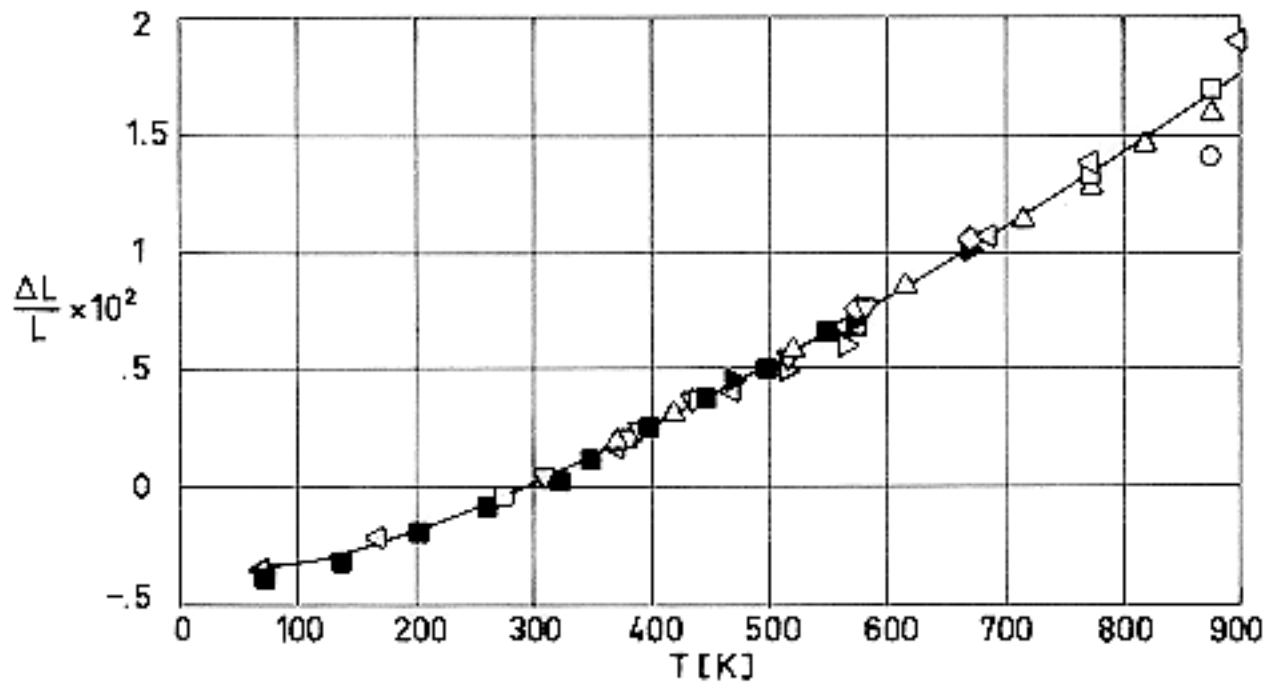
**Figure 4-4: Thermal diffusivity,  $\alpha$ , of Aluminium as a function of temperature,  $T$ .**

Explanation

Key	Description	Comments	References
○	Al - 99,9	Reported error $\pm 11\%$ .	Touloukian (1967)a [38].
□	Same as above.	Second run of the above specimen. Reported error $\pm 11\%$ .	
△	Same as above.	Third run of the above specimen. Reported error $\pm 11\%$ .	
▽	Pure. $1.9 \times 10^{-3} m^2$ square cross-section and $3.52 \times 10^{-3} m$ length.	Reported error $\pm 5\%$ .	
▷	Pure.		

## 3.2.4. Thermal expansion.

Effect of temperature on thermal expansion: Figure 4-5.



Note: non-si units are used in this figure

**Figure 4-5: Linear thermal expansion,  $\Delta L / L$ , of Aluminium as a function of temperature,  $T$ .**

Explanation

Key	Description	Comments	References
○			Touloukian (1967)a [38].
□	Al - 99,99 Annealed above 873 K.		
■	Al - 99,99		
△	Al - 99,9 Annealed 2 h at 893 K and cooled slowly.		
▽	99,952 Al - 0,019 Cu - 0,015 Fe - 0,014 Si. Cast in graphite mold.		
▷	Chemically pure.	X-ray diffraction	
◁			

Key	Description	Comments	References
		method.	
◁	99,989 Al - 0,004 each Si, Cu - 0,003 Fe.		
▶	Pure. Pressed rod made of sintered aluminium powder.		
◇	Al - 99,5		

Mean coefficient of linear thermal expansion,  $\beta$ .

The available information concerning thermal expansion coefficients of these alloys seems to indicate that there is no noticeable influence of the aluminium content on  $\beta$ . Values given below correspond to Al - 99,99.

T [K]	73-293	123-293	173-293	223-293	293-373	293-473	293-573	293-673	293-773
$\beta \times 10^6$ [K <sup>-1</sup> ]	18,0	19,9	21,0	21,8	23,6	24,5	25,5	26,4	27,4

From Pennington (1961) [29].

### 3.2.5. Melting range

Al - 99,99: 933 K. (Pennington (1961) [29]).

Al - 99,5: 919 K - 930 K. (Kappelt (1961) [23]).

Al - 99,0: 916 K - 930 K. (Kappelt (1961) [23]).

## 3.3. Thermal radiation properties

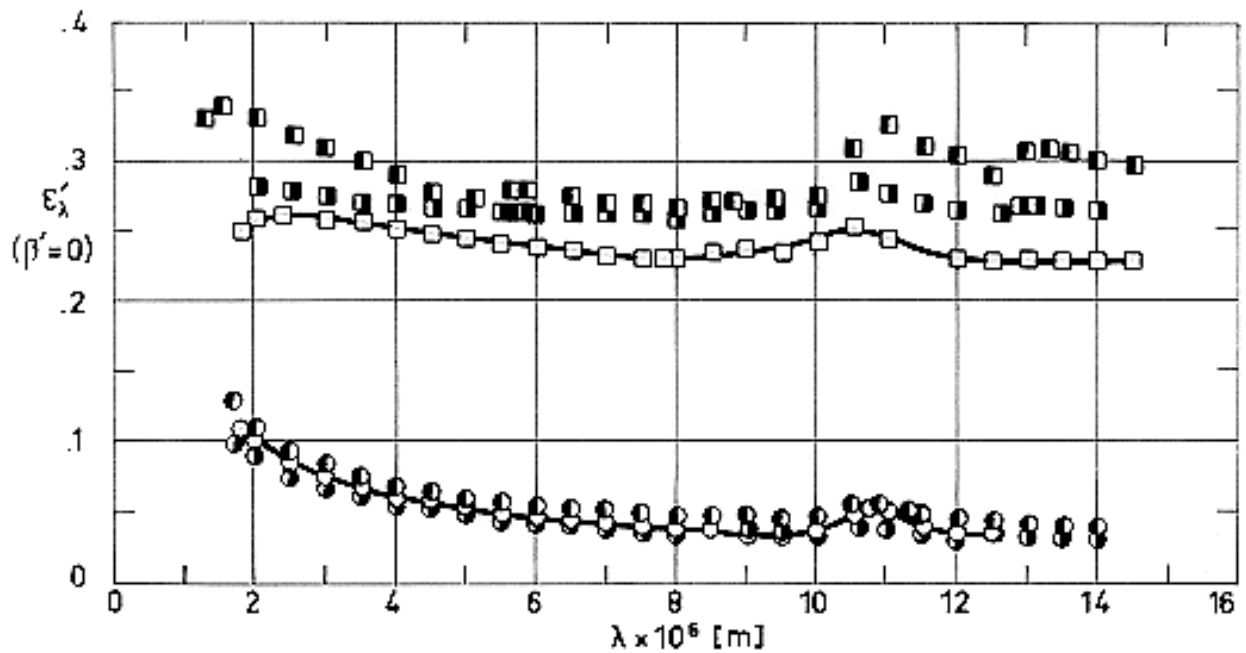
### 3.3.1. Emittance

Data concerning emittance have been arranged as indicated in the following Table.

3.3.1.1. Directional spectral emittance.				
Clause	Heading	Data presented	Fig.	Table
3.3.1.1.1.	Normal $\beta' = 0$	Al - 99,7	Figure 4-6	
		Aluminium conversion coatings.	Figure 4-7	
3.3.1.1.2.	Angular (non-normal) $\beta' \neq 0$	Al - 99,0	Figure 4-7	

<b>3.3.1.2. Directional total emittance.</b>				
3.3.1.2.1.	Normal $\beta' = 0$	Aluminium.		Table 4-1
		Aluminium. Effect of temperature.	Figure 4-9	
		Aluminium contact coatings.		Table 4-2 <sup>a</sup>
		Aluminium conversion coatings.		Table 4-3 <sup>a</sup>
		Aluminium conversion coatings. Effect of anodizing thickness.	Figure 4-10	
<b>3.3.1.4. Hemispherical total emittance.</b>				
	$\omega' = 2\pi$	Aluminium. Effect of temperature.	Figure 4-11	
		Aluminium contact coatings.		Table 4-4
		Aluminium conversion coatings. Effect of anodizing thickness.	Figure 4-12	

<sup>a</sup> Solar absorptance,  $\alpha_s$ , has been also included in this Table in order to save space.



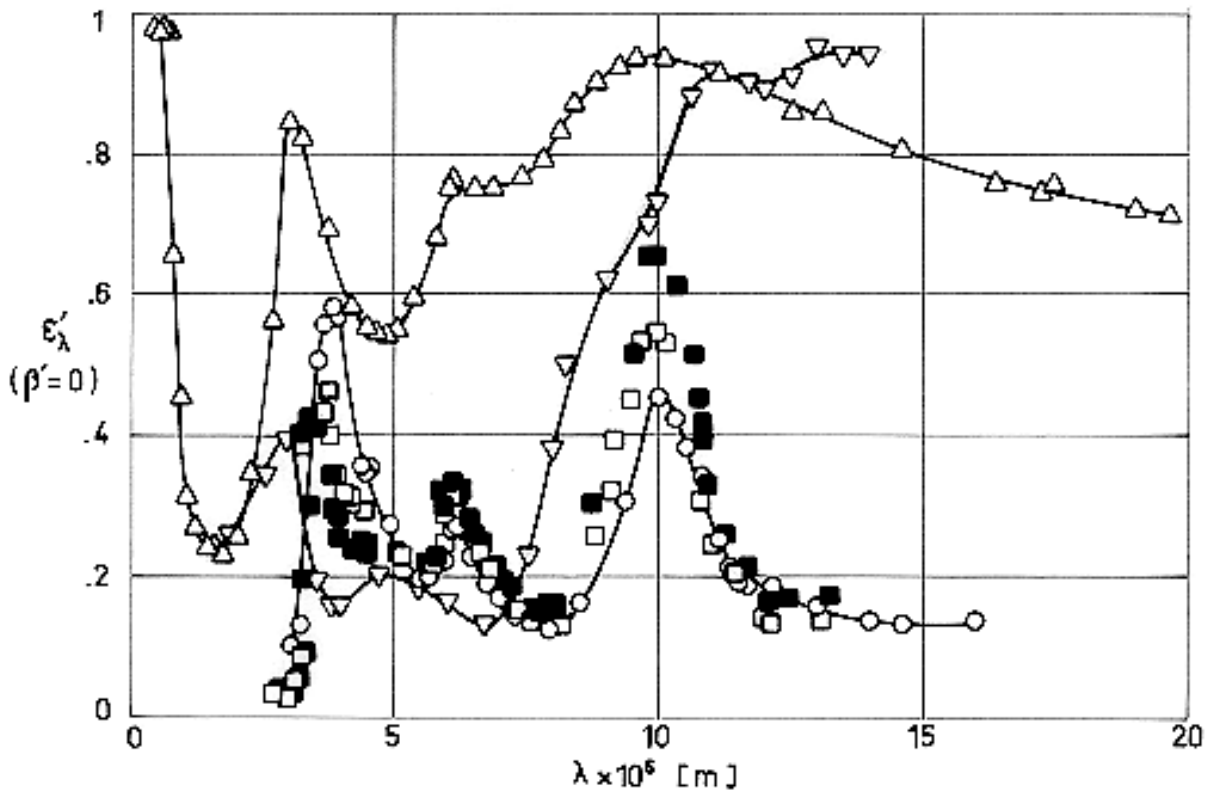
Note: non-si units are used in this figure

**Figure 4-6: Normal spectral emittance,  $\epsilon'_\lambda$ , of Aluminium as a function of wavelength,  $\lambda$ .**

Explanation

Key	Description	Comments	References
○	99,7 Al - 0,11 Fe - 0,11 Si - 0,01 Cu - 0,01 Mg - <0,01 Mn, Ni, Zn. Cylindrical tube. Heated at 467 K for 15 h. Polished. Surface roughness: $7,62 \times 10^{-8}$ m (center line average).	Sample temperature: $T = 599$ K. Data from smooth curve. Reported error $\pm 20\%$ (in the wavelength range $2 \times 10^{-6}$ to $10^{-5}$ m).	Touloukian & DeWitt (1970) [42].
●	Same as ○ except heated at 697 K for 20 h.	Same as ○ except $T = 697$ K.	
●	Same as ○ except heated at 805 K for 15 h.	Same as ○ except $T = 805$ K.	
□	Same specimen as ○ except heated at 462 K for 25 h. Roughness and knurled with grade 180 silicon carbide paper. Surface roughness: $2,92 \times 10^{-6}$ m (centre line average).	$T = 462$ K. Data from smooth curve. Reported error $\pm 10\%$ (in the wavelength range $2 \times 10^{-6}$ to $10^{-5}$ m).	

Key	Description	Comments	References
■	Same as □ except heated at 598 K for 22 h.	Same as □ except $T = 599$ K.	
■	Same as □ except heated at 715 K for 27 h.	Same as □ except $T = 715$ K.	



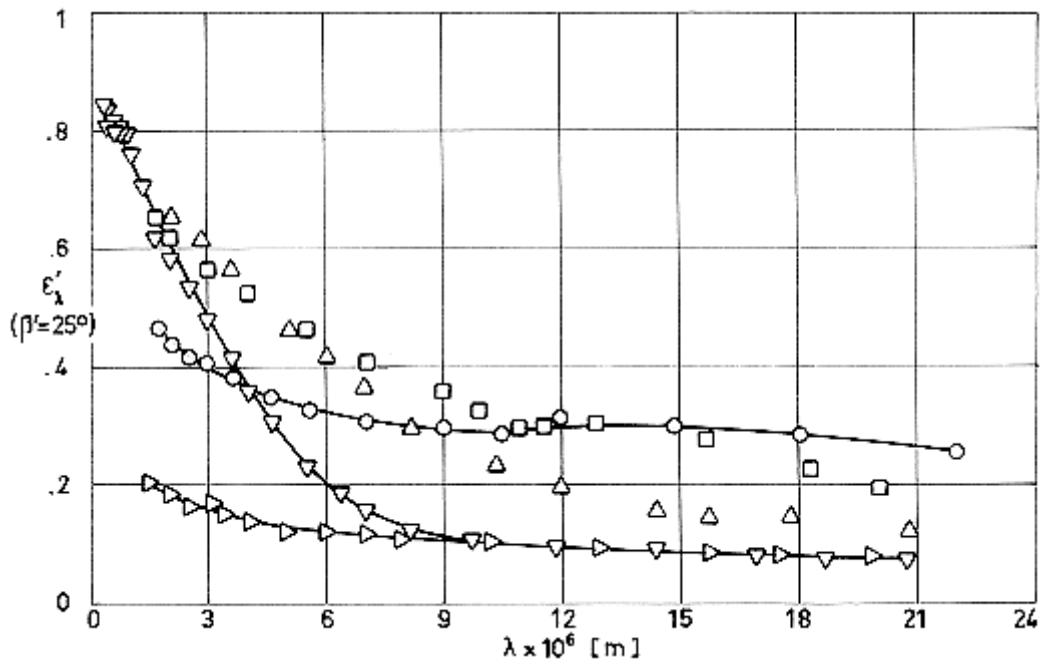
Note: non-si units are used in this figure

Figure 4-7: Normal spectral emittance,  $\epsilon_{\lambda}'$ , of Aluminium conversion coatings as a function of wavelength,  $\lambda$ .

Explanation

Key	Description	Comments	References
○	Alodine 401.45. Reaction of an aluminium surface with an aqueous solution of chromic, phosphoric, and hydrofluoric acid. Substrate: Al - 99,8 (Echo II).	Sample temperature: $T = 295$ K. Data from smooth curve. Converted from $R(2\pi, 0)$ .	Touloukian, DeWitt & HERNICZ (1972) [43].
□	Same as ○ except reacted for 20 s in a 1 N		

Key	Description	Comments	References
	sodium hydroxide solution at 298 K, then washed in water and dried in air.		
■	Same as □ . Reacted for 40 s.		
△	Black anodized.	$T = 323$ K. Data from smooth curve. Converted from $R(2\pi,0)$ .	
▽	Al - 99.7. Anodized 30 min at $10^{-2}$ A.m $^{-2}$ in 4 N analar sulphuric acid at 293 K, sealed for 30 min in boiling distilled water. Anodizing thickness $2,54 \times 10^{-6}$ m. Heated at 456 K for 15 h.	$T = 461$ K. Data from smooth curve. Reported error $\pm 10\%$ .	



Note: non-si units are used in this figure

Figure 4-8: Angular spectral emittance,  $\epsilon'_{\lambda}$ , of Aluminium as a function of wavelength,  $\lambda$ .

Explanation

Key	Description	Comments	References
○	Al - 99.0. Nominal composition. Sandblasted with 120 mesh alumina (mesh opening $1,25 \times 10^{-4}$ m).	Sample temperature:	Touloukian & DeWitt (1970) [42].

Key	Description	Comments	References
□	Same as ○ except sandblasted with 320 mesh alumina (mesh opening $4,6 \times 10^{-5}$ m).	$T = 306$ K. Authors assumed $\alpha = \varepsilon = 1 - \rho$ . $\rho (25^\circ, 2\pi)$ .	
△	Same as ○ except sandblasted with 600 mesh alumina (mesh opening $2,4 \times 10^{-5}$ m).		
▽	Same as ○ except sandblasted with 1000 mesh alumina (mesh opening $1,4 \times 10^{-5}$ m).		
▷	Same as ○ except sanded with 280 mesh silicon carbide paper.		

**Table 4-1: Normal Total Emittance of Aluminium**

Alloy	$T$ [K]	$\varepsilon'$ ( $\beta' = 0$ )	Comments	References
Al - 99,99	298	0,03		Pennington (1961) [29]
Al - 99,0		0,05	Polished	Zerlaut, Carrol & Gates (1966) [47].
Al -		0,21	Foil, vapor blasted, wet.	
Al - 99,0		0,33	Sandblasted.	
Al -	311	0,065	Bright foil roughened with abrasive cloth.	Touloukian (1967)a [38].
Al -	373	0,18	Sheet, rough polished.	
Al - 99,99		0,02	Foil ( $1,27 \times 10^{-4}$ m thick) GMC Bright dip for 10 min at 350 K.	Bevans (1969) [14].
Al -	296	0,04	Polished.	TRW (1970) [44].
Al -	298	0,055 to 0,070	Rough plate.	
Al -		0,04	Bare metal.	Scollon & Carpitella (1970) [33].
Al - 99,0	370	0,022	Polished with MgO and water, measured in vacuum ( $2,1 \times 10^{-2}$ Pa).	Touloukian & DeWitt (1970) [42].
Al - 99,99	425,4	0,037	Rolled, polished.	



Alloy	T [K]	$\epsilon'$ ( $\beta' = 0$ )	Comments	References
Al - 99,99	647	0,045	Same as above.	
Al - 99,99	780	0,0497	Same as above.	
Al - 99,99	414	0,0486	Highly polished.	
Al - 99,99	610	0,0576	Same as above.	
Al - 99,99	733	0,065	Same as above.	
Al -	366	0,028	Foil.	
Al -	311	0,045	Foil, embossed (Pattern No. 1).	
Al -	311	0,056	Foil, embossed (Pattern No. 2).	
Al -	311	0,047	Foil, embossed (Pattern No. 3).	
Al -	311	0,056	Foil, embossed (Pattern No. 4).	
Al -	311	0,061	Foil, embossed (Pattern No. 5).	
Al - 99,9	311	0,045	0,002 Si, 0,0001 Fe, 0,001 Cu, 0,0003 Na, 0,0003 Ca, 0,0003 Mg. Electrolytically brightened, density 2698 kg.m <sup>-3</sup> at 298 K. aluminium foil reference ( $\epsilon = 0,05$ ).	
Al -	311	0,035 to 0,050	Foil, bright; etched in hot sodium hydroxide solution 0,5 to 2 min, and dipped in nitric acid.	
Al -	311	0,044	Foil, bright; roughened with abrasive cloth (No. 120 Aloxite cloth).	
Al -	311	0,063	Foil, bright; roughened with abrasive cloth (No. 120 Aloxite cloth).	
Al -	311	0,066	Foil, bright; roughened with abrasive cloth (No. 120 Aloxite cloth).	
Al -	311	0,04	Foil, surface film formed by means of exposure to corrosive attack; foil-covered cardboard taken from foil-insulated dry-ice cabinet	

Alloy	T [K]	$\epsilon'$ ( $\beta' = 0$ )	Comments	References
			exposed to weather on beach during 8 months.	
Al -	311	0,05	Foil; suspended vertically in the laboratory for 3 years and measured with the accumulated dust and fume.	
Al -	311	0,09	Foil; chemically oxidized by treating with hot solution of sodium carbonate and chromate.	
Al -	311	0,10	Foil; lacquer coated; heated to partially decompose lacquer and color in brown.	
Al -	311	0,10	Foil after 2 years exposure to salt spray and moisture at seashore.	
Al -	373	0,09	Commercial sheet.	
Al -	373	0,095	Sheet, polished.	

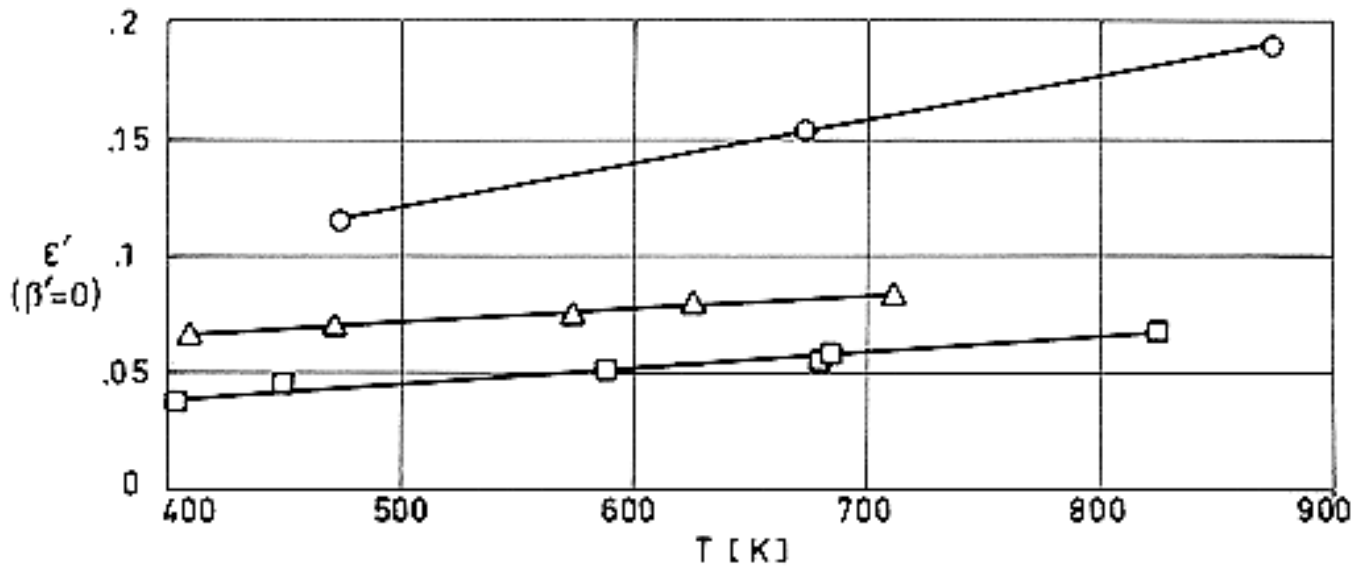
**Table 4-2: Normal Total Emittance and Normal Solar Absorptance of Aluminium Contact Coatings**

Alloy	T [K]	$\epsilon'$ ( $\beta' = 0$ )	$\alpha_s$ ( $\beta = 0$ )	Comments	References
Al -		0,03	0,10	Vacuum deposited (opaque thickness) on aluminium sheet with resin undercoat.	Bevans (1969) [14].
Al -		0,03	0,09	Vacuum deposited (opaque thickness) on aluminium foil, Reynolds Wrapp.	
Al -		0,04	0,21	Vacuum deposited (opaque thickness) on Beryllium foil.	
Al -		0,03	0,09	Vacuum deposited (opaque thickness) on Mylar film $2,5 \times 10^{-5}$ m thick.	
Al -		0,014	0,08	$10^{-7}$ to $2 \times 10^{-7}$ m thick aluminium	Scollon & Carpitella

Alloy	T [K]	$\epsilon'$ ( $\beta = 0$ )	$\alpha_s$ ( $\beta = 0$ )	Comments	References
				vapor deposited on unspecified surface. Polished surface. Measured in vacuum.	(1970) [33].
Al -		0,051	0,15	Same as above. Measured in air.	
Al -		0,024	0,13	Vapor deposited aluminium on Mylar.	
Al -		$\leq 0,05$	$\leq 0,13$	Vapor deposited aluminium on $1,2 \times 10^{-5}$ m thick Kapton. Data for metallic side. Silicone pressure sensitive adhesive. Schjeldahl.	
Al -		$\leq 0,06$	0,10 to 0,14	Vapor deposited aluminium on Kapton . Data for metallic side. Silicone pressure sensitive tape. Schjeldahl G-103500 tape.	
Al -		0,13 to 0,17	0,12 to 0,16	Vapor deposited aluminium on $1,2 \times 10^{-5}$ m thick Kapton plus nylon tulle. Data for metallic surface. Acrylic pressure sensitive adhesive. Second surface reflector. Schjeldahl G-102000 tape.	
Al -		0,025	0,11	$1,5 \times 10^{-7}$ m thick evaporated aluminium on Quartz.	McCargo, Spradley, Greenberg & McDonald (1971) [26].

**Table 4-3: Normal Total Emittance and Normal Solar Absorptance of Aluminium Conversion Coatings**

Alloy	T [K]	$\epsilon'$ ( $\beta' = 0$ )	$\alpha_s$ ( $\beta = 0$ )	Comments	References
Al - 99,99		0,77	0,20	Hard anodized, $8 \times 10^{-6}$ m thick, with sulphuric acid electrolyte 11% by weight, at 270 K.	Bevans (1969) [14].
Al - 99,99		0,79	0,14	Soft anodized, $1,3 \times 10^{-5}$ m thick, with sulphuric acid electrolyte 15% by weight, at 270 K.	
Al - 99,7		0,82	0,24	Soft anodized, $1,3 \times 10^{-5}$ m thick, with sulphuric acid electrolyte 16% by weight, at 294 K.	
Al - 99,7		0,74	0,40	Anodized, $8 \times 10^{-6}$ m thick, with chromic acid electrolyte 5% by weight, at 308 K, anodizing voltage 40V DC, 120 min.	
Al - 99,99		0,08	0,27	Anodized, citric acid electrolyte $1 \text{ kg.m}^{-3}$ ammonium citrate, at 295 K, anodizing voltage: 300V DC, 60 min.	
Al - 99,7		0,86	0,31	Anodized, $2 \times 10^{-5}$ m thick, oxalic acid solution 3% by weight, at 311 K, anodizing voltage: 30V DC, 60 min.	
Al - 99,99		0,39	0,33	Anodized, sulphamic acid electrolyte $100 \text{ kg.m}^{-3}$ , at 294 K, anodizing voltage: 45V DC, 30 min.	
Al - 99,99		0,77	0,64	Anodized, sulphamic acid electrolyte $100 \text{ kg.m}^{-3}$ , at 294 K, anodizing voltage: 15V DC, 30 min.	
Al - 99,99		0,03	0,27	Anodized, sulphamic acid electrolyte $100 \text{ kg.m}^{-3}$ , at 294 K, anodizing voltage: 5,5V DC, 15 min.	
Al -		0,73	0,70	Chromic acid anodized. Chemical surface finish. Degradation caused by deposition of outside contaminants (73 h in low earth orbit on board Apollo 9).	
Al -		0,90		Carbon black impregnated anodized coating. Chemical surface finish.	

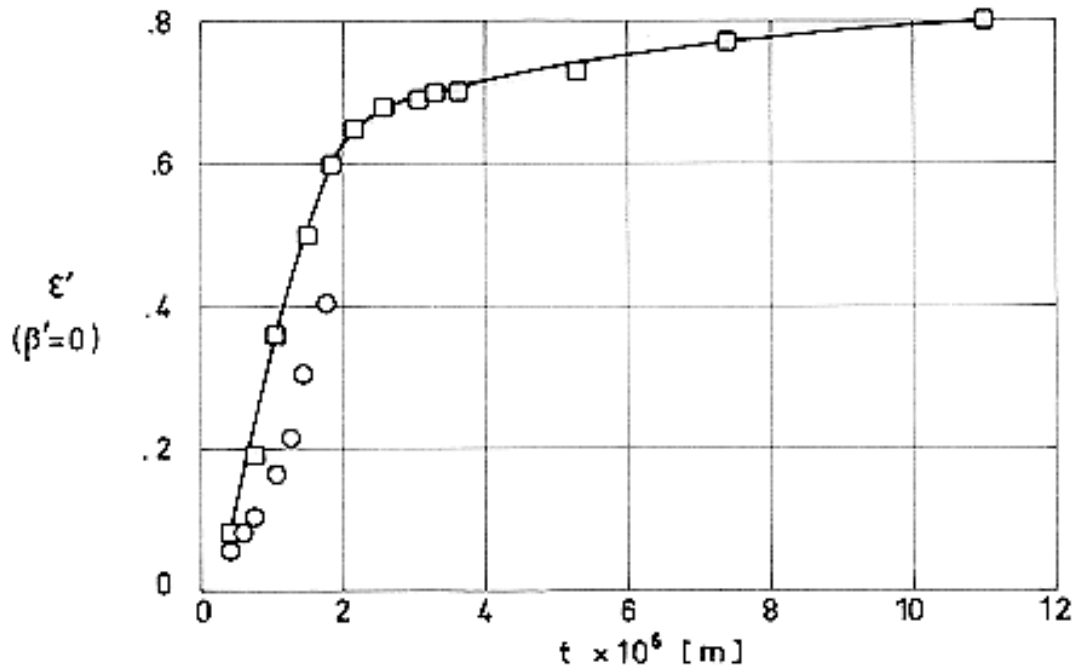


Note: non-si units are used in this figure

Figure 4-9: Normal total emittance,  $\epsilon'$ , of Aluminium as a function of temperature,  $T$ .

Explanation

Key	Description	Comments	References
○	Cleaned, polished, and oxidized.		Touloukian & DeWitt (1972) [158].
□	Pure. Highly polished.	Reported error 2%.	
△	Pure. Rolled, as received.		

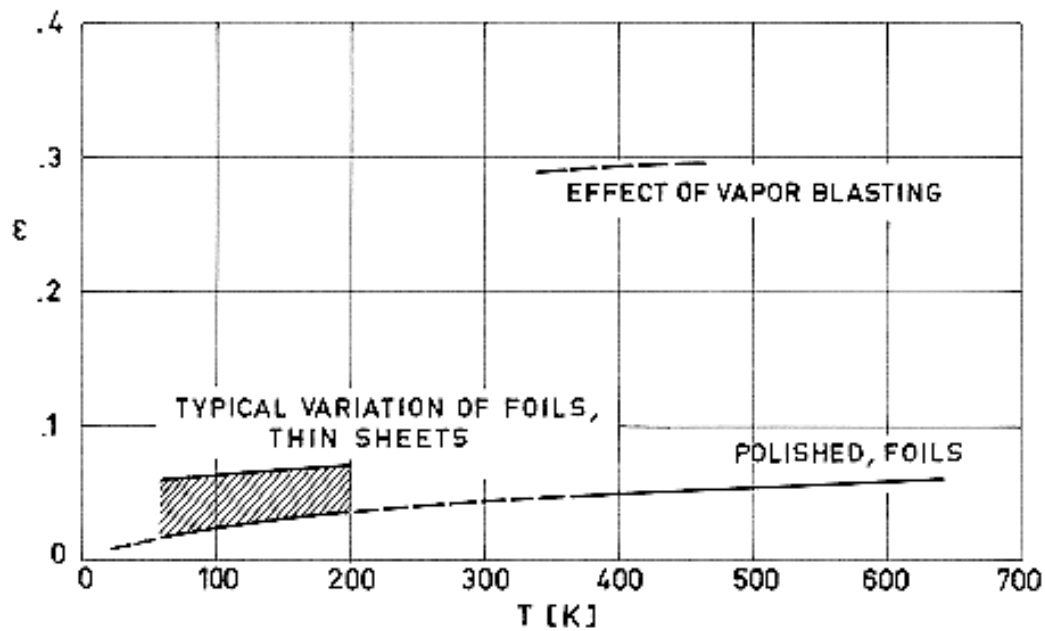


Note: non-si units are used in this figure

**Figure 4-10: Normal total emittance,  $\epsilon'$ , of Aluminium anodized as a function of anodizing thickness,  $t_c$ .**

Explanation

Key	Description	Comments	References
○	Barrier-layer anodic coating on a high aluminium substrate. Substrate cleaned, electropolished in a flouboric acid solution, anodized in aqueous ammonium tartrate solution, then immersed in a phosphoric acid solution.	Sample temperature $T \sim 298$ K. Measured in vacuum ( $\sim 1,33 \times 10^{-4}$ Pa).	Touloukian, DeWitt & Hemicz (1972) [43].
□	Foil oxidized electrolytically in 15% sulphuric acid.	$T = 311$ K. Measured relative to Aluminium.	



Note: non-si units are used in this figure

**Figure 4-11: Summary of data concerning the hemispherical total emittance,  $\epsilon$ , of Aluminium as a function of temperature,  $T$ . From Touloukian & DeWitt (1970) [42].**

**Table 4-4: Hemispherical Total Emittance of Aluminium Contact Coatings.**

$T$ [K]	$\epsilon$	Comments
76	0,04	Aluminium; plastic Mylar ( $1,27 \times 10^{-5}$ m thick) and aluminium substrates; produced by vaporizing aluminium on both sides of Mylar. Measured in vacuum ( $1,3 \times 10^{-4}$ to $1,3 \times 10^{-5}$ Pa). Authors assumed $\alpha = \epsilon$ for 300 K blackbody incident radiation. Reported error 5%.
76	0,07	Aluminium; stainless steel substrate; Al sprayed on substrate. Measured in vacuum ( $1,3 \times 10^{-4}$ to $1,3 \times 10^{-5}$ Pa). Authors assumed $\alpha = \epsilon$ for 300 K blackbody incident radiation. Reported error 5%.
76	0,06	Aluminium; stainless steel substrate; Al sprayed on substrate; wire brushed. Measured in vacuum ( $1,3 \times 10^{-4}$ to $1,3 \times 10^{-5}$ Pa). Authors assumed $\alpha = \epsilon$ for 300 K blackbody incident radiation. Reported error 5%.
76	0,04	Aluminium plastic Mylar ( $1,27 \times 10^{-5}$ m thick) and aluminium substrate; Al vapor deposited on both sides of Mylar. Measured in vacuum ( $1,3 \times 10^{-4}$ Pa). Authors assumed $\alpha = \epsilon$ for 294 K blackbody radiation.

$T$ [K]	$\epsilon$	Comments
76	0,043	Similar to above specimen and conditions.
773-1273	0,69-0,78	Aluminium; iron substrate; substrate sandblasted and degreased; coated to a surface density of $75 \text{ kg.m}^{-2}$ with aluminium powder suspension; sintered at 1223 K in vacuum. Measured in vacuum ( $6,7 \times 10^{-4} \text{ Pa}$ ). Data extracted from smooth curve. Reported error 2,5%.
378-486	0,33-0,27	Aluminium ( $1,27 \times 10^{-4}$ to $2,03 \times 10^{-4} \text{ m}$ thick); Al substrate; sprayed. Measured in vacuum (0,13 Pa). Reported error 3%.
333	0,047	Aluminium; Mylar substrate. Measured in vacuum ( $6,7 \times 10^{-4} \text{ Pa}$ ). Reported error <3,5%.
300-415	0,06	Aluminium ( $10^{-6} \text{ m}$ thick); Mylar ( $1,2 \times 10^{-5} \text{ m}$ thick) and stainless steel ( $2,5 \times 10^{-4} \text{ m}$ thick) substrates; Mylar cemented to stainless steel; Al vapor deposited. Measured in vacuum ( $1,3 \times 10^{-5} \text{ Pa}$ ). Reported error 5%.
258-348	0,0428-0,0454	Aluminium ( $2 \times 10^{-7} \text{ m}$ thick); stainless steel substrate; Al vapor deposited on hand-polished substrate; property measured by steady-state calorimetric method. Mentioned below as specimen 1.
248-348	0,0293-0,0311	Same specimen and conditions as 1 except property measured by transient calorimetric method; property of second side of sample assumed.
303	0,024	Same specimen and conditions as 1 except property calculated from $\rho$ ( $10^\circ$ , $10^\circ$ ) measured by specular method relative to a front surface aluminized mirror.
300	0,0482	Same specimen and conditions as 1 except property calculated from $\rho$ ( $7,5^\circ$ , $2\pi$ ) measured by ellipsoid method.
200-400	0,0224-0,0237	Same specimen and conditions as 1 except property calculated from $\rho$ ( $2\pi-75^\circ$ , $15^\circ$ ). Specimen placed at the center of a heated cavity, so that the angle of viewing can be varied from $15^\circ$ to $75^\circ$ . (Millard & Streed (1969) [27]).
295	0,0279	Same specimen and conditions as 1 except property measured by a portable Quick Emittance Device.
295	0,041	Same specimen and conditions as 1 except property measured by a portable emissometer.
~298	0,0334	Polyester film ( $6,35 \times 10^{-6} \text{ m}$ thick) double aluminized. Coating thickness of emitting surface $t_{e1} = 4,55 \times 10^{-8} \text{ m}$ . Coating thickness of second surface $t_{e2} = 3,78 \times 10^{-8} \text{ m}$ .

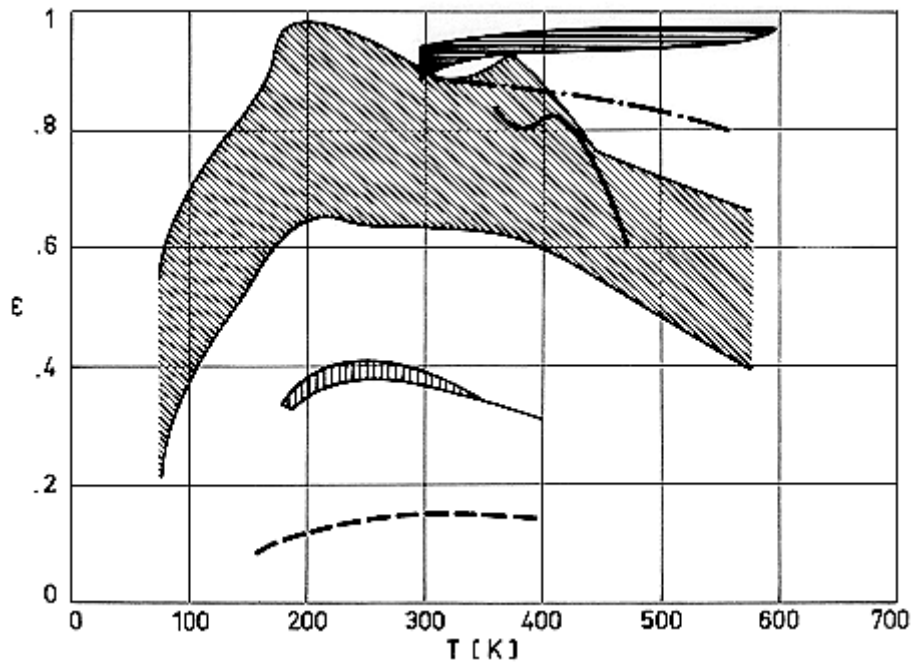


<i>T</i> [K]	$\epsilon$	Comments
~298	0,0335	Similar to above except opposite side measured.
~298	0,0335	Similar to above except $t_{c1} = 4,53 \times 10^{-8}$ m. $t_{c2} = 3,95 \times 10^{-8}$ m.
~298	0,0378	Similar to above except opposite side measured.
~298	0,0300	Similar to above except $t_{c1} = 4,5 \times 10^{-8}$ m. $t_{c2} = 3,95 \times 10^{-8}$ m.
~298	0,0331	Similar to above except opposite side measured.
~298	0,0369	Similar to above except $t_{c1} = 4,5 \times 10^{-8}$ m. $t_{c2} = 4 \times 10^{-8}$ m.
~298	0,0358	Similar to above except opposite side measured.
~298	0,0335	Similar to above except $t_{c1} = 4,56 \times 10^{-8}$ m. $t_{c2} = 3,95 \times 10^{-8}$ m.
~298	0,0243	Similar to above except opposite side measured.
307	0,0246	Aluminium; quartz substrate. Measured in vacuum ( $1,3 \times 10^{-4}$ Pa) maintained by diffusion pump.
307	0,0143	Polyester film ( $6,35 \times 10^{-6}$ m thick) single-aluminized; vacuum deposited. Measured in vacuum as above.
307	0,0543	Polyester film ( $6,35 \times 10^{-6}$ m thick) double-aluminized; vacuum deposited. Measured in vacuum as above.
307	0,0543	Similar to above except opposite side measured.
307	0,0613	Polyester film ( $6,35 \times 10^{-6}$ m thick) single-aluminized; vacuum deposited. Measured in vacuum as above.
307	0,0609	Similar to above specimen and conditions.
307	0,0450	Polyester film ( $6,35 \times 10^{-6}$ m thick) single-aluminized. $t_{c1} = 2,35 \times 10^{-8}$ m. Vacuum deposited. Measured in vacuum as above.
307	0,0532	Polyester film ( $6,35 \times 10^{-6}$ m thick) double-aluminized; vapor deposited. Measured in vacuum as above.
307	0,0773	Polyester film ( $6,35 \times 10^{-6}$ m thick) double-aluminized. $t_{c1} = 3,34 \times 10^{-8}$ m. $t_{c2} = 2,48 \times 10^{-8}$ m. Vapor deposited. Measured in vacuum as above.
307	0,0513	Polyester film ( $6,35 \times 10^{-6}$ m thick) double-aluminized. $t_{c1} = 2,48 \times 10^{-8}$ m. $t_{c2} = 3,34 \times 10^{-8}$ m. Vapor deposited. Measured in vacuum as above.
307	0,0466	Polyester film ( $6,35 \times 10^{-6}$ m thick) single-aluminized. Vacuum deposited. Measured in vacuum as above.

<i>T</i> [K]	$\epsilon$	Comments
307	0,0377	Aluminium Mylar and aluminium substrates; aluminium vacuum deposited on both sides of the Mylar. Measured in vacuum as above.
307	0,472	Aluminium; reinforced polyester film substrate (aluminized scrim). Measured in vacuum as above.
307	0,0248	Aluminium; quartz substrate. Measured in vacuum as above.
307	0,0176	Polyester film ( $6,35 \times 10^{-6}$ m thick) double-aluminized. Measured in vacuum as above.
307	0,041	Polyester film ( $6,35 \times 10^{-6}$ m thick) double-aluminized. Measured in vacuum as above.
307	0,0416	Polyester film ( $6,35 \times 10^{-6}$ m thick) double-aluminized; vapor deposited. Measured in vacuum as above.
307	0,0422	Similar to above specimen and conditions.
307	0,0398	Similar to above specimen and conditions.
307	0,0333	Polyester film ( $6,35 \times 10^{-6}$ m thick) double-aluminized. $t_{c1} = 4,55 \times 10^{-8}$ m. $t_{c2} = 3,78 \times 10^{-8}$ m. Vapor deposited. Measured in vacuum as above.
307	0,0334	Polyester film ( $6,35 \times 10^{-6}$ m thick) double-aluminized. $t_{c1} = 4,53 \times 10^{-8}$ m. $t_{c2} = 3,95 \times 10^{-8}$ m. Vapor deposited. Measured in vacuum as above.
307	0,0229	Polyester film ( $6,35 \times 10^{-6}$ m thick) double-aluminized. $t_{c1} = 4,5 \times 10^{-8}$ m. $t_{c2} = 3,8 \times 10^{-8}$ m. Vacuum deposited. Measured in vacuum as above.
307	0,0369	Polyester film ( $6,35 \times 10^{-6}$ m thick) double-aluminized. $t_{c1} = 4,5 \times 10^{-8}$ m. $t_{c2} = 4 \times 10^{-8}$ m. Vacuum deposited. Measured in vacuum as above.
307	0,0334	Polyester film ( $6,35 \times 10^{-6}$ m thick) double-aluminized. $t_{c1} = 4,56 \times 10^{-8}$ m. $t_{c2} = 3,95 \times 10^{-8}$ m. Vapor deposited. Measured in vacuum as above.
307	0,0335	Polyester film ( $6,35 \times 10^{-6}$ m thick) double-aluminized. $t_{c1} = 3,78 \times 10^{-8}$ m. $t_{c2} = 4,55 \times 10^{-8}$ m. Vapor deposited. Measured in vacuum as above.
307	0,0347	Polyester film ( $6,35 \times 10^{-6}$ m thick) double-aluminized. $t_{c1} = 3,95 \times 10^{-8}$ m. $t_{c2} = 4,53 \times 10^{-8}$ m. Vapor deposited. Measured in vacuum as above.
307	0,0381	Polyester film ( $6,35 \times 10^{-6}$ m thick) double-aluminized. $t_{c1} = 3,8 \times 10^{-8}$ m. $t_{c2} = 4,5 \times 10^{-8}$ m. Vacuum deposited. Measured in vacuum as above.
307	0,0224	Polyester film ( $6,35 \times 10^{-6}$ m thick) double-aluminized. $t_{c1} = 3,95 \times 10^{-8}$ m. $t_{c2} = 4,56 \times 10^{-8}$ m. Vapor deposited. Measured in vacuum as above.

$T$ [K]	$\epsilon$	Comments
307	0,0349	Polyester film ( $6,35 \times 10^{-6}$ m thick) double-aluminized; vapor deposited. Measured in vacuum as above.
307	0,0337	Similar to above specimen and conditions.
307	0,035	Similar to above specimen and conditions.
307	0,0835	Similar to above specimen and conditions.
307	0,0306	Similar to above specimen and conditions.
307	0,0284	Similar to above specimen and conditions.
307	0,0369	Similar to above specimen and conditions.
307	0,0369	Similar to above specimen and conditions.
307	0,0270	Similar to above specimen and conditions.
307	0,0289	Similar to above specimen and conditions.
307	0,0326	Polyester film ( $6,35 \times 10^{-6}$ m thick) single-aluminized; vacuum deposited. Measured in vacuum as above.
307	0,03	Similar to above specimen and conditions.
307	0,0337	Similar to above specimen and conditions.
307	0,0231	Polyester film single-aluminized. $t_{cl} = 2,18 \times 10^{-8}$ m. Measured in vacuum as above.
307	0,0722	Polyester film single-aluminized. $t_{cl} = 3 \times 10^{-9}$ m. Measured in vacuum as above.
307	0,0399	Polyester film single-aluminized. $t_{cl} = 1,08 \times 10^{-8}$ m. Measured in vacuum as above.
333	0,038	Polyester film single-aluminized. Measured in vacuum. ( $6,7 \times 10^{-4}$ Pa).
77	0,043	Aluminium household type foil wrapped loosely; cleaned with acetone. Measured in vacuum. ( $\sim 1,3 \times 10^{-3}$ Pa).

NOTE From Touloukian, DeWitt & HERNICZ (1972) [43].



Note: non-si units are used in this figure

**Figure 4-12: Summary of data concerning the hemispherical total emittance,  $\epsilon$ , of Aluminium conversion coatings vs. temperature,  $T$ . From Touloukian, DeWitt & HERNICZ (1972) [43].**

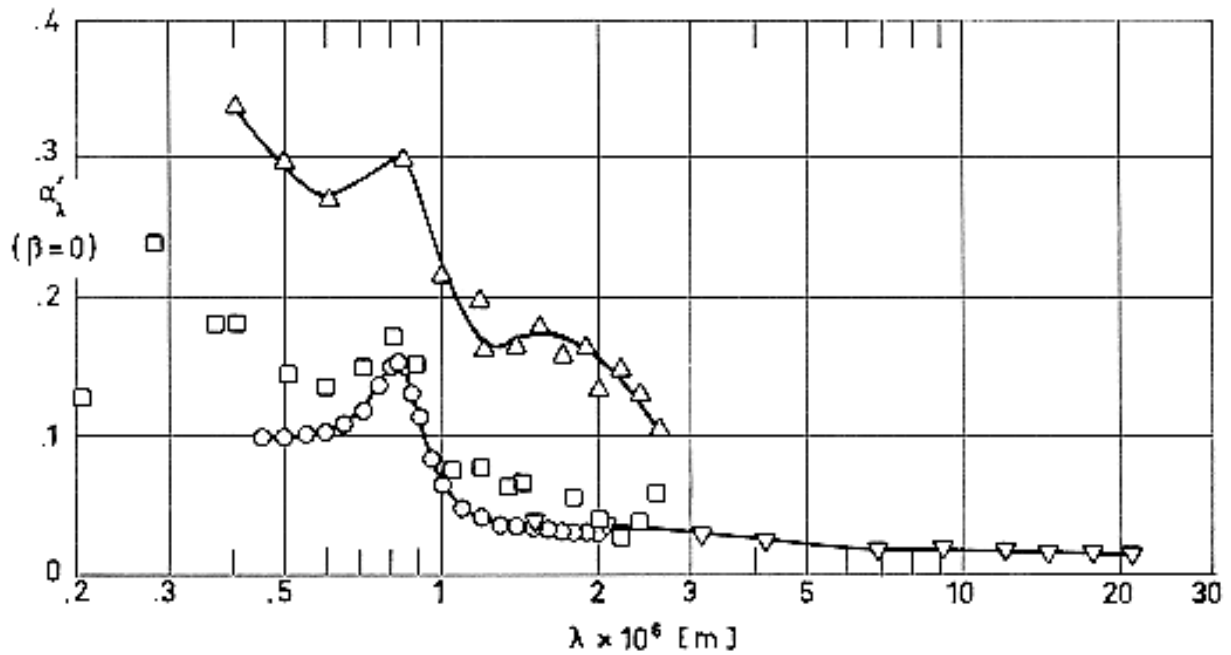
Explanation

Key	Description	Comments
	Anodized. Layer of carbon deposited into pores of the surface.	Measured in vacuum ( $1,33 \times 10^{-5}$ Pa).
	Al - 99,99, anodized in sulphuric acid. Polished substrate. Coating thickness: $2,54 \times 10^{-6}$ - $2,54 \times 10^{-5}$ m.	$\epsilon$ increases when coating thickness increases.
	Al - 99,99. Electropolished in fluoboric acid solution, then anodized in ammonium tartrate solution.	
	Anodized. Dull surface.	Measured in vacuum. Reported error $\pm 5\%$ .
	Vapor blasted after anodization.	Measured in vacuum. Reported error $\pm 5\%$ . Blasting decreases $\epsilon$ less than 6%.
	Al - 99,99. Substrate alkaline electropolished (sodium phosphate and sodium carbonate) 15 min at 353 K and 12 V DC, then anodized 15 min at 18 V DC in 10% sulphuric acid.	Measured in vacuum.

## 3.3.2. Absorptance

Data concerning absorptance have been arranged as indicated in the following Table.

<b>3.3.2.1. Directional spectral absorptance.</b>				
<b>Clause</b>	<b>Heading</b>	<b>Data Presented</b>	<b>Fig.</b>	<b>Table</b>
3.3.2.1.1.	Normal $\beta = 0$	Aluminium. A limited amount of information corresponding to $\beta = 25^\circ$ is also presented.	Figure 4-13	
<b>3.3.2.2. Directional total absorptance.</b>				
3.3.2.2.1.	Normal $\beta = 0$	Aluminium. A single value is included in the same Table as the hemispherical total absorptance.		Table 4-5
<b>3.3.2.4. Hemispherical total absorptance.</b>				
	$\omega = 2\pi$	Aluminium		Table 4-5
<b>3.3.2.5. Solar absorptance.</b>				
3.3.2.5.1.	Normal $\beta = 0$	Aluminium.		Table 4-6
		Aluminium contact coatings.		Table 4-2
		Aluminium conversion coatings.		Table 4-3, Table 4-7
3.3.2.5.2.	Angular (non- normal) $\beta \neq 0$	Aluminium conversion coatings.		Table 4-8
<b>3.3.2.6. Absorptance to emittance ratio.</b>				
		Aluminium conversion coatings. Degradation effects.	Figure 4-14	



Note: non-si units are used in this figure

**Figure 4-13: Directional spectral absorptance,  $\alpha_{\lambda}'$ , of Aluminium as a function of wavelength,  $\lambda$ . Data points  $\nabla$  correspond to  $\beta = 25^\circ$ .**

Explanation

Key	Description	Comments	References
○	Evaporated film; evaporation rate $3 \times 10^{-8} \text{ m.s}^{-1}$ at $2,66 \times 10^{-3} \text{ Pa}$ . Aged 8 d before measurement	$\beta \sim 10^\circ$ Sample temperature: $T = 298 \text{ K}$ . Measured in vacuum. Reported error $\pm 1,4\%$ .	Touloukian & DeWitt (1970) [42].
□		$T \sim 298 \text{ K}$ Data from smooth curve.	
△	Polished.		
▽	Foil.	$\beta = 25^\circ$ $T = 306 \text{ K}$ . Measured in dry nitrogen. Heated cavity at approximately $1056 \text{ K}$ with platinum reference. Authors assumed $\alpha = 1 - R$ .	

**Table 4-5: Hemispherical total Absorptance of Aluminium.**

$T$ [K]	$T_b^a$ [K]	$(\omega = 2\pi)$	Comments
2	298	0,0111	Normal total absorptance ( $\beta \sim 0$ ) of specimen electropolished. Reported error 1%.
76	300	0,018	Kaiser foil ( $2,54 \times 10^{-5}$ m thick), unannealed. Measured in vacuum ( $1,33 \times 10^{-4}$ to $1,33 \times 10^{-5}$ Pa). Reported error 5%.
76	300	0,018	Cockron home foil ( $3,81 \times 10^{-5}$ m thick). Same vacuum and error as above.
76	300	0,021	Hurwich home foil ( $3,81 \times 10^{-5}$ m thick). Same vacuum and error as above.
76	300	0,022	Same as above except measured on bright side.
76	300	0,028	Sheet ( $5,08 \times 10^{-4}$ m thick). Cold acid cleaned. Same vacuum and error as above.
76	300	0,026	Alcoa No. 2 reflector plate ( $5,08 \times 10^{-4}$ m thick). Same vacuum and error as above.
76	300	0,032	Same as above except sanded with fine emery.
76	300	0,035	Same as above except cleaned with alkali
76	300	0,045	Sheet ( $5,08 \times 10^{-4}$ m thick). Cleaned with wire brush, emery paper, steel wool and cold acid. Same vacuum and error as above.
76	300	0,060	Same as above except wire brush cleaned.
76	300	0,140	Same as above except liquid honed.
76	300	0,029	Same as above except hot acid cleaned (Alcoa process).
76	294	0,0204	Cockron foil ( $3,81 \times 10^{-5}$ m thick). Measured in vacuum ( $< 1,33 \times 10^{-4}$ Pa).
76	294	0,0200	Same as above.
76	294	0,0615	Sheet ( $5,08 \times 10^{-4}$ m thick). Cleaned with wire brush. Same vacuum as above.
76	294	0,0615	Same as above except cleaned with wire brush, emery paper, and steel wool.
76	294	0,0452	Same as above except cleaned with wire brush, emery paper, steel wool and cold acid.

$T$ [K]	$T_b^a$ [K]	$(\omega = 2\pi)$	Comments
76	294	0,0356	Same as above except alkali cleaned.
76	294	0,0327	Alcoa No. 2 reflector plate ( $5,08 \times 10^{-4}$ m thick, $\varepsilon = 0,3$ for visible light at 298 K). Same vacuum as above.
76	294	0,0317	Sheet ( $5,08 \times 10^{-4}$ m thick). Cold acid cleaned. Same vacuum as above.
76	294	0,0283	Same as above.
76	294	0,0217	Hurwich home foil ( $3,81 \times 10^{-5}$ m thick). Measured on bright side in vacuum ( $< 1,33 \times 10^{-4}$ Pa).
76	294	0,0212	Same as above except measured on mat side.
76	294	0,0204	Cockron home foil ( $3,81 \times 10^{-5}$ m thick). Same vacuum as above.
76	294	0,0186	Same as above.
76	294	0,0213	Kaiser foil ( $2,54 \times 10^{-5}$ m thick). Unannealed. Same vacuum as above.
76	294	0,0184	Same as above.
76	294	0,0186	Kaiser home foil ( $1,91 \times 10^{-4}$ m thick). Unannealed. Same vacuum as above.
76	294	0,0294	Foil ( $5,08 \times 10^{-5}$ m thick). Hot acid cleaned (Alcoa process). Same vacuum as above.

<sup>a</sup>  $T_b$  is the temperature of the emitting blackbody.

NOTE From Touloukian & DeWitt (1970) [42].



**Table 4-6: Normal Solar Absorptance of Aluminium**

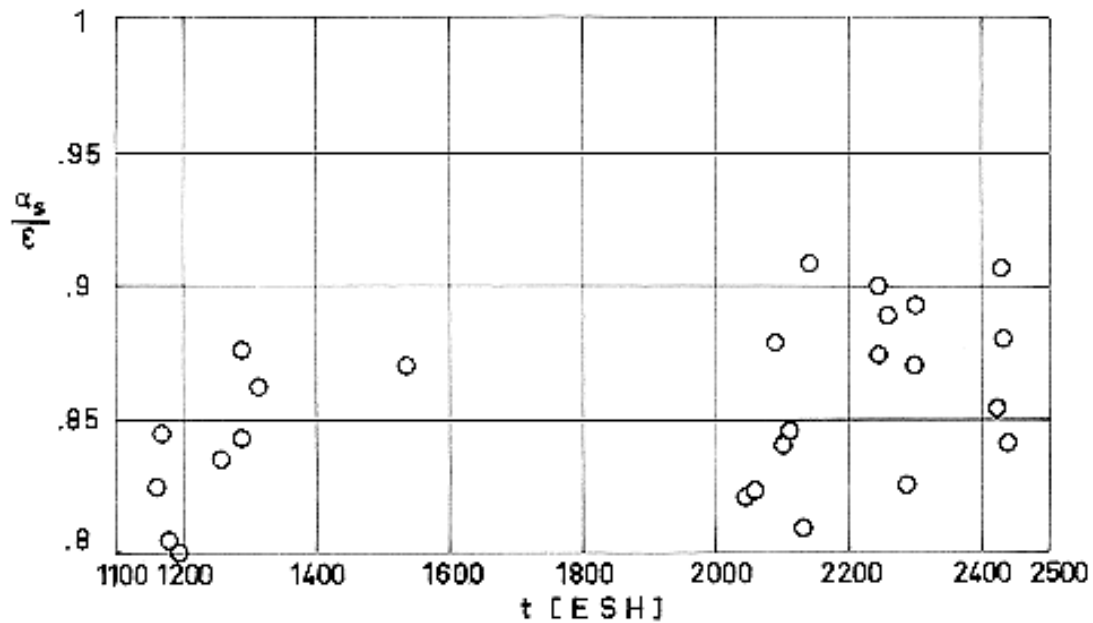
Alloy	T [K]	$\alpha_s$ ( $\beta = 0$ )	Comments	References
Al - 99,0		0,30	Polished	Zerlaut, Carrol & Gates (1966) [47].
Al - 99,0		0,48	Sandblasted	
Al -		0,42	Foil; vapor blasted, wet.	
Al - 99,99		0,08	Foil ( $1,27 \times 10^{-4}$ m thick) GMC Bright dip for 10 min at 350 K.	Bevans (1969) [14].
Al -		0,15	Bare metal.	Scollon & Carpitella (1970) [33].
Al - 99,99	298	0,096	Electropolished. Computed from spectral reflectance.	Touloukian & DeWitt (1970) [42].
Al - 99,99	298	0,104	Same as above except hydrogen ion bombarded ( $0,25 \times 10^{24}$ ions.m <sup>-2</sup> ).	
Al - 99,99	298	0,123	Same as above except hydrogen ion bombarded ( $0,84 \times 10^{24}$ ions.m <sup>-2</sup> ).	
Al - 99,99	298	0,133	Same as above except hydrogen ion bombarded ( $1,67 \times 10^{24}$ ions.m <sup>-2</sup> ).	
Al - 99,99	298	0,151	Same as above except hydrogen ion bombarded ( $3,20 \times 10^{24}$ ions.m <sup>-2</sup> ).	
Al - 99,99	298	0,170	Same as above except hydrogen ion bombarded ( $4,92 \times 10^{24}$ ions.m <sup>-2</sup> ).	
Al - 99,99	298	0,204	Same as above except hydrogen ion bombarded ( $7,45 \times 10^{24}$ ions.m <sup>-2</sup> ).	
Al - 99,99	298	0,236	Same as above except hydrogen ion bombarded ( $9,86 \times 10^{24}$ ions.m <sup>-2</sup> ).	

**Table 4-7: Normal Solar Absorptance of Aluminium Conversion Coatings.**

$T$ [K]	Basic Conditions	Variables Investigated	$\alpha_s$ ( $\beta = 0$ )
~ 298	Barrier-layer anodic coating on a high-purity aluminium substrate. Coating applied as follows: substrate thoroughly cleaned, electropolished in a fluoboric acid solution, anodized in aqueous ammonium tartrate solution diluted with ethyl alcohol, then immersed in a phosphoric acid solution. Measured in vacuum ( $1,33 \times 10^{-4}$ Pa). Computed from spectral reflectance data.	Anodizing voltage, Coating thickness 361 V, $4,7 \times 10^{-7}$ m 1089 V, $1,43 \times 10^{-6}$ m 1208 V, $1,58 \times 10^{-6}$ m 1360 V, $1,78 \times 10^{-6}$ m	0,129 0,122 0,142 0,129-0,136
~ 298	1199 aluminium anodized in sulphuric acid. Substrate polished in phosphoric/nitric acid bath for 2 min at 364 K. Computed from spectral reflectance data.	Anodizing time, Coating thickness 10 min, $8,36 \times 10^{-6}$ m 15 min, $9,38 \times 10^{-6}$ m 20 min, $10,96 \times 10^{-6}$ m 25 min, $13,21 \times 10^{-6}$ m	0,12 0,14 0,16 0,17
~ 298	Al - 99,99 anodized in sulphuric acid. Substrate polished by Alzak process. Computed from spectral reflectance data.	Anodizing time, Coating thickness Heat treatment 15 min, $9,38 \times 10^{-6}$ m Same as above except heat treated 96 h at 589 K in vacuum ( $6,65 \times 10^{-3}$ Pa). 25 min, $9,38 \times 10^{-6}$ m Same as above except heat treated 96 h at 589 K in vacuum ( $6,65 \times 10^{-3}$ Pa).	0,16 0,18 0,18 0,22
	Barrier anodized Al - 99,99 (~ $2,54 \times 10^{-4}$ m thick). Data from smooth curve. Absorptance computed from spectral reflectance measured in situ.	Simulated flight time of UV radiation exposure.  10 h 74,6 h 596 h	0,109 0,116 0,126
281	Alzak anodized aluminium ( $3,81 \times 10^{-6}$ m thick). Absorptance computed from normal spectral reflectance. Property measured in air.	Effect of electron exposure. Unexposed sample ( $T = 298$ K). 20 keV electrons ( $10^{14} - 5 \times 10^{15}$ e.m <sup>-2</sup> .s <sup>-1</sup> ; $3 \times 10^{18}$ e.m <sup>-2</sup> , in dark in vacuum ( $1,33 \times 10^{-6}$ Pa), maintained by ion pump. $10^{19}$ e.m <sup>-2</sup> $10^{20}$ e.m <sup>-2</sup>	0,13 0,14 0,14 0,16

T [K]	Basic Conditions	Variables Investigated	$\alpha_s$ ( $\beta = 0$ )
		Unexposed sample ( $T = 298$ K). 80 keV electrons ( $10^{14}$ – $5 \times 10^{15}$ e.m <sup>-2</sup> .s <sup>-1</sup> ; $10^{19}$ e.m <sup>-2</sup> , in dark in vacuum ( $1,33 \times 10^{-6}$ Pa), maintained by ion pump. $10^{20}$ e.m <sup>-2</sup>	0,14 0,15 0,16
77	Barrier anodized Al - 99,99 ( $2,54 \times 10^{-4}$ m thick). Exposed to vacuum ( $6,65 \times 10^{-7}$ – $2,66 \times 10^{-5}$ Pa), maintained with diffusion pump. Absorptance computed from $R(2\pi, 0^\circ)$ . Property measured in situ.	Effect of UV radiation and electron exposure. Unexposed sample. 6 sun intensity UV radiation; 350 ESH Electron radiation ( $8,6 \times 10^{14}$ – $1,6 \times 10^{16}$ e.m <sup>-2</sup> .s <sup>-1</sup> ); $5,8 \times 10^{19}$ e.m <sup>-2</sup> . Simultaneous exposure: Electron radiation ( $3,5 \times 10^{14}$ e.m <sup>-2</sup> .s <sup>-1</sup> ); $5,8 \times 10^{19}$ e.m <sup>-2</sup> . 8 sun intensity UV radiation; 350 ESH	0,17 0,16 0,20
77	Al - 99,99; sluphuric acid-anodized. Exposed to vacuum ( $6,65 \times 10^{-7}$ – $2,66 \times 10^{-5}$ Pa), maintained with diffusion pump. Absorptance computed from $R(2\pi, 0^\circ)$ . Property measured in situ.	Effect of UV radiation and electron. Unexposed sample. 6 sun intensity UV radiation; 350 ESH Electron radiation ( $8,6 \times 10^{14}$ – $1,6 \times 10^{16}$ e.m <sup>-2</sup> .s <sup>-1</sup> ); $5,8 \times 10^{19}$ e.m <sup>-2</sup> . Simultaneous exposure: Electron radiation ( $3,5 \times 10^{14}$ e.m <sup>-2</sup> .s <sup>-1</sup> ); $5,8 \times 10^{19}$ e.m <sup>-2</sup> . 8 sun intensity UV radiation; 350 ESH	0,20 0,28 0,20 0,27

NOTE From Touloukian, DeWitt & HERNICZ (1972) [43].



Note: non-si units are used in this figure

**Figure 4-14: Absorptance to emittance ratio,  $\alpha_s/\epsilon$ , of Aluminium conversion coatings as a function of the exposure time,  $t$ .**

Explanation

Key	Description	Comments	References
○	Alodine Aluminium.	Deduced from in-flight data concerning the temperature of substrate on board Pegasus II. Initial value $\alpha_s/\epsilon = 0,85$ , estimated from Fig. 82 of Schafer & Bannister which leads with Pegasus I flight data.	Schafer & Bannister (1967) [32]. Touloukian, DeWitt, Hernicz (1972) [43].

**Table 4-8: Angular Solar absorptance of Aluminium**

$\beta^\circ$	15	30	45	60
$\alpha_s$	0,190	0,208	0,243	0,254

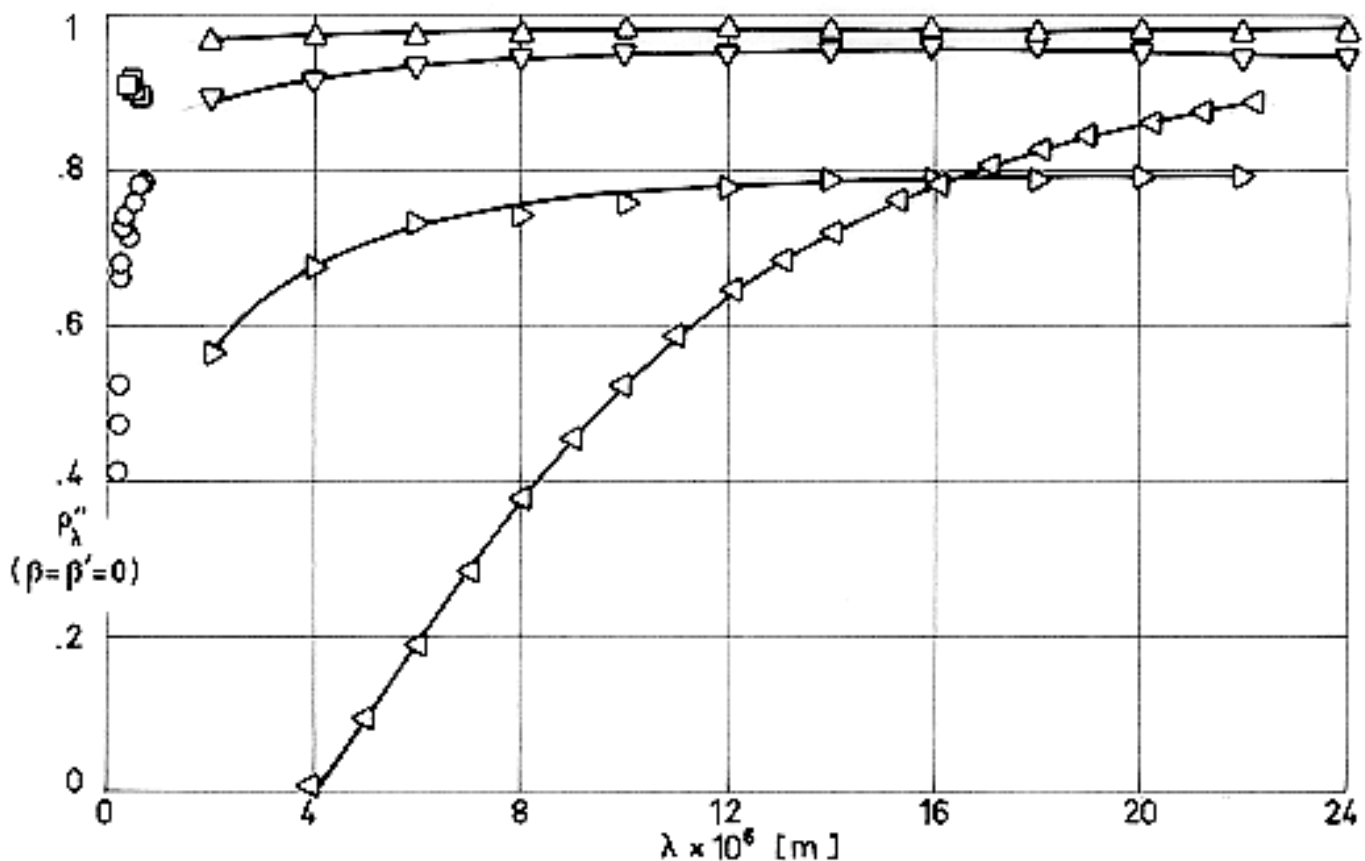
Al - 99,99. Foil ( $5,1 \times 10^{-5}$  m thick) bright dipped, anodized on both sides ( $7,6 \times 10^{-6}$  m thick) in dilute sulphuric acid. Computed from spectral reflectance data for above atm. conditions.

## 3.3.3. Reflectance

Data concerning reflectance have been arranged as indicated in the following Table.

<b>3.3.3.1. Bidirectional spectral reflectance.</b>				
<b>Clause</b>	<b>Heading</b>	<b>Data Presented</b>	<b>Fig.</b>	<b>Table</b>
3.3.3.1.1.	Normal-normal $\beta=\beta'=0$	Aluminium.	Figure 4-15	
		Aluminium contact coatings.	Figure 4-16	
		Aluminium conversion coatings. Effect of thickness.	Figure 4-17	
3.3.3.1.2.	Angular (non-normal) $\beta=\beta'\neq 0$	Aluminium contact coatings. ( $\beta\sim 18^\circ$ )	Figure 4-18	
		Aluminium conversion coatings. (any $\beta$ , given $\lambda$ )	Figure 4-19	
<b>3.3.3.2. Directional-hemispherical spectral reflectance.</b>				
3.3.3.2.1.	Normal-hemispherical $\beta=0 \omega'=2\pi$	Aluminium	Figure 4-20	
		Aluminium conversion coatings. Effect of thickness.	Figure 4-21	
		Aluminium conversion coatings. UV exposure effect.	Figure 4-22	
		Aluminium conversion coatings. Electron exposure effect.	Figure 4-23	
		Aluminium conversion coatings. Simultaneous UV-electron exposure effect.	Figure 4-24	
		Aluminium conversion coatings. Proton exposure effect.	Figure 4-25	
3.3.3.2.2.	Angular-hemispherical $\beta\neq 0 \omega'=2\pi$	Aluminium conversion coatings.	Figure 4-26	

<b>3.3.3.3. Hemispherical-directional spectral reflectance.</b>				
3.3.3.3.1.	Angular-hemispherical $\omega=2\pi \beta'=0$	Aluminium contact coatings.	Figure 4-27	
<b>3.3.3.5. Bidirectional total reflectance.</b>				
3.3.3.5.2.	Angular (non-normal)	Aluminium.	Figure 4-28	
<b>3.3.3.8. Bidirectional solar reflectance.</b>				
3.3.3.8.1.	Normal-normal $\beta=\beta'=0$	Aluminium conversion coatings.		Table 4-9
<b>3.3.3.9. Directional-hemispherical solar reflectance.</b>				
3.3.3.9.1.	Normal-hemispherical $\beta=0 \omega'=2\pi$	Aluminium, both bulk and contact coatings.		Table 4-10

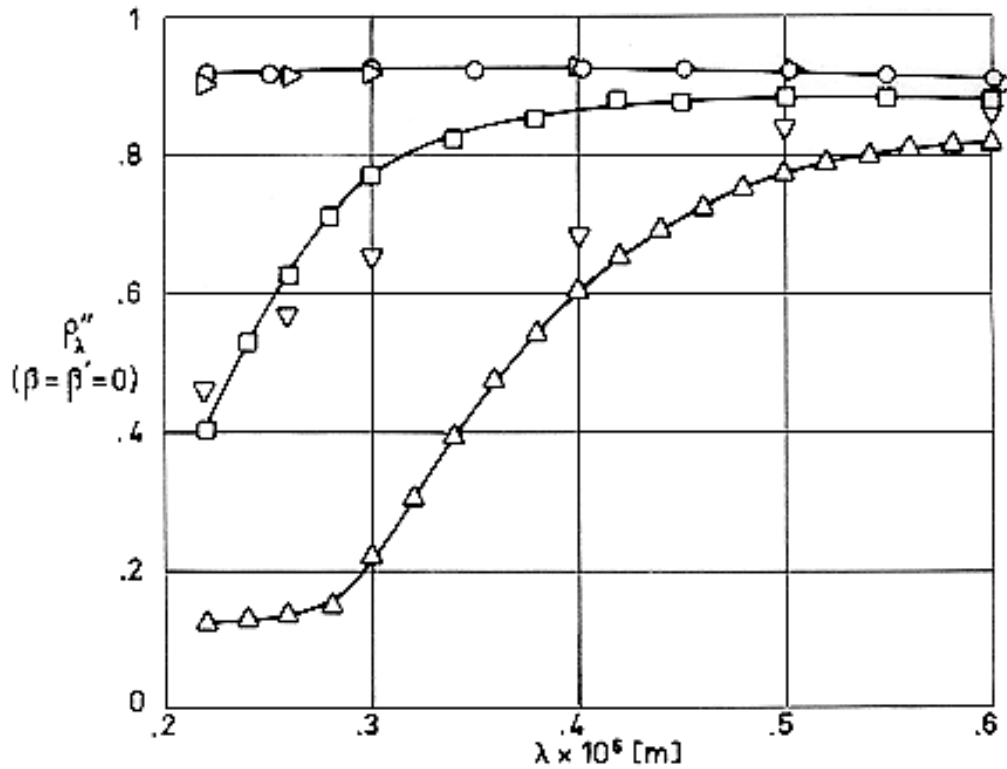


Note: non-si units are used in this figure

**Figure 4-15: Normal - normal spectral reflectance,  $\rho_{\lambda}''$ , of Aluminium as a function of wavelength,  $\lambda$ .**

## Explanation

Key	Description	Comments	References
○	Disc. Cold worked, annealed, etch tested, polished, stored in a solution of NaOH+NaF, washed and dried.	Sample temperature: $T = 298$ K. Reported error 2%.	Touloukian & DeWitt (1970) [42].
□		$\beta = \beta' = 7^\circ$ $T = 298$ K. Measured in air. Reported error <0,16%	
△	Polished.	$T = 298$ K.	
▽	Same as △. Cratered. Avg. crater diameter: $1,23 \times 10^{-4}$ m. Depth: $2,89 \times 10^{-4}$ m.		
▷	Same as △. Cratered. Avg. crater diameter: $5,4 \times 10^{-5}$ m. Depth: $1,83 \times 10^{-4}$ m.		
◁	Aluminized dense flint. Flint ground with M 303,5 grinding powder with average particle size of $1,1 \times 10^{-5}$ m.	$\beta = \beta' \sim 5^\circ$ $T = 298$ K. Al mirror reference, $\omega' = 0,03$ sr.	



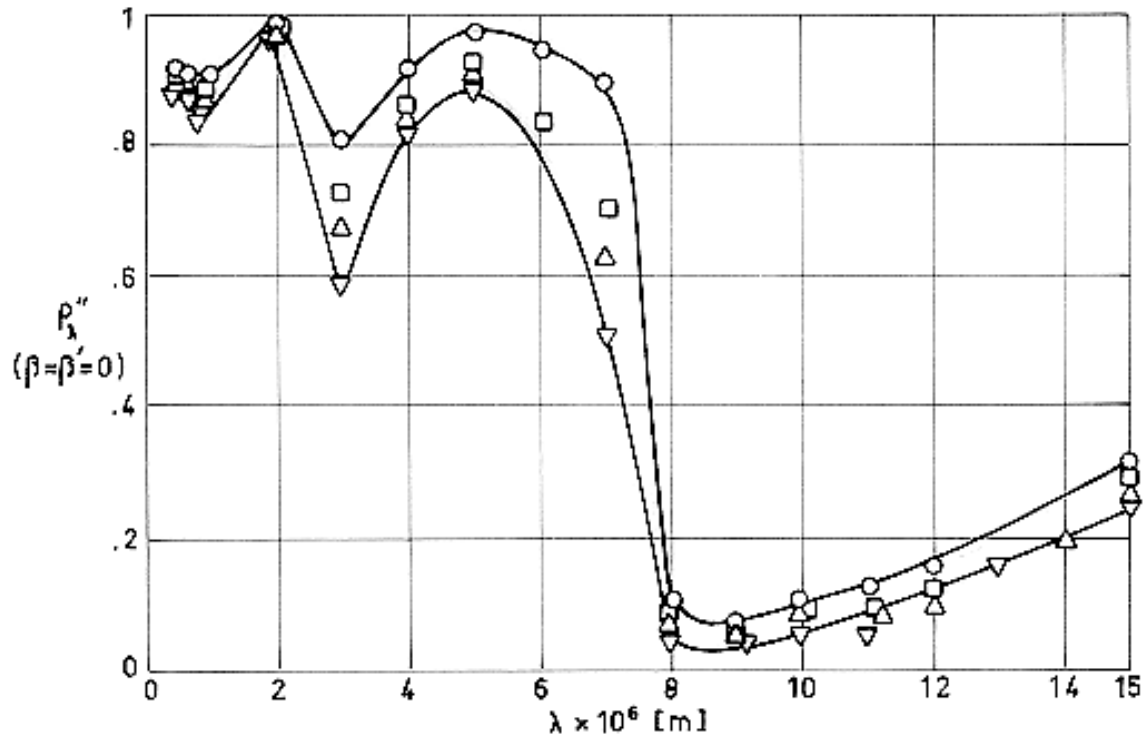
Note: non-si units are used in this figure

Figure 4-16: Normal - normal spectral reflectance,  $\rho_{\lambda}''$ , of Aluminium contact coatings as a function of wavelength,  $\lambda$ .

Explanation

Key	Description	Comments	References
○	Al - 99,99 ( $6 \times 10^{-8}$ – $7 \times 10^{-8}$ m thick). Glass substrate. Deposited in vacuum ( $1,33 \times 10^{-3}$ – $2,66 \times 10^{-3}$ Pa) for $t_d = 7$ s.	Sample temperature: $T = 298$ K. Data from smooth curve. Reported error 3%. $t_d$ is the deposition time.	Touloukian, DeWitt & Hernicz (1972) [43].
□	Same as ○ except $t_d = 180$ s.		
△	Same as ○ except $t_d = 145$ s.		
▽	Al - 99,99 ( $\sim 7 \times 10^{-8}$ m thick). Glass substrate. Deposited in vacuum ( $1,33 \times 10^{-3}$ – $2,66 \times 10^{-3}$ Pa) at $10^{-9}$ – $1,5 \times 10^{-9}$ $\text{m.s}^{-1}$ with substrate temperature 473 K.		
▷	Al - 99,99 ( $\sim 6 \times 10^{-8}$ m thick). Glass substrate. Deposited in vacuum ( $1,33 \times 10^{-3}$ Pa) at $3 \times 10^{-8}$ $\text{m.s}^{-1}$ with $60^\circ$ angle of vapor incidence.		





Note: non-si units are used in this figure

**Figure 4-17: Effect of coating thickness on normal - normal spectral reflectance,  $\rho_{\lambda}''$ , of Aluminium conversion coatings as a function of wavelength,  $\lambda$ .**

Explanation

Key	Description	Comments	References
$\circ$	Al - 99,99, anodized in sulphuric acid. Polished substrate. Coating thickness, $t_c = 8,4 \times 10^{-6}$ m.	$T \sim 298$ K.	Touloukian, DeWitt & Hernicz (1972) [43].
$\square$	Same as $\circ$ except $t_c = 9,4 \times 10^{-6}$ m.		
$\triangle$	Same as $\circ$ except $t_c = 11,4 \times 10^{-6}$ m.		
$\nabla$	Same as $\circ$ except $t_c = 13,2 \times 10^{-6}$ m.		

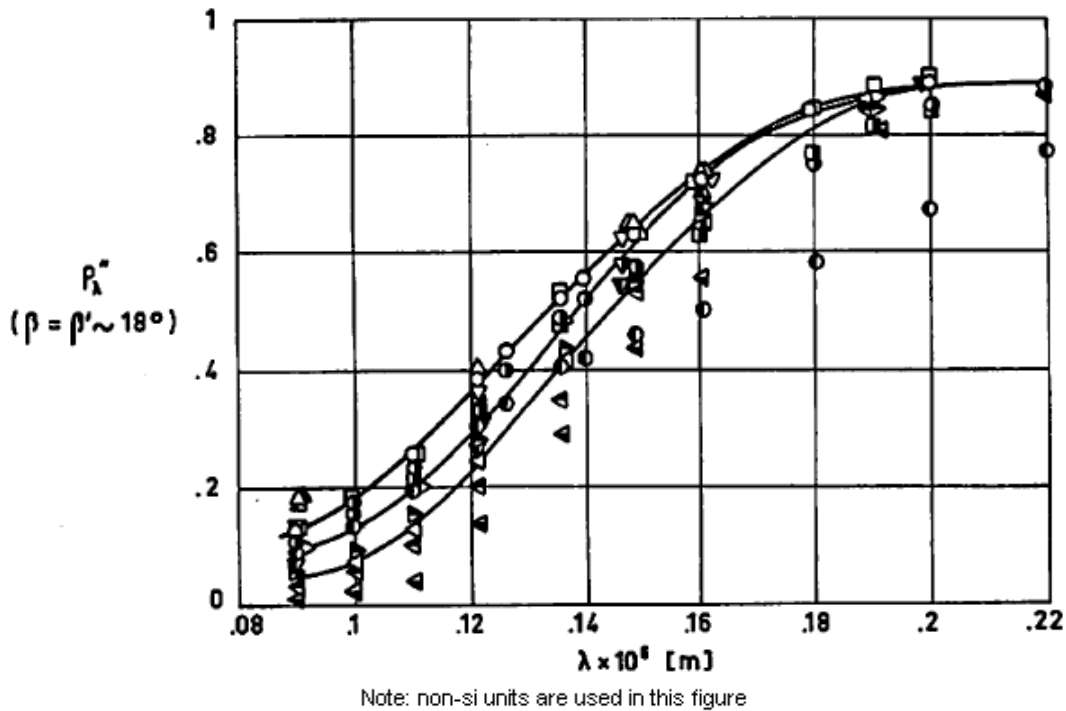
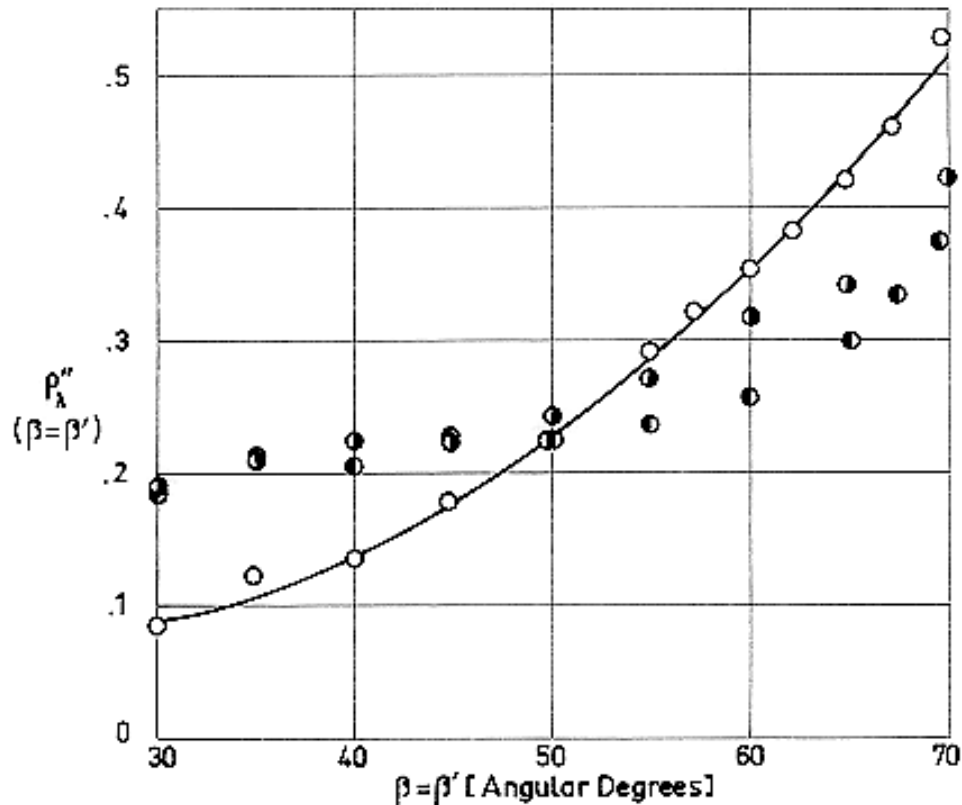


Figure 4-18: Bidirectional reflectance,  $\rho_{\lambda}''$ , of Aluminium contact coatings as a function of wavelength,  $\lambda$ .

Explanation

Key	Description	Comments	References
○	Evaporated film ( $8 \times 10^{-8}$ m thick). Substrate cleaned by a high-voltage DC glow discharge. Evaporated at $1,33 \times 10^{-3}$ Pa for 2 s. Exposed to air for 24 h.	Sample temperature: $T \sim 298$ K.	Touloukian, DeWitt & Hernicz (1972) [43].
●	Same as ○ except evaporation time 55 s.		
◐	Same as ○ except evaporation time 130 s.		
□	Evaporated film ( $9 \times 10^{-8}$ m thick). Substrate cleaned as ○. Evaporated at $1,33 \times 10^{-3}$ Pa for 2 s using Al - 99.99. Film 24 h old when measurement was made.		
◼	Same as □. Al - 99,5 used for evaporation.		
△	Evaporated film ( $8 \times 10^{-8}$ m thick). Substrate cleaned as ○. Substrate temperature at deposition 308 K. Film 2-3 h old.	$T \sim 298$ K.	

Key	Description	Comments	References
▲	Same as Δ except substrate at 323 K at time of deposition		
▲	Same as Δ except substrate at 373 K at time of deposition		
▽	Evaporated film. Substrate cleaned as ○ . Aged 10 h before measurement.	<i>T</i> ~ 298 K. Data from smooth curve.	
▽	Same as ▽ except aged 100 h.		
▽	Same as ▽ except aged 1000 h.		
▷	Evaporated film. Substrate cleaned as ○ . Stored in dry air for 63 d before measurement.		
▷	Same as ▷ except stored in normal air (30-50% humidity) for 63 d before measurement.		
◁	Evaporated film. Substrate cleaned as ○ ; prepared under optimum conditions. Placed 0,2 m from a 435-W quartz mercury burner and irradiated for 20 h in dry air.		
◁	Same as ◁ except irradiated for 20 h in normal air (30% humidity).		
◁	Same as ◁ except irradiated for 20 h in moist air (>90% humidity).		



Note: non-si units are used in this figure

**Figure 4-19: Bidirectional spectral reflectance,  $\rho_{\lambda}''$ , of Aluminium conversion coatings as a function of zenith angles,  $\beta$  and  $\beta'$ , of incident and reflected radiations.**

Explanation

Key	Description	Comments	References
○	Aluminium evaporated on Pyrex glass substrate at about $4 \times 10^{-8} \text{ m.s}^{-1}$ at pressures $1,33 \times 10^{-3}$ – $2,66 \times 10^{-3}$ Pa. Coating thickness $3 \times 10^{-7} \text{ m}$ . Anodized in a bath of freshly prepared 3% ammonium tartrate solution with a pure Al cathode. Rinsed in distilled water and dried.	$T = 298 \text{ K}$ . $\lambda = 5,07 \times 10^{-8} \text{ m}$ .	Touloukian, DeWitt & Hernicz (1972) [43].
●	Same as above.	$T = 298 \text{ K}$ . $\lambda = 7,62 \times 10^{-8} \text{ m}$ .	
●	Same as above.	$T = 298 \text{ K}$ . $\lambda = 1,032 \times 10^{-7} \text{ m}$ .	

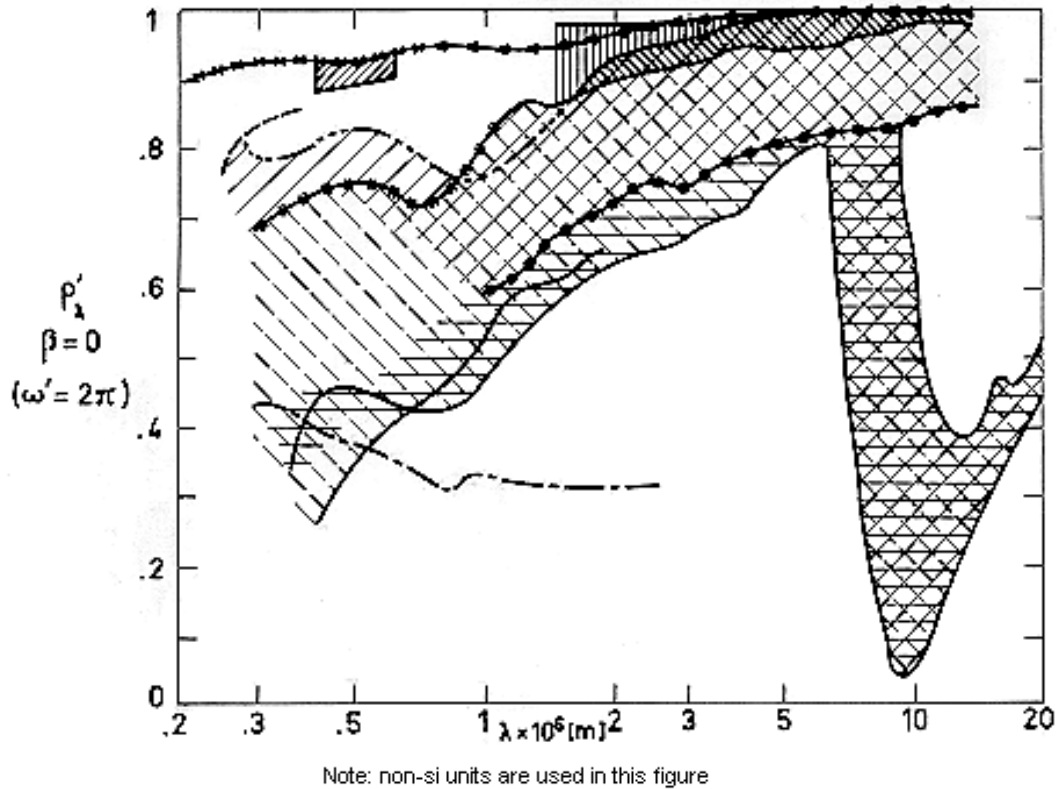
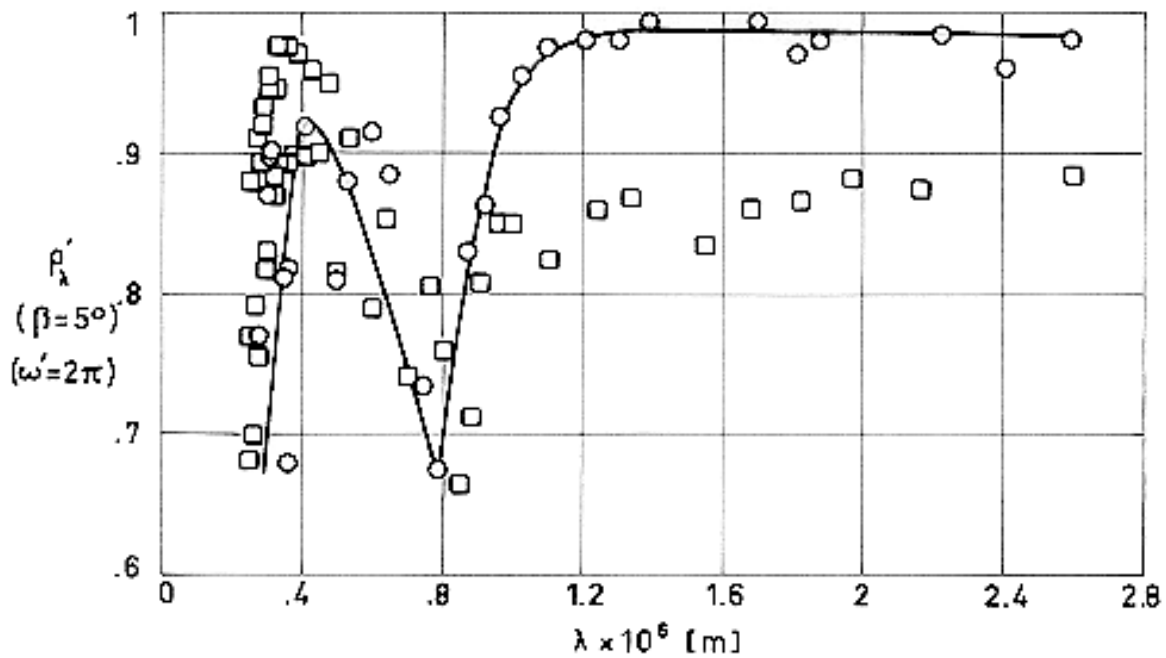


Figure 4-20: Summary of data concerning normal - hemispherical spectral reflectance,  $\rho_{\lambda}'$ , of Aluminium vs. wavelength,  $\lambda$ . From Touloukian & DeWitt (1970) [42].

Explanation

Key	Description	Comments
	Al - 99.0. Vacuum deposited on glass. Freshly prepared.	$\beta = 10^\circ$ . $T = 298 \text{ K}$ .
	Foil.	
	Mechanically polished, electro polished.	$T = 298 \text{ K}$ .
	Mill finished, electro polished.	Measured in vacuum ( $1,33 \times 10^{-4} \text{ Pa}$ ).
	Mechanically polished only.	
	Polished.	$T = 298 \text{ K}$ .
	Evaporated on Mylar ( $2 \times 10^{-7} \text{ m}$ thick).	$T = 298 \text{ K}$ .
	Film vacuum deposited on glass.	$\beta = 7^\circ$ . $T = 298 \text{ K}$ .

Key	Description	Comments
----	Acid etched.	$\beta \sim 5^\circ$ . $T = 298$ K.
*****	Sandblasted.	$T = 298$ K.
●●●●●	Polished, roughened (roughness $\sim 1,27 \times 10^{-8}$ m).	$\beta = 5^\circ$ . $T = 300$ K.
-----	Foil. Diffuse reflectance.	$T = 298$ K.

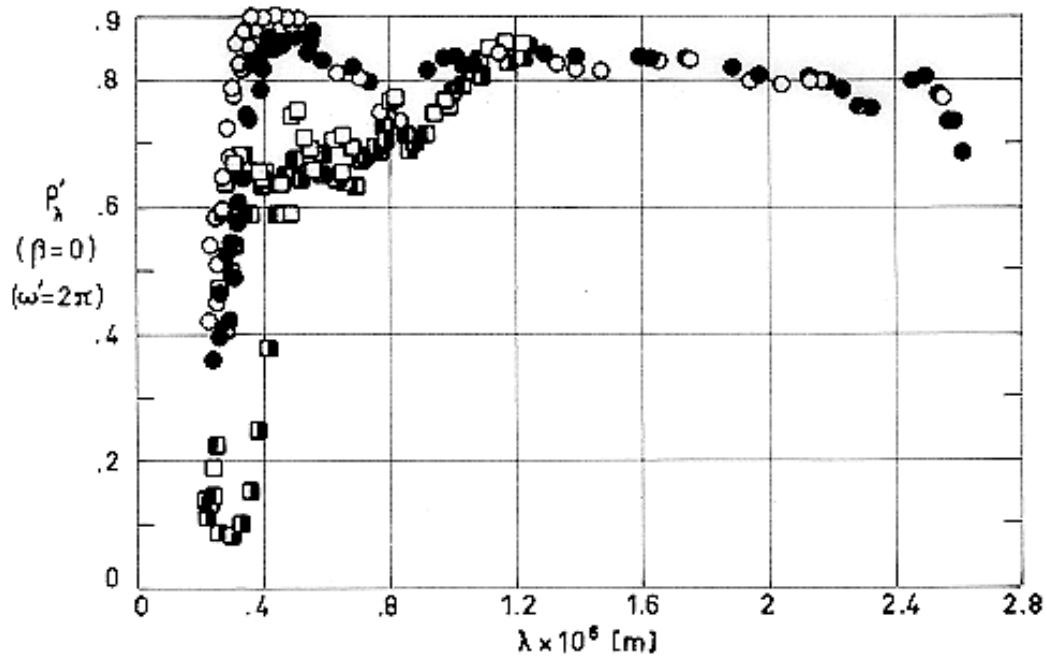


Note: non-si units are used in this figure

Figure 4-21: Normal - hemispherical spectral reflectance,  $\rho'_\lambda$ , of Aluminium conversion coatings as a function of wavelength,  $\lambda$ .

Explanation

Key	Description	Comments	References
○	Barrier-layer anodic coated Al - 99,99. Coating thickness $3,9 \pm 0,015$ $10^{-7}$ m.	$T \sim 298$ K. Measured in vacuum ( $1,33 \times 10^{-4}$ Pa). Data from smooth curve.	Touloukian, DeWitt & HERNICZ (1972) [43].
□	Same as ○ except coating thickness $1,6 \times 10^{-6}$ – $1,7 \times 10^{-6}$ m.	Same as ○ except measured relative to MgO.	

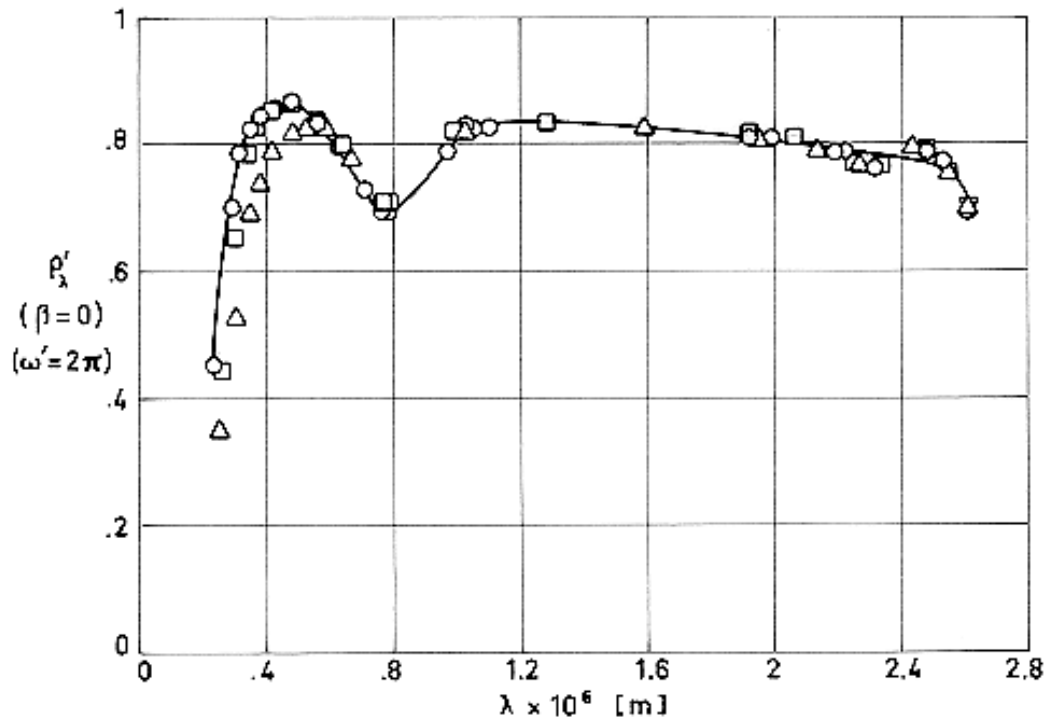


Note: non-si units are used in this figure

Figure 4-22: Effect of UV exposure on normal - hemispherical spectral reflectance,  $\rho'_{\lambda}$ , of Aluminium conversion coatings as a function of wavelength,  $\lambda$ .

Explanation

Key	Description	Comments	References
○	Al - 99,99 (2,54x10 <sup>-4</sup> m thick), barrier anodized.	T = 77 K. Exposed to vacuum (6,65x10 <sup>-7</sup> -2,66x10 <sup>-5</sup> Pa). from R(2π,0) measured in situ. Data from smooth curve.	Touloukian, DeWitt & HERNICZ (1972) [43].
●	Same as ○.	Same as ○. 350 ESH exposure at 6 sun, in vacuum.	
□	Alodine 401-45. Reaction of Aluminium surface with aqueous solution of chromic, phosphoric, and hydrofluoric acid.	T = 300 K. Data from smooth curve.	
▣	Similar to □.	T = 300 K. 353 h exposure at 3-4 suns. Substrate temperature during exposure: T <sub>s</sub> = 278 K.	
▤	Similar to □.	Same as ▣ except 358 h exposure. T <sub>s</sub> = 248 K.	



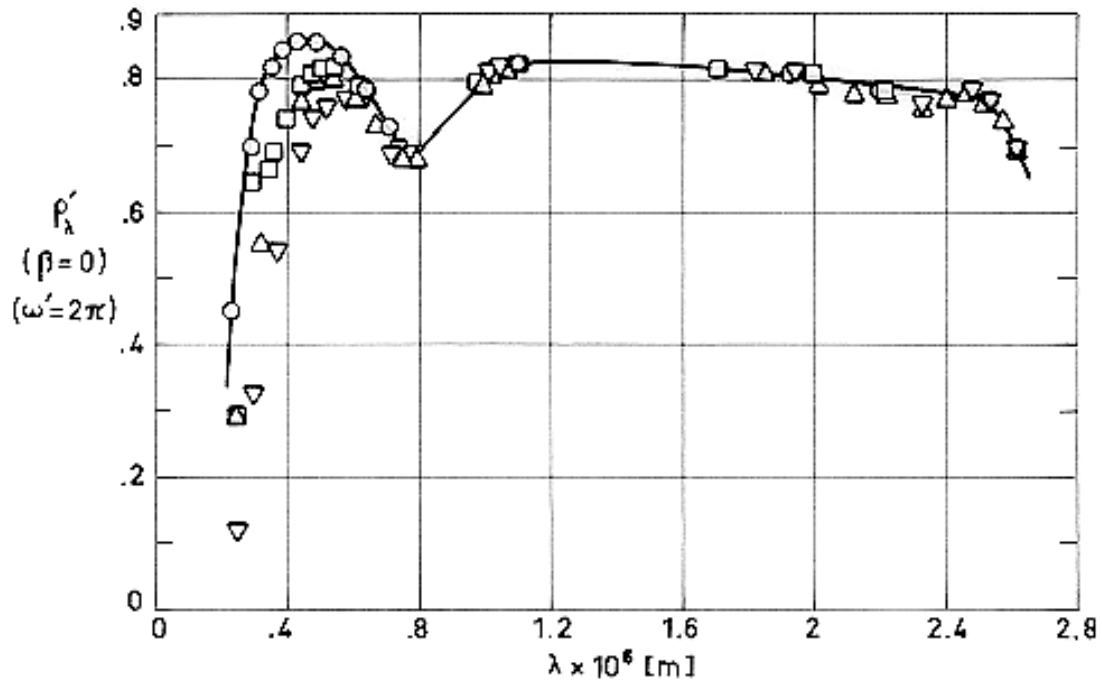
Note: non-si units are used in this figure

**Figure 4-23: Effect of electron exposure on normal - hemispherical spectral reflectance of Aluminium conversion coatings as a function of wavelength,  $\lambda$ .**

Explanation

Key	Description	Comments	References
○	Al - 99,99 anodized in sulphuric acid.	$T = 77$ K. Exposed to vacuum ( $6,65 \times 10^{-7}$ – $2,66 \times 10^{-5}$ Pa), maintained by diffusion pump. Calculated from $R(2\pi,0)$ measured in situ. Data from smooth curve.	Touloukian, DeWitt & HERNICZ (1972) [43].
□		Same as ○ except exposed to electron radiation ( $8,6 \times 10^{14}$ – $1,6 \times 10^{16}$ e.m <sup>-2</sup> .s <sup>-1</sup> ) in vacuum $5,8 \times 10^{19}$ e.m <sup>-2</sup> .	
△		Same as □ except total dose $1,2 \times 10^{20}$ e.m <sup>-2</sup> .	



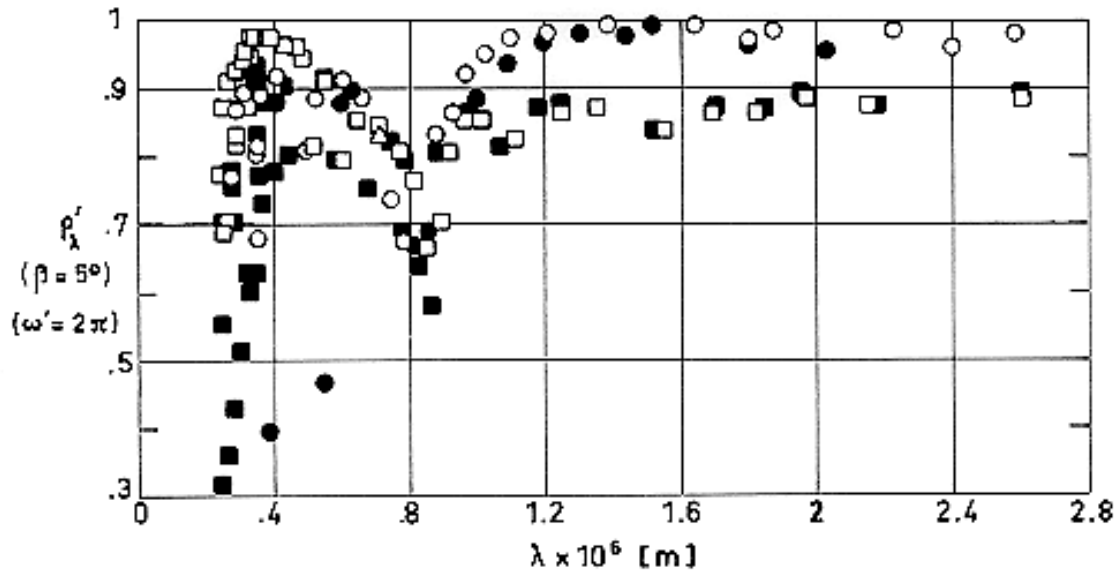


Note: non-si units are used in this figure

**Figure 4-24: Effect of simultaneous UV - electron exposure on normal - hemispherical spectral reflectance,  $\rho'_\lambda$ , of Aluminium conversion coatings as a function of wavelength,  $\lambda$ .**

Explanation

Key	Description	Comments	References
○	Al - 99,99 anodized in sulphuric acid.	$T = 77$ K. Exposed to vacuum ( $6,65 \times 10^{-7}$ – $2,66 \times 10^{-5}$ Pa), maintained by diffusion pump. Calculated from $R(2\pi, 0)$ measured in situ. Data from smooth curve.	Touloukian, DeWitt & HERNICZ (1972) [43].
□		Same as ○ except: UV 8 sun intensity in vacuum 66 ESH electron $3,5 \times 10^{14}$ e.m <sup>-2</sup> .s <sup>-1</sup> ; $1,2 \times 10^{19}$ e.m <sup>-2</sup> .	
△		Same as ○ except total dose: UV 130 ESH electron $2,3 \times 10^{19}$ e.m <sup>-2</sup> .	
▽		Same as ○ except total dose: UV 310 ESH electron $5,8 \times 10^{19}$ e.m <sup>-2</sup> .	

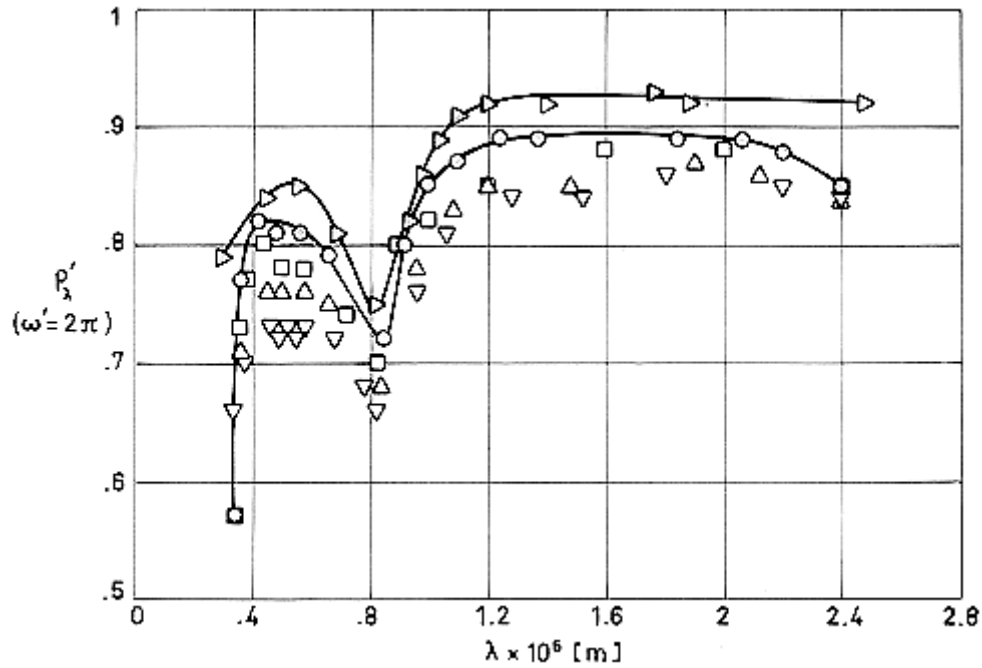


Note: non-si units are used in this figure

Figure 4-25: Effect of proton exposure on normal - hemispherical spectral reflectance,  $\rho'_\lambda$ , of Aluminium conversion coatings as a function of wavelength,  $\lambda$ .

Explanation

Key	Description	Comments	References
○	Al - 99,99, barrier-layer anodic coated. Coating thickness (3,9± 0,015)×10 <sup>-7</sup> m.	T ~ 298 K. Measured in vacuum (1,33×10 <sup>-4</sup> Pa). Data from smooth curve.	Touloukian, DeWitt & HERNICZ (1972) [43].
●		Same as ○ except irradiated in vacuum at 300 K with 8,7 keV protons to a total dose of 9,25×10 <sup>20</sup> p.m <sup>-2</sup> .	
□	Same as ○ except coating thickness 1,6×10 <sup>-6</sup> –1,7×10 <sup>-6</sup> m.	Same as ○. Measured relative to MgO.	
■		Same as □ except irradiated in vacuum at 300 K with 8,7 keV protons to a total dose of 10 <sup>20</sup> p.m <sup>-2</sup> .	

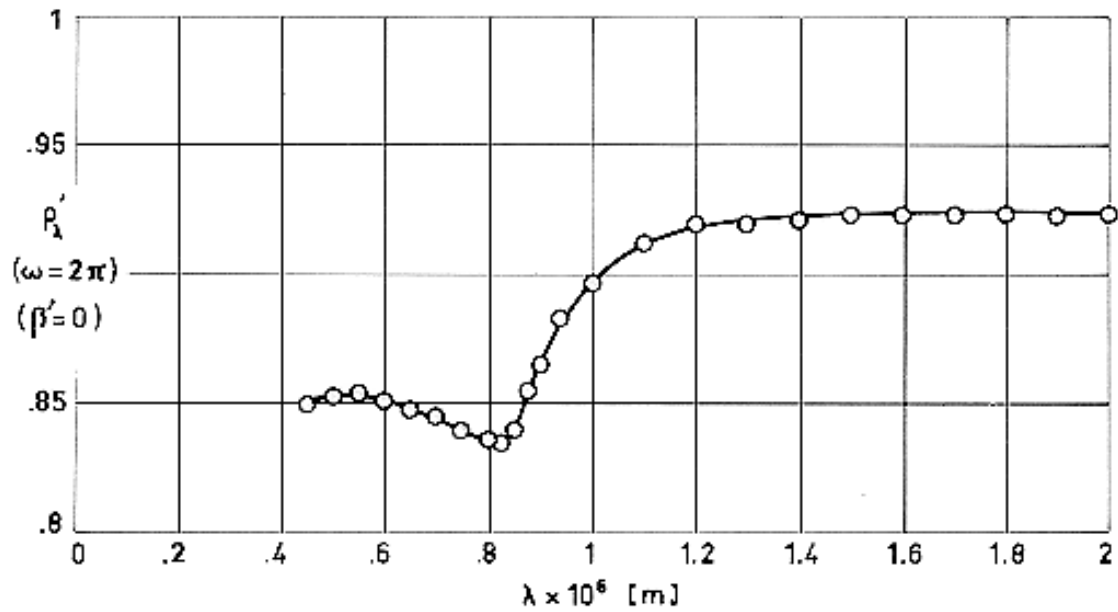


Note: non-si units are used in this figure

**Figure 4-26: Directional - hemispherical spectral reflectance,  $\rho_{\lambda}'$ , of Aluminium conversion coatings as a function of wavelength,  $\lambda$ .**

Explanation

Key	Description	Comments	References
○	Al - 99.99. Foil $5,1 \times 10^{-5}$ m thick. Bright dipped and anodized on both sides ( $7,6 \times 10^{-6}$ m thick) in dilute sulphuric acid.	$\beta = 15^\circ$ . $T = 298$ K.	Touloukian, DeWitt & Hemicz (1972) [43].
□		$\beta = 30^\circ$ . $T = 298$ K.	
△		$\beta = 45^\circ$ . $T = 298$ K.	
▽		$\beta = 60^\circ$ . $T = 298$ K.	
▷		$\beta = 15^\circ$ . $T = 298$ K.	

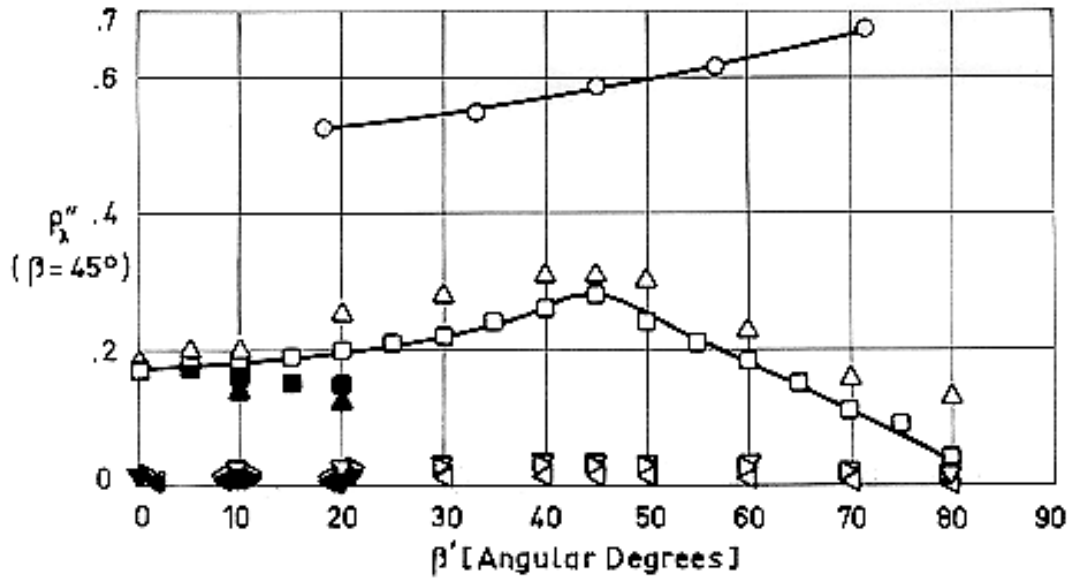


Note: non-si units are used in this figure

Figure 4-27: Hemispherical - normal spectral reflectance,  $\rho_{\lambda}'$ , of Aluminium contact coatings as a function of wavelength,  $\lambda$ .

Explanation

Key	Description	Comments	References
○	Evaporated film on mechanically polished and electropolished stainless steel.	$T = 298$ K.	Touloukian & DeWitt (1970) [42].



Note: non-si units are used in this figure

**Figure 4-28: Bidirectional total reflectance,  $\rho''$ , of Aluminium as a function of the viewing zenith angles,  $\beta$ .**

Explanation

Key	Description	Comments	References
○		$T = 298$ K. Angle of viewing within $2,5^\circ$ of angle of specular reflection.	Touloukian & DeWitt (1970) [42].
□	Sandblasted.	$T = 298$ K. $\beta = 45^\circ$ . $\theta = \theta' = 0$ . Tungsten filament lamp source.	
■		Same as □ except $\theta' = 180$ .	
△	Different sample, same as □.	Same as □.	
▲		Same as □ except $\theta' = 180$ .	
▽		Same as △ except green filter.	
▼		Same as ▽ except $\theta' = 180$ .	
▷		Same as △ except amber filter.	
▶		Same as ▷ except $\theta' = 180$ .	
◁		Same as △ except blue filter.	
◀		Same as ◁ except $\theta' = 180$ .	

**Table 4-9: Normal-Normal Solar Reflectance of Aluminium Conversion Coatings.**

$T$ [K]	$\rho''_s$ ( $\beta=\beta'=0$ )	Comments
~ 293	0,84	Al - 99,99 anodized 15 min in sulphuric acid; coating thickness $9,38 \times 10^{-6}$ m; substrate polished by Alzak process (electrolytic fluoboric acid bath); calculated from spectral reflectance data.
~ 298	0,82	Similar to above specimen and conditions except heat treated (24 h at 589 K) in vacuum ( $6,65 \times 10^{-3}$ Pa).
~ 298	0,81	Similar to above specimen and conditions except heat treated (48 h at 589 K) in vacuum ( $6,65 \times 10^{-3}$ Pa).
~ 298	0,82	Similar to above specimen and conditions except heat treated (96 h at 589 K) in vacuum ( $6,65 \times 10^{-3}$ Pa).
~ 298	0,82	Similar to above specimen and conditions except anodized 25 min; coating thickness $1,32 \times 10^{-5}$ m. Mentioned below as specimen 1.
~ 298	0,78	Similar to specimen 1 except heat treated (24 h at 589 K) in vacuum ( $6,65 \times 10^{-3}$ Pa).
~ 298	0,77	Similar to specimen 1 except heat treated (48 h at 589 K) in vacuum ( $6,65 \times 10^{-3}$ Pa).
~ 298	0,78	Similar to specimen 1 except heat treated (96 h at 589 K) in vacuum ( $6,65 \times 10^{-3}$ Pa).
~ 298	0,88	Al - 99,99 anodized 10 min in sulphuric acid; coating thickness $8,36 \times 10^{-6}$ m; substrate polished in phosphoric/nitric acid bath for 2 min at 364 K; calculated from spectral reflectance data.
~ 298	0,86	Similar to above specimen and conditions except anodizing time 15 min; coating thickness $9,38 \times 10^{-6}$ m.
~ 298	0,84	Similar to above specimen and conditions except anodized time 20 min; coating thickness $1,09 \times 10^{-5}$ m.
~ 298	0,83	Similar to above specimen and conditions except anodized time 25 min; coating thickness $1,32 \times 10^{-5}$ m.

NOTE From Touloukian, DeWitt &amp; HERNICZ (1972) [43].

**Table 4-10: Normal-Hemispherical Solar Reflectance of Both Bulk Aluminium and Contact Coatings**

$T$ [K]	$\rho''_s$ ( $\beta=0$ ) ( $\omega'=2\pi$ )	Comments
298	0,90	Pure aluminium on optical flat ( $2 \times 10^{-7}$ m thick); measured in air.
298	0,88	Aluminium foil Reynolds Wrap-heavy duty: measured in air.
298	0,88	Reynolds Wrap-heavy duty foil; measured in air.
298	0,90	Pure Al; $0,3 \times 10^{-6}$ m thick opaque layer on glass; freshly prepared; MgO reference; computed from spectral data. Mentioned below as specimen 1.
298	0,01	Above specimen and conditions; diffuse component only.
298	0,91	Different sample, same as 1 specimen and conditions.
298	0,01	Above specimen and conditions; diffuse component only.
298	0,89	Aluminium film on $6,35 \times 10^{-6}$ m thick Mylar; measured in air.
298	0,88	Aluminium film on $6,35 \times 10^{-6}$ m thick Mylar; measured in air.

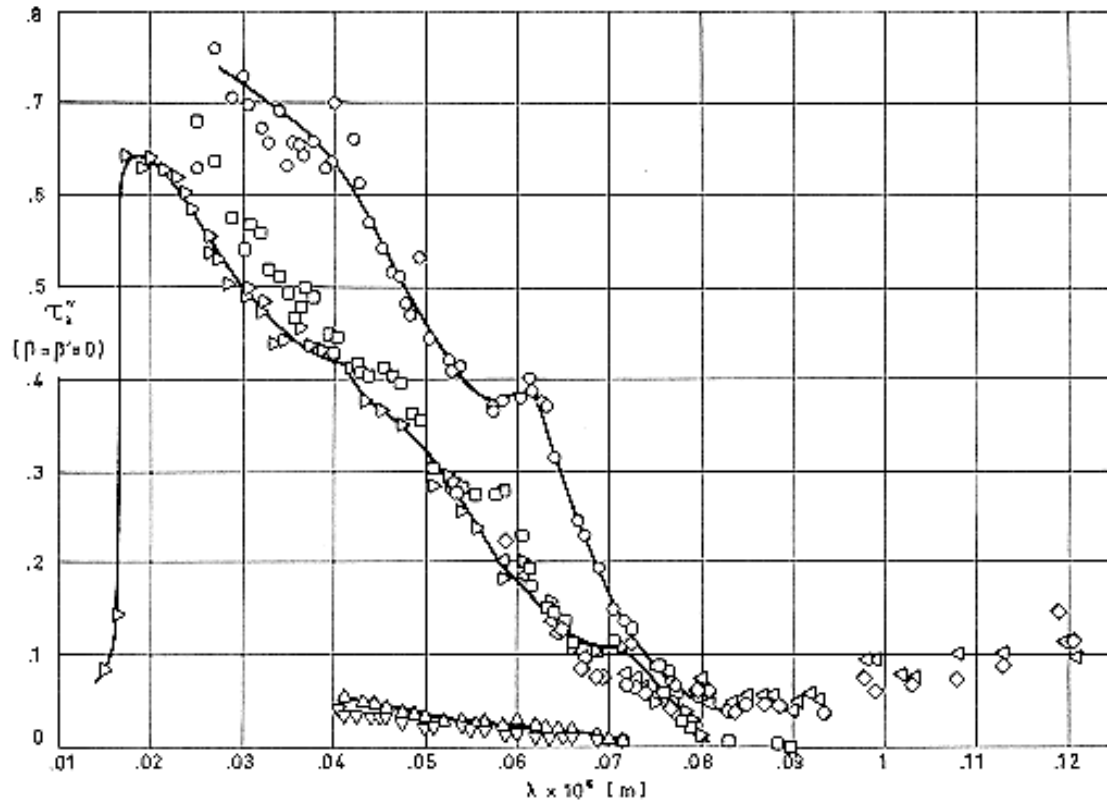
NOTE From Touloukian & DeWitt (1970) [42].

### 3.3.4. Transmittance

#### 3.3.4.1. Directional spectral transmittance

##### 3.3.4.1.1. Normal-normal spectral transmittance of Aluminium

( $\beta = \beta' = 0$ ): Figure 4-29.



Note: non-si units are used in this figure

**Figure 4-29: Normal - normal spectral transmittance,  $\tau_{\lambda}''$ , of Aluminium as a function of wavelength,  $\lambda$ .**

#### Explanation

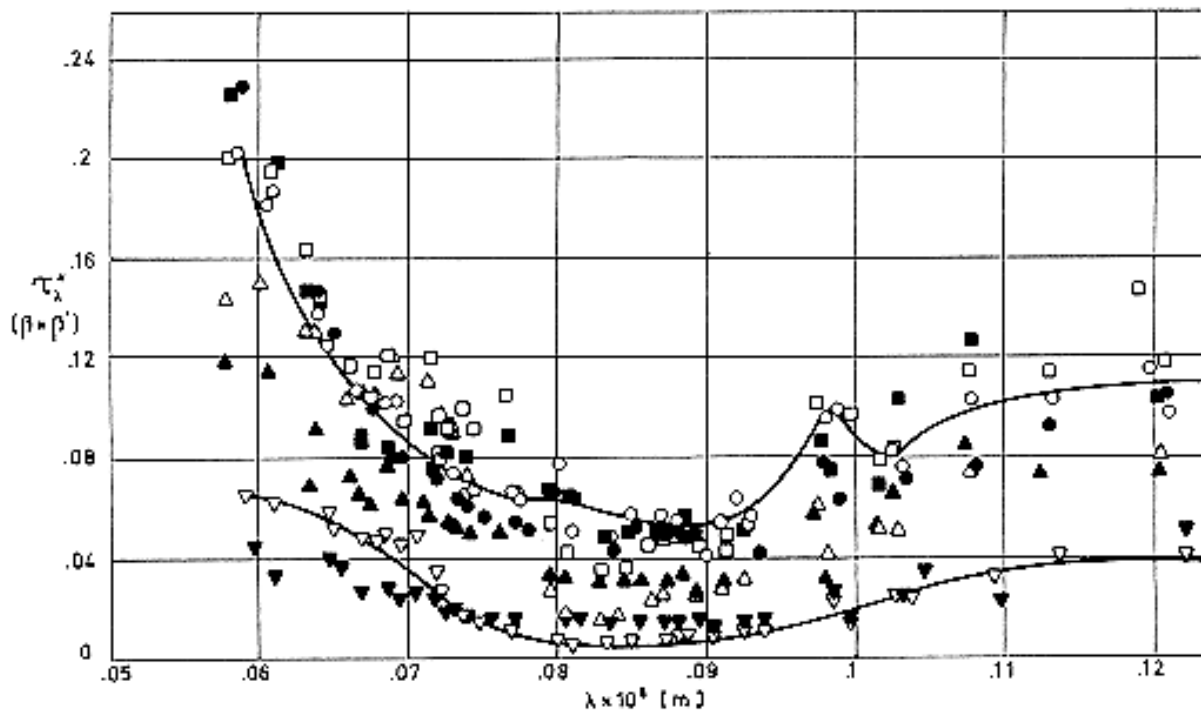
Key	Description	Comments	References
○	Evaporated film $(6 \pm 0,5) \times 10^{-8}$ m thick. Glass slide substrate at room temperature at evaporation. Evaporated at $2,67 \times 10^{-3}$ Pa in $10^{-15}$ s.	Sample temperature: $T = 298$ K. Reported error $\sim 10\%$ at $\lambda > 3,5 \times 10^{-8}$ m $< 25\%$ at $\lambda < 3,5 \times 10^{-8}$ m	Touloukian & DeWitt (1970) [42]
□	Same as ○ except film thickness $(1 \pm 0,1) \times 10^{-7}$ m.		
△	Evaporated film $4,7 \times 10^{-8}$ m thick. Unsupported. Exposed to air at atmospheric pressure.	$T = 298$ K.	
▽	Same as △ except film thickness $1,38 \times 10^{-7}$ m.		
▷	Unbacked film ( $\sim 8 \times 10^{-8}$ m thick).	$T = 298$ K.	



Key	Description	Comments	References
	Slight oxide layer.	Measured in vacuum ( $<1,33 \times 10^{-3}$ Pa).	
$\triangleleft$	Unbacked foil ( $3 \times 10^{-8}$ m thick). Evaporated in vacuum ( $4 \times 10^{-4}$ Pa). Exposed to air.	$T = 298$ K. Condensed spark discharge in argon light source. p-polarization dominant. Data uncorrected for partial polarization effects.	
$\diamond$		Same as $\triangleleft$ except s-polarization dominant.	

### 3.3.4.1.2. Angular spectral transmittance ( $\beta \neq 0$ ).

Effect of angle  $\beta$  on angular spectral transmittance of Aluminium: Figure 4-30.



Note: non-si units are used in this figure

**Figure 4-30: Angular spectral transmittance,  $\tau_{\lambda}^{\alpha}$ , of Aluminium as a function of wavelength,  $\lambda$ .**

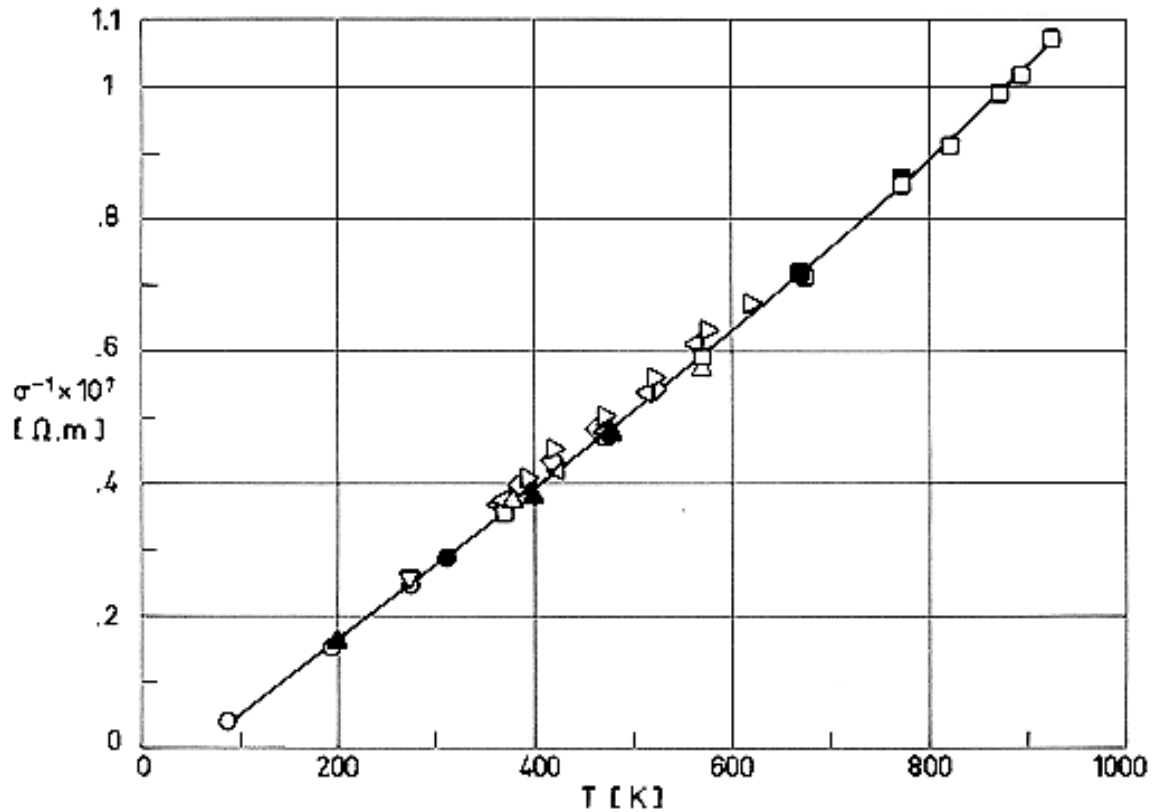
## Explanation

Key	Description	Comments	References
○	Unbacked foil (3x10 <sup>-8</sup> m thick). Evaporated in vacuum (4x10 <sup>-4</sup> Pa). Exposed to air.	$\beta=\beta'=0$ . Sample temperature: $T = 298$ K. Condensed spark discharge in argon light source. p-polarization dominant. Data uncorrected for partial polarization effects.	Touloukian & DeWitt (1970) [42]
●		Same as ○ except s-polarization dominant.	
□		Same as ○ except $\beta=\beta'=20^\circ$ .	
■		Same as □ except s-polarization dominant.	
△		Same as ○ except $\beta=\beta'=30^\circ$ .	
▲		Same as △ except s-polarization dominant.	
▽		Same as ○ except $\beta=\beta'=45^\circ$ .	
▼		Same as ▽ except s-polarization dominant.	

## 3.4. Other physical properties

## 3.4.1. Electrical resistivity

Effect of temperature on electrical resistivity: Figure 4-31.



Note: non-si units are used in this figure

Figure 4-31: Electrical resistivity,  $\sigma^{-1}$ , of Aluminium as a function of temperature,  $T$ .

Explanation

Key	Description	Comments	References
○	Traces of Mg, Si, Fe, and Cu.		Touloukian (1967)a [38].
□	99,9 Al - 0,05 Si - 0,03 B.		
△	0,04 Si - 0,03 Fe, traces of Cu, Ti, annealed 1 h at 723 K.	Furnace cooled.	
▽			
▷	Al - 99.5. Cast at 973 K into molds at 473 K, rolled and drawn. Turned into rods.		
◁	Al - 99,9, 0,038 Fe - 0,03 Si - 0,002 Cu. Same treatment as ▷.		
◇	Al - 99,99, 0,003 Fe - 0,0027 Si - 0,0024 Cu. Same treatment as ▷.		

Key	Description	Comments	References
●	SP grade.		
■	Al - 99,6.		
▲	Pure.		

#### 4. ENVIRONMENTAL BEHAVIOR

##### 4.1. Prelaunch

Aluminium surface is very susceptible to increase  $\alpha_s$  and  $\varepsilon$  caused by contamination. The surface should be protected from physical abuse, atmospheric exposure and caustic contaminants; cleanliness is of the utmost importance.

From Breuch (1967) [16].

##### 4.2. Postlaunch

No known restrictions other than structural.

Adhesive backed bright aluminium foils should not be used externally during ascent nor in areas where the peak ascent temperature is expected to exceed 460 K.

Pressure-sensitive aluminium tapes, if placed externally, should be fastened mechanically on both ends to avoid blistering. These tapes can be used internally where peak temperatures of up to 700 K are anticipated, and externally for temperatures below 670 K.

From Breuch (1967) [16].

#### 5. CHEMICAL PROPERTIES

##### 5.1. Solution potential (vs. decinormal calomel electrode)

Al - 99,5: 0,84 V, any condition.

Al - 99,0: 0,83 V, any condition.

From Kappelt (1961) [23].

##### 5.2. Corrosion resistance

These alloys are very stable because they become covered by a thin oxide film which is very resistant and protective. Thicker, more protective oxide coatings can be deposited by chemical or electrolytic treatments.

Corrosion resistance of these alloys is very good in interiors, rural, marine or industrial environments. (Kappelt (1961) [23]).

#### 6. FABRICATION

6.2. Forming. Excellent.

6.3. Welding. Good.

6.4. Machining. Excellent.

6.5. Heat treatment. These alloys are non-heat-treatable.

From Kappelt (1961) [23].

## 7. AVAILABLE FORMS AND CONDITIONS

These alloys are available in any standard product form such as: sheet, plate, strip, bar, tubing, wire extrusions, and forgings in a wide range of sizes from foils less than  $2,5 \times 10^{-5}$  m thick to big forgings.

## 8. USEFUL TEMPERATURE RANGE

Continuous structural use should be limited to temperatures below 400 K.

The temperature range of aluminized plastic films is normally controlled by the linear expansion of the film, which in the case of Mylar is extremely high above 310 K.

## 9. APPLICATIONS

Structural elements, foils, bushing and gear, tanks, sealing, wires, honeycombs (both cores and faces), thin wall tubing. As coating on Mylar, Teflon, Kapton, .... To protect aluminium alloys (alclad).

# 4.3 Aluminium-Copper alloys

ALLOY Al - 4,3 Cu - 1,5 Mg - 0,6 Mn.

## 1. TYPICAL COMPOSITION, PERCENT

Cr	Cu	Fe	Mg	Mn	Ni	Si	Ti+Zr	Zn	Others		Al
									Each	Total	
	3,8		1,2	0,3	-						Balance
0,1	4,9	0,5	1,8	0,9		0,5	0,2	0,2	0,5	0,15	

## 2. OFFICIAL DESIGNATIONS

AECMA	ISO	AFNOR	AMS	BS	DIN
Al-P13	Al-Cu4Mg1	A-U4G1	2024	2L 65	AlCuMg2 3. 1354

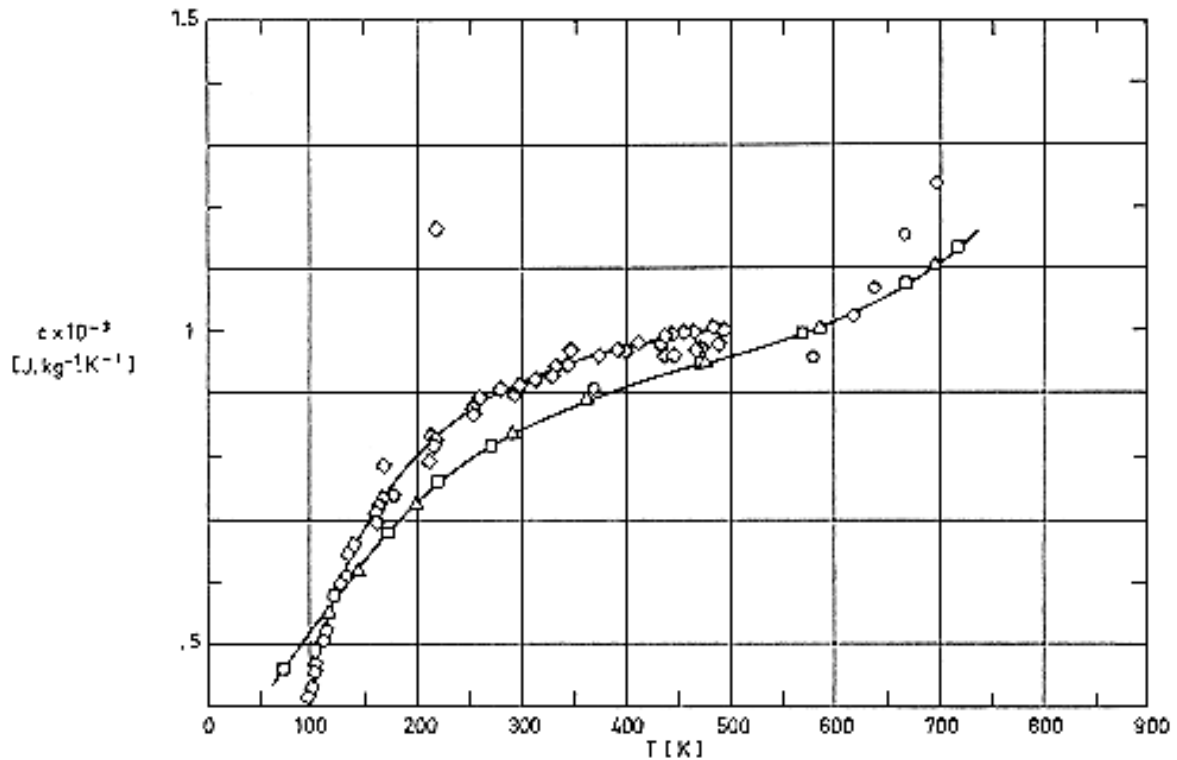
## 3. PHYSICAL PROPERTIES

3.1. Density.  $\rho = 2770 \text{ kg}\cdot\text{m}^{-3}$ . (Kappelt (1961) [23], ASMH (1974)c [10].

3.2. Thermal properties

3.2.1. Specific heat.

Effect of temperature on specific heat: Figure 4-32.



Note: non-si units are used in this figure

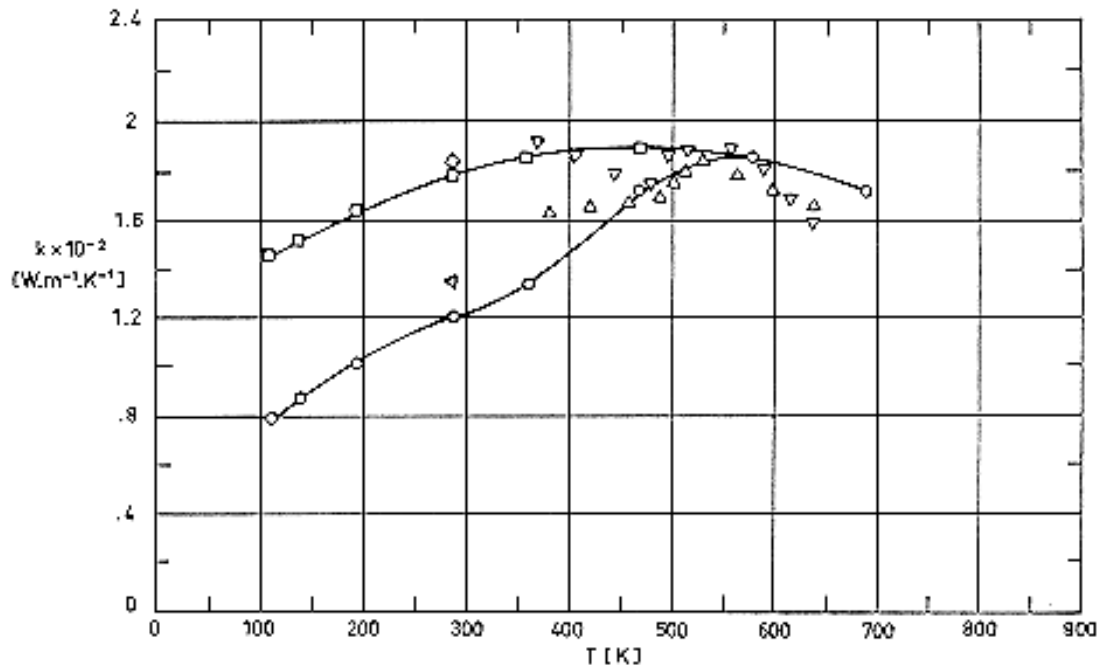
**Figure 4-32: Specific heat,  $c$ , of Al - 4,3 Cu - 1,5 Mg - 0,6 Mn as a function of temperature,  $T$ .**

Explanation

Key	Description	Comments	References
○	4,32 Cu - 0,29 Si - 0,14 Fe, and traces of other impurities. Hot worked, annealed several hours at 773 K in vacuum and cooled in 10 d. Heating rate during test 2 K.min <sup>-1</sup> .		Touloukian (1967)b [39].
□	93,4 Al - 4,5 Cu - 1,5 Mg - 0,6 Mn. Condition - T4.	Sealed under helium atmosphere.	
△	Same as □. Condition - T4.		
▽	Nominal composition. Hanova liquid platinum was applied on both surfaces of the specimen; on front surface for opaqueness and on rear surface for good conductivity. In addition front surface was undercoated with Parson black to obtain constant absorptance.	Reported error ≤ 5%.	

## 3.2.2. Thermal conductivity.

Effect of temperature on thermal conductivity: Figure 4-33.



Note: non-si units are used in this figure

**Figure 4-33: Thermal conductivity,  $k$ , of Al - 4,3 Cu - 1,5 Mg - 0,6 Mn as a function of temperature,  $T$ .**

Explanation

Key	Description	Comments	References
○	Nominal composition. Condition - T4. Density 2787 kg.m <sup>-3</sup> . As received.		Touloukian (1967)b [39].
□	Same as ○. Measured after heating to 575 K.		
△	4,5 Cu - 1,5 Mg - 0,6 Mn. Heated from virgin conditions to maximum temperature of 648 K.	Reported error ± 4%.	
▽	Same as △. Cooled to room temperature and then repeated the above heat treatment.		
◁	Same as ▽. Condition - T4 - T3.	Reported error ± 5%.	
◇	Same as ▽. Condition - 0 annealed.		

Thermal conductivity integrals: Figure 4-34.

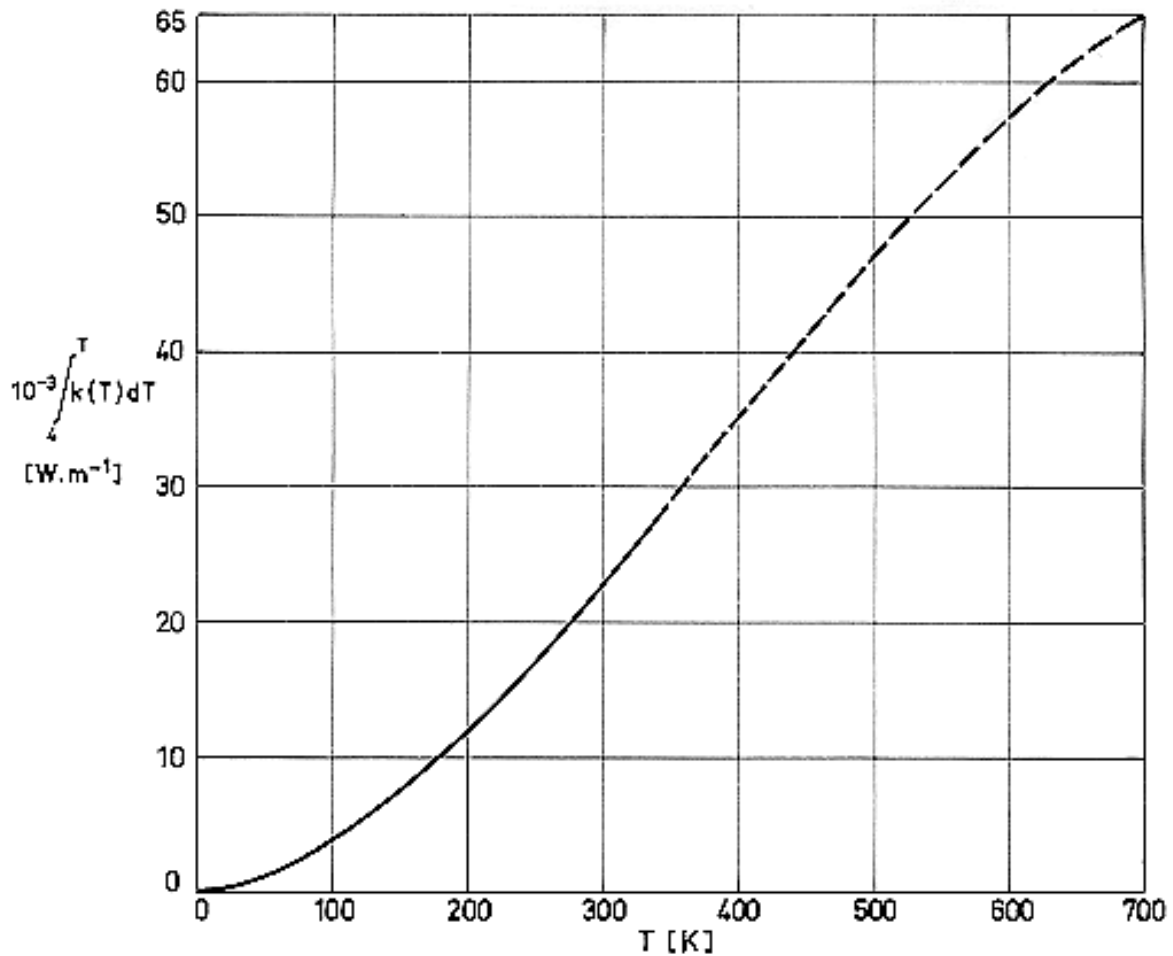


**Figure 4-34: Thermal conductivity integrals of Al - 4,3 Cu - 1,5 Mg - 0,6 Mn as a function of temperature,  $T$ .**

Explanation

Solid line: From Coston (1967) [18].

Dashed line: Calculated, by the compiler, by fitting the experimental data points  $\circ$  and  $\triangleleft$  of Figure 4-33 with the least-squares method, and integrating the expression,  $k(T) = 74,44 - 2,30 \times 10^{-2}T + 9,96 \times 10^{-4}T^2 - 1,09 \times 10^{-6}T^3$  ( $r = 0,977$ ), which is then obtained;  $r$  is the correlation coefficient giving the goodness of the fit.

3.2.3. Thermal diffusivity.

Effect of temperature on thermal diffusivity: Figure 4-35.



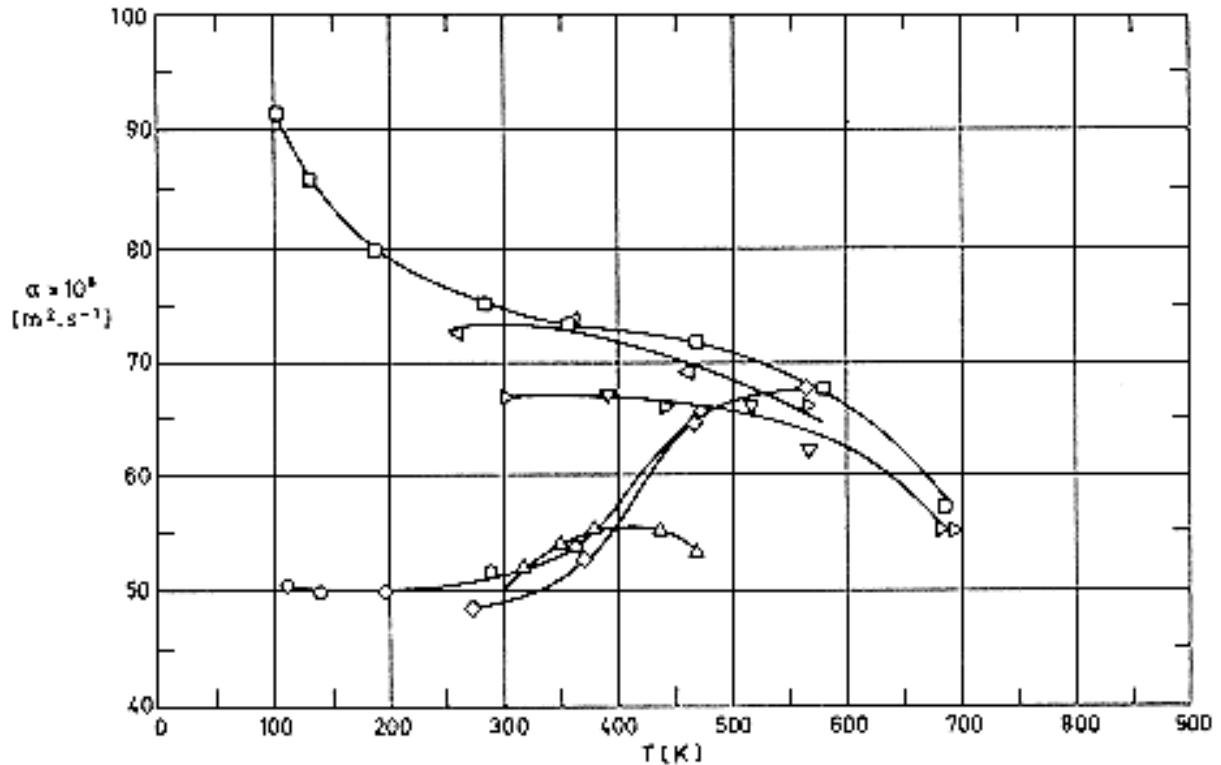


**Figure 4-35: Thermal diffusivity,  $\alpha$ , of Al - 4,3 Cu - 1,5 Mg - 0,6 Mn as a function of temperature,  $T$ .**

Explanation

Key	Description	Comments	References
○	4,5 Cu - 1,5 Mg - 0,6 Mn. Condition - T4. As received.		Touloukian (1967)b [39].
□	Same as ○. Heated above 575 K.		
△	3,8 - 4,9 Cu - 1,2 - 1,8 Mg - 0,3 - 0,9 Mn - 0,5 max Fe - 0,5 max Si - 0,25 max Zn - 0,1 max Cr and 0,15 max other in total. Condition - T86.	Measured after five exposures to radiation and followed by cooling.	
▽	Same as △.	Measured after eight exposures to radiation and followed by cooling.	
▷	Same as △.	Measured after ten exposures to radiation and followed by cooling.	

Key	Description	Comments	References
◁	4,5 Cu - 1,5 Mg - 0,6 Mn. Annealed at 723 K.		
◇	4,5 Cu - 1,5 Mg - 0,6 Mn. Condition - T4.		

### 3.2.4. Thermal expansion.

Effect of temperature on thermal expansion: Figure 4-36.

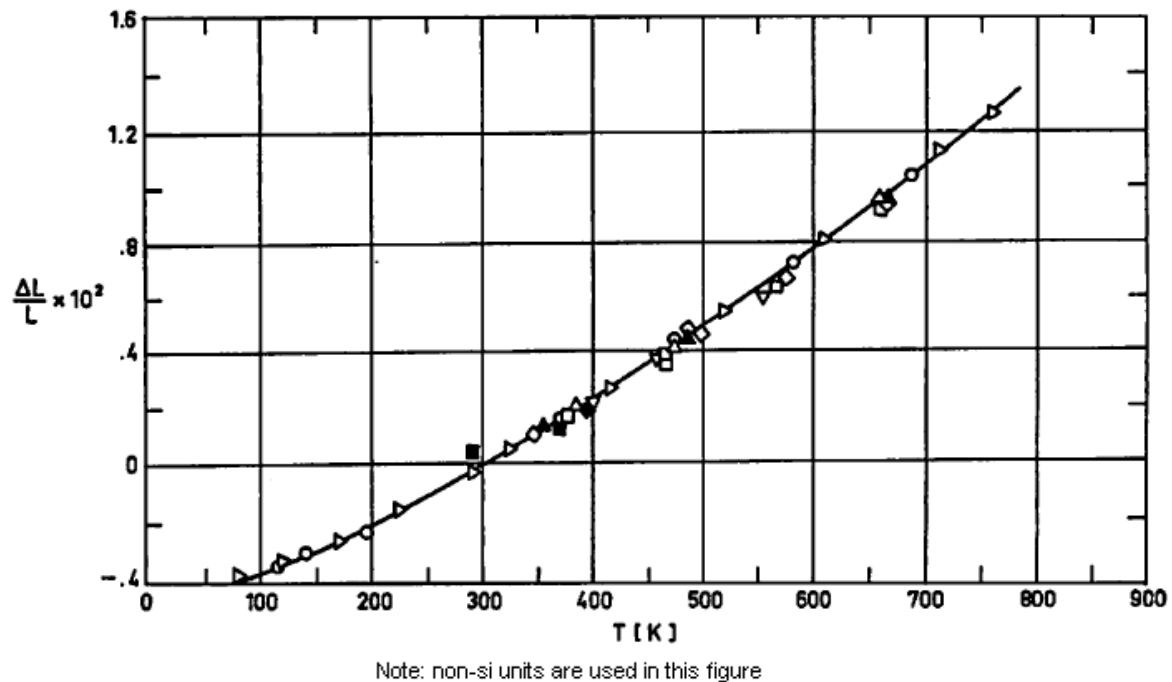


**Figure 4-36: Linear thermal expansion,  $\Delta L / L$ , of Al - 4,3 Cu - 1,5 Mg - 0,6 Mn as a function of temperature,  $T$ .**

Explanation

Key	Description	Comments	References
○	Nominal composition. Condition - T4.	Tested in vacuum.	Touloukian (1967)b [39].
□	93,09 Al - 4,41 Cu - 1,41 Mg - 0,67 Mn - 0,25 Fe - 0,10 Si - 0,02 Zn, and 0,01 Ni, Cr, Pb, Bi each. Solution heat-treated 1 h at 766,5 K, water quenched, and aged at room temperature.	Heating.	
■		Cooling.	
△	Same as □. Aged 100 h a 644 K.	Heating.	
▲	Same as △.	Cooling.	

Key	Description	Comments	References
◇	Same as □. Aged 500 h at 700 K.	Heating.	
◆		Cooling.	
▽	2,31 Cu - 1,46 Mg - 1,23 Fe - 1,20 Ni - 0,88 Si - 0,07 Ti . Wrought, heated 2 h at 798 K, quenched, aged 16 h at 443 K, quenched.		
▷	4,5 Cu - 1,5 Mg - 0,6 Mn. Condition - T4.	Tested at 1,5 - 2,5 K.min <sup>-1</sup> rise in argon.	

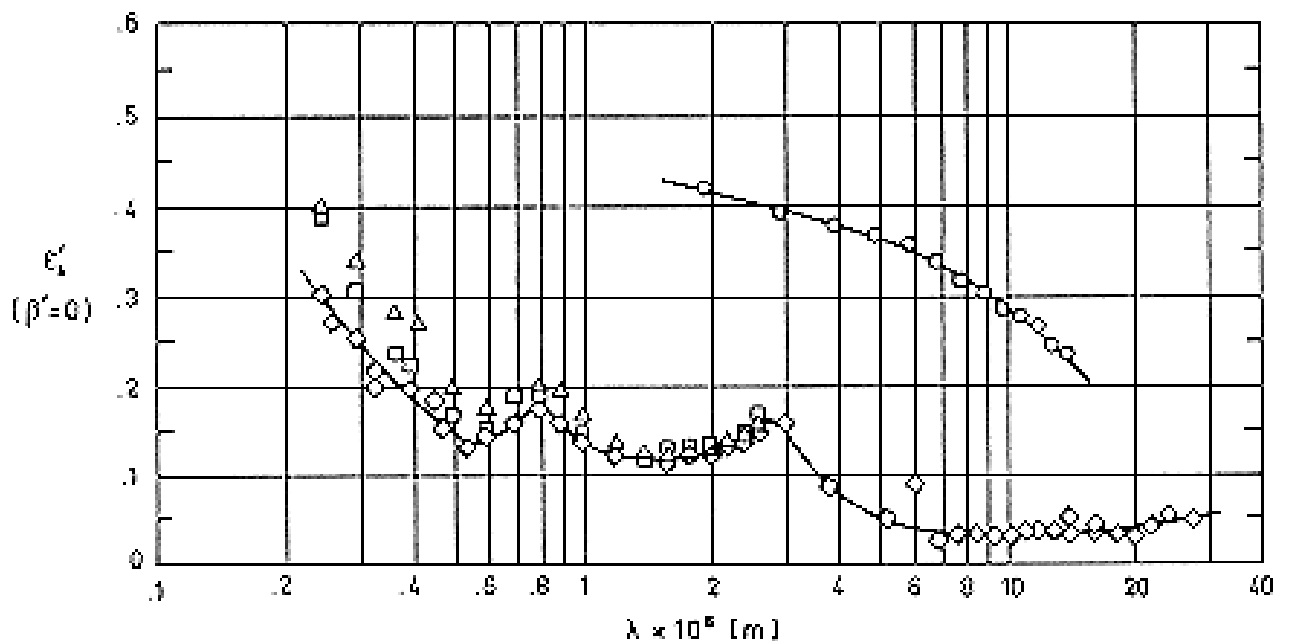
### 3.2.5. Melting range.

773 K -913 K. (ALCAN (1965) [2]).

### 3.3. Thermal radiation properties

#### 3.3.1. Emittance.

##### 3.3.1.1.1. Normal spectral emittance ( $\beta' = 0$ ): Figure 4-37



Note: non-si units are used in this figure

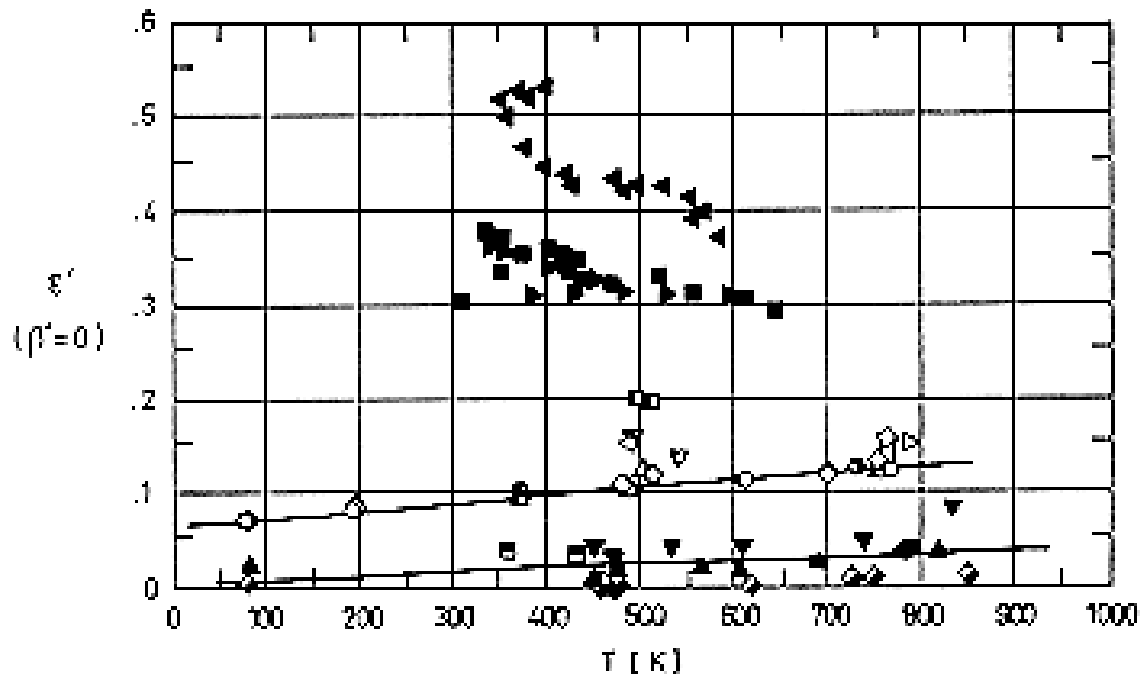
**Figure 4-37: Normal - spectral emittance,  $\epsilon'_{\lambda}$ , of Al - 4,3 Cu - 1,5 Mg - 0,6 Mn as a function of wavelength,  $\lambda$ .**

## Explanation

Key	Description	Comments	References
○	4,5 Cu - 1,5 Mg - 0,6 Mn. Ultrasonically machined. Oxidized in air at 823 K for 2 h.	Sample temperature: $T = 823$ K. Measured in air. Reported error $\pm 4\%$ .	Touloukian (1967)b [39].
△	Same as ○. Surface roughness: $9,9 \times 10^{-8}$ m and $7,1 \times 10^{-8}$ m in $x$ and $y$ directions respectively.	$T = 323$ K. Measured in nitrogen.	
□	Same as ○. Surface roughness: $4,6 \times 10^{-8}$ m and $3,8 \times 10^{-8}$ m in $x$ and $y$ directions respectively.		
◇	Same as ○. Surface roughness: $1,52 \times 10^{-7}$ m and $1,7 \times 10^{-7}$ m in $x$ and $y$ directions respectively.		

 3.3.1.2.1. Normal total emittance ( $\beta' = 0$ ).

Effect of temperature on normal total emittance: Figure 4-38.



Note: non-si units are used in this figure

**Figure 4-38: Normal total emittance,  $\varepsilon'$ , of Al - 4,3 Cu - 1,5 Mg - 0,6 Mn as a function of temperature,  $T$ .**

Explanation

Key	Description	Comments	References
○	4,5 Cu - 1,5 Mg - 0,6 Mn. As received, wiped.	Measured in helium ( $1,33 \times 10^{-3}$ Pa). Cycle 1 heating.	Touloukian (1967)b [39].
△		Cycle 1 cooling.	
□		Cycle 2 heating.	
▽		Cycle 2 cooling.	
◇	Same as above. Scrubbed, washed, and wiped.	Same as ○.	
◁		Cycle 1 cooling.	
▷		Cycle 2 heating.	
●		Cycle 2 cooling.	
▲	Same as above. Polished to a mirror like finish and washed.	Same as ○.	
■		Cycle 1 cooling.	

Key	Description	Comments	References
◆		Cycle 2 heating.	
▼		Cycle 2 cooling.	
●		Cycle 3 heating.	
■		Cycle 3 cooling.	
◆	4,5 Cu - 1,5 Mg - 0,6 Mn. Alclad As received.	Measured in vacuum ( $6,7 \times 10^{-3}$ Pa). Reported error $\pm 10\%$ .	
▲	Same as above. Cleaned with liquid detergent or polished with fine polishing compounds on a buffing wheel.		
▼	Same as above. Oxidized in air at red heat for 30 min.		
◀	4,5 Cu - 1,5 Mg - 0,6 Mn. Weathered using flat shield.		
▶	Same as above. Weathered using conical shield.		
■			
■		Constant over temperature range 361-433 K. Reported error $\pm 10\%$ .	

The influence of anodizing is given in Table 4-11.

**Table 4-11: Normal Total Emittance of Al – 4,3 Cu – 1,5 Mg – 0,6 Mn, Anodized**

$T$ [K]	$\beta^\circ$	$\varepsilon'$	Comments
373	$\sim 0$	0,55	Anodized in chromic acid. Measured in vacuum ( $<1,3 \times 10^{-3}$ Pa).
300	$\sim 0$	0,78	$1,6 \times 10^{-3}$ m thick. Anodized in sulphuric acid (coating thickness $\sim 1,3 \times 10^{-5}$ m). Calculated from reflectance measured in air. mentioned below as specimen 1.
300	$\sim 0$	0,78	Similar to 1 except exposed to vacuum ( $1,3 \times 10^{-6}$ Pa) for 300 h. Vacuum maintained by ion pump. Measured in air after exposure.
300	$\sim 0$	0,78	Similar to 1 except exposed to UV radiation in vacuum ( $1,3 \times 10^{-3}$ Pa) for 300 h. Vacuum maintained by oil-diffusion pump. $H_2$ gas UV source. Measured in air after exposure.
300	$\sim 0$	0,78	Similar to above except He gas UV source.

NOTE From Touloukian, DeWitt & HERNICZ(1972) [43].

#### 3.3.1.4. Hemispherical total emittance: Table 4-12.

**Table 4-12: Hemispherical Total Emittance of Al – 4,3 Cu – 1,5 Mg – 0,6 Mn**

$T$ [K]	$\varepsilon$	Comments
303	0,052	Measured in air.
303	0,26	Different sample, same as above specimen and conditions except weathered.
373	0,063	Prefinished with 600 grit aluminium oxide power on felt; electro polished; measured in vacuum ( $1,3 \times 10^{-3}$ Pa).
373	0,041	Above specimen and conditions except ion bombarded ( $3,2 \times 10^{24}$ ions/m <sup>2</sup> ).
373	0,053	Above specimen and conditions except ion bombarded ( $6,5 \times 10^{24}$ ions/m <sup>2</sup> ).
373	0,062	Above specimen and conditions except ion bombarded ( $9,8 \times 10^{24}$ ions/m <sup>2</sup> ).
278	0,02	As received.
278	0,06	Different sample, same as above specimen and conditions except machine polished and degreased.

NOTE From Touloukian & DeWitt (1970) [42].

#### 3.3.2. Absorptance

## 3.3.2.5. Solar absorptance

## 3.3.2.5.1. Normal solar absorptance: Table 4-13.

**Table 4-13: Normal Solar Absorptance of Al – 4,3 Cu – 1,5 Mg – 0,6 Mn**

$T$ [K]	$\beta^\circ$	$\alpha_s$	Comments
311	~ 0	0,45	Heated to 310 K; clean and smooth surface; measured in air at sea level. Mentioned below as sample 1.
311	~ 0	0,58	Above specimen and conditions except reheated to 560 K.
311	~ 0	0,67	Above specimen and conditions except reheated to 755 K.
311	~ 0	0,25	Different sample, same specimen and conditions as 1, except heated to 307 K; polished; surface free from scratches.
311	~ 0	0,18	Above specimen and conditions except reheated to 560 K.
311	~ 0	0,43	Above specimen and conditions except reheated to 755 K.
311	~ 0	0,49	Different sample, same specimen and conditions as 1, except heated to 324 K; cleaned with methyl alcohol.
311	~ 0	0,46	Above specimen and conditions except reheated to 603 K.
311	~ 0	0,73	Above specimen and conditions except reheated to 755 K.
298	9	0,242	As received; computed from spectral reflectance data for sea level condition. Mentioned as sample 2.
298	9	0,236	Above specimen and conditions except computed for above atmosphere conditions.
298	9	0,228	Different sample, same specimen and conditions as 2, except cleaned with liquid detergent.
298	9	0,220	Above specimen and conditions except computed for above atmosphere conditions.
298	9	0,302	Different sample, same specimen and conditions as 2, except polished.
298	9	0,290	Above specimen and conditions except computed for above atmosphere conditions.
298	9	0,568	Different sample, same specimen and conditions as 2, except oxidized in air at red heat for 0,5 h.
298	9	0,548	Above specimen and conditions except computed for above atmosphere conditions.



$T$ [K]	$\beta^\circ$	$\alpha_s$	Comments
278	$\sim 0$	0,27	As received; extraterrestrial. Reported error 10%.
278	$\sim 0$	0,31	Different sample, same as above specimen and conditions except machine polished and degreased. Reported error 10%.
297		0,20± 0,05	Alloy sheet (nonclad). Chemically cleaned. From Breuch (1967) [16].
297		0,22± 0,05	Alloy sheet (clad). Chemically cleaned. From Breuch (1967) [16].
323		0,16	Alloy sheet (nonclad). Surface roughness $0,152 \times 10^{-6}$ m and $0,178 \times 10^{-6}$ m in $x$ and $y$ directions respectively. Calculated by the compiler from data of Figure 4-37.

NOTE All data are from Touloukian & DeWitt (1970) [42], unless otherwise stated.

The influence of anodizing is given in Table 4-14.

**Table 4-14: Normal Solar Absorptance of Al – 4,3 Cu – 1,5 Mg – 0,6 Mn, Anodized**

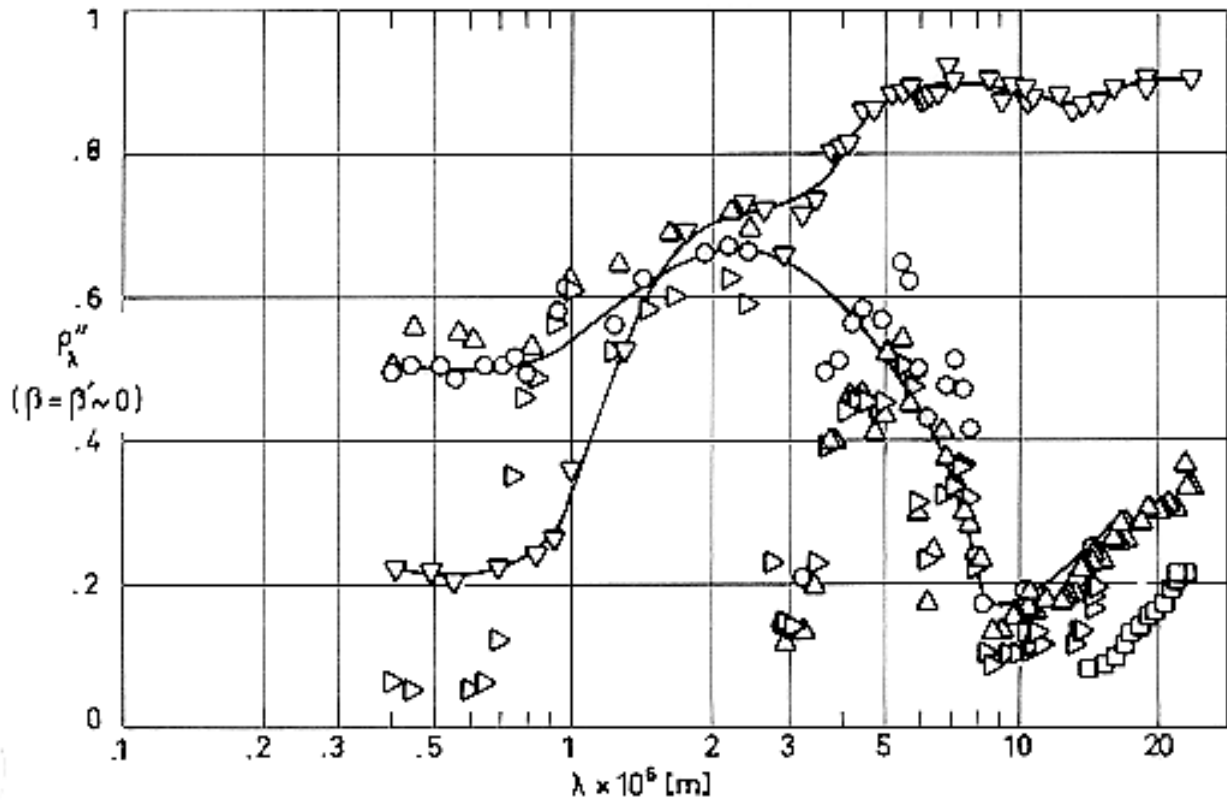
$T$ [K]	$\beta^\circ$	$\alpha_s$	Comments
300	$\sim 0$	0,15	Anodized in sulphuric acid; coating thickness $\sim 1,27 \times 10^{-5}$ m; absorptance calculated from reflectance measured in air. Mentioned below as sample 1.
300	$\sim 0$	0,16	Similar to above specimen and conditions except exposed to vacuum ( $1,33 \times 10^{-6}$ Pa) for 300 h; vacuum maintained by ion pump; properly measured in air after vacuum exposure.
300	$\sim 0$	0,18	Similar specimen and conditions as 1, except exposed to vacuum ( $1,33 \times 10^{-6}$ Pa) for 300 h; vacuum maintained by oil-diffusion pump; properly measured in air after vacuum exposure.
300	$\sim 0$	0,26	Similar to above specimen and conditions except exposed to UV radiation in vacuum for 300 h; $H_2$ gas UV source.
300	$\sim 0$	0,31	Similar to above specimen and conditions except He gas UV source.

NOTE From Touloukian, DeWitt & HERNICZ (1972) [43].

### 3.3.3. Reflectance.

#### 3.3.3.1. Bidirectional spectral reflectance.

##### 3.3.3.1.1. Normal-normal spectral reflectance ( $\beta = \beta' = 0$ ) of alloy anodized: Figure 4-39.



Note: non-si units are used in this figure

**Figure 4-39: Normal-normal spectral reflectance,  $\rho_{\lambda}''$ , of Al-4,3 Cu-1,5 Mg-0,6 Mn, anodized, as a function of wavelength,  $\lambda$ .**

Explanation

Key	Description	Comments	References
○	Nominal composition.	Sample temperature: $T = 298$ K. Data from smooth curve.	Touloukian, DeWitt & Hernicz (1972) [43].
□	Anodized in sulphuric acid.		
△	Same as ○ except substrate chem-milled.		
▽	Same as ○ except anodized in chromic acid.		
▷	Same as ○ except anodized in black chromic acid.		

3.3.3.2. Directional-hemispherical spectral reflectance.

Normal-hemispherical spectral reflectance ( $\beta = 0$ ,  $\omega' = 2\pi$ ): Figure 4-40.

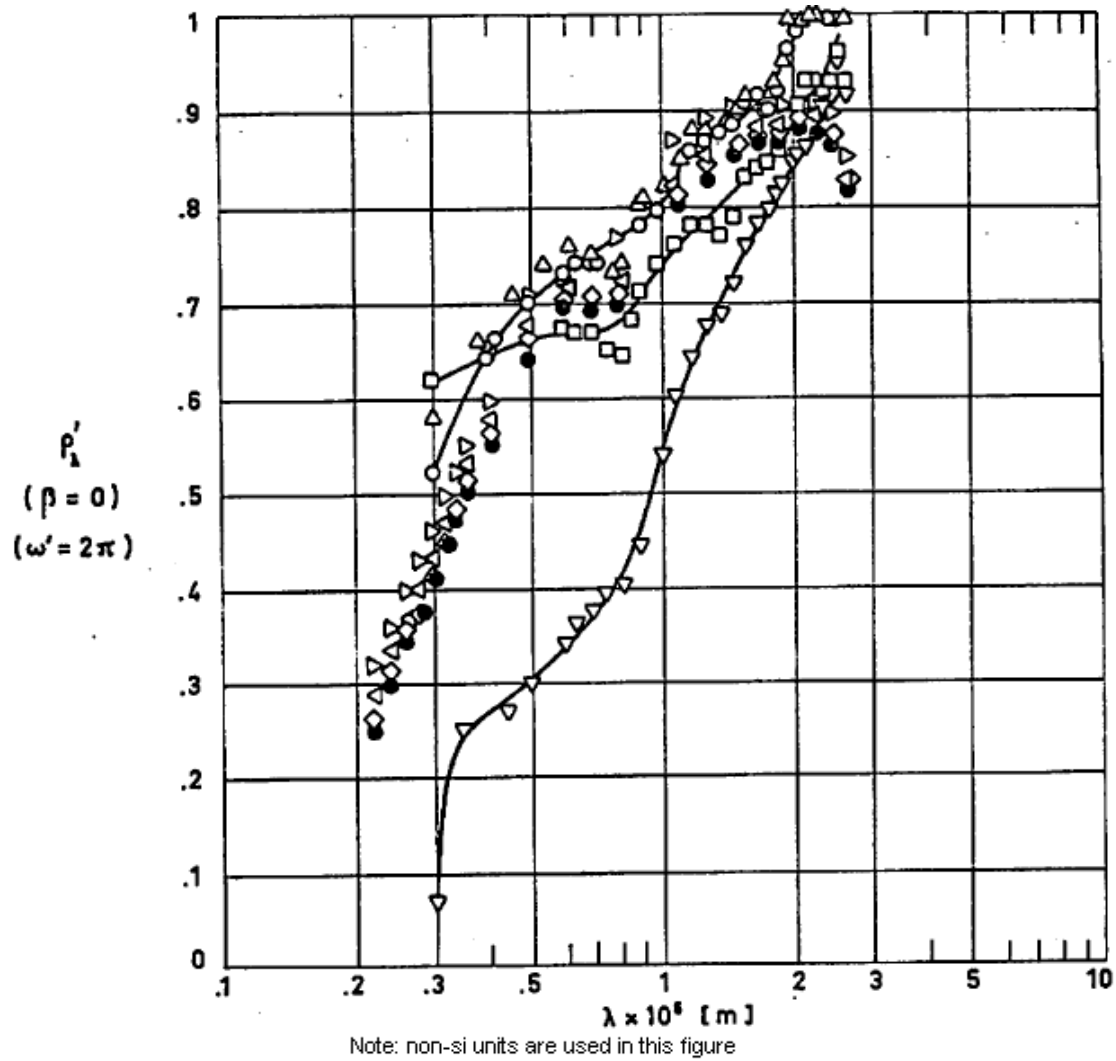


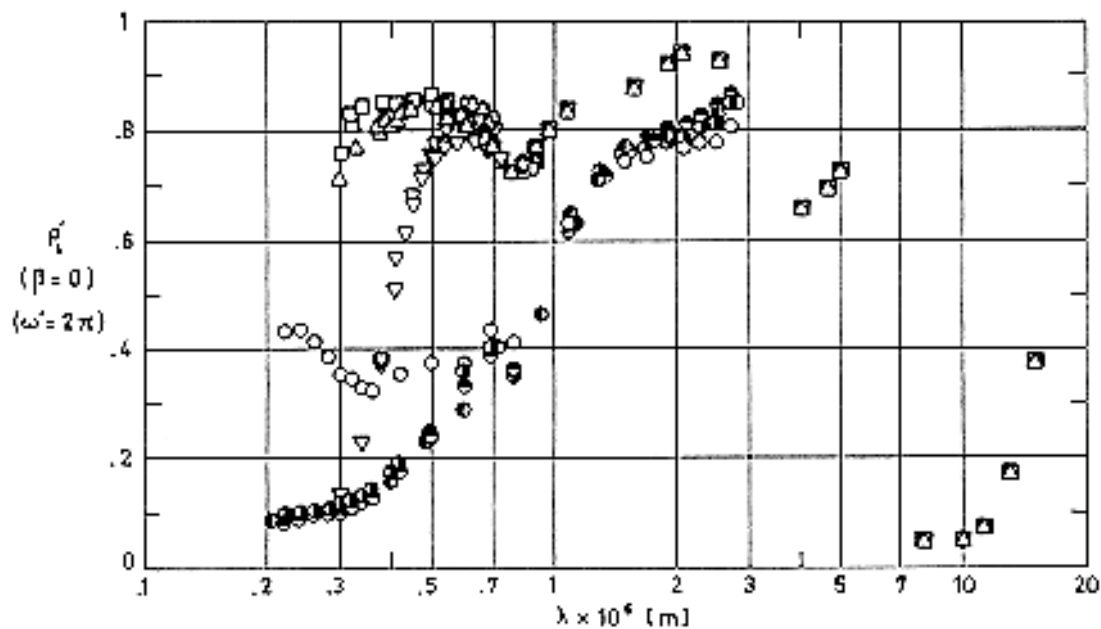
**Figure 4-40: Normal - hemispherical spectral reflectance,  $\rho_{\lambda}'$ , of Al - 4,3 Cu - 1,5 Mg - 0,6 Mn as a function of wavelength,  $\lambda$ .**

Explanation

Key	Description	Comments	References
○	Nominal composition. As received.	$\beta = 9^\circ$ Sample temperature: $T = 298$ K. Data from smooth curve. Reported error $\pm 4\%$ .	Touloukian & DeWitt (1972) [158].
□	Same as ○ except polished.		
△	Same as ○ except cleaned with liquid detergent.		
▽	Same as ○ except oxidized in air at red heat for 30 min.		
▷	Nominal composition. Cleaned.	$T = 378$ K. Measured in vacuum ( $1,33 \times 10^{-3}$ Pa).	
◁	Same as above except exposed to UV		

Key	Description	Comments	References
	radiation for 20 h; G.E. Type UA-3 lamp source.	Measured relative to MgO.	
◇	Same as ▷ except exposed to UV radiation for 60 h. Same radiation source as ◁.		
●	Same as ▷ except exposed to UV radiation for 100 h. Same radiation source as ◁.		

Normal-hemispherical spectral reflectance ( $\beta = 0$ ,  $\omega' = 2\pi$ ) of alloy anodized: Figure 4-41.



Note: non-si units are used in this figure

**Figure 4-41: Normal - hemispherical spectral reflectance,  $\rho_{\lambda}'$ , of Al - 4,3 Cu - 1,5 Mg - 0,6 Mn, anodized, as a function of wavelength,  $\lambda$ .**

Explanation

Key	Description	Comments	References
○	Nominal composition. Anodized. Cleaned.	Sample temperature: $T = 378$ K. Measured in vacuum ( $1,33 \times 10^{-3}$ Pa) relative to MgO.	Touloukian, DeWitt & Hernicz (1972) [43].
●		Same as ○ except exposed to UV radiation for 20 h. Source: G.E. UA-3 lamp.	

Key	Description	Comments	References
●		Same as ○ except exposed to UV radiation for 60 h.	
◐		Same as ○ except exposed to UV radiation for 100 h.	
□	Nominal composition. Sheet $\sim 1,59 \times 10^{-3}$ m thick anodized in sulphuric acid. Coating thickness $\sim 1,27 \times 10^{-5}$ m.	$T = 300$ K. Data from smooth curve. The data correspond to two different tests.	
△		Same as □ except exposed to vacuum ( $1,33 \times 10^{-6}$ Pa) for 300 h. Vacuum maintained by ion pump. Measured in air after vacuum exposure.	
▽		Same as □ except exposed to UV radiation in vacuum for 300 h; H <sub>2</sub> gas UV source.	

3.3.3.6. Normal-hemispherical total reflectance

3.3.3.9.2. Normal-hemispherical solar reflectance ( $\beta = 0$ ,  $\omega' = 2\pi$ ) of alloy anodized: Table 4-15.

**Table 4-15: Normal Hemispherical Solar Reflectance of Al – 4,3 Cu – 1,5 Mg – 0,6 Mn, Anodized**

$T$ [K]	$\beta^\circ$	$\omega'$	$\rho'_s$	Comments
298	$\sim 0$	$2\pi$	0,28	Anodized in chromic acid. Mentioned below as specimen 1.
298	$\sim 0$	$2\pi$	0,30	Similar to above specimen and conditions except calculated from spectral data.
298	$\sim 0$	$2\pi$	0,31	Similar to 1 specimen and conditions except anodized in black chromic acid.
298	$\sim 0$	$2\pi$	0,29	Similar to 1 specimen and conditions except calculated from spectral data.
298	$\sim 0$	$2\pi$	0,56	Similar to 1 specimen and conditions except anodized in sulphuric acid. Mentioned below as specimen 2.
298	$\sim 0$	$2\pi$	0,53	Similar to above specimen and conditions except calculated from spectral data.
298	$\sim 0$	$2\pi$	0,64	Similar to 2 specimen and conditions except substrate was chem-milled.
298	$\sim 0$	$2\pi$	0,57	Similar to above specimen and conditions except calculated from spectral data.

NOTE From Touloukian, DeWitt & HERNICZ (1972) [43].

### 3.4. Other physical properties

#### 3.4.1. Electrical resistivity (at room temperature).

Condition	0	T3-T4	T6-T81
$\sigma^{-1} \cdot 10^6$ [ $\Omega \cdot m$ ]	0,0345 <sup>a,b</sup>	0,0574 <sup>a,b</sup>	0,045 <sup>c</sup>

<sup>a</sup> Kappelt (1961) [23]

<sup>b</sup> ASMH (1974)c [10]

<sup>c</sup> Aluminium Association (1969) [5].

The coefficient giving the variation of electrical resistivity with temperature is in the range  $2 \times 10^{-3} \text{ K}^{-1}$ . (ASMH (1974)c [10]) to  $2,6 \times 10^{-3} \text{ K}^{-1}$ . (Touloukian (1967)b [39]).

#### 4. ENVIRONMENTAL BEHAVIOR

##### 4.1. Prelaunch

Aluminium surface is very susceptible to increase in  $\alpha$  and  $\varepsilon$  caused by contamination. The surface should be protected from physical abuse, atmospheric exposure and caustic contaminants; cleanliness if of the utmost importance.

##### 4.2. Postlaunch

There are no known restrictions, other than structural.

From Breuch (1967) [16].

#### 5. CHEMICAL PROPERTIES

##### 5.1. Solution potential (vs. decinormal calomel electrode)

Condition	T3-T4	T8
Sol. Pot. V	-0,68	-0,8

NOTE From REYNOLDS METALS Co (1961) [30].

##### 5.2. Corrosion resistance

It is poor in marine or industrial environments, sufficient in rural and urban environments, and good indoors.

#### 6. FABRICATION

6.2. Forming. Medium.

6.3. Welding. Poor.

6.4. Machining. Good.

6.5. Heat treatment. Good.

6.6. Anodizing. Poor.

From García-Poggio et al. (1972) [20].

#### 7. AVAILABLE FORMS AND CONDITIONS

This alloy is available in the full commercial range of sizes for sheet, strip, plate, rod, bar, forgings, tubing, wire, extrusions and structural shapes.

#### 8. USEFUL TEMPERATURE RANGE

Some disagreement seems to exist in the literature regarding the maximum operating temperature of this alloy. Although temperatures as high as 425 K are quoted for long term structural purposes (any temper condition), and even higher values for intermittent loading (475 K, T4 conditions), it is advisable not to use this alloy (T3, T4 conditions) in a corrosive environment at temperatures above 340 K for several hours, or above 365 K for more than a few minutes.

#### 9. APPLICATIONS

Gear materials in antenna drive, instruments, structural purposes, and thermal surfaces.

## 4.4 Aluminium-Magnesium alloys

ALLOY Al - 1 Mg - 0,6 Si.

### 1. TYPICAL COMPOSITION, PERCENT

Cr <sup>a</sup>	Cu	Fe	Mg	Mn	Si	Ti	Zn	Others		Al
								Each	Total	
0,15	0,15	-	0,8	-	0,4	-	-	-	-	Balance
0,35	0,4	0,7	1,2	0,15	0,8	0,15	0,25	0,05	0,15	

<sup>a</sup> Sometimes this alloy contains Mn (0,2% - 0,8%) instead of Cr.

### 2. OFFICIAL DESIGNATIONS

AECMA	ISO	AFNOR	AMS	BS	DIN
Al-P34	Al-Mg1SiCu	-	6061	H20	AlMgSi1, 3,2315

### 3. PHYSICAL PROPERTIES

3.1. Density.  $\rho = 2700 \text{ kg.m}^{-3}$ . (Kappelt (1961) [23]).

3.2. Thermal properties

3.2.1. Specific heat

From room temperature to 373 K. Conditions 0 and T6.

$c = 963 \text{ J.kg}^{-1}.\text{K}^{-1}$ . (ASMH (1974)c [10]).

3.2.2. Thermal conductivity

At room temperature.

Condition	0	T4	T6
$k$ [W.m <sup>-1</sup> .K <sup>-1</sup> ]	180 <sup>a</sup> 172 <sup>b</sup>	155 <sup>a,b</sup> -	167 <sup>a</sup> 155 <sup>b</sup>

<sup>a</sup> From ASMH (1974)c [10].

<sup>b</sup> From Kappelt (1961) [23].

3.2.4. Thermal expansion coefficient

Mean coefficient of linear thermal expansion,  $\beta$ , between 293 K and given temperature.



$T$ [K]	293 <sup>a</sup>	393	493	593
$\beta \times 10^6$ [K <sup>-1</sup> ]	21,8	23,4	24,3	25,4

<sup>a</sup> Lower limit in this case is 213 K: From Kappelt (1961) [23].

3.2.5. Melting range. 855 K - 922 K. (ASMH (1974)c [10]).

3.3. Thermal radiation properties

3.3.1. Emittance

3.3.1.2. Normal total emittance ( $\beta' = 0$ ): Table 4-16.

**Table 4-16: Normal Total Emittance of Al – 1 Mg – 0,6 Si**

$T$ [K]	$\epsilon'$	Comments
	0,03	Sheet $3,17 \times 10^{-3}$ m thick, cleaned and degreased.
	0,76	Anodized with chromic acid electrolyte 5% by weight, at 308 K, anodizing voltage: 40V DC, 120 min. Resulting coating thickness: $10^{-5}$ m.
	0,07	Anodized with citric acid electrolyte, $1 \text{ kg} \cdot \text{m}^{-3}$ ammonium citrate, at 295 K, anodizing voltage: 200V DC, 45 min.
	0,81	Anodized with oxalic acid electrolyte, 3% by weight, at 311 K, anodizing voltage: 30V DC, 60 min. Resulting coating thickness: $10^{-5}$ m.
	0,80	Hard anodized, $7,6 \times 10^{-6}$ m thick, with sulphuric acid electrolyte 15% by weight, at 269 K.
	0,82	Soft anodized, $7,6 \times 10^{-6}$ m thick, with sulphuric acid electrolyte 17% by weight, at 293 K.

NOTE From Bevans (1969) [14].

## 3.3.1.4. Hemispherical total emittance: Table 4-17.

**Table 4-17: Hemispherical Total Emittance of Al – 1 Mg – 0,6 Si**

<i>T</i> [K]	$\epsilon$	Comments
294	0,06± 0,03 <sup>a</sup>	Nonclad sheet, chemically cleaned.
278	0,09± 0,06 <sup>a</sup>	Forging, chemically cleaned.
323	0,10± 0,06 <sup>a</sup>	Forging, chemically cleaned.
223	0,10± 0,06 <sup>a</sup>	Weld area, chemically cleaned.
278	0,10± 0,06 <sup>a</sup>	Weld area, chemically cleaned.
323	0,11± 0,06 <sup>a</sup>	Weld area, chemically cleaned.
278	0,04 <sup>b</sup>	As received.
278	0,04 <sup>b</sup>	Different sample, same as above specimen and conditions except machine polished and degreased.
278	0,41 <sup>b</sup>	Different sample, same as above specimen and conditions except sandblasted (120 size grit). Reported error: 10%.
302	0,0506 <sup>b</sup>	Buffed; measured in vacuum ( $2,67 \times 10^{-5}$ Pa). Error below 7,7%.
303	0,0500 <sup>b</sup>	Above specimen and conditions; second trial. Error below 7,7%.
302	0,0506 <sup>b</sup>	Above specimen and conditions; third trial. Error below 7,7%.
302	0,049 <sup>b</sup>	Above specimen and conditions; different analysis of observed data. Error below 7,7%.
302	0,0501 <sup>b</sup>	Above specimen and conditions; second trial. Error below 7,7%.

<sup>a</sup> From Breuch (1967) [16].

<sup>b</sup> From Touloukian & DeWitt (1970) [42].

## 3.3.2. Absorptance

## 3.3.2.5. Solar absorptance

## 3.3.2.5.1. Normal solar absorptance: Table 4-18.

**Table 4-18: Normal Solar Absorptance of Al – 1 Mg – 0,6 Si**

$T$ [K]	$\beta^\circ$	$\alpha_s$	Comments
294		$0,16 \pm 0,04^a$	Nonclad sheet, chemically cleaned.
294		$0,19 \pm 0,06^a$	Sheet sanded and chemically cleaned.
		$0,37^b$	$3,17 \times 10^{-3}$ m thick sheet cleaned and degreased.
		$0,48^b$	Hard anodized, $7 \times 10^{-6}$ m thick, with sulfuric acid electrolyte, 15% by weight, at 269 K.
		$0,38^b$	Soft anodized, $7 \times 10^{-6}$ m thick, with sulfuric acid electrolyte, 17% by weight, at 293 K.
		$0,42^b$	Anodized with oxalic acid electrolyte, 3% by weight, at 311 K, anodizing voltage: 30V DC, 60 min. Resulting coating thickness: $10^{-5}$ m.
		$0,37^b$	Anodized with citric acid electrolyte, $1 \text{ kg} \cdot \text{m}^{-3}$ ammonium citrate, at 295 K, anodizing voltage: 200 V DC, 45 min.
		$0,48^b$	Anodized with chromic acid electrolyte, 5% by weight, at 308 K, anodizing voltage: 40V DC, 120 min. Resulting coating thickness: $10^{-5}$ m.
278	$\sim 0$	$0,41^c$	As received; extraterrestrial. Reported error 10%.
278	$\sim 0$	$0,35^c$	Different sample, same as above specimen and conditions except machine polished and degreased. Same reported error as above.
278	$\sim 0$	$0,60^c$	Different sample, same as above specimen and conditions except sandblasted (120 size grit). Same reported error as above.

<sup>a</sup> From Breuch (1967) [16].

<sup>b</sup> From Bevans (1969) [14].

<sup>c</sup> From Touloukian & DeWitt (1970) [42].

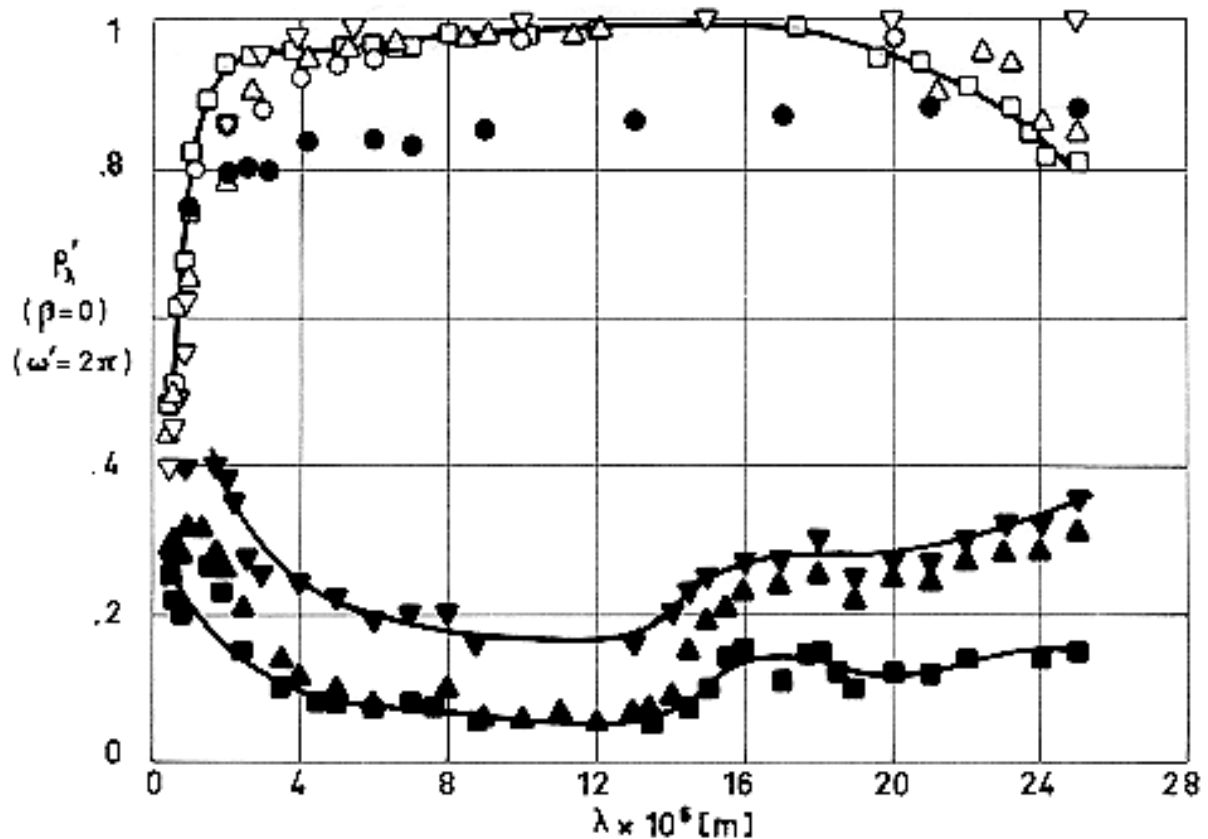
## 3.3.3. Reflectance

## 3.3.3.1. Bidirectional spectral reflectance

Normal-hemispherical spectral reflectance ( $\beta = 0, \omega' = 2\pi$ ):

Data concerning different surface conditions are given in the following figures:

As received: Figure 4-42



Note: non-si units are used in this figure

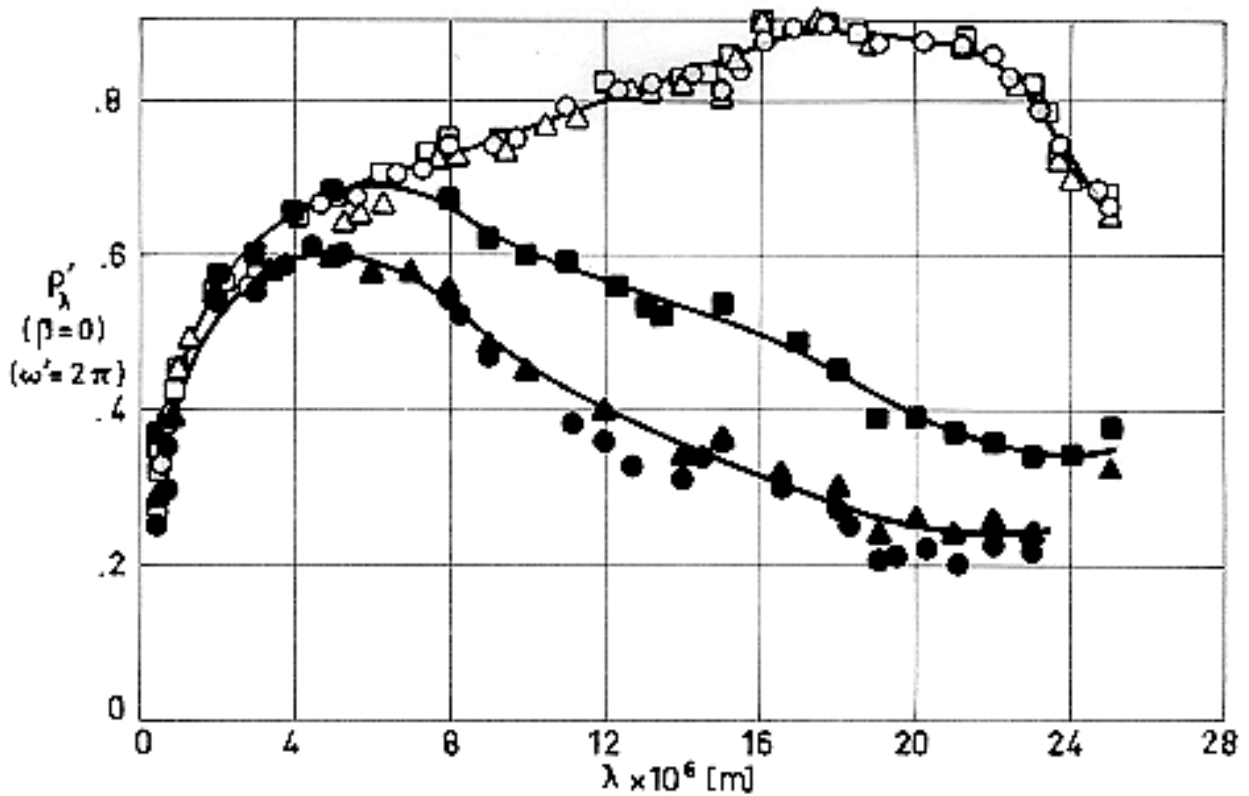
Figure 4-42: Normal-hemispherical spectral reflectance,  $\rho_{\lambda}'$ , of Al-1 Mg-0,6 Si, as received, as a function of wavelength,  $\lambda$ .

Explanation

Key	Description	Comments	References
○	Nominal composition. Surface roughness: $1,5 \times 10^{-6}$ m RMS.	$T = 298$ K. Converted from $R(2\pi, 0)$ .	Touloukian & DeWitt (1970) [42]
●	Same as above except surface roughness: $12,5 \times 10^{-6}$ m RMS.		
□	Nominal composition. Cleaned.	$T \sim 322$ K.	

Key	Description	Comments	References
■	Same as above. Diffuse component only.	Data from smooth curve. Hohlraum at 1273 K. (Gier & Dunkle). Converted from $R(2\pi,0)$ . Reported error <2%.	
△	Same as ○. Exposed to vacuum ( $5,32 \times 10^{-6}$ Pa) for 24 h.		
▲	Same as above. Diffuse component only.		
▽	Same as ○. X-Ray exposed in vacuum ( $5,32 \times 10^{-6}$ Pa) for 24 h.		
▼	Same as above. Diffuse component only.		

Grit blasted: Figure 4-43.



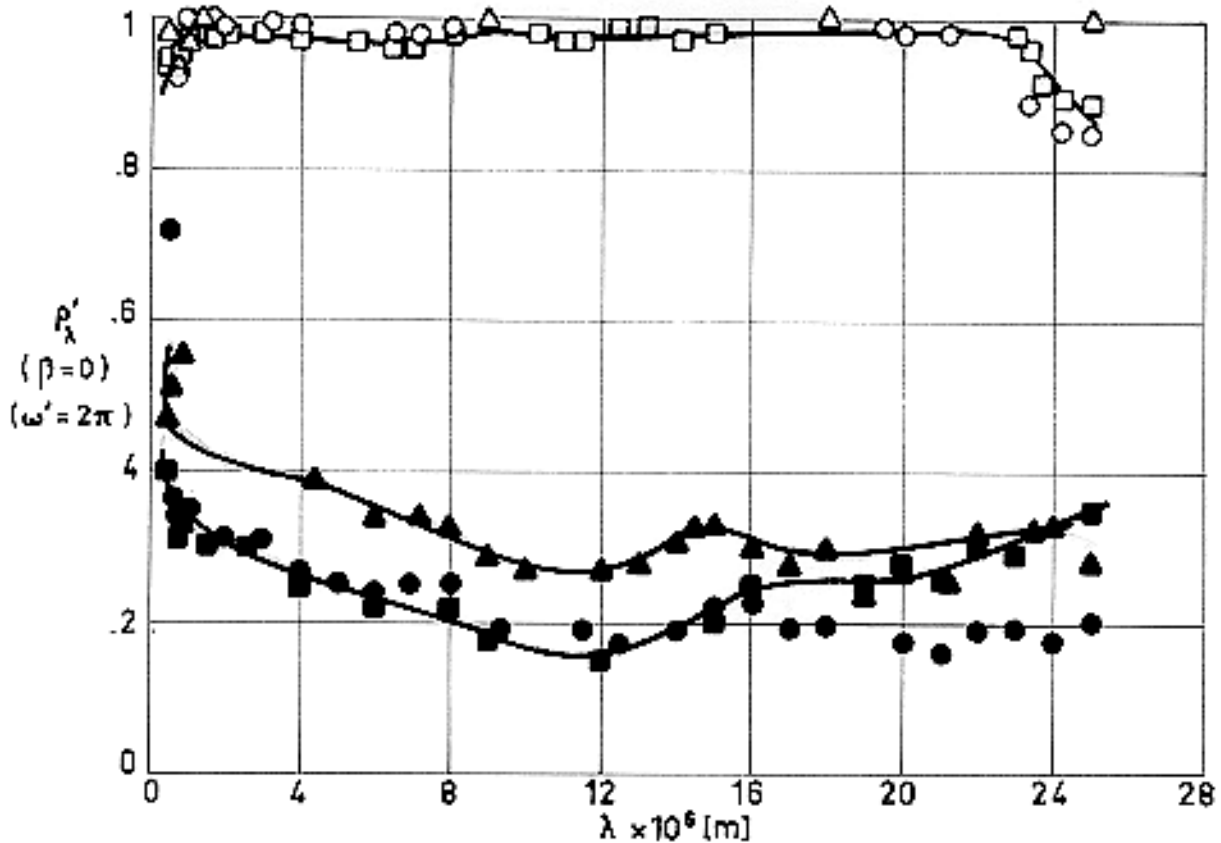
Note: non-si units are used in this figure

Figure 4-43: Normal-hemispherical spectral reflectance,  $\rho_{\lambda}'$ , of Al-1 Mg-0,6 Si, grit blasted, as a function of wavelength,  $\lambda$ .

## Explanation

Key	Description	Comments	References
○	Nominal composition. Blasted using silicon carbide, air pressure $0,76 \times 10^6$ Pa to $0,83 \times 10^6$ Pa for 30 to 45 s.	T~ 322K. Data from smooth curve. Hohlraum at 1273 K. (Gier & Dunkle). Converted from $R(2\pi,0)$ . Reported error <2%.	Touloukian & DeWitt (1970) [42]
●	Same as above. Diffuse component only.		
□	Same as ○ except chem-milled using the Turco 9H process for 3 min; blasted as above.		
■	Same as above. Diffuse component only.		
△	Same as ○ except chem-polished using the Alcoa process with a 2 min immersion at 358 K; blasted as above.		
▲	Same as above. Diffuse component only.		

Chemically polished: Figure 4-44.



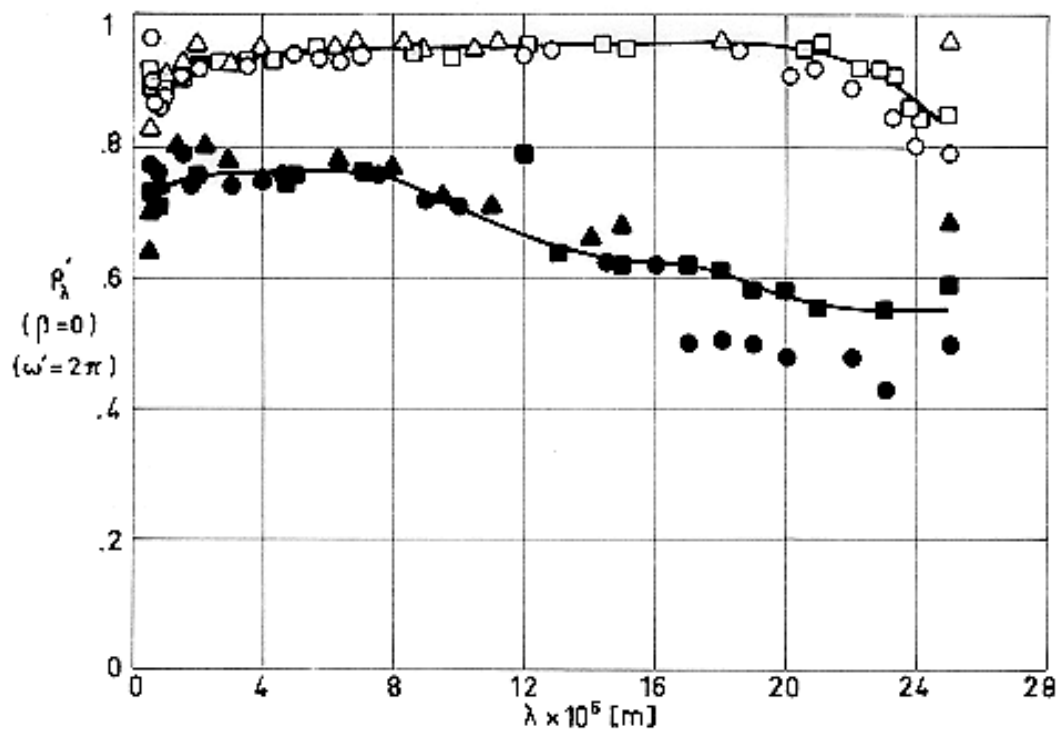
Note: non-si units are used in this figure

Figure 4-44: Normal-hemispherical spectral reflectance,  $\rho_{\lambda}'$ , of Al-1 Mg-0,6 Si, chemically polished, as a function of wavelength,  $\lambda$ .

Explanation

Key	Description	Comments	References
○	Nominal composition. Polished using the Alcoa Process with a 2 min immersion at 358 K.	T~ 322K. Data from smooth curve. Hohlraum at 1273 K. (Gier & Dunkle). Converted from $R(2\pi,0)$ . Reported error <2%.	Touloukian & DeWitt (1970) [42]
●	Same as above. Diffuse component only.		
□	Same as ○. Exposed to vacuum ( $5,32 \times 10^{-6}$ Pa) for 24 h.		
■	Same as above. Diffuse component only.		
△	Same as ○. X-Ray exposed in vacuum ( $5,32 \times 10^{-6}$ Pa) for 24 h.		
▲	Same as above. Diffuse component only.		

Chemically milled: Figure 4-45.



Note: non-si units are used in this figure

**Figure 4-45: Normal - hemispherical spectral reflectance,  $\rho_{\lambda}'$ , of Al - 1 Mg - 0,6 Si, chemically milled, as a function of wavelength,  $\lambda$ .**

Explanation

Key	Description	Comments	References
○	Nominal composition. Chem-milled using the Turco 9H process for 3 min.	T~ 322K. Data from smooth curve. Hohlraum at 1273 K. (Gier & Dunkle). Converted from $R(2\pi,0)$ . Reported error <2%.	Touloukian & DeWitt (1970) [42]
●	Same as above. Diffuse component only.		
□	Same as ○. Exposed to vacuum ( $5,32 \times 10^{-6}$ Pa) for 24 h.		
■	Same as above. Diffuse component only.		
△	Same as ○. X-Ray exposed in vacuum ( $5,32 \times 10^{-6}$ Pa) for 24 h.		
▲	Same as above. Diffuse component only.		



### 3.4. Other physical properties

#### 3.4.1. Electrical resistivity

Condition	0	T4	T6
$\sigma^{-1} \times 10^{-9}$ [ $\Omega \cdot m$ ]	3,83 <sup>a</sup> 3,71 <sup>b</sup>	4,31 <sup>a</sup> 4,29 <sup>b</sup>	4,31 <sup>a</sup> 4,11 <sup>b</sup>

<sup>a</sup> From Kappelt (1961) [23].

<sup>b</sup> From ASMH (1974)c [10].

## 4. ENVIRONMENTAL BEHAVIOR

### 4.1. Prelaunch

Aluminium surface is very susceptible to increase in  $\alpha_s$  and  $\varepsilon$  caused by contamination. The surface should be protected from physical abuse, atmospheric exposure and caustic contaminants; cleanliness if of the utmost importance. (Breuch (1967) [16]).

### 4.2. Postlaunch

No known restrictions other than structural. (Breuch (1967) [16]).

## 5. CHEMICAL PROPERTIES

### 5.1. Solution potential (vs. decinormal calomel electrode)

T4 Condition: -0,80 V.

T6 Condition: -0,83 V.

From Kappelt (1961) [23].

### 5.2. Corrosion resistance

This alloy is ranked among the best of the heat treatable alloys concerning corrosion resistance. In general, resistance to corrosion is not significantly affected by variations in the heat treatment. (ASMH (1974)c [10]).

## 6. FABRICATION

6.2. Forming. Good.

6.3. Welding. Good.

6.4. Machining. Good.

6.5. Heat treatment. Good.

6.6. Anodizing. Excellent.

From García-Poggio et al. (1972) [20].

## 7. AVAILABLE FORMS AND CONDITIONS

This alloy is available in the full commercial range of sizes for sheets, strip, plate, rod, bar, forgings, tubing extrusion and structural shapes. (ASMH (1974)c [10]).

## 8. USEFUL TEMPERATURE RANGE

Continuous structural use should be limited to temperatures below 425 K, whatever the temper conditions. Short term utilization temperatures up to 475 K can be achieved using T4 or T6 conditions. (ASMH (1974)c [10]).

## 9. APPLICATIONS

For electrical power systems, tubing, structural elements, whip antennas, heat pipes, solar absorbers.

## 4.5 Aluminium-Zinc alloys

ALLOY Al - 5,7 Zn - 2,5 Mg - 1,6 Cu.

### 1. TYPICAL COMPOSITION, PERCENT

Cr	Cu	Fe	Mg	Mn	Si	Ti	Zn	Others		Al
								Each	Total	
0,18 0,40	1,2 2,0	0,7	2,1 2,9	0,3	0,5	0,2	5,1 6,1	0,5	0,15	Balance

### 2. OFFICIAL DESIGNATIONS

AICMA	ISO	AFNOR	AMS	BS	DIN	UNE
Al-P42		A-Z5GU	7075		AlZnMgCu 1,5 3,4365	Al-5ZnMgCu UNE 38-371

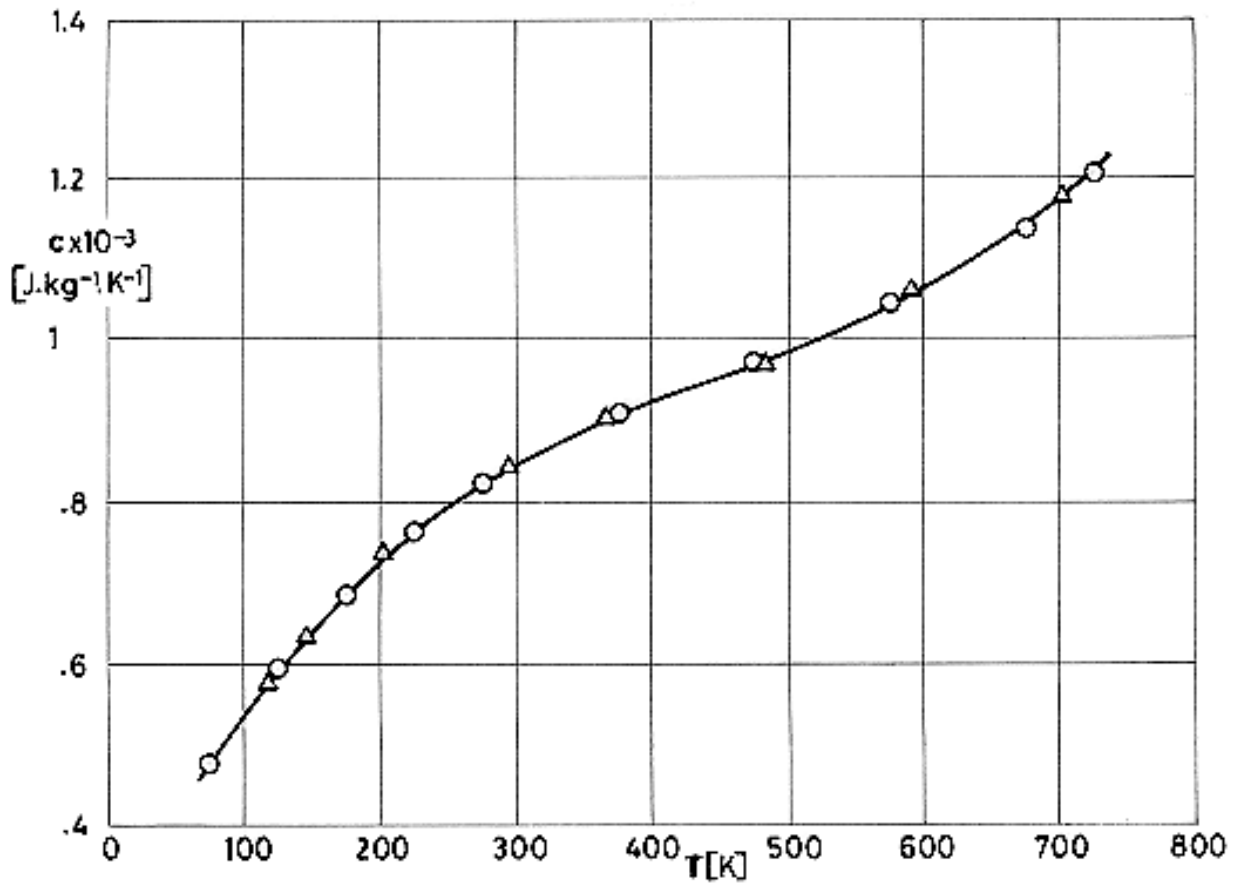
### 3. PHYSICAL PROPERTIES

3.1. Density.  $\rho = 2800 \text{ kg.m}^{-3}$ . (ASMH (1974)c [10]).

3.2. Thermal properties

3.2.1. Specific heat

Effect of temperature on specific heat: Figure 4-46



Note: non-si units are used in this figure

Figure 4-46: Specific heat,  $c$ , of Al - 5,7 Zn - 2,5 Mg - 1,6 Cu as a function of temperature,  $T$ .

Explanation

Key	Description	Comments	References
○	Al Alloy 75 S - T6 (Canadian commercial designation). 5,5 Zn, 2,5 Mg, 1,5 Cu, 0,3 Cr, 0,2 Mn, Al balance.		Touloukian (1967)c [40].
△	Al alloy 7075-T6. 5,5 Zn, 2,5 Mg, 1,5 Cu, 0,3 Cr, Al balance.	Sealed under helium atmosphere.	

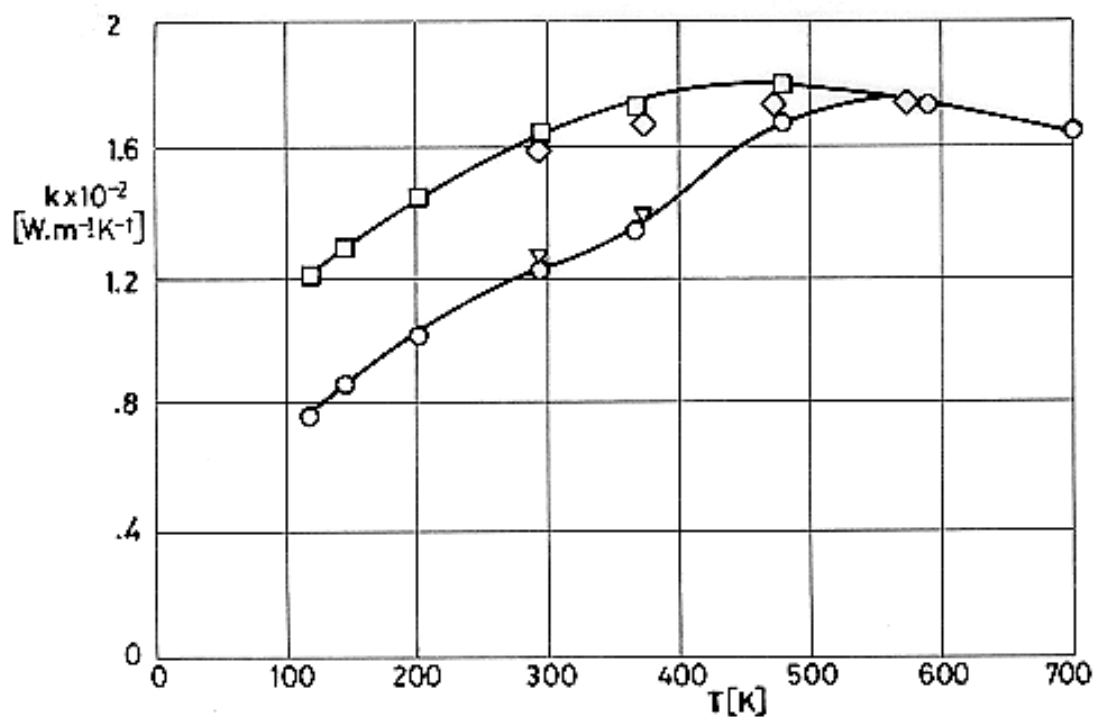
### 3.2.2. Thermal conductivity

At 298 K.

Condition	$k$ [W.m <sup>-1</sup> .K <sup>-1</sup> ]
T6	130
T73	155
T76	150

NOTE From McCall (1979) [25].

Effect of temperature on thermal conductivity: Figure 4-47.



Note: non-si units are used in this figure

**Figure 4-47: Thermal conductivity,  $k$ , of Al - 5,7 Zn - 2,5 Mg - 1,6 Cu as a function of temperature,  $T$ .**

Explanation

Key	Description	Comments	References
○	Al alloy 7075-T6 (Alcoa). 5,6 Zn, 2,5 Mg, 1,6 Cu, 0,3 Cr, Al balance. $\rho = 2800 \text{ kg.m}^{-3}$ .	As received.	Touloukian (1967)c [40].
□		After heating above 575 K.	

Key	Description	Comments	References
◇	Al Alloy RR77 (British designation). 4,96 Zn, 2,54 Mg, 2,2 Cu, 0,54 Mn, 0,31 Fe, 0,26 Si, trace Ti, Al balance.	Wrought, 2 h solution heat treatment at 720 K, quenched in water at 340 K, aged 4 h at 408 K and aircooled.	
▽		As received.	

See also [ECSS-E-HB-31-01 Part 14, clause 8.4](#), where  $k$  is given in the temperature range 25 K - 300 K.

Thermal conductivity integral: Figure 4-48.

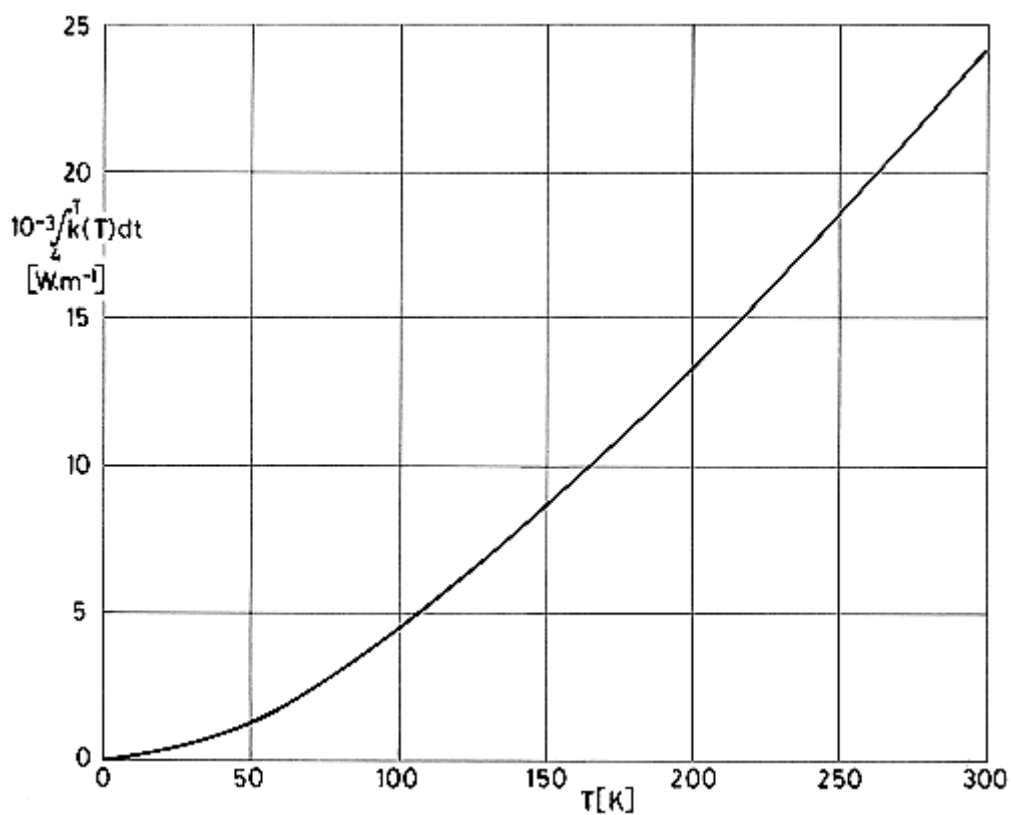


**Figure 4-48: Thermal conductivity integral of Al – 5,7 Zn – 2,5 Mg – 1,6 Cu as a function of temperature,  $T$ .**

Explanation

Description	Comments	References
Al alloy 75 S (Canadian commercial designation).		Coston (1967) [18].

3.2.3. Thermal diffusivity.

Effect of temperature on thermal diffusivity: Figure 4-49.

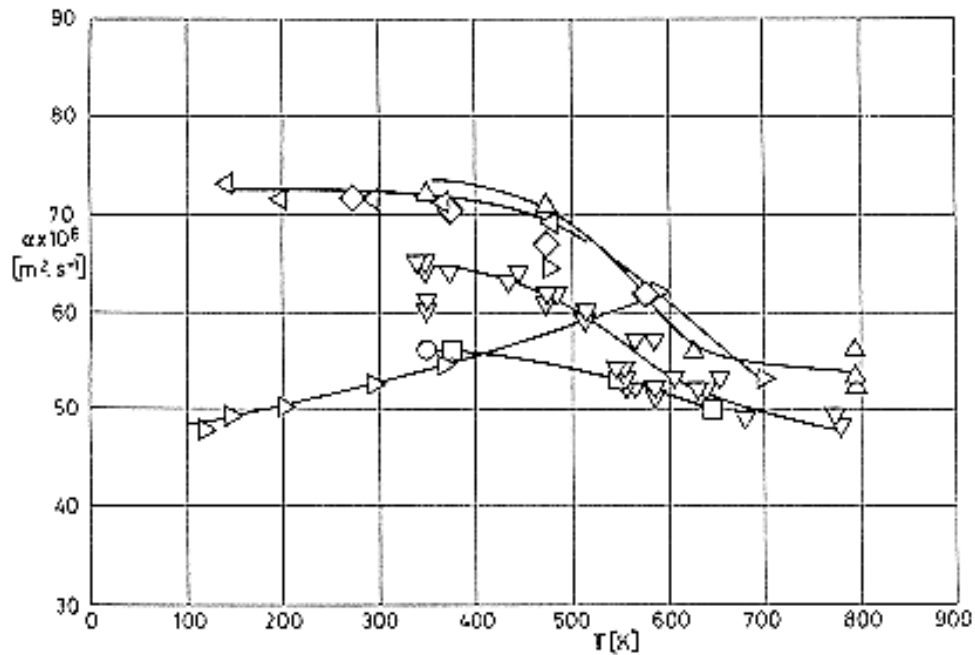


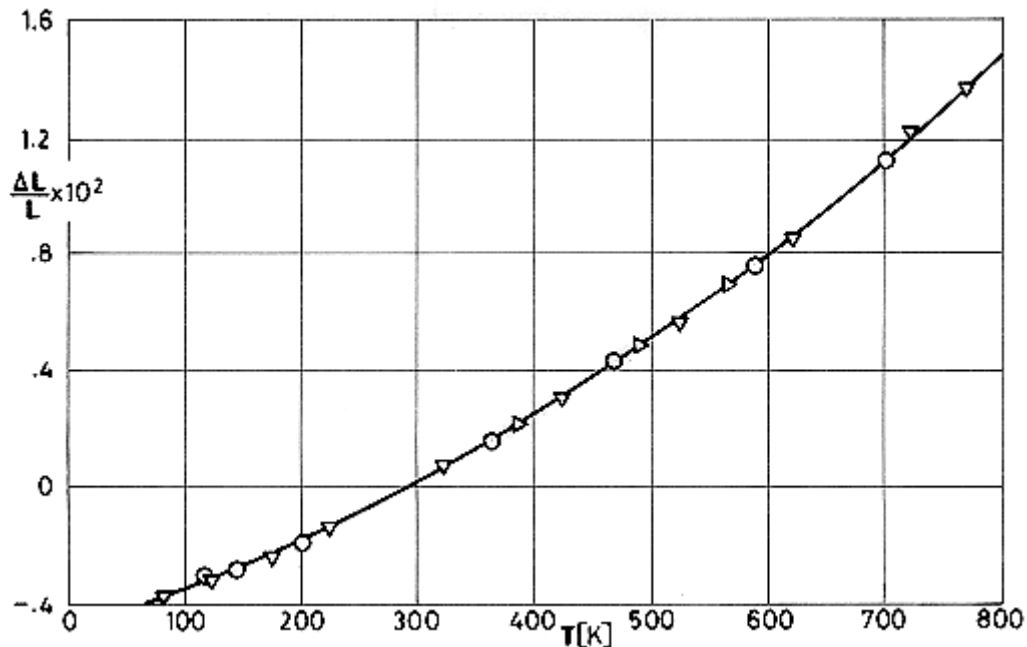
**Figure 4-49: Thermal diffusivity,  $\alpha$ , of Al - 5,7 Zn - 2,5 Mg - 1,6 Cu as a function of temperature,  $T$ .**

Explanation

Key	Description	Comments	References
○	Al alloy 7075-T6. Nominal composition.	Measured after exposure to radiation and followed by cooling.	Touloukian (1967)c [40].
□		Measured after another exposure to radiation and followed by cooling.	
△		Measured after the third cycle of exposure.	
▽		Averaged values on measurements after from 4 <sup>th</sup> to 8 <sup>th</sup> exposure cycles.	
▷	Al alloy 7075-T6. 5,6 Zn, 2,5 Mg, 1,6 Cu, Al balance.	As received.	
◁		Heated above 575 K.	
◇	Al alloy 75S (Canadian commercial designation). 5,5 Zn, 2,5 Mg, 1,5 Cu, 0,3 Cr, 0,2 Mn.	Annealed at 720 K.	

## 3.2.4. Thermal expansion.

Effect of temperature on thermal expansion: Figure 4-50.



Note: non-si units are used in this figure

**Figure 4-50: Linear thermal expansion,  $\Delta L / L$ , of Al - 5,7 Zn - 2,5 Mg - 1,6 Cu as a function of temperature,  $T$ .**

Explanation

Key	Description	Comments	References
○	Al alloy 7075-T6 (Alcoa). 5,1-6,1 Zn, 2,1-2,9 Mg, 1,2-2,0 Cu, 0,7 Fe, 0,5 Si, Al balance.	Tested in vacuum.	Touloukian (1967)c [40].
▽	Al alloy 75S-T6 (Canadian commercial designation). 5,6 Zn, 2,5 Mg, 1,6 Cu, 0,3 Cr, Al balance. $\rho = 2800 \text{ kg.m}^{-3}$ .	Tested at 1,5-2,5 K/min rise in argon.	
▷	Al alloy RR77 (British designation). 4,96 Zn, 2,54 Mg, 2,20 Cu, 0,54 Mn, 0,31 Fe, 0,26 Si and trace Ti, Al balance.	Wrought, 2 h solution heat treatment at 720 K, quenched in water at 340 K, aged 4 h at 408 K and aircooled.	

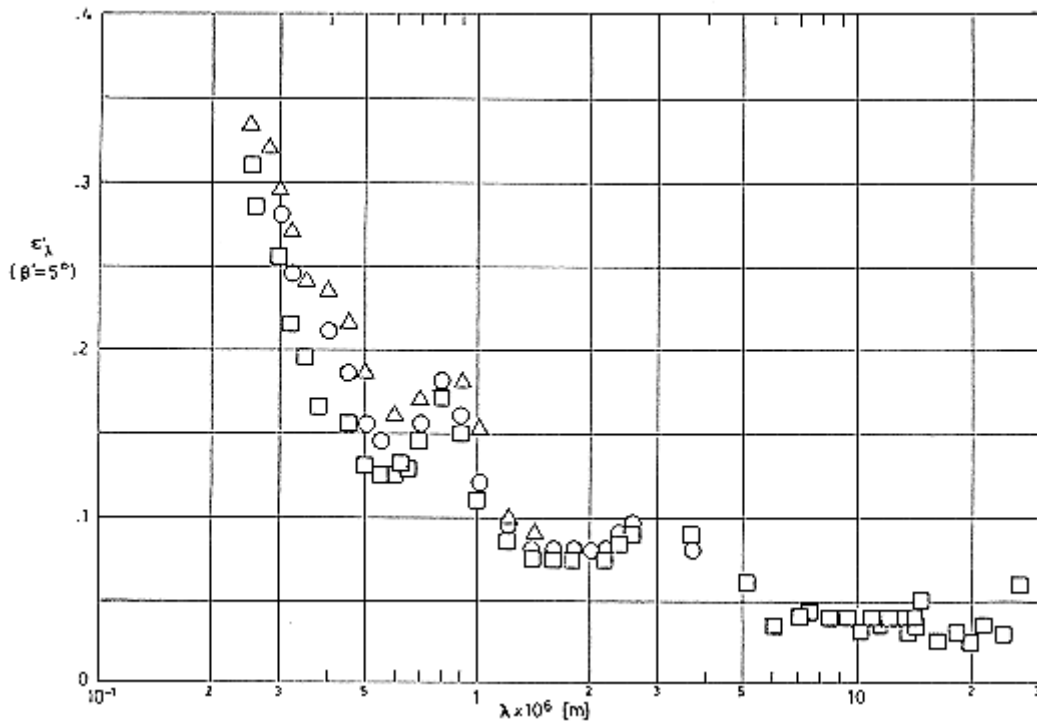
## 3.2.5. Melting range.

750 K - 910 K. (ASMH (1974)c [10]).

### 3.3. Thermal radiation properties

#### 3.3.1. Emittance

##### 3.3.1.1. Normal spectral emittance ( $\beta' = 0$ ): Figure 4-51.



Note: non-si units are used in this figure

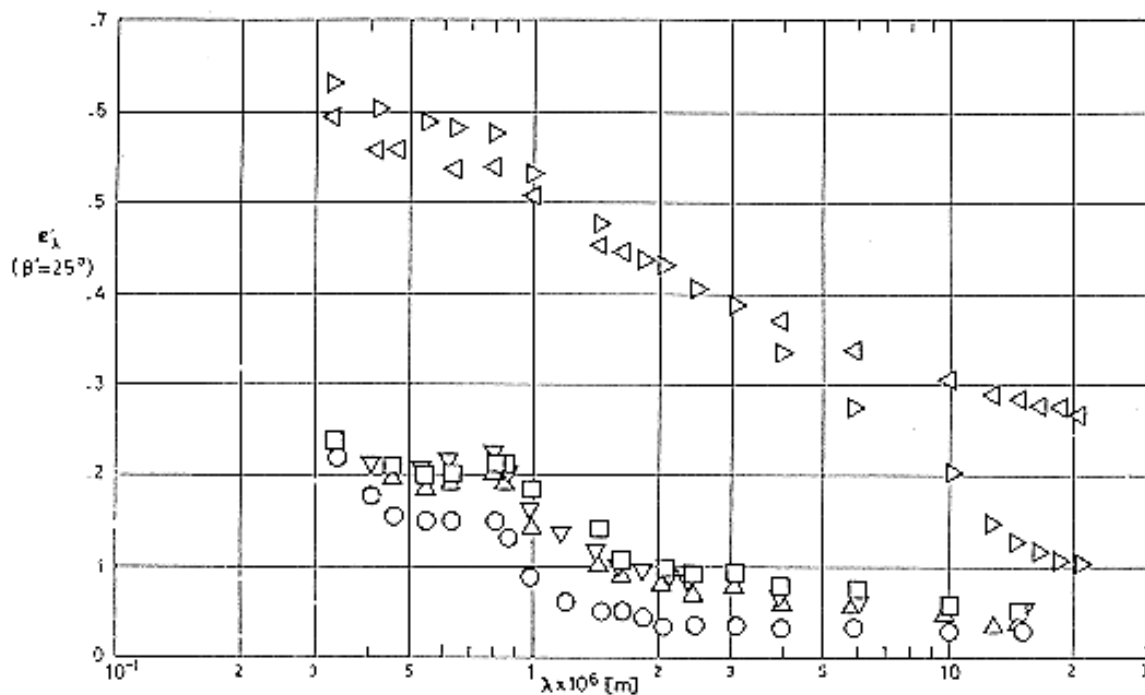
**Figure 4-51: Normal spectral emittance,  $\epsilon'_{\lambda}$ , of Al - 5,7 Zn - 2,5 Mg - 1,6 Cu as a function of wavelength,  $\lambda$ .**

Explanation

Key	Description	Comments	References
○	Al alloy 7075. 5,6 Zn, 2,5 Mg, 1,6 Cu, 0,3 Cr, Al balance. Surface roughness $0,081 \times 10^{-6}$ m – $0,112 \times 10^{-6}$ m (center line average).	Sample temperature: $T = 323$ K. Measured in nitrogen. Computed by $\epsilon = 1 - R(2\pi, 5^\circ)$ .	Touloukian & DeWitt (1970) [42]
□	Different sample, same as ○ specimen and conditions except surface roughness $0,048 \times 10^{-6}$ m – $0,064 \times 10^{-6}$ m (center line average).		



Key	Description	Comments	References
△	Different sample, same as ○ specimen and conditions except surface roughness $0,081 \times 10^{-6} \text{ m}$ – $0,113 \times 10^{-6} \text{ m}$ (center line average).		

 3.3.1.1.2. Angular spectral emittance ( $\beta' = 25^\circ$ ): Figure 4-52.


Note: non-si units are used in this figure

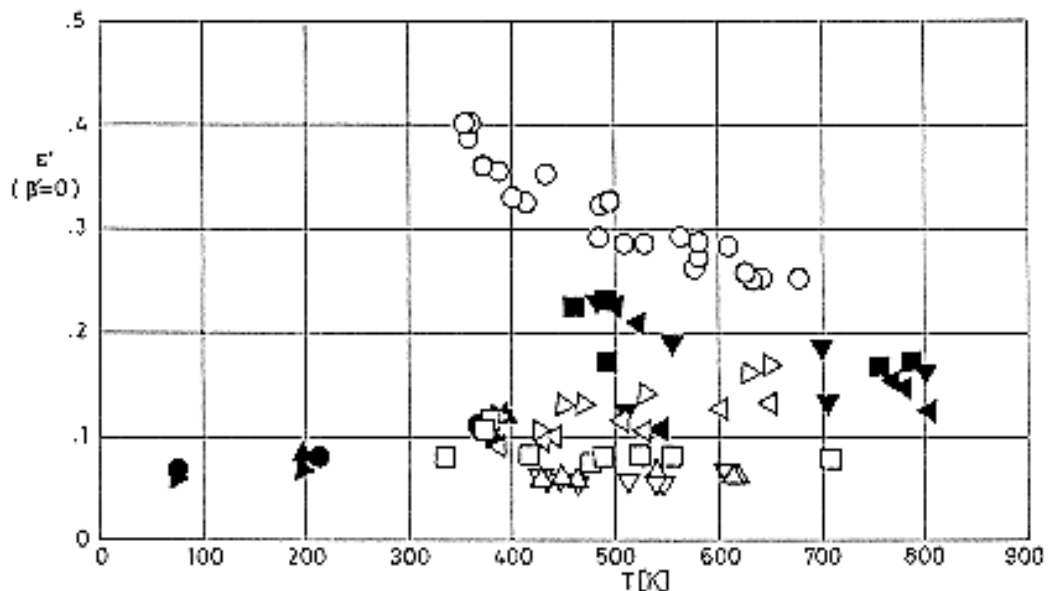
**Figure 4-52: Angular spectral emittance,  $\epsilon'_{\lambda}$ , of Al - 5,7 Zn - 2,5 Mg - 1,6 Cu as a function of wavelength,  $\lambda$ .**

## Explanation

Key	Description	Comments	References
○	Al alloy 7075-T6. 5,6 Zn, 2,5 Mg, 1,6 Cu, 0,3 Cr, Al balance. Polished. Surface roughness $0,051 \times 10^{-6} \text{ m}$ – $0,102 \times 10^{-6} \text{ m}$ (RMS).	Sample temperature: $T = 306 \text{ K}$ .	Touloukian & DeWitt (1970) [42]
□	Al alloy 7075-T6. 5,6 Zn, 2,5 Mg, 1,6 Cu, 0,3 Cr, Al balance. Sanded with 150 grit paper (grit sieve opening $104 \times 10^{-6} \text{ m}$ ). Surface roughness: in line $0,254 \times 10^{-6} \text{ m}$ –	Authors assumed $\epsilon = \alpha = 1 - \rho$	

Key	Description	Comments	References
	0,381x10 <sup>-6</sup> m, across 1,78x10 <sup>-6</sup> m – 2,29x10 <sup>-6</sup> m (RMS).	(25°, 2π).	
△	Al alloy 7075-T6. 5,6 Zn, 2,5 Mg, 1,6 Cu, 0,3 Cr, Al balance. Sanded with 80 grit paper (grit sieve opening 175x10 <sup>-6</sup> m). Surface roughness: in line 0,508x10 <sup>-6</sup> m – 1,52x10 <sup>-6</sup> m, across 3,81x10 <sup>-6</sup> m – 4,32x10 <sup>-6</sup> m (RMS).		
▽	Al alloy 7075-T6. 5,6 Zn, 2,5 Mg, 1,6 Cu, 0,3 Cr, Al balance. Sanded with 40 grit paper (grit sieve opening 42x10 <sup>-6</sup> m). Surface roughness: in line 1,27x10 <sup>-6</sup> m – 2,54x10 <sup>-6</sup> m, across 6,86x10 <sup>-6</sup> m – 7,62x10 <sup>-6</sup> m (RMS).		
▷	Al alloy 7075-T6. 5,6 Zn, 2,5 Mg, 1,6 Cu, 0,3 Cr, Al balance. Sandblasted with 250 mesh silicon carbide (mesh opening 60x10 <sup>-6</sup> m). Surface roughness 0,254x10 <sup>-6</sup> m – 0,381x10 <sup>-6</sup> m (RMS).		
◁	Al alloy 7075-T6. 5,6 Zn, 2,5 Mg, 1,6 Cu, 0,3 Cr, Al balance. Sandblasted with 60 mesh silicon carbide (mesh opening 250x10 <sup>-6</sup> m). Surface roughness 6,35x10 <sup>-6</sup> m – 7,62x10 <sup>-6</sup> m (RMS).		

Effect of temperature on normal total emittance: Figure 4-53.



Note: non-si units are used in this figure

Figure 4-53: Normal total emittance,  $\epsilon'$ , of Al - 5,7 Zn - 2,5 Mg - 1,6 Cu as a function of temperature,  $T$ .

## Explanation

Key	Description	Comments	References
○	Al alloy 75-ST (alclad) (Canadian Commercial designation). 5,6 Zn, 2,5 Mg, 1,6 Cu, 0,3 Cr, Al balance.	Effect of viewing configuration change was apparent.	Touloukian & DeWitt (1970) [42].
□		Another change in viewing configuration.	
△		Another change in viewing configuration.	
▽	Different sample, same as above specimen and conditions. Unpolished.		
▷	Different sample, same as white ○ specimen and conditions. Polished with aerobright and Bon Ami.		
◁	Same as above. Repeated measurement one day later.		
●	Al alloy 75-ST (alclad) (Canadian Commercial designation). 5,6 Zn, 2,5 Mg, 1,6 Cu, 0,3 Cr, Al balance. Cleaned with methyl alcohol.	Heating. Measuring in air (0,133 Pa).	
■	Different sample, same as above specimen and conditions.	Measured in argon (0,133 Pa).	
▲	Different sample, same as black ○ specimen and conditions except scrubbed with Bon Ami and a wet cloth, washed and dried, wiped with toluene and alcohol.		
▼	Different sample, same as above specimen and conditions.	Measured in argon (0,133 Pa).	
►	Different sample, same as black ○ specimen and conditions except polished and then finished with a wool bulf and rouge and washed. Surface free from scratches.		
◄	Different sample, same as above specimen and conditions.	Measured in argon (0,133 Pa).	

3.3.1.4. Hemispherical total emittance

75-ST (Alclad) (Canadian commercial designation). Nominal composition.

Sample temperature: 303 K.

Unpolished surface. Measured in air.

$\epsilon = 0,02$  (Touloukian (1967)c [40]). See Table 4-19.

**Table 4-19: Hemispherical Total Emittance of Al – 5,7 Zn – 2,5 Mg – 1,6 Cu Conversion Coatings.**

T [K]	$\epsilon$	Comments.
293	0,234	Alodined Al alloy 7075-T6, 5,6 Zn, 2,5 Mg, 1,6 Cu, 0,3 Cr, Al balance. Substrate sandblasted. Measured in vacuum ( $6,67 \times 10^{-4}$ Pa).
259	0,117	Similar to above specimen and conditions except substrate alclad.
273	0,100	Similar to above specimen and conditions except substrate smooth and unclad.
307	0,091	
313	0,091	
217	0,790	Al alloy 7075-T6 Martin Hardcoate anodize. 5,6 Zn, 2,5 Mg, 1,6 Cu, 0,3 Cr, Al balance. Measured in vacuum ( $6,67 \times 10^{-4}$ Pa).
242	0,849	
285	0,869	
313	0,856	

NOTE From Touloukian, DeWitt & HERNICZ (1972) [43].

## 3.3.2. Absorptance

## 3.3.2.5. Solar absorptance

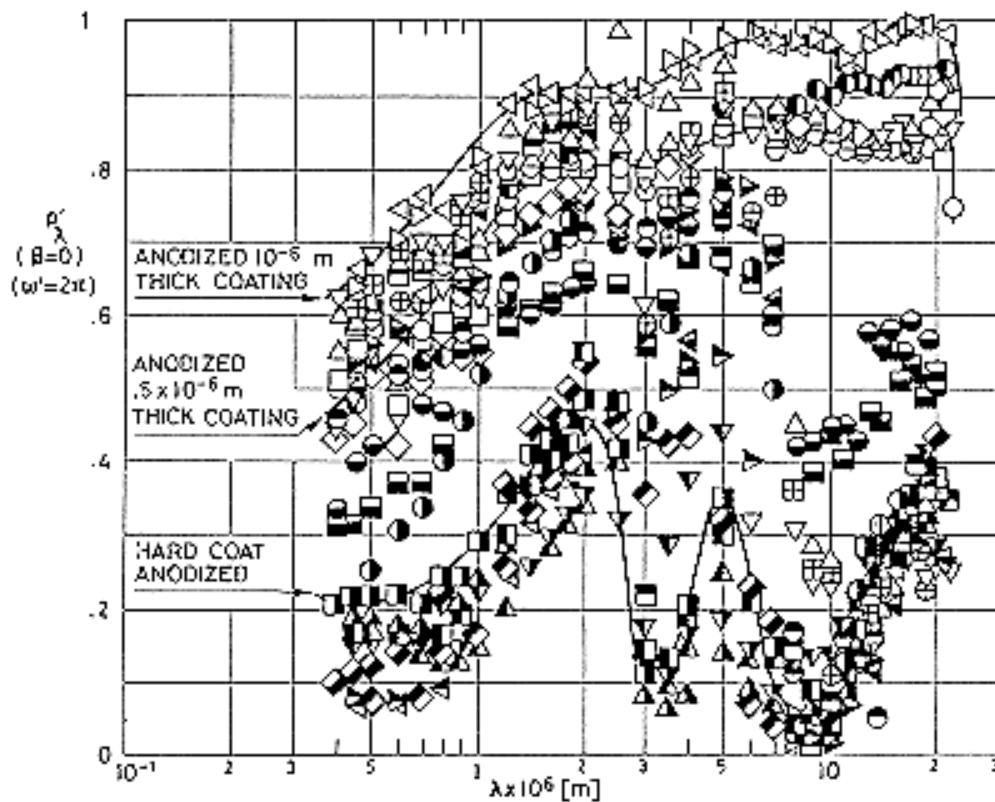
## 3.3.2.5.1. Normal solar absorptance: Table 4-20.

**Table 4-20: Normal Solar Absorptance and Normal-Hemispherical Solar Reflectance of Al – 5,6 Zn – 2,5 Mg 1,6 Cu.**

$T$ [K]	$\beta^\circ$	$\alpha_s$	$\rho_s'$	Comments
311	$\sim 0$	0,46	0,538	Al alloy 75-ST (Canadian commercial designation). 5,6 Zn, 2,5 Mg, 1,6 Cu, 0,3 Cr, Al balance. Heated to 324 K. Clean and smooth surface. $\alpha_s$ measured in air at sea level. $\rho_s'$ from $\alpha_s$ .
311	$\sim 0$	0,61	0,391	Above specimen and conditions except reheated to 559 K.
311	$\sim 0$	0,64	0,358	Above specimen and conditions except reheated to 795 K.
311	$\sim 0$	0,34	0,659	Different sample. Same specimen and conditions as in the first case except heated to 314 K. Polished. Surface free from scratches.
311	$\sim 0$	0,24	0,756	Above specimen and conditions except reheated to 567 K.
311	$\sim 0$	0,51	0,489	Above specimen and conditions except reheated to 783 K.
311	$\sim 0$	0,59	0,409	Different sample. Same specimen and conditions as in the first case except heated to 319 K. Cleaned with methyl alcohol.
311	$\sim 0$	0,66	0,341	Above specimen and conditions except reheated to 617 K.
311	$\sim 0$	0,63	0,371	Above specimen and conditions except reheated to 755 K.
298	$\sim 0$		0,67	Al alloy 75-ST (Canadian commercial designation). 5,6 Zn, 2,5 Mg, 1,6 Cu, 0,3 Cr, Al balance. Measured in air.

NOTE From Touloukian & DeWitt (1970) [42].

## 3.3.3. Reflectance

 3.3.3.2.1. Normal-hemispherical spectral reflectance ( $\beta = 0, \omega' = 2\pi$ ): Figure 4-54.


Note: non-si units are used in this figure

**Figure 4-54: Normal-hemispherical spectral reflectance,  $\rho'_\lambda$  of Al - 5,7 Zn - 2,5 Mg - 1,6 Cu conversion coatings, as a function of wavelength,  $\lambda$ .**

## Explanation

Key	Description	Comments	References
○	Al alloy 7075. Nominal composition.	Sample temperature: $T = 298$ K. Mechanically and electropolished, boric acid anodized, $10^{-6}$ m thick coating. Measured in $\sim 10^{-4}$ Pa vacuum. Converted from $R(2\pi, 0^\circ)$ .	Touloukian (1967)c [40]. Touloukian, DeWitt & Hernicz (1972) [43].
△		$T = 422$ K. Same specimen and conditions as ○.	
□		$T = 589$ K. Same specimen and conditions as ○.	
▽		$T = 714$ K.	

Key	Description	Comments	References
		Same specimen and conditions as ○.	
◇		$T = 298$ K. Same specimen and conditions as ○ after high temperature runs.	
△		$T = 298$ K. Treated as ○ except shorted anodizing time (1/3 standard). $0,5 \times 10^{-6}$ m thick coating.	
▽		$T = 298$ K. Mechanically polished and boric acid anodized. Measured in $\sim 10^{-4}$ Pa vacuum. Converted from $R(2\pi, 0^\circ)$ .	
●		$T = 298$ K. Mill finished, electropolished and boric acid anodized. Measured in $1,33 \times 10^{-1}$ Pa vacuum.	
▲	Al alloy 7075. 5,1-6,1 Zn, 2,1-2,9 Mg, 1,2-2,0 Cu, 0,7 Fe, 0,5 Si,	$T = 298$ K. Mechanically polished and electropolished, hard coat anodized. Measured in $\sim 10^{-4}$ Pa vacuum. Converted from $R(2\pi, 0^\circ)$ .	
■	0,18-0,4 Cr, 0,3 Mn, 0,2 Ti, Al	$T = 298$ K. Treated as above and sealed.	
▼	balance.	$T = 422$ K. Same specimen and conditions as above.	
◆		$T = 589$ K. Same specimen and conditions as above.	
▲		$T = 714$ K. Same specimen and conditions as above.	
▽		$T = 298$ K. Same specimen and conditions as above after high temperature runs.	
■		$T = 298$ K. Treated as ▲ and heated in air at 700 K for 30 min.	
●		$T = 298$ K. Mechanically polished and electropolished, hard coat anodizing (1/3 standard time).	
▲	Al alloy 7075.	$T = 298$ K. Mill finished and electropolished, hard coat anodized, sealed. Measured in $\sim 10^{-4}$ Pa vacuum. Converted from	

Key	Description	Comments	References
		$R(2\pi, 0^\circ)$ .	
▼		$T = 298$ K. Mechanically polished hard coat anodized. Measured in $\sim 1,33 \times 10^{-4}$ Pa vacuum. Converted from $R(2\pi, 0^\circ)$ .	
◆		$T = 298$ K. Treated as ▼ except shorter anodizing (1/3 standard) and sealed.	
▲		$T = 298$ K. Mechanically and electropolished, sulfuric acid anodized. Measured in $\sim 10^{-4}$ Pa vacuum. Converted from $R(2\pi, 0^\circ)$ .	
▽		$T = 422$ K. Same specimen and conditions as above.	
●		$T = 589$ K. Same specimen and conditions as above.	
●		$T = 714$ K. Same specimen and conditions as above.	
■		$T = 298$ K. Same specimen and conditions as above after high temperature runs.	
■		$T = 298$ K. Mechanically and electropolished, sulfuric acid anodized, $1,4 \times 10^{-6}$ m thick coating, sealed. Measured in $\sim 10^{-4}$ Pa vacuum. Converted from $R(2\pi, 0^\circ)$ .	
⊗		$T = 298$ K. Same as above except not sealed.	
▲		$T = 298$ K. Same as above except shorter anodizing time ( $\frac{1}{4}$ standard).	
▽		$T = 298$ K. Same as above and sealed.	
⊗		$T = 298$ K. Mechanically and polished, sulfuric acid anodized 1/3 standard time, sealed. Measured in $\sim 10^{-4}$ Pa vacuum. Converted from $R(2\pi, 0^\circ)$ .	



3.3.3.9.1. Normal-hemispherical solar reflectance. See Table 4-20 above.

### 3.4. Other physical properties

#### 3.4.1. Electrical resistivity (at room temperature).

Condition	T6	T73	T76
$\sigma^{-1} \times 10^6$ [ $\Omega \cdot m$ ]	0,052	0,043	0,045

NOTE From McCall (1979) [25].

## 4. ENVIRONMENTAL BEHAVIOR

### 4.1. Prelaunch

This alloy is normally coated. The surface condition is as important as the material. The production of the coating should be carefully controlled.

### 4.2. Postlaunch

No known restrictions other than structural.

## 5. CHEMICAL PROPERTIES

### 5.1. Solution potential (vs. decinormal calomel electrode).

Condition	T6	T73	T76
Sol.Pot. [V] <sup>a</sup>	-0,83	-0,84	-0,84

<sup>a</sup> Varies  $\pm 0,02$  V with quenching rate.

NOTE From McCall (1979) [25].

### 5.2. Corrosion resistance

This alloy should be protected at least on faying surfaces.

Condition	Stress-Corrosion Cracking
T6, T651, T652, T6510, T6511	Service failures with sustained tension stress acting on short transverse direction relative to grain structure. Limited failures in laboratory tests of long transverse specimens.
T73, T7351	No known instance of failure in service. Limited failures in laboratory tests of short transverse specimens.

NOTE From McCall (1979) [25].

Assemblies of this alloy with magnesium alloys require protective insulation (Braun (1979) [15]).

## 6. FABRICATION

6.2. Forming. Cold workability is poor.

6.3. Welding.

Gas. no commonly used methods have been developed.

Arc. Limited weldability because of crack sensitivity or loss in resistance to corrosion and mechanical properties.

Resistance Spot and Seam. Welbadle with special techniques or for specific applications which justify trials or development testing.

Brazing. No commonly used methods have been developed.

Soldering. Solderability is poor.

These characteristics do not change significantly with heat treatment.

From McCall (1979) [25].

6.4. Machining. Machinability of this alloy is good (compared to others of the same series) and can be improved through heat treatment.

6.5. Heat treatment.

Treatment	Forging	Annealing	Quenching and Aging	
			Quenching	Aging
Usual temperatures and times.	650 K - 720 K	Full annealing: 690 K, followed by 6 h at 500 K for long term storage. Stress relieve annealing: 610 K.	738 K $\pm$ 5 K in water	24 h at 393 K $\pm$ 5 K.

NOTE From UNE (1982) [45].

6.6. Anodizing. This alloy can be anodized to increase corrosion resistance, prior to painting or plating, or to increase emittance (see Table 4-19). Any of the three principal types of anodizing processes (chromic acid, sulfuric acid or hard anodizing) can be used (Ball (1982) [12]).

## 7. AVAILABLE FORMS AND CONDITIONS

This alloy is available in the full commercial range of sizes for sheets; plates; extrude rods, bars and wires; extruded shaped; extruded tubes; cold finished rods, bars and wires; drawn tubes and forgings (McCall (1979) [25]).

## 8. USEFUL TEMPERATURE RANGE

The tensile strength of this alloy (T6) decreases markedly above 400 K (McCall (1979) [25]).

This alloy is not normally used in applications involving cryogenic temperatures. Information on its behavior at low temperatures is scanty. Tensile properties and fracture roughness at temperatures down to 4 K and results of fatigue-life tests are given by Campbell (1980) [17]. Other alloys of the Aluminium 7000 series exhibit good behavior at temperatures as low as 20 K (Develay et al (1967) [19]).

## 9. APPLICATIONS

Aircraft and other structures, many presently operating commercial jets (Simenz & Guess (1980) [34]).

Aircraft structural parts and other highly stresses structural applications where very high strength and good resistance to corrosion is required.

Caution should be exercised in T6 temper applications where sustained tensile stresses are encountered, either residual or applied, particularly in the transverse grain direction. In such instances the T73 temper should be considered at some sacrifice in tensile strength (McCall (1979) [25]).

## 10. OTHER QUOTATIONS

These alloys have been explicitly quoted in the following pages of this Handbook.

[ECSS-E-HB-31-01 Part 4, clause 5.2](#), Al alloy 7075-T6

Thermal joints conductance. Bare joints.

[ECSS-E-HB-31-01 Part 12, clause 5.2.2.2](#), Al alloy 7075

Used in bellows for louvers actuators.

[ECSS-E-HB-31-01 Part 14, clause 6.3.3](#), Al alloy 7075

Figure of Merit,  $\sigma/k$ , of supporting materials at cryogenic temperatures.

[ECSS-E-HB-31-01 Part 14, clause 8.4](#), Al alloy 75 S (Canadian commercial designation)

Thermal conductivity in the temperature range 25 K - 300 K.

[ECSS-E-HB-31-01 Part 14, clause 9.3.1](#), Al alloy V95 (USSR designation)

Data sources of mechanical properties at cryogenic temperatures.

[ECSS-E-HB-31-01 Part 14, clause 9.3.2](#), Al alloy 7075-T73

Susceptibility to hydrogen embrittlement.

## 4.6 Magnesium-Zink-Thorium alloys

ALLOY Mg - 5,7 Zn - 1,8 Th - 0,7 Zr.

### 1. TYPICAL COMPOSITION, PERCENT

Cu	Ni	Th	Zn	Zr	Others	Mg
- 0,10	- 0,01	1,4 2,2	5,2 6,2	0,5 1	- 0,30	Balance

### 2. OFFICIAL DESIGNATIONS

AECMA	ISO	AFNOR	AMS	BS	DIN
			4438B		MgZn6Th2Zr, 3,5114

### 3. PHYSICAL PROPERTIES

3.1. Density.  $\rho = 1860 \text{ kg}\cdot\text{m}^{-3}$ . (Rhines (1961)).

3.2. Thermal properties

3.2.1. Specific heat

From 293 to 373 K,  $c = 962 \text{ J}\cdot\text{kg}^{-1}\cdot\text{K}^{-1}$ . (Rhines (1961)).

3.2.2. Thermal conductivity

$T \text{ [K]}$	293	320	395	445
$[\text{W}\cdot\text{m}^{-1}\cdot\text{K}^{-1}]$	109 <sup>a</sup>	113 <sup>b</sup>	123 <sup>b</sup>	127 <sup>b</sup>

<sup>a</sup> From Rhines (1961).

<sup>b</sup> From Touloukian (1967)c [40].

3.2.4. Thermal expansion

Mean coefficient of linear expansion,  $\beta$ .

From 293 K to 473 K,  $\beta = 27,1 \times 10^{-6} \text{ K}^{-1}$ . (Rhines (1961)).

$\beta = 27,6 \times 10^{-6} \text{ K}^{-1}$ . (Smithells (1962) [35]).

$\beta = 27,2 \times 10^{-6} \text{ K}^{-1}$ . (ASMH (1974)d [11]).

3.2.5. Melting range.

773 K - 903 K. (Smithells (1962) [35]).

3.3. Thermal radiation properties

3.3.1. Emittance

3.3.1.2. Normal total emittance ( $\beta' = 0$ ).

No data available. For polished Magnesium:  $\varepsilon' = 0,07$ . (Scollon & Carpitelle (1970) [33]).

3.3.2. Absorptance.

3.3.2.5. Solar absorptance.

3.3.2.5.1. Normal solar absorptance.

No data available. For polished Magnesium:  $\alpha_s = 0,27$ . (Scollon & Carpitelle (1970) [33]).

3.4. Other physical properties

3.4.1. Electrical resistivity at 293 K.  $\sigma^{-1} = 6,5 \times 10^{-8} \Omega\cdot\text{m}$ . (Rhines (1961)).

### 5. CHEMICAL PROPERTIES

5.2. Corrosion resistance.

Although this alloy will corrode in industrial, marine and moist environments, it will perform satisfactorily with suitable surface protection and painting. (ASMH (1974)d [11]).

## 6. FABRICATION

6.1. Casting. Good, even into complicated shapes.

6.3. Welding. Good, by argon arc process. Should not be gas-welded.

6.4. Machining. Excellent. This alloy can be chemically milled by sulphuric, nitric or hydrochloric acids of 5 percent strength.

6.5. Heat treatment. Good in SO<sub>2</sub> atmosphere. This alloy is normally used in T-5 condition.

From ASMH (1974)d [11].

## 7. AVAILABLE FORMS AND CONDITIONS

Sand, permanent mold and die castings. Normally used in T-5 condition. (ASMH (1974)d [11]).

## 8. USEFUL TEMPERATURE RANGE

This alloy shows excellent structural characteristics up to 425 K. Above this temperature the strength drops sharply.

## 9. APPLICATIONS

This alloy should be considered for any aerospace application requiring a high strength-to-weight ratio at temperatures up to 420 K. In addition, it has excellent dimensional stability at service temperatures up to the quoted value. (ASMH (1974)d [11]).

Safety precautions should be directed to the prevention of fires, burns, and explosions. (ASMH (1974)d [11]).

# 4.7 Titanium-Aluminium-Tin alloys

ALLOY Ti -5 Al - 2,5 Sn.

## 1. TYPICAL COMPOSITION, PERCENT

Al	C	Fe	H	N	O	Sn	Ti
4	-	-	-	-	-	2	Balance
6	0,1	0,5	0,02	0,07	0,3	3	

## 2. OFFICIAL DESIGNATIONS

AECMA	ISO	AFNOR	AMS	BS	DIN
			4926		

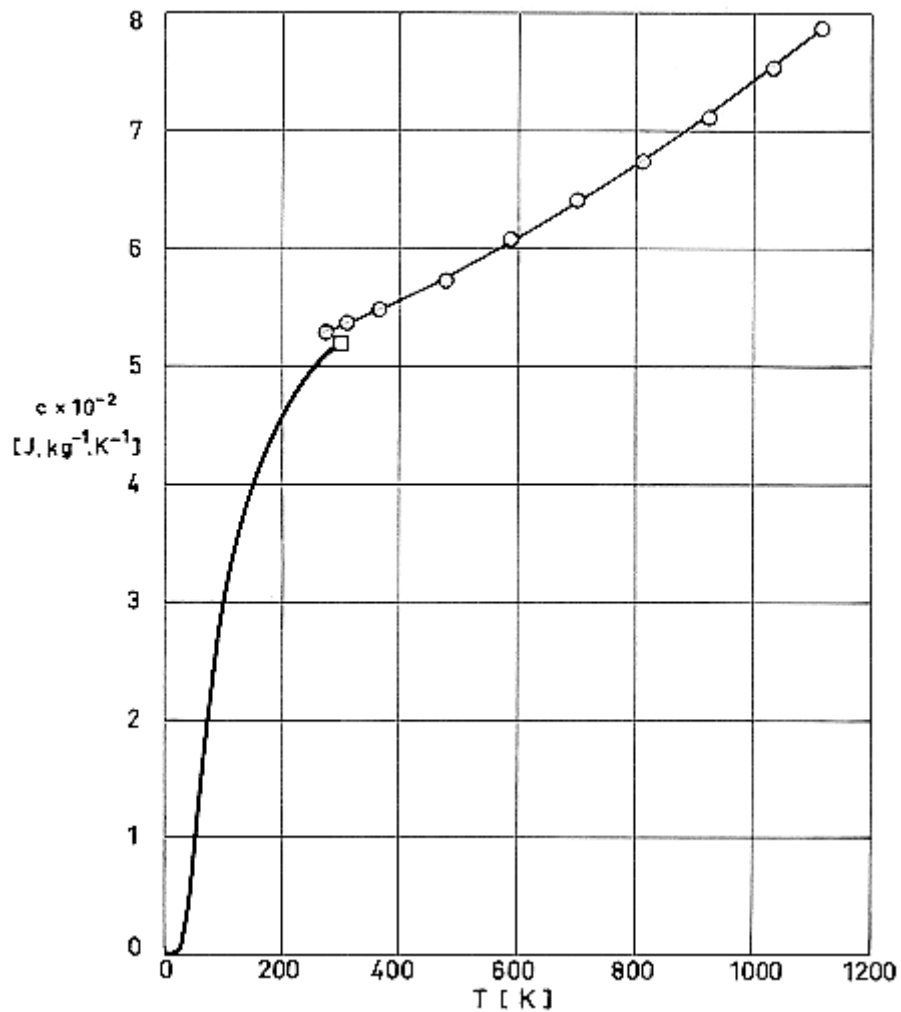
## 3. PHYSICAL PROPERTIES

3.1. Density.  $\rho = 4460 \text{ kg.m}^{-3}$ . (Stuart Lyman (1961) [36]).

3.2. Thermal properties

## 3.2.1. Specific heat

Effect of temperature on specific heat: Figure 4-55.


 Figure 4-55: Specific heat,  $c$ , of Ti - 5 Al - 2,5 Sn as a function of temperature,  $T$ .

Explanation

Key	Description	Comments	References
○	Nominal composition.		Stuart Lyman (1961) [36].
□	Nominal composition.		Coston (1967) [18].
—	Titanium.		Coston (1967) [18].

## 3.2.2. Thermal conductivity

Effect of temperature on thermal conductivity: Figure 4-56.

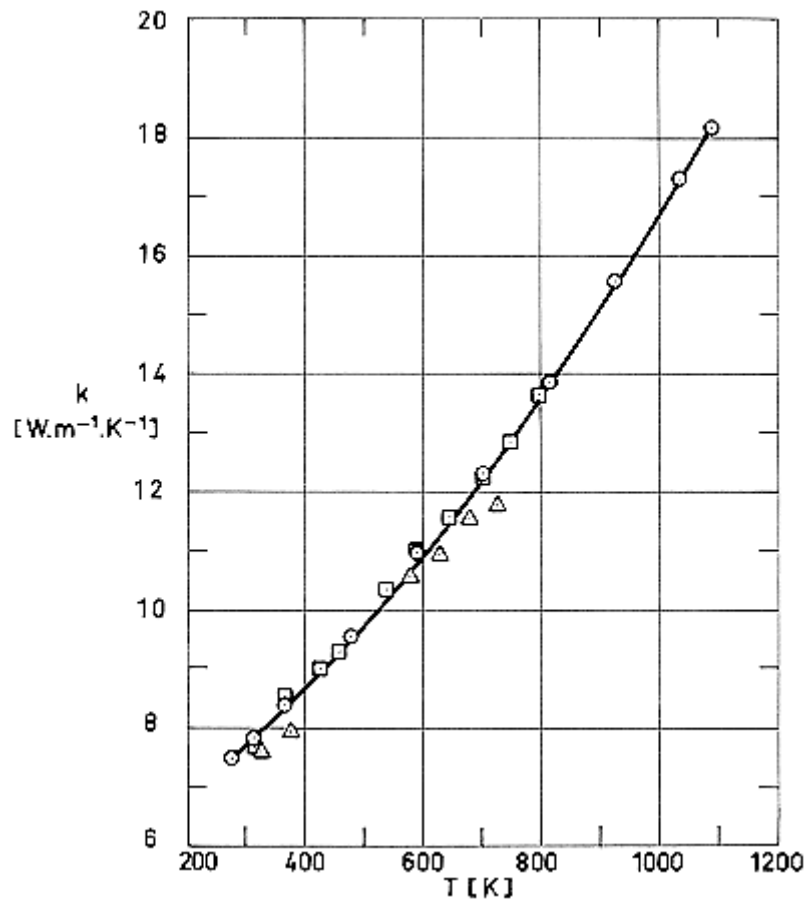


Figure 4-56: Thermal conductivity,  $k$ , of Ti - 5 Al - 2,5 Sn as a function of temperature,  $T$ .

Explanation

Key	Description	Comments	References
○	Nominal composition.		Stuart Lyman (1961) [36].
□	Nominal composition. Mild annealed.	Reported error $\pm 5\%$ .	Touloukian (1967)c [40].
△	Nominal composition.		

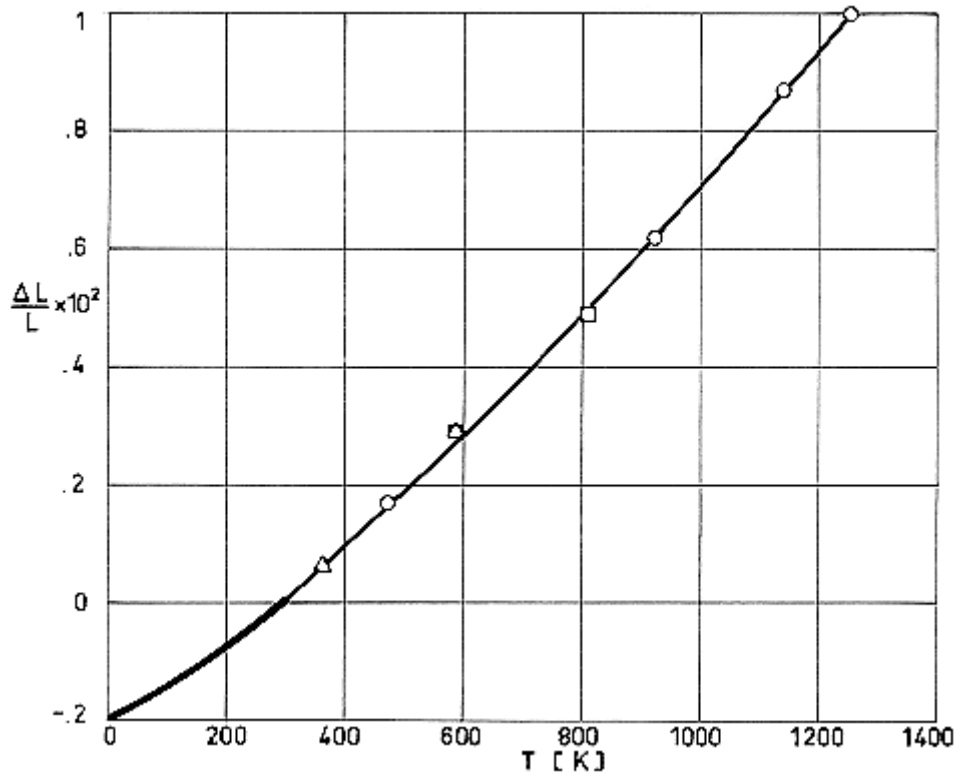
### 3.2.4. Thermal expansion

Mean coefficient of linear expansion,  $\beta$ , between 293 K and given temperature.

T [K]	366	477	588	700	811	922	1033	1144	1255
$\beta \times 10^6$ [K <sup>-1</sup> ]	9,4	9,4	9,5	9,5	9,7	9,9	10,1	10,3	10,3

NOTE From Stuart Lyman (1961) [36].

Effect of temperature on thermal expansion: Figure 4-57.



Note: non-si units are used in this figure

**Figure 4-57: Thermal linear expansion,  $\Delta L/L$ , of Ti - 5 Al - 2,5 Sn as a function of temperature,  $T$ .**

Explanation

Key	Description	Comments	References
○	Nominal composition.		Touloukian (1967)c [40].
□	Nominal composition. Density 4460-4480 kg.m <sup>-3</sup> . Alpha phase.		
△	Same as above except low oxygen content.		
—	Nominal composition.		Cosoton (1967) [18].



## 3.2.5. Melting range

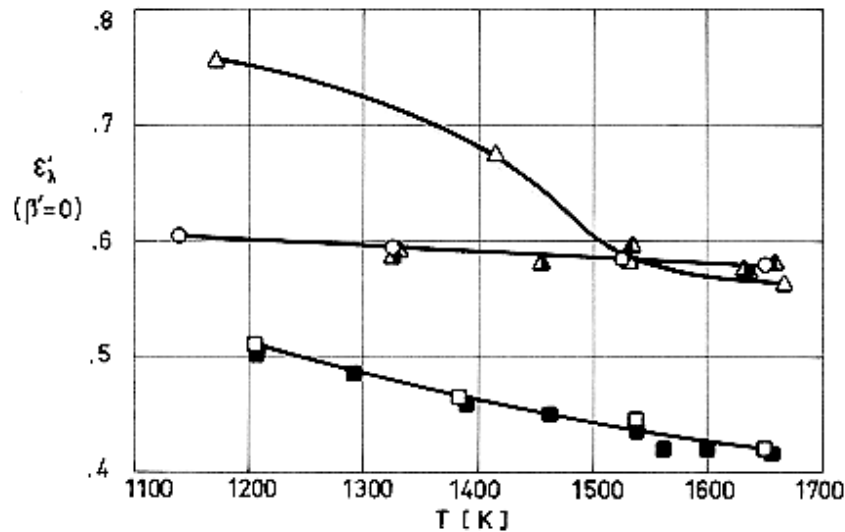
1822 K - 1922 K. (Stuart Lyman (1961) [36]).

## 3.3. Thermal radiation properties

## 3.3.1. Emittance.

 3.3.1.1.1. Normal spectral emittance ( $\beta' = 0$ ).

Effect of temperature on normal emittance for a particular wavelength: Figure 4-58.



Note: non-si units are used in this figure

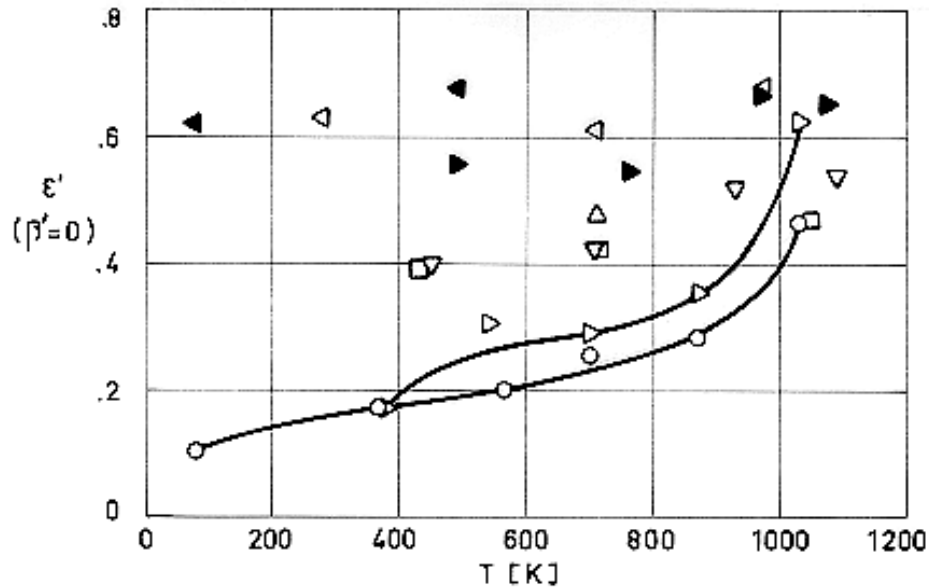
**Figure 4-58: Normal spectral emittance,  $\epsilon_{\lambda}'$ , of Ti - 5 Al - 2,5 Sn as a function of temperature,  $T$ , for  $\lambda = 6,65 \times 10^{-7}$  m.**

Explanation

Key	Description	Comments	References
○	As received. Cleaned with liquid detergent.	Measured in vacuum ( $6,65 \times 10^{-2}$ Pa). Increasing temperature.	Touloukian & DeWitt (1970) [42].
□	Same as above except polished.		
■	Same as above. Cycle 2.		
△	Same as ○ except oxidized in air at red heat for 30 min.		
▲	Same as above. Cycle 2.		
▲	Same as △. Cycle 3.		

3.3.1.2. Normal total emittance ( $\beta' = 0$ ).

Effect of temperature on normal total emittance: Figure 4-59.



Note: non-si units are used in this figure

**Figure 4-59: Normal total emittance,  $\epsilon'$ , of Ti - 5 Al - 2,5 Sn as a function of temperature,  $T$ .**

Explanation

Key	Description	Comments	References
○	Nominal composition. Polished.	Measured in air. Cycle 1.	Touloukian (1967)c [40].
□		Cycle 2 heating.	
△		Cycle 2 cooling.	
▽		Cycle 3.	
▷	Nominal composition. Oxidized at 922 K for 30 min.	Measured in air. Cycle 1.	
▶		Cycle 2.	
◁		Cycle 3 heating.	
◀		Cycle 3 cooling.	

3.3.2. Absorptance

3.3.2.5. Solar absorptance

3.3.2.5.1. Normal solar absorptance: Table 4-21.

**Table 4-21: Normal Solar Absorptance of Ti – 5 Al – 2,5 Sn**

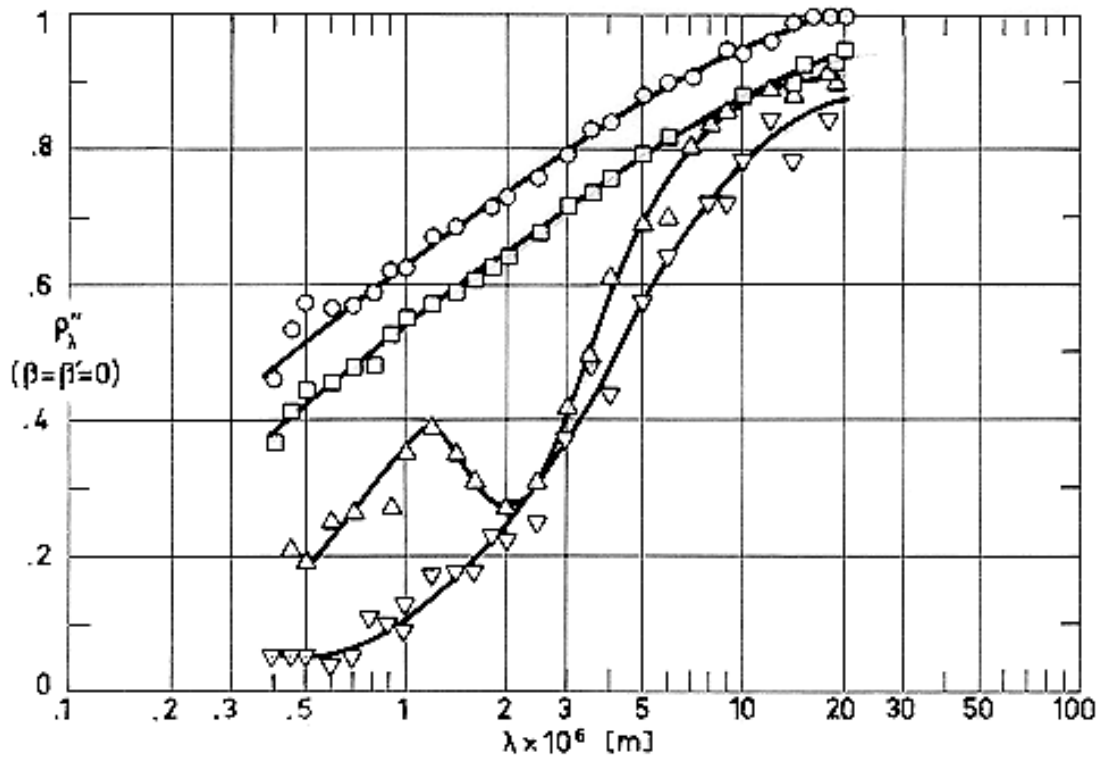
$T$ [K]	$\beta$ (°)	$\alpha_s$	Comments
298	9	0,592	As received; computed from spectral reflectance data for sea level conditions. Mentioned below as specimen 1.
298	9	0,588	Above specimen and conditions except computed for above atmosphere conditions.
298	9	0,489	Different sample, same as 1 specimen and conditions except cleaned.
298	9	0,486	Above specimen and conditions except computed for above atmosphere conditions.
298	9	0,759	Different sample, same as 1 specimen and conditions except oxidized. Mentioned below as specimen 2.
298	9	0,730	Above specimen and conditions except computed for above atmosphere conditions.
298	9	0,511	Different sample, same as 2 specimen and conditions except polished.

NOTE From Touloukian & DeWitt (1970) [42].

3.3.3. Reflectance.

3.3.3.1. Bidirectional spectral reflectance.

Normal-normal spectral reflectance ( $\beta = \beta' = 0$ ): Figure 4-60.



Note: non-si units are used in this figure

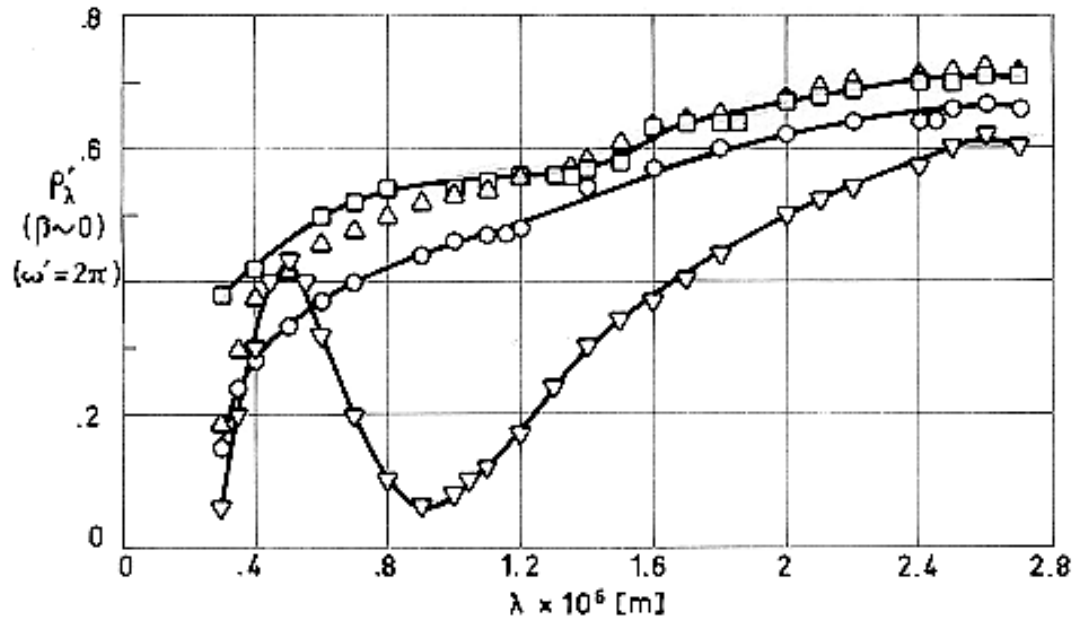
**Figure 4-60: Normal-normal spectral reflectance,  $\rho_{\lambda}''$ , of Ti - 5 Al - 2,5 Sn as a function of wavelength,  $\lambda$ .**

Explanation

Key	Description	Comments	References
○	Nominal composition. Mechanically and electropolished.	Measured in vacuum (1,33x10 <sup>-3</sup> Pa). T = 298 K.	Touloukian (1967)c [40].
□	Same as ○ except mechanically polished.		
△	Same as ○ except mechanically polished; pickled, anodized in NaOH, and sealed. 4x10 <sup>-7</sup> m thick coating.	Measured in vacuum (1,33x10 <sup>-3</sup> Pa). T = 755 K.	
▽			

3.3.3.2. Directional-hemispherical spectral reflectance.

Normal-hemispherical spectral reflectance ( $\beta = 0$ ,  $\omega' = 2\pi$ ): Figure 4-61.



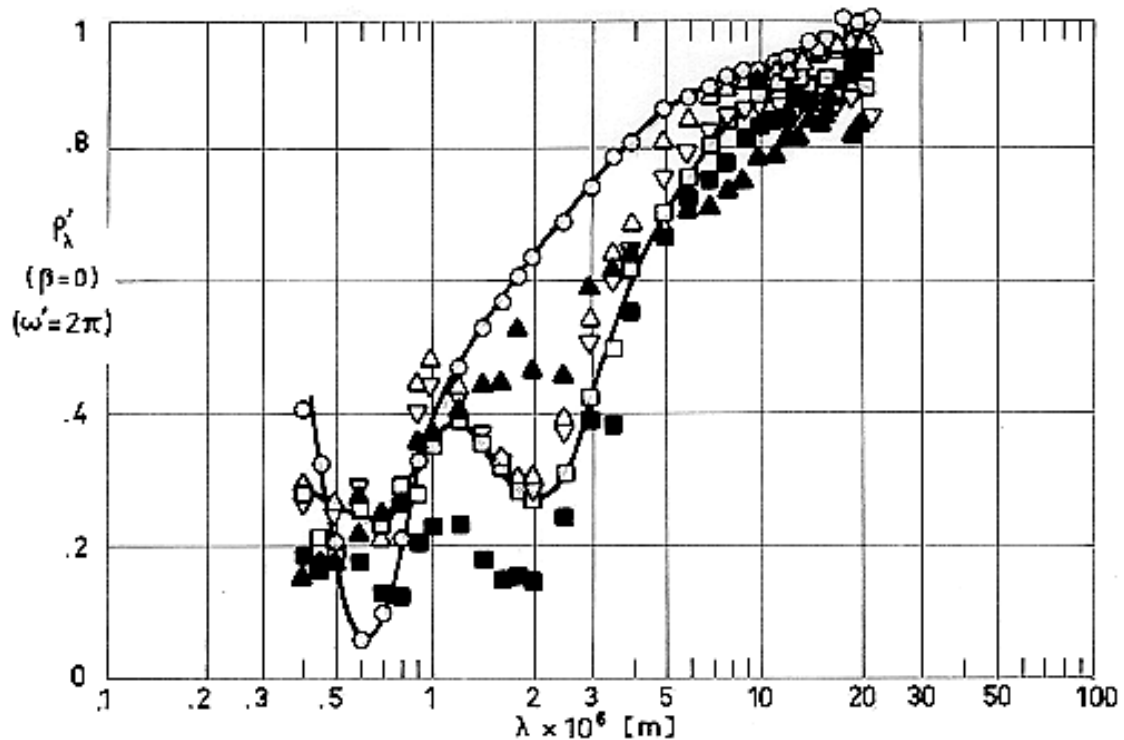
Note: non-si units are used in this figure

Figure 4-61: Normal - hemispherical spectral reflectance,  $\rho_{\lambda}'$ , of Ti - 5 Al - 2,5 Sn as a function of wavelength,  $\lambda$ .

Explanation

Key	Description	Comments	References
○	Nominal composition. As received.	$\beta = 9$ . $T = 298 \text{ K}$ .	Touloukian & DeWitt (1970) [42].
□	Same as ○ except cleaned.		
△	Same as ○ except polished.		
▽	Same as ○ except oxidized at 922 K.		

Effect of anodizing on thermal-hemispherical spectral reflectance): Figure 4-62.



Note: non-si units are used in this figure

Figure 4-62: Normal - hemispherical spectral reflectance,  $\rho_{\lambda}'$ , of Ti - 5 Al - 2,5 Sn, anodized, as a function of wavelength,  $\lambda$ .

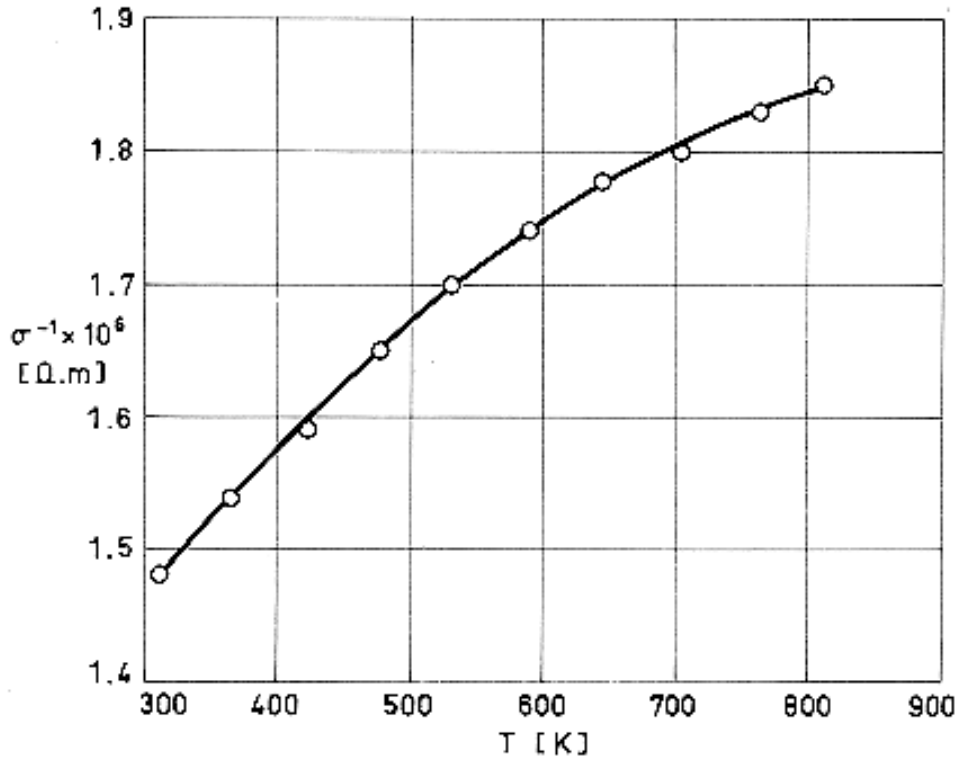
Explanation

Key	Description	Comments	References
○	Anodized in sulphuric acid for 20 min. Substrate mechanically and electro polished.	Measured in vacuum ( $\sim 1,33 \times 10^{-4}$ Pa). Converted from $R(2\pi, 0^\circ)$ . $T = 298$ K.	Touloukian, DeWitt & HERNICZ (1972) [43].
□	Anodized in sodium hydroxide for 20 min. Substrate mechanically polished and pickled.	Same as above except $T = 589$ K.	
■		Same as above except $T = 589$ K.	
△	Same as above except electropolished instead of pickled.	Same as ○.	
▲		Same as ○ except $T = 978$ K.	
▽	Same as □ except anodized in sodium hydroxide for 6,7 min.	Same as ○.	

### 3.4. Other physical properties

#### 3.4.1. Electrical resistivity.

Effect of temperature on electrical resistivity: Figure 4-63.



Note: non-si units are used in this figure

**Figure 4-63: Electrical resistivity,  $\sigma^{-1}$ , of Ti - 5 Al - 2,5 Sn as a function of temperature,  $T$ .**

Explanation

Key	Description	Comments	References
○	Nominal composition. Mild annealed.	Reported error $\pm 5\%$ .	Touloukian (1967)c [40].

3.4.2. Magnetic properties. This alloy is non-magnetic.

Relative permeability:  $\mu/\mu_0 = 1,00005$  measured at  $1,6 \times 10^3 \text{ A.m}^{-1}$ . (ASMH (1974)e [9]).

## 5. CHEMICAL PROPERTIES

5.1. Solution potential (vs. decinormal calomel electrode)

Data not available. Solution potential of Ti pure is +0,20 V (Ross (1972) [31]).

## 5.2. Corrosion resistance

This alloy is highly resistant to corrosion. It has excellent resistance to hot oxidation up to 900 K. It resists the attack by normal acids (except fuming nitric) or alkalis at room and even higher temperatures. (Ross (1972) [31]).

## 6. FABRICATION

6.2. Forming. Good. In sheet forming the minimum bending radius is 5 times the thickness.

6.3. Welding. Good, using TIG or MIG processes.

6.4. Machining. Possible with slow speeds, coarse feeds, and sharp tools.

6.5. Heat treatment. Good. This alloy can only be annealed.

From ASMH (1974)e [9].

## 7. AVAILABLE FORMS AND CONDITIONS

Available in full range of sizes for sheet, strip, plate, bar forgings, wire, extrusions and castings. (ASMH (1974)e [9]).

## 8. USEFUL TEMPERATURE RANGE

The structural use of this alloy should be limited to temperatures below 580 K. The extra-low-interstitial grade (ELI) is recommended for low temperatures uses (as low as 20 K). Fresh fracture surfaces of this alloy, when in contact with liquid oxygen, burn expontaneously, and the reaction may spread at a high rate. (ASMH (1974)e [9]).

## 9. APPLICATIONS

Structural elements, fasteners, bolts and, generally speaking, when high temperature precludes the use of aluminium alloys. Also used in pressure vessels for liquid hydrogen and liquid helium.

# 4.8 Titanium-Aluminium-Tin alloys

Alloy Ti - 6 Al - 2 Sn - 4 Zr - 2 Mo.

## 1. TYPICAL COMPOSITION, PERCENT

Al	Mo	Sn	Zr	Fe	O <sub>2</sub>	H <sub>2</sub>	N <sub>2</sub>	C	Others		Al
									Each	Total	
5,5 6,5	1,8 2,2	1,8 2,2	3,6 4,4	0,25	0,12	0,015	0,05	0,05	0,10	0,40	Balance

## 2. OFFICIAL DESIGNATIONS

AICMA	ISO	AFNOR	AMS	BS	DIN	UNE
			Ti6242			Ti-6Al4ZrMoSn UNE 38-718



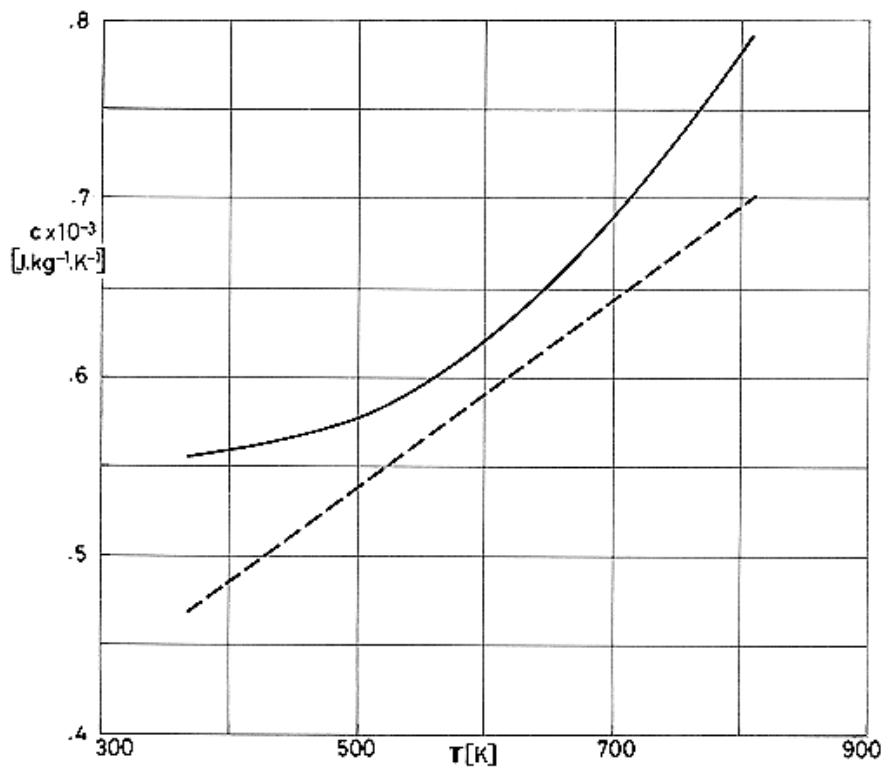
### 3. PHYSICAL PROPERTIES

3.1. Density.  $\rho = 4540 \text{ kg}\cdot\text{m}^{-3}$ . (UNE (1984) [46]).

3.2. Thermal properties

3.2.1. Specific heat.

Effect of temperature on specific heat: Figure 4-64.



Note: non-si units are used in this figure

**Figure 4-64: Specific heat,  $c$ , of Ti - 6 Al - 2 Sn - 4 Zr - 2 Mo as a function of temperature,  $T$ .**

Explanation

Key	Description	Comments	References
—	Nominal Composition. Sheet. $10^{-3}$ m thick. Duplex annealed: 1170 K, 30 min, air cool +1060 K, 15 min, air cool.		ASMH (1974).
- -	Nominal Composition. Bar. 0,0286 m in diameter. Duplex annealed: 1170 K, 1h, air cool +870 K, 8 h, air cool.		

## 3.2.2. Thermal conductivity

Effect of temperature on thermal conductivity: Figure 4-65.

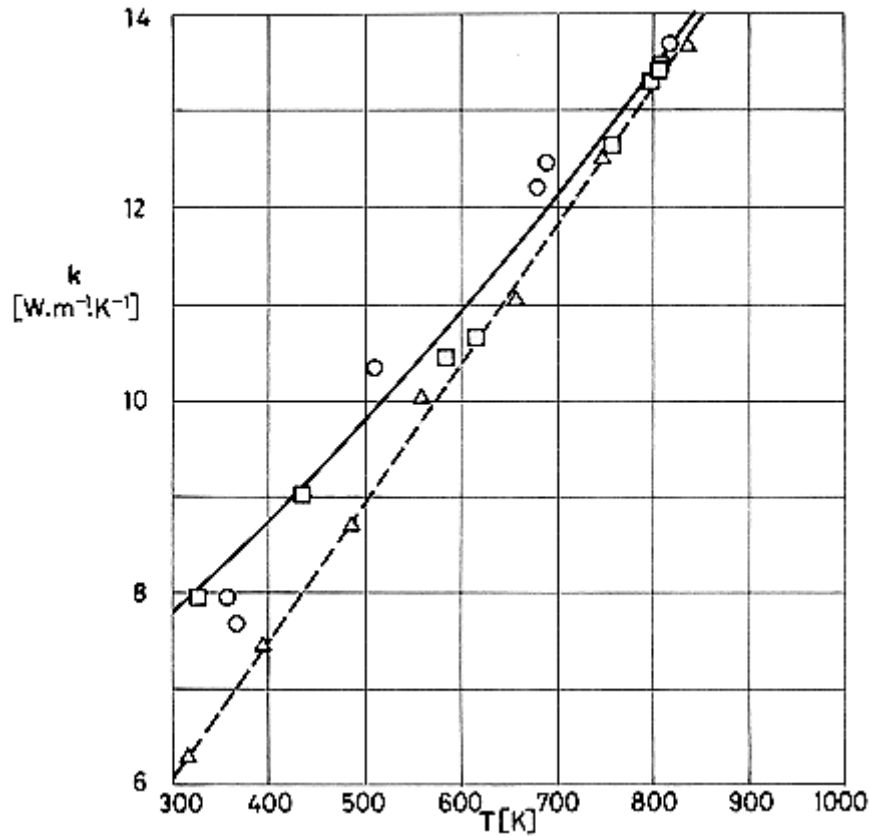


Figure 4-65: Thermal conductivity,  $k$ , of Ti - 6 Al - 2 Sn - 4 Zr - 2 Mo as a function of temperature,  $T$ .

Explanation

Key	Description	Comments	References
○ —	Nominal Composition. Sheet. 10 <sup>-3</sup> m thick. Duplex annealed: 1170 K, 30 min, air cool +1060 K, 15 min, air cool.	Measured parallel to rolling direction.	ASMH (1978) .
□ —	Same as above specimen and conditions.		
△ - -	Nominal Composition. Bar. 0,108 m in diameter. Duplex annealed: 1170 K, 1h, air cool +870 K, 8 h, air cool.	Measured parallel to long direction.	

## 3.2.3. Thermal diffusivity

## 3.2.4. Thermal expansion

Effect of temperature on thermal expansion: Figure 4-66.

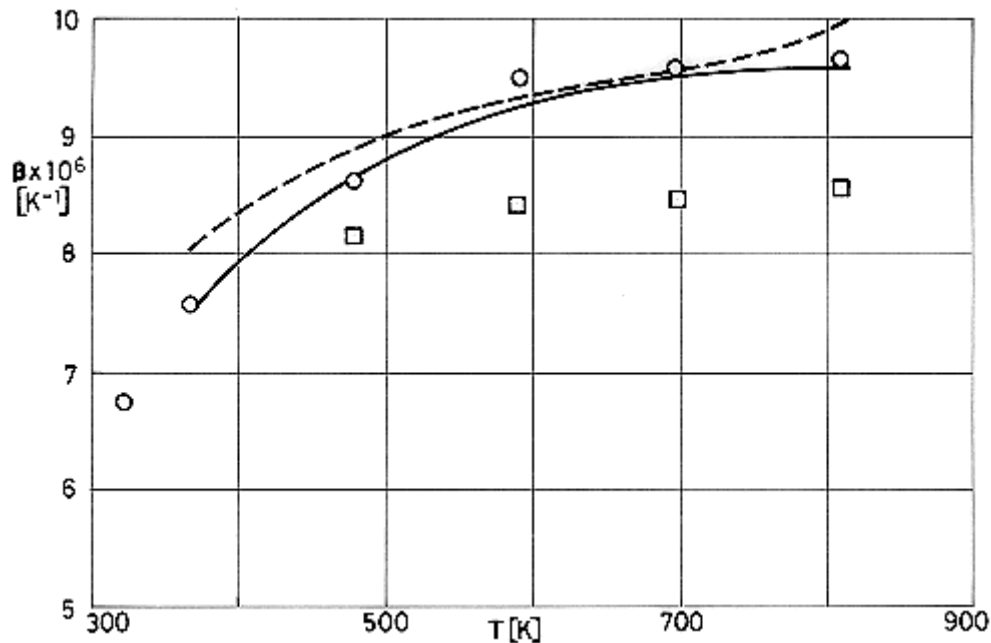


**Figure 4-66: Mean coefficient of linear thermal expansion,  $\beta$ , of Ti - 6 Al - 2 Sn - 4 Zr - 2 Mo from room temperature to temperature  $T$ .**

Explanation

Key	Description	Comments	References
—	Nominal Composition. Sheet. $10^{-3}$ m thick. Duplex annealed: 1170 K, 30 min, air cool +1060 K, 15 min, air cool.	Measured in longitudinal and transverse direction.	ASMH (1978).
- -	Nominal Composition. Bar. 0,0286 m in diameter. Duplex annealed: 1170 K, 1h, air cool +870 K, 8 h, air cool.	Measured in longitudinal direction. Average ascending-descending temperatures	
○	Nominal composition. Cast compressor casing. As cast.		
□	Nominal Composition. Package forging. Duplex annealed: 1230 K, 1h, air cool +870 K, 8 h, air cool.		

### 3.2.5. Melting range.

Alloy 6,2 Al, 2 Sn, 4,2 Zr, 1,8 Mo, 0,06 Fe, 0,124 O, 0,008 N, 0,0052 H, 0,02 C, Ti balance.

<b>T [K]</b>	<b>Solidus <sup>a,c</sup></b>	<b>Liquidus <sup>b,c</sup></b>
<b>Range</b>	1845-1890	1970-2010
<b>Average</b>	1860	1920

<sup>a</sup> Four determinations.

<sup>b</sup> Two determinations.

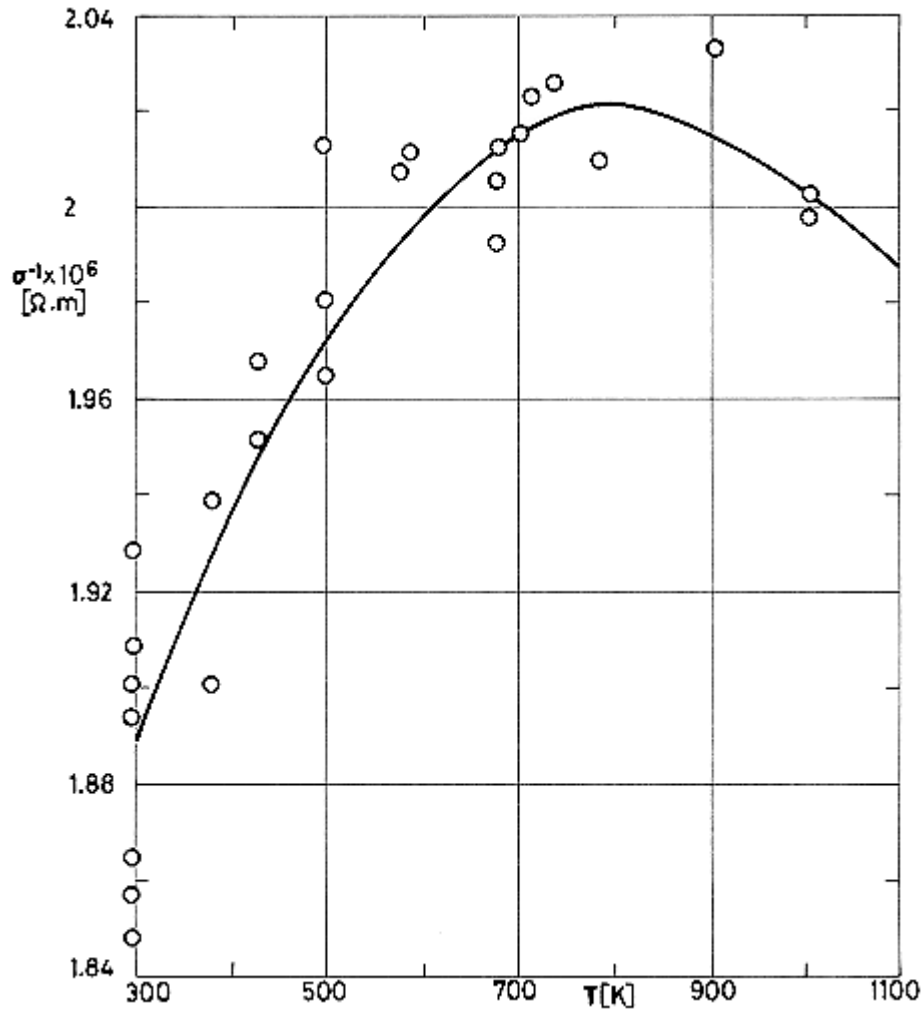
<sup>c</sup> Temperature measurement accuracy  $\pm 19$  K. Some diffusion of support tray material (Nb) into sample may have caused slight elevation of solidus and liquidus temperatures.

NOTE From ASMH (1978).

## 3.4. Other physical properties

### 3.4.1. Electrical resistivity.

Effect of temperature on electrical resistivity: Figure 4-67.



### 3.4.2. Magnetic properties.

This alloy is non-magnetic.

### 5.2. Corrosion resistance

This alloy is susceptible to solid salt stress corrosion at elevated temperatures and exhibits delayed failure of cracked specimens at room temperature in aqueous salt environments. Stress corrosion characteristics can depend on alloy processing and heat treatment (ASMH (1978)).

The application of a nickel base protective coating to this alloy yielded limited results because of formation and growth of intermetallic Ni<sub>3</sub>Ti and NiTi phases. (Tien et al. (1973) [37]).

## 6. FABRICATION

### 6.1. Casting

Acceptable castings by the induction melting technique cannot be obtained with the use of graphite crucibles and molds due to surface reaction with the mold. This problem is at present circumvented by multiple consumable electrode arc melting under vacuum in water-cooled copper crucibles. A skin of solid titanium, the "skull", is formed providing a non reactive wall between the melt and the crucible.

(ASMH (1978)).

### 6.2. Forming

bending. Bend properties are equivalent to those for similar alloys.

Forging. Forgeability of this alloy is similar to Ti - 6 Al - 4 V.

(ASMH (1978)).

### 6.3. Welding

Fusion welding by either TIG or MIG process can be performed on any of the heat treated conditions of this alloy. Weldment properties are inferior to those of Ti - 6 Al - 4 V (Betner (1980) [13]).

This alloy produces a weld the properties of which are difficult to predict and markedly different from the unwelded metal. Tests seem to indicate that weld properties may vary with ingot source, gage of material welded, weld cooling rate and, possibly, prior heat treatment.

(ASMH (1978)).

### 6.4. Machining

Good, within the group of Ti alloys (UNE (1984) [46]).

### 6.5. Heat treatment

This alloy is used in either a duplex or triplex annealed conditions. The heating cycles of duplex annealing for sheets are specified in the Explanations of Figure 4-64 to Figure 4-67. A final 870 K heating cycle for triplex annealed sheet and duplex annealed bar and forges, followed by 8 h air cool is sometimes referred as stabilization age. (ASMH (1978)).

## 7. AVAILABLE FORMS AND CONDITIONS

Ingot, bloom bar, billet, sheet, plate, wire (ASMH (1978)).

## 8. USEFUL TEMPERATURE RANGE

This alloy possesses good strength properties up to 800 K and appears metallurgically stable up to 700 K. These are disappointingly low values relative to the melting point of titanium (1900 K to 1950 K).

No service experience of this alloy at temperatures below 273 K has been gained.

## 9. APPLICATIONS

Blades and discs of the compressor section of jet engines, and air-frame applications requiring good strength, fracture toughness, erosion properties and improved creep resistance at temperatures up to 800 K.

## 4.9 Titanium-Aluminium-Vanadium alloys

ALLOY Ti - 6 Al - 4 V.

### 1. TYPICAL COMPOSITION, PERCENT

Al	C	Fe	H	N	O	V	Ti
5,5 6,75	- 0,1	- 0,4	- 0,015	- 0,07	- 0,3	3,5 4,5	Balance

### 2. OFFICIAL DESIGNATIONS

AECMA	ISO	AFNOR	AMS	BS	DIN
Ti - P63			4911 4928	TA 10	TiAl6V4, 3,7164

### 3. PHYSICAL PROPERTIES

3.1. Density.  $\rho = 4430 \text{ kg.m}^{-3}$ . (Stuart Lyman (1961) [36]).

3.2. Thermal properties

3.2.1. Specific heat.

Effect of temperature on specific heat: Figure 4-68.

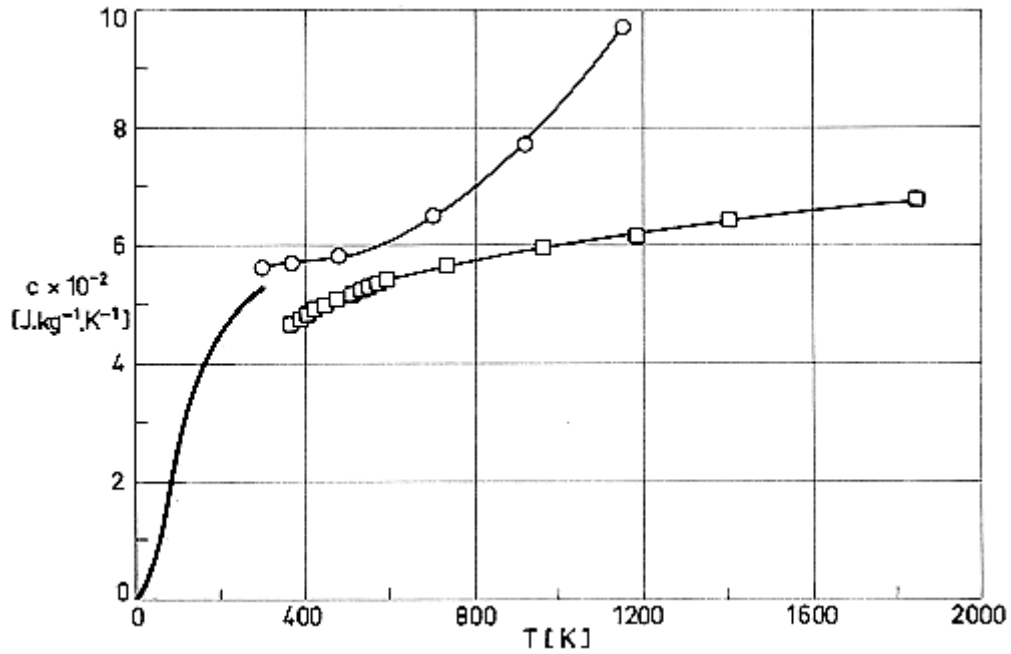


Figure 4-68: Specific heat,  $c$ , of Ti - 6 Al - 4 V as a function of temperature,  $T$ .

Explanation

Key	Description	Comments	References
○	Nominal composition.		Stuart Lyman (1961) [36].
□	Nominal composition. Solution heat treated at 1200 K for 20 min, oil-quenched and aged at 755 K for 4 h, and then cooled in air.	Reported error <2%.	Touloukian (1967)c [40].
—	Nominal composition.	Data from smooth curve.	Coston (1967) [18].

### 3.2.2. Thermal conductivity

Effect of temperature on thermal conductivity: Figure 4-69.



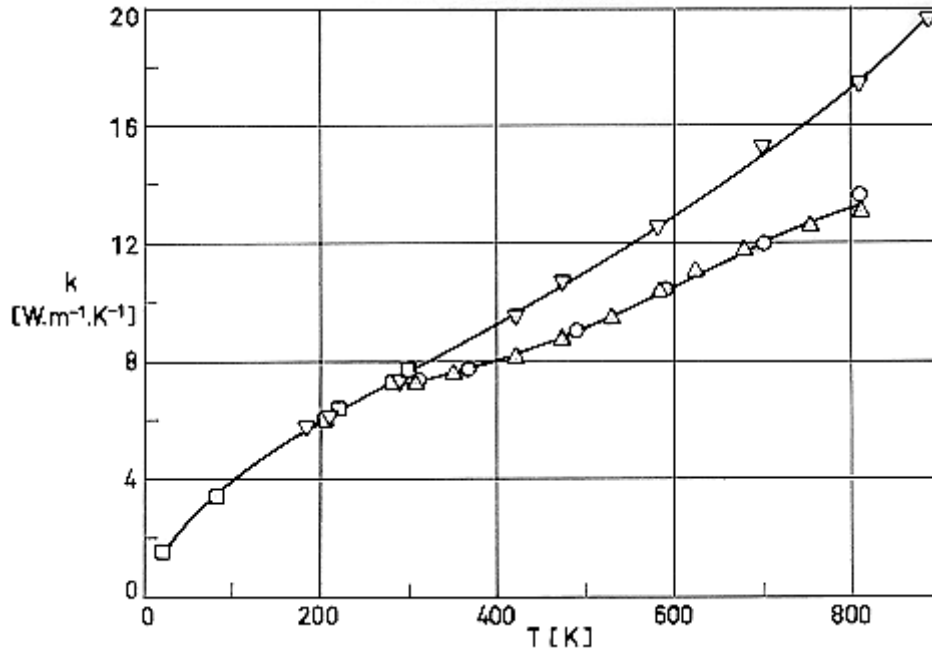
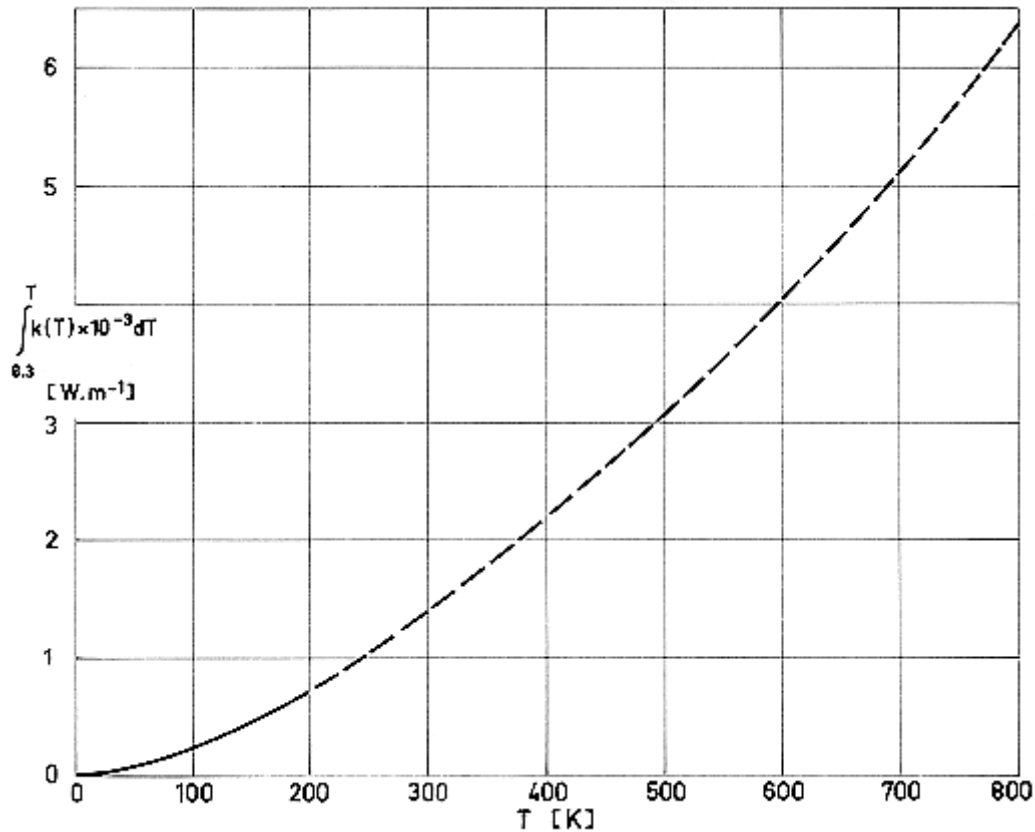


Figure 4-69: Thermal conductivity,  $k$ , of Ti - 6 Al - 4 V as a function of temperature,  $T$ .

Explanation

Key	Description	Comments	References
○	Nominal composition.		Stuart Lyman (1961) [36].
□	Nominal composition.		Coston (1967) [18].
△	In a mild annealed condition.	Reported error $\pm 5\%$ .	Touloukian (1967)c [40].
▽	Nominal composition. Sheet no. 1777 A-1.		

Thermal conductivity integrals: Figure 4-70



**Figure 4-70: Thermal conductivity integrals of Ti - 6 Al - 4 V as a function of temperature,  $T$ .**

#### Explanation

Solid line: From Coston (1967) [18].

Dashed line: Calculated, by the compiler, by fitting the experimental data points  $\circ$ ,  $\square$  and  $\triangle$  of Figure 4-69 with the least-squares method, and integrating the expression,  $k(T) = 6,33 + 3,67 \times 10^{-6} T^2$  ( $r = 0,995$ ) which is then obtained;  $r$  is the correlation coefficient giving the goodness of the fit.

#### 3.2.3. Thermal diffusivity

Effect of temperature on thermal diffusivity: Figure 4-71.

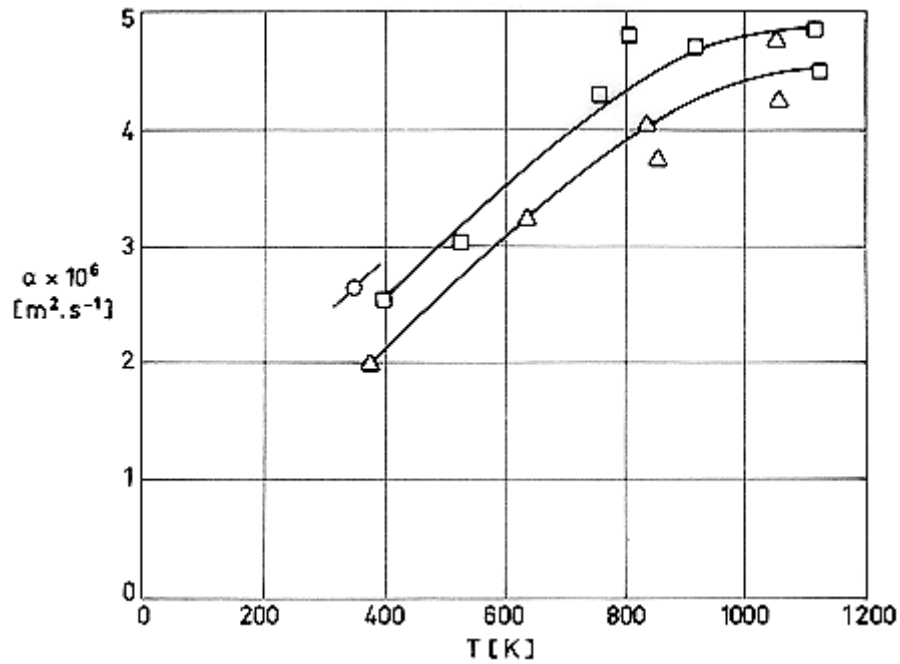


Figure 4-71: Thermal diffusivity,  $\alpha$ , of Ti - 6 Al - 4 V as a function of temperature,  $T$ .

Explanation

Key	Description	Comments	References
○	Nominal composition.	Exposed to radiation and followed by cooling.	Touloukian (1967)c [40].
□	Nominal composition.	Measured after three exposures to radiation.	
△	Nominal composition.	Measured after five exposures to radiation.	

### 3.2.4. Thermal expansion.

Mean coefficient of linear thermal expansion,  $\beta$ , between 294 K and given temperature.

$T$ [K]	366	477	588	700	811
$\beta \times 10^6$ [K <sup>-1</sup> ]	9,1	10,2	10,2	10,2	10,2

NOTE From Stuart Lyman (1961) [36].

Effect of temperature on thermal expansion: Figure 4-72.

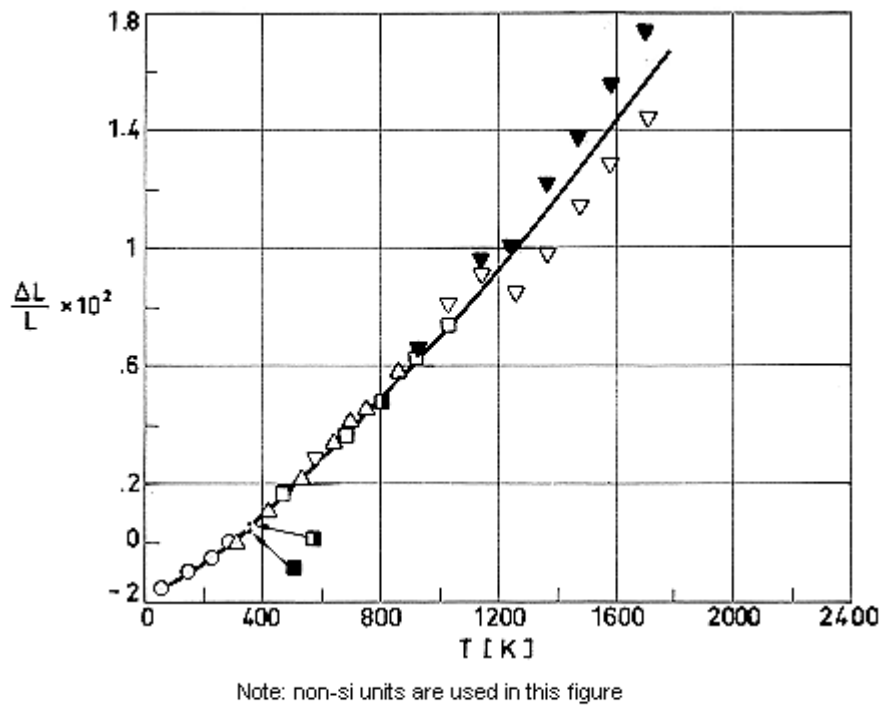


**Figure 4-72: Thermal linear expansion,  $\Delta L/L$ , of Ti - 6 Al - 4 V as a function of temperature,  $T$ .**

Explanation

Key	Description	Comments	References
○		From smooth curve.	Coston (1967) [18].
□	Nominal composition. Density $4430 \text{ kg.m}^{-3}$		Touloukian (1967)c [40].
■	Same as above. Alpha-beta alloy.		
▣	Same as above. Low C content.		
△	Machined; solution treated, 1200 K, 20 min; oil-quenched; aged 755 K, 4 h, and air-cooled. Sample $2,54 \times 10^{-3} \text{ m}$ in diameter and $5 \times 10^{-2} \text{ m}$ length.	Average data of three samples with permanent expansion from 0,011 to 0,025 percent.	
▽	Prepared from sponge. Sample $1,59 \times 10^{-2} \text{ m}$ in diameter. Annealed.	Measured in vacuum ( $\cong 4 \times 10^{-2} \text{ Pa}$ ). Beta-transus temperature 1270 K. Heating data.	

Key	Description	Comments	References
▼		Cooling data.	

### 3.2.5. Melting range.

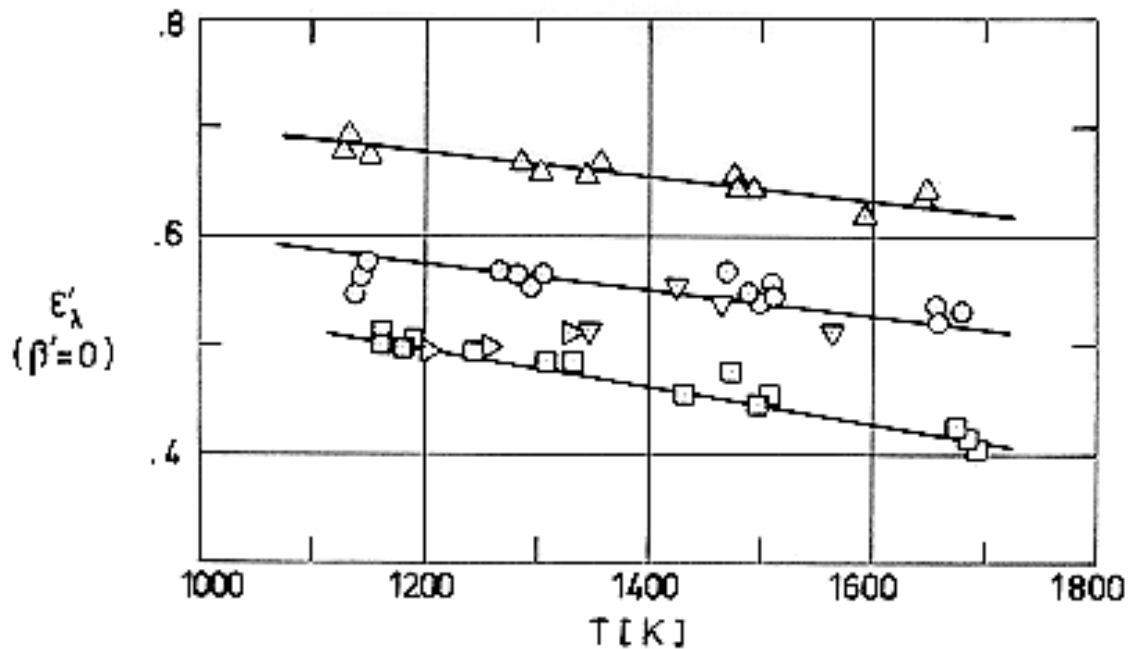
1877 K - 1933 K. (Stuart Lyman (1961) [36]).

### 3.3. Thermal radiation properties

#### 3.3.1. Emittance.

##### 3.3.1.1. Normal spectral emittance ( $\beta' = 0$ ).

Effect of temperature on normal spectral emittance: Figure 4-73.



Note: non-si units are used in this figure

Figure 4-73: Normal spectral emittance,  $\epsilon_{\lambda}'$ , of Ti - 6 Al - 4 V as a function of temperature,  $T$ .

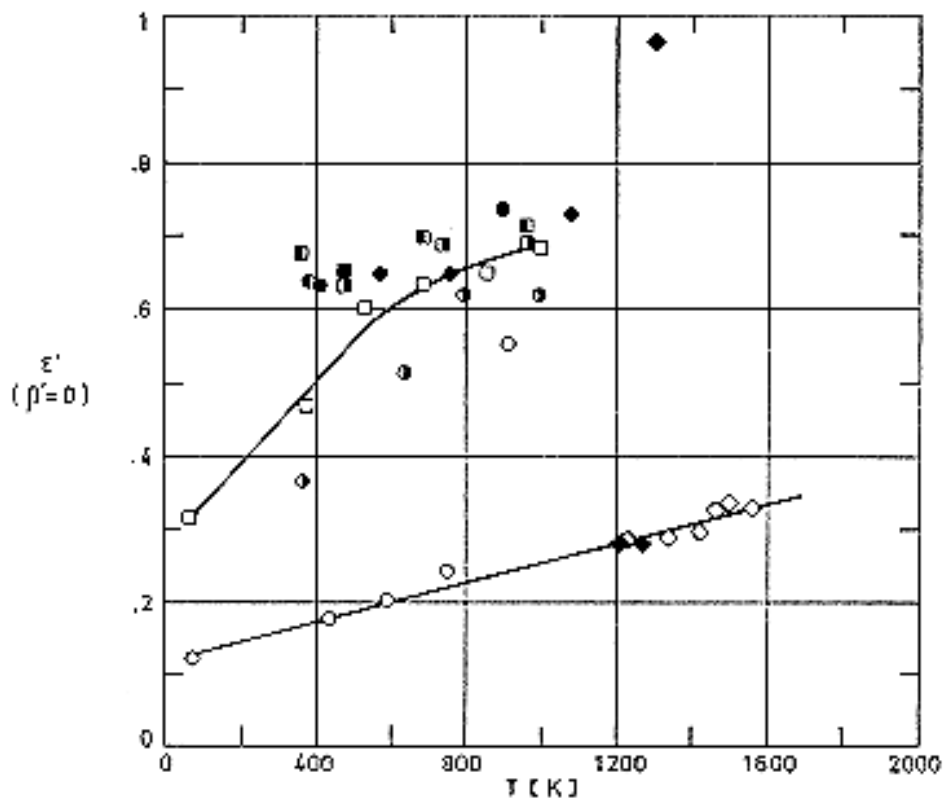
#### Explanation

Key	Description	Comments	References
○	Nominal composition.	Measured in vacuum. Same data for as received and cleaned (with a liquid detergent). $\lambda = 6,65 \times 10^{-7}$ m.	Touloukian (1967)c [40].

Key	Description	Comments	References
□	Same composition as above. polished with fine polishing compounds.	Measured in vacuum. $\lambda = 6,65 \times 10^{-7}$ m.	
△	Same composition as above. oxidized in air at red heat for 30 min.	Measured in vacuum. $\lambda = 6,65 \times 10^{-7}$ m.	
▽	Nominal composition. Surface roughness: $2 \times 10^{-6}$ - $3 \times 10^{-6}$ m RMS. Polished.	Measured in vacuum (0,4 - 0,53 Pa). Heating. $\lambda = 6,5 \times 10^{-7}$ m.	
▷	Same as above.	Same as above. Cooling. $\lambda = 6,5 \times 10^{-7}$ m.	

### 3.3.1.2. Normal total emittance ( $\beta = 0$ ).

Effect of temperature on normal total emittance: Figure 4-74.



Note: non-si units are used in this figure

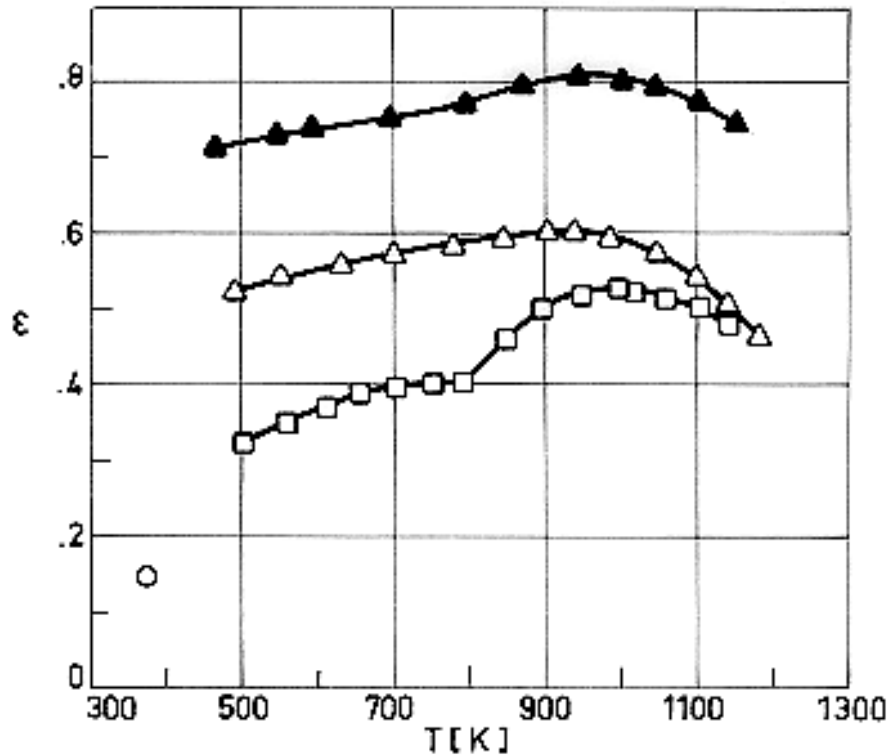
**Figure 4-74: Normal total emittance,  $\epsilon'$ , of Ti - 6 Al - 4 V as a function of temperature,  $T$ .**

## Explanation

Key	Description	Comments	References
○	Nominal composition. Polished.	Measured in air. Cycle 1.	Touloukian (1967)c [40].
◐		Cycle 2 heating.	
◑		Cycle 2 cooling.	
●		Cycle 3.	
□	Nominal composition. Oxidized at 922 K for 30 min.	Measured in air. Cycle 1.	
◻		Cycle 2.	
◼		Cycle 3 heating.	
■		Cycle 3 cooling.	
◇	Nominal composition. Surface roughness: $2 \times 10^{-6}$ - $3 \times 10^{-6}$ m RMS. Polished.	Measured in vacuum (0,4 - 0,53 Pa). Heating.	
◆		Cooling.	

## 3.3.1.4. Hemispherical total emittance

Effect of temperature on normal total emittance: Figure 4-75.



Note: non-si units are used in this figure

**Figure 4-75: Hemispherical total emittance,  $\epsilon$ , of Ti - 6 Al - 4 V as a function of temperature,  $T$ .**

Explanation

Key	Description	Comments	References
○	Nominal composition. Pre-finished with 600 grit silicon carbide paper, electropolished.	Measured in vacuum ( $1,33 \times 10^{-3}$ Pa). The effect of ion bombardment, quoted in the source, is too small to be distinguishable in the figure.	Touloukian & DeWitt (1970) [42].
□	Nominal composition. Rough surface, as received.	Data from smooth curve. Reported error >6%.	
△	Same as above except preheated at 1150 K in air.	Reported error >6%.	
▲	Rough surface. As received.	Data from smooth curve. Reported error >6%.	



## 3.3.2. Absorptance

## 3.3.2.5. Solar absorptance

## 3.3.2.5.1. Normal solar absorptance: Table 4-22.

**Table 4-22: Normal Solar Absorptance of Ti – Al – 4 V**

$T$ [K]	$\beta$ (°)	$\alpha$	Comments
298	9	0,568	As received; computed from spectral reflectance data for sea level conditions. Mentioned below as specimen 1.
298	9	0,563	Above specimen and conditions except computed for above atmosphere conditions.
298	9	0,509	Different sample, same specimen and conditions as 1, except cleaned.
298	9	0,508	Above specimen and conditions except computed for above atmosphere conditions.
298	9	0,515	Different sample, same specimen and conditions as 1, except polished.
298	9	0,511	Above specimen and conditions except computed for above atmosphere conditions.
298	9	0,878	Different sample, same specimen and conditions as 1, except oxidized.
298	9	0,869	Above specimen and conditions except computed for above atmosphere conditions.
298	~ 0	0,444	Computed from spectral reflectance.
298	~ 0	0,474	Above specimen and conditions except hydrogen ion bombarded ( $1,10 \times 10^{23}$ ions.m <sup>-2</sup> ).
298	~ 0	0,507	Above specimen and conditions except hydrogen ion bombarded ( $4,70 \times 10^{23}$ ions.m <sup>-2</sup> ).
298	~ 0	0,515	Above specimen and conditions except hydrogen ion bombarded ( $1,27 \times 10^{24}$ ions.m <sup>-2</sup> ).
298	~ 0	0,512	Above specimen and conditions except hydrogen ion bombarded ( $3,07 \times 10^{24}$ ions.m <sup>-2</sup> ).
298	~ 0	0,512	Above specimen and conditions except hydrogen ion bombarded ( $7,70 \times 10^{24}$ ions.m <sup>-2</sup> ).
298	~ 0	0,511	Above specimen and conditions except hydrogen ion bombarded

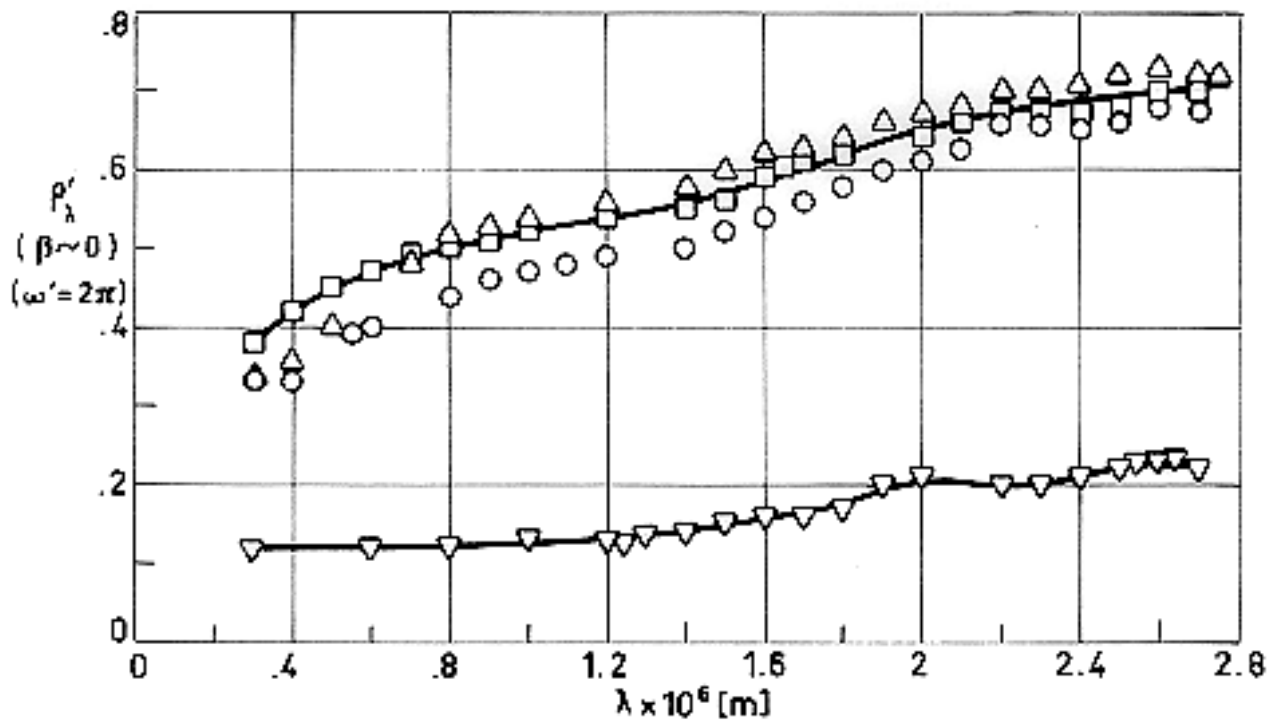
$T$ [K]	$\beta$ (°)	$\alpha$	Comments
			( $9,87 \times 10^{24}$ ions.m <sup>-2</sup> ).

NOTE From Touloukian, DeWitt & HERNICZ (1972) [43].

### 3.3.3. Reflectance.

#### 3.3.3.2. Directional-hemispherical spectral reflectance.

Normal-hemispherical spectral reflectance ( $\beta \sim 0$ ,  $\omega' = 2\pi$ ): Figure 4-76.



Note: non-si units are used in this figure

**Figure 4-76: Normal - hemispherical spectral reflectance,  $\rho_{\lambda}'$ , of Ti - 6 Al - 4 V as a function of wavelength,  $\lambda$ .**

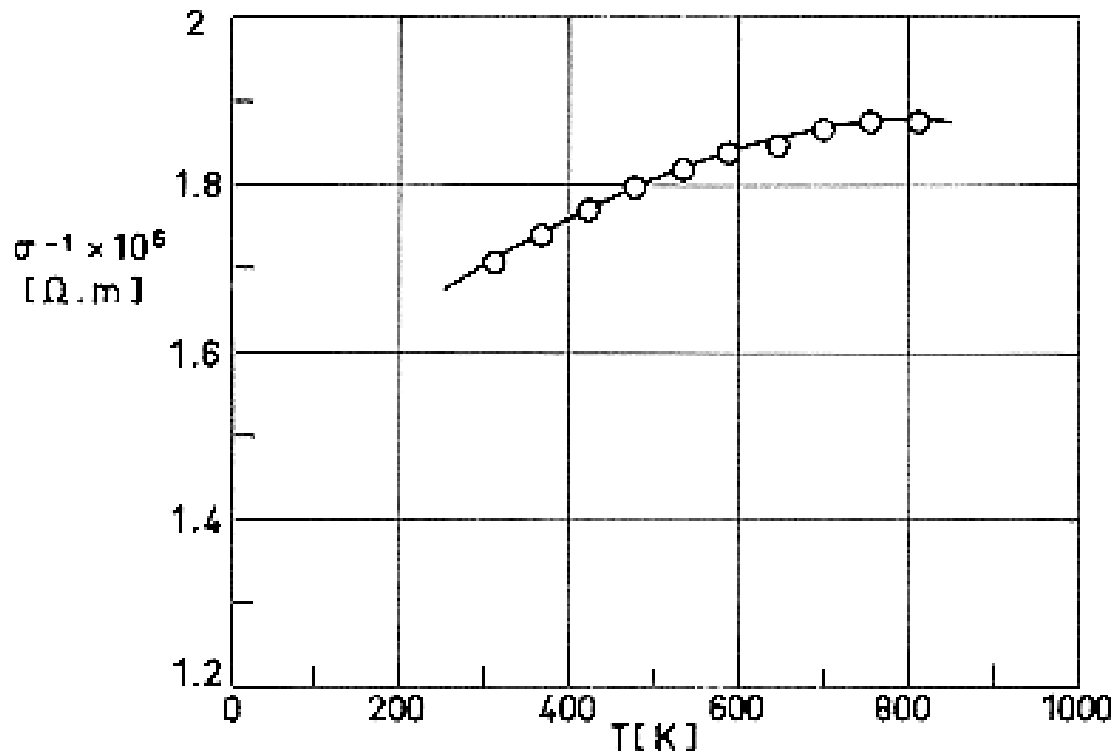
Explanation

Key	Description	Comments	References
○	Nominal composition, as received.	$\beta = 9^\circ$ . $T = 298$ K.	Touloukian & DeWitt (1970) [42].
□	Same as ○ except cleaned.		
△	Same as ○ except polished.		
▽	Same as ○ except oxidized at 922 K for 30 min.		

## 3.4. Other physical properties.

## 3.4.1. Electrical resistivity.

Effect of temperature on electrical resistivity: Figure 4-77.



Note: non-si units are used in this figure

**Figure 4-77: Electrical resistivity,  $\sigma^{-1}$ , of Ti - 6 Al - 4 V as a function of temperature,  $T$ .**

Explanation

Key	Description	Comments	References
○	Nominal composition. Mild annealed.		Touloukian (1967)c [40].

3.4.2. Magnetic properties. This alloy is non-magnetic.

 Relative Permeability:  $\mu/\mu_0 = 1,00005$  measured at  $1,6 \times 10^3 \text{ A} \cdot \text{m}^{-1}$ . (ASMHI (1974)e [9]).

## 5. CHEMICAL PROPERTIES

5.1. Solution potential (vs. decinormal calomel electrode)

Data not available. Solution potential of Ti pure is +0,20 V. (Ross (1972) [31]).

## 5.2. Corrosion resistance

This alloy is highly resistant to corrosion. It has excellent resistance to hot oxidation up to 800 K. It can not be attacked by normal acids (except fuming nitric) and alkalis at room temperature, and has considerable resistance to many acids at high temperature. (Ross (1972) [31]).

## 6. FABRICATION

6.2. Forming. Good. In sheet forming the minimum bending radius is 6 times the thickness.

6.3. Welding. Good, using TIG or MIG processes.

6.4. Machining. Possible with slow speeds, coarse feeds, and sharp tools.

6.5. Heat treatment. Good.

## 7. AVAILABLE FORMS AND CONDITIONS

It is available in the full commercial range of sizes for sheet, plate, bar, forgings, wire, extrusions, and casting in the annealed and solution treated conditions (ASMH (1974)e [9]).

## 8. USEFUL TEMPERATURE RANGE

the structural use of this alloy should be limited to the temperature range 116 K - 670 K. The extra-low-interstitial grade (ELI) is recommended for low temperature uses. Fresh fracture surfaces of this alloy, when in contact with liquid oxygen, burn expontaneously, and the reaction may spread at a high rate. (ASMH (1974)e [9]).

## 9. APPLICATIONS

Structural elements, fasteners, bolts and, generally speaking, those applications where high temperatures precludes the use of aluminium alloys.

Representative cost of this alloy (sheet stock) is compared with those of other typical metals in Table 4-23. Structural data are also included as a guide to cost effectiveness estimation.

**Table 4-23: Cost of Ti – 6 Al – 4 – V compared with those of other structural metallic materials.**

Material	$\rho$ [kg.m <sup>-3</sup> ]	$\sigma_{ult} \times 10^{-8}$ a [Pa]	$E \times 10^{-10}$ b [Pa]	$\sigma_{ult} \cdot \rho^{-1} \times 10^{-6}$ [m <sup>2</sup> .s <sup>-2</sup> ]	$E \cdot \rho^{-1} \times 10^{-8}$ [m <sup>2</sup> .s <sup>-2</sup> ]	Cost US \$.kg <sup>-1</sup>
<b>Al Alloy 2024-T6</b>	2770	3,93	7,24	0,142	0,262	1,3
<b>Mg Alloy HK 31</b>	1800	2,25	4,48	0,126	0,250	12,4
<b>Ti Alloy Ti - 6 Al - 4 V</b>	4430	8,94	10,90	0,202	0,246	26,5
<b>Stainless Steel 301 XHSR</b>	8030	17,30	20,70	0,216	0,258	2,5
<b>Beryllium hot rolled.</b>	1860	4,83	30,30	0,262	1,64	772,0

<sup>a</sup>  $\sigma_{ult}$ , Ultimate tensile strength.

<sup>b</sup>  $E$ , Modulus of Elasticity.

NOTE From Adams (1974) [51].

## 4.10 Nickel-Chrome-Cobalt-Molybdenum alloys

ALLOY Ni - 19 Cr - 11 Co - 10 Mo - 2 Ti.

### 1. TYPICAL COMPOSITION, PERCENT

Al	B	C	Cr	Co	Fe	Mn	Mo	Si	S	Ti	Ni
1,4	0,003	-	18	10	-	-	9	-	-	3	Balance
1,6	0,010	0,12	20	12	5	0,1	10,5	0,5	0,015	3,5	

### 2. OFFICIAL DESIGNATIONS

AECMA	ISO	AFNOR	ASM	BS	DIN

This alloy is known as René 41, which is a trade mark.

### 3. PHYSICAL PROPERTIES

3.1. Density.  $\rho = 8190 \text{ kg.m}^{-3}$ . (room temp.) (Alloy Digest (1958) [3]).

3.2. Thermal properties

3.2.1. Specific heat.

Effect of temperature on specific heat: Figure 4-78.

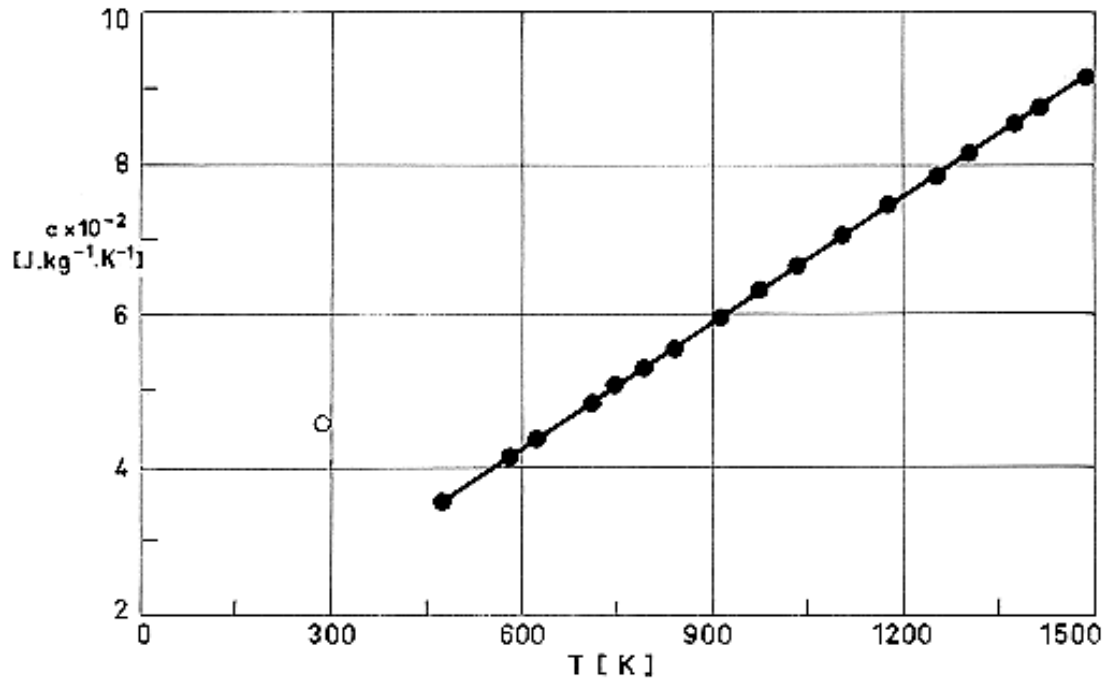


Figure 4-78: Specific heat,  $c$ , of Ni - 19 Cr - 11 Co - 10 Mo - 3 Ti as a function of temperature,  $T$ .

Explanation

Key	Description	Comments	References
○			Alloy Digest (1958) [3].
●	Nominal composition. Solution heat treated at 1350 K and water quenched.	Under helium atmosphere. Reported error 3%.	Touloukian (1967)c [40].

### 3.2.2. Thermal conductivity

Effect of temperature on thermal conductivity: Figure 4-79.

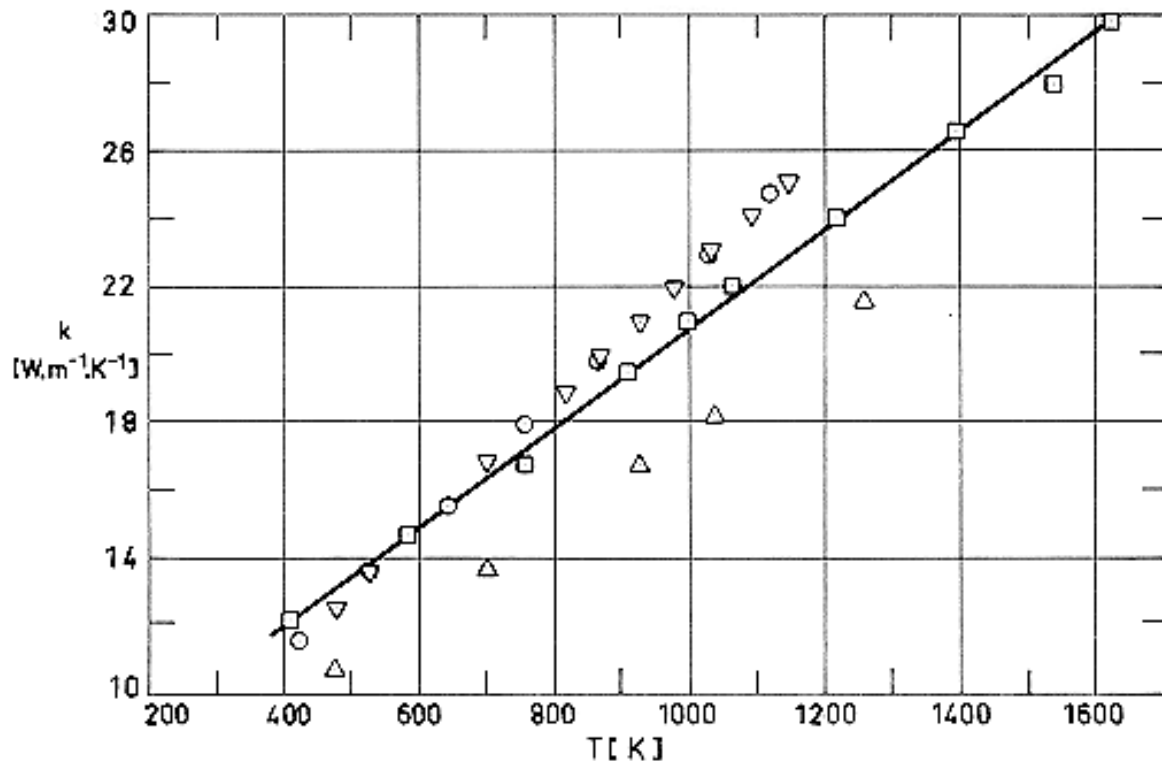


Figure 4-79: Thermal conductivity,  $k$ , of Ni - 19 Cr - 11 Co - 10 Mo - 3 Ti as a function of temperature,  $T$ .

Explanation

Key	Description	Comments	References
○			Harris (1961) [21].
□	Nominal composition.	Sample contained in five disks of $2,54 \times 10^{-2}$ m diameter. Reported error <5%.	Touloukian (1967)c [40].
△	Nominal composition.		
▽			

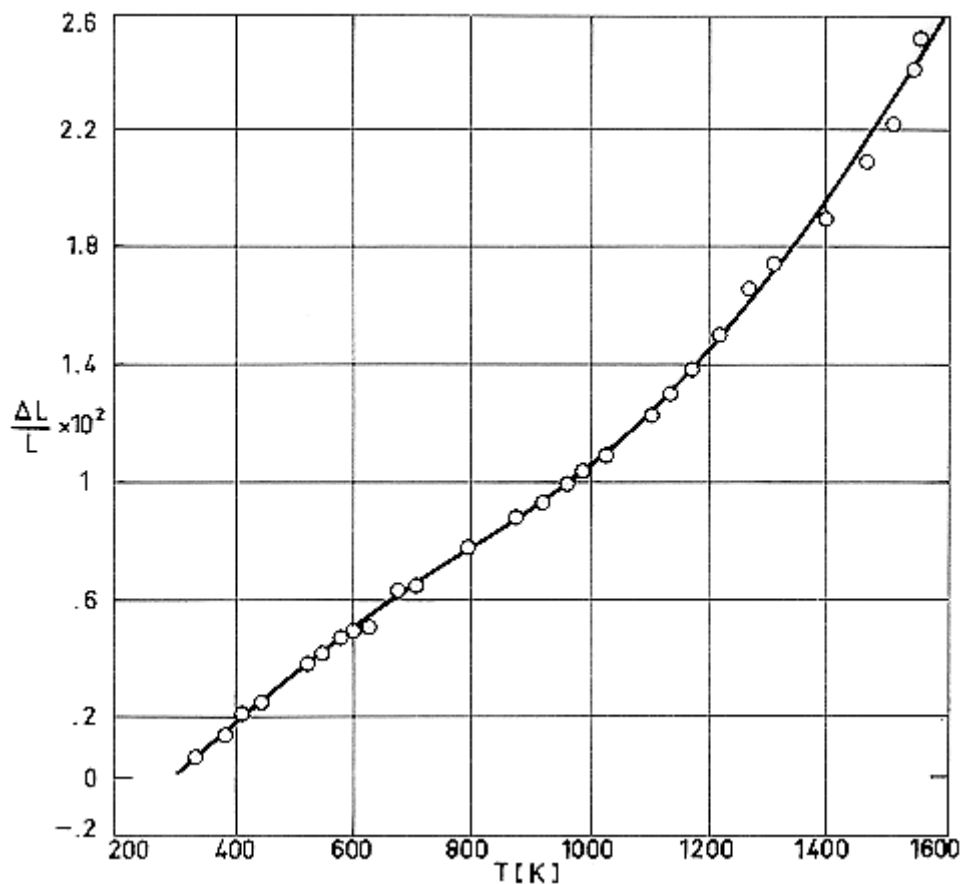
## 3.2.4. Thermal expansion

 Mean coefficient of linear thermal expansion,  $\beta$ , between 293 K and given temperature.

T [K]	422	644	866	1033	1200	1311
$\beta \times 10^6$ [K <sup>-1</sup> ]	12,15	12,82	13,72	14,78	16,2	17,28

NOTE From Harris (1961) [21].

Effect of temperature on thermal expansion: Figure 4-80.



Note: non-si units are used in this figure

**Figure 4-80: Thermal linear expansion,  $\Delta L/L$ , of Ni - 19 Cr - 11 Co - 10 Mo - 3 Ti as a function of temperature,  $T$ .**

Explanation

Key	Description	Comments	References
○	Nominal composition. Solution-treated at 1350 K and water-quenched.		Touloukian (1967)c [40].

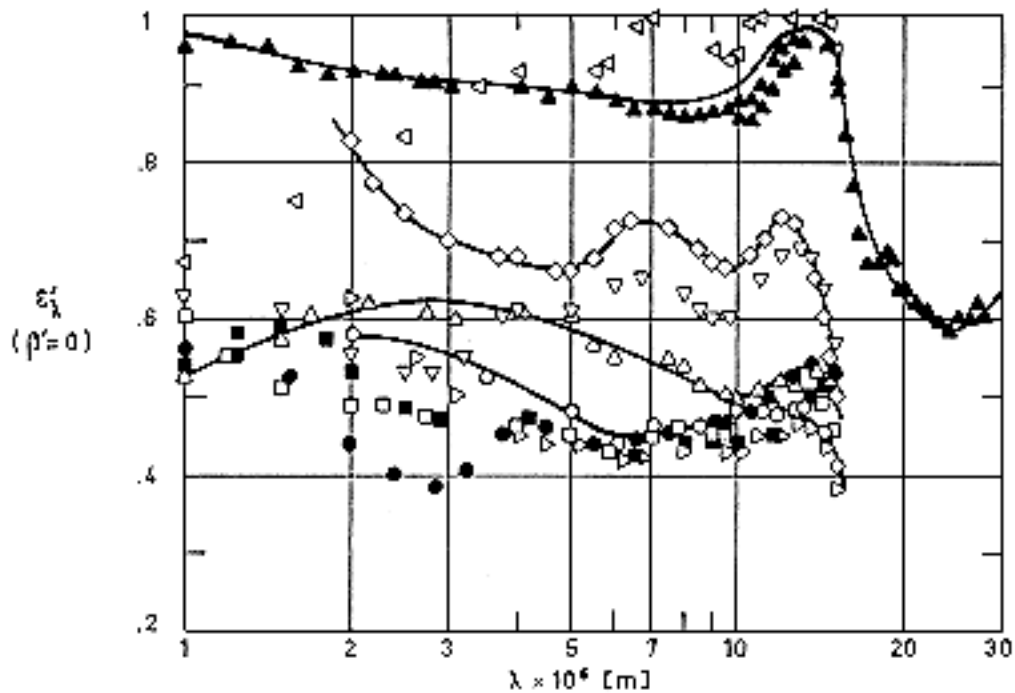


## 3.2.5. Melting range

1580 K - 1616 K. (ASMH (1974)e [9]).

## 3.3. Thermal radiation properties

## 3.3.1. Emittance.

 3.3.1.1. Normal spectral emittance ( $\beta' = 0$ ). Figure 4-81.


Note: non-si units are used in this figure

**Figure 4-81: Normal spectral emittance,  $\varepsilon'_\lambda$ , of Ni - 19 Cr - 11 Co - 10 Mo - 3 Ti as a function of wavelength,  $\lambda$ .**

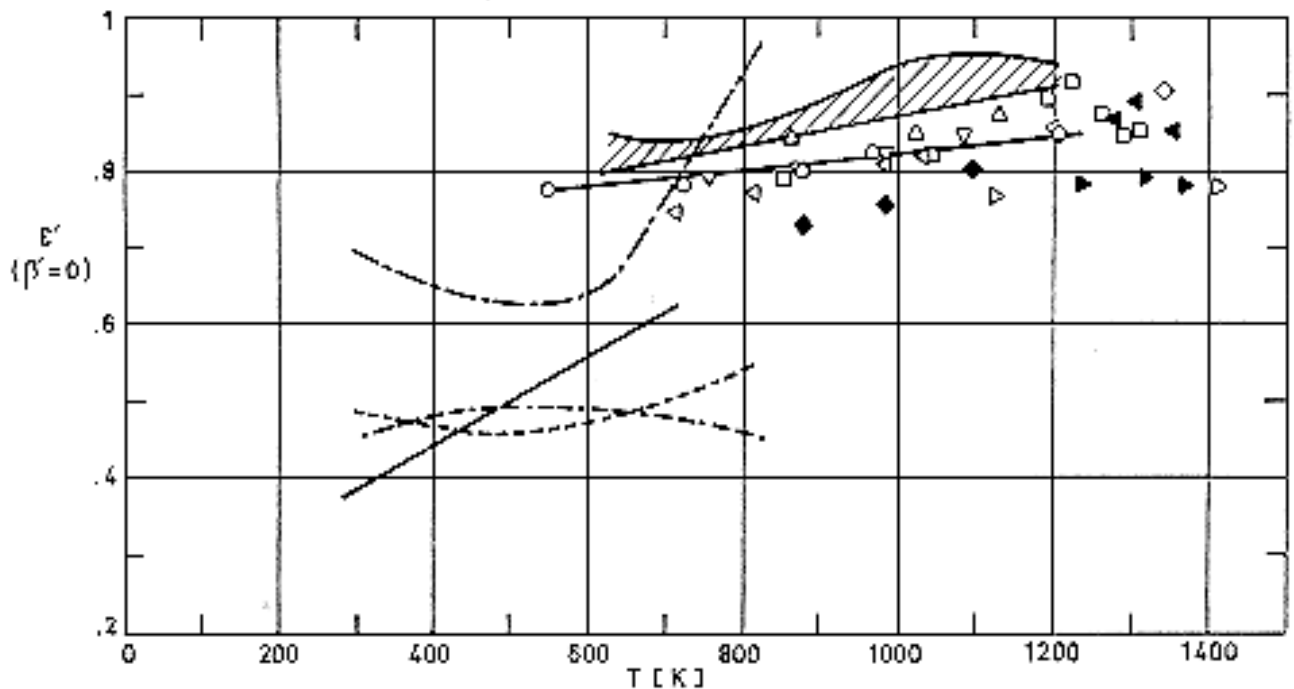
Explanation

Key	Description	Comments	References
○	Nominal composition. As received.	Sample temperature: $T = 523,2$ K.	Touloukian (1967)c [40].
□		$T = 773,2$ K.	
△		$T = 1023$ K.	
◇	Nominal composition. Heated in air at 1255 K for 30 min.	$T = 523,2$ K.	
▽		$T = 773,2$ K.	
◁		$T = 1023$ K.	

Key	Description	Comments	References
▷	Nominal composition. Heated in vacuum ( $1,01 \times 10^{-2}$ Pa) at 1255 K for 30 min.	$T = 523,2$ K.	
●		$T = 773,2$ K.	
■		$T = 1023$ K.	
▲	Nominal composition. Well oxidized.	$T = 1041,5$ K.	

 3.3.1.2. Normal total emittance ( $\beta' = 0$ ).

Effect of temperature on normal total emittance: Figure 4-82.



Note: non-si units are used in this figure

**Figure 4-82: Normal total emittance,  $\varepsilon'$ , of Ni - 19 Cr - 11 Co - 10 Mo - 3 Ti as a function of temperature,  $T$ .**

Explanation

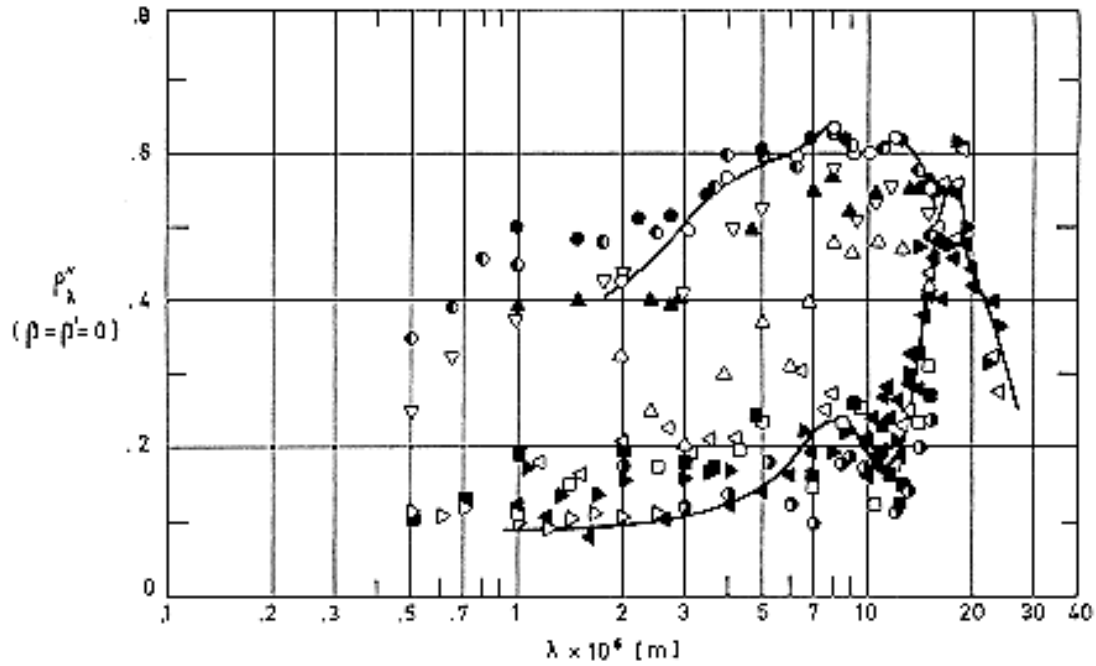
Key	Description	Comments	References
○	Nominal composition. Surface roughness (fully aged):	Measured in decreasing temperatures.	Touloukian (1967)c [40].

Key	Description	Comments	References
□	1) fine structure $2 \times 10^{-6}$ m high. 2) coarse structure $5 \times 10^{-6}$ m high at $2 \times 10^{-4}$ m intervals. Cleaned in 1 to 1 water-diluted HF solution for 1 h, oxidized 3 h at 1200 K in air.	Measured in increasing temperatures. The specimen was heated by gas for temperatures higher than 1227,6 K.	
△		Above specimen measured in decreasing temperatures.	
▽	Nominal composition.	Chromel-Alumel thermocouple mounted off center on the face. Electrically heated specimen.	
▷		Same as above.	
▶		Gas fired stand.	
◁		Same as ▽ . Electrically heated stand.	
◀		Same as ▽ . Gas fired stand.	
◇		Same as ▽ . Gas fired stand. Based on optical pyrometer.	
◆	Similar specimen.	Same as ▽ . Electrically heated stand.	
▬	As received.	Averaged over the wavelength range $2 \times 10^{-6}$ m - $15 \times 10^{-6}$ m.	
▬▬	Heated in air 30 min at 1255 K.		
▬▬▬	Heated in vacuum 30 min at 1255 K.		
▨	Oxidized in air 30 min at 1340 K and 16 h at 1030 K.		
▬	Solution treated in argon atmosphere 30 min at 1340 K. Air cooled, aged in argon 16 h at 1030 K, oxidized.		

### 3.3.3. Reflectance.

#### 3.3.3.1. Bidirectional spectral reflectance.

Normal-normal spectral reflectance ( $\beta = \beta' = 0$ ): Figure 4-83.



Note: non-si units are used in this figure

**Figure 4-83: Normal-normal spectral reflectance,  $\rho''_{\lambda}$  of Ni - 19 Cr - 11 Co - 10 Mo - 3 Ti as a function of wavelength,  $\lambda$ . Data points  $\triangleright$  correspond to normal-hemispherical reflectance while  $\blacktriangleright$ ,  $\triangleleft$ ,  $\blacktriangleleft$  correspond to hemispherical-normal reflectance.**

#### Explanation

Key	Description	Comments	References
○	Nominal composition, as received.	523,2 K source. Sample temperature below 322 K.	Touloukian (1967)c [40].
●		773,2 K source. Sample temperature below 322 K.	
◐	Same as ○. Heated in air at 1255 K for 30 min.	523,2 K source. Sample temperature below 322 K.	
◑		1273 K source. Sample temperature below 322 K.	
□		773,2 K source. Sample temperature below 322 K.	
■		1273 K source. Sample temperature below 322 K.	

Key	Description	Comments	References
△	Same as above. Heated in vacuum ( $10^{-2}$ Pa) at 1255 K for 30 min.	523,2 K source. Sample temperature below 322 K.	
▲		773,2 K source. Sample temperature below 322 K.	
▽		1273 K source. Sample temperature below 322 K.	
▷	Nominal composition. Surface roughness: 1) fine structure $2 \times 10^{-6}$ m high. 2) coarse structure $5 \times 10^{-6}$ m high at $2 \times 10^{-4}$ m intervals.	$\beta = 4^\circ$ $\omega' = 2\pi$ Sample temperature: 294,3 K.	
▶		$\omega = 2\pi$ $\beta' = 7^\circ$ Sample temperature: 294,3 K.	
◁	Cleaned in 1 to 1 water-diluted HF solution for 1 h, oxidized 3 h at 1200 K in air.	Same as above although sample temperature is 828,1 K.	
◀	Same as above. Well oxidized.	$\omega = 2\pi$ $\beta' = 7^\circ$	

### 3.4. Other physical properties

#### 3.4.1. Electrical resistivity. Table 4-24

**Table 4-24: Electrical Resistivity of Ni – 19Cr – 11Co – 10Mo – 3Ti<sup>a</sup>**

T [K]	Condition	$\sigma^{-1} \times 10^6$ [ $\Omega \cdot m$ ]
19	Solution treated.	1,18
17	Solution treated.	1,20
194	Solution treated.	1,23
273	Solution treated.	1,27
293 <sup>b</sup>	Solution treated.	1,31
293 <sup>b</sup>	Solution treated. Heat treated at 1340 K during 4 h. Air cooled.	1,25
293 <sup>b</sup>	Solution treated at 1030 K during 16 h. Air cooled.	1,26
293 <sup>b</sup>	Solution treated at 1450 K during 30 min. Air cooled.	1,33
293 <sup>b</sup>	Solution treated at 1170 K during 4 h. Air cooled.	1,34

<sup>a</sup> A sheet 1,9x10<sup>-2</sup> m thick was used in any case.

<sup>b</sup> It appears in the source as "room temperature".

NOTE From ASMH (1974)e [9].

### 3.4.2. Magnetic properties

Relative Permeability:  $\mu/\mu_0 < 1,002$  measured at  $1,6 \times 10^{-3}$  A.m<sup>-1</sup> at room temperature (ASMH (1974)e [9]).

## 4. ENVIRONMENTAL BEHAVIOR

### 4.1. Prelaunch

Highly polished surfaces of this alloy are very susceptible to increase in  $\alpha_s$  and  $\varepsilon$ , by fingerprinting and surface oxidation. Permanent damage may be caused unless contamination is immediately removed and the surface is protected.

### 4.2. Postlaunch

Ascent heating is very likely to increase  $\alpha_s$  and  $\varepsilon$ .

(From Breuch (1967) [16]).

## 5. CHEMICAL PROPERTIES

### 5.2. Corrosion resistance

This alloy is highly corrosion and oxidation resistant (Alloy Digest (1958) [3]).

## 6. FABRICATION

6.2. Forming. Good in the annealed condition. Bad in the age hardening condition. (ASMH (1974)e [9]).

6.3. Welding. Good in inert gas shielded arc (ASMH (1974)e [9]) for electron beam with preheating. (Harris (1961) [21]). Sections thicker than  $1,3 \times 10^{-2}$  m are recommended in the last case.

6.4. Machining. Good with tungsten carbide tools in age hardening condition. (Alloy Digest (1958) [3]).

6.5. Heat treatment. Good. (ASMH (1974)e [9]).

### 6.6. Anodizing

## 7. AVAILABLE FORMS AND CONDITIONS

Bar, sheet, plate, flats and billets.

## 8. USEFUL TEMPERATURE RANGE

This alloy has excellent properties even at temperature as high as 1250 K. Nevertheless, structural use should be limited to temperatures below 1150 K, and even below 950 when thin sheets are used.

## 9. APPLICATIONS

For structural elements (high speed airframes) and antennas.

## 4.11 Iron-Nickel alloys

ALLOY Fe - 36 Ni.

### 1. TYPICAL COMPOSITION, PERCENT

C	Mn	Ni	Si	Fe
- 0,12	- 0,5	34,5 36	- 0,5	Balance

### 2. OFFICIAL DESIGNATIONS

AECMA	ISO	AFNOR	AMS	BS	DIN
					Ni 36 1,3912

This alloy is often known as Invar, which is a trade mark.

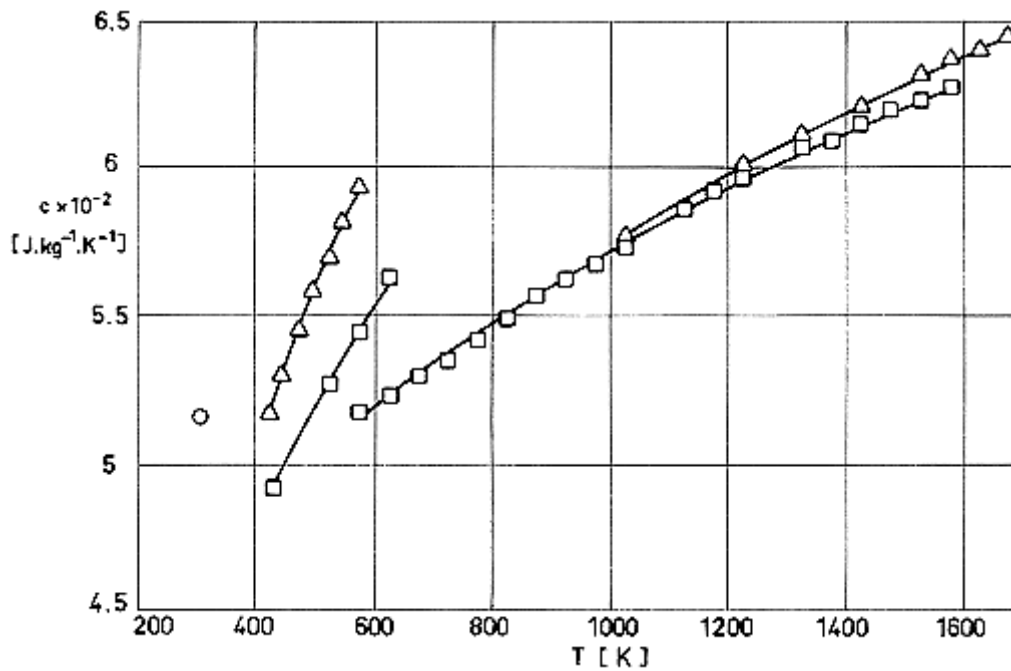
### 3. PHYSICAL PROPERTIES

3.1. Density.  $\rho = 8082 \text{ kg.m}^{-3}$ . (Alloy Digest (1964) [4]).

3.2. Thermal properties

3.2.1. Specific heat.

Effect of temperature on specific heat: Figure 4-84.



Note: non-si units are used in this figure

Figure 4-84: Specific heat,  $c$ , of Fe - 36 Ni (Invar) as a function of temperature,  $T$ .

Explanation

Key	Description	Comments	References
○			Hunter (1961) [22].
□	Fe - 29,5 Ni, prepared from electrolytically deposited pure iron and pure nickel.	Vacuum melted.	Touloukian (1967)d [41].
△	Fe - 39 Ni, prepared from electrolytically deposited pure iron and pure nickel.		

3.2.2. Thermal conductivity.

293 K - 373 K,  $k = 10,96 \text{ W.m}^{-1}.\text{K}^{-1}$ . (Hunter (1961) [22]).

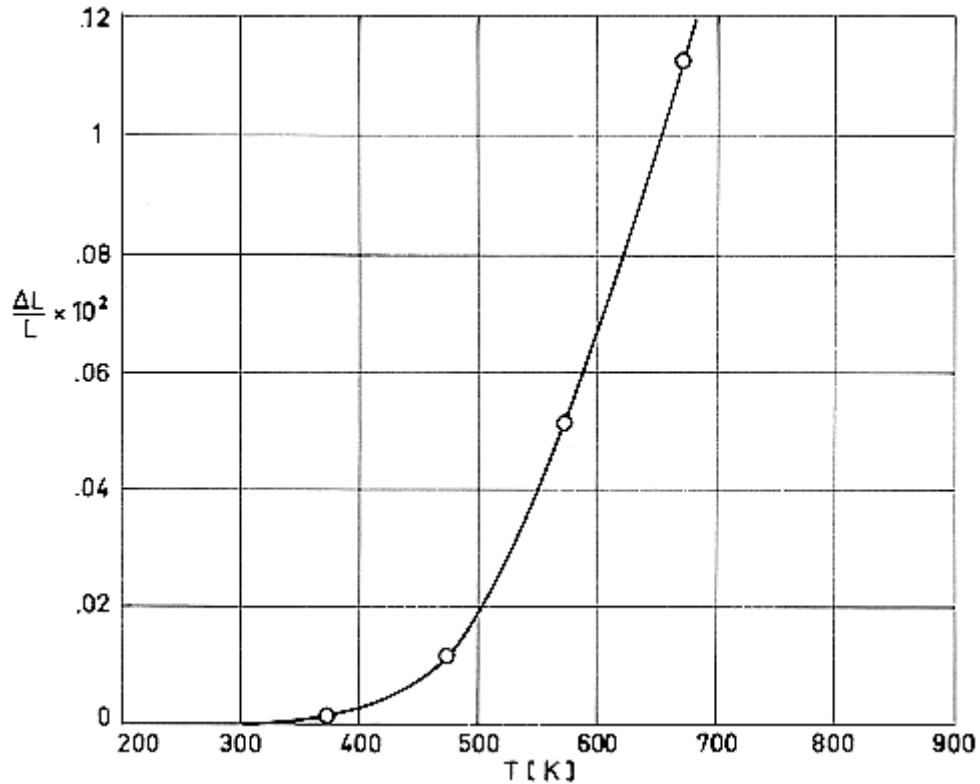
$k = 10,47 \text{ W.m}^{-1}.\text{K}^{-1}$ . (Alloy Digest (1964) [4]).

$k = 13,50 \text{ W.m}^{-1}.\text{K}^{-1}$ . (Anon (1973) [6]).

3.2.4. Thermal expansion

Effect of temperature on thermal expansion: Figure 4-85.





Note: non-si units are used in this figure

**Figure 4-85: Linear thermal expansion,  $\Delta L/L$ , of Fe - 36 Ni (Invar) as a function of temperature,  $T$ .**

#### Explanation

Key	Description	Comments	References
○	Nominal composition. Vacuum-melted, hot-rolled at 1470 K from $7,5 \times 10^{-2}$ to $2 \times 10^{-2}$ m, reheated to 1270 K, water-quenched, cold-rolled to $10^{-3}$ m, aged 8 h at 370 K, and cooled slowly.		Touloukian (1967)d [41].

## 3.2.4.1. Effect of alloying elements on thermal expansion coefficient: Figure 4-86

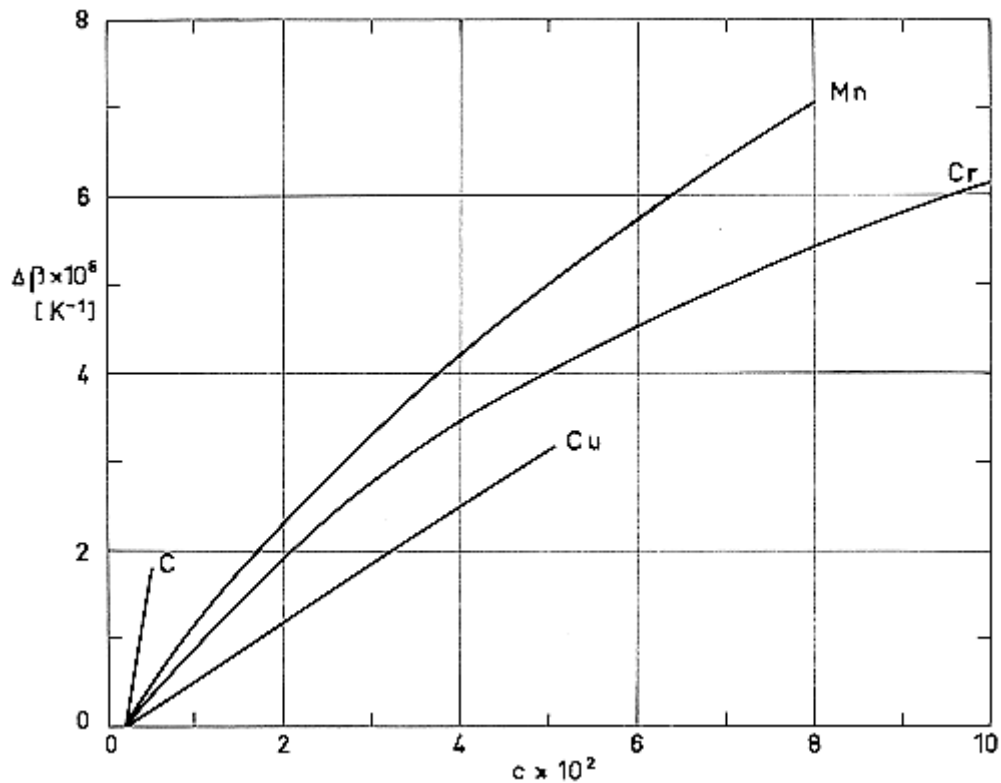


Figure 4-86: Effect of the concentration of alloying elements,  $c$ , on the value of the coefficient of linear expansion,  $\beta$ . From MOND NICKEL Co.

## 3.2.4.2. Effect of heat treatment on linear thermal expansion coefficient: Table 4-25.

Table 4-25: Linear thermal expansion coefficient of Fe – 36 Ni under different temper conditions.

Condition	Temp. Range [K]	$\beta \times 10^6$ [K <sup>-1</sup> ]
After forging	290-373	1,66
	290-523	3,11
Quenched from 1100 K	291-373	0,64
	291-523	2,53
Quenched from 1100 K, tempered.	288-373	1,02
	288-523	2,43
Cooled from 1100 K to room temperature in 19 h.	288-373	2,01
	288-523	2,89

NOTE From Hunter (1961) [22].

### 3.2.5. Melting range.

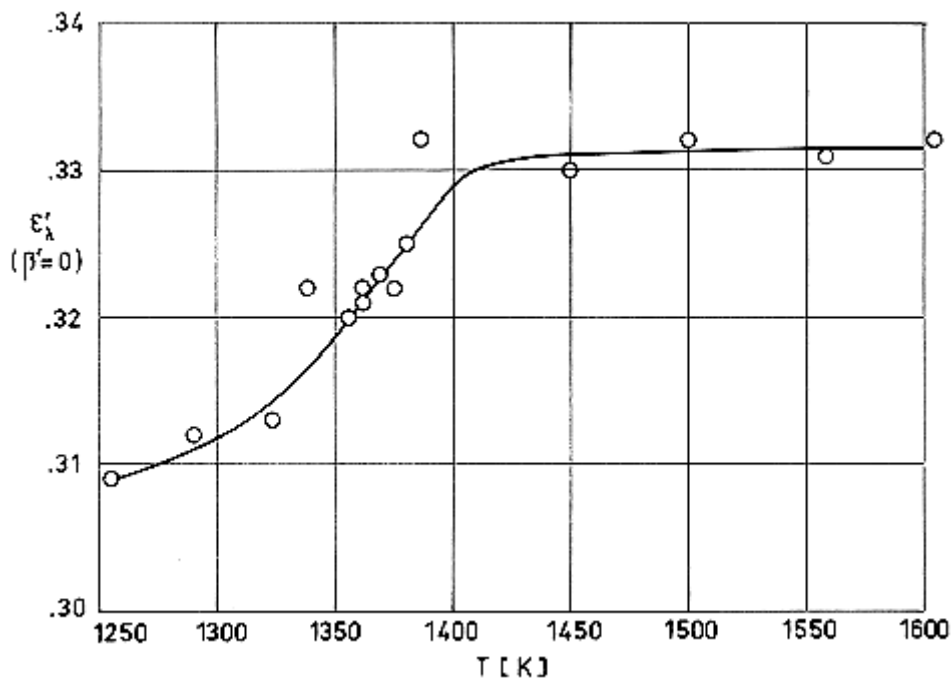
Solidus temperature: 1698 K. (Hunter (1961) [22]).

## 3.3. Thermal radiation properties

### 3.3.1. Emittance.

#### 3.3.1.1.1. Normal spectral emittance ( $\beta' = 0$ ).

Effect of temperature on normal emittance for a particular wavelength: Figure 4-87.



Note: non-si units are used in this figure

**Figure 4-87: Normal emittance,  $\epsilon'_\lambda$ , of Fe - 36 Ni (Invar), for  $\lambda = 6,7 \times 10^{-7}$  as a function of temperature,  $T$ .**

Explanation

Key	Description	Comments	References
○	Nominal composition. Powders were mixed in desired proportions, compressed at $4,8 \times 10^8$ Pa and 298 K, heated at 1373 K in flowing hydrogen; cold rolled, then heated in hydrogen at 1273 K.		Touloukian (1967)d [41].

### 3.4. Other physical properties

## 3.4.1. Electrical resistivity.

 $\sigma^{-1} = (0,80 \pm 0,05) \times 10^{-6} \Omega \cdot m$ . (Hunter (1961) [22]).

Temperature coefficient of electrical resistivity:

 $\alpha = 1,2 \times 10^{-3} K^{-1}$ . (Hunter (1961) [22]).

## 3.4.2. Magnetic properties. Table 4-26 and Table 4-27.

**Table 4-26: Magnetic Properties of Fe – 36 Ni under different temper conditions.**

Condition	Field Strength $H [A \cdot m^{-1}]$	Normal Induction $B [T]$	Relative Permeability $(\mu/\mu_0) \times 10^{-3}$
Annealed	8	0,020	1
	32	0,950	2,2
	64	0,310	3,7
	95	0,440	3,5
	103	0,445	3,4
Hard drawn	160	0,030	1,7
	320	0,160	2,9
	480	0,400	4,4
	640	0,560	4,5
	800	0,650	4,3

NOTE From Alloy Digest (1964) [4].

**Table 4-27: Relative Permeability of Fe – 36 Ni, measured at 400 A.m<sup>-1</sup>**

$T [K]$	$(\mu/\mu_0) \times 10^{-3}$
255	1,800
283	1,715
311	1,630
339	1,545
367	1,450
389	1,360

From Alloy Digest (1964) [4].

## 3.4.2.1. Loss of magnetism

Condition	$T_i^a$ [K]	$T_f^a$ [K]
Annealed	435	544
Quenched	478	544

<sup>a</sup>  $T_i$  initial temperature;  $T_f$  minimum temperature of complete loss.

NOTE From Hunter (1961) [22].

## 5. CHEMICAL PROPERTIES

5.2. Corrosion resistance. This alloy resists the atmospheric corrosion and those produced by fresh water and by salt water. (Anon. (1973) [6]).

## 6. FABRICATION

6.2. Forming. This alloy has almost unlimited capacity for plastic deformation, either hot or cold. (Alloy Digest (1964) [4]).

6.2.1. Hot working can be performed below 1530 K, (Alloy Digest (1964) [4]), however, as has been reported by Hunter (1961) [22], careful handling is required to avoid cracking and breaking up.

6.2.2. Invar which has been subjected to cold working or machining may require a stress-relieving heat treatment for stabilization. (Alloy Digest (1964) [4]).

6.3. Welding. May be successfully welded by any of the commonly used methods. (Alloy Digest (1964) [4]).

6.4. Machining. Is somewhat difficult. (Alloy Digest (1964) [4]).

6.5. Heat treatment. A reducing atmosphere should be used. (Hunter (1961) [22]).

## 7. AVAILABLE FORMS AND CONDITIONS

Hot rolled and cold drawn bars, wires, strips, and forgings.

## 8. USEFUL TEMPERATURE RANGE

This alloy retains its characteristic low expansiveness provided that temperature is maintained below 475 K. For applications at temperatures above this value, higher nickel alloys are recommended. (Alloy Digest (1964) [4]).

## 9. APPLICATIONS

Because Invar has unusually low thermal expansion, it is used for instruments requiring constant distances between points, glass to metal seals, thermostatic and other temperature control or indicating devices, bimetals, etc.

Invar has positive thermoelastic coefficients over a large temperature range. This anomaly is useful in developing alloys with nearly temperature-invariant elastic constants.

Invar is also a candidate low-temperature material. Its elastic properties between room temperature and liquid helium temperature have been reported by Ledbetter, Naimon & Weston (1977) [24].

# 5

## Composite materials

---

### 5.1 List of symbols

$D,$	Diffusion Coefficient. [ $\text{m}^2.\text{s}^{-1}$ ] Radiation Dose Absorbed. [ $\text{rad}$ , 1 $\text{rad} = 10^{-2} \text{ J.kg}^{-1}$ ]
$E,$	Elasticity Modulus. [ $\text{Pa}$ ]
$Fo,$	Fournier Number, $Fo = at/L^2$ .
$G,$	Relative Moisture Content.
$L,$	Length, Sample Thickness. [ $\text{m}$ ]
$Le,$	Lewis-Semenov Number. $Le = \rho Dc/k$
$M,$	Moisture Content.
$N,$	Number of Thermal Cycles.
$Q,$	Volume Gas Flow Rate. [ $\text{m}^3.\text{s}^{-1}$ ]
$R,$	Electrical Resistance. [ $\Omega$ ] Sunspot Number (Wolf Number). Introduced in clause 5.13.2.5.
$Re,$	Atomic Oxygen Reaction Efficiency. [ $\text{m}^3.\text{atom}^{-1}$ ]
$R'_{\lambda}(\beta, \theta),$	Directional Hemispherical Spectral Reflectance Factor.
$T,$	Temperature. [ $\text{K}$ ]
$T_M,$	Maximum Continius Service Temperature. [ $\text{K}$ ]
$T_{MI},$	Maximum Intermittent Service Temperature. [ $\text{K}$ ]
$T_d,$	Deflection Temperature. [ $\text{K}$ ]
$T_g,$	Glass Transition Temperature. [ $\text{K}$ ]
$X,$	Mole Fraction. Strength. [ $\text{Pa}$ ]

$c,$	Specific Heat. [ $\text{J.kg}^{-1}.\text{K}^{-1}$ ]
$k,$	Thermal Conductivity. [ $\text{W.m}^{-1}.\text{K}^{-1}$ ]
$p,$	Pressure. [Pa]
$t,$	Time. [s], [h], [d]
$\alpha,$	Thermal Diffusivity. [ $\text{m}^2.\text{s}^{-1}$ ]. $\alpha = k/\rho c$
$\alpha_s,$	Solar Absorptance.
$\alpha'(\beta, \theta),$	Directional Total Absorptance.
$\alpha'_\lambda(\beta, \theta),$	Directional Spectral Absorptance.
$\beta,$	Coefficient of Linear Thermal Expansion. [ $\text{K}^{-1}$ ] Angle Between Surface Normal and Direction of Incident Flux. [Angular degrees]
$\beta',$	Angle Between Surface Normal and Direction of Emergent Flux. [Angular degrees]
$\varepsilon,$	Hemispherical Total Emittance.
$\varepsilon'(\beta', \theta'),$	Directional Total Emittance.
$\varepsilon'_\lambda(\beta', \theta'),$	Directional Spectral Emittance.
$\theta,$	Circumferential Angle of Incident Flux. [Angular degrees]
$\theta',$	Circumferential Angle of Emergent Flux. [Angular degrees]
$\lambda,$	Wavelength. [m]
$\nu,$	Poisson's Ratio.
$\rho,$	Density. [ $\text{kg.m}^{-3}$ ] Electrical resistivity. [ $\Omega.\text{m}$ ]
$\rho'_\lambda(\beta, \theta),$	Directional-Hemispherical Spectral Reflectance.
$\sigma_t,$	Tensile Strength. [Pa]
$\tau,$	Dimensionless temperature. introduced in clause 5.12.1.5.
$\tau'(\beta, \theta),$	Directional-Hemispherical Total Transmittance.
$\varphi,$	Volume Fraction. Particle Flux. [ $\text{m}^2.\text{s}^{-1}$ ] Relative Humidity.

$\omega$ ,	Frequency. [ $s^{-1}$ ]
$\omega'$ ,	Solid Angle of Emitted, Reflected or Transmitted Radiation Beam. [Steradians]

## Subscripts

<b>f</b> ,	Fiber.
<b>m</b> ,	Matrix.
<b>o</b> ,	Initial value. 0° Angle in Angle Plyed Laminates.
<b>s</b> ,	Solar.
<b>v</b> ,	Void.
<b><math>\theta</math></b> ,	Angle $\theta$ with Fibers in Unidirectional Laminates. [degrees]
<b>1</b> ,	Parallel to Fibers in Unidirectional Laminates.
<b>2</b> ,	Normal to Fibers, in Plane of Laminate, Unidirectional Laminates.
<b>3</b> ,	Normal to Plane of Laminate, Unidirectional Laminates.

## Acronyms

<b>A-glass</b> ,	High-Alkali Glass.
<b>ABM</b> ,	Apogee Boost Motor.
<b>APC</b> ,	Aromatic Polymer Composite.
<b>AS</b> ,	High Tensile. Surface Treated Fiber.
<b>ASTM</b> ,	American Society for Testing Materials.
<b>ATC</b> ,	Accelerated Thermal Cycling.
<b>BDMA</b> ,	Benzyl-Dimethylamine.
<b>BMI</b> ,	Bismaleimide.
<b>BTDE</b> ,	Dimethylester of 3,3',4,4' Benzophenonetetracarboxylic Acid.
<b>C-glass</b> ,	Chemical Glass.



---

<b>CD,</b>	Direct Current.
<b>CF,</b>	Carbon Fiber.
<b>CPI,</b>	Condensation-Reaction Polyimide.
<b>CTE,</b>	Coefficient of Thermal Expansion.
<b>CVCM,</b>	Collected Volatile Condensable Material.
<b>CVD,</b>	Chemical Vapor Deposition.
<b>D-glass,</b>	Dielectric Glass.
<b>DDM,</b>	Diaminodiphenylmethane.
<b>DDS,</b>	Diaminodiphenyl Sulfone.
<b>DMP,</b>	Tri-dimethylaminomethylphenol.
<b>DSC,</b>	Differential Scanning Calorimetry.
<b>E-glass,</b>	Electrical Glass.
<b>ESCA,</b>	Electron Spectroscopy Chemical Analysis.
<b>ESD,</b>	Equivalent Sun Days.
<b>ESH,</b>	Equivalent Sun Hours.
<b>FEP,</b>	Fluorinated Ethylene-Propylene.
<b>FM,</b>	
<b>FWPF,</b>	Fine Weave Pierced Fabric.
<b>HHPA,</b>	Hexahydrophthalic Anhydride.
<b>HM,</b>	High-modulus same as Type I Carbon Fiber.
<b>HMS,</b>	High Modulus. Surface Treated.
<b>HS,</b>	High Strength same as Type II Carbon Fibers.
<b>HT,</b>	High Tensile.
<b>HTS,</b>	Intermediate Tensile and Modulus. Surface Treated.
<b>IM,</b>	Intermediate Modulus.
<b>IMFP,</b>	Inelastic Mean Free Path.
<b>INTELSAT,</b>	Interim Telecommunications Satellite.
<b>IPN,</b>	Interpenetrating Polymer Network.

---

<b>IR,</b>	Infrared.
<b>KEL-F,</b>	Polychlorotrifluoroethylene.
<b>LEO,</b>	Low Earth Orbit.
<b>LMSC,</b>	Lockheed Missiles & Space Company.
<b>MBMI,</b>	Methyl-substituted Bismaleimide.
<b>MDA,</b>	4,4'-Methylenedianiline.
<b>MEA,</b>	Monoethylamine.
<b>MEK,</b>	Methylethyl ketone.
<b>MLI,</b>	Multilayer Insulation.
<b>MMAB,</b>	m-Aminibenzamide.
<b>mPDA,</b>	Metaphenylene Diamine.
<b>NBS,</b>	National Bureau of Standards (now National Institute of Standards and Technology).
<b>NE,</b>	Monomethylester of 5-Norbornene-2,3-Dicarboxylic Acid.
<b>NMA,</b>	Nadic Methyl Anhydride.
<b>OP,</b>	
<b>PAN,</b>	Polyacrylonitrile.
<b>PBT,</b>	Polybutylene Terephthalate.
<b>PCU,</b>	
<b>PEEK,</b>	Polyether Etherketone.
<b>PES,</b>	Polyether Sulfone.
<b>PET,</b>	Polyethylene Terephthalate.
<b>PMR,</b>	(In situ) Polymerization of Monomeric Reactants.
<b>PP,</b>	Polypropylene.
<b>PPS,</b>	Polyphenylene Sulfide.
<b>PTFE,</b>	Polytetrafluorethylene.
<b>PVA,</b>	Polyvinyl Alcohol.
<b>PVF,</b>	Polyvinyl Fluoride.

---

RPPR,	Reflection Pulsed Photothermal Radiometry.
S-glass,	High-Strength Glass.
SH,	Solar Hours.
SPELDA,	Structure Porteuse Externe de Lancement Double ARIANE.
STS,	Space Transportation System.
TAC,	Triallylcyanurate.
TEA,	Triethanolamine.
TFE,	Tetrafluoroethylene.
TML,	Total Mass Loss.
TPPR,	Transmission Pulsed Photothermal Radiometry.
TPRL,	Thermophysical Properties Research Laboratories (Purdue University).
UHM,	Ultrahigh Modulus.
UV,	Ultra Violet.
VHM,	Very High Modulud.
WCB,	
WYP,	
XAS,	Super A Surface Treated Fiber.
XPS,	X-ray Photoelectron Spectroscopy.
YM-31A,	High Modulus Glass.
4H-1,	Glass.

## 5.2 List of matrices, prepregs and laminates quoted in this clause

The materials listed below have been identified by using both references where the property data have been reported and brochures from manufacturers or vendors.

Many products appear in the list, although their production has been discontinued, only because interesting information on them has been collected. No claim is made that these products can be presently found in the market and delivered by the quoted manufacturer.

### 5.2.1 Matrices, adhesives, potting, moulding compounds

TRADE NAME	DESCRIPTION	MANUFACTURER (OR DEVELOPER)
Araldite CY 203/HT 872	MS Epoxy Resin + Hardener	CIB
Araldite CY 209/HT 972	MS Epoxy Resin + Hardener	CIB
Araldite LY 556	Epoxy	CIB
Araldite LY 556/HY 906 DY 070	MS Epoxy Resin + Hardener + Accelerator	CIB
Araldite LY 556/HY 917 DY 070	MS Epoxy Resin + Hardener + Accelerator	CIB
Araldite LY 556/HY 972	MS Epoxy Resin + Hardener	CIB
Araldite LY 558	Epoxy Novolac	CIB
Araldite LY 558/HT 973	Epoxy NovolaC + HT973 hardener	CIB
Araldite LY 564/HY 560	MS Epoxy Resin + Hardener	CIB
Araldite LY 564/HY 2954	MS Epoxy Resin + Hardener	CIB
Araldite LY 1927GB/HY 1927GB	MS Epoxy Resin + Hardener	CIB
Araldite MY 750/DDM	Epoxy + Diaminodiphenylmethane hardener (HT972)	CIB
Araldite XD 893/HY 932	MS Epoxy Resin + Hardener	CIB
Araldite 501/TEA	Epoxy + Triethanolamine hardener	CIB
BMI-1/MBMI-1	Bismaleimide/Methyl-substituted Bismaleimide	HCC
BMI-1/MMAB	Bismaleimide/m-Aminobenzamide	HCC
BMI-2/MBMI-2	Bismaleimide/Methyl-substituted Bismaleimide	HCC

TRADE NAME	DESCRIPTION	MANUFACTURER (OR DEVELOPER)
Castolite	TAC Polyester (Mold. Cpnd.)	CAS
Code 69	Epoxy System (for prepregs only)	FOT
Comco	Nylon 6/6 Polyamide	BOU
Copec	Polyester Carbonate	ALR
CRC 350A	Novolac base Epoxy	CNS
Delrin	Acetal (diethylaldehyde) (Mold. Cpnd.)	DUP
DER 332/DDS	Epoxy + DDS (Diaminodiphenil-sulfone) hardener	DOW
DER 332/DMP30	Epoxy + DMP30 (tris-dymethylamino methyl-phenol) hardener	DOW
DER 332/T403	Bisphenol A Epoxy + T403 (Aliphatic Polyeter Triamine) Jeffamine hardener	DOW, JEF
DLS 351/BF <sub>3</sub> 400	Epoxy + Epikure BF3400 (boron trifluoride ethylamine complex) hardener	CIB, SHL
Ekonol	Aromatic Polyester	CRB
EF-2	Epoxy system (also known as Polaris formulation) Epon 828 + Epon 1031 (1:1) Hardener: 90 pbw NMA (Nadic Methyl Anhydride), 0,5 pbw BDMA (Benzyl Dimethyl Amine)	SHL
Epikote 210/ BF <sub>3</sub> 400	Epoxy + Epikure BF3400 (boron trifluoride ethylamine complex) hardener (for prepregs only)	SHL, CIB
Epikote 828	Epoxy	SHL
Epikote 828/ BF <sub>3</sub> 400	Epoxy + Epikure BF3400 (boron trifluoride ethylamine complex) hardener	SHL
Epikote 828/ BF <sub>3</sub> MEA	Epoxy + Boron trifluoride monoethylamine complex hardener	SHL
Epikote 828/ NMA/K61B	Epoxy + NMA (Nadic Methyl Anhydride) hardener + K61B accelerator	SHL
Epocryl 332	Polyester	ASH

TRADE NAME	DESCRIPTION	MANUFACTURER (OR DEVELOPER)
Epocryl 480	Polyester	ASH
Epon 828	Epoxy	SHL
Epon 1031	Epoxy	SHL
Epoxin 162	Epoxy	BAS
ERL 4221/ HHPA+BDMA	Epoxy + HHPA (accelerator) + BDMA (hardener)	UCC
ERL 4221+DDM+Resorcinol	Epoxy + DDM (hardener) + Resorcinol (accelerator)	UCC
ERLA 4617/mPDA	Epoxy + mPDA hardener	BKX,ANC
E719	Epoxy	USP
Ferro CE-339	Epoxy	FER
Ferro CE-3305	Epoxy	FER
Ferro E-293	Epoxy	FER
Fiberite 934	Epoxy	FIB
Fiberite 1034	Epoxy	FIB
Fiberite 1034C	Epoxy	FIB
Fibredux 914	Epoxy Adhesive	CIB
Fibredux 914C	Epoxy System (for prepregs only)	CIB
FM-1000	Epoxy Adhesive	ACC
GAC 3320	Epoxy	GAC
GAC 3330	Epoxy	GAC
Hercules 3002	Epoxy	HER
Hercules 3501-5	Epoxy	HER
Hercules HA 43	Epoxy	HER
Hexcel C-1000	Polyhydroxybenzoate	HEX

TRADE NAME	DESCRIPTION	MANUFACTURER (OR DEVELOPER)
Hexcel F155	Epoxy	HEX
Hexcel F263	Epoxy	HEX
Hexcel I-2000	Polyhydroxybenzoate	HEX
HT 424	Epoxy-Phenolic Adhesive	ACC
Hysol 6000-OP	Epoxy	HYS
H70E	Alumina filled Epoxy Adhesive	EPO
H70S	Alumina filled Epoxy Adhesive	EPO
Igelit-PCU	Polyvinylchloride-Acrylic	BAS
KEL-F	Polychlorotrifluoroethylene (Mold. Cpnd.)	MMM
Lexan	Polycarbonate (Mold. Cpnd.)	GEC
Narmco 5505	Epoxy	WCN
Nylon FM-1	Polyamide	DUP
Nylon 6	Polyamide	FBR,LNP
Nylon 6/6	Polyamide	FBR,LNP,PPC
Nylon 6/10	Polyamide	FBR,LNP
Palatal P51	Polyester	BASF
PBT	PBT	Many
PBT S600	PBT	CIB
PET	PBT	Many
PMR-P1	PMR Polyimide	NASA
PMR-P6	PMR Polyimide	NASA
PMR-P7	PMR Polyimide	NASA
PMR-15	PMR Polyimide	NASA
Polypenco 101	Nylon 6/6 Polyamide	PPC

TRADE NAME	DESCRIPTION	MANUFACTURER (OR DEVELOPER)
PP	Polypropilene	HOE
PPS	PPS	Many
PR 279	Epoxy	PRC
PR 286	Epoxy	MMM
P13N	Polyimide	TRW (devel.)
P1700	Polysulfone	UCC,CNS
Radel	Polyphenylsulfone (Mold. Cpnd.)	UCC
Resin 2	100 pbw EPON 828 + 127 pbw EPON 1031 300, pbw NMA, 3 pbw BDMA	NASA (devel.)
Rezolin EP0 93L	Epoxy	HHA
Rezolin EP0 58/970	Epoxy	HHA
Rigidite 5208 (Narmco)	Epoxy (for prepregs only)	WCN
Ryton	PPS (Mold. Cpnd.)	PHP
Semi-IPN	Dicyanate	ALR
TAC Polyester	Triallylcyanurate	Many
Teflon FEP	FEP	DUP
Teflon TFE	TFE	DUP
Torlon 2000	Polyamide/imide (Mold. Cpnd.)	AOC
Torlon 4203	Polyamide/imide (Mold. Cpnd.)	AOC
Trolitul Luv M150	Polyvinyl Carbazol Polyester (Luvican)	BAS
Udel	PES (Mold. Cpnd.)	UCC
Upjohn 2080	Polyimide	UJC
Vicotex 108	Epoxy	CTH
Victrex	PES	ICI



TRADE NAME	DESCRIPTION	MANUFACTURER (OR DEVELOPER)
XD 893/HY 932	MS Epoxy Resin + Hardener	CIB
XD 927	Epoxy	CIB
HD7818/T403	Bisphenol F Epoxy Resin + Jeffamine T403 Hardener	DOW JEF
Xylok 237	Epoxy	ARL
3M SP288	Epoxy	MMM
3501	Epoxy System (Hercules 3501)	COU
948A1	Epoxy	FIB

## LIST OF NOT YET IDENTIFIED MATERIALS

TRADE	DESCRIPTION
P2000	PES
3110	Epoxy
HBRF 55A	Epoxy

**5.2.2 Prepregs, laminates and films**

TRADE	DESCRIPTION	MANUFACTURER
APC 2-2022	Hércules AS4 Carbon/PEEK	ICI
Azdel PP	Glass/PP	AZD
Azmet PBT	Glass/PBT	AZD
CTL-37-9X	Glass/Phenolic	CTL
CTL-91-LD	Glass/Phenolic	CTL
C6000/P1700	Graphite/Polysulfone	CNS,UCC
E720	Glass/Epoxy	SPI
Ferro CE 339/HMS	Graphite/Epoxy Prepreg	FER

TRADE	DESCRIPTION	MANUFACTURER
Ferro CPH 2209	Glass/Phenolic Prepreg	FER
Fiberite HY-E-1334	Graphite/Epoxy	FIB
Fibredux 914C	HTS Carbon /Redux 914 epoxy	CIB
Fibredux 914K-49	Kevlar 49/Epoxy Prepreg	CIB,BRO
GE101	Glass/Epoxy	ELI
G10	Glass/Epoxy Laminate	ATL,MCA,SYN, UOP,WEC,WEI
G11	Glass/Epoxy Laminate	SYN,WEI
Hercules 2002M	HM Graphite/Epoxy Prepreg	HER
Hercules 3002M	HM Graphite/Epoxy	HER
Hercules 3002T	HT Graphite/Epoxy	HER
Hexcel F155	Glass/Epoxy Prepreg	HEX
Hexcel F161	Glass/Epoxy Prepreg	HEX
Hexcel F164	Kevlar 49/Epoxy Prepreg	HEX
Hexcel F174	Glass/Polyimide Prepreg	HEX
Ironside 101	Graphite/Phenolic	MIL
Kapton	Polyimide (Film)	DUP
Kapton F	Polyimide (Film)	DUP
Kapton H	Polyimide (Film)	DUP
Kevlar/145-6	Kevlar 49/Epoxy	BRO
Kevlar 49/E719	Kevlar 49/Epoxy Prepreg	USP
Monsanto	Graphite/Phenolic	MON
Mylar	PET (Film)	DUP
Narmco T300/5208	Graphite/Epoxy Prepreg	WCN
Narmco 4018	Nylon Fabric/Phenolic Prepreg	WCN

TRADE	DESCRIPTION	MANUFACTURER
Narmco 4033	Quartz Fabric/Phenolic Prepreg	WCN
Narmco 4047	Carbon Fabric/Phenolic Prepreg	WCN
Narmco 4065	Lightweight Quartz Fabric/ Acrylonitrile Butadiene Phenolic Prepreg	WCN
Narmco 5505	Boron/Epoxy	WCN
PMR-15	Polyimide Prepreg	FER,FIB,HEX,USP
Scotchcal	Mylar, PET (Film)	MMM
Scotchply XP251-S	Glass/Epoxy	MMM
Skybond 703	Kevlar/Polyimide	MON
Tedlar	PVF (Film)	DUP
Thornel T300/934	Graphite-Epoxy Prepreg Tape	FIB
Thornel 75	Carbon/Epoxy Prepreg	UCC
Torayca P-301A	T300A/Epikote 828/BF <sub>3</sub> MEA Prepreg	TOR
T300/3M SP288	Graphite/Epoxy	MMM
T50(PAN)/Hexcel F263	Graphite/Epoxy	HEX
Vicotex 100	Graphite/Epoxy Prepreg	BRO
3M DuPont 5134	Kevlar 49/Epoxy	MMM
3M SP290	Boron/Epoxy	MMM
3M SP306	Kevlar 49/Epoxy	MMM
75S (Pitch)/948 A1	Graphite/Epoxy	FIB

### 5.2.3 Code list of manufacturers (or developers)

ACC, American Cyanamid Company

ALR, Allied Resin Corporation

ANC, Anchor Chemicals Limited

AOC, Amoco Chemicals Corporation

ARL, Advanced Resin Limited

ASH, Ashland Oil Incorporated  
ATL, Atlantic Laminates  
AZD, Azdel Incorporated  
BAS, BASF  
BKX, Bakelyte Xylonite Limited  
BOU, Boulder Plastics, Incorporated  
BRO, Brochier S.A. (Ciba-Geigy)  
CAS, The Castolite Company  
CIB, Ciba-Geigy, Limited. Ciba Corporation  
CNS, Celanese Corporation  
CRB, Carborundum Company, Plastics & Adhesives Department  
COU, Courtaulds  
CTH, Consultech Limited  
CTL, Cincinnati Testing Laboratories, Incorporated  
DOW, DOW Chemical Company  
DUP, E.I. du Pont de Nemours and Company, Incorporated  
ELI, Electroply, Incorporated  
EPO, Epoxy Technology Inc.  
FBR, Fiberfil Division, Dart Industries  
FER, Ferro Corporation  
FIB, Fiberite Corporation  
FOT, Fothergill and Harvey, Limited  
GAC, Goodyear Aerospace Corporation  
GEC, General Electric Company  
HCC, HC Chem. Research & Service Corporation  
HER, Hercules Incorporated  
HEX, Hexcel Products Incorporated  
HHA, Hecht, Heyworth and Alcan (Chemical) Limited  
HOE, Hoechst AG  
HYS, Hysol Division, The Dexter Corporation  
ICI, Imperial Chemical Industries  
JEF, Jefferson Chemical Company  
LNP, Liquid Nitrogen Processing Corporation  
MCA, The Mica Corporation  
MIL, Milliken & Company  
MMM, Minnesota Mining & Manufacturing Company

MON, Monsanto Company

NASA, National Aeronautics and Space Administration

PHP, Phillips 66 Petroleum Company

PPC, The Polymer Corporation

PRC, Products Research & Chemical Corporation

SHL, Shell Chemicals, UK Limited. Shell Chemical Company

SPI, Stevens Products Incorporated

SYN, Synthane Taylor Incorporated

TOR, Toray

TRW, Thompson-Ramo-Wooldrige

UCC, Union Carbide Corporation

UJC, Upjohn Company

UOP, Universal Oil Products

USP, U.S. Polymeric Incorporated

WCN, Whittaker Corporation, Narmco Materials Division

WEC, Westinghouse Electric Corporation, Micarta Division

WEI, Westinghouse Electric Corporation, Industrial Plastics Division

### **5.3 General introduction**

Composites are materials that consist of two or more constituents deliberately combined to form heterogeneous structures with intended (synergic) properties.

We will not consider in this item:

1. Metal alloys, dispersion-strengthened materials, copolymers, conventional cements, rubber tire materials, plywood, asphalt, some glasses, nuclear materials.
2. Properties other than thermal, thermo-optical, degradation and aging. Mechanical related properties are also out of the scope of this item.
3. High temperature properties. Main emphasis is placed on the behavior of composites at or near room temperature, or lower.

## 5.3.2 Composition

Composite materials could consist of either an additive constituent (fibers, particles) embedded in a matrix, or layers of two or more different materials.

### 5.3.2.1 Reinforcements

Reinforcing materials supply the basic strength of the composite.

Reinforcements could be:

a. Fibers.

Glass Fibers. They are mainly based on silica ( $\text{SiO}_2$  content is larger than 50 % in any case). Depending on the chemicals added, different types of glass arise: A-glass (high alkali, 72 % of  $\text{SiO}_2$ ), C-glass (chemically resistant, it resists to acids), D-glass (good dielectrical properties, high dielectric permittivity or dielectric constant), E-glass (good electrical properties, low electrical resistivity, it resists to alkalis and to moisture), S-glass (high strength), YM-31A (high modulus).

High Silica and Quartz Fibers.

Metal Fibers and Wires.

Amorphous Metals (or Metallic Glasses). They are non-crystalline metallic solids formed by rapid quenching, sputtering, vacuum evaporation or other methods. They exhibit at least one small dimension to ease rapid quenching. Their properties are distinctly different from those of the corresponding crystalline alloys, particularly very high strength and high compressive or bending ductility.

Carbon and Graphite Fibers. Carbon fibers are produced by pyrolysis of an organic precursor fiber in an inert atmosphere at temperatures beyond 1200 K. The aim of these fibers could either be to obtain high strength (HS or Type II carbon fiber), high modulus (HM or Type I), or both (HMS).

The process of pyrolyzation in an inert atmosphere at temperatures in excess of 2000 K (and holding the fibers under tension) is called graphitization. Its aim is to obtain fibers with higher moduli. From this point of view the cut-line between carbon and graphite fibers is not clearly delineated (the same product may be identified as carbon or as graphite depending on the reference). Although the distinction between both is far from crucial, in this clause we will mainly follow the nomenclature used in the corresponding source.

GY70, from Celanese (now BASF Structural Materials), is the graphite fiber most often used in spacecraft.

Multiphase Fibers. These are filaments, produced by CVD processes of boron on a filament substrate such as tungsten. These fibers are attractive for use at high temperatures because of their chemical stability.

Ceramic Fibers. These are continuous length filaments of alumina, boron carbide or silicon carbide.

Aramid Fibers. Aramid fibers are produced from aromatic polyamides. Their main features are low weight, high temperature strength and high modulus. They are resistant to flame and high temperatures and can be easily woven. Kevlar, from E.I. du Pont de Nemours and Company, is the most extensively used Aramid fiber. Unfortunately, it buckles under moderate compressive

forces, absorbs water and deteriorates under ultra-violet radiation. Another Aramid, Nomex, is also produced by DuPont.

**Directionally-Solidified Eutectics.** Metallic fibers can be produced by directional solidification of cast alloys. This process usually involves eutectic alloys in which the molten material exhibits two or more phases during solidification at constant temperature.

In directional solidification the material structure is characterized by longitudinal single crystals which, because of their ordered arrangement, provide to the material a very high strength.

**Whiskers.** Whiskers are short discontinuous ceramic or metallic single crystal fibers which exhibit a very large strength and elastic strains greater than 1%. They can be used to reinforce metal matrices. However, their very fine size makes whiskers extremely difficult to handle and fabricate into fiber reinforced composites.

b. Fillers.

Solid Microspheres.

Hollow Microspheres.

Flakes.

### 5.3.2.2 Matrices

Matrices serve two fundamental purposes: 1) holding the reinforcement phase, and 2) distributing the stress to the reinforcement constituents.

Matrices could be:

a. Metal matrix materials such as Aluminium, Titanium or Magnesium.

Fiber reinforced superalloy matrix composites have been developed for improved materials at elevated temperatures. Fibers considered for such use include: refractory metal alloy wires, carbon filaments, boron filaments, submicron diameter ceramic whiskers, continuous length ceramic filaments, ...

The theoretical specific strength potential of refractory alloy fiber reinforced superalloys is less than that of ceramic fiber reinforced superalloys, nevertheless the use of ceramic fibers has been unsuccessful to date. The more ductile metal fiber systems are more tolerant of fiber-matrix reactions and thermal expansion mismatches.

b. Polymer matrix materials.

Polymer matrix materials can be thermosetting, thermoplastic and thermosetting-plastic.

Thermosetting polymers are synthetic products which undergo a permanent and irreversible change during curing. The cure is accomplished by heat, pressure and catalytic and/or hardener agents. Several thermosetting polymers are capable of curing at ambient conditions.

The most used thermosetting products in the aerospace industry are: Epoxies with excellent mechanical properties, Phenolics for their heat resistance and, for low performance applications, Polyesters.

Thermoplastic polymers soften, and even melt, at high temperatures but reversibly regain rigidity after cooling. The most commonly used are the Polyamide resins (Nylon) having outstanding toughness, low friction and good chemical resistance. Polysulfone resins are also used because they exhibit good transparency and high heat resistance.

Thermosetting-plastic polymers behave either as thermosetting or as thermoplastic depending on the applied curing process. The sole thermosetting-plastic polymers used in spacecraft are

the polyimides which exhibit outstanding resistance to heat and a low coefficient of thermal expansion.

- c. Ceramic and Glass matrix materials which are only used at high temperatures.
- d. Carbon/carbon composites, also known as C/C or G/G composites, offer a superior potential as high performance engineering materials at elevated temperatures where resistance to thermal shock coupled with high strength is of importance. However, carbon/carbon composites are susceptible to oxidation degradation at high temperatures for a long period of service and, also, the achievement of controllable quality from suitable design and processing is, at present, uncertain.

From Weeton, Peters & Thomas (1987) [164], Petrasek, Signorelli, Caufield & Tien (1989) [136], Hsu & Chen (1989) [105].

### 5.3.3 Commercial fiber product names, descriptions and manufacturers

TRADE NAME	DESCRIPTION	MANUFACTURER
Alphaquartz	Quartz fibers	Alpha Associates, Inc.
Astroquartz	Quartz fibers - 99,5% SiO <sub>2</sub>	J.P. Stevens & Co.
Fiberglas	Glass fiber	Owens-Corning
Celion C6S	Chopped carbon fiber - sized	BASF Structural Materials <sup>a</sup>
Celion G50	High-modulus carbon fiber - sized	BASF Structural Materials
Celion 1000	High-strength carbon fiber - sized	BASF Structural Materials
Celion 3000	High-strength carbon fiber - sized	BASF Structural Materials
Celion 6000	High-strength carbon fiber - sized	BASF Structural Materials
Celion 12000	High-strength carbon fiber - sized	BASF Structural Materials
Fortafil 3(C)	Chopped or continuous carbon fiber -sized	Great Lakes Carbon
Fortafil 3(O)	Chopped or continuous carbon fiber -sized	Great Lakes Carbon
Fortafil 5(O)	Chopped or continuous carbon fiber -sized	Great Lakes Carbon
Grafil XA-S	Standard high-performance and high-strain grade carbon/graphite fibers	Hysol Grafil Co.
Kureca	Carbon fiber	Kureha Chem.
Microfil 40	Ultrahigh-strength carbon fiber	Fiber Materials, Inc.
P-VS-0053	Pitch-carbon fiber	Union Carbide



TRADE NAME	DESCRIPTION	MANUFACTURER
P-VSB-32	Pitch-carbon fiber	Union Carbide
Pan 50	PAN-carbon fiber	Union Carbide
Panex CF-30	Chopped carbon fiber - sized	Stackpole
Panex CFP 30-05	Carbon fiber paper	Stackpole
Panex KFB	Carbon "Jersey Knit" fabric	Stackpole
Panex PWB-3	Plain weave carbon fabric	Stackpole
Panex PWB-6	Spun yarn plain weave fabric	Stackpole
Panex SWB-8	Spun yarn 8-harness satin weave carbon fiber	Stackpole
Panex WRB-14	Spun yarn 2 x 2 basketweave carbon fabric	Stackpole
Panex 30	Continuous carbon - filament	Stackpole
Panex 30R	Carbon fiber yarn - roving	Stackpole
Panex 30Y/300d	Carbon fiber yarn - roving	Stackpole
Panex 30Y/800d	Carbon fiber yarn	Stackpole
Pyrofil	Carbon fiber	Mitsubishi R.
Rigilor	Carbon fiber	SEROFIM
Sigrafil	Carbon fiber - fabric	Sigri Elektro
Thornel T40	PAN-carbon, continuous fiber	Union Carbide
Thornel T50	PAN-carbon, continuous fiber	Union Carbide
Thornel T300	PAN-carbon, continuous fiber	Union Carbide
Thornel T500	PAN-carbon, continuous fiber	Union Carbide
Thornel 75	Carbon fiber	Union Carbide
Thornel 400	Carbon fiber	Union Carbide
Thornel 700	PAN-carbon fiber	Union Carbide
Toray	Carbon fiber - fabric	Toray

TRADE NAME	DESCRIPTION	MANUFACTURER
VSA-11 (VS-0032)	Mesophase-pitch fiber	Union Carbide
Celion GY70	High-modulus unidirectional graphite fiber tape	BASF Structural Materials
Celion GY80	High-modulus PAN-based graphite fiber	BASF Structural Materials
Grafil	Graphite fabric	Courtaulds
Grafil HM-S/6K	Graphite fibers	Hysol Grafil Co
Grafil HM-S/10K	Graphite fibers	Hysol Grafil Co
Grafil IM-S	Graphite fibers	Hysol Grafil Co
HDG	High-density isotropic graphite	Fiber Materials, Inc.
Hi-Tex	Graphite fibers	Hitco Materials Inc.
Hi-Tex HS	Graphite fibers	Hitco Materials Inc.
Magnamite	Chopped graphite fiber	Hercules
Magnamite A193-P	Plain weave graphite fabric	Hercules
Magnamite A370-5H	5-harness graphite satin weave fabric	Hercules
Magnamite A370-8H	8-harness graphite satin weave fabric	Hercules
Magnamite AS1	Continuous graphite fiber	Hercules
Magnamite AS2	Continuous graphite fiber	Hercules
Magnamite AS4	Continuous graphite fiber	Hercules
Magnamite AS6	Continuous graphite fiber	Hercules
Magnamite HMS	Continuous graphite fiber	Hercules
Magnamite HMU	Continuous graphite fiber	Hercules
Magnamite HTS	Graphite fiber	Hercules
Magnamite IM6	Continuous carbon fiber	Hercules
Microfil 55	High-strength/high-modulus graphite fiber	Fiber Materials, Inc.

TRADE NAME	DESCRIPTION	MANUFACTURER
Ekonol	Liquid crystal polymer (LCP)	Sumitomo Chemical
Fortafil OPF(C)	Oxidized polyacrylonitrile chopped fiber	Great Lakes Carbon
Fortafil OPF(O)	Oxidized polyacrylonitrile chopped fiber	Great Lakes Carbon
Kevlar 29	Aramid fiber	du Pont de Nemours
Kevlar 49	High-modulus aramid fiber	du Pont de Nemours
Kevlar 149	Higher modulus less water absorbent	du Pont de Nemours
PBO	Ordered polymer fiber	Dow Chemical
Spectra	Polyethylene fiber	Allied Signal Technologies (Fibers Division)
Spectra-900	High-tenacity, high-modulus polyethylene and polypropylene fiber	Allied Signal Technologies (Fibers Division)
Twaron	Aramid fiber	Enka (Akzo Group)
Vectran	Liquid crystal polymer (LCP)	Hoechst
Ribtec-GR 304	Stainless steel fiber	Ribtec
Ribtec-HT	Stainless steel fiber	Ribtec
Ribtec-LR 430	Stainless steel fiber	Ribtec
Ribtec-OC 330	Stainless steel fiber	Ribtec
Ribtec-OS 446	Stainless steel fiber	Ribtec
Ribtec-310	Stainless steel fiber	Ribtec
ALBF-1	Bulk alumina fibers	Zircar
APA-1	Alumina papers	Zircar
APA-2	Alumina papers	Zircar
APA-3	Alumina papers	Zircar
Fiberfrax	Standard ceramic fiber - 49,5% Al <sub>2</sub> O <sub>3</sub> , 48,3% SiO <sub>2</sub> , 0,85-1,1% F <sub>2</sub> O <sub>3</sub> , 1,00-1,83% TiO <sub>2</sub>	Standard Oil Engineered Materials Co.
Fibermax	Mullite ceramic fiber - 72% Al <sub>2</sub> O <sub>3</sub> , 27% SiO <sub>2</sub> , 0,02% F <sub>2</sub> O <sub>3</sub> , 0,001% TiO <sub>2</sub>	Standard Oil Engineered Materials Co.

TRADE NAME	DESCRIPTION	MANUFACTURER
FP Alumina	Polycrystalline alumina	du Pont de Nemours
Nextel 312	Polycrystalline metal oxide fibers - 62% Al <sub>2</sub> O <sub>3</sub> , 24% SiO <sub>2</sub> , 14% B <sub>2</sub> O <sub>3</sub>	Minnesota Mining
Nextel 440	70% Al <sub>2</sub> O <sub>3</sub> , 28% SiO <sub>2</sub> , 2% B <sub>2</sub> O <sub>3</sub>	Minnesota Mining
Nicalon	SiC fiber	Nippon Carbon
Saffil	Alumina fibers	Imperial Chem. Inds.
ZYBF-2	Zirconia bulk fibers	Zircar
ZYK-15	Zirconia fabric	Zircar
ZYW-15	Zirconia fabric	Zircar
ZYW-30A	Satin weave zirconia - sized	Zircar
SCW	SiC whisker	Tateho Chemical Industries Co. Ltd.
SNW	Si <sub>3</sub> N <sub>4</sub> whisker	Tateho Chemical Industries Co. Ltd.
X PV1	"Cobweb" whisker - predominately amorphous silica	S.M. Huber

<sup>a</sup> Formerly Celion Fibers, Celanese Corporation.

NOTE From SENER (1984) [147], Weeton, Peters & Thomas (1987) [164], Brown (1989) [64].

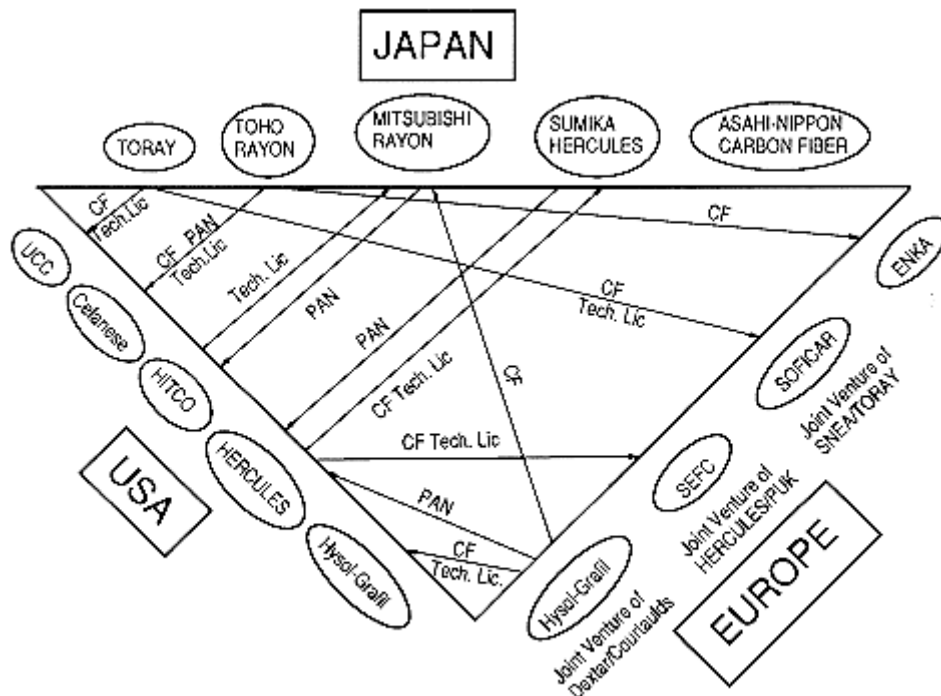


Figure 5-1: International ties between Carbon Fiber manufacturers. From SENNER (1984) [147].

### 5.3.4 Geometry of fiber reinforcement. fabrics. abridged designation

The length, shape, composition and orientation of the fibers in fiber reinforced composite materials can be very varied (see, for instance, Weeton, Peters & Thomas (1987) [164]). Particular emphasis is placed here on those configurations the properties of which are collected in the present clause.

Continuous fiber reinforcements can be one-dimensional, when the fibers are unidirectionally oriented in monolayer tapes (or in tapes stacked together but with the fibers in the same orientation), two-dimensional when the tapes are stacked into plies with different orientations (cross plied when the fibers are at right angles, angle plied at other angles), see Figure 5-2, or three-dimensional where non-interlacing straight filaments (or tapes) are positioned or woven in a predesigned multidirectional structure pattern, Figure 5-3.

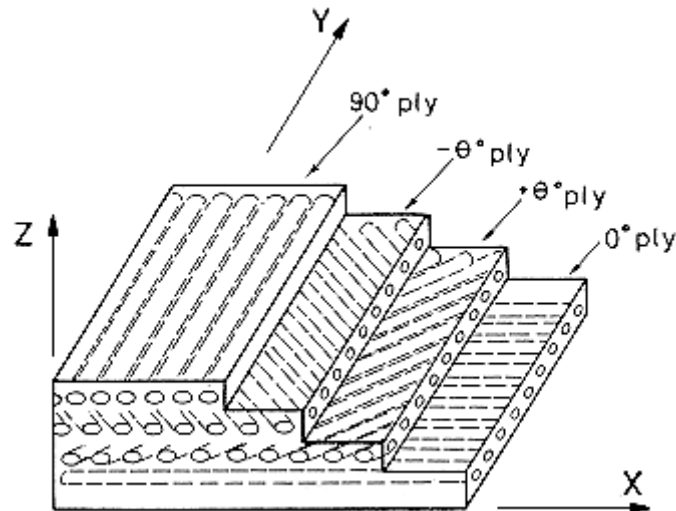


Figure 5-2: Schematic of an angle plied laminate. From Chamis (1987) [67].

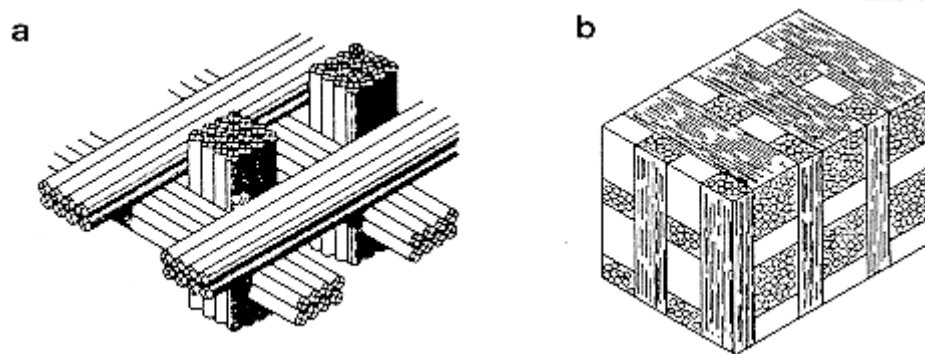


Figure 5-3: Schematic of a tri-orthogonally fiber reinforced composite. a) Straight filaments. From Domínguez (1987) [82]. b) Tapes. From Aboudi (1984) [49].

Hybrid stratified laminates are characterized by a single matrix (usually) and two or more dissimilar fibers. In intralaminar hybrid two reinforcements are in the same ply. An interlaminar hybrid has plies reinforced with different fibers.

Fabric weaves are planar systems made by interlacing yarns or fibers as in the textile industry. Fabrics are introduced to improve the in-plane isotropic characteristics of a ply and to allow manufacturing complex curvature surfaces. Different types of fabric weaves are shown in Figure 5-4.

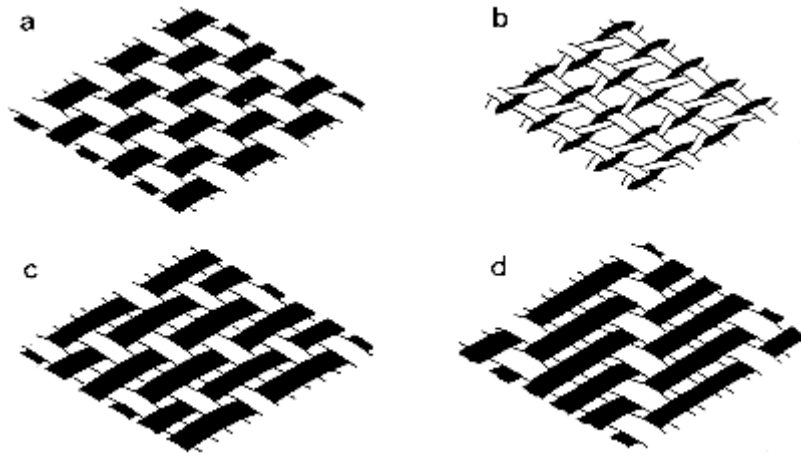


Figure 5-4: Main types of woven fabrics. Lengthwise (warp) yarns and crosswise (fill) yarns can be interlaced to produce woven fabrics. A fabric construction of 16 x 14 means 16 warp ends per inch and 14 fill ends per inch. a) Plain weave. Very stable. Small yarn slippage. b) Leno weave. Minimizes distortion with few yarns. c) Twill. The fabric has a broken diagonal line and, consequently, greater pliability than a plain weave. d) Crowfoot satin. Pliable and comfortable to contoured surfaces. From Domínguez (1987) [82], Weeton, Peters & Thomas (1987) [164].

An abridged designation is used to identify the laminates according to the reinforcement arrangement. The convention used for laminates with a single type of reinforcing fibers is introduced, by means of simple examples, in Table 5-1.

**Table 5-1: Abridged Designation of Single Reinforcement Laminates**

Description of the Ply Sequence	Abridged Designation	Comments
45°,0°,90°	(45/0/90) <sub>T</sub>	T = total laminate Any angle ply should be identified.
45°,0°,0°,90°	(45/0 <sub>2</sub> /90) <sub>T</sub>	Total. A given ply appears twice.
45°,0°,90°,90°,0°,45°	(45/0/90) <sub>S</sub>	S = symmetrical laminate. No ply contains the symmetry plane.
0°,90°,45°,90°,0°	(0/90/ $\overline{45}$ ) <sub>S</sub>	Symmetrical. The central ply (45°) contains the symmetry plane.
0°,90°,-90°,0°	(0/90) <sub>Q</sub>	Antisymmetrical. No ply contains the antisymmetry plane.
90°,0°,-90°	(90/ $\overline{0}$ ) <sub>Q</sub>	Antisymmetrical. The central ply (0°) contains the antisymmetry plane.
45°,0°,90°,-90°,-90°,90°,0°,45°	(45/0/±90) <sub>S</sub>	Symmetrical. Consecutive balanced plies. No ply contains the symmetry plane.
45°,0°,-90°,90°,-90°,90°,0°,-45°	(45/0/ $\mp$ 90) <sub>Q</sub>	Antisymmetrical. Consecutive balanced plies. No ply contains the antisymmetry plane.
45°,0°,90°,45°,0°,90°,90°,0°,45°,90°,0°,45°	(45/0/90) <sub>2S</sub>	Symmetrical. Double sequence.

When fabrics and tapes are stacked in a laminate, fabrics are given in parenthesis. Thus, (45/(0)/90/(45))<sub>T</sub> indicates that the sequence is: tape at 45°, fabric at 0°, tape at 90° and fabric at 45°.

For hybrid laminates the convention is the same but the reinforcing material is specified by means of initials and digits as subscripts. Thus: (45<sub>K49</sub>/0<sub>T300</sub>) indicates that one of the plies, at 45°, is reinforced by Kevlar 49 and the other, at 0°, by Graphite T300.

The matrix-fiber composition of a composite material is represented by the initials representing the fibers followed by those used to identify the matrix. For example: T300/SP288 is a graphite (T300) epoxy (SP288) reinforced material.

Epoxy resin systems consist of a resin and a hardener or curing agent. They can be supplied as two independent products, to be mixed before use, or as a mixture which can be thermally activated.

Two-product systems are identified as it is indicated in the following example: DER 332/T403, where DER 332 is the resin (Bisphenol A, epoxy) and T403 the hardener.



In addition to the angular arrangement of plies a new angle appears because of the anisotropy of most composite materials. For an unidirectional laminate the properties in the plane of laminate can be measured parallel to the fibers and normal to the fibers.

Scalar variables are identified by a single subscript which indicates the direction, 1, 2 or 3 (see Figure 5-5) in which they have been measured.

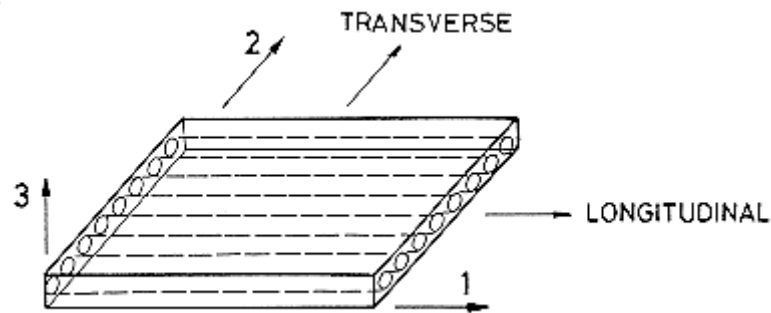


**Figure 5-5: Longitudinal (to fibers) and transverse directions for the measurement of composite properties. From Chamis (1987) [67].**

For plies stacked with different orientations, in-plane variables are usually referred to the  $0^\circ$  direction.

## 5.4 Physical properties

### 5.4.1 Density

#### 5.4.1.1 Calculation formula for composites

The density,  $\rho$ , of a composite in terms of those of the fiber,  $\rho_f$ , and of the matrix,  $\rho_m$ , is given by

$$\rho = \rho_f \varphi_f + \rho_m \varphi_m \quad \rho = \rho_f \varphi_f + \rho_m \varphi_m \quad [5-1]$$

where  $\varphi$  is the volume ratio.

#### 5.4.1.2 Tabulated data

Densities of fibers are given in Table 5-2 and those of matrices in Table 5-3.

**Table 5-2: Density,  $\rho_f$  [kg.m<sup>-3</sup>], of High-Strength Fibers**

Type	$\rho_f \times 10^{-3}$ [kg.m <sup>-3</sup> ]	References
Glass Fibers A-glass	2,50	SENER (1984) [147]
C-glass	2,49	
D-glass	2,16	
E-glass	2,55	Weeton, Peters & Thomas (1987) [164]
S-glass	2,49	
4H-1 glass	2,66	
YM-31A	2,84	SENER (1984) [147]
Quartz (fused silica)	2,19	Weeton, Peters & Thomas (1987) [164]
Carbon Fibers Carbon PAN	1,72-1,80	Weeton, Peters & Thomas (1987) [164]
Carbon/Graphite pitch	1,99-2,16	
Graphite I	1,75	Beardmore et al. (1980) [62]
Graphite II	1,85	

Type	$\rho_f \times 10^{-3}$ [kg.m <sup>-3</sup> ]	References	
Celion G50	1,78	SENER (1984) [147]	
Celion GY70	1,95		
Celion ST	1,77	ESA (1989) [88]	
Celion 1000, 3000, 6000	1,76	SENER (1984) [147]	
Celion 6000 (unsized)	1,78	Scola & Laube (1988) [146]	
Celion 6000 (epoxy sized)	1,78		
Courtaulds XAS	1,71	SENER (1984) [147]	
Fenax ST3 (Enka/TOHO)	1,77	ESA (1989) [88]	
Fortafil 3 (0)	1,73	SENER (1984) [147]	
Fortafil 3	1,71		
Fortafil 3T	1,80		
Fortafil 4T	1,70		
Fortafil 5	1,80		
Fortafil 5T	1,80		
Fortafil 6T	1,90		
Grafil AS	1,76		
Grafil HMS (6K)	1,86		ESA (1989) [88]
Grafil HTS	1,77		SENER (1984) [147]
GY-70	1,96	ESA (1989) [88]	
G40-600 (IM Celanese)	1,78		
Hercules AS	1,77	SENER (1984) [147]	
Hercules AS4	1,80	ESA (1989) [88]	
Hercules AS6	1,83		
Hercules HTS	1,80	SENER (1984) [147]	

Type	$\rho \times 10^{-3}$ [kg.m <sup>-3</sup> ]	References
Hercules HMS	1,88	
Hercules IM6 1200	1,73	ESA (1989) [88]
Hercules IM7	1,78	
Hi-Tex 1500, 3000, 6000, 12000	1,80	SENER (1984) [147]
Modmor I S	1,90	
Modmor II S	1,77	
Modmor III S	1,65	
Modmor IV S	1,80	
Panex 1/4CF-30	1,73	
Panex 30	1,74	
Panex 30A	1,78	
Panex 30C	1,78	
Panex 30R	1,75	
Panex 30Y/800d	1,75	
Rigilor	1,75	
Rigilor AG	1,95	
Sigrafil HF	1,80	
Sigrafil HM	2,00	
Thornel 50 <sup>a</sup>	1,67	
Thornel 50S <sup>a</sup>	1,67	
Thornel 75 <sup>a</sup>	1,82	
Thornel 75S <sup>a</sup>	1,82	
Thornel 300	1,76	
Thornel 300 WYP 90-1/0	1,75	

Type	$\rho_f \times 10^{-3}$ [kg.m <sup>-3</sup> ]	References
Thornel 400	1,78	
Toray T300B	1,72	
Toray T300C	1,74	
Toray T300R (unsized)	1,73	Scola & Laube (1988) [146]
Toray T400	1,80	ESA (1989) [88]
Toray T800	1,80	
Torayca M40	1,85	SENER (1984) [147]
Torayca T300	1,78	
Toraica T500	1,78	
Aramid Fibers Kevlar 29	1,44	Weeton, Peters & Thomas (1987) [164]
Kevlar 49	1,44	
Kevlar 49/HBRF 55A	1,23	Elias & Waugh (1981)
Nomex	1,38	SENER (1984) [147]
Twaron HM (ENKA AG)	1,45	ESA (1989) [88]
Other Organic Fibers Polyamide	1,13	Weeton, Peters & Thomas (1987) [164]
Polyester-Dacron Type 68	1,38	
Nylon Du-Pont 728	1,13	
Spectra-900	0,97	
Processed mineral fiber	2,68	
Fibrafrax	2,60	
Fibermax	2,99	
Metal Wires Aluminium	2,68	
Beryllium	1,85	Rosato (1982) [145]

Type	$\rho_f \times 10^{-3}$ [kg.m <sup>-3</sup> ]	References
Boron	2,52	
Molybdenum	10,2	
Steel	7,81	
Tantalum	16,6	
Titanium	4,71	
Tungsten	19,2	Weeton, Peters & Thomas (1987) [164]
René 41	8,25	
Amorphous Metals Fe <sub>80</sub> B <sub>20</sub>	7,40	Davis (1978) [78]
Fe <sub>80</sub> P <sub>16</sub> C <sub>3</sub> B <sub>1</sub>	7,30	
Fe <sub>40</sub> Ni <sub>40</sub> P <sub>14</sub> B <sub>6</sub>	7,51	
Ni <sub>49</sub> Fe <sub>29</sub> P <sub>14</sub> B <sub>6</sub> Si <sub>2</sub>	7,65	
Pd <sub>80</sub> Si <sub>20</sub>	10,3	
Multiphase <sup>b</sup> Boron	2,63	Weeton, Peters & Thomas (1987) [164]
B <sub>4</sub> C Boron Carbide	2,35	
SiC Silicon Carbide	3,46-3,52	
SiC on B	~ 3	
TiB <sub>2</sub> Titanium Diboride	4,48	
Polycrystalline Inorganic (Bulk or Fiber) Al <sub>2</sub> O <sub>3</sub> Alumina	3,16	Weeton, Peters & Thomas (1987) [164]
ZrO <sub>2</sub> Zirconia	4,84	
BN Boron Nitride	1,91	
WC Tungsten Carbide	15,70	
TiB <sub>2</sub> Titanium Diboride	4,5±0,1	

Type	$\rho_f \times 10^{-3}$ [kg.m <sup>-3</sup> ]	References
ZrC Zirconium Carbide	6,56	Weeton, Peters & Thomas (1987) [164]
TiC Titanium Carbide	4,92	
ZrB <sub>2</sub> Zirconium Diboride	6,10	
SiO <sub>2</sub> Silica	2,54	
Whiskers Graphite	2,10	
Al <sub>2</sub> O <sub>3</sub> Alumina	3,98	
BeO Beryllium Oxide	3,01	
SiC Silicon Carbide	3,22	
B <sub>4</sub> C Boron Carbide	2,51	

<sup>a</sup> Precursor RAYON.

<sup>b</sup> Deposited on 0,127 x 10<sup>-3</sup> m diameter Tungsten core wire.

**Table 5-3: Density,  $\rho_m$  [kg.m<sup>-3</sup>], of Matrices**

Type	T [K]	$\rho_m \times 10^{-3}$ [kg.m <sup>-3</sup> ]	References
<u>Epoxy</u> Typical		1,12	Weast (1976) [163]
Code 69		1,268	ESA (1989) [88]
Fibredux 914		1,304	
Hexcel F155		1,336	Balis Crema, Balboni & Castellani (1986) [59]
Hysol 6000-OP	267	1,21	Touloukian (1967) [157]
3501		1,280	ESA (1989) [88]
<u>Phenolic</u> Typical	363	1,27	Touloukian (1967) [157]
50% Resin type S		1,37	
40% Resin type S		1,40	

Type	T [K]	$\rho_m \times 10^{-3}$ [kg.m <sup>-3</sup> ]	References
<u>Polyester</u> Typical		1,50-2,10	Weast (1976) [163]
Castolite	267	1,23	Touloukian (1967) [157]
<u>Polyamide</u> Nylon 6		1,13-1,14	Skinner & Goldhar (1968) [149]
Nylon 6/6		1,13-1,15	
Nylon 6/10		1,07-1,09	
<u>Polysulfone</u> Typical		1,24-1,25	
<u>Polyimide</u> Typical		1,44	Economy, Nowak & Cottis (1970) [86]

## 5.5 Thermal properties

### 5.5.1 Specific heat

#### 5.5.1.1 Measuring methods

The specific heat,  $c$ , can be measured by Differential Scanning Calorimetry (DSC) or with a conventional calorimeter.

In the DSC method a small, usually powdered, sample of given mass is heated in a platinum alloy cup. A second cup contains a reference material of known mass and specific heat (which are not too different from those of the sample material). The cups are mounted on a solid aluminium block which contains heaters and temperature sensors. The sample-holder can be heated independently.

The temperature of both samples is raised (or decreased) at a constant rate, and from the amount of power required to keep the sample holder at any instant at the same temperature as the reference holder, the specific heat of the sample is deduced.

When a conventional calorimeter is used, a given mass of a sample is heated up to a given temperature, which is fixed beforehand. The heat source is a thermally insulated reservoir holding a liquid at a higher temperature. The specific heat of the material is deduced from the liquid temperature loss.

#### 5.5.1.2 Calculation formula for composites

The specific heat,  $c$ , of a composite in terms of those of the fiber,  $c_f$ , and of the matrix,  $c_m$ , is given by

$$c = \frac{1}{\rho} (\rho_f \varphi_f c_f + \rho_m \varphi_m c_m) \quad [5-2]$$



$\rho$  and  $\varphi$  being respectively the density and the volume fraction.

5.5.1.3. Tabulated data

**Table 5-4: Specific Heat,  $c_f$  [J.kg<sup>-1</sup>.K<sup>-1</sup>], of High-Strength Fibers**

Type	Temperature [K]					
	290	300	370	480	670	
<u>Glass Fibers</u> Fused Silica	963 <sup>c,d</sup>	745 <sup>a,b</sup>				Table 5-5
C-glass <sup>a,d</sup>	887					
D-glass <sup>a,d</sup>	732					
E-glass <sup>a,d</sup>	803					
S-glass <sup>a,d</sup>	737					
S-2-glass <sup>a,d</sup>	737					
<u>Carbon Fibers</u> A graphite <sup>d</sup>	710					
HM graphite <sup>d</sup>	710					
VHM graphite <sup>d</sup>	710					
UHM P75 graphite <sup>e</sup>	1000					
UHM P100 graphite <sup>e</sup>	1000					
UHM P120 graphite <sup>e</sup>	1000					
Fortafil 3 <sup>f</sup>		921				
Fortafil 5 <sup>f</sup>		879				
Grafil <sup>f</sup>	710					
Magnamite AS1 <sup>f</sup>		712				
Magnamite HTS <sup>f</sup>		712				

Type	Temperature [K]					
	290	300	370	480	670	
Thornel 300 <sup>f</sup>		712				
<u>Aramid Fibers</u> Kevlar <sup>d</sup>						Table 5-6
Kevlar 49/HBRF 55a <sup>g</sup>			1172	1507		
<u>Metal Wires</u> Aluminium <sup>d</sup>	960					
Boron <sup>d</sup>	840					
<u>Amorphous Metals</u> Fe <sub>81,5</sub> B <sub>14,5</sub> Si <sub>4</sub> <sup>f</sup>					270	
Fe <sub>75</sub> C <sub>10</sub> P <sub>15</sub> <sup>f</sup>	494					
Pd <sub>82</sub> Si <sub>18</sub> <sup>f</sup>	670					

<sup>a</sup> Determined on bulk.

<sup>b</sup> From Johnson (1961) [109].

<sup>c</sup> Determined on fibers.

<sup>d</sup> From Weeton, Peters & Thomas (1987) [164]. Temperature not given.

<sup>e</sup> From AMOCO (1990) [52]. The number after P stands for the fiber  $E_f$  in millions of lb.in<sup>-2</sup>.

<sup>f</sup> From Karlsson (1983) [111].

<sup>g</sup> From Elias & Waugh (1981) .

**Table 5-5: Fused Silicia**

Temperature [K]	$c_f$ [J.kg <sup>-1</sup> .K <sup>-1</sup> ]
50	96,8 <sup>a,b</sup>
100	261 <sup>a,b</sup>
200	543 <sup>a,b</sup>
290	963 <sup>c,d</sup>
300	745 <sup>a,b</sup>

- <sup>a</sup> Determined on bulk.
- <sup>b</sup> From Johnson (1961) [109].
- <sup>c</sup> Determined on fibers.
- <sup>d</sup> From Weeton, Peters & Thomas (1987). Temperature not given.

**Table 5-6: Kevlar <sup>d</sup>**

Temperature [K]	$c_f$ [J.kg <sup>-1</sup> .K <sup>-1</sup> ]
270	1220
320	1600
370	1990
420	2370
470	2620
520	2740
570	2840

- <sup>d</sup> From Weeton, Peters & Thomas (1987). Temperature not given.

**Table 5-7: Specific Heat,  $c_m$  [ $J.kg^{-1}.K^{-1}$ ], of Matrices**

Type	T [K]	$c_m$ [ $J.kg^{-1}.K^{-1}$ ]	References
Epoxy Typical ( $1200 kg.m^{-3}$ )	290	1200	GENIUM (1986) [91]
	500	3100	
	560	1500	
DER 332/T403 (100:36)	290	1750	Chiao & Moore (1974) [68]
DER 332/DMP30 (2%)	230	960	Touloukian (1967) [157]
	250	1050	
	310	1260	
	370	1460	
	420	1800	
	480	2340	
	500	3060	
	530	2220	
	560	1460	
	590		
	620		
Polyamide Nylon 6		1670	Anon. (1969) [53]
Nylon 6/6		1260-2090	
Nylon 6/10		1260-2090	
Polyimide Typical		1050	Chamis (1987) [67]

**Table 5-8: Specific Heat,  $c$  [J.kg<sup>-1</sup>.K<sup>-1</sup>], of Composite Materials**

Matrix	Fiber		Temperature [K]									
	Type	Volume $\phi$	30	80	210	220	250	270	290	300	320	350
Epoxy DER 332/T403 <sup>a</sup>	E-glass Unidirec.	0,700			640		750		850		900	950
NASA Resin 2 <sup>b</sup>	S-901 Glass			179						1935		
Narmco 4033	Quartz Fabric								1000			
Narmco 4065	Light Weight Quartz Fabric								1300			
Narmco 4047	Carbon Fabric								1200			
DER 332/T403 <sup>d</sup>	Kevlar 49 Unidirec.	0,600				840	930	1020		1120	1190	1300
XD7818/T403 <sup>d</sup>	Kevlar 49 Unidirec.	0,600				860	940	1030		1120	1200	2650
Narmco 4018	Nylon Fabric							1400				
Narmco 5505 <sup>b</sup>	0,14x10 <sup>-3</sup> m Boron			154						1275		
Not identified	P75 <sup>e</sup>	0,600							1300			
Al		0,450							920			
SiC		0,600							750			
Graphite		0,600							790			
15V coal tar pitch <sup>f</sup>	HM Carbon	0,490	19	111								

- a From Clements & Moore (1978) [73].
- b From Collings & Smith (1978) [75].
- c From Penton (1966) [135].
- d From Clements & Chiao (1977) [71].
- e From Amoco (1990) [52]. The number after P stands for the fiber  $E_f$  in millions of lb.in<sup>-2</sup>.
- f Composite is Textron FWPF. Data from smooth curve in the 30 K to 100 K range. From Yang & Migone (1989) [167].

For additional information on the specific heat of glass-reinforced, graphite-epoxy, boron-epoxy and of other advanced composites, at room temperature and below, see clause 5.5.

## 5.5.2 Thermal conductivity

### 5.5.2.1 Measuring methods

Thermal conductivity can be measured at constant or at varying temperature. In the first instance two different types of apparatus can be used depending on whether the thermal conductivity is large or small.

When the thermal conductivity is large, the so-called Searle's bar system is used. See Figure 5-6a

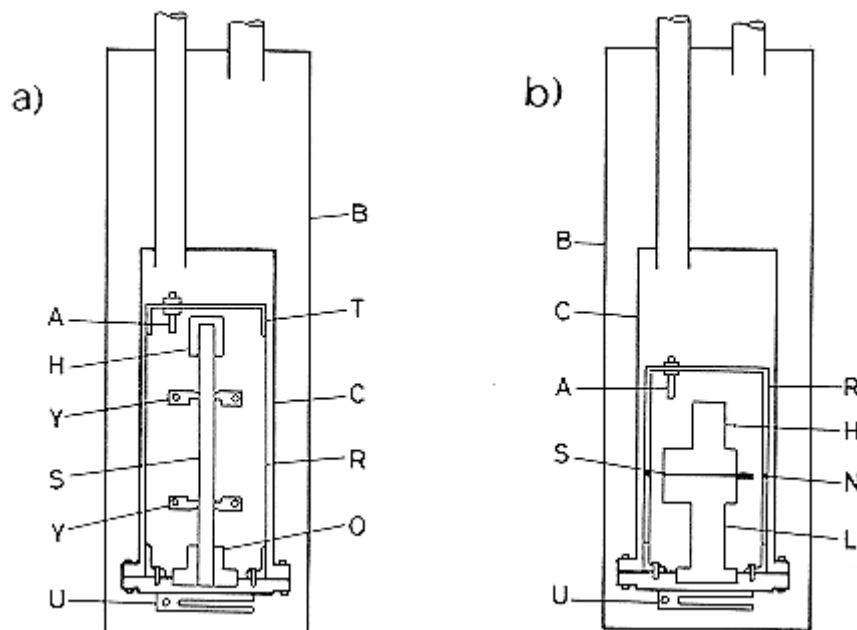


**Figure 5-6: Cryostat assemblies for measuring the thermal conductivity,  $k$ . a) High- $k$  samples. b) Low- $k$  samples. From Pilling, Yates, Black & Tattersall (1979) [137]. For explanation see text.**

A cryostat assembly, suspended from the top cap of a Dewar vessel by means of three stainless steel tubes, encloses a copper specimen chamber, C, surrounded by an outer brass can, B. The specimen, S, shaped as a bar, is held axially by a copper mounting block, O, located at the center of the base of the specimen chamber. Another, slightly different, mounting block can be used to hold an electrolytic iron reference bar.

The upper copper block, H, thermally decoupled from the surrounding, is electrically heated. Both the heated holder and the bar are surrounded by a stainless steel radiation shield, R, which terminates in a copper top cap, T, with a thermal anchoring port, A, for the electrical connections.

A copper block, U, is hard soldered to the base of the specimen chamber to house a platinum resistance thermometer. The temperature gradient along the specimen can be measured through thermometer yokes, Y, in thermal contact with the specimen.

Apiezon vacuum grease is used to achieve good thermal contact between the various demountable components. The specimen chamber is evacuated and sealed to the bottom plate by Loctite Stud Lock which provides access when changing specimens.

Temperatures between 80 K and 270 K can be achieved, with liquid nitrogen in the Dewar, by means of a series of five heating coils wound on the outside of the specimen chamber, C. The temperature is monitored, within a few milli degrees, with the sensor located in the copper block, U, which activates the heating coils.

The temperature gradient along the radiation shield, R, should be identical to that along the specimen. To this aim the base of the shield was in thermal contact with the specimen holder whereas a differential thermocouple placed between H and T activates a heating coil wound on the top section of the radiation shield.

When the thermal conductivity is small, disc-shaped samples are used as in the Lee's disc arrangement, Figure 5-6b.

Now the outer brass can, B, the specimen chamber, C, and the temperature sensor, U, are the same as before.

The specimen disc, S, is sandwiched between two copper blocks which contain the platinum resistance thermometers. The upper block terminates on a pillar, H, to which a heater is wound. The lower block, L, fits into the base of the specimen chamber.

Good thermal contact between the various surfaces is achieved by a low vapour-pressure grease.

The radiation shield, R, consists of two equal diameter cylindrical copper shells separated by a nylon insert, N, the length and axial position of which are the same as those of the specimen.

The temperature equality between the lower part of the shield and the lower sandwich block is achieved by thermally connecting them through the base of the specimen chamber, and that between the upper part of the shield and the upper sandwich block is achieved with the aid of a differential thermocouple which actuates a heater wound to the upper part of the shield.

When the temperature changes, the thermal conductivity is measured continuously by use of a two-plate apparatus, Figure 5-7.

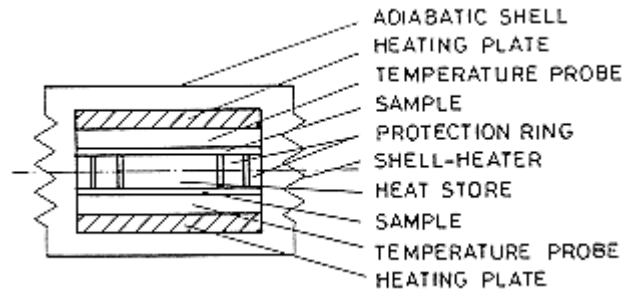


**Figure 5-7: Facility used to measure the thermal conductivity,  $k$ , of a sample as a function of temperature in the range 90 K to 410 K. Temperature changes continuously. From Ott (1981) [132].**

The samples lie between the temperature probe plates and the heat store. The heat flows from the outer plates to the central heat store through temperature probes and samples. An adiabatic shell, kept at the heat store temperature, shields the system.

Helium and Nitrogen, are used in order to obtain a reliable thermal contact between the plates.

Since the temperature changes with time, both the sample specific heat and heat store influence the flux and should be taken into account. The specific heat is deduced from the measurements.

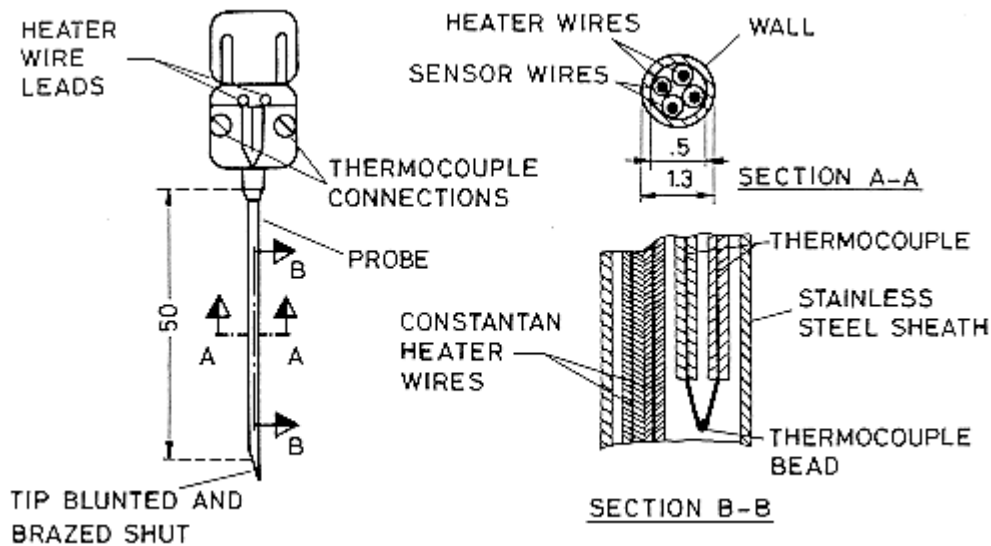
In the case of polymer melts, material characteristics could change due to degradation when exposed to high temperatures for the extended periods of time required by the measurements.

The measurements can be made quickly, before the effects of thermal degradation become apparent, by use of the Line Source Method which is based on the transient flow of heat in cylindrical geometries (Lobo & Cohen (1990) [120]).

The thermal conductivity is deduced (independently of the specific heat) from the change in temperature during a time interval at a fixed point close to the cylinder axis. This method has been used to measure the thermal conductivity of unreinforced and reinforced materials in the temperature range 290 K to 500 K. The reproducibility of the results is better than 10 %. The results agree reasonably close with others found in the literature.

The probe consists in heater and measurement wires which are encased in a thin steel hypodermic needle 0,05 m long and  $1,3 \times 10^{-3}$  m in diameter, Figure 5-8: Hypodermic probe to measure the thermal conductivity of polymer melts. All the dimensions are in mm. From Lobo & Cohen (1990) [120]. Heater elements are 36 gauge constantan thermocouple wires (TFE sheathed) which extend all along the probe. Temperature is measured with 36 gauge J-type thermocouple wires (TFE sheathed) which are spot welded or brazed. Care should be taken to place the thermocouple bead halfway down the casing length and in physical contact with the wall.





Note: non-si units are used in this figure

**Figure 5-8: Hypodermic probe to measure the thermal conductivity of polymer melts. All the dimensions are in mm. From Lobo & Cohen (1990) [120].**

Since the power output of the probe heater is too small a booster heater is used to heat up the sample to its initial temperature.

For molten samples a concentric barrel heater is used. After the barrel heater has attained the desired temperature level, the sample is introduced through the top. Once the sample is melted, the probe is inserted axially down the center of the barrel and the temperature monitored until steady state is attained.

For measurements below the melting point the barrel heater is inconvenient and a circulation oil or fluidized sand bath may be used. The samples are prepared by melting the polymer into small vials in an oven under vacuum. The probe is inserted into the molten polymer which is allowed to solidify slowly. The sample with imbedded probe is then placed in the bath and reading may be taken at different temperatures.

To account for the deviation of the experimental setup from the ideal situation, a probe constant factor is obtained by calibration against materials of known thermal conductivity.

### 5.5.2.2 Calculation formulae for composites

The longitudinal (direction 1) thermal conductivity,  $k_1$ , of the composite in terms of those of the fiber,  $k_f$  and of the matrix,  $k_m$ , is given as follows:

$$k_1 = \varphi_f k_f + \varphi_m k_m \quad [5-3]$$

The transverse thermal conductivity,  $k_2 = k_3$ , of the composite in terms of the thermal conductivities of the constituents:

$$k_2 = k_3 = \left(1 - \sqrt{\varphi_f}\right) k_m + \frac{\sqrt{\varphi_f} k_m}{1 - \sqrt{\varphi_f} \left(1 - \frac{k_m}{k_{f_2}}\right)} \quad [5-4]$$

When voids exist in the matrix  $k_m$  should be substituted by  $k'_m$

$$k'_m = \left(1 - \sqrt{\phi_f}\right) k_m + \frac{\sqrt{\phi_v} k_m}{1 - \sqrt{\phi_v} \left(1 - \frac{k_m}{k_v}\right)} \quad [5-5]$$

For the thermal conductivity in a direction forming an angle  $\theta$  with the fibers,  $k_\theta$ :

$$k_\theta = k_1 \cos^2 \theta + k_2 \sin^2 \theta \quad [5-6]$$

For a composite material with  $n_1$  layers of fibers forming an angle  $\theta_1$  with the measurement direction, and  $n_2$  layers of fibers forming an angle  $\theta_2$ :

$$k = \frac{n_1}{n_1 + n_2} k_{\theta_1} + \frac{n_2}{n_1 + n_2} k_{\theta_2} \quad [5-7]$$

From Karlsson (1983) [111], Chamis (1987) [67].

### 5.5.2.3 Tabulated data

**Table 5-9: Longitudinal (1) and Transverse (2) Thermal Conductivity, of High-Strength Fibers. Tabulated Data are  $k_{f1}$  [W.m<sup>-1</sup>.K<sup>-1</sup>]/ $k_{f2}$ [W.m<sup>-1</sup>.K<sup>-1</sup>], of Fibers**

Type	Temperature [K]						
	270	290	300	370	380	470	670
Glass Fibers E-Glass			1,9/2,2 <sup>a</sup>				
S-2 Glass			2,6/2,7 <sup>a</sup>				
Carbon Fibers Grafil		105/-					
GY70			140/-				
Fortafil 3			20/-				
Fortafil 5			144/-				
Magnamite AS1			6/-				
Thornel P			83/-				
Thornel 300			21/9				

Type	Temperature [K]						
	270	290	300	370	380	470	670
P 130X <sup>b</sup>	920/-	905/-	890/-	790/-	760/-	660/-	
Aramid Fibers Kevlar <sup>c</sup>			0,48/0,41	0,52/0,46		0,57/0,57	
Kevlar 49/HBRF 55A <sup>d</sup>					-/21		
Amorphous Metals Fe <sub>81,5</sub> B <sub>14,5</sub> Si <sub>4</sub>							14
Fe <sub>80</sub> B <sub>20</sub>	6,5						
Fe <sub>74</sub> C <sub>10</sub> P <sub>15</sub>			5,9				
Fe <sub>73</sub> Mo <sub>10</sub> B <sub>17</sub>	7,1						
Zr <sub>70</sub> Co <sub>30</sub>	5,1						
Zr <sub>70</sub> Ni <sub>30</sub>	3,8						
Zr <sub>10</sub> Be <sub>40</sub> Ti <sub>50</sub>	3,5						
Pd <sub>82</sub> Si <sub>18</sub>			21				
Pd <sub>78</sub> Cu <sub>6</sub> Si <sub>16</sub>	9,2						

<sup>a</sup> Deduced from k of an unidirectional composite.

<sup>b</sup> P 130X is an Amoco Advanced Pitch-Based Fiber. Data from smooth curve in McGuire & Vollerin (1990) [127]. See also Figure 5-10.

<sup>c</sup> Measured on fibers only. Corrected value for a specific density 1,45.

<sup>d</sup> From Elias & Waugh (1981).

NOTE All data, unless otherwise stated, are from Karlsson (1983) [111].

**Table 5-10: Thermal Conductivity,  $k_m$  [ $\text{W}\cdot\text{m}^{-1}\cdot\text{K}^{-1}$ ], of Matrices**

Type	Temperature [K]						
	270	290	300	350	470	570	
<u>Epoxy</u> Araldite LY556 <sup>a</sup>	0,230	0,234	0,236				Table 5-11
Araldite MY 750/DDM <sup>b</sup>		0,29± 0,06					
DER 332/T403 (100:36) <sup>c</sup>			0,134				Table 5-12
Epitoke 210/BF <sub>3</sub> 400 <sup>b</sup>	0,226						Table 5-13
Epoxin 162 <sup>a</sup>	0,245	0,247	0,248				Table 5-14
Hysol 6000-OP <sup>d</sup>		0,196					
H 70E <sup>e</sup>		1,4					
H 70S <sup>e</sup>		1,2					
<u>Phenolic</u> Typical <sup>d</sup>		0,245					
50% Resin type S <sup>d</sup>		0,356					
40% Resin type S <sup>d</sup>		0,377					
<u>Polyester</u> Typical <sup>f</sup>			0,16				
Castolite <sup>d</sup>	0,175						
Palatal P51 <sup>a</sup>	0,192	0,193	0,193				Table 5-15
<u>Polyamide</u> Nylon 6 <sup>a</sup>	0,215	0,219	0,220				Table 5-16
Comco, Nylon 6/6 <sup>g,h</sup>			0,366				Table 5-17
Polypenco 101,Nylon 6/6 <sup>g,h</sup>			0,342				Table 5-18
<u>Polysulfone</u> Typical <sup>f</sup>			0,26				
<u>Polyphenylene Sulfide</u> <sup>f</sup>			0,29				
<u>Polypropylene</u> <sup>a</sup>	0,193	0,195	0,195				Table 5-19

Type	Temperature [K]						
	270	290	300	350	470	570	
<u>Polymide</u> Kapton <sup>i</sup>			0,156	0,163	0,178	0,189	

- <sup>a</sup> Curve fitting to experimental points given by Ott (1981) [132].
- <sup>b</sup> From Pilling, Yates, Black & Tattersall (1979) [137].
- <sup>c</sup> From Chiao & Moore (1974) [68].
- <sup>d</sup> From Touloukian (1967) [157].
- <sup>e</sup> From Epo-Tek (1989) [87].
- <sup>f</sup> From Karlsson (1983) [111].
- <sup>g</sup> Rod. Measured along direction of extrusion.
- <sup>h</sup> From Ashworth, Loomer & Kreitman (1973) [54].
- <sup>i</sup> From GENIUM (1986) [91].

**Table 5-11: Araldite LY556**

Temperature [K]	$k_m$ [W.m <sup>-1</sup> .K <sup>-1</sup> ]
100	0,162
140	0,187
175	0,203
180	0,205
220	0,219
260	0,228
270	0,230
290	0,234
300	0,236
320	0,239
340	0,243

- <sup>a</sup> Curve fitting to experimental points given by Ott (1981) [132].

**Table 5-12: DER 332/T403 (100:36) <sup>c</sup>**

Temperature [K]	$k_m$ [W.m <sup>-1</sup> .K <sup>-1</sup> ]
300	0,134
320	0,174
340	0,210

<sup>c</sup> From Chiao & Moore (1974) [68].

**Table 5-13: Epitoke 210/BF<sub>3</sub>400 <sup>b</sup>**

Temperature [K]	$k_m$ [W.m <sup>-1</sup> .K <sup>-1</sup> ]
175	0,194
180	0,196
220	0,207
260	0,222
270	0,226

<sup>b</sup> From Pilling, Yates, Black & Tattersall (1979) [137].

**Table 5-14: Epoxin 162 <sup>a</sup>**

Temperature [K]	$k_m$ [W.m <sup>-1</sup> .K <sup>-1</sup> ]
100	0,179
140	0,207
175	0,223
180	0,225
220	0,237
260	0,244
270	0,245
290	0,247

Temperature [K]	$k_m$ [W.m <sup>-1</sup> .K <sup>-1</sup> ]
300	0,248
320	0,250
340	0,252

<sup>a</sup> Curve fitting to experimental points given by Ott (1981) [132].

**Table 5-15: Palatal P51 <sup>a</sup>**

Temperature [K]	$k_m$ [W.m <sup>-1</sup> .K <sup>-1</sup> ]
100	0,156
140	0,171
175	0,180
180	0,182
220	0,188
260	0,192
270	0,192
290	0,193
300	0,193
320	0,193
340	0,192

<sup>a</sup> Curve fitting to experimental points given by Ott (1981) [132].

**Table 5-16: Nylon 6 <sup>a</sup>**

Temperature [K]	$k_m$ [W.m <sup>-1</sup> .K <sup>-1</sup> ]
100	0,166
140	0,182
175	0,193
180	0,195
220	0,205
260	0,213
270	0,215
290	0,219
300	0,220
320	0,223
340	0,226

<sup>a</sup> Curve fitting to experimental points given by Ott (1981) [132].



**Table 5-17: Comco, Nylon 6/6 <sup>g,h</sup>**

Temperature [K]	$k_m$ [ $\text{W}\cdot\text{m}^{-1}\cdot\text{K}^{-1}$ ]
1	0,00193
20	0,0948
40	0,184
60	0,245
80	0,278
100	0,297
140	0,324
180	0,337
220	0,348
260	0,355
300	0,366
320	0,370
340	0,370

<sup>g</sup> Rod. Measured along direction of extrusion.

<sup>h</sup> From Ashworth, Loomer & Kreitman (1973).

**Table 5-18: Polypenco 101, Nylon 6/6 <sup>g,h</sup>**

Temperature [K]	$k_m$ [W.m <sup>-1</sup> .K <sup>-1</sup> ]
1	0,00193
20	0,0948
40	0,175
60	0,228
80	0,263
100	0,284
140	0,305
180	0,316
220	0,328
260	0,329
300	0,342
320	0,353
340	0,357

<sup>g</sup> Rod. Measured along direction of extrusion.

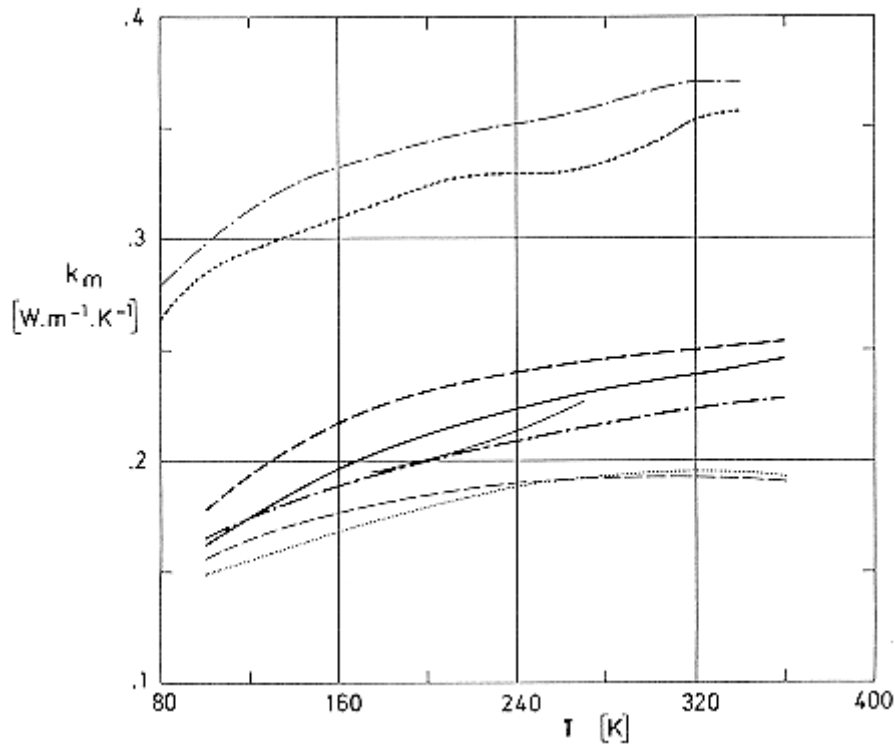
<sup>h</sup> From Ashworth, Loomer & Kreitman (1973).

**Table 5-19: Polypropylene <sup>a</sup>**

Temperature [K]	$k_m$ [W.m <sup>-1</sup> .K <sup>-1</sup> ]
100	0,148
140	0,162
175	0,173
180	0,174
220	0,185
260	0,192
270	0,193
290	0,195
300	0,195
320	0,196
340	0,195

<sup>a</sup> Curve fitting to experimental points given by Ott (1981) [132].

See also Figure 5-9.

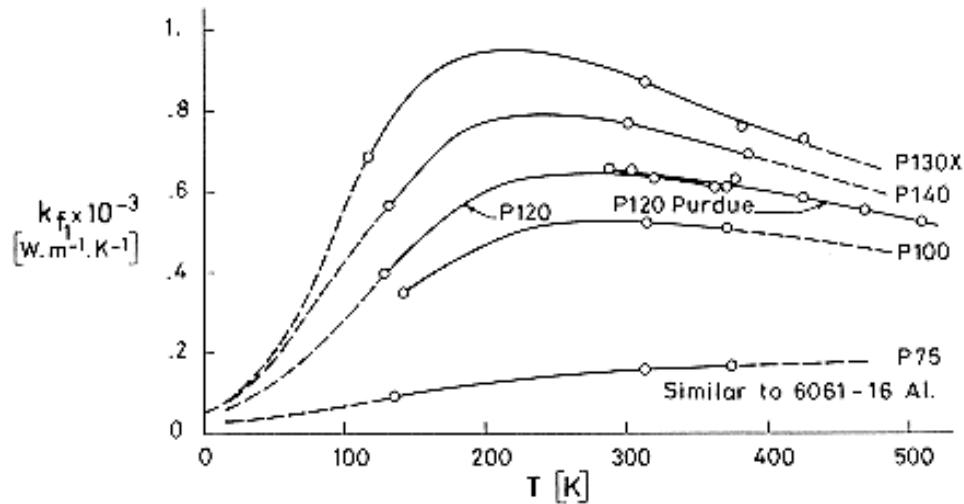


Note: non-si units are used in this figure

**Figure 5-9: Thermal conductivity,  $k_m$ , of different matrices as a function of temperature,  $T$ . Numerical values are given in Table 5-10.**

Explanation

Key	Description	References
	Araldite LY 556	Ott (1981) [132]
	Epikote 210/BF <sub>3</sub> 400	Pilling, Yates, Black & Tattersall (1979) [137]
	Epoxin 162	Ott (1981) [132]
	Palatal P51	
	Nylon 6	
	Comco, Nylon 6/6	Ashworth, Loomer & Kreitman (1973) [54]
	Polypenco 101, Nylon 6/6	
	PP Polypropylene	Ott (1981) [132]



Note: non-si units are used in this figure

**Figure 5-10: Longitudinal thermal conductivity,  $k_f$ , of several advanced pitch graphite fibers vs. temperature,  $T$ . The fiber designation is from Amoco Performance Products; the number stands for the fiber elasticity modulus in millions of lbs.in<sup>-2</sup>. All the data, unless otherwise stated, are from LMSC. Pitch precursor graphite fibers have a structure which approaches that of a single crystal of graphite and, thus, their thermal conductivity is very large. From McGuire & Vollerin (1990) [127].**

**Table 5-20: Characteristics of Composite Materials (Thermal Conductivity can be found following the links)**

Spec. No.	Matrix	Fiber		Fiber Volume $\phi_f$	Void Content $\phi_v$	Direction of measurement
		Type (Manufacturer)	Fiber angle (°) of Weave			
Table 5-21	Araldite LY 556	Glass Roving	0	0,586		Parallel to fibers
Table 5-21						Perpendicular to fibers
Table 5-22	DER 332/T403	E-Glass Type 30 Nomenclature 410AA-450 (Owens-Corning)	0	0,600		Parallel to fibers
Table 5-22						Perpendicular to fibers
Table 5-22						
Table				0,650		Parallel to fibers
Table						Perpendicular

Spec. No.	Matrix	Fiber		Fiber Volume $\varphi_f$	Void Content $\varphi_v$	Direction of measurement
		Type (Manufacturer)	Fiber angle (°) of Weave			
5-22						to fibers
Table 5-22				0,700		Parallel to fibers
Table 5-22						Perpendicular to fibers
Table 5-23		S-2 Glass Fiberglass P263A (Owens-Corning)	0	0,600		Parallel to fibers
Table 5-23						Perpendicular to fibers
Table 5-23				0,650		Parallel to fibers
Table 5-23				0,700		Parallel to fibers
Table 5-24	Epoxin 162	Glass, Roving (Owens-Corning)	0	0,455		Parallel to fibers
Table 5-24	Palatal P51			0,484		Parallel to fibers
Table 5-24				0,487		Perpendicular to fibers
Table 5-24	Nylon 6	Short glass		0,195		Parallel to fibers
Table 5-24	PP	Long glass		0,300		Parallel to fibers
Table 5-25	Epoxy DOW	YM-31A-glass	0			Parallel to fibers
Table 5-25		Roving, HTS finish	57/303			Parallel to plane of cloth
Table 5-26	Narmco 4033	Quartz (Whittaker Corp. (prepreg))	Weave			Parallel to plane of cloth
Table 5-26	Narmco 4065	Light Weight Quartz (Whittaker Corp. (prepreg))	Weave			Parallel to plane of cloth
Table 5-27	Epikote 210/BF3400	Morganite HMS Carbon	0	0,607	0,001	Parallel to fibers

Spec. No.	Matrix	Fiber		Fiber Volume $\varphi_f$	Void Content $\varphi_v$	Direction of measurement	
		Type (Manufacturer)	Fiber angle (°) of Weave				
Table 5-27		(Modmor)		0,579	0,003	Perpendicular to fibers	
Table 5-27			90	0,557	0,008	Parallel to one set of fibers	
Table 5-27				0,561	0,000	Bisecting angle between fibers	
Table 5-27		Morganite HTS Carbon (Modmor)	0	0,584	0,023	Parallel to fibers	
Table 5-27				0,459	0,000	Perpendicular to fibers	
Table 5-27				0,591	0,003	Perpendicular to fibers	
Table 5-27				0,719	0,000	Perpendicular to fibers	
Table 5-27				90	0,621	0,012	Parallel to one set of fibers
Table 5-27				0,593	0,028	Bisecting angle between fibers	
Table 5-27							
Table 5-28	Phenolic Monsanto	Graphite WCB Style Fabric	0			Parallel to fibers	
Table 5-29	Hercules 2002M (prepreg)	HM Graphite (Hercules)	0	0,510	0,019	0°	
Table 5-29						90°	
Table 5-29						0/90	
Table 5-29						±30	
Table 5-29						±45	
Table 5-29						±60	
Table 5-29						0/±60	

Spec. No.	Matrix	Fiber		Fiber Volume $\varphi_f$	Void Content $\varphi_v$	Direction of measurement
		Type (Manufacturer)	Fiber angle (°) of Weave			
Table 5-29			0/90/±45			
Table 5-29			0/±45			
Table 5-30	Araldite CY 203	Thornell T300 (Union Carbide)	90/0 <sub>s</sub> /90	0,620		0°
Table 5-30	HT 872 Hardener					
Table 5-30	Narmco 4047	Carbon (Whittaker Corp.)	Weave			Parallel to plane of cloth
Table 5-31	Hercules HA 43	Rayon G2206 Carbon (Hitco)	Weave	0,530		Parallel to plane of cloth
Table 5-31	Epoxy decomposed under heating (Carbon matrix)					Perpendicular to plane of cloth
Table 5-31		PAN M/74/01/C Carbon (Morganite)	Weave	0,440		Parallel to plane of cloth and one set of fibers
Table 5-31						Perpendicular to plane of cloth
Table 5-31	Araldite LY 558			0,450		Parallel to plane of cloth and one set of fibers
Table 5-31	Epoxy decomposed under heating (Carbon matrix)					Perpendicular to plane of cloth
Table 5-32	DER 332/T403	Kevlar 49 (du Pont)	0	0,650		Parallel to fibers
Table 5-32						Perpendicular to fibers
Table 5-32	XD7818/T403			0,600		Perpendicular to fibers
Table 5-32	Narmco 4018	Nylon (Whittaker Corp. (prepreg))	Weave			Parallel to plane of cloth



Spec. No.	Matrix	Fiber		Fiber Volume $\varphi_f$	Void Content $\varphi_v$	Direction of measurement
		Type (Manufacturer)	Fiber angle (°) of Weave			
Table 5-32	CTL-91-LD Phenolic	SN-19 Nylon	YN-25 Style			

**Table 5-21: Smoothed values of the Thermal conductivity,  $k$  [ $\text{W}\cdot\text{m}^{-1}\cdot\text{K}^{-1}$ ], of the Composite Specimens Characterized in Table 5-9.**

Spec. No.	Temperature [K]									Comments
	100	150	200	220	250	270	300	320	350	
1	0,367	0,487	0,567	0,591	0,617	0,631	0,645	0,653	0,662	(1)
2	0,270	0,355	0,400	0,412	0,427	0,435	0,447	0,456	0,468	

NOTE References: Ott (1981) [132].

(1) Fiber rovings impregnated and wrapped on a metal frame by a winding machine with constant feed. Plates cut out of the wound composite were used for measuring the thermal conductivity perpendicular to the fibers. For the measurements in the fiber direction approximately 30 plane polished plates were stacked together with the resin, and the plates cut out of the block perpendicular to the fiber direction. Measurements as in Figure 5-6. Curve fitting to experimental points by the compiler.

**Table 5-22: Smoothed values of the Thermal conductivity,  $k$  [ $\text{W}\cdot\text{m}^{-1}\cdot\text{K}^{-1}$ ], of the Composite Specimens Characterized in Table 5-9.**

Spec. No.	Temperature [K]				Comments
	250	290	320	350	
3	1,06	1,17	1,26	1,35	(2)
4	~ 0,5	~ 0,55	~0,6	~0,65	
5	1,14	1,26	1,35	1,44	
6	0,53	0,59	0,63	0,68	
7	1,23	1,35	1,44	1,53	
8	0,50	0,56	0,58	0,61	

NOTE References: Clements & Moore (1978) [73]

(2) 100 pbw resin - 45 pbw hardener. Cured 16 h at 330 K. Filament-wound molded rod specimens for longitudinal measurements,  $6 \times 10^{-3}$  m dia, 0,120 m long. Tubes o.d.  $37 \times 10^{-3}$  m, i.d.  $2,5 \times 10^{-3}$  m,  $65 \times 10^{-3}$  m long for transverse measurements. Data valid within  $\pm 20\%$ . Exploring low cost fabrication of large parts.

**Table 5-23: Smoothed values of the Thermal conductivity,  $k$  [ $\text{W}\cdot\text{m}^{-1}\cdot\text{K}^{-1}$ ], of the Composite Specimens Characterized in Table 5-9.**

Spec. No.	Temperature [K]						Comments
	220	250	270	300	320	350	
9			1,50±0,26	1,58±0,26	1,67±0,26	1,75±0,26	(3)
10	0,477	0,509	0,540	0,571	0,601	0,634	
11			1,62±0,26	1,70±0,26	1,80±0,26	1,88±0,26	
12			1,7±0,26	1,82±0,26	1,92±0,26	2,00±0,26	

NOTE References: Clements & Moore (1979) [74]

(3) Specimens as above. Longitudinal values are valid within  $\pm 26\%$ . Continuing study on the exploration of low cost fabrication of large parts.

**Table 5-24: Smoothed values of the Thermal conductivity,  $k$  [ $\text{W}\cdot\text{m}^{-1}\cdot\text{K}^{-1}$ ], of the Composite Specimens Characterized in Table 5-9.**

Spec. No.	Temperature [K]									Comments
	100	150	200	220	250	270	300	320	350	
13	0,338	0,459	0,528	0,548	0,571	0,584	0,599	0,605	0,606	(1) (4)
14	0,352	0,450	0,510	0,527	0,548	0,560	0,576	0,585	0,591	
15	0,249	0,308	0,342	0,352	0,363	0,370	0,379	0,384	0,393	
16	0,166	0,185	0,200	0,205	0,211	0,215	0,220	0,223	0,227	
17	0,182	0,204	0,222	0,227	0,232	0,234	0,234	0,232	0,228	

NOTE References: Ott (1981) [132]

(1) Fiber rovings impregnated and wrapped on a metal frame by a winding machine with constant feed. Plates cut out of the wound composite were used for measuring the thermal conductivity perpendicular to the fibers. For the measurements in the fiber direction approximately 30 plane polished plates were stacked together with the resin, and the plates cut out of the block perpendicular to the fiber direction. Measurements as in Figure 5-6. Curve fitting to experimental points by the compiler.

(4) Nylon 6 samples furnished by BASF AG, PP samples from Hoechst AG. Measurements as in (1).

**Table 5-25: Smoothed values of the Thermal conductivity,  $k$  [ $\text{W}\cdot\text{m}^{-1}\cdot\text{K}^{-1}$ ], of the Composite Specimens Characterized in Table 5-9.**

Spec. No.	Temperature [K]									Comments
	100	120	150	170	200	220	250	270	290	
18	0,215	0,234	0,260	0,274	0,288	0,294	0,301	0,310	0,327	(5)
19	0,214	0,236	0,263	0,279	0,300	0,314	0,330	0,337	0,338	

NOTE References: Hertz & Haskins (1965) [101]

<sup>(5)</sup> Cure temperature 420 K. Curing pressure  $14 \times 10^5$  Pa to  $1,6 \times 10^3$  Pa. Stops. Measured in Nitrogen (similar values are obtained in Helium). From smooth curve.

**Table 5-26: Smoothed values of the Thermal conductivity,  $k$  [ $\text{W}\cdot\text{m}^{-1}\cdot\text{K}^{-1}$ ], of the Composite Specimens Characterized in Table 5-9.**

Spec. No.	Temperature [K]		Comments	References
	290	530		
20	0,32	0,36	(6)	Penton (1966)
21	0,072	0,079		

<sup>(6)</sup> Re-entry shield.

**Table 5-27: Smoothed values of the Thermal conductivity,  $k$  [ $\text{W}\cdot\text{m}^{-1}\cdot\text{K}^{-1}$ ], of the Composite Specimens Characterized in Table 5-9.**

Spec. No.	Temperature [K]									Comments
	80	100	120	150	170	200	220	250	270	
22		12,0	17,2	24,6	29,5	36,6	41,1	47,1	50,6	<sup>(7)</sup>
23						1,331	1,413	1,410	1,463	
24	(3.30)	5,30	7,40	10,9	13,1	16,1	18,0	20,7	22,6	
25	(3.64)	5,64	7,75	11,0	13,1	16,2	18,0	20,6	22,0	
26	(1.55)	2,27	3,05	4,25	5,08	6,35	7,20	8,48	9,33	
27						0,485	0,514	0,574	0,607	
28						0,575	0,623	0,701	0,747	
29						0,829	0,926	1,048	1,133	
30	(0.94)	1,45	1,95	2,70	3,20	3,96	4,46	5,21	5,73	
31	(1.02)	1,46	1,94	2,71	3,28	4,17	4,79	5,75	6,39	

NOTE References: Pilling, Yates, Black & Tattersall (1979) [137]

<sup>(7)</sup> Resin in a solution of MEK and 20% hardener is heated in vacuum oven at 400 K. Oven is pumped from 10 min. Resin poured in a mould and oven cured for 1 h. Once void free resin is cured at 420 K for 2 h. For longitudinal measurements the Searle's bar technique was used (see paragraph 2.5.2.1). Bar specimens  $6 \times 10^{-3}$  m  $\times$   $6 \times 10^{-3}$  m  $\times$  0,1 m. For transverse measurements the Lee's disc method was used (see paragraph 2.5.2.1). Discs  $35 \times 10^{-3}$  dia. The estimated error was  $\pm 3\%$  at 80 K increasing to  $\pm 4\%$  at 270 K for the HMS reinforced bars, and  $\pm 5\%$  at 80 K to  $\pm 7\%$  -  $\pm 10\%$  at 270 K for HTS reinforced bars. The error in the Lees' disc method was  $\pm 3\%$  to  $\pm 10\%$  over the temperature range. Parenthetical values have been apparently extrapolated. The work aims at obtaining data for immediate technological application and evaluating the available prediction methods.

**Table 5-28: Smoothed values of the Thermal conductivity,  $k$  [ $\text{W}\cdot\text{m}^{-1}\cdot\text{K}^{-1}$ ], of the Composite Specimens Characterized in Table 5-9.**

Spec. No.	Temperature (K)			Comments	References
	100	150	200		
32	0,428	0,667	0,887	( <sup>8</sup> )	Hertz & Haskins (1965)

(<sup>8</sup>) Cure temperature 435 K. Curing pressure  $14 \times 10^6$  Pa to  $1,6 \times 10^3$  Pa. Stops. Measured in Nitrogen. From smooth curve.

**Table 5-29: Smoothed values of the Thermal conductivity,  $k$  [ $\text{W}\cdot\text{m}^{-1}\cdot\text{K}^{-1}$ ], of the Composite Specimens Characterized in Table 5-9.**

Spec. No.	Temperature (K)								Comments	References
	170	220	270	290	300	330	370	420		
33	31,5	35,5	37,0	38,9		41,5	44,3	47,4	(9)	Friend, Poesch & Leslie (1972)
34	0,69	0,78	0,81	0,85		0,88	0,93	0,95		
35					19,9					
36					29,4					
37					19,9					
38					10,4					
39					19,9					
40					19,9					
41					26,3					

(9) Values for Specs. No. 35 to 41 have been calculated.

**Table 5-30: Smoothed values of the Thermal conductivity,  $k$  [ $\text{W}\cdot\text{m}^{-1}\cdot\text{K}^{-1}$ ], of the Composite Specimens Characterized in Table 5-9.**

Spec. No.	Temperature (K)												Comments	References
	100	150	170	220	250	270	290	300	320	330	350	530		
42	8,6	21,0	26,0	39,0	47,0	51,0	55,0	57,0	60,0	62,0	64,0		(10)	Reibaldi (1985)
43	7,4	19,0	24,0	36,0	43,0	47,0	51,0	53,0	56,0	57,0	60,0		(11)	
44							0,68					0,70	(6)	Penton (1966)

(6) Re-entry shield.

**Table 5-31: Smoothed values of the Thermal conductivity,  $k$  [ $\text{W}\cdot\text{m}^{-1}\cdot\text{K}^{-1}$ ], of the Composite Specimens Characterized in Table 5-9.**

Spec. No.	Temperature (K)				Comments	References
	2	10	40	80		
45	0,0042	0,023	0,25		(12)	Nicholls & Rosenberg (1984)
46	0,0027	0,016	0,15	0,47		
47	0,0059	0,027	0,25	0,87		
48	0,0027	0,013	0,098	0,27		
49	0,0050	0,022	0,23	0,84		
50	0,0022	0,013	0,089	0,22		

(12) Sheets formed by layers of woven CF cloth held by an epoxy matrix. Epoxy decomposed by heating. Matrix density increased by CVD in a Xylene atmosphere at 1400 K. Searle's bar (see paragraph 2.5.2.1). Data smoothed by the compiler. Low  $k$  composites for cryogenic temperatures.

**Table 5-32: Smoothed values of the Thermal conductivity,  $k$  [ $\text{W}\cdot\text{m}^{-1}\cdot\text{K}^{-1}$ ], of the Composite Specimens Characterized in Table 5-9.**

Spec. No.	Temperature (K)										Comments	References
	100	150	220	250	270	290	300	320	350	530		
51			2,62	2,84	3,05		3,22	3,31	3,34		(13)	Clements & Moore (1977)
52				0,27	0,33		0,35	0,37	0,39			
53			0,63	0,73	0,83		0,93	1,03	1,13			
54						0,14				0,19	(6)	Penton (1966)
55	1,99	0,241	0,276	0,275	0,268		0,262				(8)	Hertz & Haskins (1965)

(6) Re-entry shield.

(8) Cure temperature 435 K. Curing pressure  $14 \times 10^6$  Pa to  $1,6 \times 10^3$  Pa. Stops. Measured in Nitrogen. From smooth curve.

(13) Filament wound specimens. 100 pbw resin, 45 pbw hardener. Cured at 290 K for 24 h and then at 360 K for 16 h. Data for specs. Nos. 51 and 52 are quite different from each other.

For additional information on the thermal conductivity of glass-reinforced, graphite-epoxy, boron-epoxy and of other advanced composites, at room temperature and below, see clause 5.5.

## 5.5.3 Thermal diffusivity

### 5.5.3.1 Measuring methods

Although the thermal diffusivity,  $\alpha = k/\rho c$ , can be deduced from the variables in the right-hand side, there exist several methods for direct measurement, starting with that by Ångström, more than 100 years old (see Landis (1964) [116]) for two simple experimental versions of the same basic idea). In this method the end ( $x = 0$ ) of a long slender bar is subjected to periodic temperature changes. Heating is supplied by a bunsen burner flame, but the bar end is periodically shielded from it by a plate which has a hole cut and which rotates slowly around a vertical axis, Figure 5-11. The same bar end is cooled by cold water for equal time intervals. After the initial starting transients have died out, the temperature at any section along the bar can also vary periodically although at a reduced amplitude and with a phase shift.

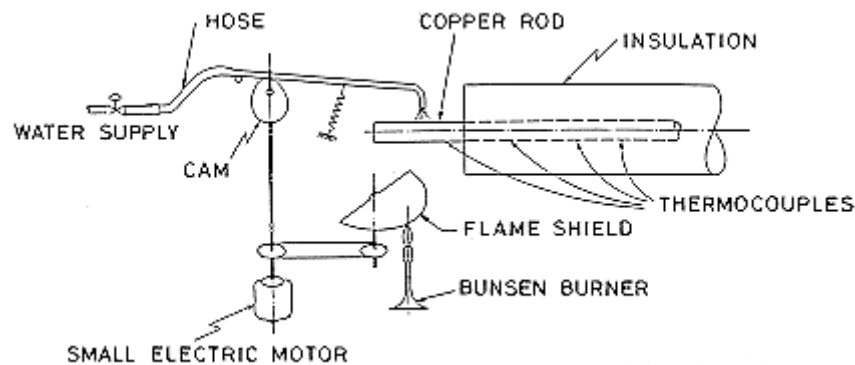


**Figure 5-11: Typical assembly for measuring the thermal diffusivity,  $\alpha$ , of a long slender bar by use of the Ångström method. From Landis (1964) [116].**

If  $\omega$  is the input frequency (1 to 2 cycles per minute) and considering only the conductive heat transfer along the bar, the phase shift at  $x = L$  is  $(\omega/2\alpha)^{1/2}L$  (Carslaw & Jaeger (1959) [65]), from which  $\alpha$  can be deduced. The analysis is quite simple if the bar end temperature changes as a pure sinusoid, this however is difficult to achieve experimentally and higher harmonics appear in the experimental periodic function which should be analyzed numerically.

The so called Transmission Pulsed Photothermal Radiometry (TPPR or "flash" method), also based on the application of a time-dependent heat input, is used worldwide, since the early sixties, for measuring  $\alpha$  and has been applied to composite materials. See Taylor, Groot & Shoemaker (1981) [152], Balageas (1988) [57] and the references therein, Pujolá & Balageas (1986) [140], ...

In this technique, the front face of a small disc-shaped sample is heated (by a laser, a flash lamp or an electron beam) during a short enough time to be considered as a pulse, Figure 5-12. The temperature of the rear face at instant  $t$  is a known function of the Fourier number,  $Fo = \alpha t/L^2$ ,  $L$  being the sample thickness, so that,  $\alpha$  can be deduced from the measured temperature history of the rear face.

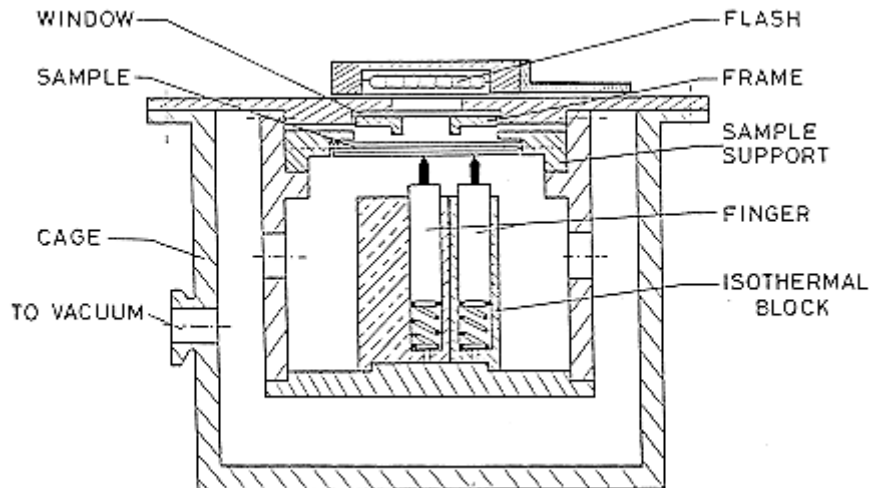


**Figure 5-12: Typical assembly for measuring the thermal diffusivity,  $\alpha$ , of a disc shaped sample. From Lachi, Legrand & Degiovanni (1988) [115].**

The effects of heat losses to the environment, pulse shape, and temperature-dependent properties should be accounted for.

In the Reflection Pulsed Photothermal Radiometry (RPPR), which is a variant of the flash method, the evolution of the front face is analyzed in order to calculate  $\alpha$ . According to Balageas, Déom & Boscher (1988) [56] both methods (transmission and reflection) seem up to now to be equivalent.

An apparatus, used at TPRL (Purdue University) has been described by Taylor, Groot & Shoemaker (1981) [152]. The apparatus consists of a Korad K2 laser, a high vacuum system including a bell jar with windows for viewing the sample, a tantalum tube heater surrounding the sample-holding assembly, a spring-loaded thermo-couple and an IR detector. The electronic subsystem consists in the appropriate biasing circuits, amplifiers, A-D converters, crystal clocks and a minicomputer-based data acquisition system capable of accurately taking data in the 40 microsecond and longer time domain. The computer controls the experiment, collects the data, calculates the results and compares the raw data with the theoretical model.

The application of the technique to composite materials is discussed by Luc & Balageas (1984) [124]. For sufficiently thick samples an equivalent homogeneous medium is defined (Balageas & Luc (1986) [58]).



**5.5.3.2 Tabulated data**
**Table 5-33: Thermal diffusivity,  $\alpha_f \times 10^6$  [m<sup>2</sup>.s<sup>-1</sup>], of High-Strength Fibers**

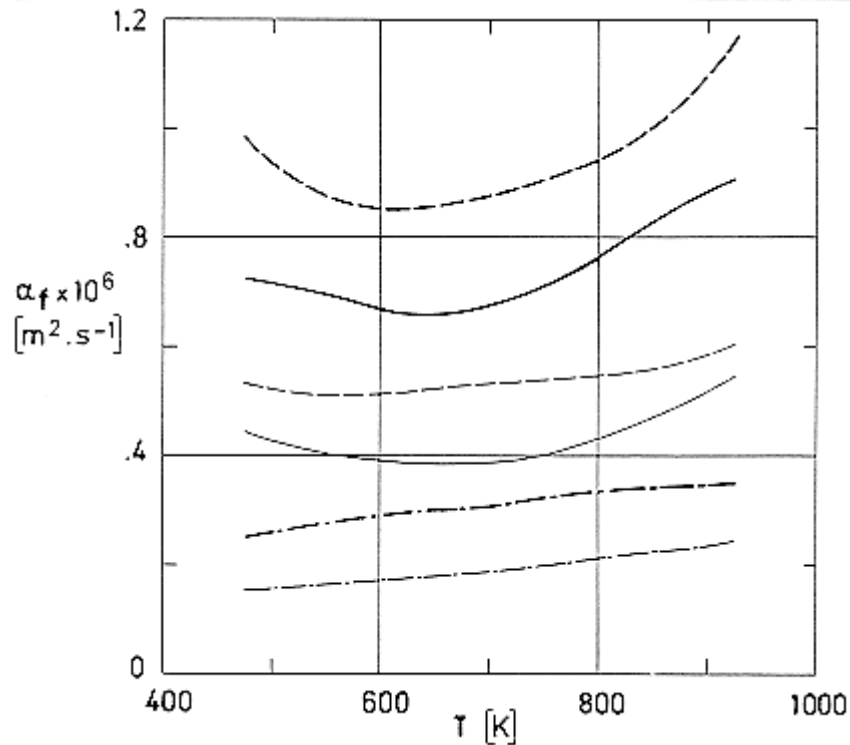
Type	Manufacturer (Supplier)	Direction of Measurement	Temperature [K]		References
			300		
E-Glass <sup>a</sup>	Owens-Corning	Parallel to fiber	0,928		Table 5-2, Table 5-4, Table 5-9
Fiber Glass Cloth	Owens-Corning	Perpendicular to plane of cloth		Other Temp.	Touloukian(1967) [157]
				Other Temp.	
Silica <sup>a</sup> Cloth FLRG 2502-1	Fabric Res. Lab, Inc.	Perpendicular to plane of cloth		Other Temp.	
				Other Temp.	
Fortafil 3	Great Lakes Carbon	Parallel to fibers	12,7		Table 5-2, Table 5-4, Table 5-9
Fortafil 3 Grafil HM	Hysol Grafil Co.		91,0		
			77,8		
Graphite <sup>a</sup> Cloth	National Carbon Co.	Perpendicular to plane of cloth		Other Temp.	Touloukian (1967) [157]
				Other Temp.	
Graphite (PAN) Cloth	Woven by Fiber Materials Inc. Rigidized, Densified and graphitized by G.E.	Perpendicular to plane of cloth	96,5	Other Temp.	Tayalor, Groot & Shoemaker (1981) [152]
			91,8	Other Temp.	

<sup>a</sup> Data displayed in Figure 5-13.

**Table 5-34: Thermal diffusivity,  $\alpha_f \times 10^6$  [m<sup>2</sup>.s<sup>-1</sup>], of High-Strength Fibers**

Type	Manufacturer (Supplier)	Thickness L x 10 <sup>3</sup> [m]	Direction of Measurement		References
			Perpendicular to plane of laminate	Parallel to plane of laminate	
Vicotex 100 <sup>b</sup> Graphite/Epoxy	Brochier	1,7	0,404	1,3	Lachi, Legrand & Degiovanni (1988) [115]  De Giovanni (1990) [79]
APC-2-2022 <sup>b</sup> Hercules AS4 Carbon/ PEEK 150 P	Imperial Chemical Industries	1,8	0,670	2,5	
		5,3	0,540	2,5	
T300/914 <sup>b</sup> Carbon fiber tape/Epoxy	Toray/Ciba- Geigy	2,1	0,470	1,6	
		3,9	0,470	1,8	
		6,0	0,450	1,6	
Lyvertex G803 <sup>b</sup> HT Carbon Fabric	Brochier	6,2	0,410	1,7	
Fibredux 914K-49 <sup>b</sup> Kevlar 49/Epoxy	Du Pont/Ciba (Brochier)	0,9	0,160	0,670	
		1,6	0,165	0,620	
		2,2	0,145	0,610	
		2,9	0,148	0,660	
		3,8	0,145	0,650	
		4,4	0,145	0,650	
		5,1	0,148	0,730	
		6,0	0,149	0,680	
Kevlar/145-S Epoxy <sup>b</sup>	Du Pont/Brochier	5,6	0,147	0,700	

<sup>b</sup> T = 300 K. Ambient pressure: 10<sup>5</sup> Pa. Flash method.



Note: non-si units are used in this figure

**Figure 5-13: Thermal diffusivity,  $\alpha_f$ , of different fiber cloths as a function of temperature,  $T$ . Numerical values are given in Table 5-33 From Touloukian (1967) [157].**

Explanation

Key	Description
————	Glass cloth. 8 harness satin. 57 yarns.in <sup>-1</sup> x 54 picks.in <sup>-1</sup> Mass/Area = 0,30 kg.m <sup>-2</sup> , $L = 0,42 \times 10^{-3}$ m, $p = 1,21 \times 10^5$ Pa.
————	As above. $p = 1,56 \times 10^3$ Pa.
- - - -	Silica cloth. Twill weave. 57 warp.in <sup>-1</sup> x 52 filling yarns.in <sup>-1</sup> Mass/Area = 0,25 kg.m <sup>-2</sup> , $L = 0,50 \times 10^{-3}$ m, $p = 1,21 \times 10^5$ Pa.
- - - -	As above. $p = 0,56 \times 10^3$ Pa.
—•—	Graphite cloth. Plain weave. 26,9 warp.in <sup>-1</sup> x 22,7 filling yarns.in <sup>-1</sup> Mass/Area = 0,26 kg.m <sup>-2</sup> , $L = 0,62 \times 10^{-3}$ m, $p = 1,20 \times 10^5$ Pa.
—•—	As above. $p = 2,16 \times 10^3$ Pa.

**Table 5-35: Thermal diffusivity,  $\alpha_m$  [ $\text{m}^2.\text{s}^{-1}$ ], of Matrices**

Type	T [K]	$\alpha_m \times 10^6$ [ $\text{m}^2.\text{s}^{-1}$ ]	References
<u>Epoxy</u> Araldite <sup>a</sup>	90	0,25	Tsatis (1988) [160]
	300	0,048	
Hysol 6000-OP	267	0,13	Touloukian (1967) <sup>b</sup> [157]
<u>Phenolic</u> Typical <sup>c</sup>	363	0,13	
50% Resin type S		0,17	
40% Resin type S		0,18	
<u>Polyester</u> Castolite	267	0,12	Table 5-3, Table 5-7, Table 5-10
Trolitul Luv M150 $\rho = 1190 \text{ kg.m}^{-3}$	363	0,10	
<u>Polyamide</u> Nylon 6	300	0,12	
Nylon 6/6		0,15-0,26	
<u>Polyvinylchloride</u> Igelit PCU $\rho = 1390 \text{ kg.m}^{-3}$	363	0,090	Touloukian (1967) <sup>b</sup> [157]

<sup>a</sup> Standard two tubes pack adhesive. 1:1. Cured several days at room temperature. Angstrom method. 10% accuracy.

<sup>b</sup> From a low resolution figures:  $\Delta\alpha_m = 10^{-8} \text{ m}^2.\text{s}^{-1}$  corresponds to  $10^{-3} \text{ m}$  in the figure.

<sup>c</sup> Pressed.  $\rho = 1270 \text{ kg.m}^{-3}$ .

**Table 5-36: Thermal diffusivity,  $\alpha \times 10^6$  [m<sup>2</sup>.s<sup>-1</sup>], of Composite Materials**

Matrix	Fiber	Fiber Volume, $\varphi$	Temperature [K]					Comments	References	
			290	330	370	590	Other			
Epoxy	Glass Fabric	0,70			0,110	0,107		a	Touloukian (1967) [157]	
TAC Polyester	Glass Fabric	0,70			0,018	0,026				
Phenolic	Glass Fabric				0,670	0,515				
CTL-37-9X Phenolic	181 Glass Fabric						Table 5-37	b		
Ironside 101 Phenolic	Graphite Mat			0,14				c		
	WC-101 Graphite Cloth			0,31				d		
	Graphite Cloth	0,47 to 0,53						Table 5-38	e	
								Table 5-38	f	
								Table 5-38	g	
							Table 5-38	h		
CTL-91 LD Phenolic	Graphite Mat	0,47 to 0,53					Table 5-38	i		
Carbon	Torayca Carbon (Three dimensional)	Fibers in direction 1: $\varphi = 0,25$	260					j	Balageas, Deom & Boscher (1988) [56]	
		Directions 2,3: $\varphi = 0,22$	310					k		

- a Pressed 500 kg.m<sup>-2</sup> at 450 K for 1 h, then postcured at 450 K for 16 h. From smooth curve.
- b From smooth curve. Highly scattered data points. Reported error 9% - 11%.
- c 6 sheets of graphite mat. Disc-shaped 3,2 x 10<sup>-2</sup> m<sup>2</sup>, 3,6 x 10<sup>-3</sup> m thick,  $\rho = 1060 \text{ kg.m}^{-3}$ . Pressed 500 kg.m<sup>-2</sup> at 450 K for 1 h, then postcured at 450 K for 16 h. From smooth curve. Low resolution figure.
- d 13 sheets of graphite cloth, Disc-shaped 3,2 x 10<sup>-2</sup> m<sup>2</sup>, 4,1 x 10<sup>-3</sup> m thick,  $\rho = 1280 \text{ kg.m}^{-3}$ . Cured and postcured as above. From smooth curve. Low resolution figure.
- e Pressed 500 kg.m<sup>-2</sup> at 465 K for 1 h, then postcured at 465 K for 12 h. Measured at side 1. From smooth curve. Low resolution figure.
- f Same as above. Measured at side 2. From smooth curve. Low resolution figure.
- g Same as above. Measured at side 5. From smooth curve. Low resolution figure.
- h Same as above. Measured at side 6. From smooth curve. Low resolution figure.
- i Sample size 0,115 m x 0,115 m x 4,6 x 10<sup>-3</sup> m. Cured and postcured as above. From smooth curve. Low resolution figure.
- j  $L = 1,62 \times 10^{-3} \text{ m}, 3,21 \times 10^{-3} \text{ m}, 4,81 \times 10^{-3} \text{ m}, 6,42 \times 10^{-3} \text{ m}, 8,2 \times 10^{-3} \text{ m}, \rho = 1900 \text{ kg.m}^{-3}$ .  $\alpha_{min}$  at the beginning of the temperature rise extrapolated to  $L = 0$ . TPPR method parallel to direction 1.
- k  $L = 1,62 \times 10^{-3} \text{ m}, 3,2 \times 10^{-3} \text{ m}, 4,8 \times 10^{-3} \text{ m}, 6,42 \times 10^{-3} \text{ m}$ . Same as above. Measured parallel to direction 2.

**Table 5-37: Thermal diffusivity,  $\alpha \times 10^6 \text{ [m}^2\cdot\text{s}^{-1}\text{]}$ , of Composite Materials**

Temperature [K]	Matrix: CTL-37-9X Phenolic <sup>b</sup> Fiber: 181 Glass Fabric
350	0,69
400	0,69
450	0,69
500	0,692
550	0,693
600	0,694

NOTE References: Touloukian (1967) [157]

<sup>b</sup> From smooth curve. Highly scattered data points. Reported error 9% - 11%.

**Table 5-38: Thermal diffusivity,  $\alpha \times 10^6$  [m<sup>2</sup>.s<sup>-1</sup>], of Composite Materials**

Temperature [K]	Fiber Volume, $\varphi$ : 0,47 to 0,53				
	Matrix: Ironside 101 Phenolic Fiber: Graphite Cloth				Matrix: CTL-91 Phenolic Fiber: Graphite Mat
	e	f	g	h	i
425				0,46	0,58
450				0,45	0,52
500	0,98		0,72	0,42	0,42
550	0,95		0,60	0,39	0,36
600	0,86	0,62	0,52	0,36	0,32
650	0,74	0,58	0,45	0,32	0,30
700	0,64	0,55	0,40	0,28	0,28
750	0,58	0,52	0,37	0,24	0,26
800	0,56	0,49	0,35	0,21	0,25
850	0,59	0,48	0,33	0,19	0,23
900	0,73	0,47	0,28	0,18	0,21
950		0,47	0,29	0,20	0,21
1000				0,22	0,22

NOTE References: Touloukian (1967) [157]

<sup>e</sup> Pressed 500 kg.m<sup>-2</sup> at 465 K for 1 h, then postcured at 465 K for 12 h. Measured at side 1. From smooth curve. Low resolution figure.

<sup>f</sup> Same as above. Measured at side 2. From smooth curve. Low resolution figure.

<sup>g</sup> Same as above. Measured at side 5. From smooth curve. Low resolution figure.

<sup>h</sup> Same as above. Measured at side 6. From smooth curve. Low resolution figure.

<sup>i</sup> Sample size 0,115 m x 0,115 m x 4,6 x 10<sup>-3</sup> m. Cured and postcured as above. From smooth curve. Low resolution figure.

## 5.6 Thermo-elastic properties

### 5.6.1 Coefficient of linear thermal expansion

#### 5.6.1.1 Measuring methods

Several methods have been used for measuring the thermal expansion of matrices and composites.

In the capacitive method the sample is bonded to a flat plate. The outer surface of the sample is kept planar and parallel to a second flat plate. The capacity of the electrical capacitor thus formed is measured as a function of temperature.

In the interferometric method the sample, usually shaped as a hollow cylinder, is held between two optical flats, the distance between which can be measured interferometrically. For interferometric measurements the Fizeau fringes produced by a Fabry-Perot interferometer are much sharper than those produced by interferometers using two interfering beams. Thus, this method is normally used for measurements at low temperatures when the thermal expansions are small.

The ambient temperature is controlled, either continuously or in steps, by means of a thermostat. The temperature range through which the specimens are cycled is traversed at least twice, ascending and descending. Sample temperatures are measured by thermo-couples.

The experimental arrangement used by James & Yates (1965) [108] to measure the thermal expansion of Caesium Iodide at low temperatures is shown in Figure 5-14a.

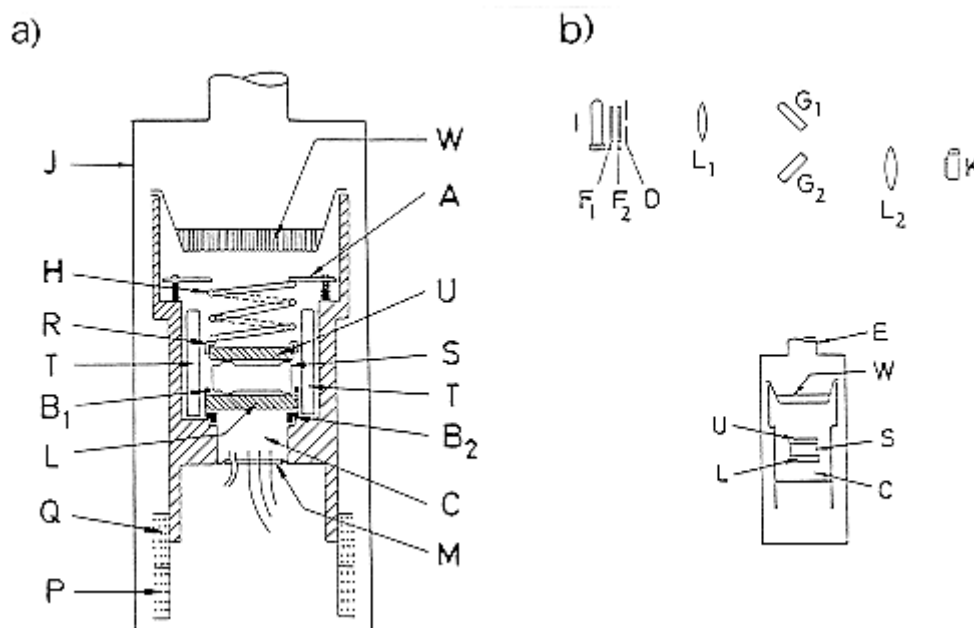


**Figure 5-14: Experimental arrangement for the interferometric measurement of the thermal expansion. a) Specimen chamber assembly. b) Optical system. From James & Yates (1965) [108]. For explanation see text.**



Two quartz optical flats, U and L, having thicknesses  $4,5 \times 10^{-3}$  m and diameters  $27 \times 10^{-3}$  m and  $30 \times 10^{-3}$  m respectively are shown in the figure in contact with the specimen, S. The two faces of U and the upper face of L are polished flat. In addition the two faces of U are cut at an angle of  $40^\circ$  to each other. Finally, the lower face of U is partially aluminized and the upper face of L is fully aluminized to enhance fringe visibility.

The L flat is placed between two brass rings,  $B_1$  and  $B_2$ , connected to each other by three metal strips (not shown).  $B_1$  surrounds the specimen, S, while  $B_2$  is located in a groove within the specimen chamber, C. Lateral movement of the U flat is controlled by the grooved collar, R. The whole assembly is slightly compressed by means of the spring, H, the lower extremity of which is soldered to R and the upper extremity to the ring A, which is positioned and controlled by three spring-loaded levelling screws (two of them are shown).

The top of the specimen chamber, C, is sealed by the  $6 \times 10^{-3}$  m thick optically-flat glass window W,  $45 \times 10^{-3}$  m in diameter.

The specimen chamber, C, is supported from the top of the brass jacket, J, by three adjustable tubes (not shown). J is immersed in liquid nitrogen or liquid hydrogen. The space between C and J is evacuated and the temperature monitored to within 0,01 K with the aid of a heater, P, and of the sensing element, Q.

The specimen temperature is measured by an Indium resistance thermometer, T, the leads of which enter C by a metal-glass seal, M. The same seal is used for the Helium exchange gas duct. This exchange gas enhances the thermal conduction between specimen and thermometer.

The optical system is shown schematically in Figure 5-14b.

I is the light source.  $F_1$  and  $F_2$  are filters, D is a diaphragm and  $L_1$  a lens.  $G_1$  and  $G_2$  are respectively a fully aluminized and a partially aluminized glass plate.

The light beam is collimated and reflected into U and L down a tube, E, of internal diameter  $25 \times 10^{-3}$  m, lined with black paper. The emerging light is focused by the objective,  $L_2$ , on the camera, K. Approximately six interference fringes are formed in the image. The arrangement used by Pojur & Yates (1973) [138] is similar. Now the upper flat is substituted by a  $45^\circ$  prism, and the specimens are placed in between. The lower flat rests on a stainless steel holder and lateral movement of both components is prevented by means of vertical guiding rods. Different sample geometries can be used with this arrangement.

Sample sizes are more or less limited in the different arrangements used, but the length range of reported measurements is very wide. Typically  $5 \times 10^{-3}$  m to  $50 \times 10^{-3}$  m long,  $5 \times 10^{-3}$  m to  $20 \times 10^{-3}$  m wide and  $10^{-3}$  m to  $5 \times 10^{-3}$  m thick.

The thermal expansion of amorphous metals ribbons in the thickness range  $30 \times 10^{-6}$  m to  $350 \times 10^{-6}$  m can be measured by holding the ribbon between two fused silica pillars so that the thermal expansion of the beam formed by the sample and the two supporting bars is measured. Particular attention should be paid to keep the sample straight at any time.

The linear thermal expansion of fibers can be deduced from that of unidirectional composites reinforced with such fibers. In other technique the fiber is kept under constant tension between two holding blocks, the distance between which is measured as a function of temperature.

Strain gauge techniques have been used also. Any size of specimen including structures and components can be tested, and measurements are made in several directions simultaneously.

The technique is limited to the temperature capability of the strain gauge and of the bond line, but measurements in the temperature range from 12 K to 450 K have been reported (Valentich (1985) [161]).

The active gauge used to measure the thermal expansion will be compensated for the effects of apparent thermal strain. This can be done by mounting an identical gauge on a low-expansion fused silica standard reference kept at the sample temperature when the reading is made.

A facility to measure the linear thermal expansion of composite structures (rods, panels or even structural assemblies) up to 0,7 m in length has been described by Aalders (1989) [48].

The thermal expansion is measured by means of inductive dilatometers, which consist in a coil system through which a rod-shaped magnet moves. These sensors, Sony-Magnascale, have a resolution of  $5 \times 10^{-7}$  m.

The test specimens are cooled and heated exclusively by radiation. The temperature range is 150 K to 390 K and the achievable uniformity in temperature is 2 K above 273 K over a 0,7 m test sample and 5 K at 140 K.

The maximum diameter of the test area is 0,15 m and, thus, five samples plus one reference rod can be measured at a time, with  $\beta$  values possibly as low as  $10^{-8}$  K<sup>-1</sup>, and all having distinctly different linear thermal expansions.

The measurements can be performed either changing the temperature in steps from one extreme to the other, with one or two intermediate steps, or under (slowly varying, below 20 K/h) transient conditions.

The whole system is contained in a vacuum chamber, Figure 5-15. The sample platform and the sensor ring are attached to the supporting ring by means of appropriate supporting rods which are thermally decoupled from each other.

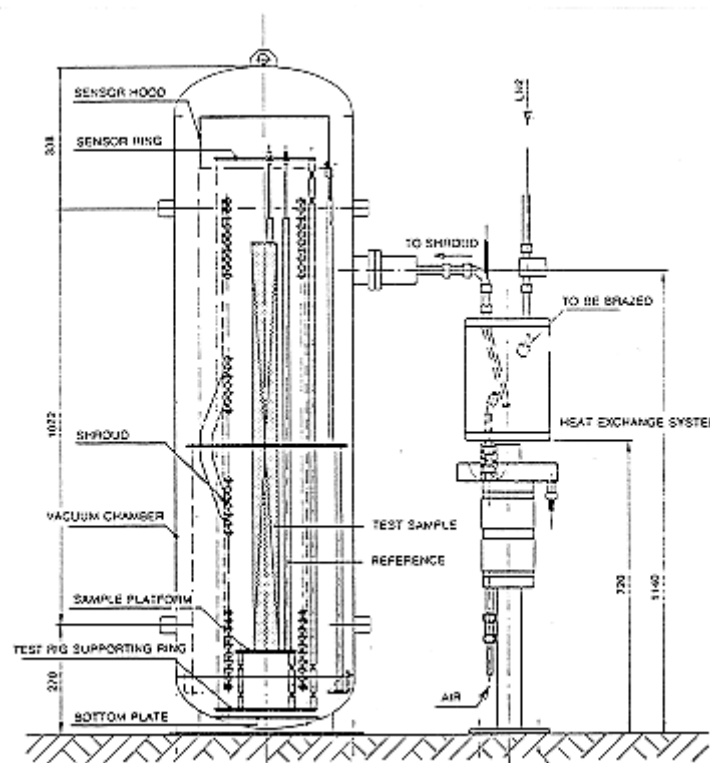


**Figure 5-15: The ESTEC CTE 1000 facility for the measurement of the linear thermal expansion of structure up to 0,7 m long. All the dimensions are in mm.**

**From Aalders (1989) [48].**

The sensor ring is placed in the upper part of the vacuum chamber and is kept at constant temperature by means of a temperature-controlled sensor hood.

The sample(s) together with an Invar ( $\beta \approx 10^{-7} \text{ K}^{-1}$ ) reference rod, are surrounded by a free-standing double bifilar coil shroud which is thermally controlled by a heat exchange system which delivers air at any given temperature between 80 K and 390 K. Heat transfer between coil shroud and sample(s) takes place by radiation only. In order to keep the rods at nearly ambient temperature, the shroud is thermally decoupled from the supporting rods by a 20-layer insulation blanket. MLI blankets, with appropriate openings, are also placed on top and bottom of the shroud and on the bottom of the hood.

The shroud is 0,4 m longer than the sample(s) so that its lower end surrounds the sample platform, whereas the upper end is placed 0,2 m above the sample end.

The test sample(s) and the Invar reference rod are glued to the platform by means of small patches of epoxy. The distance from the top of each test sample and the sensor ring ( $\approx 0,450 \text{ m}$  long) is bridged by an Invar extension rod glued to the sample. The sensor magnetic rod is pressed into the top of the extension rod which has area restrictions to ensure that the sensor ring is thermally decoupled from the test specimen.

The thermal expansion of the test sample is deduced from the change in length of the sample plus the extension rod. In its turn, the thermal expansion of the extension rod is deduced from that of the reference rod, made of the same material and held at the same temperature.

The same facility can be used to study other phenomena yielding length changes and can be scaled up to accommodate samples three or four times as long.

### 5.6.1.2 Calculation formulae for composites

The longitudinal linear thermal expansion,  $\beta_1$ , of the composite in terms of the linear thermal expansions of the constituents, fiber, subscript f, and matrix, subscript m, is given by

$$\beta_1 = \frac{\varphi_f \beta_{f_1} E_{f_{11}} + \varphi_m \beta_m E_m}{\varphi_f E_{f_{11}} + \varphi_m E_m} \quad [5-8]$$

where  $E$  [Pa] is the modulus of elasticity.

The transverse linear thermal expansion,  $\beta_2 = \beta_3$ , is given by:

$$\beta_2 = \beta_3 = \beta_{f_2} \sqrt{\varphi_f} + \left(1 - \sqrt{\varphi_f}\right) \left(1 + \varphi_f \nu_m \frac{E_{f_{11}}}{\varphi_f E_{f_{11}} + \varphi_m E_m}\right) \beta_m \quad [5-9]$$

where  $\nu_m$  is the Poisson's ratio of the matrix.

For the thermal expansion in a direction forming an angle  $\theta$  with the fibers,  $\beta_\theta$

$$\beta_\theta = \beta_1 \cos^2 \theta + \beta_2 \sin^2 \theta \quad [5-10]$$

Usually  $\beta_1 \approx \beta_f$  and  $\beta_2 \approx \beta_m$ .

From Karlsson (1983) [111], Chamis (1987) [67].

**5.6.1.3 Tabulated data**
**Table 5-39: Linear thermal expansion,  $\beta_f$  [K<sup>-1</sup>], and elasticity modulus,  $E_f$  [Pa], of high-strength fibers**

Type	T [K]	$\beta_f \times 10^6$ [K <sup>-1</sup> ]		$E_{f11} \times 10^{-9}$ [Pa]	References	
		$\beta_{f1}$	$\beta_{f2}$			
Glass Fibers C-glass	290	7,2 <sup>a</sup>		69,0 <sup>b</sup>	Weeton, Peters & Thomas (1987) [164] unless otherwise stated	
D-glass	290	3,1 <sup>a</sup>		51,7 <sup>c</sup>		
E-glass	290	5 <sup>a</sup>		72,4 <sup>b</sup> , 85,5 <sup>d</sup>		
	810			81,4 <sup>d</sup>		
S-glass	290	5,6 <sup>a</sup>		85,5 <sup>b</sup>		
S-2-glass	290	5,6 <sup>a</sup>		86,9 <sup>b</sup> , 93,1 <sup>d</sup>		
	810			89,0 <sup>d</sup>		
Quartz (fused silica)	290			71,7		Weast (1976) [163]
	290-590	0,55				
	100	-0,56			$\beta_f$ from smooth curve in Karlsson (1983) [111]	
	250	0,36				
	300	0,60				
	500	0,65				
	600	0,61				
	750	0,50				
Carbon Fibers Celanese 950	290-1700		13,1 <sup>e</sup>		$\beta_f$ from Karlsson (1983) [111] unless otherwise stated	
Celanese Celion ST				234 <sup>f</sup>		
Celanese GY 70						517 <sup>f</sup>
	290-420	-1,7	18			
Celanese G40-						300 <sup>f</sup>

Type	T [K]	$\beta_f \times 10^6 [K^{-1}]$		$E_{f11} \times 10^{-9}$ [Pa]	References
		$\beta_{f1}$	$\beta_{f2}$		
600					
Fortafil 3	290-420	-0,11		230 <sup>g</sup>	
Fortafil 5		-0,50		345 <sup>g</sup>	
Fortafil HM	290-420	-1,1			$\beta_f$ from Karlsson (1983) [111] and $E_{f11}$ from Weeton, Peters & Thomas (1987) [164] unless otherwise stated
Hercules AS-1	290-1700		12,5 <sup>e</sup>		
Hercules HT	290-420	-0,63			
Hercules HM		-0,10			
Hercules HM-3000	290-1700		10,9 <sup>e</sup>		
Hercules AS-4				234 <sup>f</sup>	
Hercules AS-6				248 <sup>f</sup>	
Hercules IM6 1200				278 <sup>f</sup>	
Hercules IM7				303 <sup>f</sup>	
Hitco HT	290-420	-1,0			
Hitco HM		-1,3			
Hysol Grafil XA-S (standard)				235 <sup>f</sup>	
Hysol Grafil XA-S (HS)				235 <sup>f</sup>	
Hysol Grafil XA-S	290	-0,26	26 <sup>h</sup>	234	
Hysol Grafil HT/HM		(-1) - (-1,2)	17-27		
Hysol Grafil Apollo HS				245 <sup>f</sup>	

Type	T [K]	$\beta_f \times 10^6$ [K <sup>-1</sup> ]		$E_{f11} \times 10^{-9}$ [Pa]	References
		$\beta_{f1}$	$\beta_{f2}$		
Hysol Grafil HMS (6K)				370 <sup>f</sup>	
Hysol Grafil Apollo HM				390 <sup>f</sup>	
Hysol Grafil Apollo IM				275 <sup>f</sup>	
Magnamite AS1	290-420	-0,4		230	
Magnamite HTS		-0,4			
Magnamite HMS		-0,5		345	
Modmor HT	290	-0,73	28		
		-0,54			
Modmor HM		-1,1			
Thornel HT		-1,1			
Thornel HM		-1,4			
Thornel VHM		-1,3			
Toray T50		-1,22 <sup>e</sup>	6,7 <sup>e</sup>		
Toray T300 & T400				235 <sup>f</sup>	
Toray T800				294 <sup>f</sup>	
Toray M40				392 <sup>f</sup>	
UCC P55	290-1700		12,0 <sup>e</sup>		
	290	-1,37 <sup>e</sup>	11,8 <sup>e</sup>		
UCC P75		-1,48 <sup>e</sup>	12,4 <sup>e</sup>		

Type	T [K]	$\beta_f \times 10^6 [K^{-1}]$		$E_{f11} \times 10^{-9} [Pa]$	References
		$\beta_{f1}$	$\beta_{f2}$		
UCC P100		-1,48 e	9,4 e		
Aramid Fibers Kevlar 49				124	From Weeton, Peters & Thomas (1987) [164]
	270-370	-2	59		
	370-470	-4			
	470-530	-5			
Kevlar 29				83	
Fenax ST3 (ENKA/TOHO)				235 <sup>f</sup>	
Twaron HM (ENKA AG)				125 <sup>f</sup>	
Metal Wires Boron	290	5,0 <sup>i</sup>	5,0 <sup>i</sup>	400	$\beta_f$ from Karlsson (1983) [64] $E_f$ from Chamis (1987) [67]
	290-460	3,6			
Amorphous Metals Fe <sub>78</sub> B <sub>20</sub> Mo <sub>2</sub>	290	8,6			$\beta_f$ from Karlsson (1983) [111]
Fe <sub>75</sub> P <sub>15</sub> C <sub>10</sub>		9,0			
Fe <sub>40</sub> Ni <sub>40</sub> B <sub>20</sub>		6,6			
Fe <sub>40</sub> Ni <sub>40</sub> P <sub>14</sub> B <sub>6</sub>		13,8		125	$\beta_f$ from Steinberg, Tyagy & Lord (1980) [150]. $E_f$ from Davis (1978) [78]
		13,1 <sup>j</sup>			
		11,3 <sup>k</sup>			
		10,9 <sup>l</sup>			
		10,5 <sup>m</sup>			
Fe <sub>40</sub> Ni <sub>38</sub> B <sub>10</sub> Mo <sub>4</sub>		10			$\beta_f$ from Karlsson (1983) [111] $E_f$ from Davis (1978) [78]
Ni <sub>36</sub> Fe <sub>32</sub> Cr <sub>14</sub> P <sub>12</sub> B <sub>6</sub>		14		141	
Ni <sub>49</sub> Fe <sub>29</sub> P <sub>14</sub> B <sub>6</sub> Si <sub>2</sub>	12,4		132	$\beta_f$ from Steinberg,	

Type	T [K]	$\beta_f \times 10^6$ [K <sup>-1</sup> ]		$E_{f11} \times 10^{-9}$ [Pa]	References
		$\beta_{f1}$	$\beta_{f2}$		
		12,2 <sup>j</sup>			Tyagy & Lord (1980)[150]. $E_f$ from Davis (1978) [78]
		11,0 <sup>k</sup>			
		10,7 <sup>l</sup>			
		10,1 <sup>m</sup>			
CO <sub>84</sub> B <sub>16</sub> -CO <sub>79</sub> B <sub>21</sub>		14			$\beta_f$ from Karlsson (1983) [111]
Pd <sub>82</sub> Si <sub>18</sub>		15			

- a Determined on bulk gas.
- b Determined on glass fibers, without heat compaction.
- c From SENER (1984) [147].
- d Determined on glass fibers, after heat compaction.
- e From Dresselhaus, Dresselhaus, Sugihara, Spain & goldberg (1988) [84].  $\beta_{f2}$  data from T up to 1700 K were obtained with fibers held under a preload tension of  $7 \times 10^6$  Pa.
- f From ESA (1989) [88].
- g From Weeton, Peters & Thomas (1987) [164].
- h Calculated from Graphite.
- <sup>l</sup> Composition dependent.
- <sup>j</sup> Annealing treatment, T = 520 K, t = 10 min.
- <sup>k</sup> Annealing treatment, T = 520 K, t = 50 min.
- <sup>l</sup> Annealing treatment, T = 570 K, t = 50 min.
- <sup>m</sup> Annealing treatment, T = 620 K, t = 15 min.

**Table 5-40: Linear thermal expansion,  $\beta_m$  [K<sup>-1</sup>], elasticity modulus,  $E_m$  [Pa] and Poisson's ratio,  $\nu_m$ , of matrices**

Type	T [K]	$\beta_m \times 10^6$ [K <sup>-1</sup> ]	$E_m \times 10^{-9}$ [Pa]			$\nu_m$	References
			Tensile	Compr.	Flex.		
Epoxy Typical	290	45-90	> 2,0			0,38±0,006	$\beta_m$ and $E_m$ from Weast (1976) [163], $\nu_m$ from Chamis (1987) [67]
Araldite 501/TEA Triethanolamine	50	19					Calculated by the
	90	29					



Type	T [K]	$\beta_m \times 10^6$ [K <sup>-1</sup> ]	$E_m \times 10^{-9}$ [Pa]			$\nu_m$	References
			Tensile	Compr.	Flex.		
2cc hardener/40 g resin Cured: 8 h at 390 K 24 h at 450 K	130	36					compiler from $\Delta L/L$ in Touloukian (1967) [157]. $\nu_m$ for Araldite from Lemaitre & Chaboche (1985) [119]. Neither cure nor ambient temperature are given.
	170	42					
	210	47					
	250	52					
	290	60				0,4	
	330	72					
Fibredux 914	90		6,47±0,24				SENER (1984) [147]
	130		5,71±0,53				
	170		5,28±1,19				
	230		4,27±0,28			0,40	
	270					0,41	
	290		3,32±0,18				
	300					0,39	
	370					0,38	
	420					0,38	
Code 69 <sup>a</sup>	230		4,6±0,5	3,3±0,1		0,38±0,01	$\beta_m$ from Yates et al. (1978b) [168] $E_m$ and $\nu_m$ from SENER (1984) [147]
	290		4,1±0,3	2,9±0,1		0,39±0,01	
	340	49,0	3,7±0,5	2,5±0,1		0,38±0,01	
	360	52,0	4,0±0,6	2,5±0,1		0,38±0,006	
	390		3,6±0,6	2,3±0,1		0,39±0,01	
	420	63,6	3,2±0,4	2,2±0,1		0,38±0,01	
CRC 350A	290	50				0,40	Kalnin (1974) [110]
	370	60					
DER 332/T403 (100:36)	220-290	52					Chiao & Moore (1974). [68] For $E_m$ cure is 16 h at 330 K
	290		3,24	3,49	1,26 <sup>b</sup>		
	330-350	74					
Epikote 828/BF <sub>3</sub> 400	290	65	3,43 <sup>c</sup>			0,38 <sup>c</sup>	$\beta_m$ from

Type	T [K]	$\beta_m \times 10^6$ [K <sup>-1</sup> ]	$E_m \times 10^{-9}$ [Pa]			$\nu_m$	References
			Tensile	Compr.	Flex.		
							Karlsson (1983) [111]. $E_m$ and $\nu_m$ from Ishikawa et al. (1977) [106].
ERLA 4617/mPDA <sup>d</sup>	290	34					Karlsson (1983) [111]
Ferro CE-3305	290-370	65					
Fibredux 914C <sup>e</sup>	230		5,9±2,2	3,2±0,1		0,40±0,006	SENER (1984) [147]
	290		4,0±0,3	2,7±0,1		0,39	
	340	51,5	4,0±0,6	2,3±0,1		0,39±0,006	
	360	53,8	3,2±0,3	2,1±0,1		0,38±0,012	
	390		2,6±0,3	2,1±0,05		0,39±0,03	
	420	65,5	2,5±0,3	1,8±0,1		0,39±0,031	
GAC 3320	290	48					Karlsson (1983) [111]
GAC 3330	290	46					
Hercules 3501 (Courtaulds)	230		4,1±0,7	3,0±0,2		0,39±0,005	ESA (1989) [88]
	290		4,1±0,7	3,0±0,2		0,39±0,006	
	340		3,0±0,3	2,6±0,1		0,38±0,012	
	360		4,1±0,7	2,4±0,1		0,38±0,016	
	390		3,2±0,4	2,3±0,1		0,38±0,016	
	420		3,0±0,3	2,2±0,05		0,40±0,006	
Hercules 3501-5	270-360	27±2 <sup>f</sup>					Adamson (1980) [51]
	270-350	31±2 <sup>g</sup>					
		63±2 <sup>h</sup>					
Hexcel F155		53	3,29				Balis, Crema, Barboni & Castellani (1986) [59]
Narmco 5505	290	72					Karlsson (1983) [111]
	460	114					
PR 279	290	39					Karlsson (1983) [111]

Type	T [K]	$\beta_m \times 10^6$ [K <sup>-1</sup> ]	$E_m \times 10^{-9}$ [Pa]			$\nu_m$	References	
			Tensile	Compr.	Flex.			
PR 286	300	48,1					Strife & Prewo (1979) [151]	
	420	79,4						
	300-420	66,1						
CRC 350A	290	47					Karlsson (1983) [111]	
3110	290	46						
Phenolic Typical	290	60-80	0,028-0,034					Skinner & Goldhard (1968) [149]
Polyester Epocryl 332	290	80					Karlsson (1983) [111]	
Epocryl 480		75						
Hexcel C-1000		52						
Hexcel I-2000		29						
PBT		70-110						
PBT S600		80						
PET		130						
Polyamide Nylon 6			86			0,97-2,6		
Nylon 6/6		81	3,28 <sup>i</sup>		2,8 <sup>i</sup>			
Nylon 6/10		90	1,9-2,1		1,9 <sup>i</sup>			
Nylon FM 1	0	0,58					Calculated by the compiler from $\Delta L/L$ in Touloukian (1967) [157]	
	40	19						
	80	32						
	120	42						
	160	50						
	200	59						
	240	69						
	280	82						
320	100							
Nylon 6	240	85						

Type	T [K]	$\beta_m \times 10^6$ [K <sup>-1</sup> ]	$E_m \times 10^{-9}$ [Pa]			$\nu_m$	References
			Tensile	Compr.	Flex.		
	280	130					
	320	180					
	360	200					
Nylon 6/6	240	62					
	280	74					
	320	120					
	360	150					
<u>Polysulfone</u> Typical	290	56	2,5	2,6		0,413	$b_m$ and $E_m$ from Skinner & Goldhard (1968) [149]. $\nu_m$ from Hartwig (1988) [99]
PPS		43-49					Karlsson (1983) [111]
P2000		55					
Radel		55					
Ryton		54					
Udel		56					Weeton, Peters & Thomas (1987) [164]
<u>Polyimide</u> Typical	290	36	3,4			0,35	Chamis (1987) [67]
PMR-15		50,4	3,2				SENER (1984) [147]
PMR-P1 i		50,4	3,2				Hanson & Chamis (1974) [96]
P13N		45					Karlsson (1983) [111]
Upjohn 2080		50					
<u>Polyamide/imide</u> Torlon 2000		34					
Torlon 4203		36					

- a Spec. No. 45, Table 5-49. See also Figure 5-12.
- b Shear modulus. From torsion tests.
- c Hardener is BF<sub>3</sub>MEA.
- d Spec. No. 21, Table 5-42. See also Figure 5-16.
- e Spec. No. 115, Table 5-57. See also Figure 5-16.
- f Measured dry.
- g Saturated at 350 K but measured dry.
- h Saturated at 350 K but measured at the same moisture concentration.
- i Dry, as molded.
- j For three different monomers (MDA, NE and BTDE with methylalcohol as the solvent).

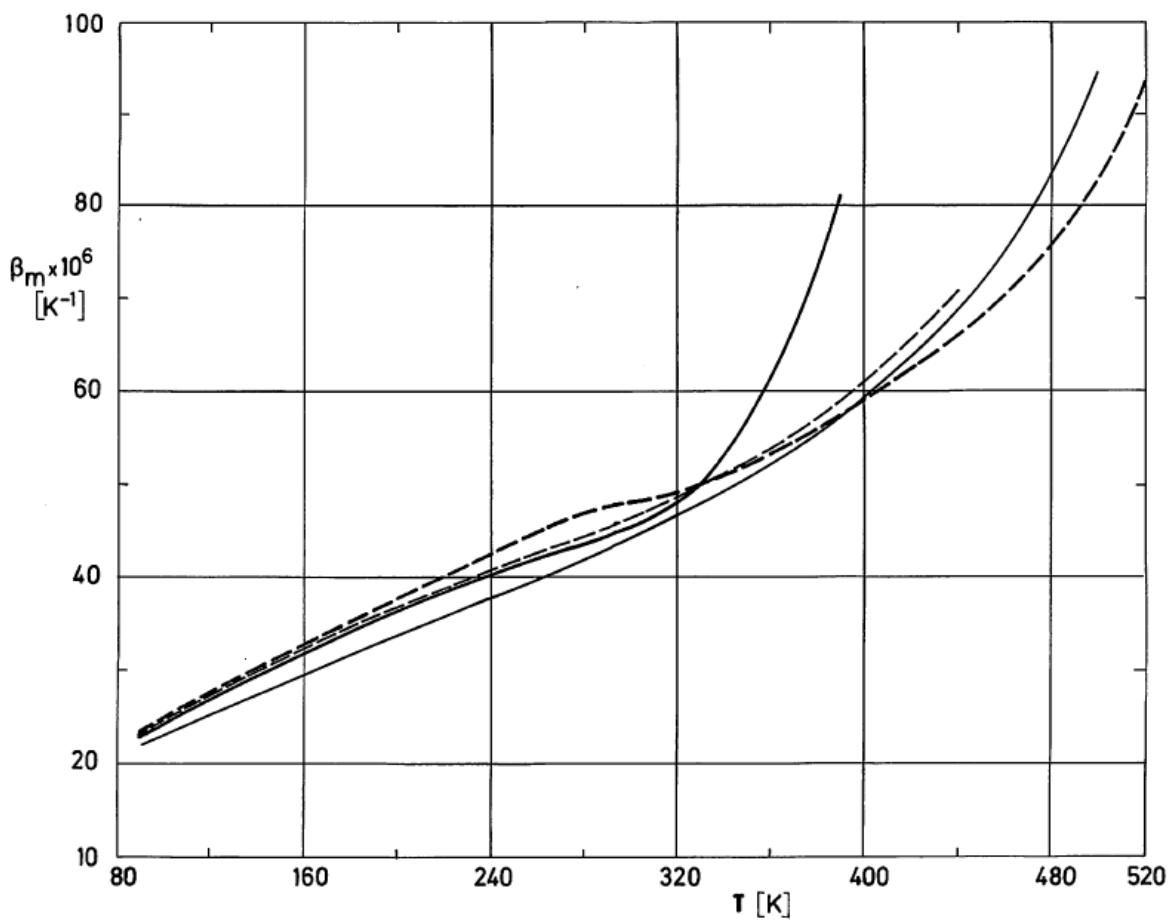






Figure 5-16: Linear thermal expansion,  $\beta_m$ , as a function of temperature,  $T$ , for four different epoxy matrices. Numerical values are given in Table 5-41.

## Explanation

Key	Description	Spec. No. Table 5-41	References
	ERLA 4617/mPDA	21	Rogers, Phillips, Kingston-Lee, Yates, Overy, Sargent & McCalla (1977) [144].
	DLS 351/BF <sub>3</sub> 400	38	Yates, Overy, Sargent, McCalle, Kingston-Lee, Phillips & Rogers (1978)a [170]
	Code 69	45	Yates, McCalla, Sargent, Rogers, Phillips & Kingston-Lee (1978)b [169]
	Fibredux 914C	115	Parker, Chandra, Yates, Dootdon & Walters (1981) [133].

**Table 5-41: Arrangements of the Data on Linear Thermal Expansion,  $\beta$ , of Composite Materials Compiled in Table 5-42 to Table 5-60**

Content	Table or Figure
Characterization of glass or carbon reinforced specimens	Table 5-42
Smoothed values of $\beta$ , curing and measuring of glass or carbon reinforced specimens	Table 5-41
More relevant trends of glass or carbon reinforced specimens	Figure 5-17 to Figure 5-19
Characterization of carbon reinforced specimens	Table 5-49
Smoothed values of $\beta$ , curing and measuring of carbon reinforced specimens	Table 5-49
More relevant trends of carbon reinforced specimens	Figure 5-20 to Figure 5-22
Characterization of carbon reinforced specimens	Table 5-54
Smoothed values of $\beta$ , curing and measuring or carbon reinforced specimens	Table 5-54
More relevant trends of carbon reinforced specimens	Figure 5-23 to Figure 5-25
Characterization of carbon reinforced specimens	Table 5-57

Content	Table or Figure
Smoothed values of $\beta$ , curing and measuring or carbon reinforced specimens	Table 5-57
More relevant trends of carbon reinforced specimens	Figure 5-26 to Figure 5-28
Characterization of aramid fiber reinforced and miscellany specimens	Table 5-60
Smoothed values of $\beta$ , curing and measuring or aramid fiber reinforced and miscellany specimens	Table 5-60
More relevant trends of aramid fiber reinforced and miscellany specimens	Figure 5-29 to Figure 5-31

**Table 5-42: Characterization of Composite Materials (Linear Thermal Expansion is given following the links).**

Spec. No.	Matrix	Fiber		Fiber volume $\varphi_f$	Void content $\varphi_v$	Direction of measurement
		Type (Manufacturer)	Fiber angle (°) or Weave			
Table 5-43	DER 332/T403	E-glass Type 30 Nomenclature 410AA-450 (Owens-Corning)	0	0,600	0,000	Parallel to fibers
Table 5-43						Perpendicular to fibers
Table 5-43				0,650	Parallel to fibers	
Table 5-43					Perpendicular to fibers	
Table 5-43				0,700	Parallel to fibers	
Table 5-43					Perpendicular to fibers	
Table 5-44		S-2 glass Fiberglass P263A (Owens-Corning)	0	0,600		Parallel to fibers
Table 5-44						Perpendicular to fibers
Table 5-44				0,650	Parallel to fibers	
Table					Perpendicular to	

Spec. No.	Matrix	Fiber		Fiber volume $\varphi_f$	Void content $\varphi_v$	Direction of measurement
		Type (Manufacturer)	Fiber angle (°) or Weave			
5-44						fibers
Table 5-44				0,700		Parallel to fibers
Table 5-44						Perpendicular to fibers
Table 5-45	EF-2	7576 E-glass VM 665 finish 120 fibers in warp 24 fibers in weft 0,28 x 10 <sup>-3</sup> m thick	Woven 11 plies per laminate	0,670 to 0,730		0°
Table 5-45						90°
Table 5-45		7781 E-glass Volan A finish 60 fibers in warp 54 fibers in weft 0,22 x 10 <sup>-3</sup> m thick	Woven 14 plies per laminate			0°
Table 5-45						90°
Table 5-45		Both types above stacked	(07576/07781/ ± 307576/07576/ +307781/(07781)2/07576)S			0°
Table 5-45						90°
Table 5-46	Narmco 4033	Quartz (Whittaker Corp.)	Weave	-		Parallel to plane of cloth
Table 5-46	Narmco 4065	Light weight quartz (Whittaker Corp.)		-		
Table 5-47	ERLA 4617/mPDA	No fibers		0,000	0,000	
Table 5-47		HTS PT112/21Z Carbon fiber (Courtaulds)	0	0,494	0,019	Parallel to fibers
Table 5-47						Perpendicular to fibers
Table 5-47						45° to fibers
Table 5-47		HTS PT112/21Z (prepreg) (Courtaulds)	90	0,500	0,000	Parallel to one set of fibers
Table 5-47						Bisecting angle between fibers
Table	Perpendicular to					



Spec. No.	Matrix	Fiber		Fiber volume $\varphi_f$	Void content $\varphi_v$	Direction of measurement			
		Type (Manufacturer)	Fiber angle (°) or Weave						
5-47						laminate			
Table 5-48		HTS PT112/21Z (Courtaulds)	63	0,529	0,042	Bisecting acute angle			
Table 5-48						Bisecting obtuse angle			
Table 5-48		HMS QM218/622W Carbon fiber (Courtaulds)	0	0,504	0,016	Parallel to fibers			
Table 5-48						Perpendicular to fibers			
Table 5-48						90	0,520	0,000	Parallel to one set of fibers
Table 5-48									Bisecting angle between fibers
Table 5-48									Perpendicular to laminate
Table 5-48						66	0,526	0,002	Bisecting acute angle
Table 5-48									Bisecting obtuse angle
Table 5-48									Perpendicular to laminate

**Table 5-43: Smoothed values of the Linear Thermal Expansion Coefficient,  $\beta \times 10^6$  [K<sup>-1</sup>], of the Specimens characterized in Table 5-85.**

Spec. No. <sup>g</sup>	Temperature (K)					References
	210	250	290	320	350	
1 <sup>a</sup>	6,57± 0,53					Clements & Moore (1978)
2 <sup>b</sup>	23,4	25,9	30,0	35,3	104,0	
3 <sup>a</sup>	6,31± 0,51					
4 <sup>b</sup>	20,2	22,4	25,6	30,5	90,0	
5 <sup>a</sup>	6,07± 0,49					
6 <sup>b</sup>	17,1	18,9	21,6	25,8	76,0	

<sup>a</sup> Data displayed in Figure 5-17

<sup>b</sup> Data displayed in Figure 5-18

<sup>g</sup> Comments: 100 p DER 332/45 p T403. 16h/330 K.

For longitudinal tests: filament wound and moulded rods  $6 \times 10^{-3}$  m dia., 0,120 m long.

For transverse tests: tubes with  $25 \times 10^{-3}$  m inner diameter,  $6 \times 10^{-3}$  m wall thickness and approximately  $65 \times 10^{-3}$  m long.

95% confidence limits for the second set of data given in the Ref. are in error. Rapid increase of  $\beta$  above 320 K attributable to resin.

**Table 5-44: Smoothed values of the Linear Thermal Expansion Coefficient,  $\beta \times 10^6$  [K<sup>-1</sup>], of the Specimens characterized in Table 5-85.**

Spec. No. <sup>g</sup>	Temperature (K)						References
	220	250	270	300	320	350	
7 <sup>a</sup>	3,52± 0,38						Clements & Moore (1979)
8 <sup>b</sup>	23,5± 0,8	24,3± 0,8	26,3± 0,8	28,9± 0,8	32,7± 3,4	98± 21	
9 <sup>a</sup>	3,52± 0,38						
10 <sup>b</sup>	19,9± 0,8	21,3± 0,8	23,2± 0,8	25,1± 0,8	27,6± 3,4	77± 21	
11 <sup>a</sup>	3,38± 0,38						
12 <sup>b</sup>	21,3± 0,8	23,4± 0,8	24,9± 0,8	27,6± 0,8	29,6± 3,4	86± 21	

<sup>a</sup> Data displayed in Figure 5-17

<sup>b</sup> Data displayed in Figure 5-18

<sup>c</sup> Comments: 100 p DER 332/45 p T403. 16h/330 K.

For longitudinal tests: filament wound and moulded rods  $6 \times 10^{-3}$  m dia., 0,120 m long.

For transverse tests: tubes with  $25 \times 10^{-3}$  m inner diameter,  $6 \times 10^{-3}$  m wall thickness and approximately  $65 \times 10^{-3}$  m long.

95% confidence limits for the second set of data given in the Ref. are in error. Rapid increase of  $\beta$  above 320 K attributable to resin.

**Table 5-45: Smoothed values of the Linear Thermal Expansion Coefficient,  $\beta \times 10^6$  [K<sup>-1</sup>], of the Specimens characterized in Table 5-85.**

Spec. No. <sup>h</sup>	Temperature (K)		References
	80 K - 295 K	295 K - 360 K	
13	6,59	8,07	Klich & Cockrell (1983)
14	15,51	16,32	
15	10,82	12,70	
16	10,87	14,37	
17	8,58	10,66	
18	12,78	16,02	

<sup>h</sup> Comments: Prepregs 7,5 h/440 K Max. Temp.,  $5,2 \times 10^5$  Pa Max. Pres.  $12,7 \times 10^{-3}$  m x  $25,4 \times 10^{-3}$  x 0,152 m long. ASTM D696-70 test. Measurements in LN, in room temp. water, in 370 K water. Periodic micrometric readings. Cryogenic wind tunnel fan.

**Table 5-46: Smoothed values of the Linear Thermal Expansion Coefficient,  $\beta \times 10^6$  [K<sup>-1</sup>], of the Specimens characterized in Table 5-85.**

Spec. No.	Temperature (K)	Comments	References
	290 K - 530 K		
19	6,1	Re-entry thermal shields. Density of Narmco 4065 depends on curing process.	Penton (1966)
20	16,0		

**Table 5-47: Smoothed values of the Linear Thermal Expansion Coefficient,  $\beta \times 10^6$  [K<sup>-1</sup>], of the Specimens characterized in Table 5-85.**

Temperature [K]	Spec. No. <sup>i, k</sup>						
	21	22 <sup>c</sup>	23 <sup>c</sup>	24	25 <sup>d</sup>	26 <sup>d</sup>	27 <sup>d</sup>
90	23,1	0,33	16,6	(8.3)	2,78		22,4
100	24,3	0,30	17,9	9,0	2,84	(3.06)	23,8
120	26,8	0,25	20,2	10,1	2,95	3,20	26,6
140	29,3	0,19	22,1	11,1	3,07	3,32	29,1
160	31,6	0,13	24,1	12,1	3,21	3,45	31,9
180	33,8	0,06	25,6	12,9	3,35	3,58	34,2
200	36,1	0,00	27,0	13,7	3,51	3,71	36,8
220	38,3	-0,04	28,3	14,3	3,67	3,86	38,9
240	40,0	-0,08	29,1	14,8	3,86	4,00	40,9
260	41,8	-0,14	29,9	15,0	4,09	4,16	42,9
280	43,2	-0,18	30,8	15,1	4,35	4,33	46,0
300	45,0	-0,26	32,7	15,9	4,66	4,53	50,5
320	47,8	-0,22	36,0	17,6	5,15	4,76	57,3
340	53,3	0,02	41,1	20,7	5,55	5,02	68,3
360	62,1	0,12	48,1	25,1	5,65	5,35	83,4
380	73,7	0,02	58,6	31,9	5,55	5,80	104
390	81,1	-0,08	67,0	37,0	5,42	6,11	118
400		-0,22		44,9	5,25	6,50	136
410		-0,42			4,98	6,98	161
420		-0,66			4,61		
430		-1,10			4,06		
440					3,23		

<sup>c</sup> Data displayed in Figure 5-29.

<sup>d</sup> Data displayed in Figure 5-19.

<sup>i</sup> Comments: 50 p ERLA 4617/50 p mPDA in MEK. Pure resin: 2,5 h/400 K + 2 h/440 K + 6 h/500 K.

Composite: 2,5 h/400 K, removed, cut, 2 h/440 K + 6 h/500 K.  $5 \times 10^{-3} \times 6 \times 10^{-3} \times 13 \times 10^{-3}$  m long.

Each temperature region traversed twice. Interferometric measurements. Parenthetical values are extrapolated.

Investigation of the influence of fiber type and orientation.

<sup>k</sup> References: Rogers, Phillips, Kingston-Lee, Yates, Overy, Sargent & McCalla (1977) [144]

**Table 5-48: Smoothed values of the Linear Thermal Expansion Coefficient,  $\beta \times 10^6$  [K<sup>-1</sup>], of the Specimens characterized in Table 5-85.**

Temperature [K]	Spec. No. <sup>i, k</sup>									
	28	29	30 <sup>c,e</sup>	31 <sup>c,f</sup>	32 <sup>d</sup>	33 <sup>d</sup>	34 <sup>d</sup>	35	36	37
90	-1,3	7,2		19,0	1,43	1,20	26,5	-1,7	8,4	26,1
100	-1,4	7,8	-0,20	20,0	1,44	1,25	28,0	-2,0	8,7	27,5
120	-1,7	8,7	-0,28	21,9	1,45	1,33	31,0	-2,4	9,3	30,1
140	-1,9	9,4	-0,36	23,6	1,48	1,39	33,3	-2,6	10,0	32,9
160	-2,1	10,1	-0,47	25,4	1,52	1,42	35,8	-2,8	10,6	35,2
180	-2,2	10,8	-0,56	27,0	1,57	1,46	38,0	-3,0	11,2	37,8
200	-2,4	11,3	-0,57	28,4	1,64	1,50	40,0	-3,1	11,8	40,0
220	-2,4	11,7	-0,52	29,9	1,72	1,56	42,0	-3,1	12,4	42,0
240	-2,5	12,1	-0,46	31,1	1,83	1,63	43,7	-3,2	13,0	44,0
260	-2,6	12,1	-0,37	32,1	1,97	1,72	45,0	-3,4	13,6	45,7
280	-2,06	12,4	-0,30	33,1	2,14	1,82	46,2	-3,7	14,2	47,3
300	-2,07	13,4	-0,26	33,9	2,40	1,95	48,3	-4,2	14,9	49,5
320	-3,0	15,0	-0,26	34,6	2,67	2,11	54,0	-5,0	16,4	54,6
340	-3,7	17,6	-0,28	36,4	2,75	2,30	64,0	-6,2	19,2	67,8
360	-4,8	21,5	-0,36	40,3	2,42	2,59	82,0	-8,2	25,6	96,0
380	-7,4	27,7	-0,46	47,5	1,60	3,10	125	-15,1		156
390	-10,4	32,6	-0,52	53,4	0,54					208

Temperature [K]	Spec. No. <sup>i,k</sup>									
	28	29	30 <sup>c,e</sup>	31 <sup>c,f</sup>	32 <sup>d</sup>	33 <sup>d</sup>	34 <sup>d</sup>	35	36	37
400	-14,6		-0,63	62,9						265
410	-22,1		-0,73							
420			-0,90							
430			-1,10							
440			-1,47							

<sup>c</sup> Data displayed in Figure 5-29.

<sup>d</sup> Data displayed in Figure 5-19.

<sup>e</sup> Data displayed in Figure 5-30.

<sup>f</sup> Data displayed in Figure 5-31.

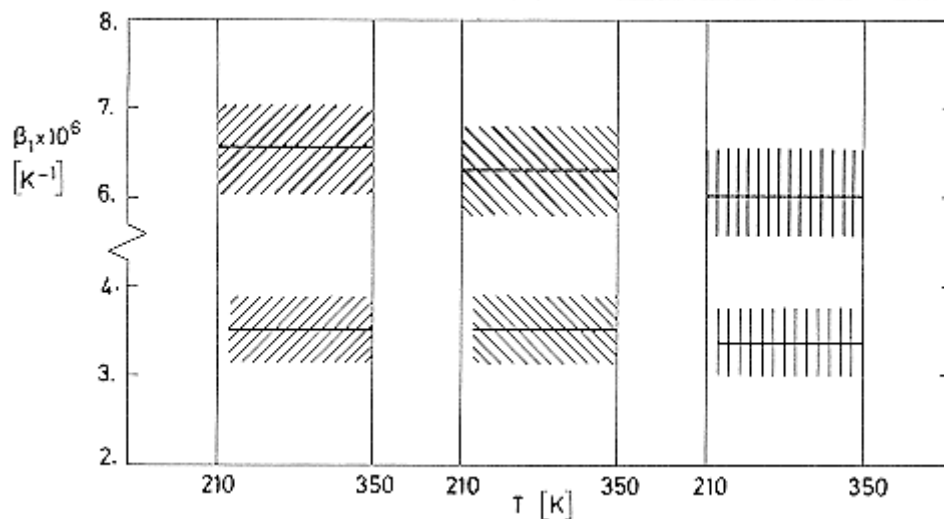
<sup>i</sup> Comments: 50 p ERLA 4617/50 p mPDA in MEK. Pure resin: 2,5 h/400 K + 2 h/440 K + 6 h/500 K.

Composite: 2,5 h/400 K, removed, cut, 2 h/440 K + 6 h/500 K.  $5 \times 10^{-3} \times 6 \times 10^{-3} \times 13 \times 10^{-3}$  m long.

Each temperature region traversed twice. Interferometric measurements. Parenthetical values are extrapolated.

Investigation of the influence of fiber type and orientation.

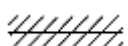
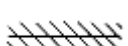
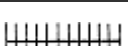
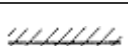


<sup>k</sup> References: Rogers, Phillips, Kingston-Lee, Yates, Overy, Sargent & McCalla (1977) [144].



Note: non-si units are used in this figure

**Figure 5-17: Linear thermal expansion coefficient measured parallel to fibers,  $\beta_1$ , as a function of temperature,  $T$ , for some composite materials formed by the same matrix, DER 332/T403, and two different glass fiber reinforcements. Upper and lower limits of the shadowed regions are for 95% confidence.**

Explanation

Spec. No.	Key	Fiber	$\varphi$	Reference
1		E-Glass	0,600	Clements & Moore (1978) [73]
3			0,650	
5			0,700	
7		S-2-Glass	0,600	Clements & Moore (1979) [74]
9			0,650	
11			0,700	

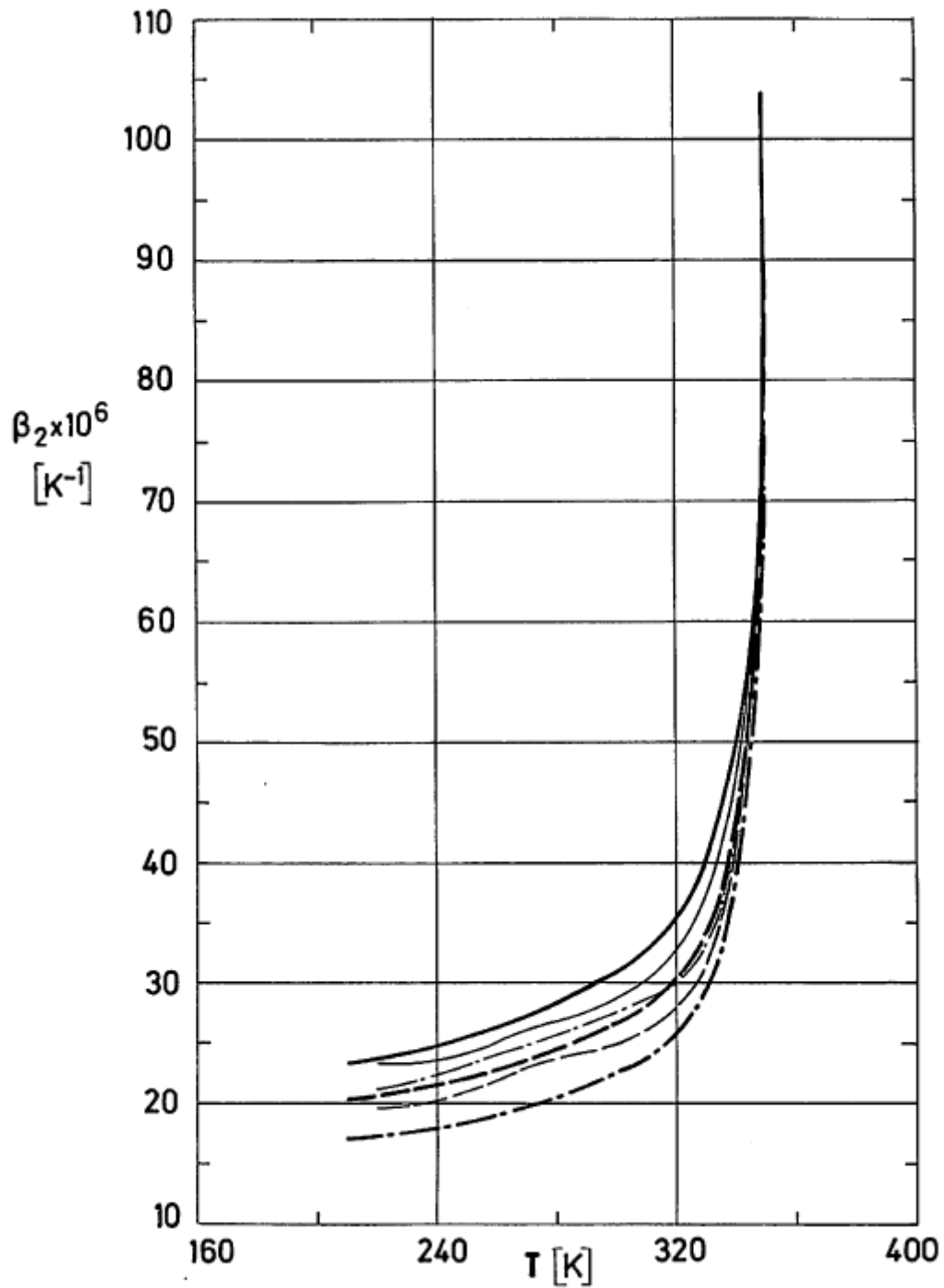


Figure 5-18: Linear thermal expansion coefficient measured perpendicular to fibers,  $\beta_2$ , as a function of temperature,  $T$ , for some composite materials formed by the same matrix, DER 332/T403, and two different glass fiber reinforcements.



## Explanation

Spec. No.	Key	Fiber	$\varphi$	Reference
2		E-Glass	0,600	Clements & Moore (1978) [73]
4			0,650	
6			0,700	
8		S-2-Glass	0,600	Clements & Moore (1979) [74]
10			0,650	
12			0,700	

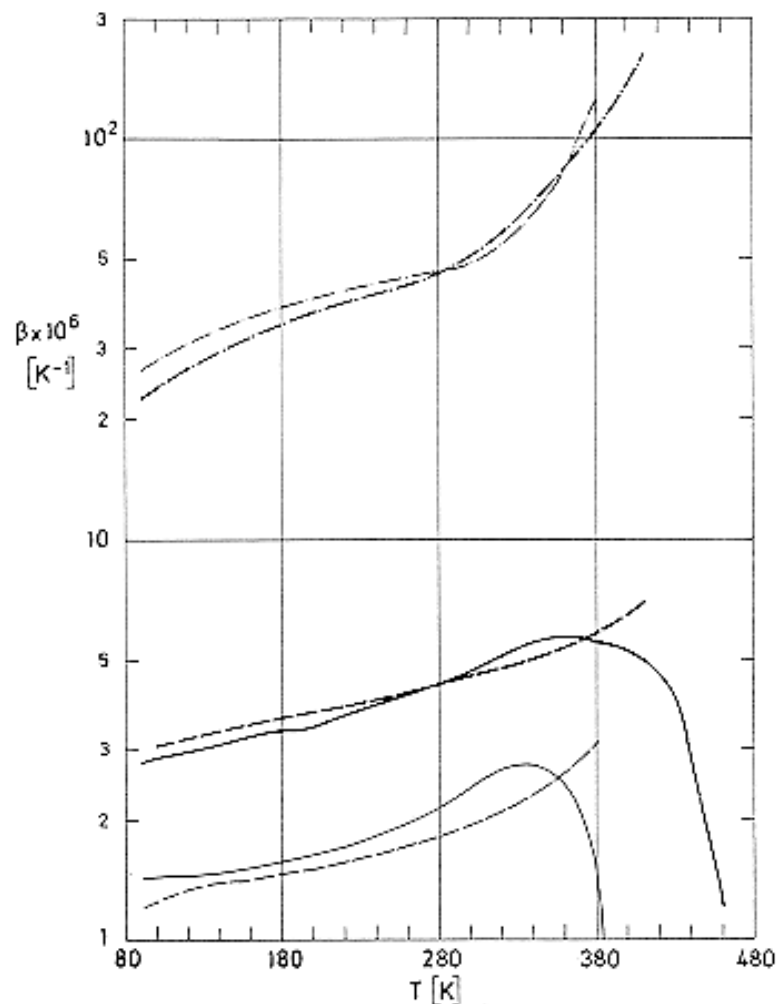








Figure 5-19: Linear thermal expansion coefficient measured in different directions,  $\beta$ , as a function of temperature,  $T$ , for similar carbon fiber reinforced composite materials. The matrix is ERLA 4617/mPDA. From Rogers, Phillips, Kingston, Lee, Yates, Overy, Sargent & McCalla (1977) [144].

## Explanation

Spec. No.	Key	Fiber	Fiber Angle [°]	$\phi_f$	Direction of Measurement
25		HTS PT112/21Z (prepreg)	90	0,500	Parallel to one set of fibers
26					Bisecting angle between fibers
27					Perpendicular to laminate
32		HMS QM218/622W		0,520	Parallel to one set of fibers
33					Bisecting angle between fibers
34					Perpendicular to laminate

**Table 5-49: Characterization of Composite Materials (Linear Thermal Expansion is given following the links).**

Spec. No.	Matrix	Fiber		Fiber volume $\phi_f$	Void content $\phi_v$	Direction of measurement	
		Type (Manufacturer)	Fiber angle (°) or Weave				
Table 5-50	DLS 351/BF <sub>3</sub> 400	(No fibers)		0,000	0,000		
Table 5-50		HTS PT112/21Z (Courtaulds)		0	0,515	0,022	Parallel to fibers
Table 5-50							Perpendicular to fibers
Table 5-50							Parallel to fibers
Table 5-50							Perpendicular to fibers
Table 5-50							Parallel to fibers
Table 5-50							Perpendicular to fibers
Table 5-50							Parallel to fibers
Table 5-50	Perpendicular to fibers						
Table 5-51	Code 69	(No fibers)		0,000	0,000		
Table		HTS PT112/21Z	0	0,589	0,000	Parallel to fibers	

Spec. No.	Matrix	Fiber		Fiber volume $\varphi_f$	Void content $\varphi_v$	Direction of measurement
		Type (Manufacturer)	Fiber angle (°) or Weave			
5-51		(Courtaulds)				
Table 5-51						Perpendicular to fibers
Table 5-51						In plane of laminate
Table 5-51						Perpendicular to laminate
Table 5-51						Bisecting acute angle
Table 5-51						Bisecting obtuse angle
Table 5-51						Perpendicular to laminate
Table 5-51	DLS 351/BF <sub>3</sub> 400		90	0,614	0,018	In plane of laminate
Table 5-51						Perpendicular to laminate
Table 5-52	Code 69	Grafil HTS 130 SC/10000 (Courtaulds)	(0/± 45) <sub>80</sub>	0,560	0,070	0°, in plane of laminate
Table 5-52						90°, in plane of laminate
Table 5-52						Perpendicular to laminate
Table 5-53	DLS 351/BF <sub>3</sub> 400	Type II Carbon fiber (Morganite)	16 plies of plain weave woven from 5000-end carbon tows	0,601	0,030	Parallel to warp
Table 5-53						Parallel to weft
Table 5-53						Perpendicular to laminate
Table 5-53			15 plies of 5000-end twill weave	0,611	0,036	Parallel to warp
Table 5-53						Parallel to weft
Table 5-53						Perpendicular to laminate

Spec. No.	Matrix	Fiber		Fiber volume $\varphi_f$	Void content $\varphi_v$	Direction of measurement
		Type (Manufacturer)	Fiber angle (°) or Weave			
Table 5-53		Grafil E/XAS XA: Super A type S: Surface treated E: Sized with uncured epoxy (Shell Epikote 834) (Courtaulds)	25 plies of twill weave woven from 3000-end fiber	0,600	0,005	Parallel to warp
Table 5-53						Parallel to weft
Table 5-53						Perpendicular to laminate
Table 5-53			25 plies of 5 ShaftSatin 3000-end fiber. The warp tows of each ply in the same direction	0,591	0,022	Parallel to warp
Table 5-53						Parallel to weft
Table 5-53						Perpendicular to laminate
Table 5-53			As above. Warp tows of even plies at right-angles to those of odd plies	0,587	0,009	Perpendicular to direction having 13 warps and 12 wefts
Table 5-53						Perpendicular to direction having 12 warps and 13 wefts
Table 5-53			Unidirectional unwoven fibers. 3000-end fiber	0,619	0,013	Parallel to fibers
Table 5-53						Perpendicular to fibers

**Table 5-50: Smoothed Values of the Linear Thermal Expansion Coefficient,  $\beta \times 10^6$  [K<sup>-1</sup>], of the Specimens Characterized in Table 5-49.**

Temperature [K]	Spec. No. <sup>d, e</sup>						
	38	39 <sup>a</sup>	40 <sup>b</sup>	41 <sup>a</sup>	42 <sup>b</sup>	43 <sup>a</sup>	44 <sup>b</sup>
90	23,3	-0,18	15,7	-0,53	14,0	-0,41	10,0
100	24,6	-0,22	16,7	-0,61	14,9	-0,44	10,5
120	27,3	-0,27	18,6	-0,70	16,5	-0,50	11,6
140	30,0	-0,29	20,5	-0,75	18,1	-0,57	12,6
160	32,5	-0,31	22,1	-0,75	19,7	-0,65	13,5
180	35,0	-0,30	23,7	-0,71	21,2	-0,71	14,4
200	37,6	-0,29	25,1	-0,62	22,4	-0,74	15,2
220	40,0	-0,26	26,5	-0,50	23,5	-0,74	16,0
240	42,5	-0,22	27,7	-0,35	24,6	-0,72	16,6
260	44,8	-0,18	28,7	-0,25	25,5	-0,69	17,2
280	47,0	-0,12	29,5	-0,20	26,3	-0,64	17,7
300	48,0	-0,05	30,1	-0,20	26,6	-0,57	18,0
320	49,3	0,02	30,5	-0,42	27,1	-0,56	18,3
340	51,0	0,09	31,3	-0,46	27,8	-0,59	18,4
360	53,4	0,14	32,7	-0,30	28,7	-0,58	19,0
380	56,0	0,19	34,9	-0,04	29,8	-0,52	19,9
400	59,0	0,22	37,8	-0,15	31,5	-0,35	21,3
420	62,5	0,24	41,3	0,19	33,5	-0,24	23,3
440	66,0	0,24	45,2	0,13	36,1	-0,18	26,1
460	70,2	0,20	49,5	0,02	39,4	-0,16	30,0
480	75,8	0,09	54,3	-0,15	43,9	-0,21	36,3
500	82,5	-0,13		-0,44	50,6		

Temperature [K]	Spec. No. <sup>d, e</sup>						
	38	39 <sup>a</sup>	40 <sup>b</sup>	41 <sup>a</sup>	42 <sup>b</sup>	43 <sup>a</sup>	44 <sup>b</sup>
510	-0,30		-0,80				
520	-0,55						

<sup>a</sup> Data displayed in Figure 5-20.

<sup>b</sup> Data displayed in Figure 5-21.

<sup>d</sup> Comments: 80 p DLS 351/1,2 p BF<sub>3</sub>400 at 400 K. 0,5 h vacuum oven + 0,25 h mould outgas/400 K. Vacuum released. Then 0,25 h/400 K + 2,5 h/420 K + 15 h/460 K. Specimen sizes and measurements as above. Investigation of the influence of  $\varphi$ .

<sup>e</sup> References: Yates, Overy, Sargent, McCalla, Kingston-Lee, Phillips & Rogers (1978)a [170].

**Table 5-51: Smoothed Values of the Linear Thermal Expansion Coefficient,  $\beta \times 10^6$  [K<sup>-1</sup>], of the Specimens Characterized in Table 5-49.**

Temperature [K]	Spec. No. <sup>f, g</sup>									
	45	46	47	48 <sup>c</sup>	49 <sup>c</sup>	50	51	52	53 <sup>c</sup>	54 <sup>c</sup>
90	22,0	-0,08	13,0	1,56	19,2	-1,00	7,8	18,0	1,29	18,7
100	23,0	-0,08	13,9	1,58	20,2	-1,10	8,1	19,0	1,33	19,6
120	25,1	-0,09	15,5	1,63	22,2	-1,37	8,9	20,9	1,41	21,7
140	27,3	-0,12	17,0	1,68	24,1	-1,66	9,6	22,4	1,47	23,7
160	29,5	-0,18	18,4	1,73	26,0	-1,92	10,3	24,5	1,53	25,7
180	31,6	-0,24	19,7	1,78	27,9	-2,18	11,0	26,2	1,59	27,6
200	33,7	-0,26	20,9	1,85	29,8	-2,39	11,8	28,1	1,67	29,6
220	35,8	-0,24	22,1	1,92	31,7	-2,59	12,5	30,0	1,77	31,5
240	37,8	-0,19	23,1	1,99	33,5	-2,76	13,2	31,9	1,88	33,3
260	39,7	-0,11	24,1	2,05	35,5	-2,90	13,9	33,6	2,03	35,0
280	41,7	-0,10	25,1	2,13	37,5	-3,02	14,7	35,4	2,18	36,6
300	43,9	-0,20	26,0	2,21	39,1	-3,18	15,4	37,1	2,24	38,1
320	46,3	-0,39	26,9	2,30	41,0	-3,27	16,1	39,9	2,23	39,5

Temperature [K]	Spec. No. <sup>f, g</sup>									
	45	46	47	48 <sup>c</sup>	49 <sup>c</sup>	50	51	52	53 <sup>c</sup>	54 <sup>c</sup>
340	49,0	-0,40	27,8	2,39	42,9	-3,37	16,8	42,8	2,14	40,8
360	52,0	-0,32	28,6	2,50	44,9	-3,42	17,5	46,4	2,02	41,9
380	55,4	-0,19	29,8	2,61	47,0	-3,50	18,3	50,8	1,98	42,9
400	59,1	0,01	31,1	2,74	49,5	-3,56	19,0	53,5	2,07	44,7
420	63,6	0,21	32,7	2,90	52,5	-3,70	19,7	55,2	2,26	47,0
440	69,1	0,26	35,1	3,16	55,9	-4,03	20,5	57,7	2,68	50,4
460	75,7	0,23	38,5	3,56	60,2	-4,65	21,2	64,0	3,16	56,1
480	83,8	0,10	44,4	4,21	66,8	-6,22	(21,9)	86,4	3,40	65,0
490	89,2	0,01	49,7	3,80	72,0	-8,65		109	2,95	70,9
500	(95,0)	-0,12		2,66	82,3			137	2,28	78,9
510				1,53				175	1,59	90,9
520				0,44					0,72	

<sup>c</sup> Data displayed in Figure 5-22.

<sup>f</sup> Comments: Code 69 as received. Several days in vacuum. several hours mould outgas/350 K. Vacuum released. Then 2 h/350 K + 1 h/440 K + 5 h/500 K. DLS 351/BF<sub>3</sub>400 as above. Investigation of the behaviour of a resin of direct technological interest.

<sup>g</sup> References: Yates, McCalla, Sargent, Rogers, Phillips & Kingston-Lee, (1978)b [168].

**Table 5-52: Smoothed Values of the Linear Thermal Expansion Coefficient,  $\beta \times 10^6$  [K<sup>-1</sup>], of the Specimens Characterized in Table 5-49.**

Temperature [K]	Spec. No. <sup>h,i</sup>		
	55	56	57
90	-0,14	4,15	17,0
100	-0,16	4,25	17,9
120	-0,16	4,49	19,5
140	-0,12	4,72	21,2
160	-0,07	5,00	22,8
180	-0,06	5,29	24,6
200	-0,07	5,62	26,3
220	-0,11	5,94	27,9
240	-0,17	6,32	29,7
260	-0,24	6,74	31,4
280	-0,28	7,18	33,2
300	-0,30	7,48	36,3
320	-0,29	7,68	39,4
340	-0,22	7,77	41,2
360	-0,08	7,78	42,3
380	0,17	7,87	42,9
400	0,56	7,98	43,5
420	1,06	8,11	45,0
440	1,33	8,31	47,0
460	0,56	8,78	51,8
480	0,13	9,67	63,3
490	-0,01	10,3	76,2



Temperature [K]	Spec. No. <sup>h,i</sup>		
	55	56	57
500	-0,13	11,2	95,0
510	-0,30	12,5	
520	-0,52		

<sup>h</sup> Comments: Resin cure, specimen sizes and measurements as above. Investigation of ply multidirectional effects.

<sup>i</sup> References: Yates, McCalla, Sargent, Rogers, Kingston-Lee & Phillips (1978)c [169].

**Table 5-53: Smoothed Values of the Linear Thermal Expansion Coefficient,  $\beta \times 10^6$  [K<sup>-1</sup>], of the Specimens Characterized in Table 5-49.**

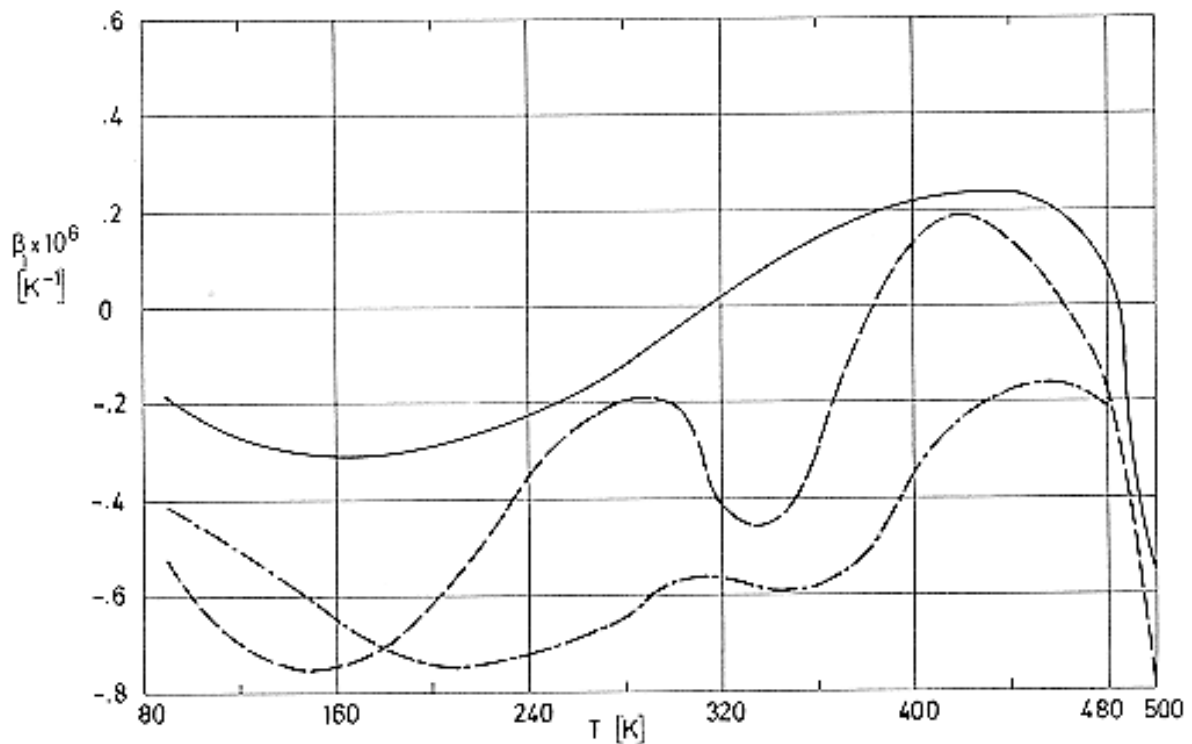
Temp. [K]	Spec. No. <sup>i,k</sup>															
	58	59	60	61	62	63	64	65	66	67	68	69	70	71	72	73
90	1,68	2,71	16,1	1,48	2,35	17,7	1,61	1,65	18,2	2,10	2,11	19,3	2,22	2,20	0,38	14,9
100	1,77	2,73	17,1	1,48	2,35	18,7	1,62	1,68	19,3	2,15	2,14	20,3	2,22	2,22	0,37	15,7
120	1,89	2,81	19,1	1,49	2,37	20,7	1,64	1,74	21,5	2,22	2,20	22,6	2,24	2,25	0,33	17,3
140	1,96	2,90	21,1	1,50	2,39	22,7	1,67	1,80	23,5	2,26	2,26	24,6	2,26	2,28	0,28	18,7
160	1,92	3,00	22,9	1,52	2,43	24,4	1,70	1,86	25,5	2,29	2,32	26,5	2,29	2,32	0,24	20,3
180	1,89	3,11	24,8	1,54	2,47	26,2	1,74	1,93	27,5	2,32	2,37	28,5	2,34	2,36	0,21	21,8
200	1,92	3,25	26,5	1,56	2,53	27,8	1,78	2,00	29,5	2,37	2,41	30,3	2,40	2,42	0,18	23,3
220	2,00	3,41	28,1	1,60	2,61	29,3	1,84	2,08	31,4	2,45	2,47	31,8	2,49	2,49	0,16	24,9
240	2,13	3,62	29,7	1,69	2,69	30,7	1,88	2,17	33,3	2,58	2,60	33,5	2,62	2,57	0,17	26,4
260	2,23	3,90	31,1	1,84	2,80	31,9	1,98	2,26	35,0	2,77	2,80	35,2	2,77	2,68	0,20	27,9
280	2,28	4,24	32,4	2,07	2,92	34,0	2,07	2,37	36,9	2,95	3,00	36,9	2,95	2,84	0,25	29,4
300	2,35	4,18	34,6	2,44	3,06	37,7	2,17	2,49	39,0	2,70	3,08	38,1	3,02	3,00	0,31	31,0
320	3,05	3,54	39,2	2,85	3,23	39,2	2,29	2,66	41,5	2,62	3,02	38,9	2,89	2,93	0,37	32,5
340	2,93	3,45	40,0	3,16	3,44	39,6	2,40	2,89	44,2	2,85	2,87	39,2	2,71	2,72	0,43	34,1
360	1,99	4,16	41,6	3,38	3,67	42,0	2,52	3,17	46,8	3,08	2,91	39,8	2,72	2,72	0,49	35,6

Temp. [K]	Spec. No. <sup>i,k</sup>															
	58	59	60	61	62	63	64	65	66	67	68	69	70	71	72	73
380	2,19	4,48	45,3	3,55	3,96	46,0	2,62	3,30	50,3	3,27	3,49	41,8	3,45	3,28	0,53	37,5
400	2,07	4,42	49,6	3,66	4,23	50,3	2,72	3,32	54,2	3,41	4,10	47,9	3,97	3,79	0,47	39,7
420	1,32	3,90	53,7	3,72	4,33	(55,0)	2,80	3,24	60,3	3,50	4,03	59,1	4,12	3,96	0,34	42,3
440	0,87	2,47	57,6	3,66	3,86		2,87	2,94	71,5	3,37	3,55	74,2	3,95	3,89	0,14	45,6
450			59,4					2,58	82,5		2,96			(3,58)	(0,03)	

<sup>i</sup> Comments: DLS 351/BF<sub>3</sub>400 cured as in Specs. No. 38 to 44. Specimens were rectangular parallelepipeds.

Dimensions so chosen that the pattern revealed in the surface layers was a representative unit of the overall pattern. Experimental procedure and measurements as above. Parenthetical values have been extrapolated. Investigation of the influence of fiber weave in fabric reinforcement.

<sup>k</sup> References: Rogers, Kingston-Lee, Phillips, Yates, Chandra & Parker (1981) [143].

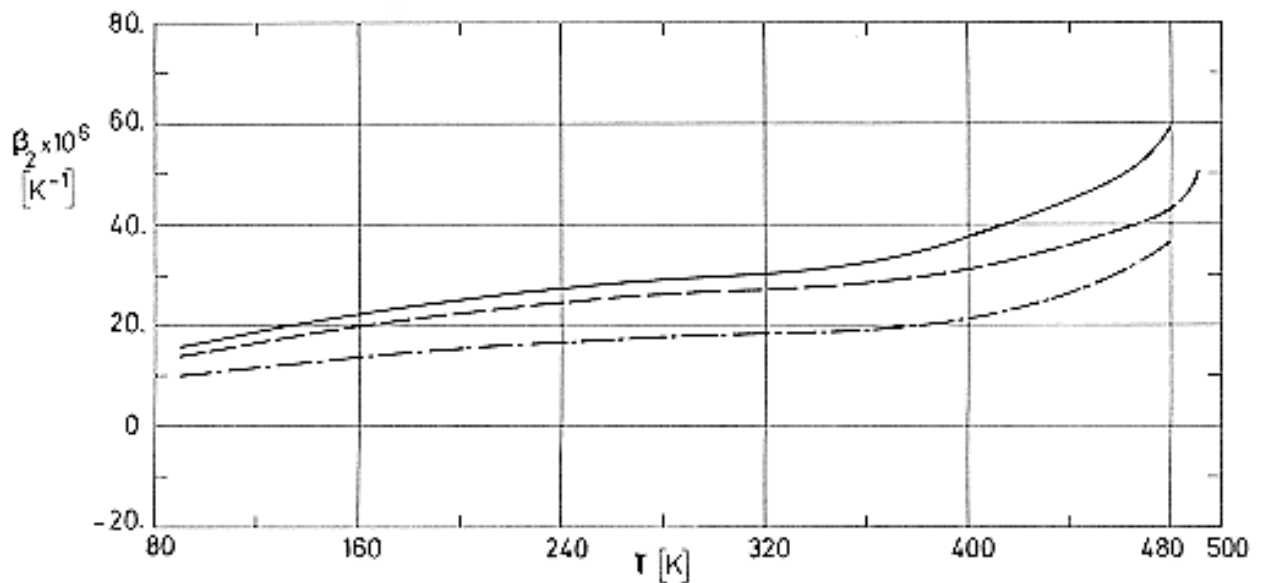


Note: non-si units are used in this figure

**Figure 5-20: Linear thermal expansion coefficient measured parallel to fibers,  $\beta_l$ , as a function of temperature,  $T$ , for different fiber volume ratios,  $\phi$ . Fiber: Courtaulds HTS PT112/21Z; Matrix: DLS 351/BF<sub>3</sub>400.**

## Explanation

Spec. No.	Key	$\varphi_f$	Reference
39		0,515	Yates, Overy, Sargent, McCalla, Kingston-Lee, Phillips & Rogers (1978)a [170]
41		0,607	
43		0,789	



Note: non-si units are used in this figure

**Figure 5-21: Linear thermal expansion coefficient measured perpendicular to fibers,  $\beta_2$ , as a function of temperature,  $T$ , for different fiber volume ratios,  $\varphi_f$ .  
 Fiber: Courtaulds HTS PT112/21Z; Matrix: DLS 351/BF<sub>3</sub>400.**

## Explanation

Spec. No.	Key	$\varphi_f$	Reference
40		0,515	Yates, Overy, Sargent, McCalla, Kingston-Lee, Phillips & Rogers (1978)a [170]
42		0,607	
44		0,789	

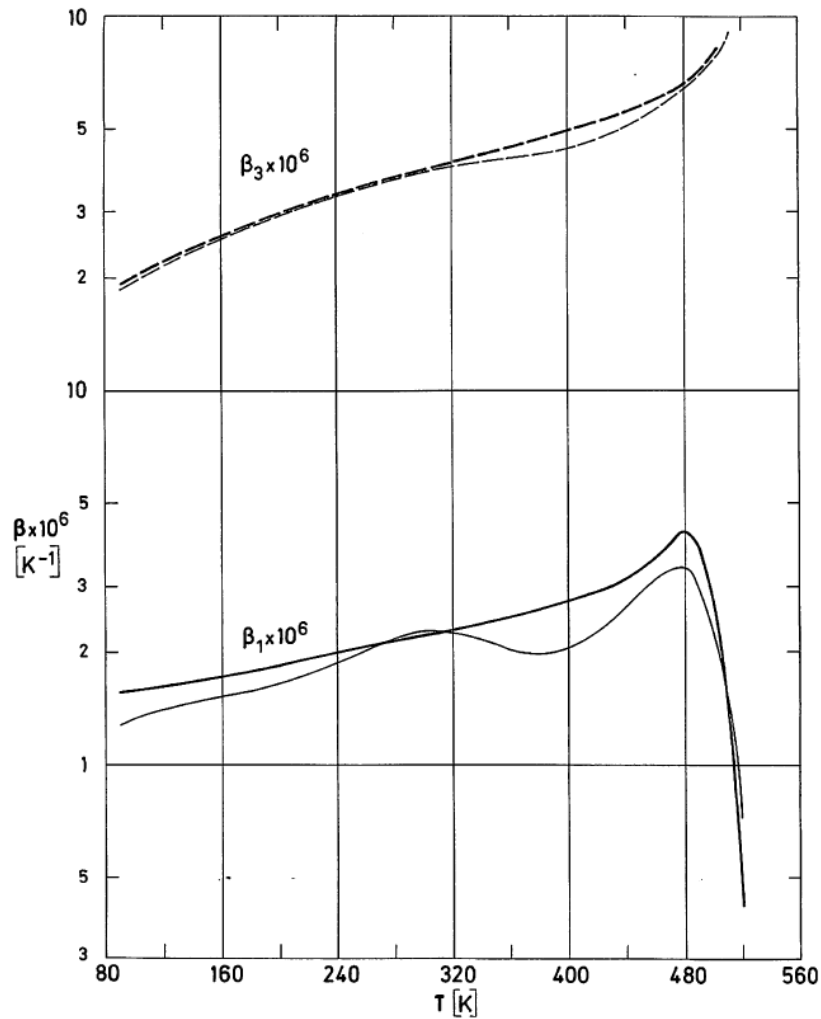


Figure 5-22: Linear thermal expansion coefficient measured either in plane of laminate,  $\beta_l$ , or perpendicular to it,  $\beta$ , as a function of temperature,  $T$ , for similar carbon fibers reinforced composite materials. The fiber is carbon HTS PT112/21Z. From Yates, McCalla, Sargent, Rogers, Phillips & Kingston-Lee (1978)b [169].

Explanation

Spec. No.	Key	Matrix	Fiber Angle [°]	$\varphi$	$\beta$	Direction of Measurement
48		Code 69	90	0,589	$\beta_l$	In plane of laminate
49					$\beta$	Perpendicular to laminate
53		DLS 351/BF <sub>3</sub> 400		0,614	$\beta_l$	In plane of laminate
54					$\beta$	Perpendicular to laminate

**Table 5-54: Characterization of Composite Materials (Linear Thermal Expansion is given following the links).**

Spec. No.	Matrix	Fiber		Fiber volume $\phi_f$	Void content $\phi_v$	Direction of measurement			
		Type (Manufacturer)	Fiber angle (°) or Weave						
Table 5-55	CRC 350A	GY70 (Celion Fibers Celanese Corp.)	0	0,600	0,006	Parallel to fibers			
Table 5-55						Perpendicular to fibers			
Table 5-55			(90/+45/0/-45)s	0,610	0,018	0°			
Table 5-55						+45°			
Table 5-55						90°			
Table 5-55						-45°			
Table 5-55						(90/+45/0/-45)3s	0,610	0,018	0°
Table 5-55									30°
Table 5-55			45°						
Table 5-55			60°						
Table 5-55			90°						
Table 5-55			Epitoke 210/BF <sub>3</sub> 400	T300	0	0,650	Parallel to fibers		
Table 5-55	Perpendicular to fibers								
Table 5-55	Epitoke 828/NMA/K61B	Grafill HMS (Courtaulds)	0	0,570	Parallel to fibers				
Table 5-55					Perpendicular to fibers				
Table 5-55	Epitoke 828/BF <sub>3</sub> MEA(Toraica-P-301 <sup>a</sup> prepreg)	Torayca T300A (Toray)	0	0,650	Parallel to fibers				
Table					Perpendicular				

Spec. No.	Matrix	Fiber		Fiber volume $\varphi_f$	Void content $\varphi_v$	Direction of measurement
		Type (Manufacturer)	Fiber angle (°) or Weave			
5-55						to fibers
Table 5-55				0,600		0° in plane of laminate
Table 5-55						15° in plane of laminate
Table 5-55						28° in plane of laminate
Table 5-55						29° in plane of laminate
Table 5-55						42° in plane of laminate
Table 5-55						43° in plane of laminate
Table 5-55						59° in plane of laminate
Table 5-55						60° in plane of laminate
Table 5-55						74° in plane of laminate
Table 5-55						76° in plane of laminate
Table 5-55						83° in plane of laminate
Table 5-55						87° in plane of laminate
Table 5-56	Fibredux 914C	HTS carbon fiber NM565 issue 2, 132/1,55/K10 Grade SF. Average tensile modulus: $132 \times 10^9$ Pa. 10000 ends per tow. Surface treated and sized. (Courtaulds)	0	0,64	0,000	Parallel to fibers
Table 5-56						Perpendicular to fibers
Table 5-56				0,687	0,004	Parallel to fibers
Table 5-56						Perpendicular to fibers
Table 5-56				0,671	0,000	Parallel to fibers

Spec. No.	Matrix	Fiber		Fiber volume $\varphi_f$	Void content $\varphi_v$	Direction of measurement
		Type (Manufacturer)	Fiber angle (°) or Weave			
Table 5-56						Perpendicular to fibers
Table 5-56		Type II carbon fiber NM565 issue 1 as 130 SC 10000. Average tensile modulus: $130 \times 10^9$ Pa. 10000 ends per tow. Surface treated and continuous fibers. (Morganite)	0	0,619	0,0025	Parallel to fibers
Table 5-56	Perpendicular to fibers					
Table 5-56	Parallel to fibers					
Table 5-56	Perpendicular to fibers					
Table 5-56	Parallel to fibers					
Table 5-56	Perpendicular to fibers					
Table 5-56	Parallel to fibers					
Table 5-56				0,6375	<0,001	Parallel to fibers
Table 5-56						Perpendicular to fibers
Table 5-56				0,642		Parallel to fibers
Table 5-56						Perpendicular to fibers

**Table 5-55: Smoothed Values of the Linear Thermal Expansion Coefficient,  $\beta \times 10^6$  [K<sup>-1</sup>], of the Specimens Characterized in Table 5-54.**

Spec. No.	Temperature (K)						Comments	References	
	290	300	330	350	380	450			
74			-0,90				d	Kalnin (1974)	
75			29						
76			0,50						
77			0,35						
78			0,05						
79			0,30						
80			0,25						
81			0,28						
82			030						
83			0,40						
84			0,50						
85	0,2								Karlsson (1983)

Spec. No.	Temperature (K)						Comments	References
	290	300	330	350	380	450		
86	35							
87	1,0						e	Harley & Rosenberg (1981)
88	70							
89	-0,27					f	Ishikawa, Koyama & Kobayashi (1977, 1978)	
90	33,5							
91 <sup>a</sup>	0,03							
92 <sup>a</sup>	2,55							
93 <sup>a</sup>	8,45							
94 <sup>a</sup>	7,92							
95 <sup>a</sup>	17,0							
96 <sup>a</sup>	16,7							
97 <sup>a</sup>	27,7							
98 <sup>a</sup>	28,1							
99 <sup>a</sup>	34,2							
100 <sup>a</sup>	33,9							
101 <sup>a</sup>	34,6							
102 <sup>a</sup>	36,2							

<sup>a</sup> Data displayed in Figure 5-23.

<sup>d</sup> From prepreg. Curing: 6h/450 K, bag pressure  $5,2 \times 10^5$  Pa. Specimens from tape 0,075 m wide. Cured panels were trimmed, jigged and cut into  $6 \times 10^{-3}$  m wide strips along measurements direction. Bonded rectangular prisms or cast cylinders  $25 \times 10^{-3}$  m to  $45 \times 10^{-3}$  m long,  $6 \times 10^{-3}$  m to  $10^{-2}$  m wide. Netzsch dilatometer Model 402/T2. Accuracy checked with Pyrex glass and Al 6061T. Heating rate 10 K/min. Hysteresis loop and random displacement eliminated by 2-3 pretest cycles 290 K -420 K.

<sup>e</sup> Capacitive method of measurement.

<sup>f</sup> From prepreg. Curing: 8 min/420 K + 52 min/440 K,  $10^6$  Pa + 3h/440 K. Specimens  $2 \times 10^{-3}$  m x 0,01 m x 0,01 m. Specs. No. 89 and 90 were cut from bars either in the surface direction or orthogonal. Data for Spec. No. 90 is an average of eleven data given in the source. Specs. No. 91 to 102 were cut from plates 0,01 m thick. Commercial interferometric dilatometer was used with He-Ne gas laser beam as incident light. Heating from room up to 420 K at 1 K/min. Temperature measured in an electrical heating point by a thermocouple. Fair comparison with numerical predictions.



**Table 5-56: Smoothed Values of the Linear Thermal Expansion Coefficient,  $\beta \times 10^6$  [K<sup>-1</sup>], of the Specimens Characterized in Table 5-54.**

Temp. [K]	Spec. No. <sup>g h</sup>											
	103 <sup>b</sup>	104 <sup>c</sup>	105 <sup>b</sup>	106 <sup>c</sup>	107 <sup>b</sup>	108 <sup>c</sup>	109 <sup>b</sup>	110 <sup>c</sup>	111 <sup>b</sup>	112 <sup>c</sup>	113 <sup>b</sup>	114 <sup>c</sup>
80				12,4					- 0,018			
90	- 0,041	13,9	- 0,099	13,3	- 0,008	14,1	0,161	15,6	0,043	13,7	0,062	13,3
100	- 0,059	14,6	- 0,137	14,0	- 0,022	14,3	0,203	16,1	0,058	14,4	0,128	14,5
120	- 0,150	15,8	- 0,239	15,2	- 0,111	15,8	0,113	17,5	0,072	15,6	0,137	15,2
140	- 0,223	16,8	- 0,254	16,3	- 0,160	16,9	0,025	18,8	- 0,023	16,7	0,001	16,0
160	- 0,265	17,6	- 0,314	16,8	- 0,281	18,2	- 0,026	20,6	- 0,075	17,9	- 0,116	17,2
180	- 0,316	18,6	- 0,342	17,4	- 0,320	19,6	- 0,115	21,7	- 0,104	19,5	- 0,153	18,9
200	- 0,370	20,0	- 0,345	18,3	- 0,347	21,0	- 0,087	22,5	- 0,140	20,2	- 0,195	19,9
220	- 0,323	21,2	- 0,338	19,4	- 0,342	21,3	- 0,127	23,6	- 0,123	21,3	- 0,191	20,7
240	- 0,345	22,1	- 0,311	20,4	- 0,318	22,5	- 0,087	24,5	- 0,148	22,2	- 0,136	22,2
260	- 0,285	22,8	- 0,292	21,4	- 0,246	23,2	- 0,039	25,3	- 0,090	23,6	- 0,085	23,3
280	- 0,275	23,7	- 0,261	22,1	- 0,225	24,0	- 0,001	27,0	0,008	25,1	- 0,082	24,6
290	- 0,251	24,1	- 0,268	22,8	- 0,201	24,5	0,034	27,5	0,026	25,7	- 0,536	25,2
300	- 0,253	24,5	- 0,245	23,3	- 0,221	25,0	0,058	27,6	- 0,060	26,4	- 0,365	23,5
320	- 0,325	26,0	- 0,417	23,6	- 0,300	26,0	- 0,005	28,5	- 0,460	27,6	- 0,196	26,0

Temp. [K]	Spec. No. <sup>g</sup> <sup>h</sup>											
	103 <sup>b</sup>	104 <sup>c</sup>	105 <sup>b</sup>	106 <sup>c</sup>	107 <sup>b</sup>	108 <sup>c</sup>	109 <sup>b</sup>	110 <sup>c</sup>	111 <sup>b</sup>	112 <sup>c</sup>	113 <sup>b</sup>	114 <sup>c</sup>
340	- 0,410	26,9	- 0,346	24,4	- 0,201	26,7	0,022	30,4	- 0,408	29,0	- 0,073	28,2
350	- 0,407	27,6	- 0,291	24,4	- 0,191	28,1	0,005	31,3	- 0,428	29,3	0,078	28,9
360	- 0,299	28,2	- 0,286	26,4	- 0,228	27,1	0,009	32,0	- 0,013	29,4	0,012	28,9
380	- 0,284	29,4	- 0,148	26,9	- 0,262	26,5	0,048	34,8	- 0,257	30,4	0,095	29,4
400	- 0,154	28,0	0,108	30,3	- 0,249	28,5	0,220	35,8	- 0,050	31,1	0,057	29,4
420	- 0,075	28,5	0,164	29,1	- 0,124	29,1	0,193	38,3	0,035	32,0	0,194	31,4
440	0,081	29,5	0,192	30,6	0,029	30,8	0,124	42,3	0,194	36,7	- 0,100	37,3
450	0,012		0,161					50,5	0,531		- 0,182	40,8

<sup>b</sup> Data displayed in Figure 5-23.

<sup>c</sup> Data displayed in Figure 5-23.

<sup>g</sup> Prepreg. Curing: 1h/448 K,  $6,9 \times 10^5$  Pa Pressure bag + 4h/460 K. From data points in the source, smoothed by the compiler. Specimens constructed from 18 plies of prepreg. Rectangular parallelepipeds, dimensions  $9 \times 10^{-3}$  m  $\times$   $3 \times 10^{-3}$  m  $\times$   $2 \times 10^{-3}$  m. Interferometric measurements. Large data scattering when measured parallel to fibers. The aim of this work was the investigation of the behavior of two nominally identical unidirectional laminates.

<sup>h</sup> Dootson, Sargent, Wostenholm & Yates (1980) [83].

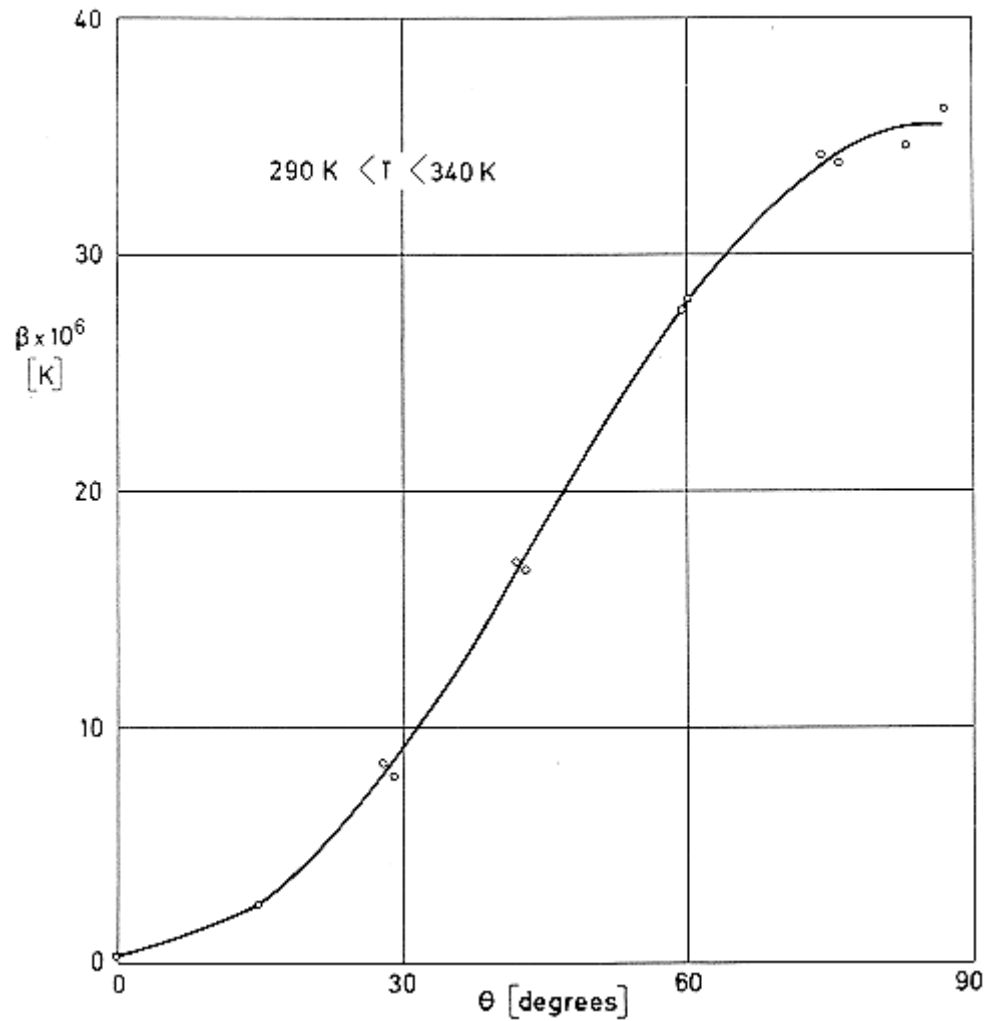
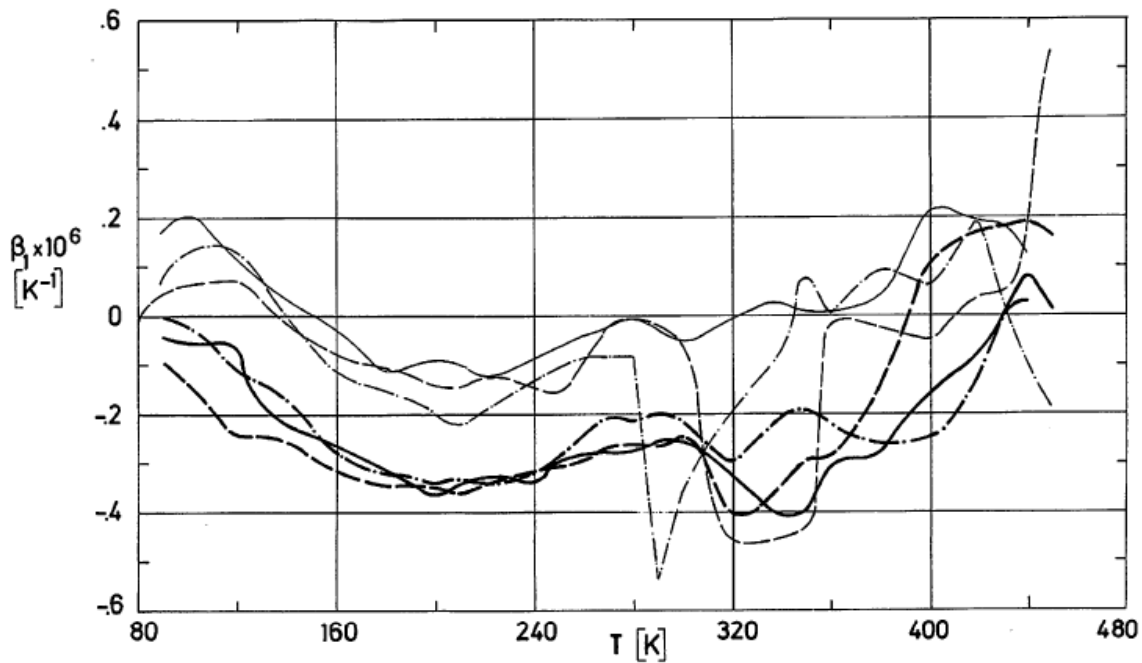


**Figure 5-23: Linear thermal expansion coefficient,  $\beta$ , of a carbon fiber reinforced unidirectional composite material, measured in plane of laminate, as a function of the direction of the measurement,  $\theta$ . Matrix is Epikote 828/BF<sub>3</sub>MEA. Fibers are Torayca T300A. Temperature range is 290 K to 340 K. From Isikawa, Koyama & Kobayashi (1977, 1978) [106] & [107].**

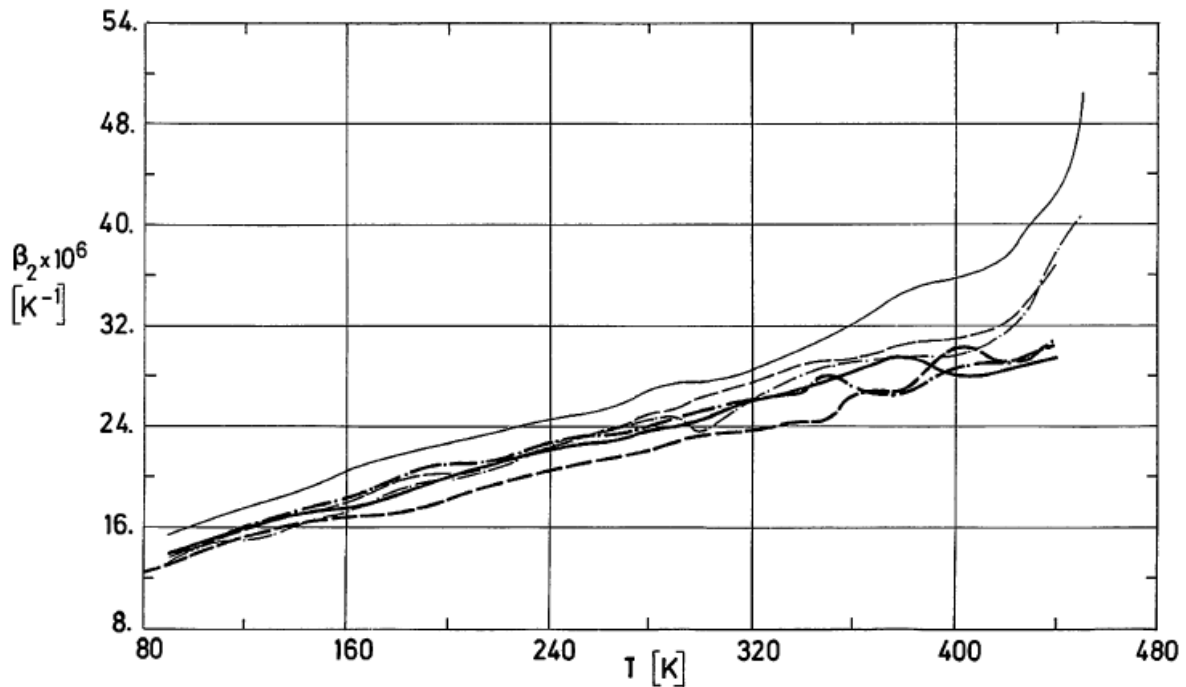


Note: non-si units are used in this figure

**Figure 5-24: Linear thermal expansion coefficient measured parallel to fibers,  $\beta_l$ , as a function of temperature,  $T$ , for two nominally identical carbon fiber reinforced composite materials produced on separate occasions and having slightly different fiber volume ratios,  $\phi$ . Fiber: HTSCarbon; Matrix: Fibredux 914C.**

Explanation

Spec. No.	Key	Fiber	$\phi_f$	$\phi_v$	Reference
103	————	Courtaulds HTS NM565	0,64	0,000	Dootson, Sargent, Wostenholm & Yates (1980) [83]
105	— — — —		0,687	0,004	
107	— • — —		0,671	0,000	
109	————	Morganite Type II NM 565	0,619	0,0025	
111	— — — —	0,6375	<0,001		
113	— • — —	0,642			



Note: non-si units are used in this figure

**Figure 5-25: Linear thermal expansion coefficient measured perpendicular to fibers,  $\beta_2$ , as a function of temperature,  $T$ , for two nominally identical carbon fiber reinforced composite materials produced on separate occasions and having slightly different fiber volume ratios,  $\phi$ . Fiber: HTSCarbon; Matrix: Fibredux 914C.**

Explanation

Spec. No.	Key	Fiber	$\phi$	Reference
104	————	Courtaulds HTS NM565	0,64	Dootson, Sargent, Wostenholm & Yates (1980) [83]
106	— — —		0,687	
108	— • —		0,671	
110	————	Morganite Type II NM565	0,619	
112	— — —		0,6375	
114	— • —		0,642	

**Table 5-57: Characterization of Composite Materials (Linear Thermal Expansion is given following the links).**

Spec. No.	Matrix	Fiber		Fiber volume $\phi_f$	Void content $\phi_v$	Direction of measurement
		Type (Manufacturer)	Fiber angle (°) or Weave			
Table 5-58	Fibredux 914C	(No fibers)		0,000		
Table 5-58		HTS, Type II 132/1,55/K10 132: compression modulus (in 10 <sup>9</sup> Pa) of an unidirectional composite, $\phi=0,66$ 1,55: minimum acceptable composite tensile strength (in 10 <sup>9</sup> Pa) K10: 10000 fibers per tow (Courtaulds)	100%; 0	0,671	<0,010	0°
Table 5-58			75%, 0; 25%, $\pm 45$	0,658		
Table 5-58			50%, 0; 50%, $\pm 45$	0,686	<0,020	
Table 5-58			25%, 0; 75%, $\pm 45$	0,693		
Table 5-58			50%, 0; 50%, 90	0,651	<0,010	
Table 5-58			25%, 90; 75%, $\pm 45$	0,693	<0,020	
Table 5-58			50%, 90; 50%, $\pm 45$	0,683		
Table 5-58			75%, 90; 25%, $\pm 45$	0,658	<0,010	
Table 5-58			100%; 90	0,675		
Table 5-59	Hercules 3002 (Hercules3002T prepreg)		HT Graphite (Hercules)	0	0,660	
Table 5-59				Perpendicular to fibers		
Table 5-59		0/90		0°		
Table 5-59		0/ $\pm 45$ /90				
Table 5-59		$\pm 30$				
Table 5-59		$\pm 45$				

Spec. No.	Matrix	Fiber		Fiber volume $\varphi_f$	Void content $\varphi_v$	Direction of measurement
		Type (Manufacturer)	Fiber angle (°) or Weave			
Table 5-59			$\pm 60$			
Table 5-59	Hercules 3002 (Hercules3002M prepreg)	HM Graphite (Hercules)	0	0,563		Parallel to fibers
Table 5-59						Perpendicular to fibers
Table 5-59			$0/\pm 60$			0°
Table 5-59	Narmco 4047	Carbon (Whittaker Corp.)	Weave	-		Parallel to plane of cloth
Table 5-59	Rigidite 5208 (Narmco)	T300 (Whittaker Corp.)	0	0,600		Parallel to fibers
Table 5-59						Perpendicular to fibers
Table 5-59			$(0/45/135/0/90)_s$			0°
Table 5-59	PMR-P1	Carbon HTS	0 6 plies	0,550		Parallel to fibers
Table 5-59						Perpendicular to fibers
Table 5-59	Hercules HA43 (carbonized)	Hotco G2206 (Rayon-based) (Hitco)	90° weave	0,530		Parallel to one set of fibers
Table 5-59						Perpendicular to plane of cloth
Table 5-59		Morganite M7401/C (pan-based) (Modmor)		0,440		Parallel to one set of fibers
Table 5-59						Perpendicular to plane of cloth
Table 5-59	LY558/HT973 (carbonized)			0,450		Parallel to one set of fibers
Table 5-59						Perpendicular to plane of cloth

**Table 5-58: Smoothed Values of the Linear Thermal Expansion Coefficient,  $\beta \times 10^6$  [K<sup>-1</sup>], of the Specimens Characterized in Table 5-57.**

Temp. [K]	Spec. No. <sup>d, e</sup>									
	115 <sup>a</sup>	116 <sup>a</sup>	117 <sup>a</sup>	118 <sup>a</sup>	119 <sup>a</sup>	120 <sup>a</sup>	121 <sup>a</sup>	122 <sup>a</sup>	123 <sup>a</sup>	124 <sup>a</sup>
80	21,7		-0,03							13,5
90							3,54			
100	25,0	0,048	-0,17	0,341	0,88	1,84	3,56	5,78	8,04	14,6
120	27,6	-0,049	-0,27	0,197	0,74	1,84	3,63	6,13	8,56	15,6
140	30,0	-0,137	-0,35	0,082	0,62	1,84	3,70	6,42	9,09	16,9
160	32,1	-0,217	-0,40	-0,005	0,54	1,84	3,79	6,67	9,62	18,1
180	35,0	-0,279	-0,43	-0,069	0,51	1,84	3,87	6,94	10,2	19,0
200	36,4	-0,316	-0,44	-0,108	0,53	1,84	3,97	7,20	10,7	20,2
220	38,4	-0,324	-0,43	-0,117	0,59	1,84	4,08	7,40	11,3	21,2
240	40,6	-0,295	-0,40	-0,101	0,68	1,85	4,19	7,65	11,7	22,6
260	42,4	-0,218	-0,41	-0,052	0,75	1,87	4,29	7,98	12,4	23,9
280	44,1	-0,141	-0,49	0,027	0,77	1,90	4,45	8,18	12,9	25,0
300	46,7	-0,128	-0,60	0,090	0,76	1,94	4,57	8,42	13,4	26,1
320	48,7	-0,141	-0,73	0,110	0,73	2,00	4,76	8,66	13,9	26,8
340	51,1	-0,179	-0,81	0,104	0,70	2,14	4,92	8,94	14,5	27,6
360	53,8	-0,234	-0,80	0,107	0,75	2,27	5,20	9,26	15,1	28,5
380	57,7	-0,257	-0,66	0,148	0,86	2,42	5,50	9,70	15,7	29,1
400	61,3	-0,251	-0,41	0,229	0,97	2,66	5,84	10,1	16,4	29,6
420	65,5	-0,183	-0,11	0,345	1,08	2,93	5,40	11,0	17,2	30,2
440	70,9	-0,080		0,473	1,22	3,32			18,0	30,9



<sup>a</sup> Data displayed in Figure 5-26.

<sup>d</sup> Comments: Spec. No. 115 from Fibredux 914C unreinforced, Specs. No. 116 to 124 from Fibredux 914C prepreg. Curing was in any case the following: 0,25 h/2x10<sup>5</sup> Pa bag pressure + 0,5 h/400 K. Pressure raised to 7x10<sup>5</sup> Pa for 0,25 h. Then 1h/440K + 4h/460 K. From smooth curves in the source. Specimens constructed from 16 plies of prepreg. Symmetrical sequence of plies. Interferometric measurements. The aim of this work was the investigation of the influence of the amount of fibers in different directions.

<sup>e</sup> References: Parker, Chandra, Yates, Dootson & Walters (1981) [133].

**Table 5-59: Smoothed Values of the Linear Thermal Expansion Coefficient,  $\beta \times 10^6$  [K<sup>-1</sup>], of the Specimens Characterized in Table 5-57.**

Spec. No.	Temperature (K)									Comments	References		
	80	290	310	370	380	420	440	450	530				
125 <sup>b</sup>	-0,36			-0,40						f	Friend, Poesch & Leslie (1972)		
126 <sup>b</sup>	22,8												
127	1,58			1,6									
128	2,05												
129 <sup>b</sup>	-2,38												
130 <sup>b</sup>	1,87												
131 <sup>b</sup>	13,6												
132	-0,54												
133	25,8												
134	0,83												
135	13											g	Penton (1966)
136 <sup>c</sup>			0,02	0,05		0,40		0,45				Karlsson (1983)	
137 <sup>c</sup>			23	30		33		37					
138 <sup>c</sup>			0,40	0,80		0,93		0,97					
139		0								h	Hanson & Chamis (1974)		
140	26,1												
141	3,1									i	Harley & Rosenberg (1981)		
142	6,7												
143	2,2												
144	7,8												
145	1,9												
146	10												

<sup>b</sup> Data displayed in Figure 5-27.

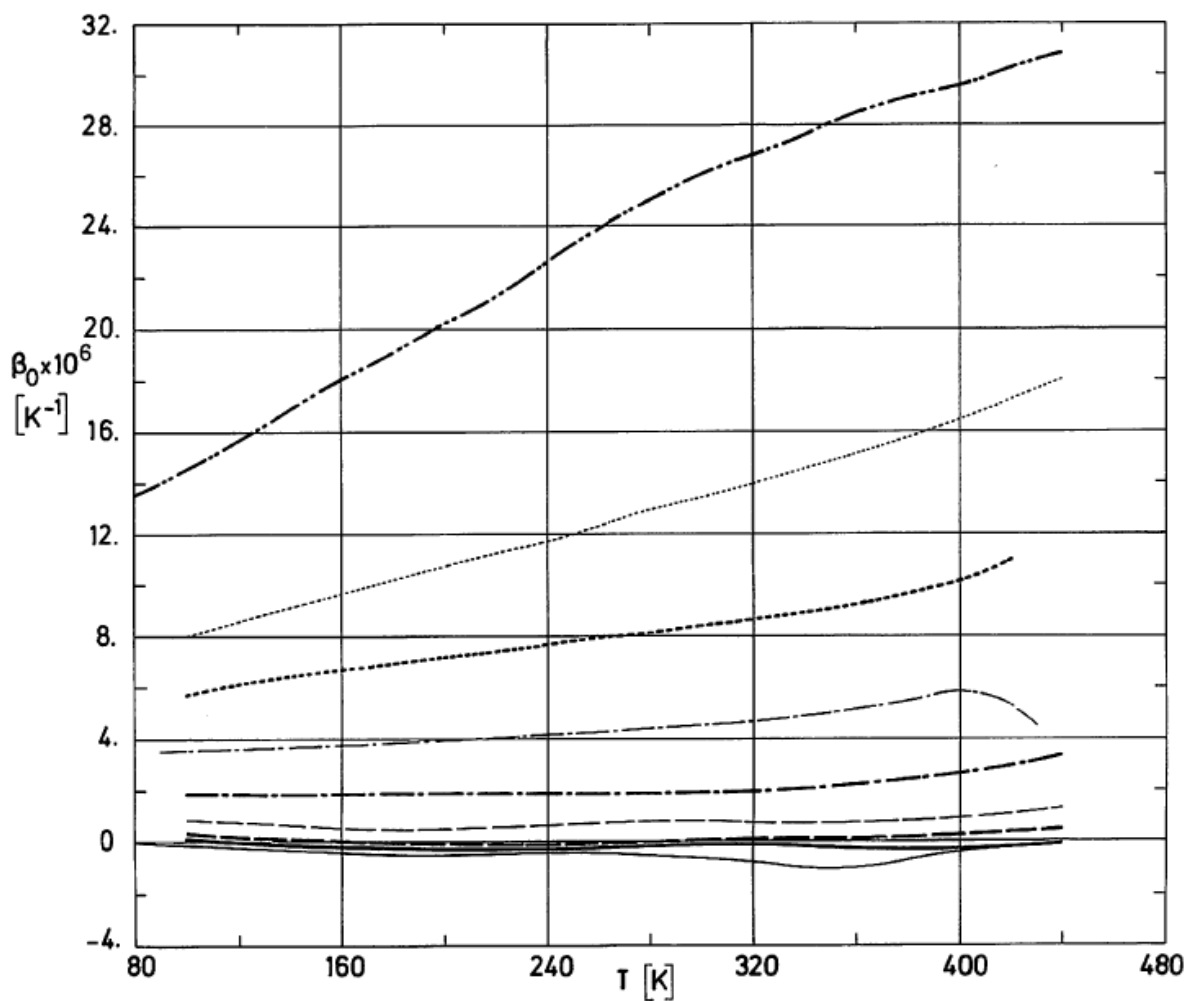
<sup>c</sup> Data displayed in Figure 5-28.

<sup>f</sup> Excellent correlation with predictions regarding the influence of angle ply. A zero thermal expansion coefficient can be obtained with  $\pm 42$  degrees orientation.

<sup>g</sup> Re-entry thermal shield. Phenolic are efficient ablative resins.










<sup>h</sup> Resin is a dried and grinded solution of MDA, NE, BTDE in methyl alcohol. Powder imidized and compacted. Prepregs.  $0,2 \times 10^{-3}$  m thick cut to mould sizes  $76,2 \times 10^{-3}$  m  $\times$   $254 \times 10^{-3}$  m. Curing: 2h/590 K,  $34,5 \times 10^5$  Pa. Imbedded strain gauge measurements.

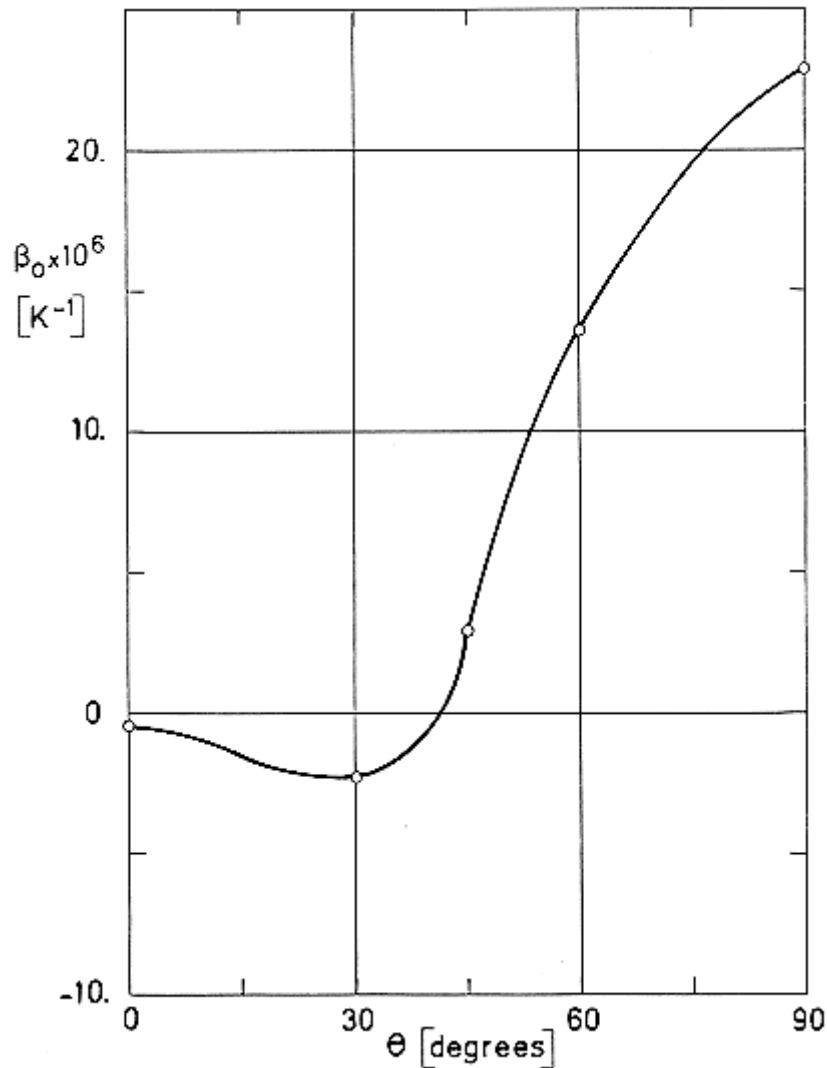
<sup>i</sup> Matrix decomposed by heating and densified by CVD in a Xylene atmosphere. Percentage of pyrocarbon pickup by weight was: 9,54 for Spec Nos. 141 and 142, 11 for Spec. Nos. 143 and 144, 27-28 for Spec. Nos. 145 and 146. Capacitive method of measurement.



**Figure 5-26: Linear thermal expansion coefficient measured in  $0^\circ$  direction,  $\beta_0$ , as a function of temperature,  $T$ , for some carbon fiber reinforced composite materials with various amounts of fibers in different directions. Fiber: Courtaulds HTS, Type II; Matrix: Fibredux 914C.**

Explanation

Spec. No.	Key	Percentage in each direction	Reference
116		100%, 0°	Parker, Chandra, Yates, Dootson & Walters (1981) [133].
117		75%, 0°, 25%; ± 45°	
118		50%, 0°, 50%; ± 45°	
119		25%, 0°, 75%; ± 45°	
120		50%, 0°, 50%; ± 90°	
121		25%, 90°, 75%; ± 45°	
122		50%, 90°, 50%; ± 45°	
123		75%, 90°, 25%; ± 45°	
124		100%, 90°	



Note: non-si units are used in this figure

**Figure 5-27: Linear thermal expansion coefficient,  $\beta_0$ , of a two-ply ( $\pm \theta$ ) carbon fiber reinforced composite material, measured in direction  $0^\circ$  of the plane of laminate, as a function of the angle ply,  $\theta$ . Matrix is Hercules 3002, fibers are Hercules HT (Hercules 3002T prepreg). Temperature range is 80 K to 450 K. From Friend, Poesch & Leslie (1972) [90].**

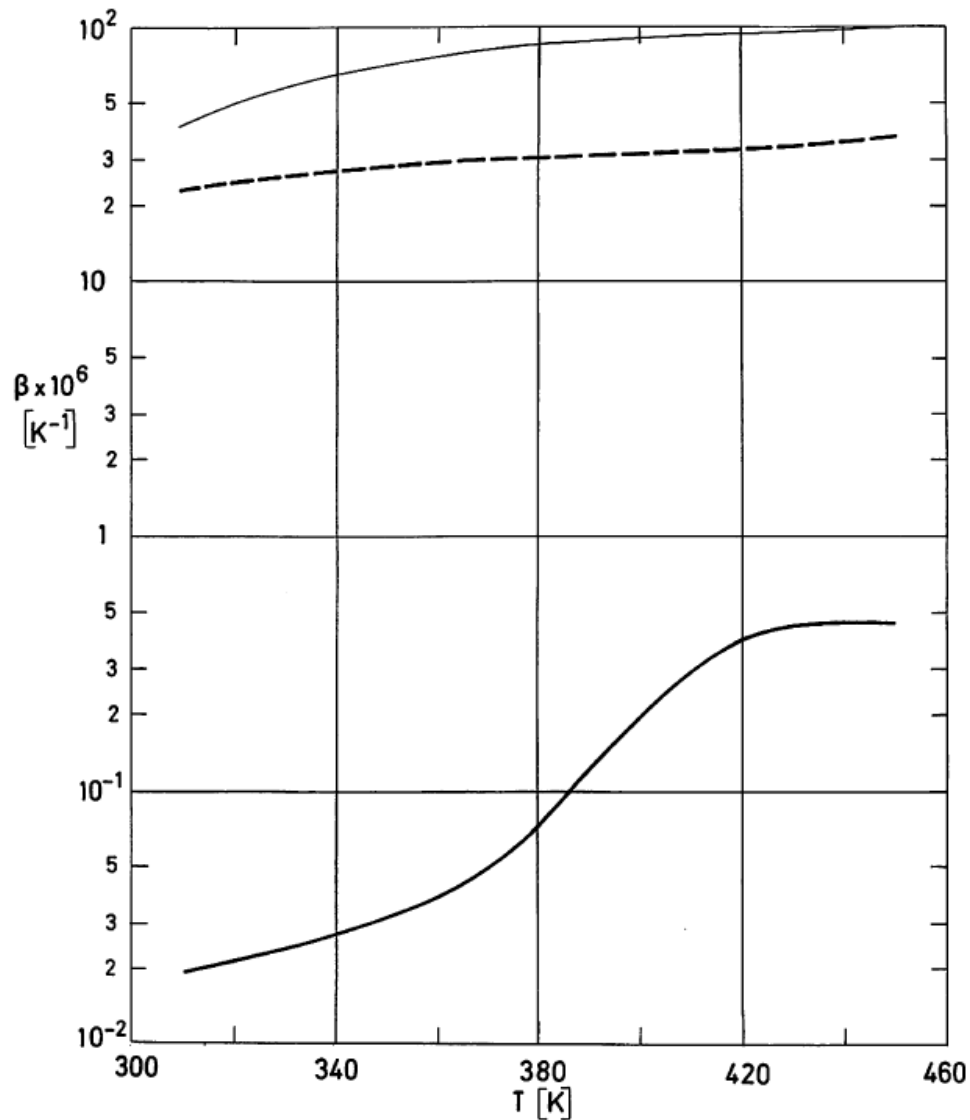


Figure 5-28: Linear thermal expansion coefficient,  $\beta$ , measured in several directions of the plane of laminate for an unidirectional and an angle plied carbon fiber reinforced composite material, as a function of temperature,  $T$ . Matrix is Narmco 5208, fibers are Narmco T300. From Karlsson (1983) [111].

Explanation

Spec. No.	Key	Fiber Angle [°]	$\phi_f$	Direction of Measurement
136		0	0,600	Parallel to fibers
137				Perpendicular to fibers
138		(0/45/135/0/90) <sub>s</sub>		0°

**Table 5-60: Characterization of Composite Materials (Linear Thermal Expansion is given following the links).**

Spec. No.	Matrix	Fiber		Fiber volume $\varphi_f$	Void content $\varphi_v$	Direction of measurement
		Type (Manufacturer)	Fiber angle (°) or Weave			
Table 5-61	DER 332/T403	Kevlar 49 (E.I. du Pont de Nemours and Company)	0	0,650 0,600		Parallel to fibers
Table 5-61			Perpendicular to fibers			
Table 5-61	XD7818/T403		0	0,600		Perpendicular to fibers
Table 5-62	Ferro E-293		0	0,600		Parallel to fibers
Table 5-62			Perpendicular to fibers			
Table 5-62	Ferro CE-3305			0,650		Parallel to fibers
Table 5-62			$\pm 45$			$0^\circ$
Table 5-62			$\pm 60$			
Table 5-62			0			Perpendicular to fibers
Table 5-62			0/+45/0/-45			$0^\circ$
Table 5-62		Style 120 fabric	Warp fill			
Table 5-62		Hexcel F155	Kevlar 49 - 285 style fabric (E.I. du Pont de Nemours and Company)			(0/90)5s
Table 5-62	[(0/90) $\pm$ 0]s			0,400		$0^\circ, 90^\circ$
Table 5-63	PR 286	Kevlar 49 (E.I. du Pont de Nemours and Company)	0	0,5		$0^\circ$
Table 5-63			30			
Table 5-63			45			
Table			60			

Spec. No.	Matrix	Fiber		Fiber volume $\varphi_f$	Void content $\varphi_v$	Direction of measurement
		Type (Manufacturer)	Fiber angle (°) or Weave			
5-63						
Table 5-63			90			
Table 5-63			$\pm 22$	0,52		
Table 5-63			$\pm 30$	0,51		
Table 5-63			$\pm 45$	0,56		
Table 5-63			$\pm 60$	0,51		
Table 5-63			$\pm 68$	0,52		
Table 5-63	3M Du Pont 5134	Kevlar (E.I. du Pont de Nemours and Company)	0	0,600		Parallel to fibers
Table 5-63	3M SP306					
Table 5-63						Perpendicular to fibers
Table 5-63	Narmco 5505	Boron	0	0,500		Parallel to fibers
Table 5-63						Perpendicular to fibers
Table 5-63	HT 424	Boron	0	0,500		Parallel to fibers
Table 5-63						Perpendicular to fibers
Table 5-63	FM-1000	Amorphous Metal 2826 HB	0	0,620		Parallel to fibers
Table 5-63						45°
Table 5-63						Perpendicular to fibers
Table 5-64	Al Alloy 6061-T6	HM Graphite VS0054	0	0,370		Parallel to fibers

Spec. No.	Matrix	Fiber		Fiber volume $\varphi_f$	Void content $\varphi_v$	Direction of measurement
		Type (Manufacturer)	Fiber angle (°) or Weave			
Table 5-64	Al Alloy 6061-0					Parallel to fibers
Table 5-64						Perpendicular to fibers

**Table 5-61: Smoothed Values of the Linear Thermal Expansion Coefficient,  $\beta \times 10^6$  [K<sup>-1</sup>], of the Specimens Characterized in Table 5-60.**

Spec. No.	Temperature (K)								Comments	References
	220	250	270	300	320	350	370	400		
147	-3,8	-3,8	-3,8	-4,0	-4,7	-6,0			d	Clements & Moore (1977)
148	61	66	72	79	87	150	214	214		
149	50	50	54	60	73	150	160	160		

<sup>d</sup> Matrix composition and curing as in Spec. Nos 1 to 12. Filament wound specimens.  $\beta_i$  is negative because the fiber shrinks with temperature.  $\beta_i$  increases rapidly above 320 K due to change in matrix.



**Table 5-62: Smoothed Values of the Linear Thermal Expansion Coefficient,  $\beta \times 10^6$  [K<sup>-1</sup>], of the Specimens Characterized in Table 5-60.**

Spec. No.	Temperature (K)									Comments	References
	80	190	290	300	340	360	370	390	450		
150	-4,1										Karlsson (1983)
151	35										
						58					
152	-4,0± 1,0										
153	-1,25± 0,30										
154	34										
155	57										
156	-2,5										
157	0										
158				4,5						e	Ballis Crema, Barboni & Castellani (1986)
159				4,4						f	Ballis Crema, Barboni, Castellani & Peroni (1987)

<sup>e</sup> Specimens  $2,5 \times 10^{-3}$  m x  $21 \times 10^{-3}$  m x 0,230 m. Heating rate 0,4 K/min. Mean values at least two heating and cooling cycles. Small hysteresis detected.

<sup>f</sup> Rectangular specimens  $5 \times 10^{-3}$  m x  $25 \times 10^{-3}$  m. 10 plies. Commercial dilatometer. Heating rate 0,5 K/min. No differences between heating and cooling.

**Table 5-63: Smoothed Values of the Linear Thermal Expansion Coefficient,  $\beta \times 10^6$  [K<sup>-1</sup>], of the Specimens Characterized in Table 5-60.**

Spec. No.	Temperature (K)										Comments	References	
	190	260	290	300	320	340	370	400	420	450			520
160 <sup>a</sup>				-2,1	(From 300 K) -2,2			-2,2				g	Strife & Prewo (1979)
161				13,1	(From 300 K) 15,6			18,9					
162				29,1	(From 300 K) 41,4			60,0					
163				45,0	(From 300 K) 58,5			67,9					
164 <sup>a</sup>				63,6	(From 300 K) 79,3			95,4					
165				-10,8	(From 300 K) -12,4			-16,2					
166				-11,7	(From 300 K) -13,7			-16,8					
167				2,6	(From 300 K) 2,7			2,4					
168				41,9	(From 300 K) 49,7			55,0					
169				57,3	(From 300 K) 68,0			80,0					
170	-2,3											Karlsson (1983)	
171	-3,5												
172	69												
173	4,5											Karlsson (1983)	
174		24					32		36				
175		5,6										Karlsson (1983)	
176		3,0											
177	13,4											Karlsson (1983)	
178	13± 7												
179	12± 0,4												

<sup>a</sup> Data displayed in Figure 5-29.

<sup>g</sup> PR-286 resin diluted with MEK /50 pwd resin). 2 h/400 K in a vacuum oven + slow heating up to 450 K then 1h/450 K. Postcured 4h/450 K in air circulating oven. Rectangular parallelepipeds  $25 \times 10^{-3}$  m  $\times$   $6,3 \times 10^{-3}$  m  $\times$   $6,3 \times 10^{-3}$  m. Measurements made by use of a single-rod quartz dilatometer referenced to a NBS fused silica standard. Slight hysteresis between heating and cooling. Data for cooling. Hysteresis decreased by decreasing the heating rate (below 2 K/min). Comparing with Specs. No. 2-11 it is seen that the thermal expansion of Kevlar/epoxy composite materials is considerable more anisotropic than that of carbon fiber/epoxy composites.

**Table 5-64: Smoothed Values of the Linear Thermal Expansion Coefficient,  $\beta \times 10^6$  [K<sup>-1</sup>], of the Specimens Characterized in Table 5-60.**

Temp. [K]	Spec. No. <sup>h, i</sup>				
	180 <sup>b</sup>	181 <sup>b</sup>		182 <sup>c</sup>	
150	2,84			2,25	2,32
190	3,29			2,52	2,64
200	3,35	0,326	3,92	2,57	2,69
220	3,41	0,643	3,58	2,66	2,75
250	3,42	1,28	2,77	2,77	2,80
260	3,42	1,54	2,46	2,80	2,80
270	3,43	1,81	2,15	2,82	2,80
290	3,45	2,39	1,52	2,87	2,80
300	3,47	2,70	1,23	2,89	2,79
320	3,58	3,35	0,743	2,93	2,80
340	3,76	4,03	0,426	2,98	2,81
350	3,90	4,38	0,354	3,00	2,83
360	4,06	4,73	0,350	3,02	2,85
370	4,26	5,09	0,423	3,05	2,89
380	4,50	5,44	0,581	3,08	2,93
390		5,79	0,832	3,14	2,99

<sup>b</sup> Data displayed in Figure 5-30.

<sup>c</sup> Data displayed in Figure 5-31.

<sup>h</sup> Comments: Specimens. Plates.  $0,81 \times 10^{-3}$  m thick (including  $0,1 \times 10^{-3}$  m thick 6061 face sheets. Considering these sheets,  $\varphi \cong 0,276$ ). Nos. 175 and 176 are annealed (750 K for 30 min). Strain gauge measurements with fused silica and Al T-6 as reference materials. Cyclic loop repeatably detected in annealed specimens, caused by elastic-plastic matrix deformation; left figures in the Table are for heating and right for cooling.  $\beta$  depends on mechanical loading when matrix deforms plastically. Data are for zero loading. Calculated by the compiler by numerical derivation of data:  $\beta = d(\Delta L/L)/dT$ .

<sup>i</sup> References: Min & Crossman (1982) [129].

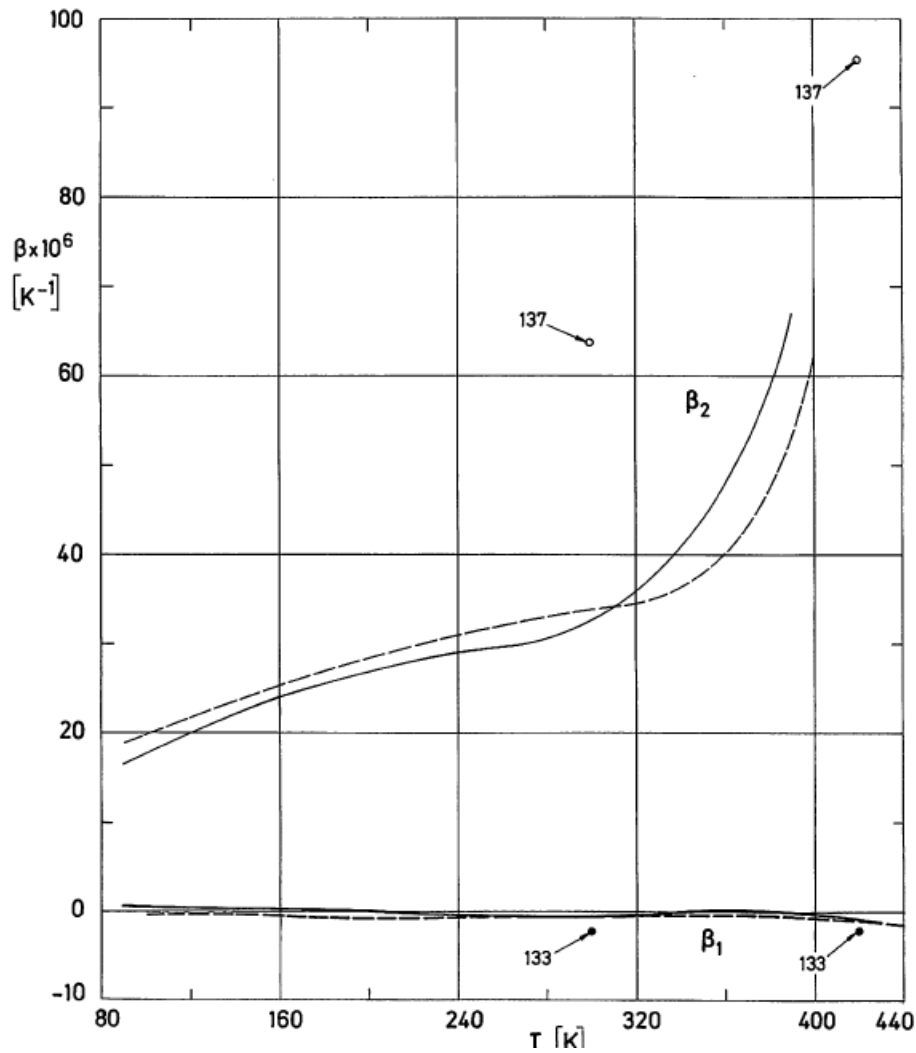
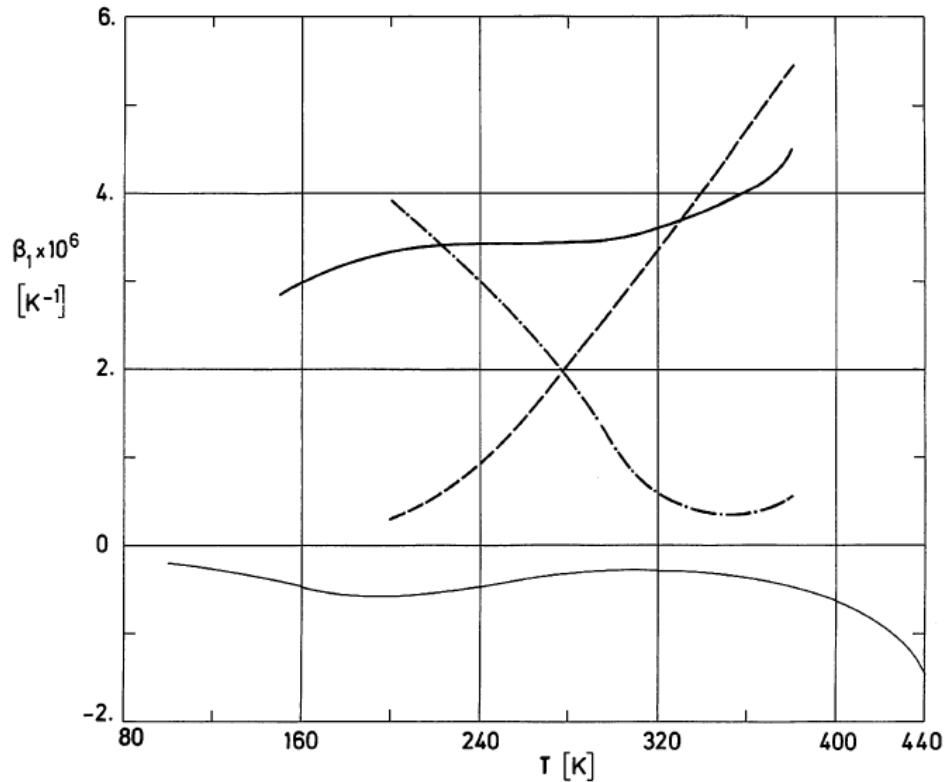


**Figure 5-29: Linear thermal expansion coefficient measured either parallel,  $\beta_1$ , or perpendicular,  $\beta_2$ , to fibers of two composites with similar epoxy matrices, but with carbon fiber or Kevlar 49 reinforcements.**

Explanation

Spec. No.	Key	Matrix	Fiber	$\varphi_f$	$\beta$	References
22		ERLA 4617/mPDA	Courtaulds HTS Carbon	0,494	$\beta_1$	Roger, Phillips, Kingston- Lee, Yates, Overy, Sargent & McCalla (1977) [144]
23					$\beta_2$	
30				0,504	$\beta_1$	
31					$\beta_2$	
160		PR 286	Kevlar 49	0,5	$\beta_1$	Strife & Prewo (1979) [151]
164					$\beta_2$	



Note: non-si units are used in this figure

**Figure 5-30: Linear thermal expansion coefficient measured parallel to fibers,  $\beta_i$ , as a function of temperature,  $T$ , for two graphite fiber-metal and one carbon fiber-epoxy composite materials.**

Explanation

Spec. No.	Key	Matrix	Fiber	$\phi_f$	Run	References
180		Al Alloy 6061-T6	HM Graphite VS0054	0,370		Min & Crossman (1982) [129]
181		Al Alloy 6061-O			Heating	
					Cooling	
30		ERLA 4617/mPDA	Courtaulds HMS Carbon	0,504		Rogers, Phillips, Kingston-Lee, Yates, Overy, Sargent & McCalla (1977) [144]

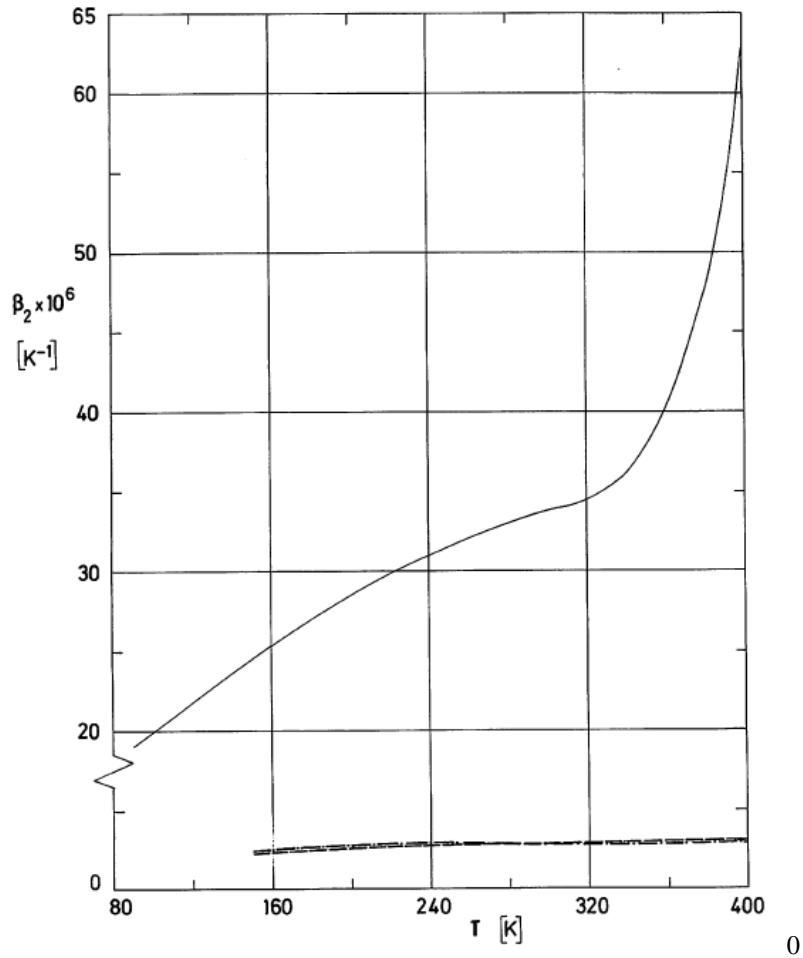


**Figure 5-31: Linear thermal expansion coefficient measured perpendicular to fibers,  $\beta_2$ , as a function of temperature,  $T$ , for graphite fiber-metal and carbon fiber-epoxy composite materials.**

Explanation

Spec. No.	Key	Matrix	Fiber	$\phi$	Run	References
182		Al Alloy 6061-O	HM Graphite VS0054	0,370	Heating	Min & Crossman (1982) [129]
					Cooling	
31		ERLA 4617/mPDA	Courtaulds HMS Carbon	0,504		Rogers, Phillips, Kingston-Lee, Yates, Overy, Sargent & McCalla (1977) [144]

For additional information on the linear thermal expansion of glass-reinforced, graphite-epoxy and of other advanced composites, at room temperature and below, see [ECSS-E-HB-31-01 Part 14, clause 8.5](#).

## 5.7 Thermal radiation properties of bare high strength fibers

Composite materials are seldom used uncovered in exposed space-craft structures. This is the reason why data on thermal radiation properties of fibers, matrices and composites are very scanty.

Bare high purity silica fabrics are stable, low outgassing thermal control coatings which have been proposed (Eagles, Babjak & Weaver (1975) [85]) to control the effects of electrostatic charging at synchronous altitudes.

Data on optical properties ( $\alpha'(\beta = 0)$ ,  $\rho'(\beta = 0)$ ,  $\tau'(\beta = 0)$ ) of woven ceramic fabrics (high purity silica, aluminoborosilicate, and silicon carbide) have been reported by Covington & Sawko (1986) [76].

Since the ceramic fabrics retain their desirable properties after exposure to temperatures of 1500 K or higher, they have been considered for use in flexible thermal protection systems in entry vehicle heat shields.

The optical properties of these materials strongly depend on fabric weight and are less affected by the fabric weave pattern.

The data from Eagles, Babjak & Weaver (1975) [85] are summarized in the following.

### 5.7.1 Sample characterization

SiO<sub>2</sub> Fabric. 8 Harness Satin Weave 0,28 × 10<sup>-3</sup> m thick on an Alclad 2024 Al alloy substrate.

Usually the fabric is not directly bonded to the spacecraft, to avoid surface contamination. Composite structures have been developed where the fabric is laminated, at 550 K, to an aluminium foil backing with a thin film of FEP as an adhesive.

### 5.7.2 Emittance

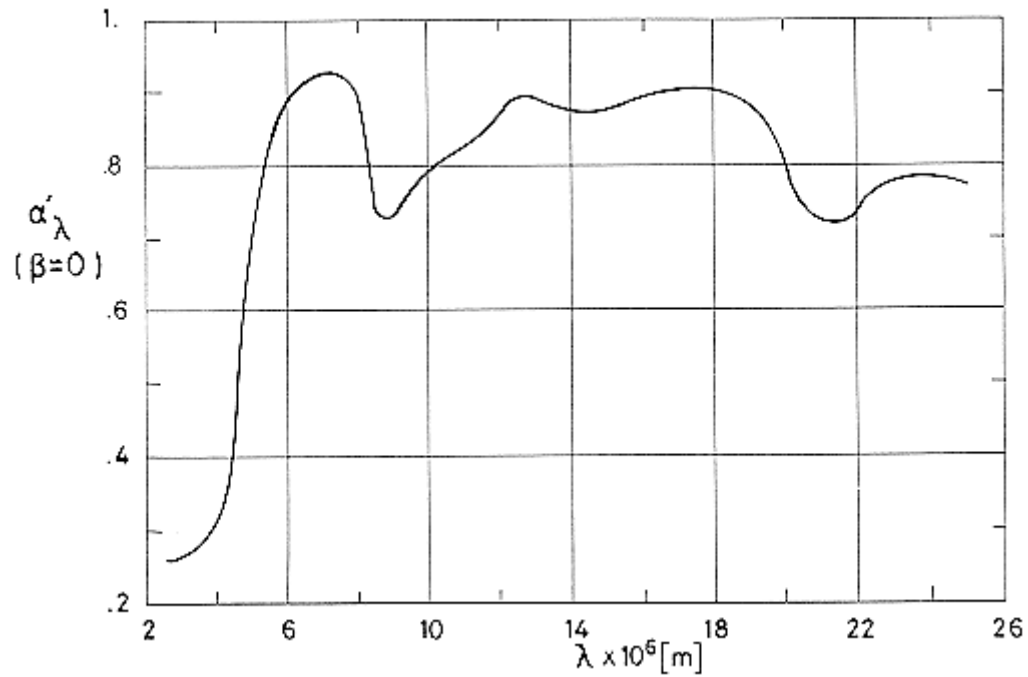
#### 5.7.2.1 Hemispherical total emittance

$$\varepsilon = 0,84 \pm 0,02$$

From spectral reflectance data in the wavelength range 2 × 10<sup>-6</sup> m to 24 × 10<sup>-6</sup> m.

Obtained by using a Pelkin Elmer Model 205 spectrophotometer fitted with a heated cavity.

The normal spectral absorptance,  $\alpha'_{\lambda}(\beta=0) = 1 - \rho'_{\lambda}(\beta=0)$ , of the same sample at 310 K is shown in Figure 5-32. From this type of data the value of the hemispherical total emittance,  $\varepsilon$ , is obtained by taking into account the Kirchhoff's law for each wavelength,  $\varepsilon'_{\lambda} = \alpha'_{\lambda}$ , and integrating over the wavelength range with the Plank's black body function as weight function.



Note: non-si units are used in this figure

**Figure 5-32: Normal spectral absorptance,  $\alpha'_\lambda$  of SiO<sub>2</sub> Fabric at 310 K vs. wavelength,  $\lambda$ . Sample is described in the text. From Eagles, Babjak & Weaver (1975) [85].**



## 5.7.3 Absorptance

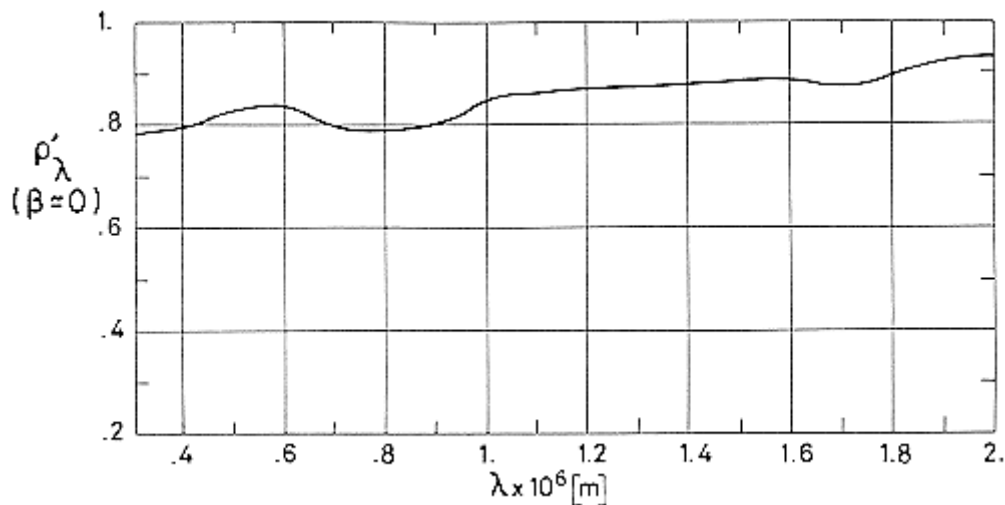
### 5.7.3.1 Solar absorptance

$$\alpha_s = 0,17$$

From spectral reflectance data in the wavelength range  $0,3 \times 10^{-6}$  m to  $2 \times 10^{-6}$  m.

Obtained by use of a Beckman DK2A spectrophotometer and integrated with the solar spectral emissive power weight function.

A reflectance curve for the same sample is shown in Figure 5-33.

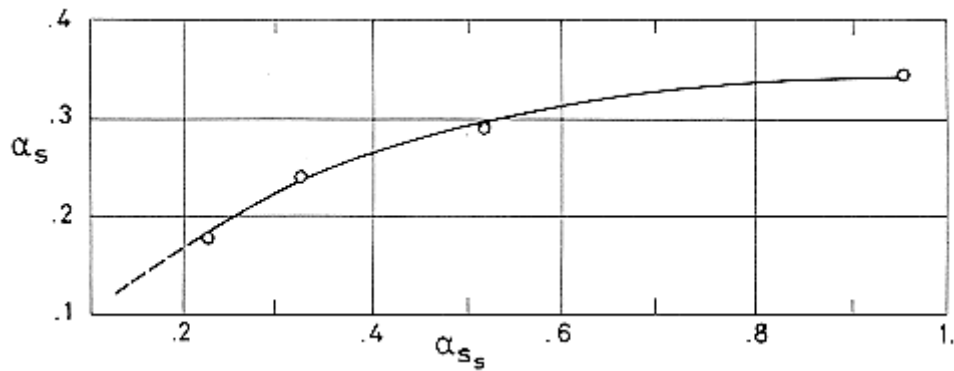


Note: non-si units are used in this figure

**Figure 5-33: Normal-hemispherical spectral reflectance,  $\rho'_\lambda$  of  $\text{SiO}_2$  Fabric vs. wavelength,  $\lambda$ . Sample is described in the text. From Eagles, Babjak & Weaver (1975) [85].**

### 5.7.3.2 Influence of the substrate on the solar absorptance

Tightly woven silica fabrics are opaque in the IR; however variations in solar absorptance occur because the fabrics have some transmittance in the visible. Thence the solar absorptance of the fabric slightly depends on that of the substrate, Figure 5-34.

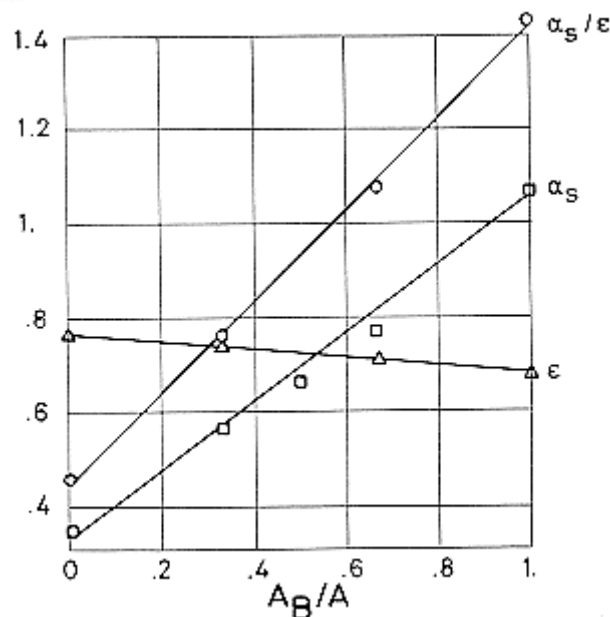


Note: non-si units are used in this figure

**Figure 5-34: Solar absorptance,  $\alpha_s$ , of SiO<sub>2</sub> Fabric-Substrate composite as a function of the solar absorptance,  $\alpha_{ss}$ , of the substrate. Sample: 16 Harness Satin Weave  $0,38 \times 10^{-3}$  m thick, on different substrates. From Eagles, Babjak & Weaver (1975) [85].**

### 5.7.3.3 Solar absorptance of mosaics

Any value of  $\alpha_s$  ( $0,2 < \alpha_s < 0,9$ ) can be obtained by use of a mosaic fabric by interweaving SiO<sub>2</sub> with carbon yarn, Figure 5-35.



Note: non-si units are used in this figure

**Figure 5-35: Absorptance/Emitatnce ratio,  $\alpha_s/\epsilon$ , solar absorptance,  $\alpha_s$ , and hemispherical total emittance,  $\epsilon$ , of various mosaics of silica and carbon yarn as functions of the exposed black to total area fraction,  $A_B/A$ . From Eagles, Babjak & Weaver (1975) [85].**

### 5.7.3.4 Effects of the space environment on absorptance

See Table 5-65. Data obtained by use of the GE Combined Radiation Effects facility.

**Table 5-65: Effect of the Space Environment on Solar Absorptance,  $\alpha_s$ , of Silica Fabrics**

Spec. No.	Description	Initial Value <sup>a</sup> $\alpha_{s0}$	Treatment <sup>b</sup> T [K]	$\Delta\alpha_s^a$ UV (376 SH)	$\Delta\alpha_s^a$ UV (995 SH)	$\Delta\alpha_s^a$ UV (1697 SH)	$\Delta\alpha_s^a$ UV (2500 SH)	$\Delta\alpha_s^a$ UV (3004 SH)
1	8 Harness Satin	0,172	810	0,012	0,023	0,029	0,029	0,029
2	Weave SiO <sub>2</sub> 0,28 x 10 <sup>-3</sup> m	0,171	920	0,010	0,016	0,019	0,019	0,019
3	thick	0,168	1120	0,007	0,012	0,014	0,014	0,014
4		0,170	1320	0,003	0,004	0,006	0,006	0,006
5	20 Harness Satin	0,196	None	0,089	0,115	0,133	0,133	0,133
6	Weave SiO <sub>2</sub> 0,20 x 10 <sup>-3</sup>	0,191	1120	0,008	0,012	0,012	0,012	0,012
7	m thick	0,191	920	0,013 <sup>c</sup>	0,013 <sup>d</sup>	0,020 <sup>e</sup>	0,020 <sup>f</sup>	0,020 <sup>g</sup>
8	Same as 2, but	0,187	1120	0,012 <sup>c</sup>	0,018 <sup>d</sup>	0,018 <sup>e</sup>	0,018 <sup>f</sup>	0,018 <sup>g</sup>
9	laminated to 0,01 x 10 <sup>-3</sup> m Al	0,188	1320	0,013 <sup>c</sup>	0,017 <sup>d</sup>	0,017 <sup>e</sup>	0,017 <sup>f</sup>	0,017 <sup>g</sup>
10	foil with 0,025 x 10 <sup>-3</sup> m FEP Teflon	0,187	1120	0,007 <sup>c</sup>	0,010 <sup>d</sup>	0,010 <sup>e</sup>	0,010 <sup>f</sup>	0,010 <sup>g</sup>
11	Same as 3, bonded to aluminium with SR-595 adhesive	0,179	None	0,009 <sup>c</sup>	0,010 <sup>d</sup>	0,010 <sup>e</sup>	0,010 <sup>f</sup>	0,010 <sup>g</sup>

<sup>a</sup> The third, subscripted figure, is added to show trend in the data.

<sup>b</sup> This treatment is required to remove the finish applied to the yarn for weaving.

<sup>c</sup> Electrons. Intensity: 15 keV. Flux:  $5 \times 10^{-2} \text{ e.m}^{-2}.\text{s}^{-1}$ , +e =  $6,1 \times 10^{17} \text{ e.m}^{-2}$ .

<sup>d</sup> Electrons. Intensity: 15 keV. Flux:  $5 \times 10^{-2} \text{ e.m}^{-2}.\text{s}^{-1}$ , +e =  $1,7 \times 10^{18} \text{ e.m}^{-2}$ .

<sup>e</sup> Electrons. Intensity: 15 keV. Flux:  $5 \times 10^{-2} \text{ e.m}^{-2}.\text{s}^{-1}$ , +e =  $8 \times 10^{18} \text{ e.m}^{-2}$ .

<sup>f</sup> Electrons. Intensity: 15 keV. Flux:  $5 \times 10^{-2} \text{ e.m}^{-2}.\text{s}^{-1}$ , +e =  $1,5 \times 10^{19} \text{ e.m}^{-2}$ .

<sup>g</sup> Electrons. Intensity: 15 keV. Flux:  $5 \times 10^{-2} \text{ e.m}^{-2}.\text{s}^{-1}$ , +e =  $2,3 \times 10^{19} \text{ e.m}^{-2}$ .

NOTE From Eagles, Babjak & Weaver (1975) [85].

Chamber pressure:  $1,3 \times 10^{-6} \text{ Pa}$ .

Chamber temperature not given.

## 5.8 Thermal radiation properties of bare composite materials

Uncoated plastic materials have been seldom used in exposed surfaces for Spacecraft or Solar Power Plants. Thus, data regarding thermo-optical properties of these materials are scarce.

### 5.8.1 Tabulated data

**Table 5-66: Normal Total Emittance,  $\varepsilon'$  ( $\beta=0$ ), and Solar Absorptance,  $\alpha_s$ , of Uncoated Plastic Materials**

Type	T [K]	$\varepsilon'$ ( $\beta=0$ )	T [K]	$\alpha_s$		References
				Above Atmosphere	Sea Level	
Glass-Fabric/Epoxy <sup>a</sup>	383	0,79		0,850	0,830	Skinner & Goldhard (1968) [149]
Glass-Fabric/Phenolic <sup>b</sup>	396	0,80		0,819	0,808	
Glass-Fabric/TAC Polyester <sup>c</sup>	383	0,82		0,577	0,532	
Glass-Fabric/Silicone <sup>d</sup>	393	0,83		0,492	0,445	
Carbon Fiber/Epoxy <sup>e</sup>		0,805		0,694		Witte & Teichman (1989) [166]
		0,815		0,704		
Scotchcal <sup>g</sup>			298	0,23		Touloukian & DeWitt (1972) [158]
				0,25		
				0,25		
Teflon TFE <sup>j</sup>	380	0,89				
	394	0,86				
	408	0,86				
	422	0,86				
	436	0,88				
	450	0,89				
	464	0,91				
	478	0,91				

- a Visually opaque.
- b MIL-R-9299C. 3 Dic. 1968. "Resin, Phenolic, Laminating".
- c MIL-R-25042B. 12 Sep. 1967. "Resin, Polyester, High Temperature Resistant, Low Pressure Laminating".
- d MIL-R-25506C. 30 Aug. 1982. "Resin Solution, Silicone, Low-Pressure Laminating".
- e Smooth. From spectral reflectance data.
- f Rough. From spectral reflectance data.
- g From spectral reflectance data for above atmosphere conditions.  $\beta' = 15^\circ$ .
- h As e, except exposed to 700 MeV protons.
- i As e, except exposed to UV (UA-2 Hg lamp) for 10 d in air.
- j  $\rho = 2,18 \times 10^{-3} \text{ kg.m}^{-3}$ . Heated at 583 K for 4 h.

## 5.9 Thermal radiation properties of coated composite materials

Data concerning two different coated carbon fiber reinforced composite materials have been collected in this clause. The main characteristics of these materials are given in Table 5-67.

**Table 5-67: Coated Composite Materials the Thermal Radiation Properties of Which Are Given in This Clause**

Spec. No.	Matrix	Fiber			Coating		Data Given	References
		Manu- facturer	Type	Fiber Angle of Weave [°]	Type	Thickness $t_c \times 10^6$ [m]		
1	Al Alloy 6531 (Baseline)				PV 100 (TiO <sub>2</sub> white paint) APA-2474 from Whittaker Corporation, Haynes Division	70	$\epsilon'_\lambda$ ( $\beta'=0$ ) vs. $\lambda$ Figure 5-36	Giommi, Marchetti, Salza & Testa (1985) [92]
2						110		
3						150		
4	Code 69	Celanese	UHM- GY70 Carbon	(0/90) <sub>s</sub>		50	$\epsilon'$ ( $\beta'=0$ ) Table 5-68	
5	90							
6	110							
7	Fiberite 934	Fiberite	T-300- 134/34 Carbon	Woven, Two Layers		25	$R'_\lambda$ ( $\beta=0$ ) vs. $\lambda$ Figure 5-37	
8						55		
9						80		
10	Narmco 5209	Thornel	T300 300 PAN	(0 <sub>s</sub> /90) <sub>s</sub>	CD Magnetron- Sputtered Al	Up to 0,25	$\epsilon'(0)$ vs. $t_c$ Figure 5-38 $\alpha_s$ vs. $t_c$ Figure 5-39 $\alpha_s/\epsilon$ vs. $t_c$ Figure 5-40	Witte & Teichman (1989) [166]

### 5.9.1 White painted composite materials

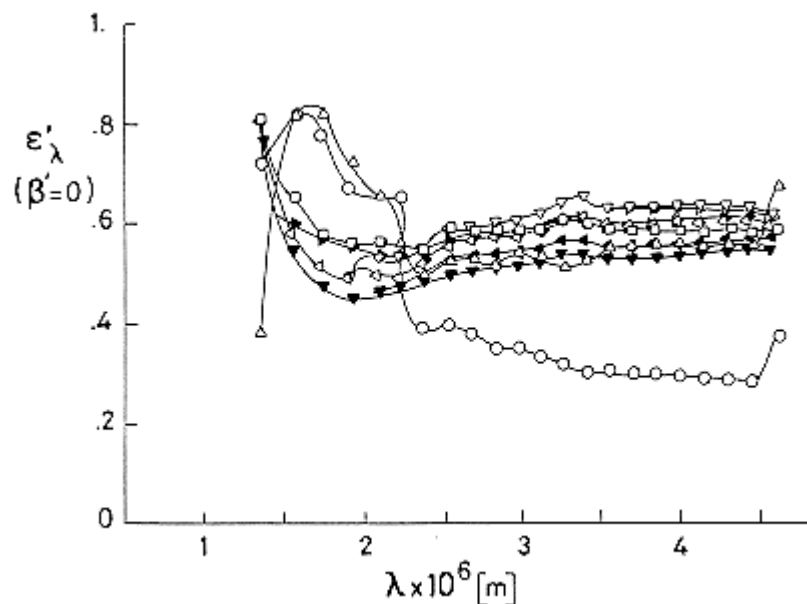
(Specs. No. 1 to 9 in Table 5-67).

Samples are discs, 0,025 m in diameter, formed by either of the followingsubstrates:

1. Al alloy 6531, cleaned with solvent. Baseline.
2. Carbon fiber-epoxy. Sanded with abrasive paper, cleaned with solvent.
3. Carbon fiber-epoxy.

#### 5.9.1.2 Normal spectral emittance

It is deduced from the ratio of sample spectral emissive power to that of a black body radiator at the same temperature and under the same wavelength and viewing conditions (or by using proper corrections if they differ from each other). Data are given in Figure 5-36.



Note: non-si units are used in this figure

**Figure 5-36: Normal spectral emittance,  $\varepsilon'_\lambda$ , of PV 100 coating on different substrates and with different thicknesses (see Table 5-67) vs. wavelength,  $\lambda$ , at 393 K. From Giommi, Marchetti, Salza & Testa (1985) [92].**

Expansion

Spec. No.	Key	Spec. No.	Key	Spec. No.	Key
1	○	4	▽	7	▼
2	□	5	▷	8	►
3	△	6	◁	9	◄

The comparison black body is an integral black body cavity the external edge of which could or could not support the sample disc. If not, the blackbody emission is analyzed by a monochromator. If the sample disc closes the cavity, it is heated from the rear by the black body cavity itself, and its radiant emission is analyzed as above. Errors are introduced in the measurements by uncertainties in the effective sample temperature.

### 5.9.1.3 Normal total emittance

Integration of the spectral measurements with the Plank's black body function as weight function and proper, Stefan-Boltzmann law, normalization, would give the normal total emittance. Unfortunately the covered wavelength range is not wide enough, thus, the normal total emittance has been measured directly by using two different methods; both consist in measuring the ratio of the sample emissive power to that of a blackbody radiator, but differ in sample heating.

The first method is similar to that used for measuring the normal spectral emittance, but the monochromator is replaced by a lock-in amplifier and a fast response bolometer (detector).

In order to cope with the uncertainties in the sample temperature, in the second method the rear face of the sample disc and a blackbody radiant cone are simultaneously heated by means of a water bath of uniform and controllable temperature. The water is held in a stainless steel container two windows of which (in the same wall) are closed by the sample disc and by the blackbody. Measurements are made by placing the detector successively in front of the sample and of the blackbody. The detector is (apparently) shielded from the stainless steel wall emission by a parallel plate with two pinholes directly facing the sample and the blackbody. Data obtained by the second method are systematically larger than those obtained by the first. The values given in Table 5-68 are calculated as the average of the results obtained by either method.

**Table 5-68: Normal Total Emittance,  $\epsilon'(\beta=0)$ , of PV 100 Coating on Different Substrates and with Different Thicknesses**

Spec. No.	$\epsilon'$	Spec. No.	$\epsilon'$	Spec. No.	$\epsilon'$
1	0,76±0,15	4	0,75±0,15	7	0,78±0,15
2	0,77±0,15	5	0,76±0,15	8	0,75±0,15
3	0,75±0,15	6	0,72±0,15	9	0,72±0,15

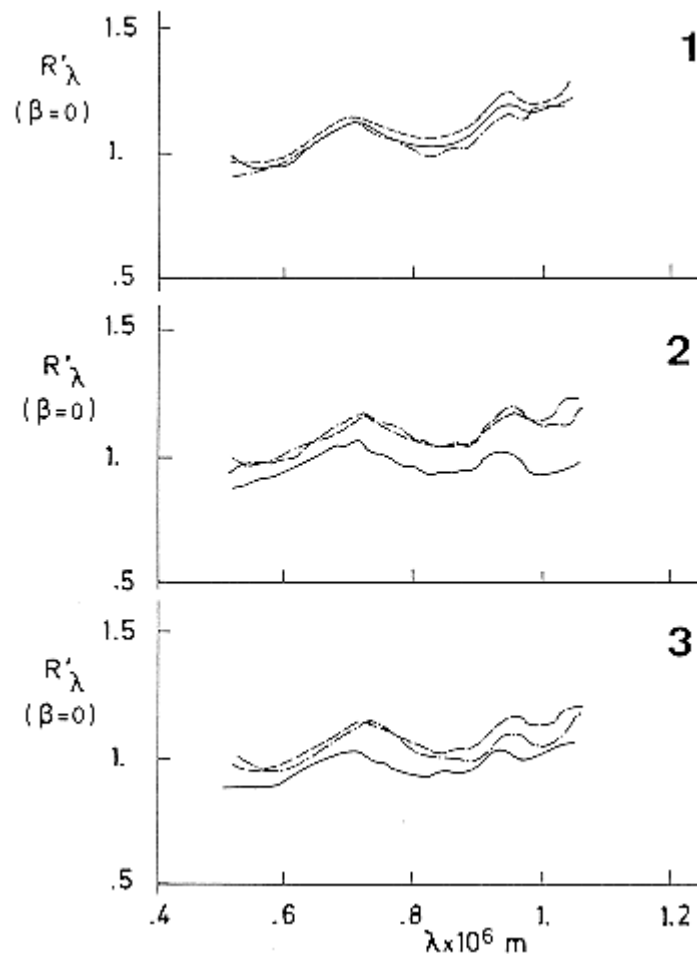
NOTE From Giommi, Marchetti, Salz & Testa (1985) [92]



### 5.9.1.4 Normal-hemispherical spectral reflectance

Measured by use of an integrating sphere reflectometer (0,25 m diameter) and a monochromator.










The so-called substitution-direct method is used to measure the normal-hemispherical spectral reflectance factor,  $R'_\lambda(\beta=0)$ , relative to MgO. In this method the sample is irradiated directly and the detector views an area of the sphere wall. A similar reading is then taken on the comparison standard of known reflectance under the same conditions. The reflectance factor,  $R'_\lambda$ , is the ratio of the flux reflected by the sample to that reflected by the standard under identical conditions of irradiation and viewing. Data for the samples introduced in Table 5-67 are given in Figure 5-37.



Note: non-si units are used in this figure

**Figure 5-37: Normal-hemispherical spectral reflectance factor,  $R'_\lambda$ , of PV 100 coating on different substrates and with different thicknesses vs. wavelength,  $\lambda$ . From Giommi, Marchetti, Salza & Testa (1985) [92].**

## Explanation

Figure	Spec. No.	Key	Figure	Spec. No.	Key	Figure	Spec. No.	Key
Figure 5-37, 1	1		Figure 5-37, 2	4		Figure 5-37, 3	7	
	2			5			8	
	3			6			9	

### 5.9.1.5 Normal solar reflectance

The normal-hemispherical total reflectance for solar radiation has been obtained (Table 5-69) by first deducing the corresponding spectral reflectance data from those of MgO and then integrating with the solar spectral emissive power (solar irradiance), properly normalized, as weight function (see, f.i., [ECSS-E-HB-31-01 Part 6 clause 5.2.5.1](#)).

**Table 5-69: Normal Solar Reflectance,  $\rho_s$  ( $\beta=0$ ), of PV 100 Coating on Different Substrates and with Different Thicknesses**

Spec. No.	$\rho_s$	Spec. No.	$\rho_s$	Spec. No.	$\rho_s$
1	0,90±0,06	4	0,83±0,06	7	0,81±0,06
2	0,91±0,06	5	0,92±0,06	8	0,90±0,06
3	0,89±0,06	6	0,93±0,06	9	0,97±0,06

NOTE From Giommi, Marchetti, Salza & Testa (1985) [92]

For the influence of coating thickness on solar absorptance of other white paints see [ECSS-E-HB-31-01 Part 6, clauses 5.2.2](#) and [5.2.3.1](#) (Zinc Oxide pigment) and [5.2.3](#) (Zinc Orthotitanate). Unfortunately, present data lack of sufficient resolution to estimate the solar absorptance.

For a comment on the optimum coating thickness of a similar coating system, see [ECSS-E-HB-31-01 Part 6, clause 5.2.1](#).

## 5.9.2 Sputtered Aluminium on graphite-epoxy composite material

(Spec. No. 10 in Table 5-67).

Samples are discs 0,025 m in diameter, cut with a diamond-impregnated core drill from a 0,650 m x 1,27 m 8 ply laminate, sanded around the edges with 600A WT silicon carbide paper, wiped quickly with 1,1,1-trichloroethane, rinsed with deionized water and stored for several weeks in a desiccator.

The laminate is fabricated from cured commercial prepreg. The resulting composite material has a smooth side (average roughness:  $0,53 \times 10^{-6}$  m along the striations,  $0,73 \times 10^{-6}$  m across) and a rough side (average roughness:  $4,3 \times 10^{-6}$  m).

The samples have been DC magnetron-sputtered with aluminium.

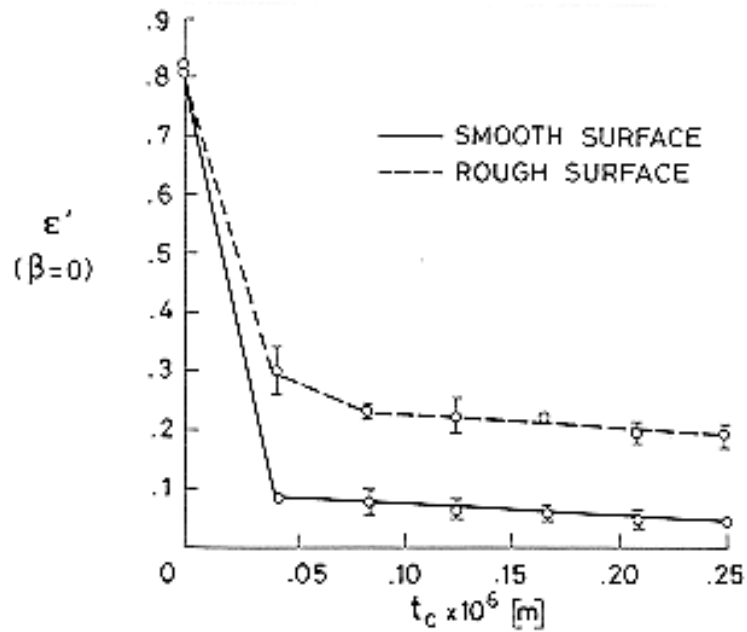
Six sputter coating runs were made. For each run ten specimens were placed in a vacuum chamber with a sapphire wafer thickness monitor in the center of the holding plate. All coatings were sputtered at 1 kW power. The chamber was evacuated, at least 30 min before sputtering, to a pressure ranging from  $50 \times 10^{-5}$  Pa to  $130 \times 10^{-5}$  Pa and backfilled with argon to a pressure of 1 Pa and then an arc was struck to form a plasma.

The coating thickness on each disc was assumed to be the same as that on the thickness monitor for each run. Actually the sputtered coating on rough surfaces tends to be nonuniform with thinner coating deposited on highly sloped surfaces than on flatter surfaces.

### 5.9.2.1 Normal total emittance

It is deduced from infrared reflectance measurements made with a Gier Dunkle DB-100 infrared reflectometer in the wavelength range of  $5 \times 10^{-6}$  m to  $25 \times 10^{-6}$  m.

For each supporting surface texture and coating thickness five specimens were measured and a mean, with a standard deviation, was calculated. The results are summarized in Figure 5-38.



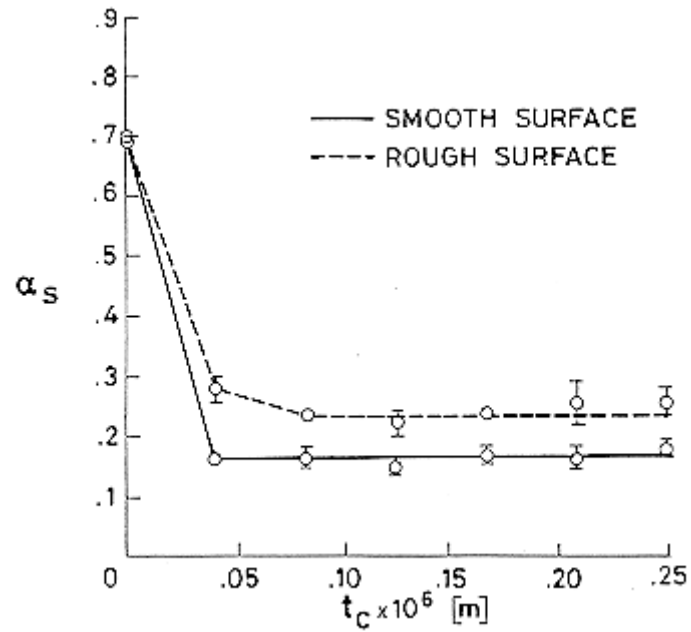
Note: non-si units are used in this figure

**Figure 5-38: Normal total emittance,  $\epsilon'(0)$ , of sputtered aluminium on T300/5209 graphite-epoxy composite material as a function of sputtered coating thickness,  $t_c$ , and for two different textures of the supporting material. From Witte & Teichman (1989) [166].**

### 5.9.2.2 Solar absorptance

It is deduced from solar reflectance ( $\alpha_s = 1 - \rho_s$ ) measured in the wavelength range of  $0,3 \times 10^{-6}$  m to  $2,5 \times 10^{-6}$  m with a Gier Dunkle MS-251 solar reflectometer. The source, optics and sphere characteristics of this instrument, as it was used, approximate the solar spectrum.

Five specimens were again measured for each supporting surface texture and coating thickness. The results are summarized in Figure 5-39.

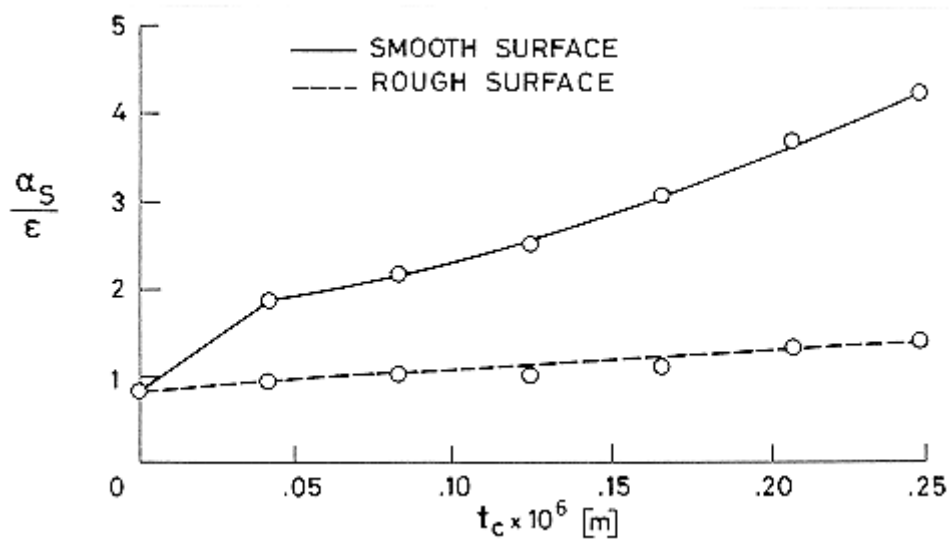


Note: non-si units are used in this figure

Figure 5-39: Normal solar absorptance,  $\alpha_s$ , of sputtered aluminium on T300/5209 graphite-epoxy composite material as a function of sputtered coating thickness,  $t_c$ , and for two different textures of the supporting material. From Witte & Teichman (1989) [166].

### 5.9.2.3 Solar absorptance to emittance ratio

The results are summarized in Figure 5-40.



Note: non-si units are used in this figure

**Figure 5-40: Solar absorptance to emittance ratio of sputtered aluminium on T300/5209 graphite-epoxy composite material as a function of sputtered coating thickness,  $t_c$ , and for two different textures of the supporting material. From Witte & Teichman (1989) [166].**

As a general rule changes in absorptance and emittance due to the sputtered coating are less for rough than for smooth substrates. In addition to the non-uniformity in the coating thickness of rough substrate specimens, which has been already mentioned, the calculations of surface area based on the roughness data indicate that the rough specimens present about 1,3 times as much surface area as the smooth ones. Under the assumption of uniform deposition rates, the coating will be thinner on rough substrates and thus its effect are reduced.

## 5.10 Operating temperature range

Maximum service temperature of organic matrix composites is determined by the resin. Metal and ceramic matrix composites suit high-temperature applications and serve the need for exceptional mechanical and thermal properties in three dimensions.

Unfilled resins have a low resistance to thermal shock at low temperatures because of their relatively high thermal expansion and low thermal conductivity. The most suitable unfilled epoxy resins for use at very low temperature generally have a glass transition temperature,  $T_g$ , just below room temperature.

The high temperature reach of composites and other structural materials are shown in Figure 5-41.

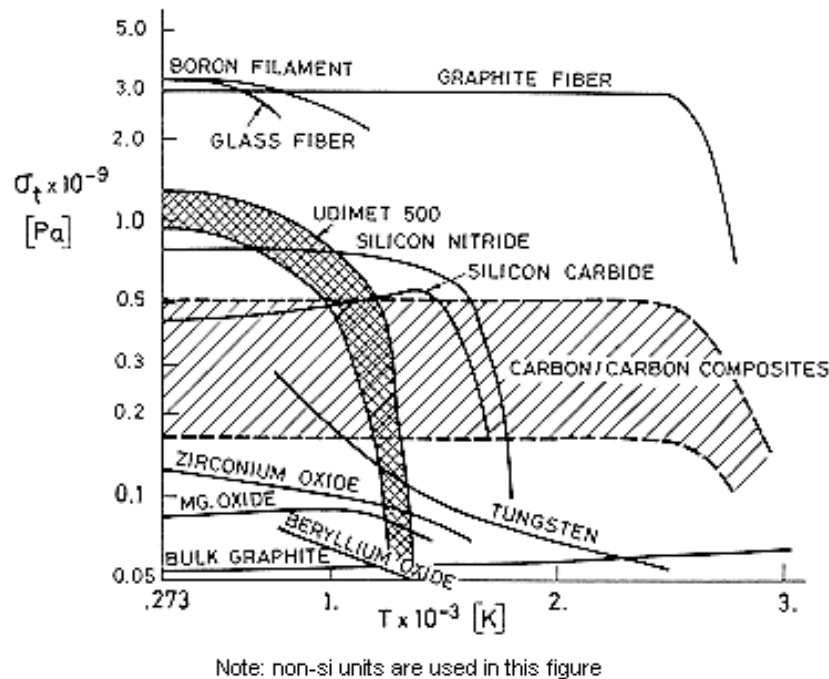


Figure 5-41: Tensile strength,  $\sigma$ , vs. temperature,  $T$ , of structural materials. Inert atmospheres. From DeMario (1985) [81].

### 5.10.1 Temperatures related to the maximum service temperature

Although the designer is usually concerned with the Maximum Continuous Service Temperature,  $T_M$ , of a given material, or with the Maximum Intermittent Service Temperature,  $T_{MI}$ , when service is anticipated to last hours, there are other characteristic temperatures which:

- Indicate structural modifications resulting in abrupt changes in the physical properties, and/or
- are easily measurable and then allow the comparison of different materials for quality control and development purposes.

The glass transition temperature,  $T_g$ , is the temperature at which the stiffness and strength of an organic resin undergo drastic reductions. Other physical properties which change abruptly at  $T_g$  are the specific heat and the coefficient of linear thermal expansion.  $T_g$  is a function of the chemical structure of the polymer. It is measured by the DSC method (see clause 5.5.1.1).

The deflection temperature,  $T_d$ , is the temperature at which a simply loaded beam deflects a given distance under a given load. Beam size, heating rate, geometry, load and deflection are specified. For ASTM D 468 see Harper (1975) [98], p. 3-14.

$T_d$  was formerly known as heat distortion temperature (HDT). It is not necessarily an upper temperature limit but rather a means to compare the relative heat resistance of polymers.

Usually, two different values of  $T_d$  are given which correspond respectively to loads of:

66 lb/in<sup>2</sup> = 4,6 x 10<sup>5</sup> Pa, or 264 lb/in<sup>2</sup> = 18,2 x 10<sup>5</sup> Pa.

Characteristic temperatures of typical matrices are given in Table 5-70.

**Table 5-70: Characteristic Temperatures of Neat and Reinforced Resins**

Type	T <sub>g</sub> [K]	T <sub>d</sub> [K]	T <sub>M</sub> [K]	T <sub>Ml</sub> [K]	References
Epoxy Typical			450		Beardmore, Harwood, Kinsman & Robertson (1980) [62]
Cured at 395 K			345	380	Weeton, Peters & Thomas (1987) [164]
Cured at 450 K			395	525	
Liquid Casting Room Cure. Flexigle			370-405	405-450	SENER (1984) [147]
Liquid Casting Room Cure. Rigid		360-475	405-430	425-475	
Liquid Casting Oven Cure. Flexible			395-430	425-475	
Liquid Casting Oven Cure. Rigid		360-475	405-450	450-475	
Moulding Compound		380-480	450-535	510-565	
Araldite LY 556/HY 906/DY 070 Oven Cure	453				
Araldite LY 556/HY 917/DY 070 Oven Cure	428				
Araldite LY 556/HY 972. Oven Cure	438				
Araldite LY 564/HY 2954. Oven Cure	448				
Araldite LY 564/HY 560. Oven Cure	373				
Araldite LY 1927GB/HY 1927GB Room or Warm Cure	388				
Araldite XD 893/HY 932.	473				



Type	T <sub>g</sub> [K]	T <sub>d</sub> [K]	T <sub>M</sub> [K]	T <sub>Mi</sub> [K]	References	
Oven Cure						
DER 332/T403, 24h/330K+24h/350K		338,5 <sup>a</sup> 335,5 <sup>b</sup>			Chiao & Moore (1974) [68]	
DER 332/T403, 16h/330K, 0,60 glass fiber	353				Clements & Moore (1978) [73]	
DER 332/T403, 16h/330K, 0,65 glass fiber	353					
DER 332/T403, 16h/330K, 0,70 glass fiber	355					
XD927 16h/350K+16h/380K		386,5			SENER (1984) [147]	
ERL 4221+HHPA+BDMA 2,5h/360K+5h/430K		447,5				
ERL 4221+DDM+Resorcinol 16h/390K+18h/450K+4h/470K		425				
Vicotex 108, 2h/400K+2h/450K		499,5				
Xylok 237, 5h/390K+2h/450K		443				
Rezolin EPO 93L, up to 4h/430K		430,5				
Rezolin EPO 58/970A, up to 3 h/530K		444				
Cyclo-Aliphatic Tri Epoxy Resin 24h/420K+4h/470K		458,5				
H70E, 1h/423K	358		425	573-673		EPO-TEK (1989) [87]
H70S, 1h/423K	358		425	573-673		
Phenolic Typical			535	590	Weeton, Peters & Thomas (1987) [164]	
Semi-IPM. Copec/2-CBA 1:1 pbw	468				Hsiue, Miller & Segal (1985) [103]	
Semi-IPN. Victrex/2-CBA 1:1 pbw	458					

Type	T <sub>g</sub> [K]	T <sub>d</sub> [K]	T <sub>M</sub> [K]	T <sub>Mi</sub> [K]	References
Cured 2-CBA	518				
<u>Polyester</u> Typical			370		Beardmore, Harwood, Kinsman & Robertson (1980) [62]
Ekonal Sinterized at 700 K, 7 x 10 <sup>7</sup> Pa			530-590	670-730	Economy, Nowak & Cottis (1970) [86]
Polycarbonate		405			Weeton, Peters & Thomas (1987) [164]
Lexan	425	412-418 <sup>a</sup> 411-416 <sup>b</sup>			T <sub>g</sub> from Hsiue, Miller & Segal (1985) [103] T <sub>d</sub> from Kazanjian (1974) [113]
Polycarbonate 0,30 glass fiber		425			Weeton, Peters & Thomas (1987) [164]
Polycarbonate, 0,30 carbon fiber		425			
<u>Polyamide</u> Nylon 6/6			415		Beardmore, Harwood, Kinsman & Robertson (1980) [62]
Nylon 6 General purpose		455 <sup>a</sup> 341-344 <sup>b</sup>	390-420		Anon. (1969) [53]
Nylon 6 0,30 fiber		491-493 <sup>a</sup> 488-489 <sup>b</sup>	390-420		
Nylon 6/6 General purpose		516 <sup>a</sup> 377 <sup>b</sup>	390-420		
Nylon 6/6 0,30 glass fiber		537 <sup>a</sup> 530 <sup>b</sup>	390-420		
Nylon 6/6 0,30 carbon fiber		530			Weeton, Peters & Thomas (1987) [164]
Nylon 6/6 0,40 glass fiber		538 <sup>a</sup> 533 <sup>b</sup>	390-420		Anon. (1969) [53]

Type	T <sub>g</sub> [K]	T <sub>d</sub> [K]	T <sub>M</sub> [K]	T <sub>Mi</sub> [K]	References
Nylon 6/10 General purpose		422 <sup>a</sup> 320 <sup>b</sup>	380-420		
Nylon 6/10 0,30 glass fiber		494 <sup>a</sup> 489 <sup>b</sup>	390-420		
<u>Polysulfone</u> Typical		445	425	450	Weeton, Peters & Thomas (1987) [164]
	461				Hsiue, Miller & Segal (1985) [103]
Polysulfone 0,30 glass fiber		460			Weeton, Peters & Thomas (1987) [164]
Polysulfone 0,30 carbon fiber		460			
Polyphenylsulfone			455	480	
<u>Polyimide</u> Typical/590K			565	645	
PMR-15	644				Pater (1988) [134]
PMR-P1	637				
PMR-P6	631				
PMR-P7	628				
BMI-1/MBMI-1, X <sub>1</sub> = 1, 6h/517K	653 <sup>d</sup> 658				Hsu, Chen, Parker & Heimbuch (1985) [104]
BMI-1/MBMI-1, X <sub>1</sub> = 0,66, /503K	553 <sup>d</sup> 603				
BMI-1/MBMI-1, X <sub>1</sub> = 0,5, 6h/486K	533 <sup>d</sup> 573				
/513KBMI-1/MBMI-1, X <sub>1</sub> = 0,33, /489K	513 <sup>d</sup> 553				
BMI-1/MBMI-1, X <sub>1</sub> = 0, 6h/486K	443 <sup>d</sup> 528				
BMI-1/MMAB, X <sub>1</sub> = 0,5 /489K	435 <sup>e</sup>				
BMI-1/MMAB, X <sub>1</sub> = 0,66 /509 K	478 <sup>e</sup>				

Type	T <sub>g</sub> [K]	T <sub>d</sub> [K]	T <sub>M</sub> [K]	T <sub>Mi</sub> [K]	References
BMI-1/MMAB, X <sub>1</sub> = 0,75 /513 K	510 <sup>e</sup>				
BMI-2/MBMI-2, X <sub>1</sub> = 1	673 <sup>e</sup>				
BMI-2/MBMI-2, X <sub>1</sub> = 0,75 /531 K	645 <sup>e</sup>				
BMI-2/MBMI-2, X <sub>1</sub> = 0,66 /527 K	621 <sup>e</sup>				
BMI-2/MBMI-2, X <sub>1</sub> = 0,5 /513 K	591 <sup>e</sup>				
BMI-2/MBMI-2, X <sub>1</sub> = 0,33 /500 K	591 <sup>e</sup>				
BMI-2/MBMI-2, X <sub>1</sub> = 0/489 K	433 <sup>e</sup>				
Polyetherimide		475			Weeton, Peters & Thomas (1987) [164]
Polyetherimide 0,30 glass fiber		440			
Polyetherimide 0,30 carbon fiber		440			
Poly (amide-imide) Typical			535		Beardmore, Harwood, Kinsman & Robertson (1980) [62]
Vinylester			370		
PBT			455		
Azmet PBT 0,35 glass fiber		491 <sup>b</sup>			Reinhard (1988) [142]
PBT		360			Weeton, Peters & Thomas (1987) [164]
PBT 0,30 glass fiber		485			
PBT 0,30 carbon fiber		485			
Azdel PP 0,40 glass fiber		430 <sup>b</sup>			Reinhard (1988) [142]

- a Applied load  $4,6 \times 10^5$  Pa.
- b Applied load  $18,2 \times 10^5$  Pa.
- c Where two values are given, upper corresponds to before and lower after postcure. Typical postcure is 16h/510K.
- d No postcure.

Upper service temperature as controlled by thermo-oxidative stability of the fibers is introduced in clause 5.13.3.1.

## 5.11 Electrical properties

### 5.11.1 Electrical resistance and electrical resistivity

We can distinguish here between electrical resistance  $R$  [Ohm] and electrical resistivity  $\rho$  [Ohm.m]. For a homogeneous and isotropic material of length  $L$  and cross-sectional area  $S$ , both are related by the following expression:

$$R = \rho \frac{L}{S} \quad [5-11]$$

The electrical resistivity,  $\rho$ , of composite materials used in aircraft and spacecraft is about three orders of magnitude higher than that of conventional metal alloys.

#### 5.11.1.1 Calculation formulae for composites

It is not possible to introduce here generally applicable simple expressions.

For a composite with continuous unidirectional fibers, the electrical resistance along the fibers is given by

$$\frac{1}{R_1} = \frac{\varphi_f}{R_f} + \frac{\varphi_m}{R_m} \quad [5-12]$$

In many cases: metals, boron, carbon fibers, ... the electrical conduction takes place through fibers ( $R_m \gg R_f$ ) and thus:

$$R_1 \approx \frac{R_f}{\varphi_f} \quad [5-13]$$

The electrical conduction in the 2 direction takes place by chance contacts between adjacent fibers. For unidirectional fibers with volume fractions of structural interest ( $\varphi_f \approx 0,60$  to  $0,65$ ) the resistivities perpendicular to the fibers are 200 to 400 times higher than those in the fiber direction (Lodge (1982) [121], Thomson (1982) [156]) and, in general, considerably smaller than that of the matrix alone.

The electrical resistance in a direction forming an angle  $\theta$  with the 1 direction (fibers) is given by (Karlsson (1983) [111])

$$R_{\theta} = R_1 \cos^2 \theta + R_2 \sin^2 \theta \quad [5-14]$$

In multidirectional layups the leakage between adjacent plies tends to reduce the difference between  $R_1$  and  $R_2$  so that a four-directional quasi-isotropic layup can be regarded as electrically isotropic in the plane of the composite.

In general, for multilayered composites formed by  $n$  plies with different orientations, the electrical resistance in the plane of the composite is given by (Karlsson (1983) [111])

$$\frac{1}{R} = \frac{1}{n} \sum_{1}^n \frac{1}{R_n} \quad [5-15]$$

where  $R_n$  is the electrical resistance of the  $n$  layer in its 1 direction.  $R_n$  depends on temperature, moisture and thermal history of the material.

The electrical resistances normal to the plane of the laminate are much higher because of the excess resin between adjacent plies.

The available body of measurements of the resistivities of a variety of samples is fairly extensive. Data are summarized in the following.

### 5.11.1.2 Tabulated data

**Table 5-71: Electrical Resistivity,  $\rho_f$  [ $\Omega \cdot m$ ], of High-Strength Fibers**

Type	T [K]	$\rho_f \times 10^6$ [ $\Omega \cdot m$ ]		References
		$\rho_{f1}$	$\rho_{f2}$	
Celion C-6S		15		Weeton, Peters & Thomas (1987) [164]
Celion G 50		10		
Celion GY 50	290	9,1		Karlsson (1983) [111]
Celion GY 70		3,1-6,5		
Celion GY 70SE		6,5		Weeton, Peters & Thomas (1987) [164]
Celion 1000		15		
Celion 3000		15		
Celion 6000		15		
Celion 12000		15		
DG 112	290	65		Karlsson (1983) [111]
Fortafil 3		60		

Type	T [K]	$\rho_f \times 10^6$ [ $\Omega \cdot m$ ]		References
		$\rho_{f1}$	$\rho_{f2}$	
Fortafil 3(C)		16,7		Weeton, Peters & Thomas (1987) [164]
Fortafil 3(O)		18,2		
Fortafil 5	290	9,5		Karlsson (1983) [111]
Fortafil 5(O)		9,5		Weeton, Peters & Thomas (1987) [164]
Grafil HT	290	13	10	Karlsson (1983) [111]
Hercules E-HTS		10		
HMG 50		14		
HMS typical		8,3		
Magnamite AS1		20		
Magnamite AS3		13		
Magnamite AS6		18,26		Weeton, Peters & Thomas (1987) [164]
Magnamite IM6		14,04		
Modmor HMS	290	7,8		Karlsson (1983) [111]
	450	6,6		
Polycarbon C	290	35		
Thornel T-50		9,5		Weeton, Peters & Thomas (1987) [164]
Thorel T-300		18		
Thornel T-500		18		
Thornel P-25W		13		
Thornel P-55S		7,5		
Thornel P-75S		5		
Thornel P-100		2,5		
Torayca	290	26-34		Karlsson (1983) [111]

Type	T [K]	$\rho_f \times 10^6$ [ $\Omega \cdot m$ ]		References
		$\rho_{f1}$	$\rho_{f2}$	
Boron		26 <sup>a</sup>	b	
Amorphous Metal		0,8-3,5		

<sup>a</sup> Depends on the manufacturing process.

<sup>b</sup> Very high values.

**Table 5-72: Electrical Resistivity,  $\rho$  [ $\Omega \cdot m$ ], of Carbon-Epoxy Composite Materials**

Fiber			T [K]	$\rho \times 10^6$ [ $\Omega \cdot m$ ]	
Type	Angle [°]	$\phi_f$		$\rho_1$	$\rho_2$
HMS	0	0,4	290	22	4350
		0,5		19	2700
		0,6		15	1960
HM	0,5	18		3850	
HTS	0	0,4		40	8300
		0,5		29	3201
		0,6		24	1700
HT	0	0,5		29	3700
E-HTS	0/90	0,65		44	--
	+45/-45			85	--
	90/90		10 <sup>5</sup>	--	
T300	0/90		150	--	
	+45/-45		200	--	
	90/90		4,4x10 <sup>4</sup>	--	
	0		40	6600	

NOTE From Karlsson (1983) [111].

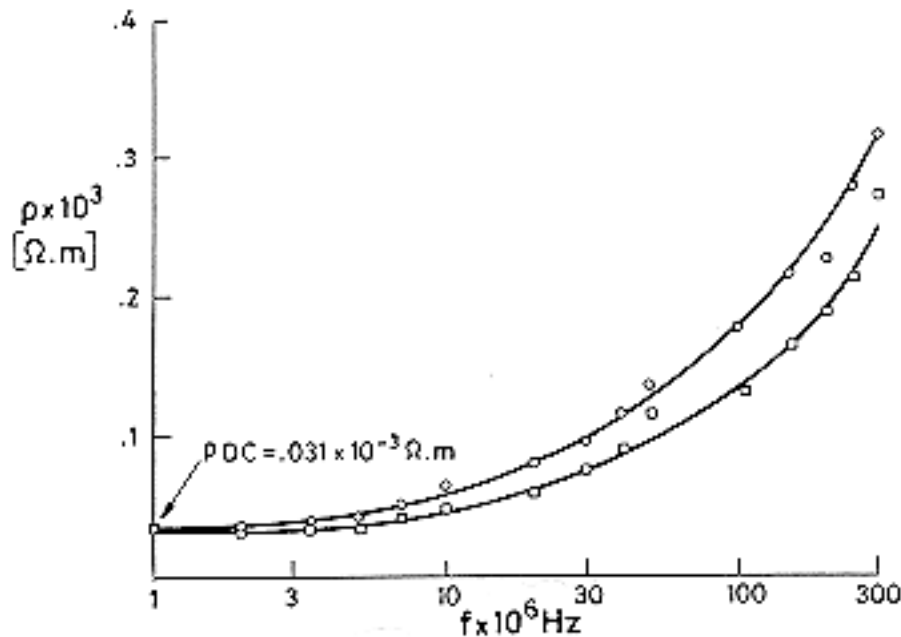


### 5.11.1.3 High-frequency effects

Electrical conduction in composites at non-zero frequencies is not clearly understood and, thus, a theoretical prediction of the high-frequency behavior of composites is at present not possible.

Nevertheless, a substantial body of measurements exists.

Typical results, given in Figure 5-42, correspond to two set of samples which differ only in their widths. The electrical resistivity is lower for the narrower samples. This is due to the skin effect for alternating current flow since in the narrower samples the loss in effective cross-sectional area will be proportionally less than in the wider samples as the frequency rises.



Note: non-si units are used in this figure

**Figure 5-42: Electrical resistivity,  $\rho$ , as a function of frequency,  $f$ , for a carbon-epoxy composite material. Fiber: Super A, Matrix: Fibredux 914C. Layup ( $0^\circ \pm 45^\circ$ ) 16 plies.**

**Sample size:  $\circ$  :>  $1,98 \times 10^{-3}$  m,  $10 \times 10^{-3}$  m,  $25 \times 10^{-3}$  m.  $\square$  :>  $1,98 \times 10^{-3}$  m,  $5,5 \times 10^{-3}$  m,  $25 \times 10^{-3}$  m.**

**From Thomson (1982) [156].**

### 5.11.1.4 Electrical behaviour of structural joints

The ease of the electrical conduction across a joint is measured by its admittance, expressed in Siemens ( $\text{Ohm}^{-1}$ ) per meter of joint.

In this clause particular emphasis is placed on the electrical behavior of composite-composite joints.

Since all the conduction in a carbon fiber composite takes place through the fibers, for a joint to be electrically conducting, the fibers of one half of the joint should be linked to the fibers on the other half.

Due to the resin rich surface layer which is squeezed out of the composite during curing, very little current flows from one panel to the other directly across the interface in composite-composite joints.

On the contrary, all the current is forced to flow across the joint via the shank of the metal fasteners through the composite/metal and metal/composite interfaces.

Bolts are used for component assembly because they sustain high mechanical loads. Hexagonal-headed bolts exhibit high electrical admittances, which depend on the bolt tightening torque, below a given torque value. The tightening pressure under the head of these bolts (combined with localized heating from the passage of the current) seems to be sufficient to break up the resin rich layer.

When high closing pressures are used on fasteners, structural damage could occur but good electrical properties could result since the fastener and the fibers are in intimate contact.

Countersink bolts (in which the head fits flush with the surface), although they contact a large area of machined carbon fiber, exhibit low admittances because the current enters the bolt via a small annulus around the base of the countersink rather than over the entire area.

Adhesive joints are much worse, from the electrical admittance point of view, than mechanically fastened joints since no metallic fastener is present and cold curing resins are electrical insulators.

Composite-metal joints present their own problems. Again bolts are used for component assembly. Among the bolted joints there are fixed configurations, with Hi-Loks, and removable configurations with nut plates. The bolt material has to be compatible with both parts to be assembled. Thus, titanium bolts are used with carbon fiber reinforced composite - Aluminium joints.

On the other hand, a bonded joint between composite material and metal is not mechanically reliable if the adhesive used needs a cure cycle. The materials should be pre stressed to cope with thermal expansion.

The following stratagems are recommended for improving the electrical performance of both composite-composite and composite-metal joints with minor effects on their structural strength.

#### COMPOSITE-COMPOSITE JOINTS

1. The protective glass cloth around the fastener impedes the conduction between fibers and bolt. The cloth layer should be locally removed. The surface could be resealed again after the fasteners have been installed.
2. Increasing the contact area by using either larger diameter fasteners or large head and tail fittings. This can result in additional weight and cost.
3. Increasing the contact area by tighter tolerances on the hole drilling. These holes are very expensive to produce and very easily damaged before final fixing. See Table 5-73.

**Table 5-73: Drill Bit Costs and Standard Drilling Hourse**

Material	Drill Bit Costs	Resharpener Potential	Standard Hours to Drill One Hole
Aluminium	High Speed Steel \$ 0,40 (Al)	10-15 times	0,0006 (Al)
Titanium	Cobalt \$ 0,70 (Ti)		
Graphite-Epoxy	Carbide Tipped \$ 3,00	3-4 times	0,03
	4 Fluted 30,00	5-6 times	

The factors that affect the cost when drilling holes in composite materials are: hole tolerance requirements, special drill bit cost, drill speed and setup time. Drill bits specifically designed for obtaining high quality holes in composite materials are available. Tighter tolerances than in standard metallic structures are required when using metallic fasteners in composite structures. Slower drill feeds should be used because of increased wear rates. Setup time is increased to avoid back face damage when the drill bit breaks-through the laminate. Removing a misplaced hole can be time consuming and costly.

NOTE From Carter III (9819) [66].

4. Electrodeposited copper down to  $5 \times 10^{-3}$  m bolt holes improves the admittance of countersink titanium bolts. Flame spraying and electrodeless deposition have been also used.
5. Conducting particle ladden coatings can be sprayed or hand painted at much less cost and in situ, although the admittance gains are much more modest.
6. Adhesive joints should be avoided although several recommendations to enhance the electrical conductivity of the joint are:
  - 6.1. Several hot curing resins have metal particles incorporated into them to improve their hot strength, Increasing the metal loading up to 70% only results in modes admittance gains. At such high metal loadings the adhesive becomes unsuitable for structural applications.
  - 6.2. Addition of metal gauzes has been attempted and modest admittance gains have been achieved.
  - 6.3. Hotspots due to passing electrical current cause local softening and even vaporization of the matrix, releasing more fibers, and increasing the admittance. Nevertheless, the structural integrity of the composite suffers with a possible loss of strength in the adhesive.

From Lodge (1982) [121].

#### COMPOSITE-METAL JOINTS

1. The presence of non-conductive sealant during a wet assembly will increase the resistivity. Tracers of this sealant should therefore be removed from both components of the joint.
2. A tenacious non conducting oxide film, that titanium bolts have, will increase the resistivity. The metal surface should therefore be uncoated and abraded in the bolt areas to improve the electrical conductivity.

3. Meshes will increase the weight of a component part since the added plies are not structural materials. A metalized carbon fiber ply should be more useful. It is a structural material which can be used instead of the last ply of the laminate.
4. The choice of a metallic protection should take into account thermomechanical distortion problems during the cure cycle.
5. Incorrect drilling can produce over size holes. On the other hand, a wrong speed drilling or feed rate can smear the resin over the ends of the fibers insulating them.
6. The current will flow under the head of the pin and will reach the metallic part through the shank of the bolt.
  - 6.1. The use of washers or metallic strips connecting more Hi-Loks will improve both the electrical conduction (admittance increases when pressure does) and the distribution of stresses around the hole.
  - 6.2. A metallic strip electrical connection of the bolt heads will increase the bolt admittance and the current will find a new preferential path. When metallic strips are to be avoided, plasma spraying can be used for the electrical connection of the screw heads.
  - 6.3. If a Ti bolt is used, the higher resistivity of this material compared with Al should be taken into account in the calculation of the cross-section.

## 5.12 Prelaunch environmental effects

### 5.12.1 Moisture absorption and desorption

The mechanical properties of composite materials, when they work close to their ultimate mechanical and thermal limits, may suffer if the material is exposed to moisture for long periods of time.

The state of knowledge regarding the so-called hydrothermal effects on carbon fiber-epoxy composite materials can be summarized as follows (Hancox (1981) [94]):

1. Carbon fibers are not attacked by water. Any action of moisture and temperature on composite materials will involve the matrix and the interface.
2. For a given material the increase in weight due to moisture absorption leads to practically the same reduction in properties no matter whether the material has been either exposed to humid air or fully immersed in water.
3. The effects of water and exposure to elevated temperatures, as measured by tensile, compressive and interlaminar shear performance, seems to be fully reversible on the removal of water. Nevertheless, irreversible changes have been noticed:
  - (a) In interlaminar shear strength and work of fracture.
  - (b) After rapid temperature changes which cause a permanent increase in moisture diffusion.
  - (c) In a decrease of both fatigue life and the incubation period during which failure is not observed in a fatigue test.
4. Although several authors noticed time dependent effects associated to microcracking in the matrix, water absorption and desorption can be predicted by use of the simple Fick's law of laminar diffusion (Bird, Stewart & Lightfoot (1960) [63]).

We will introduce in the following the analysis by Shen & Springer (1976) [148] and by Loos & Springer (1979) [122].

### 5.12.1.2 Fickian analysis of moisture absorption of composite materials

The moisture content (or weight gain),  $M$ , of the material is defined as:

$$M(t) = \frac{\text{Weight of Moist Material} - \text{Weight of Dry Material}}{\text{Weight of Dry Material}} \quad [5-16]$$

A relative moisture content,  $G$ , can be defined as:

$$G(t) = \frac{M(t) - M_o}{M_m - M_o} \quad [5-17]$$

where  $M_o$  is the initial moisture content of the material, and  $M_m$  the maximum moisture content, which is related to the ambient moisture content,  $M_a$ . See clause 5.12.1.2.

According to experimental evidence, obtained in the temperature range 322 K to 366 K by Loos & Springer (1979) [122], the maximum moisture content,  $M_m$ , seems to be insensitive to temperature.

In order to calculate  $G(t)$ , the Fick's diffusion law will be applied to a homogeneous isotropic medium which has uniform initial moisture content,  $M_o$ , and uniform initial temperature,  $T_o$ , and which is immersed in an environment with uniform moisture content,  $M_a$ , and the same temperature,  $T_o$ .

It should be realized first that mass and heat transport processes are decoupled because the Lewis-Semenov number,  $Le$ ,

$$Le = \frac{D}{\alpha} \quad [5-18]$$

which is the ratio of mass to thermal diffusivities, is here of the order of  $10^6$ , and then the temperature approaches equilibrium much faster than the moisture concentration.

The time evolution of the moisture content,  $M(t)$ , is given by Eqs. [5-19] and [5-20] below.

- (a) One-dimensional configuration

$$\frac{M(t) - M_o}{M_a - M_o} = 1 - \frac{8}{\pi^2} \sum_{p=0}^{\infty} \frac{1}{(2p+1)^2} \exp\left[-\left(\frac{(2p+1)\pi}{L}\right)^2 Dt\right] \quad [5-19]$$

where  $D$  [ $\text{m}^2 \cdot \text{s}^{-1}$ ] is the diffusion coefficient in the direction normal to the material surface. For a fiber reinforced material,  $D = D_2$  (normal to fibers).  $t$  is the time and  $L$  the thickness of the composite material when exposed on two faces (edges are assumed to be shielded by an impermeable coating in order to keep valid the one-dimensional approach). When the material is exposed on one face only,  $L$  should be twice the thickness.

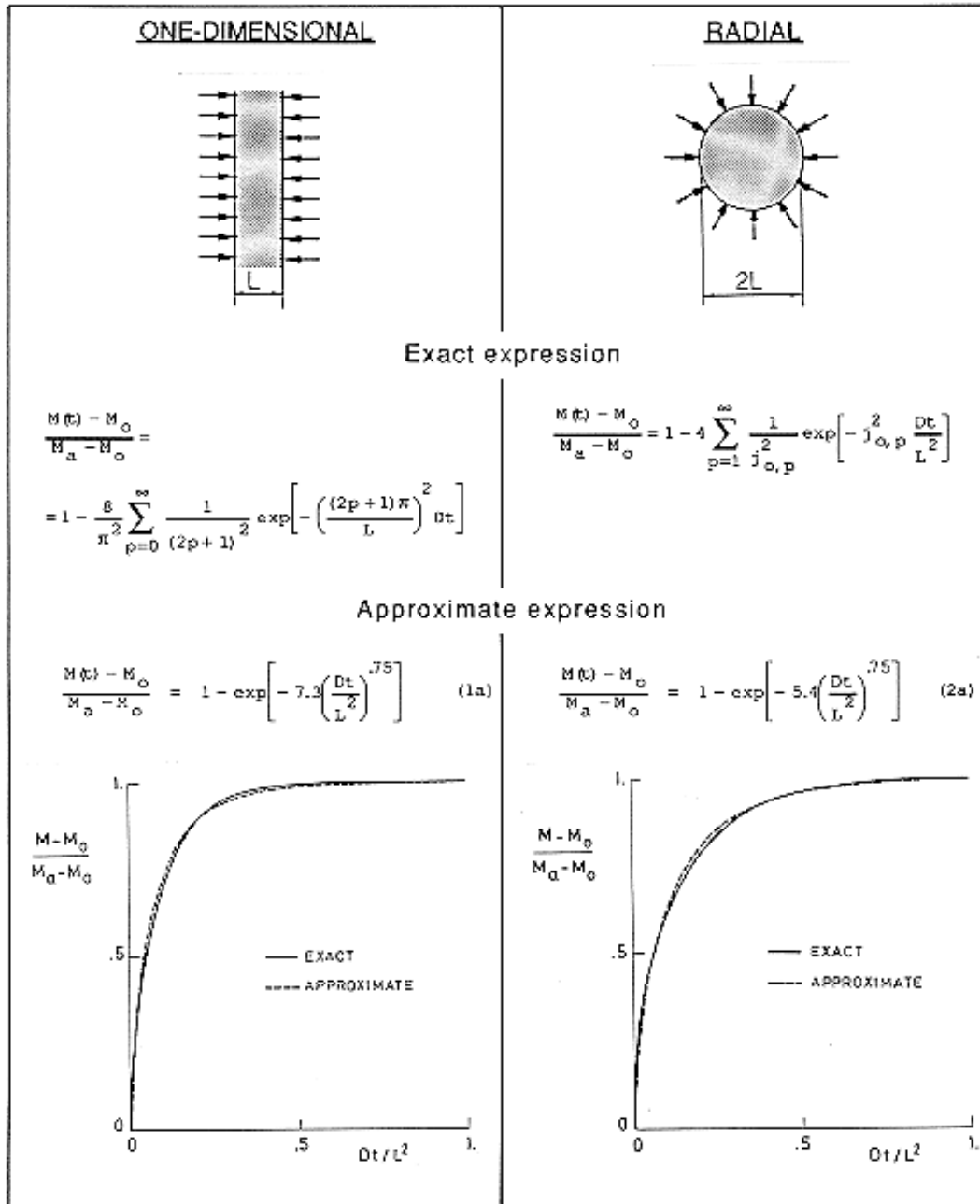
- (b) Radial configuration

Data from experiments with slender rods of diameter  $2L$  have been also reported. In order to analyze them, the simple one-dimensional model used by Shen & Springer should be slightly modified yielding the following expression

$$\frac{M(t) - M_o}{M_a - M_o} = 1 - 4 \sum_{p=1}^{\infty} \frac{1}{j_{o,p}^2} \exp\left[-j_{o,p}^2 \frac{Dt}{L^2}\right] \quad [5-20]$$

where  $j_{o,p}$  is the p-th real zero of  $J_o$  (Bessel function of first kind and order 0) (Abramowitz & Stegun (1965) [50]).

Approximate expressions of Eqs. [5-19] and [5-20] are given in Figure 5-43.



Note: non-si units are used in this figure

**Figure 5-43: One-dimensional and radial models of laminar diffusion through homogeneous-isotropic media.**

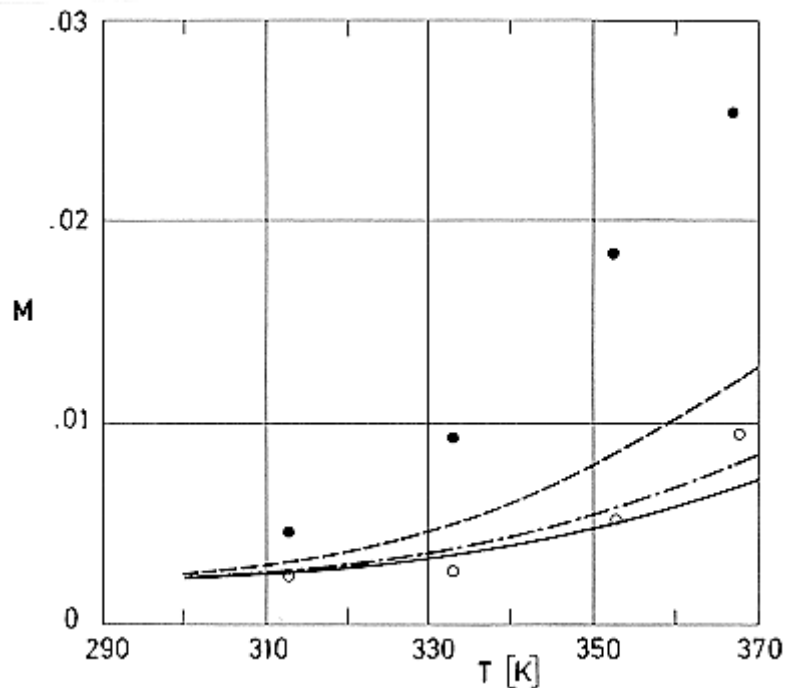
The diffusion coefficient,  $D_2$ , changes very little with the moisture content, but depends on temperature. Loos & Springer (1979) [122], based on experimental evidence, suggest the following Arrhenius-type law:

$$D_2 = D_0 e^{-C/T} \quad [5-21]$$

Values of  $D_0$  and  $C$  for typical graphite-epoxy composite materials will be given in Table 5-76.

Similar expressions are being used for predicting diffusion coefficients of gases in different materials (see f.i. Fortier & Giletti (1989) [89]).  $C$  depends on the characteristics of the carrying material and also on those of the diffusing fluid. This could be deduced from the data in Table 5-76, where, in addition, nominally identical materials have been exposed to different cure cycles.



Numerical values of the moisture content,  $M$ , for  $t = 100\text{h}$  and typical composites vs. ambient temperature,  $T$ , are shown in Figure 5-44.



Note: non-si units are used in this figure

**Figure 5-44: Moisture content,  $M$ , as a function of ambient temperature,  $T$ , after 100 h of exposure to distilled water at that temperature, for several carbon fiber reinforced composites. The specimens are infinitely large rods of  $6 \times 10^{-3}$  m diameter.  $M_0 = 0,002$  assumed.**

Explanation

Key	Description	Comments
	Spec. No. 1, Table 5-74.	Calculated by the compiler Eq. (2a), Figure 5-43
	Spec. No. 2, Table 5-74	

— • —	Spec. No. 3, Table 5-74	$M_a = M_m$ as in Table 5-75 $D_0$ and $C$ as in Table 5-76
○	Matrix: DER 332/DDS, 3h/420K Fiber: HT-S prepreg carbon $\varphi_f = 0,58$ to $0,62$ , $\varphi_v < 0,01$	Experimental Hancox (1981) [94], Fig. 4.
●	As above, except $\varphi_v = 0,05$ to $0,06$	

### 5.12.1.3 Maximum moisture content. Experimental data

Experimental evidence indicates that the maximum moisture content is insensitive to temperature but depends on the moisture content of the environment.

For a material immersed in a liquid  $M_m$  is constant.

For a material exposed to humid air,  $M_m = a\varphi^b$ ,

where  $\varphi$  is the relative humidity of the environment and  $a$  and  $b$  are experimental constants.

The experimental data which will be given in this clause were obtained with the samples characterized in Table 5-74.

**Table 5-74: Characterization of Composite Materials, the Maximum Moisture Content and Diffusion Constants of which are given in Table 5-75 and Table 5-76 respectively**

Spec. No.	Matrix	Fiber			Fiber Volume $\varphi_f$	Cure Cycle	Spec. Size
		Manu- facture	Type	Fiber Angle [°]			
1	Fiberite 1034	Fiberite	T300	0 8 ply	0,650	Vacuum bag. Temp. raised to 390 K at 2 K/min. Then 0,25h/390K+0,75h/390K and $7 \times 10^5$ Pa + 2h/450 K. Cooled under pressure to below 350 K.	$1,04 \times 10^{-3}$ m x $12,7 \times 10^{-3}$ m x 0,101 m
2	Hercules 3501-5	Hercules	AS		0,650	Vacuum bag $0,85 \times 10^5$ Pa. Temp. raised to 450 K at 1,5 K/min. At 400 K pressure raised to $5,9 \times 10^5$ Pa, 1h/450K and $5,9 \times 10^5$ Pa. Temp. lowered to 340 K at 7 K/min. Pressure released. Postcure 3h/460K.	
3	Rigidite 5208	Narmco	T300		0,700	Vacuum ba $0,74 \times 10^5$ Pa. Temp. raised to 410 K at 2	



	(Narmco)					K/min. Then 1h/410K. Temp. raised to 450 K at 2 K/min. 2h/450K and 5,9x10 <sup>5</sup> Pa. Temp. lowered to 330 K at 2 K/min. Pressure released. Postcure 4h/480K.	
--	----------	--	--	--	--	--	--

The maximum moisture content of the materials in Table 5-74, immersed either in water or in humid air, are given in Table 5-75.

**Table 5-75: Maximum Moisture Content,  $M_m$ , of the Specimens Characterized in Table 5-74**

Material	Immersed in Water		Exposed to Humid Air	
	Distilled	Saturated Salt	a	b
T300/Fiberite 1034	0,017	0,0125	0,017	1
AS/Hercules 3501-5	0,019	0,0140	0,019	1
T300/Narmco 5208	0,015	0,0112	0,015	1

NOTE From Loos & Springer (1979) [75].

#### 5.12.1.4 Transverse coefficient of diffusion. Experimental data

Values of the diffusion constants,  $D_0$  and  $C$  from Loos & Springer (1979) [122] are collected in Table 5-28. These values have been obtained by best fit to experimental data in the temperature range 300 K to 330 K. Results from other investigators, as quoted by Loos & Springer (1979) [122], have been enclosed also. Owing to variations in the material, data from different sources hardly can be compared.

**Table 5-76: Constants  $D_0$  and  $C$  for the Arrhenius Expression, of the Transverse Diffusion Coefficient,  $D_2$ , of the Specimens Characterized in Table 5-74**

Moisture Exposition	Material	$D_0 \times 10^6$ [m <sup>2</sup> .s <sup>-1</sup> ]	C [K]	References
Distilled Water	T300/Fiberite 1034	16,3	6211	Loos & Springer (1979) [122] The value of $D_0$ for AS/Hercules 3501-5 in Saturated Salt Water is from Tsai (1987) [159]
	AS/Hercules 3501-5	768	7218	
	T300/Narmco 5208	132	6750	
Saturated Salt Water	T300/Fiberite 1034	5,85	6020	
	AS/Hercules 3501-5	5,38	6472	

Moisture Exposition	Material	$D_0 \times 10^6$ [m <sup>2</sup> .s <sup>-1</sup> ]	C [K]	References
	T300/Narmco 5208	6,23	5912	
Humid Air	T300/Fiberite 1034	2,28	5554	
		0,44	5058	Shen & Springer (1976) [148]
	AS/Hercules 3501-5	6,51	5722	Loos & Springer (1979) [122]
		0,44	4768	Whitney & Browning (1978) [165]
		28,8	6445	DeIasi & Whiteside (1978) [80]
	T300/Narmco 5208	0,57	4993	Loos & Springer (1979) [122]
		0,41	5231	Augl & Berger (1976) [55]
	Fiberite 934	4,85	5113	Shen & Springer (1976) [148]
		16,4	5992	DeIasi & Whiteside (1978) [80]
	Hercules 3501-5	16,1	5690	
	Narmco 5208	2,8	5116	Augl & Berger (1976) [55]
		0,051	4060	McKague et al. (1978) [128]
		4,19	5448	DeIasi & Whiteside (1978) [80]

### 5.12.1.5 Trends in the variation of mechanical properties

Moisture absorption effects on mechanical properties of composite materials are more noticeable when they are associated to changes in temperature (hygrothermal effects).

In the absence of extensive data, the following trends have been deduced by Tsai (1987) [159] from calculations based on a micro-macro mechanics analysis for a typical laminate of given:  $E_m$ ,  $E_f$ ,  $X_m$ ,  $X_f$ ,  $\phi$ ,  $T_g$ ,  $T_c$  (curing temperature) and  $G$ .

The influence of temperature is given as a function of a dimensionless temperature,  $\tau$

$$\tau = \frac{T_g - T_s G - T}{T_g - T_s G - T_o} \quad [5-22]$$

which is based on a dry glass transition temperature,  $T_g$ , and a built-in temperature shift  $T_s = 2000$  K, due to moisture absorption.  $T$  is the operating and  $T_o$  the ambient temperature.

For unidirectional composite laminates, the following trends have been observed:

1. The swelling due to moisture absorption relieves curing stresses and increases both the limit and the ultimate strength. The effect on the first is greater than on the second.

2. The beneficial effect of moisture is partially offset by the decreasing in the glass transition temperature of the matrix by moisture absorption. In addition moisture affects the corrosion resistance of certain glass fibers.
3. A three-dimensional diagram of tensile strength versus both temperature,  $T$ , and moisture content,  $G$ , will show the same trends with different values of  $T$  as for cold conditions. The lowest values will correspond to cold/dry conditions, due to curing residual stresses. The highest values will correspond to cold/wet conditions, where absorbed moisture cancels the curing-induced stresses.

On the other hand, for a given  $G$ , the strength decreases at high temperature due to reduced matrix strength.

These considerations can not be translated directly to angle plied laminates where both layup and the nature of the applied load have as much effect as temperature and moisture.

Moisture does not seem to affect the fatigue life of carbon fiber reinforced laminates at room temperatures. No reliable fatigue data seem to exist for combined temperature and moisture.

## 5.13 Postlaunch environmental effects

### 5.13.1 Ascent

#### 5.13.1.1 Outgassing

A list of composite materials meeting Johnson Space Center vacuum stability requirements for polymeric materials is given in Table 5-77.

**Table 5-77: Outgassing Data for Typical Composite Materials**

Material	% TML	% CVCM	Cure Time [h]	Cure Temp. [K]
<u>Thermosets</u> Glass/Epoxy (E720)	0,54	0,04		
Glass/Epoxy (G10)	0,10	0,01		
Glass/Epoxy (G11)	0,61	0,03		
Glass/Epoxy (GE101)	0,48	0,05		
Glass/Epoxy (Hexcel F161)	0,30	0,02	2,75	436
Glass/Phenolic	0,64	0,00		
Glass/Phenolic (Ferro CPH 2209)	0,53	0,00	As received	
Glass Polyimide (Hexcel F174)	0,40	0,00		
S-Glass/Epoxy (Scotchply XP251-S)	0,58	0,01	0,5	413

Material	% TML	% CVCM	Cure Time [h]	Cure Temp. [K]
Silica Fiber/Silicon Rersin	0,21	0,03	16	477
Graphite/Epoxy (Fiberite HY-E-1334)	0,97	0,01	1	450
Graphite/Epoxy (Thornel T300/934)	0,62	0,00		
Kevlar 49/Epoxy (Hexcel F164)	0,00	0,00	3	450
Kevlar/Polyimide (Skybond 703)	0,85	0,00		
<u>Thermoplastics</u> Teflon FEP	0,06	0,06		
Teflon TFE	0,10	0,03		
Nylon 6/6-glass (70/30)	0,81	0,04		
Delrin (Acetal)	0,48	0,07		
KEL-F	0,03	0,01		
Polycarbonate/glass laminated	0,10	0,01		
Acrylic	0,57	0,01		
Polypropylene/glass	0,13	0,04		
Polyphenyle oxide	0,04	0,03		
Polystyrene	0,26	0,01		
Polysulfone	0,33	0,00		
Polysulfone/glass (70/30)	0,24	0,01		

NOTE From Lubin & Dastin (1982) [123].

### 5.13.2 Orbital effects

Material property degradation data under the effect of the vacuum radiation environment of space are presented here for the specimens in Table 5-78.

**Table 5-78: Characterization of Materials Tested under a Vacuum Radiation Environment**

Spec. No.	Laminate	Matrix	Fiber	Fiber Angle [°]	Fiber Volume $\varphi_f$	Environment	References
1		CY 209 Epoxy HT 972 Hardener	Thornel 75 S Carbon	0	0,50 to 0,55	UV, Electron, Proton	Bassewitz (1974) [61]
2	T300/3M SP288	3M SP288 Epoxy	T300 Graphite	0		UV, Electron, UV+Electron	Tennyson & Zimcik (1982) [154], Hansen & Tennyson (1983) [95]
3				90			
4				(±43) <sub>s</sub>			
5	3M SP306	Epoxy	Kevlar	0			
6				90			
7				(±43) <sub>s</sub>			
8	C6000/P1700	P1700 Polysulfone	C6000 (Celanese Corp.)		0,479	UV, Electron	Giori, Yamauchi, Rajan & Mell (1983) [93]
9	T300/934	Fiberite 934 Epoxy (Fibe-rite Corp.)	T300 Thornel (Hercules, Inc.)		0,475		
10	T300/5208	Rigidite 5208 (Narmco)			0,603		
11	T50(PAN)/F263 (Hexcel Corp.)	Hexcel F 263 Epoxy	T50(PAN) HM Graphite	(0/90) <sub>2S</sub>	0,6±0,02	Electron	Mauri & Crossman (1983) [125]
12	75S(Pitch)/948A1 (Fiberite Corp.)	948A1 Epoxy	VHM Graphite				
13	Kevlar 49/E719 UX Polymeric Co.	E719 Epoxy	Kevlar 49				

Only linear thermal expansion data are given, whereas trends for degradation of mechanical properties are shortly outlined.

### 5.13.2.1 Test facilities

The tests have been undertaken by use of different facilities which are described here for later reference.

TF1. Samples  $2 \times 10^{-3}$  m thick irradiated with a Xenon lamp (450 W), 8,35 Sun levels, up to 500 ESD. Sample temperature held at 323 K - 324 K during irradiation.

Samples  $0,5 \times 10^{-3}$  m thick were exposed to a dose of  $3 \times 10^9$  rad electron with a particle energy of 40 keV and subsequently to a dose of  $05 \times 10^9$  rad at 700 keV.

Samples, required for shear tests,  $10^{-2}$  m thick, were exposed to doses of  $10^9$  rad to  $5 \times 10^9$  rad, 2 MeV electrons, first on one face and then on the other.

Samples  $05 \times 10^{-3}$  m thick were exposed to proton radiation with fluxes of  $3 \times 10^9$  p.m<sup>-2</sup> up to  $23 \times 10^{20}$  p.m<sup>-2</sup>.

All the above irradiations were applied separately from each other.

TF2. Thermal vacuum radiation facility. Its working chamber is 0,46 m diameter, 0,33 m long. Operating pressure was  $1,33 \times 10^{-4}$  Pa. Temperatures from 290 K to 450 K, with 1 K difference on any sample. Thermal cycling tests were also run in hard vacuum ( $1,33 \times 10^{-4}$  Pa to  $1,33 \times 10^{-5}$  Pa).

UV radiation with UV Xenon compact arc lamp (Canrad Hanovia 976C0010) up to 180 ESD.

Up to 30 specimens are supported on a carousel arrangement which can be turned externally. When required, loading can be supplied by an external hydraulic piston.

The lower half of each sample is shielded from direct UV radiation in order to separate UV radiation from thermal vacuum effects. Since the temperatures of the shielded and unshielded parts of the sample were slightly different they are independently measured.

The high energy electron source consisted of a Strontium-90 foil contained in a plexi-glass holder mounted on the chamber wall. The front panel of this holder can be lowered from outside the chamber to allow samples directly in front of the foil to be irradiated.

Radiation dose up to  $20 \times 10^3$  rad.

TF3. A-H6 high pressure, quartz-jacketed, water cooled mercury-arc lamp.

Equivalent exposure times were 210, 480, 720, 960 ESH.

Samples held in pyrex tubes 0,038 m diameter, 0,305 m long at  $1,33 \times 10^{-5}$  Pa.

TF4. Electron Linear Accelerator of IRT Corp., San Diego, CA. 92121,12 MeV beam.

Total doses were  $5 \times 10^7$ ,  $10^8$ ,  $5 \times 10^8$ ,  $10^9$  rads.

Mean dose rate: 10,8 krad/sec. At this dose rate the irradiated samples reached a temperature of 322 K. Pressure not given.

Samples held in pyrex tubes as above.

TF5. Electron Accelerator of the Boeing Radiation Facility, Seattle, Washington.

1,5 MeV impinging on the test specimen in vacuum ( $1,33 \times 10^{-4}$  Pa to  $1,33 \times 10^{-3}$  Pa), 296 K.

This facility does not simulate the proton energy distribution in Space, the dose rate or the combined effects of electrons and protons.

Total doses:  $1 \times 10^3$  rads,  $3 \times 10^9$  rads

### 5.13.2.2 Measurement methods

MM1. Bending, pull and shear tests were performed ex situ after irradiations. The samples were held at 330 K to 340 K during the tests.

MM2. In situ measurements of thermal strains were made using bonded surface straining gauges. For low  $\beta$  configurations the strain gauges were calibrated interferometrically.

No tests on the influence of moisture contents were performed on these samples.

MM3. Ex situ.

In order to control the moisture content, the cartridge tubes containing the composite samples were dried at 390 K overnight under reduced pressure. The tubes were subsequently evacuated to  $1,33 \times 10^5$  Pa or less.

MM4. Specimen sizes:  $76 \times 10^{-3}$  m,  $13 \times 10^{-3}$  m,  $10^{-3}$  m thick.

Spec. No. 10 was cured at 450 K molded in an autoclave from commercial prepreg tape. Spec. Nos. 11 and 12 were cured at 390 K.

All specimens were maintained in the dry condition after cutting.

Tests performed before and after irradiation.

Thermal expansion was measured on a standard laboratory dilatometer over the temperature range 140 K to 390 K.

Specimens were transferred to the Boeing Radiation Facility in sealed aluminium desiccators containing Drierite. Prior to irradiation, they were degassed in vacuum. After irradiation the specimens were repackaged in the desiccators and maintained in this condition until just prior to testing.

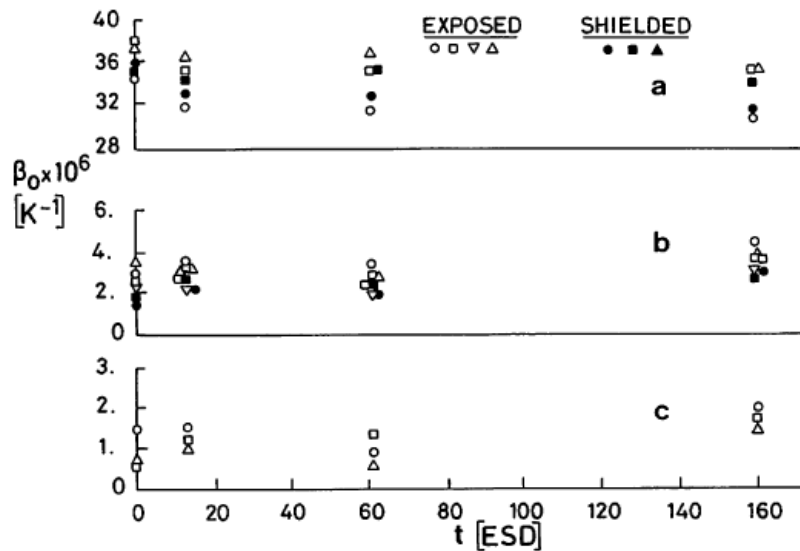
### 5.13.2.3 Radiation effects on the coefficient of linear thermal expansion

The data which will be introduced in the following are summarized in Table 5-79.

**Table 5-79: Summary of the Data Regarding Radiation Effects on the Coefficient of Linear Thermal Expansion for the Specimens Characterized in Table 5-78**

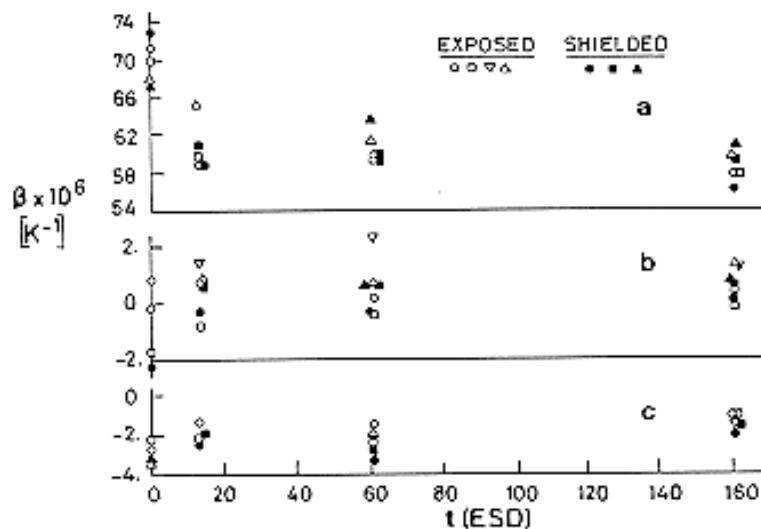
Spec. No.	Laminate	Test Facility	Measurement Method	Radiation	
				Ultraviolet	Electrons
1					
2	T300/SP288	TF2	MM2	Figure 5-45 Figure 5-47	Figure 5-47
3					
4					
5	3M SP306	TF2	MM2	Figure 5-46 Figure 5-47	
6					
7					
8	C6000/P1700	TF3 TF4	MM3		
9	T300/934				
10	T300/5208				
11	T50(PAN)/F263	TF5	MM4		Figure 5-48
12	75S(Pitch)/948A1				Table 5-80
13	Kevlar 49/E719				





Note: non-si units are used in this figure

Figure 5-45: Effect of UV radiation on linear thermal expansion,  $\beta$ , of Graphite/epoxy T300/SP 288 laminates. a)  $\theta = 90^\circ$ , b)  $\theta = (\pm 43^\circ)_s$ , c)  $\theta = 0^\circ$ . Ambient pressure  $10^{-4}$  Pa to  $10^{-5}$  Pa. From Tennyson & Zimcik (1982) [107], Hansen & Tennyson (1983) [153].



Note: non-si units are used in this figure

Figure 5-46: Effect of UV radiation on linear thermal expansion,  $\beta$ , of Kevlar/epoxy 3M SP 306 laminates. a)  $\theta = 90^\circ$ , b)  $\theta = (\pm 43^\circ)_s$ , c)  $\theta = 0^\circ$ . Ambient pressure  $10^{-4}$  Pa to  $10^{-5}$  Pa. From Tennyson & Zimcik (1982) [154], Hansen & Tennyson (1983) [95].

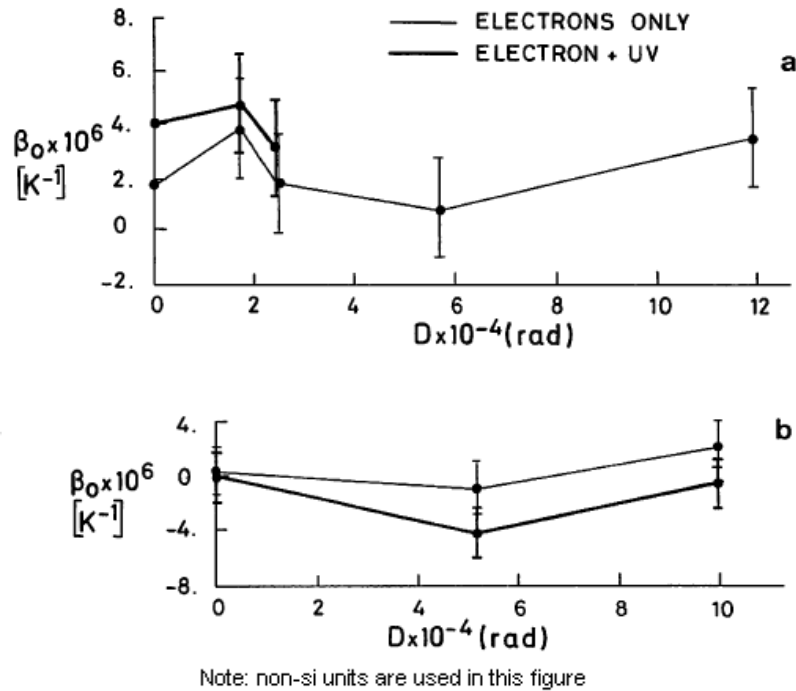


Figure 5-47: Effect of electron radiation with (thick solid line) and without (thin solid line) UV exposure, on linear thermal expansion,  $\beta_0$ , of graphite/epoxy and Kevlar/epoxy,  $\theta = (\pm 43^\circ)_s$ . Ambient pressure  $10^{-4}$  Pa to  $10^{-5}$  Pa. Exposure > 1 year and 300 ESD of UV. From Hansen & Tennyson (1983) [95].

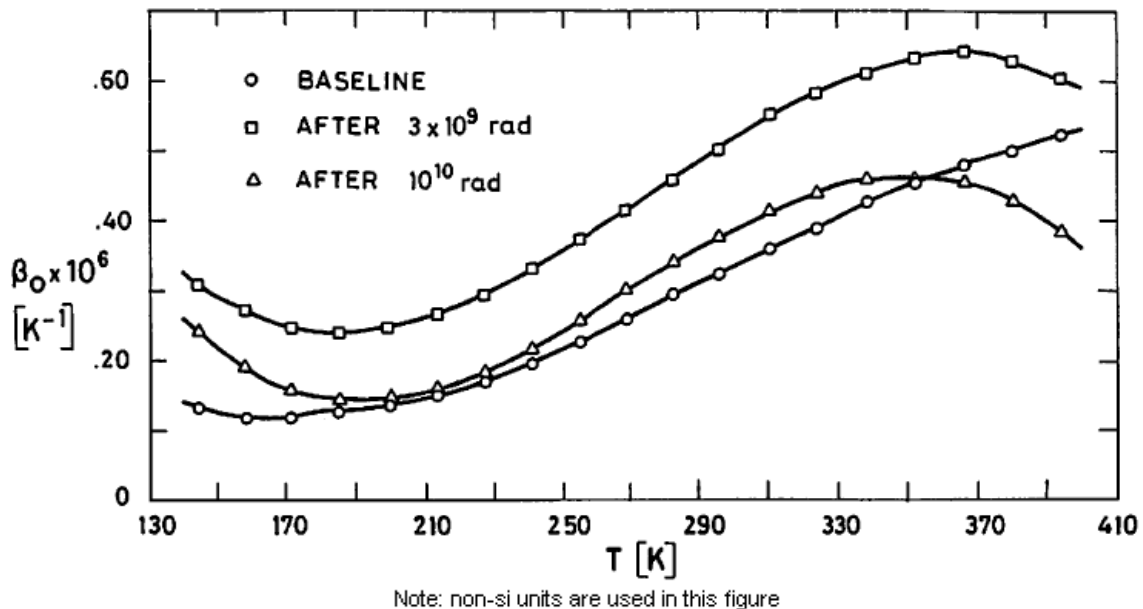


Figure 5-48: Linear thermal expansion,  $\beta_0$ , as a function of temperature,  $T$ , of T50(PAN)/F263 (0/90)<sub>2s</sub> HM graphite/epoxy laminates exposed to electron radiation. Calculated by the compiler by numerical derivation ( $\beta = d(\Delta L/L)/dT$ ) of data from Mauri & Crossman (1983) [125].

**Table 5-80: Average Values of Linear Thermal Expansion,  $\beta$ , for 75S(Pitch)/948A1(0/90)<sub>2s</sub> Graphite/Epoxy Laminates in the Temperature Range 280 K - 370 K**

Specimen	Run	$\beta_0 \times 10^6$ [K <sup>-1</sup> ]
Baseline, 2	1	0,54
	2	0,49
3 x 10 <sup>9</sup> rad, 1	1	0,49
	2	0,43
3 x 10 <sup>9</sup> rad, 2	1	0,23
	2	0,23

NOTE From Mauri & Corssman (1983) [125].

#### 5.13.2.4 Trends in the variation of mechanical properties

Spec. No. 1

UV radiations during 500 ESD resulted in a bending modulus degradation of 21 % without change in bending strength.

Electron irradiated samples suffered a 8 % degradation of the tensile modulus, a 28 % degradation of the bending modulus and a bending strength degradation of 16 %. Shear tests indicated an improvement of the shear strength up to 10<sup>9</sup> rad (2 MeV) followed by a degradation under higher doses.

No degradation was observed of the tensile modulus after proton irradiation at a dose of 20 x 10<sup>9</sup> rad. After a dose of 0,2 x 10<sup>12</sup> rad the tensile modulus experimented a decrease of 22 %.

Ref. Bassewitz (1974) [61].

Spec. Nos. 2 to 7.

UV radiations up to 160 ESD were found to produce no significant changes for the material laminates investigated.

Ref. Tennyson & Zimcik (1982) [154], Hansen & Tennyson (1983) [95].

For the dosage levels achieved up to the present ( $\approx 10^5$  rad) no change in  $\beta$  is discernible.

Ref. Hansen & Tennyson (1983) [95].

Spec. Nos. 8 to 10.

With the exception of C6000/P1700 samples, there is no evidence to indicate that UV and electron exposed samples are different from the control samples.

Ref. Giori, Yamauchi, Rajan & Mell (1983) [93].

Spec. Nos. 11 to 13.

The graphite/epoxies cured at 390 K and 450 K are not significantly altered except at the highest temperature (390 K) of the mechanical test where the 450 K curing epoxy systems experienced a degradation of matrix-dependent properties of up to 20%.

In contrast to the excellent stability shown by T50(PAN)/F263 and 75S(Pitch)/948 A1 graphite/epoxies to electron irradiation at high doses, the 390 K curing Kevlar/epoxy composite suffered severe

radiation-induced degradation in shear strength, which probably renders it unsuitable for use in external spacecraft primary structural components.

Ref. Mauri & Crossman (1983) [125].

### 5.13.2.5 Atomic oxygen effects

The operation of many satellites in low earth orbit (LEO) presents a serious problem, since continuous exposure to atomic oxygen at an orbital velocity of over  $8 \text{ km.s}^{-1}$  affects exposed organic surfaces. In connection with spacecraft, the phenomenon was discovered after one of the first Space Shuttle flights (STS-3 flight) but it was already well known from other situations of technical interest (Dauphin (1985) [77]).

Satellites such as space stations, which are expected to last 15-30 years in low earth orbit, will need protective coatings for light weight subsystems, otherwise these subsystems will disappear due to the erosion produced by atomic oxygen.

Outgassing and thermo-optical data for polymeric materials in the as-received state are of minor relevance and, for prolonged missions, knowledge of the characteristics modified by the environment is essential for appropriate planning.

According to Leger & Visentine (1986) [118], material loss is a function of the flux (number of oxygen atoms per unit area and per unit time), and is proportional to atmospheric density, orbital velocity, surface angle to velocity vector, and duration of exposure. Atmospheric density depends on altitude and on solar activity. Over a solar cycle (approximately 10 years) atmospheric density changes by several orders of magnitude. In addition, dayside heating and nightside cooling superimpose a factor of two to the change during nominal solar activity.

In addition to atomic oxygen the environment at LEO altitudes is characterized by (Haruvy (1990) [100]):

1. Ionizing radiation. Electrons with energies as high as 5 MeV and protons, up to 400 MeV.
2. UV radiation with energy fluxes of  $400 \text{ W.m}^{-2}$ .
3. Temperature cycling. More than  $10^4$  cycles.yr<sup>-1</sup> and temperature extremes of 120 K and 420 K.
4. High vacuum. Typical values of  $10^{-9}$  Pa to  $10^{-7}$  Pa, and  $10^{-4}$ Pa near the satellite due to outgassing.

The induced outgassing problem is particularly serious because of two reasons: first fragmented macromolecules of relatively high molecular weight appear, adding to the CVCM contaminating inventory. Secondly, the fragmented macromolecules are produced at the surface of the eroded material finding an easy way to migrate towards the contamination sensitive sites.

Paradoxically enough, the contamination problem worsens at low atomic oxygen fluxes or in highly sheltered areas. Since the incoming oxygen atoms are not sufficient for complete oxidation of the organic molecules, fragmented oligomers may be formed increasing the CVCM inventory.

The sensitivity of a given material to atomic oxygen is expressed by the reaction efficiency parameter,  $R_e$  [ $\text{m}^3.\text{atom}^{-1}$ ], which is the volume of material lost per incident oxygen atom. For convenience, the results are normalized to Kapton-H as a reference material.

Most of the available reaction efficiency data were obtained on material science experiments performed on board STS-5 and STS-8 Shuttle flights.

More than 300 individual samples were exposed to normal-to-the surface conditions for 41,75 h, leading to a total atomic oxygen flux of  $3,5 \times 10^{24} \text{ atom.m}^{-2}$  in the STS-8 Atomic Oxygen Effects

Experiment (Visentine, Leger, Kuminecz & Spiker (1985) [162]). The basic experimental approach consisted of exposing samples to the LEO environment and then returning them for ground-based laboratory analysis. Most of these samples were exposed in disc form ( $25,4 \times 10^{-3}$  m diameter), however film strips, woven cables and fabrics were also tested.

Reaction efficiencies, measured by mass change, of several organic films were in the range of  $3 \times 10^{-30}$  m<sup>3</sup>/atom. Effects of parameters such as temperature and solar radiation were assessed as was the importance of atmospheric ionic species on surface recession.

Reaction efficiencies so far obtained have errors of the order of 30 % to 50 %, mainly due to errors in predicting density. Since then, several ground test facilities have been designed, built and tested (Zimcik et al. (1985) [171], McCargo et al. (1985) [126], Morrison et al. (1988) [130],...) and valuable data on thin film polymeric materials, coatings and paints are beginning to appear.

Relevant data for composite materials are summarized in Table 5-81.

**Table 5-81: Atomic Oxygen Reaction Efficiency Data from Reported LEO Flights and Ground Testing**

Material	$R_e \times 10^{30}$ [m <sup>3</sup> /atom]	$R_e/(R_e)_{\text{Kapton H}}$	Comments and References
Kapton H	3,0	1	Flight data Visentine, Leger, Kuminecz & Spiker (1985) [162]
Mylar	3,0-3,6	1-1,2	
Clear Tedlar	3,2	1,1	
Polyethylene	3,3	1,1	
Teflon TFE	< 0,05	< 0,02	
Kapton F	< 0,05	< 0,02	
Fiberite 1034 C Epoxy	2,1	0,70	Flight data Leger & Visentine (1986) [118]
Narmco T300/5208 Graphite/Epoxy	2,6	0,87	
Ferro CE 339/HMS Graphite/Epoxy	3,6	1,2	Ground test data McCargo, Dammann, Cumming & Carpenter (1985) [126]
Fibertie 934 Graphite/Epoxy	4,2	1,4	
Ferro CE 339 Siloxane Coated	0,6	0,2	
PTFE/Epoxy/Fiberglass	8,4	2,8	

Generally speaking, good agreement between in-flight and laboratory simulation experimental results has been obtained for polymeric materials that are readily eroded by impingement of oxygen atoms,

and also for those almost unaffected by it. Controversy still exists regarding the vulnerability of partially erodable polymeric materials, namely fluorinated polymers (TFE and FEP).

In the case of Teflon FEP the simulation erosion rates were two orders of magnitude higher than those in space.

The total energy and the flux of the oxygen atoms eroding the polymeric materials in simulation experiments should be controlled so that the supposedly correct space data be reproduced, even in the case of the fluoropolymers.

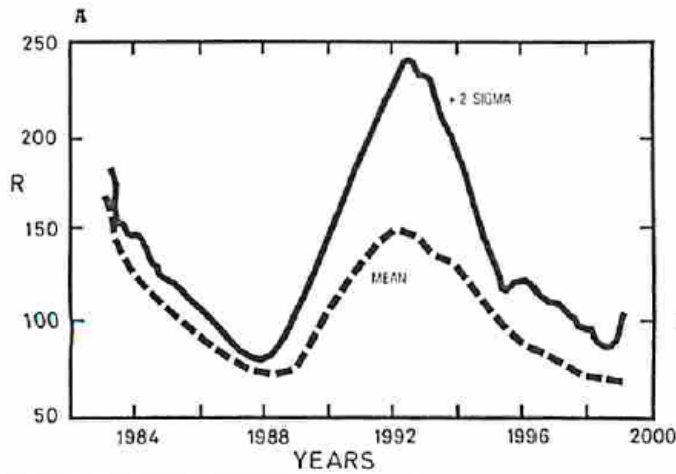
Haruvy (1990) [100] has recently noted that the following four polymers, namely: a) Kapton H (polyimide), b) Kynar (fluorocarbon), c) Teflon FEP (polyfluoroethylenepropylene), and d) Silicone Rubber (polysiloxane), exhibited in the STS experiments relative reaction efficiencies,  $R_e/(R_e)_{\text{Kapton H}}$  of 1, 0,2, 0,05 and  $\approx 0$ , respectively. What is then actually needed for a reliable prediction of material durability in LEO is a calibrated simulation facility in which these ratios are maintained.

Since the existing facilities produce the oxygen atoms by a wide variety of methods and in a wide range of energies, the calibration process should pay the attention to the energy supplied to a given flux, in order to reproduce the in-flight experimental results.

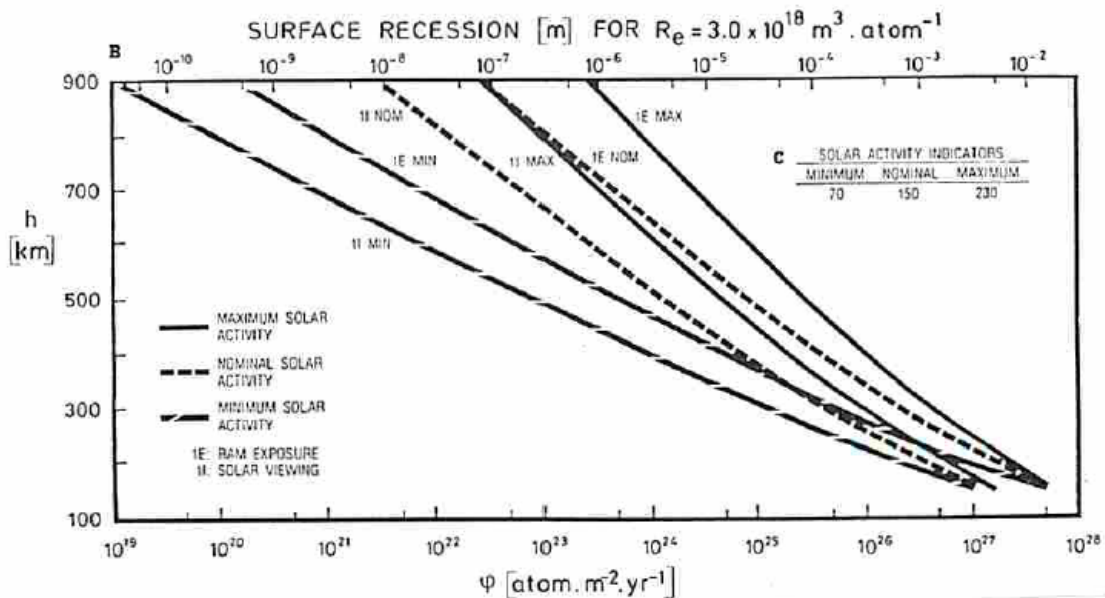
On the other hand, the gap between Kynar (0.2) and Kapton H (1.0) could well be filled with Tedlar at various degrees of fluorination.

The estimation of the material depletion by atomic oxygen can be made by using Figure 5-49. This estimation is based on the assumption of a linear relationship between atomic oxygen-induced erosion, flux and time. It has been suggested (see Haruvy (1990) [100]) that matters are not so simple and that the higher the flux the more the erosion rate increases.

The solar activity graph, A, shows mean and mean plus 2 standard deviations (+2 $\sigma$ ) activity predictions for the present solar cycle. The graph gives the solar flux index (or sunspot number,  $R^a$ ), for each year the spacecraft will be in low Earth orbit.



The flux profile graph, B, should be used in connection with the solar activity indicator, C. Two curves are shown for each one of three typical levels of activity. 1E concerns the spacecraft surface always opposite to the atomic oxygen beam, and 1I, always pointing to the Sun. Once selected the altitude, solar activity and surface orientation, the atomic oxygen flux,  $\phi$ , is deduced from abscissae in B. Multiplying this value by  $R_e$  of the concerned material gives the yearly recession, in m, of a square meter of surface material.



<sup>a</sup> The sunspot number,  $R$ , also called Wolf number, is given (Priest (1982)) by:

$$R = K(f+10g)$$

where  $f$  is the number of sunspots,  $g$  the sunspot groups, and  $K = .6$  an observer correction factor.

Note: non-si units are used in this figure

Figure 5-49: Graphs for estimating the depletion by atomic oxygen of a material of known Reaction Efficiency,  $R_e$ . From Leger & Visentine (1986) [118].

### 5.13.3 Re-entry effects

#### 5.13.3.1 Oxidation

For applications in the temperature region 550 K - 620 K, and within the Earth atmosphere, both components of a graphite fiber/high temperature polymer composite should be resistant to oxidation.

Although the graphite fiber is encapsulated in the polymer matrix, air permeates the composite material, either through the matrix or by way of interface, and can destroy the bond at the fiber/polymer interface. This particularly occurs when the polymer is more resistant to oxidation than the fiber. It is often said that a graphite fiber containing a high concentration of surface sodium shows poor thermo-oxidative stability. Fiber surface impurities could result from the PAN precursor or from the surface treatment process.

The excellent high-temperature characteristics of Graphite fiber or Carbon/Carbon composites, Figure 5-41, can be achieved in inert atmospheres only, unless protective coatings are used.

The thermo-oxidative stability of a composite material is measured through the weight loss after isothermal aging for sufficiently large time periods (Scola & Laube (1988) [146]). In this particular case samples were aged in an air circulating oven ( $Q = 6 \times 10^{-3} \text{ m}^3/\text{h}$ ) at 598 K. Periodically samples are removed for weighting and returned to the oven for aging up to a total time of 4000 h.

In order to relate the thermo-oxidative stability of the fibers to their surface composition, ESCA analysis is performed.

In ESCA technique (also known as XPS) the surface to be analyzed is irradiated with soft X-rays. Photoelectrons and Auger electrons are excited and can escape the sample surface, without loss of energy, provided that their initial deep into the surface is smaller than the Inelastic Mean Free Path (IMFP). The binding energies of these photo and Auger electrons depend on the atomic number and chemical environment of the excited atom. The IMFP, in its turn, is a function of the electron energy and of the angle between the surface and the analyzer. The depth of information, which is further restricted by the fact that electrons leave the surface of a bunch of fibers at angles between grazing and normal, is of the order of  $0 \text{ \AA} - 10 \text{ \AA}$  for electron energies to approximately 500 eV. In practice a nominal sputter depth is quoted, although the surface of a bunch of fibers is not uniformly sputtered.

Weight loss of several carbon and graphite fibers after aging in flowing air has been collected in Table 5-82.

**Table 5-82: Weight Loss, WL (%), of Carbon Fibers After Isothermal Aging in Flowing Air**

Type	T [K]	Q x 10 <sup>6</sup> [m <sup>3</sup> .s <sup>-1</sup> ]	t [h]							
			3	233	425	1001	1500	2009	3425	4512
Celion HM (99,7%C) <sup>a</sup>	670		0,05							
Celion HM (99,6%C)			0,02							
Celion 3000/6000			3-5							
Celion 6000 (unsized) <sup>b</sup>	580	1,7		2,30	6,70	27,5	47,7	65,2	94,0	
Celion 6000 (epoxy sized)				4,90	9,70	31,3	46,8	64,3	94,0	
GY70 <sup>a</sup>	670		0,1							
G40-700 (unsized) <sup>b</sup>	580	1,7		0,40	0,45	1,00	1,90	2,70	5,50	6,97



Type	T [K]	Q x 10 <sup>6</sup> [m <sup>3</sup> .s <sup>-1</sup> ]	t [h]							
			3	233	425	1001	1500	2009	3425	4512
G40-700 (epoxy sized)				1,60	1,65	1,90	2,50	2,90	4,70	5,51
Hercules AS <sup>a</sup>	670		98,7							
Hercules AS4 (unsized) <sup>b</sup>	580	1,7		2,80	5,70	23,6	51,1	78,0		
HMS <sup>a</sup>	670		3,3							
IM6 (unsized) <sup>b</sup>	580	1,7		1,30	2,10	7,50	14,3	23,5	54,1	74,1
Thornel 50 <sup>a</sup>	670		9,6							
Thornel 300			99,3							
T40R (unsized) <sup>b</sup>	580	1,7		0,15	0,19	0,30	0,45	0,60	0,67	0,78
T300R (unsized)				1,30	1,50	5,50	10,6	17,4	45,4	60,4
UCC pitch <sup>a</sup>	670		4,6							
UCC VS All pitch			0,6							
VM 0032 (UCC non-woven mat)			0,7							

<sup>a</sup> From Dresselhaus, Sugihara, Spain & Goldberg (1988) [84]

<sup>b</sup> From Scola & Laube (1988) [146]

ESCA surface analysis of a series of carbon fibers indicates that the chemical composition of their surface bears a direct relationship to oxidative stability. It could be illuminating to compare the composition as received and after oxidation of the fibers introduced in Table 5-82. This comparison has been summarized, considering only two extreme cases, in Table 5-83.

**Table 5-83: Chemical Composition, Atom (%), of both T40R and Hercules AS4 Carbon Fibers, as received and oxidized, ESCA**

Type	Sputter Depth [Å]	C	O	N	Na	S	F	Ca	Si
T40R As received	0	93,1	6,8		tr				
	50	98,6	1,2		0,3				
	100	98,8	1,1		0,2				
AS4 As received	0	70,1	24,3	5,4	0,1	0,1			
	50	90,8	5,4	3,7	0,2				
	100	93,0	3,5	3,4	0,1				
T40R Oxidized	0	94,3	3,8	tr		tr	1,8		tr
	50	96,5	1,6				1,7		
	100	97,3	1,0				1,5		
AS4 Oxidized	0	78,6	15,7	3,4		tr			2,3
	50	83,7	10,1	4,2	0,2				1,8
	100	86,9	7,4	3,8	0,1				1,7

NOTE From Scola & Laube (1988) [146].

It can be deduced from Table 5-83 that Carbon Fibers with the highest carbon content and lowest oxygen and nitrogen contents exhibit the greatest resistance to oxidation. The presence of sodium does not appear to influence the oxidative stability of the fibers, at least at levels up to 0,6 atom % according to Scola & Laube (1988) [146]. The role of other elements in influencing the oxidative stability of the fibers is not presently understood.

## 5.14 Thermal vacuum cycling

The results of several tests which have been made recently, regarding the effect of thermal vacuum cycling, with the specimens characterized in Table 5-84, are introduced here.

**Table 5-84: Characterization of Materials Tested under or after Thermal Vacuum Cycling**

Spec. No.	Laminate	Matrix	Fiber	Fiber Angle [°]	Fiber Volume $\varphi_f$	References
1 <sup>a</sup>		Rigidite 5208 Epoxy	Narmco HMS Narmco T300	0 <sub>T300</sub> [±52] <sub>SHMS</sub>		Hansen & Tennyson (1983) [95]
2	T300/3M SP288	3M SP288 Epoxy	T300 Graphite	(±22) <sub>s</sub>		Tennyson & Zimcik (1982) [154] Hansen & Tennyson (1983) [95]
3 <sup>b</sup>				(±43) <sub>s</sub>		
4 <sup>b</sup>				90		
5 <sup>b</sup>	3M SP306	Epoxy	Kevlar	0		
6				(±30) <sub>s</sub>		
7 <sup>b</sup>				(±43) <sub>s</sub>		
8				(±60) <sub>s</sub>		
9 <sup>b</sup>				90		
10	3M SP290	Epoxy	Boron	0		
11				90		
12 <sup>c</sup>		CY 203 Epoxy HT 872 Hardener	HMS		0,620	Reibaldi (1985) [141]

<sup>a</sup> Circular hybrid tubes.

<sup>b</sup> Same specimens as those in Table 5-78.

<sup>c</sup> Circular hybrid tubes. Sames as Specs. Nos. 42 & 43 in

### 5.14.1 Test facilities

TF1. A thermal-vacuum facility (SS1) with in-situ mechanical loading has been used. It consists in a cylindrical stainless steel chamber 0,51 m in diameter and 1,17 m long. Operating pressure was  $1,33 \times 10^{-4}$  Pa. Several LN<sub>2</sub> monitors and automatically controlled electric heaters allow the facility to run continuously for periods up to two weeks. Strain and temperature recordings are automated. A

mechanical loading fixture, attached to the chamber door, supplies uniaxial or torsional loading of specimens.

For long test periods (exceeding nine months) a long term thermal-vacuum cycling facility (SS2) has been developed. The working chamber is approximately .66 m in diameter, 0,76 m long. The vacuum is close to  $1,33 \times 10^{-6}$  Pa. Currently 120 flat laminates plus 38 tubes are mounted for testing. 33 of these specimens are strain gauged for monitoring thermal strains. The temperature is recorded with thermocouples. A mass spectrometer is also implemented for species determination.

TF2. Fast thermal cycling was performed by use of the accelerated thermal cycling chamber (ATC2) of ESTEC. See Larue (1982) [117] for a description of this facility. The useful dimensions for the test samples were 0,5 m x 0,5 m x 0,25 m. Six specimen tubes were accommodated inside the chamber. The acceleration factor was 50 compared to low orbit conditions. The tests were interrupted every 1000 cycles (or more often) for cutting sections of the specimens in order to monitor the microcracks.

Mechanical and thermal expansion tests were performed ex-situ.

The linear thermal expansion was measured in an old ESTEC facility. See Aalders (1989) [48] for the so called "1983 facility". It consisted of a vacuum chamber of .55 m diameter and 1,3 m long. The optics for the laser interferometer measurement system was positioned inside the shroud unit except the remote interferometer block which was outside the shroud and kept at constant temperature of 300 K monitored by a thermocouple. The interferometer and associated optics were especially prepared for vacuum use. A video recording system was used to perform a continuous monitoring of the length variation and specimen temperature.

The facility is pumped down to less than  $1,33 \times 10^{-3}$  Pa. The specimens were dried and de-gassed by heating at 340 K for 48 h. Then the laser system was adjusted and set to zero.

In order to increase the temperature from its lower end, the liquid nitrogen supply was stopped and the temperature rose, by thermal leaks, up to about 290 K. Beyond this, the heating system was activated in order to allow the specimen to reach 340 K.

### 5.14.2 Measurement methods

MM1. Thermal strains are measured in situ using bonded surface strain gauges. Laser interferometry is employed to calibrate the strain gauges in the case of tubular samples.

Circular tubes of hybrid construction were subjected to 6 months of storage in ambient laboratory or in a "dry" desiccators environment, in order to determine the extent to which initial values of the coefficient of thermal expansion,  $\beta$ , could be expected to change. Results are given in Table 5-86.  $\beta$  is measured in the axial ( $0^\circ$ ) direction.

It can be seen that significant increases in  $\beta$  are found in cases where the initial values were low.

MM2. Mechanical properties were measured before thermal cycling. In addition, a set of short compression tests was performed on the specimens after 3000 thermal cycles.

The tubes were inspected before, in-between and after thermal cycling to investigate the presence of microcracks in the matrix. Crack density was computed from the microstructure observations. The crack density increased with the number of thermal cycles (up to 2000 cycles). After extended thermal cycling (2000 to 3000 cycles) some delamination was observed.

Linear thermal expansion was measured before and after cycling by using laser interferometry.

### 5.14.3 Thermal vacuum cycling effects on the coefficient of linear thermal expansion

The data which will be introduced in the following are summarized in Table 5-85.

**Table 5-85: Thermal Vacuum Cycling Effects on the Coefficient of Linear Thermal Expansion of the Specimens Characterized in Table 5-84**

Spec. No.	Material	Test Facility	Measurement Method	Thermal Cycling		
				Storage	Thermal Ambient	Thermal Vacuum
1	Circular hybrid tube Graphite/Epoxy	TF1	MM1	Table 5-86	Table 5-87	
2	Laminate Graphite/Epoxy			Figure 5-50	Figure 5-50, Figure 5-52	
3				Figure 5-51	Figure 5-51, Figure 5-52	
4					Figure 5-52	
5				Laminate Kevlar/Epoxy		Figure 5-53, Figure 5-54
6						
7						
8						
9						
10	Laminate Boron/Epoxy				Figure 5-55	
11						
12	Circular hybrid tube Graphite/Epoxy	TF2	MM2			Figure 5-56

**Table 5-86: Effect of Storage on the Linear Thermal Expansion,  $\beta_0$ , of the Hybrid Tubes Identified as Spec. No. 1, in Table 5-84 and Table 5-85**

Sample	$\beta_0 \times 10^6 \text{ [K}^{-1}\text{]}$		
	Initial	Ambient Storage	Desiccator Storage
1	3,8	3,6	--
2	1,6	3,1	--
3	4,5	--	4,3
4	1,4	--	3,8

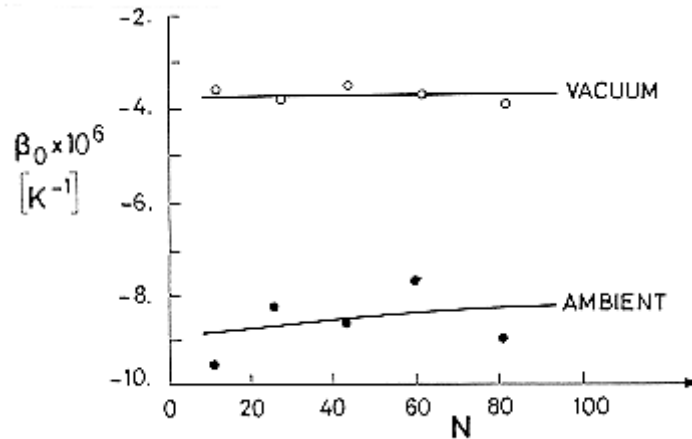
NOTE From Hansen & Tennyson (1983) [95].

**Table 5-87: Effect of Thermal Cycling (either Ambient or Vacuum) on the Linear Thermal Expansion,  $\beta_0$ , of the Hybrid Tubes Identified as Spec. No. 1 in Table 5-84 and Table 5-85<sup>a</sup>**

Sample	$\beta_0 \times 10^6 \text{ [K}^{-1}\text{]}$			
	Initial	Ambient Cycling		Vacuum Cycling
5	3,2	1060 Cycles	3,2	
6	1,6		2,5	
7	1,3		2,0	
2	1,6		177 cycles	2,63
8			77 cycles	3,94
9	1,4			3,46
10				4,19
11	1,6			3,85

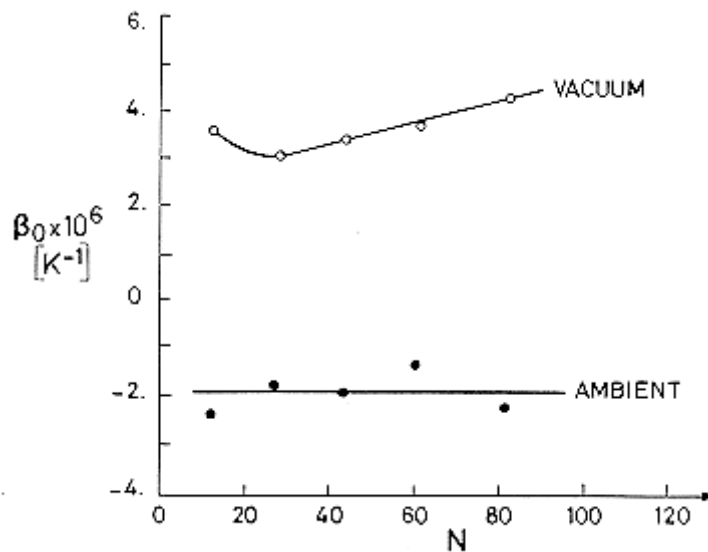
<sup>a</sup>  $300 \text{ K} \leq T \leq 370 \text{ K}$ ,  $p = 1,33 \times 10^{-4} \text{ Pa}$  to  $1,33 \times 10^{-5} \text{ Pa}$ .

NOTE From Hansen & Tennyson (1983) [95].



Note: non-si units are used in this figure

Figure 5-50: Effect of the number of thermal cycles,  $N$ , on the linear thermal expansion,  $\beta_0$ , of  $(\pm 22^\circ)_s$  T300/3M SP288 Graphite/Epoxy laminates.  $300 \text{ K} \leq T \leq 370 \text{ K}$ ,  $p = 1,33 \times 10^{-4} \text{ Pa}$  to  $1,33 \times 10^{-5} \text{ Pa}$ . From Tennyson & Zimcik (1982) [154], Hansen & Tennyson (1983) [95].



Note: non-si units are used in this figure

Figure 5-51: Effect of the number of thermal cycles,  $N$ , on the linear thermal expansion,  $\beta_0$ , of  $(\pm 43^\circ)_s$  T300/3M SP288 Graphite/Epoxy laminates.  $300 \text{ K} \leq T \leq 370 \text{ K}$ ,  $p = 1,33 \times 10^{-4} \text{ Pa}$  to  $1,33 \times 10^{-5} \text{ Pa}$ . From Tennyson (1980) [153], Tennyson & Zimcik (1982) [154], Hansen & Tennyson (1983) [95].

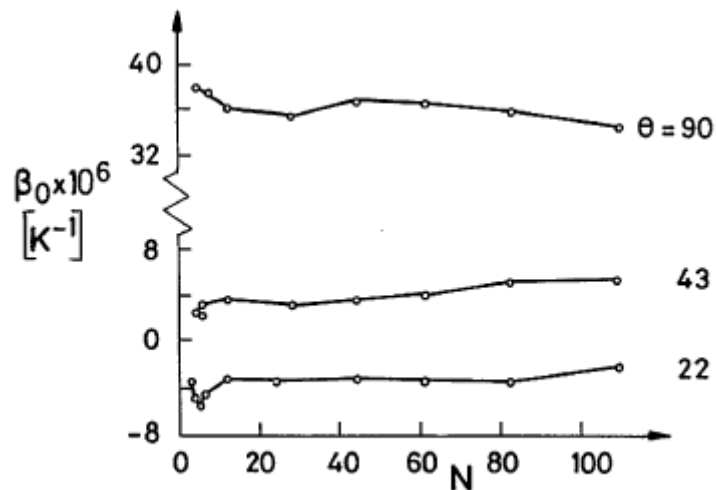
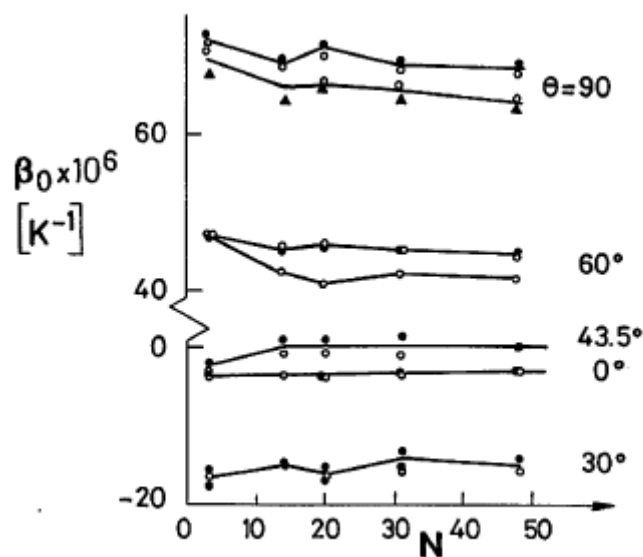


Figure 5-52: Effect of the number of thermal vacuum cycles,  $N$ , on the linear thermal expansion,  $\beta_0$ , of  $(\pm \theta^\circ)_s$  T300/3M SP288 Graphite/Epoxy laminates.  $300\text{ K} \leq T \leq 370\text{ K}$ ,  $p = 1,33 \times 10^{-4}\text{ Pa}$  to  $1,33 \times 10^{-5}\text{ Pa}$ . 50 cycles  $\approx$  220 days in vacuum. From Tennyson & Zimcik (1982) [154], Hansen & Tennyson (1983) [95].



Note: non-si units are used in this figure

Figure 5-53: Effect of the number of thermal vacuum cycles,  $N$ , on the linear thermal expansion,  $\beta_0$ , of  $(\pm \theta^\circ)_s$  3M SP306 Kevlar/Epoxy laminates.  $300\text{ K} \leq T \leq 370\text{ K}$ ,  $p = 1,33 \times 10^{-4}\text{ Pa}$  to  $1,33 \times 10^{-5}\text{ Pa}$ . 50 cycles  $\approx$  220 days in vacuum. From Tennyson & Zimcik (1982) [154], Hansen & Tennyson (1983) [95].



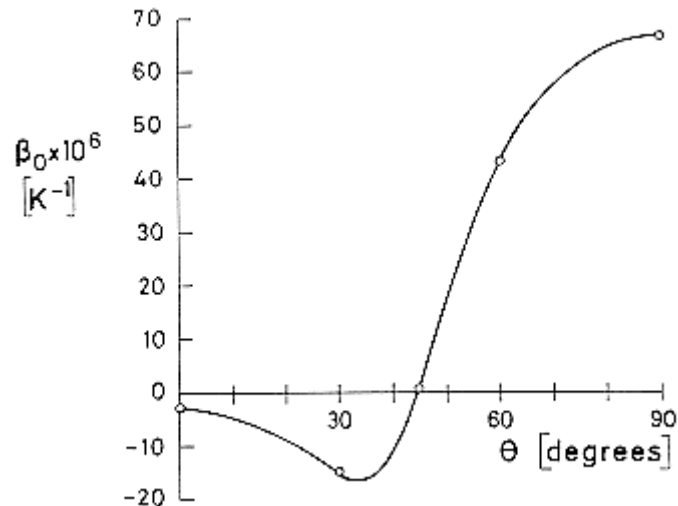


Figure 5-54: Comparison of predicted (-) and experimental (o) values of the linear thermal expansion,  $\beta_0$ , vs. fiber angle,  $\theta$ , for  $(\pm\theta^\circ)_s$  3M SP306 Kevlar/Epoxy laminates. 48 cycles  $\approx$  220 days in vacuum.  $300\text{ K} \leq T \leq 370\text{ K}$ ,  $p = 1,33 \times 10^{-4}\text{ Pa}$  to  $1,33 \times 10^{-5}\text{ Pa}$ . From Tennyson & Zimcik (1982) [171], Hansen & Tennyson (1983) [95]. Results for Graphite/Epoxy are given in Tennyson (1980) [153]. Compare also with Figure 5-27.

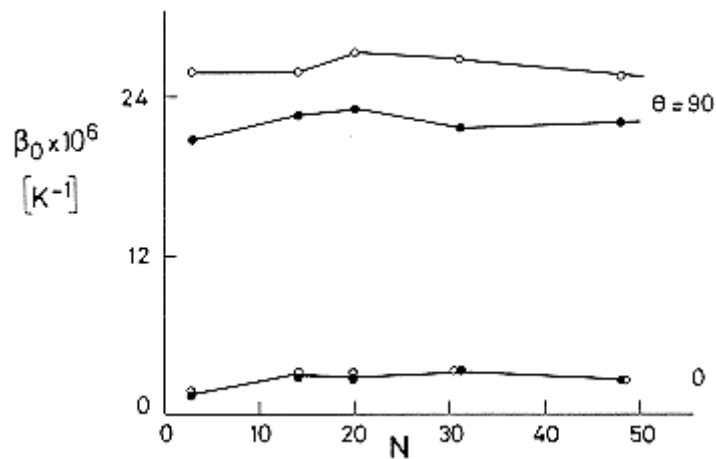
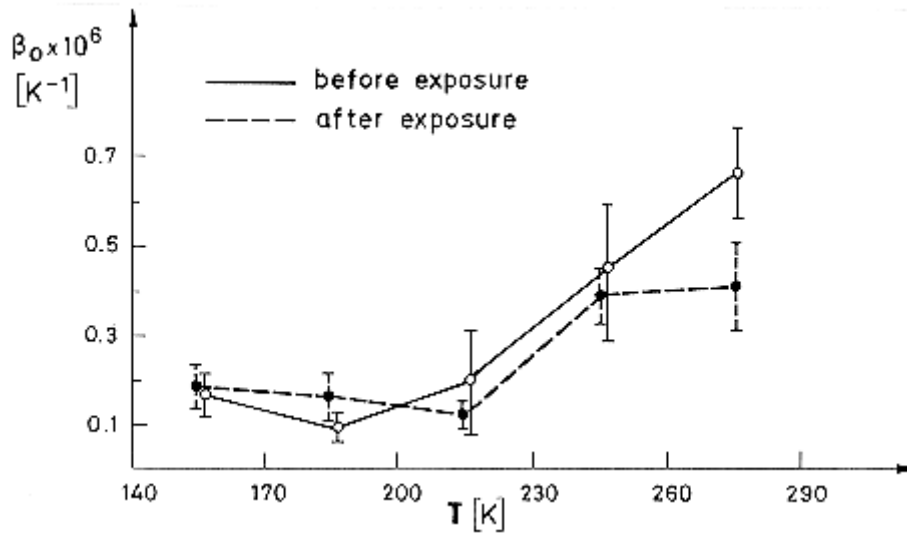


Figure 5-55: Effect of the number of thermal vacuum cycles,  $N$ , on the linear thermal expansion,  $\beta_0$ , of  $(\pm\theta^\circ)_s$  3M SP290 Boron/Epoxy laminates.  $300\text{ K} \leq T \leq 370\text{ K}$ ,  $p = 1,33 \times 10^{-4}\text{ Pa}$  to  $1,33 \times 10^{-5}\text{ Pa}$ . 50 cycles  $\approx$  220 days in vacuum. From Tennyson & Zimcik (1982) [154], Hansen & Tennyson (1983) [95].



Note: non-si units are used in this figure

**Figure 5-56: Coefficient of the linear thermal expansion,  $\beta_0$ , as a function of temperature,  $T$ , for Graphite/Epoxy circular hybrid tubes, identified as Spec. No. 12 in Table 5-84 and Table 5-85, before (solid line) and after (dashed line) thermal vacuum cycling, 3000 cycles,  $98 \text{ K} \leq T \leq 370 \text{ K}$ ,  $p = 1,33 \times 10^{-3} \text{ Pa}$ . From Reibaldi (1985) [141].**

#### 5.14.4 Trends in the variation of mechanical properties

No significant changes in mechanical properties have been reported in any case.

### 5.15 Coating application

#### 5.15.1 Pcbz conductive white paint

This thermal control coating can be applied to fiber-glass, carbon fiber or Kevlar composite materials.

The method of application as well as the main properties of this coating are given in [ECSS-E-HB-31-01 Part 6, clause 5.2.5.1](#).

#### 5.15.2 APA-2474 (TiO<sub>2</sub> white paint)

Application and properties of this coating on carbon reinforced composite materials are given in clause 5.9.

### 5.15.3 Wiederhold's Z-12321

#### 5.15.3.1 General

This coating system is widely used by the European Aeronautical industry on carbon fiber composite materials. No thermo-optical nor space environmental properties are given. The system consists of:

#### 5.15.3.2 Filling

Z-12207 Filler (from Hermann Wiederhold, Germany). It is constituted by two components to be added as follows:

100 pbw PE-F84/2,5 pbw PFH. Thinner: Z-12623, N 39400

Pot life: 40 min to 50 min at 293 K.

Tack free: 1 h at 293 K.

Final drying: 6 h to 8 h at 293 K.

#### 5.15.3.3 Priming

Z-12129 White primer (from SIKKENS, The Netherlands).

100 pbw Aerodin Primer 37045/30 pbw Hardener S 66/8

Thinner  $\leq 70$  pbw. Add thinner to reach a viscosity of 12 s - 13 s per DIN No. 4 cup (see [ECSS-E-HB-31-01 Part 6, clause 5.2.5.1](#)).

Final drying: 4 h at 293 K.

Thickness (dry):  $15 \times 10^{-6}$  m to  $25 \times 10^{-6}$  m.

#### 5.15.3.4 Thinning

Z-12607, C 25/90 S Thinner (from SIKKENS).

Formulation (percent by volume):

MEK  $30 \pm 1$

Butyl acetate  $10 \pm 1$

Cellosolve acetate  $40 \pm 1$

Toluene  $\leq 12$

Xylene  $\leq 8$

Cellosolve acetate is a trade-mark for ethylene glycol monoethyl ether acetate.

Catalyst: Z-12322, S 66/8R

This priming system resists to oils and lubricants up to 390 K, to SKYDROL 5008, to greases and to synthetic oils.

#### 5.15.3.5 Antierosion coating

Z-12536 over Z-12535 (from Hermann Wiederhold).

Z-12535 is constituted by

4 pbw N53636/1 pbw 39/1327 hardener. Thinner: 39/3460

Z-12536 is constituted by

4 pbw N53628/1 pbw 39/1327 hardener. Thinner: 39/3460

### 5.15.3.6 Finishing coating

Z-12321 (from Hermann Wiederhold).

Alternative bases: N53624, N53629, N53634, N53635, N39/2040

Catalyst: N39/1327. Thinner: Z-12607

## 5.16 Past spatial uses

### 5.16.1 Intelsat v

INTELSAT V, communication satellite (Figure 5-57), was launched on 6 December 1980 and placed in geosynchronous orbit five days later. It provides 12000 communication circuits, including telephone and television for the member nations of the INTELSAT Corporation.

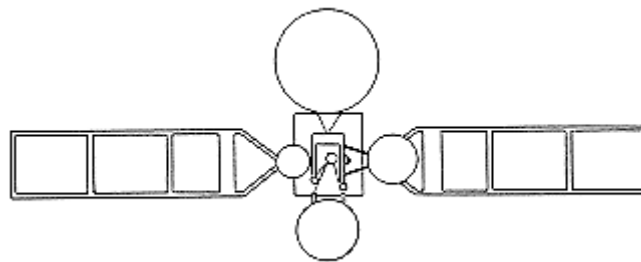


**Figure 5-57: Outline of INTELSAT V communication satellite.**

INTELSAT V was the first satellite in which extensive use of composite materials has been made (Hillesland (1980) [102]).

The requirements of low mass, low thermal expansion, stiffness, strength, and thermal stability are satisfactorily fulfilled. Over 4000 separate parts of the spacecraft, accounting for 25 % of total mass, are of composite materials.

1. Antennae. Eleven antennae (parabolic reflectors and horns) are located on the antenna tower module.

Among the four parabolic reflectors, the larger 4 GHz and 6 GHz units incorporate a thin honeycomb shell with a rib-stiffened backup structure. The skins are 2-ply from GY70 (Celanese) on the outside and Kevlar 49 in the inside bonded to a Kevlar honeycomb core. The rib stiffeners incorporate both materials bonded to the back of the reflector shell.

The two smaller parabolic reflector antennae, 11 GHz and 14 GHz, by Selenia (Italy), have GY70 face skins with aluminium honeycomb core for the sandwich structure. The surface of the reflectors are Carbon covered by a white thermal control coating.

The 4 GHz and 6 GHz horn antennae, by Mitsubishi Electric Corp. (Japan), have Carbon skins and honeycomb core sandwich using Torayca M40A Carbon.

2. 4 GHz and 6 GHz antenna feeds. Two antenna feed arrays with eighty-eight feed elements on each array, fabricated from T300 Carbon fiber/Epoxy, copper-clad in the inside surface. The feed elements are attached to a feed network array of copper-clad Carbon (GY70)/Epoxy face skins with aluminium sandwich structure and are in turn bolted to another Carbon/Epoxy skin-aluminium honeycomb core sandwich, which is part of the antenna support structure. A Kevlar aperture cover is used over the feed elements.

3. Carbon/Epoxy waveguides placed in the antenna tower module. One hundred and eighty Carbon/Epoxy pieces. Most of them are fabricated from T300 Carbon with an integral copper coating. These individual components are fabricated separately, with relatively simple tooling, and adhesively bonded to each other to form a maximum length run that can be accommodated in the antenna support module structure. These parts are in turn bolted together using Carbon flanges.

There are also thirty-nine Carbon/Epoxy waveguides in the spacecraft main body.

4. Antenna module structure. A Carbon/Epoxy structure, 3,3 m high, supports on the spacecraft the previously described systems.

The structure is fabricated out of Carbon/Epoxy tubular members of diameters  $25,4 \times 10^{-3}$  m and  $50,8 \times 10^{-3}$  m and wall thicknesses ranging from  $0,51 \times 10^{-3}$  m to  $1,90 \times 10^{-3}$  m, which are bonded together to form the truss. Carbon materials are GY70 and T300 fabric.

Five different support platforms of honeycomb sandwich construction with GY70 face skins with aluminium honeycomb core are bonded to the primary truss by Carbon/Epoxy clips.

There are over eight hundred separate piece parts in the tower fabrication.

5. Multiplexers. There are twenty-nine input fillers which make up eight multiplexers and twenty-three output fillers which make up five multiplexers per spacecraft system.

Material utilized is HMS Carbon/Epoxy. The individual parts (over 1100) are adhesively bonded together and the surface is metal-coated to fulfil electrical and moisture requirements.

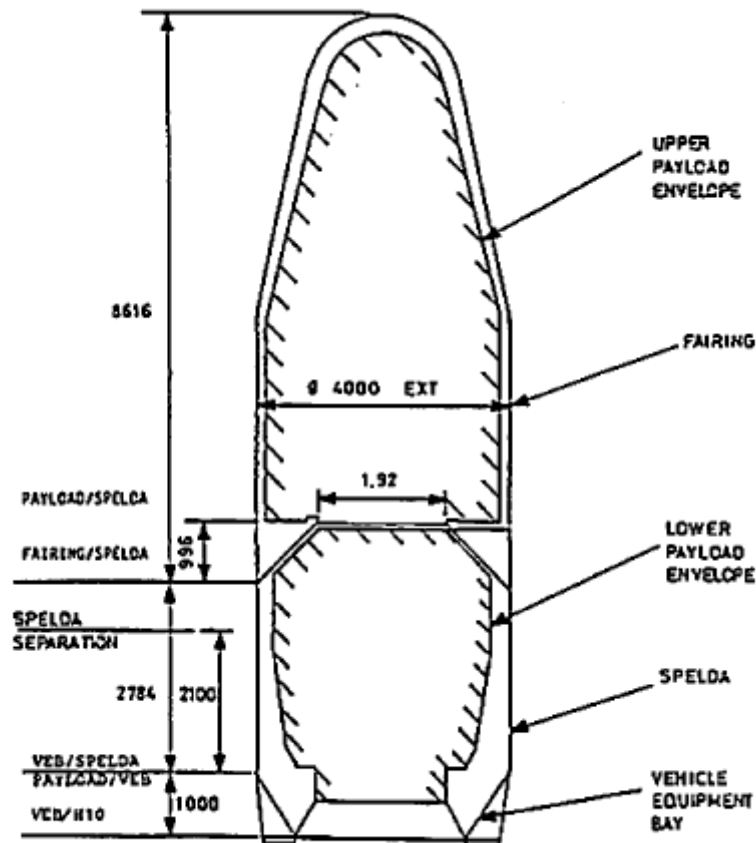
6. Solar array. Furnished by MBB (Germany). It consists of two wings, each 7 m long and 17 m wide. Each wing is assembled with three hinged panels (1,6 m x 2 m) and a yoke structure.

Each panel consists of a frame of Carbon/Epoxy edge members, aluminium honeycomb core and face skins of Carbon/Epoxy (Thornel 75) woven in an open mesh configuration and bonded to the frame and to the aluminium honeycomb core.

The yoke used to attach the panels to the spacecraft main body is Carbon/Epoxy.

### **5.16.2 Spelda (structure porteuse externe de lancement double ariane)**

SPELDA is a system for launching two satellites whilst fulfilling the functions of the external structure of ARIANE 4. It has been developed by British Aerospace. The major functions of SPELDA are (Figure 5-58):



Note: non-si units are used in this figure

**Figure 5-58: Sketch of the ARIANE 4 upper part. From Thomas & Oliver (1985) [155].**

Supporting the Upper Payload and Fairing.

Forming part of the launcher primary structure and shielding the Lower Payload. The shield separates around its circumference for deployment of the Lower Payload.

Carrying electrical signals for instrumentation and functioning of the Upper Payload and Fairing.

Giving access to the Lower Payload through the Payload Access Doors.

SPELDA structure is formed by Carbon/Epoxy faced honeycomb sandwich, Figure 5-59.

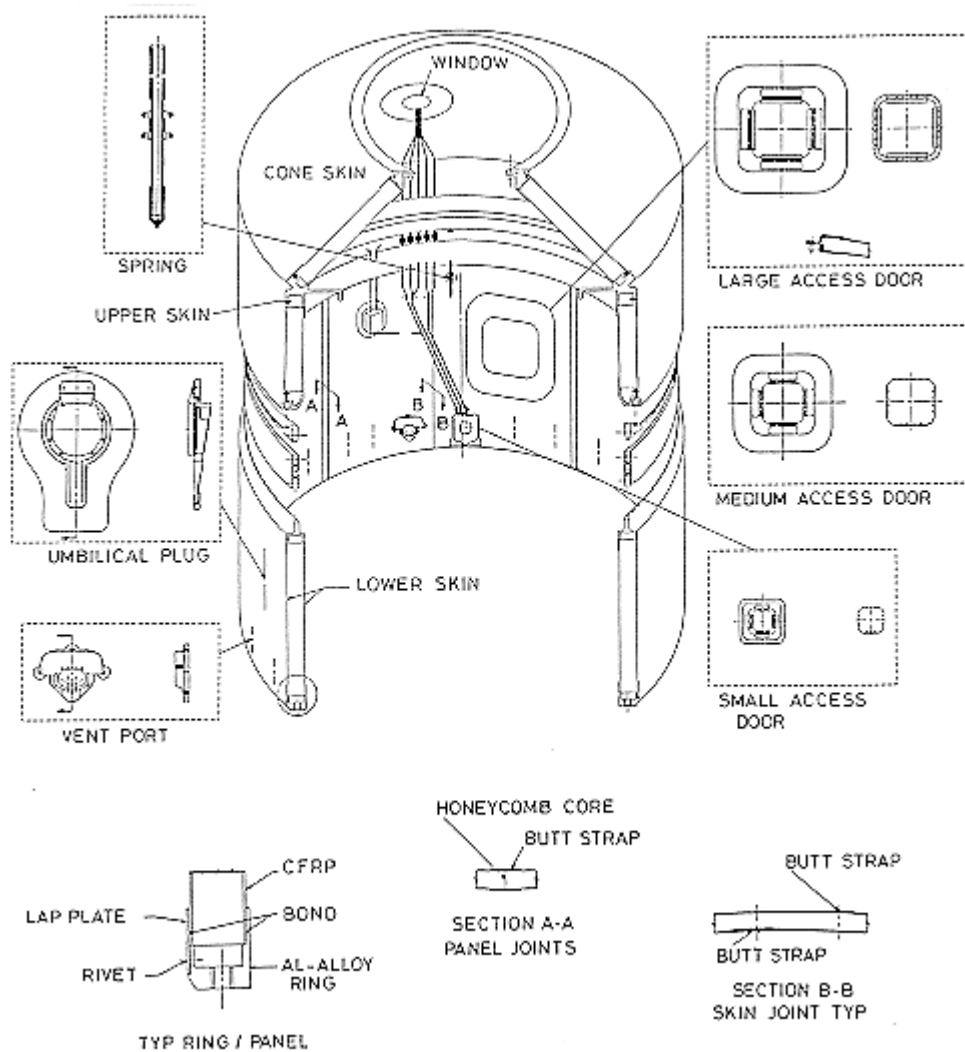


**Figure 5-59: Exploded view of SPELDA. From Thomas & Oliver (1985) [155].**

Carbon fiber is Courtaulds HMS pre-preg. Matrix is Code 69.

Honeycomb core is from expanded 5056 Al alloy with  $4,8 \times 10^{-3}$  m hexagonal cells  $0,018 \times 10^{-3}$  m foil thickness. Face skins are of Carbon/Epoxy bonded to the core.

The cylindrical and conical shell structures consist of panels bonded to each other by Carbon fiber butt straps. Each cylindrical shell is formed by three panels, each panel constructed from four separate skins. The conical shell consists of three panels of two skins each.

Ply layups.

Lower Panels and Core Panels:  $(0/60/\overline{90})_0$  fulfilling the requirements for stiffness and strength.

Upper Panels  $(0/\pm 60/\overline{90})_0$  driven by the requirement of diffusing local overload by the Fairing at the level of the Line Charge Connection Device.

The shells thus formed are bonded into forged and machined aluminium rings to complete the major SPELDA structure.

This composite materials structure fulfills the requirement imposed of mass, stiffness and strength under high loads at temperatures near 420 K.

### 5.16.3 CS-3A Japanese satellite

CS-3a is a Japanese domestic communication satellite, launched on 19 February 1988 which has a capacity of 6000 simultaneous telephone circuits. It has been developed by Mitsubishi Electrical Corporation under NASDA. CS-3a structure is sketched in Figure 5-60. The total launch mass is 1080 kg and the structure mass 53 kg. Almost all structural members are Carbon/Epoxy.

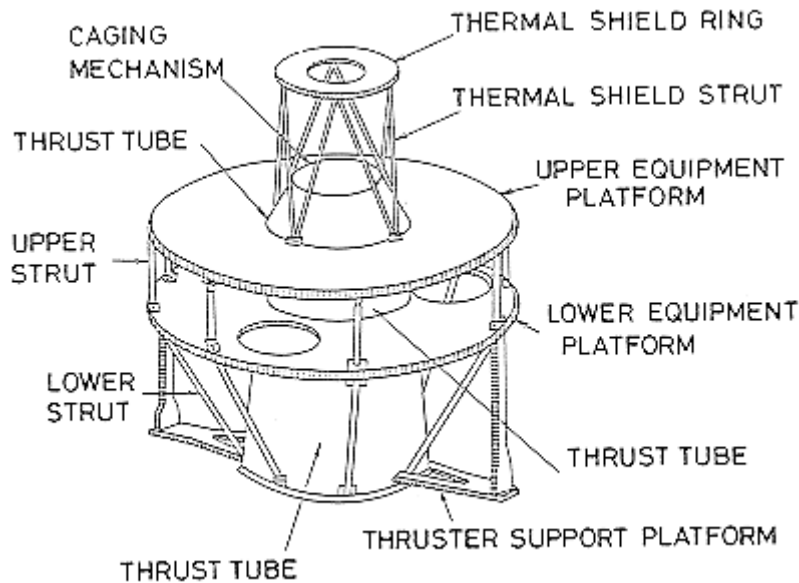


**Figure 5-60: Sketch of the CS-3a structure. From Kawashima, Inoue & Seko (1985) [112].**

1. Central Thrust Tube. The structure of the CS-3a satellite is assembled around a monocoque cone of continuously wound filament shell of Carbon/Epoxy from the rocket interface plane (bottom) to the antenna interface plane, Figure 5-61. The Apogee Boost Motor (ABM) is supported by a ring bonded inside the cone and the lower equipment platform is supported by a ring bonded outside the cone.



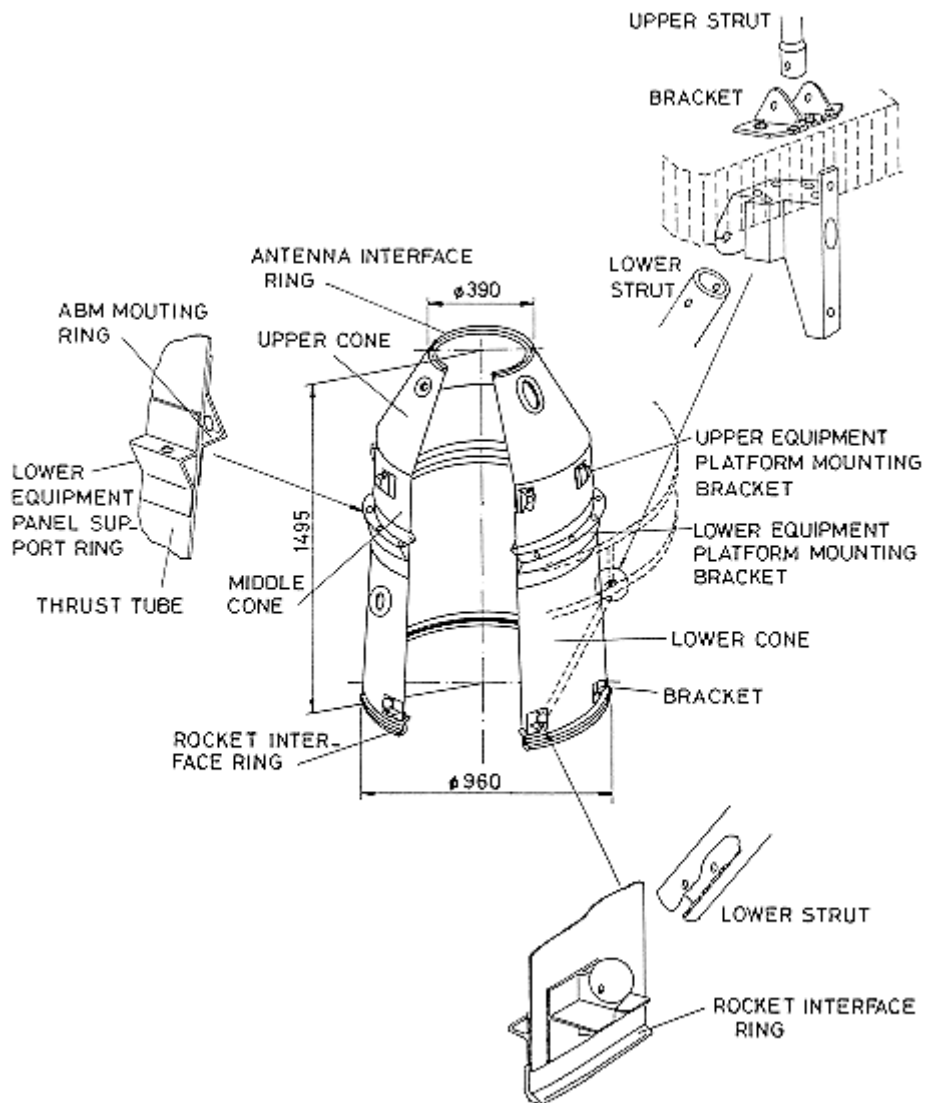


**Figure 5-61: Exploded view of CS-3a Central Thrust Tube. Prepared by the compiler after Kawashima, Inoue & Seko (1985) [112].**

The upper equipment platform is supported by eight brackets bonded to the cone. The thrust tube also supports the despun antenna assembly mounted on the top of it and has the rocket interface ring at the bottom.

Ply layups.

Below the ABM ring  $(\pm 70 / (\pm 20)_2 / \pm 70)_s$ .

Above the ABM ring  $(\pm 70^\circ / \pm 20^\circ)_s$ .

The directions  $20^\circ$  and  $70^\circ$  were chosen so as to maximize the buckling strength of the cone.

No additional details are given on the materials used except that the ABM ring can withstand a temperature of about 550 K and then its matrix is Polyimide instead of Epoxy.

The mass of the central thrust tube is 17,5 kg.

2. Joints. Up to thirty-two fairly critical brackets are used to join the equipment panels to the thrust tube. Considerably mass saving was achieved by fabricating them out of composite materials.

The configuration adopted in CS-3a is shown in Figure 5-61. Brackets and struts are all Carbon/Epoxy. The brackets attach the struts near the inner surface of these in order to diminish size. A spherical shell around the bosses allows rotating the strut around the connecting pin and transfers the strut load to the web.

More than 30 % mass savings, compared to an ordinary design, was achieved.

The joint connecting the upper and lower struts to the lower equipment platform is also shown in Figure 5-61. The brackets are composed of Carbon/Epoxy pieces (7 in the case of sketched bracket) bonded to each other.

3. Equipment Platforms. The upper and lower equipment platforms are Al alloy face sheets sandwiches.

The mass of each panel is 15 kg.

---

## Bibliography metallic materials

---

- [1] Adams, D.F., "High-Performance Composite Material Airframe Weight and Cost Estimating Relations", *Journal of Aircraft*, Vol. 11, No. 12, dec. 1974, pp. 751-757.
- [2] ALCAN, "Heat-Treatable Al-Cu-Mg Wrought Alloy 24 S", in "Aluminium Alloy Tables", 4<sup>th</sup> ed., Alcan S.A., Zürich, Switzerland, Feb. 1965.
- [3] Alloy Digest, "G-E Alloy René 41", in *Data on World Wide Metals and Alloys*", Engineering Alloy Digest, Inc., Upper Montclair, New Jersey, Nov. 1958, Filing Code: Ni-47.
- [4] Alloy Digest, "Invar", in "Data on World Wide Metals and Alloys", Engineering Alloy Digest, Inc., Upper Montclair, New Jersey, March 1964, Filing Code: Fe-24.
- [5] ALUMINIUM ASSOCIATION, "Aluminium Standards & Data 1970-71", 2<sup>nd</sup> ed., The Aluminium Association, New York, Dec. 1969, p. 35.
- [6] Anon., "1974 Materials Selector, Nonferrous Metals", *Materials Engineering*, Reinhold Publishing Company, Inc. Mid-Sep. 1973, p. 130.
- [7] ASMH, "Aluminium Alloys; Wrought, Heat Treatable (AIWT)", in "Aerospace Structural Metals Handbook", AFML-TR-68-115, J. Wolf, Ed., Mechanical Properties Data Center, Watertown, Mass., 1974, Codes 3203 & 3206.
- [8] ASMH, "Magnesium Alloys, Cast (MgWT)", in "Aerospace Structural Metals Handbook", AFML-TR-68-115, J. Wolf, Ed., Mechanical Properties Data Center, Watertown, Mass., 1974, Code 3407.
- [9] ASMH, "Nickel Base Alloys (>5% Co)(NiCo)", in "Aerospace Structural Metals Handbook", AFML-TR-68-115, J. Wolf, Ed., Mechanical Properties Data Center, Watertown, Mass., 1974, Code 4205.
- [10] ASMH, "Titanium Alloys (Ti)", in "Aerospace Structural Metals Handbook", AFML-TR-68-115, J. Wolf, Ed., Mechanical Properties Data Center, Watertown, Mass., 1974, Codes 3706 & 3707.
- [11] ASMH, "Titanium Alloys (Ti-3700)", in "Aerospace Structural Metals Handbook", AFML-TR-68-115, J. Wolf, Ed., Mechanical Properties Data Center, Watertown, Mass., 1974, Code 3718.
- [12] Ball, K., "Cleaning and Finishing of Aluminium and Aluminium Alloys", in "Metals Handbook, Vol. 5, Surface Cleaning, Finishing, and Coating", 9<sup>th</sup> ed., W.H. Cubberley et al., Eds., American Society for Metals (ASM), Metals Park, Ohio 44073, 1982, pp. 585-610.
- [13] Betner, D.R., "Properties of Titanium and Titanium Alloys", in "Metals Handbook, Vol. 3, Properties and Selection: Stainless Steels, Tool Materials and Special-Purpose Metals", 9<sup>th</sup> ed., W.H. Cubberley et al., Eds., American Society for Metals (ASM), Metals Park, Ohio 44703, 1980, pp. 372-412.

- [14] Bevans, J.T., "Aerospace Coatings for Thermal Control", Preliminary Report, Space Technology Laboratories, Inc., Redondo Beach, California, 1969.
- [15] Braun, A.H., "Selection and Applications of Magnesium Alloys", in "Metals Handbook, Vol. 2, Properties and Selection: Non Ferrous Alloys and Pure Metals", 9<sup>th</sup> ed., W.H. Cubberley et al., Eds., American Society for Metals (ASM), Metals Park, Ohio 44073, 1979, pp. 525-679.
- [16] Breuch, R.A., "Handbook of Optical Properties for Thermal Control Surfaces", LMSC-A847882, Vol. III, (NAS 8-20353), Lockheed Missiles & Space Company, Sunnyvale, California, 1967.
- [17] Campbell, J.E., "Alloys for Structural Applications at Subzero Temperatures", in "Metals Handbook, Vol. 3, Properties and Selection: Stainless Steels, Tool Materials and Special-Purpose Metals", 9<sup>th</sup> ed., W.H. Cubberley et al., Eds., American Society for Metals (ASM), Metals Park, Ohio 44073, 1980, pp. 723-746.
- [18] Coston, R.M., "Handbook of Thermal Design Data for Multilayer Insulation Systems", LMSC-A847882, Vol. II, (NAS 8-20353), Lockheed Missiles & Space Company, Sunnyvale, California, 1967.
- [19] Develay, R., Faure, A., Lehongre, S., Mugnier, D., Schroeter, D., "A Versatile Aluminium Alloy for Cryogenic Applications", in "Advances in Cryogenic Engineering", Vol. 12, K.D. Timmerhaus, Ed., Plenum Press, New York, 1967, pp. 484-495.
- [20] García-Poggio, J.A., Ramírez, P., Torre, J.M. de la, Vázquez, M., Asensi, E., Marín, C., Ciria, J., "Aleaciones Industriales de Aluminio", Instituto Nacional de Técnica Aeroespacial Esteban Terradas, Madrid, 1972.
- [21] Harris, Jr., W.J., "Wrought Heat-Resisting Alloys", in "Metals Handbook, Vol. 1, Properties and Selection of Metals", 8<sup>th</sup> ed., T. Lyman, Ed., American Society for Metals (ASM), Cleveland, Ohio, 1961, pp. 487-490.
- [22] Hunter, M.A., "Low-Expansion Alloys", in "Metals Handbook, Vol. 1, Properties and Selection of Metals", 8<sup>th</sup> ed., T. Lyman, Ed., American Society for Metals (ASM), Cleveland, Ohio, 1961, pp. 816-819.
- [23] Kappelt, G.F., "Properties of Aluminium and Aluminium Alloys", in "Metals Handbook, Vol. 1, Properties and Selection of Metals", 8<sup>th</sup> ed., T. Lyman, Ed., American Society for Metals (ASM), Cleveland, Ohio, 1961, pp. 935-958.
- [24] Ledbetter, H.M., Naimon, E.R., Weston, W.F., "Low-Temperature Elastic Properties of Invar", in "Advances in Cryogenic Engineering", Vol. 22, K.D. Timmerhaus, R.P. Reed and A.F. Clark, Eds., Plenum Press, New York, 1977, pp. 174-181.
- [25] McCall, J.L., "Introduction to Aluminium and Aluminium Alloys", in "Metals Handbook, Vol. 2, Properties and Selection: Non Ferrous Alloys and Pure Metals", 9<sup>th</sup> ed., W.H. Cubberley et al., Eds., American Society for Metals (ASM), Metals Park, Ohio 44073, 1979, pp. 3-236.
- [26] McCargo, M., Spradley, L.W., Greenberg, S.A., McDonald, S.L., "Review of the Transient Degradation/Contamination of Thermal Coatings", LMSC-D1778, (NAS 8-26004), Lockheed Missiles & Space Company, Sunnyvale, California, 1971.
- [27] Millard, J.P., Streed, E.R., "A Comparison on Infrared-Emittance Measurements and Measurement Techniques", Applied Optics, Vol. 8, No. 7, July 1969, pp. 1485-1492.
- [28] MOND NICKEL Co., "The Physical Properties of the Nickel Iron Alloys", The Mond Nickel Company Ltd., London.

- [29] Pennington, Wm.A., "Pure Metals", in "Metals Handbook, Vol. 1, Properties and Selection of Metals", 8<sup>th</sup> ed., T. Lyman, Ed., American Society for Metals (ASM), Cleveland, Ohio, 1961, p. 1197.
- [30] REYNOLDS METALS Co., "The Aluminium Data Book", Reynolds Metal Company, Richmond, Virginia, 1961, p. 49.
- [31] Ross, R.B., "Metallic Materials. Specification Handbook", E & F.N. Spon Ltd., London 1972, pp. 676-692.
- [32] Schafer, G.F., Bannister, T.C., "Thermal Control Coating Degradation Data from the Pegasus Experiment Packages", in "Progress in Astronautics and Aeronautics", Vol. 20, G.B. Heller, Ed., Academic Press, New York, 1967, pp. 457-473.
- [33] Scollon, T.R., Carpitella, M.J., "Long Life High Reliability Thermal Control Systems Study Data Handbook", Prepared under Contract NAS 8-26252 by Space Systems Organization, General Electric Company, Valley Forge Space Technology Center, Pennsylvania, 1970.
- [34] Simenz, R.F., Guess, M.K., "Structural Aluminium Materials for the 1980's", J. Aircraft, Vol. 17, July 1980, pp. 514-520.
- [35] Smithells, C.J., "Metals Reference Book", Vol II, 3<sup>rd</sup> ed., Butterworths, London, 1962, p. 701.
- [36] Stuart Lyman, W., "Properties of Titanium Alloys", in "Metals Handbook, Vol. 1, Properties and Selection of Metals", 8<sup>th</sup> ed., T. Lyman, Ed., American Society for Metals (ASM), Cleveland, Ohio, 1961, pp. 537-542 and 1153-1156.
- [37] Tien, J.K., Chesnutt, J.C., Boone, D.H., Goward, G.W., "Metallurgy of Nickel-Base Coatings on Titanium Alloys", in "Titanium Science and Technology", Vol. 4, R.I. Jaffee & H.M. Burte, Eds., Plenum Press, New York & London, 1973, pp. 2517-2525.
- [38] Touloukian, Y.S., "Thermophysical Properties of High Temperature Solid Materials", Vol. 1: Elements, The MacMillan Company, New York, 1967.
- [39] Touloukian, Y.S., "Thermophysical Properties of High Temperature Solid Materials", Vol. 2: "Nonferrous Alloys", Part I: "Nonferrous Binary Alloys", The MacMillan Company, New York, 1967.
- [40] Touloukian, Y.S., "Thermophysical Properties of High Temperature Solid Materials", Vol. 2: "Nonferrous Alloys", Part II: "Nonferrous Multiple Alloys", The MacMillan Company, New York, 1967.
- [41] Touloukian, Y.S., "Thermophysical Properties of High Temperature Solid Materials", Vol. 3: "Ferrous Alloys", The MacMillan Company, New York, 1967.
- [42] Touloukian, Y.S., DeWitt, D.P., "Thermal Radiative Properties. Metallic Elements and Alloys", Thermophysical Properties of Matter, Vol. 7, IPI/Plenum, New York, 1970.
- [43] Touloukian, Y.S., DeWitt, D.P., Hemicz, R.S., "Thermal Radiative Properties. Coatings", Thermophysical Properties of Matter, Vol. 9, IPI/Plenum, New York, 1972.
- [44] TRW, "Aerospace Fluid Component Designers' Handbook, Emissivity", Technical Documentary Report No. RPL-TOR-64-25, Feb. 1970. TRW Systems Group, Redondo Beach, California.
- [45] UNE, "Aluminio y Aleaciones de Aluminio para Forja", UNE 38-371-82, Madrid, Dec. 1982.
- [46] UNE, "Titanio y Aleaciones de Titanio para Forja", PNE 38-718-84, Madrid, 1984.

- [47] Zerlaut, G.A., Carroll, W.F., Gates, D.W., "Spacecraft Temperature-Control Coatings: Selection, Utilization and Problems Related to the Space Environment", in "Proceedings of the XVith International Astronautical Congress, Athens 1965", Gauthier-Villars, Dunod, Paris, 1966, pp. 259-313.

---

## References composite materials

---

- [48] Aalders, B.G.M., "A New Facility for Measuring the Coefficient of Thermal Expansion: CTE 1000", *ESA Journal*, Vol. 13, No. 4, 1989, pp. 383-392.
- [49] Aboudi, J., "Minimechanics of Tri-orthogonally Fibre-reinforced Composites: Overall Elastic and Thermal Properties", *Fibre Science and Technology*, Vol. 21, No. 4, 1984, pp. 277-293.
- [50] Abramowitz, M., Stegun, I.A., "Handbook of Mathematical Functions", 1<sup>st</sup> ed., Dover Publications, Inc., New York, 1965, Chap. 9, pp. 357-374.
- [51] Adamson, M.J., "Thermal Expansion and Swelling of Cured Epoxy Resin Used in Graphite/Epoxy Composite Materials", *J. Mater. Sci.*, Vol. 15, No. 7, July 1980, pp. 1736-1745.
- [52] AMOCO, "Composite Systems for Space Applications", Amoco Chemical Europe, Geneva, Switzerland, 1990, pp. 12 & 19.
- [53] Anon., "Materials Selector Issue", *Material Engineering*, Vol. 70, No. 5, Mid-Oct. 1969, pp. 190-191.
- [54] Ashworth, T., Loomer, J.E., Kreitman, M.M., "Thermal Conductivity of Nylons and Apiezon Greases", in "Advances in Cryogenic Engineering, Vol. 18", K.D. Timmerhaus, Ed., Plenum Press, New York, 1973, pp. 271-279.
- [55] Augl, J.M., Berger, A.E., "The Effect of Moisture on Carbon Fiber Reinforced Epoxy Composites. I: Diffusion", NSWC/WOL/TR 76-7, Naval Surface Weapons Center, White Oak, Maryland, 1976, pp. 1-77.
- [56] Balageas, D., Déom, A., Boscher, D., "Composite Materials Thermal Properties MEasurements by Pulsed Photothermal Radiometry", ONERA, T.P. 1988-77. Also presented to Eurotherm 4, Nancy, 28 Jun.-1er Juillet, 1988.
- [57] Balageas, D.L., "Thermal Diffusivity Measurement by Pulsed Methods", ONERA, T.,P. 1988-113.
- [58] Balageas, D.L., Luc, A.M., "Transient Thermal Behavior of Directional Reinforced Composites: Applicability Limits of Homegeneous Property Model", ONERA, T.P. 1986-47. Also published in *AIAA Journal*, Vol. 24, No. 1, Jan. 1986, pp. 109-114.
- [59] Balis Crema, L., Barboni, R., Castellani, A., "Thermoelastic Behaviour of Space Structures in Composite Materials". *Acta Astronautica*, Vol. 13, No. 9, Sept. 1986, pp. 547-552.
- [60] Balis Crema, L., Barboni, R., Castellani, A., Peroni, I., "Thermoelastic Characteristics Testing on Kevlar Samples for Spacecraft Structures", *Acta Astronautica*, Vol. 15, No. 12, Dec. 1987, pp. 997-1000.
- [61] Bassewitz, H.v., "Behaviour of Carbon Fibre Composites under Simulated Space Environment", in "Evaluation de L'Action de L'Environnement Spatial sur les Materiaux", International Conference, CNES, Toulouse, 17-21 Juin, 1974, pp. 525-537.

- [62] Beardmore, P., Hardwood, J.J., Kinsman, K.R., Robertson, R.E., "Fiber-Reinforced Composites: Engineered Structural Materials", *Science*, Vol. 208, No. 4446, 23 May 1980, pp. 833-840.
- [63] Bird, R.B., Stewart, W.E., Lightfoot, E.N., "Transport Phenomena", John Wiley & Sons, New York, 1960, Chap. 8, pp. 243-249, Chap. 16, pp. 495-504.
- [64] Brown, A.S., "Spreading Spectrum of Reinforcing Fibers", *Aerospace America*, Vol. 27, No. 1, Jan. 1989, pp. 14-18.
- [65] Carslaw, H.S., Jaeger, J.C., "Conduction of Heat in Solids", 2<sup>nd</sup> ed., Oxford at the Clarendon Press, 1959, Chap. 4, pp. 136-139.
- [66] Carter III, A.B., "Preserving the Structural Integrity of Advanced Composite Materials through the Use of Surface Mounted Fasteners", *SAMPE Journal*, Vol. 25, No. 4, July/Aug. 1989, pp. 21-25.
- [67] Chamis, C.C., "Simplified Composite Micromechanics Equations for Mechanical, Thermal and Moisture-Related Properties", in "Engineers' Guide to Composite Materials", J.W. Weeton, D.M. Peters, K.L. Thomas, Eds., American Society for Metals, Metals Park, Ohio, 1987, pp. 3-8 to 3-24.
- [68] Chiao, T.T., Moore, R.L., "A Room-Temperature-Curable Epoxy for Advanced Composites", 29<sup>th</sup> Annual Technical Conference of the Reinforced Plastic/Composites Institute (Society of the Plastics Industry, Inc., 1974), Sec. 16-B, pp. 1-7.
- [69] CIBA-GEIGY, "Araldite Matrix Systems", Sept. 1986.
- [70] Cipri, F., Pelosi, M., "A Study to Optimize the CFRP-Al Mechanical Joint in Order to Reduce Electrical Resistance", in "Behaviour and Analysis of Mechanically Fastened Joints in Composite Structures", AGARD-CP-427, Structures and Materials Panel Specialists' Meeting, Madrid, Spain, 27-29 April, 1987, Session II, pp. 10-1 to 10-11.
- [71] Clements, L.L., Chiao, T.T., "Engineering Design Data for an Organic Fibre/Epoxy Composite", *Composites*, Vol. 8, No. 2, April 1977, pp. 87-92.
- [72] Clements, L.L., Moore, R.L., "Composite Properties of an Aramid Fiber in a Room Temperature-Curable Epoxy Matrix", *Sample Quarterly*, Vol. 9, Oct. 1977, pp. 6-12.
- [73] Clements, L.L., Moore, R.L., "Composite Properties for E-glass Fibres in a Room Temperature Curable Epoxy Matrix", *Composites*, Vol. 9, No. 2, April 1978, pp. 93-99.
- [74] Clements, L.L., Moore, R.L., "Composite Properties for S-2 Glass in a Room Temperature Curable Epoxy Matrix", *SAMPE Quart.*, Vol. 10, Jan 1979, pp. 32-36. Society for the Advancement of Material and Process Engineering (SAMPE), Azusa, Calif.
- [75] Collings, E.W., Smith, R.D., "Specific Heats of Some Cryogenic Structural Materials II - Composites", in "Advanced in Cryogenic Engineering, Vol. 24", K.D. Timmerhaus, R.P. Reed, A.F. Clark, Eds. Plenum Press, New York, 1978, pp. 290-296.
- [76] Covington, M.A., Sawko, P.M., "Optical Properties of Woven Fabrics for Flexible Heat Shields", AIAA Paper No. 86-1281, AIAA 4<sup>th</sup> Joint Thermophysics and Heat Transfer Conference, June 2-4, 1986, Boston, Massachusetts.
- [77] Dauphin, J., "Fashionable Materials Subjects", in "Third European Symposium on Spacecraft Materials in Space Environment", ESTEC, Noordwijk, The Netherlands, 1-4 Oct. 1985, ESA SP-232, pp. 3-4.
- [78] Davis, L.A., "Strength, Ductility and Toughness", in "Metallic Glasses", American Society for Metals, Metals Park, Ohio 44073, 1978, Chap. 8, pp. 190-233.



- [79] Degiovanni, A., "Private Communication", LEMTA, Nancy, 10 Oct. 1990.
- [80] Delasi, R., Whiteside, J.B., "Effect of Moisture on Epoxy Resins and Composites", in "Advanced Composite Materials", Proceedings of the Symposium on Environmental Effects, Dayton, Ohio, Sept. 29-30, 1977. American Society for Testing and Materials, 1978, pp. 2-20.
- [81] DeMario, W.F., "New World for Aerospace Composites", *Aerospace America*, Vol. 24, No. 10, Oct. 1985, pp. 36-41.
- [82] Domínguez, F.S., "Woven Fabric Prepregs", in "Engineered Materials Handbook, Vol. 1: Composites", ASM International Handbook Committee, ASM International, Metals Park, Ohio, 44073, pp. 148-150, 1987.
- [83] Dootson, M., Sargent, J.P., Wostenholm, G.H., Yates, B., "Time and Temperature-Dependent Effects in the Thermal Expansion Characteristics of Carbon Fibre-Reinforced Plastics", *Composites*, Vol. 11, No. 2, April 1980, pp. 73-78.
- [84] Dresselhaus, M.S., Dresselhaus, G., Sugihara, K., Spain, I.L., Goldberg, H.A., "Graphite Fibers and Filaments", Springer Series in Material Sciences 5, Springer Verlag, Berlin, Heidelberg, New York, 1988, Chap. 5, pp. 106-119, Chap. 9, pp. 230-243.
- [85] Eagles, A.E., Babjak, S.J., Weaver, J.H., "Fabric Coatings: A New Technique for Spacecraft Passive Temperature Control", AIAA Paper No. 75-668, AIAA 10<sup>th</sup> Thermophysics Conference, Denver, Colorado, May 27-29, 1975.
- [86] Economy, J., Nowak, B.E., Cottis, S.G., "Ekonol: A High Temperature Aromatic Polyester", *SAMPE Journal*, Vol. 6, Aug.-Sep. 1970, pp. 21-27.
- [87] EPO-TEK, "Epo-Tek Epoxies, Thermally Conductive", Epoxy Technology Inc. Billerica, MA. 01821, USA, 1989.
- [88] ESA, "Composites Design Handbook for Space Structure Applications", ESA PSS-03-1101, ESTEC Noordwijk, 1989, Vol. 1, Chap. 2,000.
- [89] Fortier, S.M., Giletti, B.J., "An Empirical Model for Predicting Diffusion Coefficients in Silicate Minerals", *Science*, Vol. 245, No. 4925, Sept. 1989, pp. 1481-1484.
- [90] Friend, C.A., Poesch, J.G., Leslie, J.C., "Graphite Fiber Composites Fill Engineering Needs", 27<sup>th</sup> Annual Technical Conference. Reinforced Plastics/Composites Institute, The Society of the Plastics Industry, Inc., New York, 1972, Clause 17-E, pp. 1-8.
- [91] GENIUM, "Heat Transfer and Fluid Flow Data Books. Update No. 47", GENIUM Pub. Corp. Schenectady, N.Y., 1986, Clause 416.2.3, pp. 1-5.
- [92] Giommi, M., Marchetti, M., Salza, G., Testa, P., "Measurement of the Thermo-Optical Properties of Varying Paint Thicknesses on Carbon Fiber Composites in Spacecraft Structures", in ESA SP-232, "Third European Symposium on Spacecraft Materials in Space Environment", ESA, Paris, 1985, pp. 233-238.
- [93] Giori, C., Yamauchi, T., Rajan, K., Mell, R., "Mechanisms of Degradation of Graphite Composites in a Simulated Space Environment", AIAA Paper No. 83-0590, AIAA 21<sup>st</sup> Aerospace Sciences Meeting, Reno, Nevada, Jan. 10-13, 1983.
- [94] Hancox, N.L., "The Influence of Voids on the Hydrothermal Response of Carbon Fibre Reinforced Plastics", *J. Mater. Sci.*, Vol. 16, No. 3, March 1981, pp. 627-632.
- [95] Hansen, J.S., Tennyson, R.C., "Simulated Space Environmental Effects on Fiber-Reinforced Polymeric Composites", AIAA Paper No. 83-0590, AIAA 21<sup>st</sup> Aerospace Sciences Meeting, Reno, Nevada, Jan. 10-13, 1983.

- [96] Hanson, M.P., Chamis, C.C., "Experimental and Theoretical Investigation of HT-S/PMR-PI Composites for Application to Advanced Aircraft Engines", 29<sup>th</sup> Annual Technical Conference, 1974, Reinforced Plastic/Composites Institute, The Society of the Plastics Industry, Inc., Clause 20-C, pp. 1-10.
- [97] Harley, J.A., Rosenberg, H.M., "The Thermal Expansion of Carbon/carbon Composites", *Composites*, Vol. 11, Jan. 1981, pp. 73-75.
- [98] Harper, C.A., "Handbook of Plastics and Elastomers", 1<sup>st</sup> ed., McGraw-Hill Book Company, New York, 1975, Chap. 3, pp. 3-1 to 3-82.
- [99] Hartwig, G., "Overview of Advanced Fibre Composites", *Cryogenics*, Vol. 28, No. 4, April 1988, pp. 216-219.
- [100] Haruvy, Y., "Risk Assessment of Atomic-Oxygen-Effected Surface Erosion and Induced Outgassing of Polymeric Materials in LEO Space Systems", *ESA Journal*, Vol. 14, No. 1, 1990, pp. 109-119.
- [101] Hertz, J., Haskins, J.F., "Thermal Conductivity of Reinforced Plastics at Cryogenic Temperatures", "Advances in Cryogenic Engineering", Vol. 10, K.D. Timmerhaus, Ed., Plenum Publ. Corp., New York, 1965, pp. 163-170.
- [102] Hillesland, H.L., "Advanced Composites Hardware Utilized on the INTELSAT V Spacecraft", in "The 1980's-Payoff Decade for Advanced Materials", 25<sup>th</sup> National Sampe Symposium and Exhibition, San Diego, Calif., May 6-8, 1980, pp. 202-211. Society for the Advancement of Material and process Engineering (SAMPE), Azusa, Calif.
- [103] Hsiue, E.S., Miller, R.L., Segal, L., "A New Matrix System for Advanced Composites: Dicyanate Semi-IPN", in "Proceedings of the Fifth International Conference on Composite Materials", San Diego, CA, July 29-Aug. 1, 1985. Metallurgical Society, Inc., Warrendale, PA, 1985, pp. 1655-1665.
- [104] Hsu, M.S., Chen, T.S., Parker, J.A., Heimbuch, A.H., "New Bismaleimide Matrix Resins for Graphite Fiber Composites", *SAMPE Journal*, Vol. 21, July-Aug. 1985, pp. 11-16.
- [105] Hsu, S.E., Chen, C.I., "The Processing and Properties of Some C/C Systems", in "Superalloys, Supercomposites and Superceramics", J.K. Tien & T. Caufields, Eds., Academic Press, Inc., Boston, 1989, pp. 721-744.
- [106] Ishikawa, T., Koyama, K., Kobayashi, S., "Elastic Moduli of Carbon-Epoxy Composites and Carbon Fibers", *J. Composite Materials*, Vol. 11, July 1977, pp. 332-344.
- [107] Ishikawa, T., Koyama, K., Kobayashi, S., "Thermal Expansion Coefficients of Unidirectional Composites", *J. Composites Materials*, Vol. 12, April 1978, pp. 153-167.
- [108] James, B.W., Yates, B., "The Interferometric Measurement of the Thermal Expansion of Caesium Iodide at Low Temperatures", *Cryogenics*, Vol. 5, No. 2, April 1965, pp. 68-72.
- [109] Johnson, V.I., "Properties of Materials at Low Temperatures (Phase 1)", Pergamon Press, New York, 1961, Part II, Chap. 4, 4,402.
- [110] Kalnin, I.L., "Thermal Expansion of High Modulus Graphite Fiber/Epoxy Composites", 29<sup>th</sup> Annual Technical Conference, 1974, Reinforced Plastic/Composites Institute, The Society of the Plastics Industry, Inc., Clause 25-C, pp. 1-8.
- [111] Karlsson, T., "Litteraturundersökning AV Elektriskt Motstånd och Termiska Egenskaper hos Moderna Kompositter och i dem Ingaende Fibrer och Matriser", FOA Rapport C 20505-D6 (F9) Augusti 1983, Försvarets Forskningsanstalt - Huvudavdelning 2, Stockholm.

- [112] Kawashima, T., Inoue, T., Seko, H., "Design and Development of the Graphite Epoxy Structure for CS-3 Satellite", in ESA SP-243, "Composites Design for Space Applications", Proceedings of a Workshop, ESTEC, Noordwijk, The Netherlands, 15-18 Oct. 1985, ESA, Paris, 1985, pp. 267-274.
- [113] Kazanjian, A.R., "Review of Properties of Polycarbonate Resins", in "Polymer-Plastics Technology and Engineering", Vol. 2, L. Naturman, Ed., Marcel Dekker, Inc., New York, 1974, pp. 123-160.
- [114] Klich, P.J., Cockrell, C.E., "Mechanical Properties of a Fiberglass Prepreg System at Cryogenic and Other Temperatures", AIAA Journal, Vol. 21, No. 12, dec. 1983, pp. 1722-1728.
- [115] Lachi, M., Legrand, P., Degiovanni, A., "Mesure de la Diffusivité Thermique de Matériaux Composites en Plaques Minces", Proc. Eurotherm Seminar, No. 4, 28-30 Juin 1988, LEMTA U.A. 875 CNRS, Nancy, France.
- [116] Landis, F., "Laboratory Experiments and Demonstrations in Fluid Mechanics and Heat Transfer", Dept. of Mech. Eng., School of Engineering and Science, New York University, N.Y., 1964, Chap. II, Exp. (46), pp. 126-129.
- [117] Larue, J.C., "Accelerated Thermal Cycling of Spacecraft Solar-Cell Modules", ESA Bulletin, No. 32, Nov. 1982, pp. 70-74.
- [118] Leger, L.J., Visentine, J.T., "Protecting Spacecraft from Atomic Oxygen", Aerospace America, Vol. 24, No. 7, July 1986, pp. 32-35.
- [119] Lemaitre, J., Chaboche, J.L., "Mecanique des Matériaux Solides", 1<sup>st</sup> ed., Dunod, Paris, 1985, Chap. 4, p. 134.
- [120] Lobo, H., Cohen, C., "Measurement of Thermal Conductivity of Polymer Melts by Line-Source Method", Polym. Eng. Sci., Vol. 30, No. 2, Jan. 1990, pp. 65-70.
- [121] Lodge, K.J., "The Electrical Properties of Joints in Carbon Fibre Composites", Composites, Vol. 13, July 1982, pp. 305-310.
- [122] Loos, A.C., Springer, G.S., "Moisture Absorption of Graphite-Epoxy Composites Immersed in Liquids and in Humid Air", J. Composite Materials, Vol. 13, April 1979, pp. 131-147.
- [123] Lubin, G., Dastin, S.J., "Aerospace Applications of Composites", in "Handbook of Composites", G. Lubin, Ed., Van Nostrand Reinhold Company, New York, 1982, Chap. 28, pp. 722-743.
- [124] Luc, A.M., Balageas, D., "Comportement Thermique des Composites a Renforcement Orienté Soumis à des Flux Impulsionnels", ONERA. T.P. 1984-119. Also published in High Temperatures-High Pressures, 1984, Vol. 16, pp. 209-219.
- [125] Mauri, R.E., Crossman, F.W., "Space Radiation Effects on Structural Composites", AIAA Paper No. 83-0591, AIAA 21<sup>st</sup> Aerospace Sciences Meeting, Reno, Nevada, Jan. 10-13, 1983
- [126] McCargo, M., Dammann, R.A., Cummings, T., Carperter, C., "Laboratory Investigation of Organic Coatings for Use in a LEO Environment", in ESA SP-232, "Third European Symposium on Spacecraft Materials in Space Environment", ESA, Paris, 1985, pp. 91-97.
- [127] McGuire, C.F., Vollerin, B.L., "Thermal Management of Space Structures", in "Plastics-Metals-Ceramics", Proceedings of the 11<sup>th</sup> International European Chapter Conference of the Society for Advancement of Material and Process Engineering, Basel, Switzerland, May 29-31, 1990, H.L. Hornfeld and the Swiss Sampe Member Association, Eds., pp. 95-115.

- [128] McKague, Jr., E.L., Reynolds, J.D., Halkias, J.E., "Swelling and Glass Transition Relations in Epoxy Matrix Material in Humid Environments", *J. Applied Polymer Science*, Vol. 22, No. 6, pp. 1643-1654, June 1978.
- [129] Min, B.K., Crossman, F.W., "History-Dependent Thermomechanical Properties of Graphite/Aluminium Unidirectional Composites", in "Composite Materials: Testing and Design (Sixth Conference)", ASTM STP 787, I.M. Daniel, Ed., American Society for Testing and Materials, 1982, pp. 371-392.
- [130] Morrison, W.D., Tennyson, R.C., French, J.B., Braithwaite, T., Moisan, M., Hubert, J., "Atomic Oxygen Effects on Materials", 4<sup>th</sup> International Conference on "Spacecraft Materials in Space Environment", Toulouse, France, 6-9 Sept. 1988. A Revision copy by the same authors, "Atomic Oxygen Studies on Polymers".
- [131] Nicholls, C.I., Rosenberg, H.M., "The Thermal Conductivity of Carbon-Carbon Fibre Composites below 80K", *Cryogenics*, Vol. 24, No. 7, July 1984, pp. 355-358.
- [132] Ott, H.J., "Thermal Conductivity of Composite Materials", *Plastics and Rubber Processing and Applications*, Vol. 1, No. 1, 1981, pp. 9-24.
- [133] Parker, S.F.H., Chandra, M., Yates, B., Dootson, M., Walters, B.J., "The Influence of Distribution between Fibre Orientations upon the Thermal Expansion Characteristics of Carbon Fibre-Reinforced Plastics", *Composites*, Vol. 11, Oct. 1981, pp. 281-287.
- [134] Pater, R.H., "A Review of Dynamic Mechanical Characterization of High Temperature PMR Polyimides and Composites", in "Polymer Composites for Automotive Applications", SP-748, Society Automotive Engineers, Inc. Warrendale, PA, Feb. 1988.
- [135] Penton, A.P., "Changing Patterns and New Technology for Non-Metallic Thermal Protection Materials for Atmospheric Re-Entry Vehicles", 21<sup>st</sup> Annual Meeting, 1966, Reinforced Plastics Division, The Society of the Plastics Industry, Inc., Clause 8-A, pp. 1-8.
- [136] Petrasek, D.W., Signorelli, R.A., Caufield, T., Tien, J.K., "Fiber Reinforced Superalloys", in "Superalloys, Supercomposites and Superceramics", J.K. Tien & T. Caufields, Eds., Academic Press, Inc., Boston, 1989, pp. 625-670.
- [137] Pilling, M.W., Yates, B., Black, M.A., Tattersall, P., "The Thermal Conductivity of Carbon Fibre-Reinforced Composites", *J. Mater. Sci.*, Vol. 14, No. 6, June 1979, pp. 1326-1338.
- [138] Pojur, A.F., Yates, B., "Thermal Expansion at Elevated Temperatures. I: Apparatus for Use in the Temperature Range 300-800 K: The Thermal Expansion of Copper", *J. Phys. E.: Sci. Instruments*, Vol. 6, No. 1, January 1973, pp. 63-66.
- [139] Priest, E.R., "Solar Magneto-Hydrodynamics", 1<sup>st</sup> ed., Reidel Publishing Company, London 1982, Chap. 1, pp. 52-53.
- [140] Pujolá, R.M., Balageas, D.L., "Derniers Développements de la Méthode Flash Adaptée aux Matériaux Composites à Renforcement Orienté", ONERA, T.P. 1986-130. Also published in *High Temperatures-High Pressures*, 1985, Vol. 17, pp. 623-632.
- [141] Reibaldi, G.G., "Thermomechanical Behaviour of CFRP Tubes for Space Structures", *Acta Astronautica*, Vol. 12, No. 5, May 1985, pp. 323-333.
- [142] Reinhard, D., "Reinforced Thermoplastics Composites in Transportation Applications", in "Polymer Composites for Automotive Applications", SP-748, Society Automotive Engineers, Inc. Warrendale, PA, Feb. 1988.
- [143] Rogers, K.F., Kingston-Lee, D.M., Phillips, L.N., Yates, B., Chandra, M., Parker, S.F.H., "The Thermal Expansion of Carbon Fibre-Reinforced Plastics. Part 6. The Influence of

- Fibre Weave in Fabric Reinforcement", *J. Mater. Sci.*, Vol. 16, No. 10, Oct. 1981, pp. 2803-2818.
- [144] Rogers, K.F., Phillips, L.N., Kingston-Lee, D.M., Yates, B., Overy, M.J., Sargent, J.P., McCalla, B.A., "The Thermal Expansion of Carbon Fibre-Reinforced Plastics. Part. 1: The Influence of Fibre Type and Orientation", *J. Mater. Sci.*, Vol. 12, No. 4, April 1977, pp. 718-734.
- [145] Rosato, D.V., "An Overview of Composites", in "Handbook of Composites", G. Lubin, Ed., Van Nostrand Reinhold Company, New York, 1982, Chap. 1, pp. 1-14.
- [146] Scola, D.A., Laube, B.L., "A comparison of Thermo-Oxidative Stability of Commercial Graphite Fibers for Composite Applications", in "Polymer Composites for Automotive Applications", SP-748, Society Automotive Engineers, Inc. Warrendale, PA, Feb. 1988.
- [147] SENER, "Composites Design Handbook, Vols. I, II", ESTEC Contract 5816/84/NL/PB(SC), 1984.
- [148] Shen, C.H., Springer, G.S., "Moisture Absorption and Desorption of Composite Materials", *J. Composite Materials*, Vol. 10, Jan. 1976, pp. 2-20.
- [149] Skinner, W., Golghar, J.D., "An Introduction to the Plastic Industry", in "Environmental Effects on Polymeric Materials. Vol. 1: Environments", D.V. Rosato and R.T. Schwartz (eds.), Interscience Publishers, New York, 1968, pp. 41, 157.
- [150] Steinberg, J., Tyagy, S., Lord, Jr., A.E., "Effect of Annealing on the Thermal Expansion of  $\text{Fe}_{40}\text{Ni}_{40}\text{P}_{14}\text{B}_6$  and  $\text{Fe}_{29}\text{Ni}_{49}\text{P}_{14}\text{B}_6\text{Si}_2$ ", *J. Non-Crystalline Solids*, Vol. 41, No. 2, 1980, pp. 279-282.
- [151] Strife, J.R., Prewo, K.M., "The Thermal Expansion Behavior of Unidirectional and Bidirectional Kevlar/Epoxy Composites", *J. Composite Materials*, Vol. 13, Oct. 1979, pp. 264-277.
- [152] Taylor, R.E., Groot, H., Shoemaker, R.L., "Thermophysical Properties of Fine Weave Carbon/Carbon Composites", AIAA Paper No. 81-1103, AIAA 16<sup>th</sup> Thermophysics Conference, Palo Alto, Calif., June 23-25, 1981.
- [153] Tennyson, R.C., "Composite Materials in a Simulated Space Environment", AIAA Paper No. 80-0678-CP, AIAA/ASME/ASCE/AHS 21<sup>st</sup> Structures, Structural Dynamics & Materials Conference, Seattle, Washington, May 12-14, 1980.
- [154] Tennyson, R.C., Zimcik, D.G., "Space Environmental Effects on Polymer Matrix Composite Structures", in "Spacecraft Materials in a Space Environment", ESA SP-178, ESA, Paris, 1982, pp. 215-226.
- [155] Thomas, N.G., Oliver, W.T., "The Development of the ARIANE 4 SPELDA", in ESA SP-243, "Composites Design for Space Applications", Proceedings of a Workshop, ESTEC, Noordwijk, The Netherlands, 15-18 Oct. 1985, ESA, Paris, 1985, pp. 251-263.
- [156] Thomson, J.M., "The Electrical Properties of Carbon Fibre Composites", in "Practical Considerations of Design, Fabrication and Tests of Composite Materials", AGARD-LS-124, Lecture Series presented 11-12 October 1982 in Oporto, Portugal, 14-15 October 1982 in London, U.K. and 18-19 October in Ankara, Turkey, pp. 9-1 to 9-5.
- [157] Touloukian, Y.S., "Thermophysical Properties of High Temperature Solid Materials", Vol. 6: Intermetallics, Cermets, Polymers, and Composite Systems, The MacMillan Company, New York, 1967, Polymers, pp. 939-1093, Composite Systems, pp. 1095-1231.

- [158] Touloukian, Y.S., DeWitt, D.P., "Thermal Radiative Properties, Nonmetallic Solids", Thermophysical Properties of Matter, Vol. 7, IFI/Plenum, New York-Washington, 1972, pp. 1711-1731.
- [159] Tsai, S.W., "Composite Design", 3<sup>rd</sup> ed., Think Composites, Dayton OH, 1987, Chap. 17, pp. 17-7 to 17-11.
- [160] Tsatis, D.E., "Thermal Diffusivity of Araldite", Cryogenics, Vol. 28, No. 9, Sept. 1988, pp. 609-610.
- [161] Valentich, J., "Thermal Expansion of Solids from -261°C to 173°C Using Strain Gauges", Cryogenics, Vol. 25, No. 2, Feb. 1985, pp. 63-67.
- [162] Visentine, J.T., Leger, L.J., Kuminecz, J.F., Spiker, I.J., "STS-8 Atomic Oxygen Effects Experiment", AIAA Paper No. 85-0415, AIAA 2<sup>nd</sup> Aerospace Sciences Meeting, Reno, Nevada, Jan. 14-17, 1985.
- [163] Weast, R.C., "Handbook of Chemistry and Physics", 57<sup>th</sup> ed., CRC Press, Cleveland, Ohio, 1976, pp. C-797, C-799, F-801.
- [164] Weeton, J.W., Peters, D.M., Thomas, K.L., "Engineers Guide to composite Materials", American Society for Metals, Metals Park, Ohio, 1986.  
Section 1: Introduction to Composite Materials, pp. 1-1 to 1-6.  
Section 5: Property Data: Reinforcements, pp. 5-1 to 5-39.  
Section 6: Property Data: Polymer Matrix Composites, pp. 6-1 to 6-68.
- [165] Whitney, J.M., Browning, C.E., "Some Anomalies Associated with Moisture Diffusion in Epoxy Matrix Composite Materials", in "Advanced Composite Materials - Environmental Effects", ASTM STP 658, J.R. Vinson, Ed., American Society for Testing and Materials, 1978, pp. 43-60.
- [166] Witte, Jr., W.G., Teichman, L.A., "Optical Properties of Sputtered Aluminium on Graphite/Epoxy Composite Materials", NASA TM 101620, NASA Langley Research Center, Aug. 1989.
- [167] Yang, G., Migone, A.D., "Low Temperature Specific Heat Measurement of a Carbon-Carbon Composite", Cryogenics, Vol. 29, No. 12, Dec. 1989, pp. 1154-1155.
- [168] Yates, B., McCalla, B.A., Sargent, J.P., Rogers, K.F., Kingston-Lee, D.M., Phillips, L.N., "Thermal Expansion of Carbon Fibre-Reinforced Plastics. Part 4: Ply Multidirectional Effects", J. Mater. Sci., Vol. 13, No. 10, Oct. 1978, pp. 2226-2232.
- [169] Yates, B., McCalla, B.A., Sargent, J.P., Rogers, K.F., Phillips, L.N., Kingston-Lee, D.M., "The Thermal Expansion of Carbon Fibre-Reinforced Plastics. Part 3: The Influence of Resin Type", J. Mater. Sci., Vol. 13, No. 10, Oct. 1978, pp. 2217-2225.
- [170] Yates, B., Overy, M.J., Sargent, J.P., McCalla, B.A., Kingston-Lee, D.M., Phillips, L.N., Rogers, K.F., "The Thermal Expansion of Carbon Fibre-Reinforced Plastics. Part 2: The Influence of Fibre Volume Fraction", J. Mater. Sci., Vol. 13, No. 2, Feb. 1978, pp. 433-440.
- [171] Zimcik, D.G., Tennyson, R.C., Kok, L.J., Maag, C.R., "The Effect of Low Earth Orbit Space Environment on Polymeric Spacecraft Materials", in ESA SP-232, "Third European Symposium on Spacecraft Materials in Space Environment", ESA, Paris, 1985, pp. 81-89.